

Natural products modulate the sensitivity of cancer to Anti-PD-1 based immunotherapy

Edited by

Qian Ba, Hang Ma, Jean Christopher Chamcheu and Xiaoguang Li

Published in

Frontiers in Pharmacology

Frontiers in Oncology



FRONTIERS EBOOK COPYRIGHT STATEMENT

The copyright in the text of individual articles in this ebook is the property of their respective authors or their respective institutions or funders. The copyright in graphics and images within each article may be subject to copyright of other parties. In both cases this is subject to a license granted to Frontiers.

The compilation of articles constituting this ebook is the property of Frontiers.

Each article within this ebook, and the ebook itself, are published under the most recent version of the Creative Commons CC-BY licence. The version current at the date of publication of this ebook is CC-BY 4.0. If the CC-BY licence is updated, the licence granted by Frontiers is automatically updated to the new version.

When exercising any right under the CC-BY licence, Frontiers must be attributed as the original publisher of the article or ebook, as applicable.

Authors have the responsibility of ensuring that any graphics or other materials which are the property of others may be included in the CC-BY licence, but this should be checked before relying on the CC-BY licence to reproduce those materials. Any copyright notices relating to those materials must be complied with.

Copyright and source acknowledgement notices may not be removed and must be displayed in any copy, derivative work or partial copy which includes the elements in question.

All copyright, and all rights therein, are protected by national and international copyright laws. The above represents a summary only. For further information please read Frontiers' Conditions for Website Use and Copyright Statement, and the applicable CC-BY licence.

ISSN 1664-8714
ISBN 978-2-8325-2621-7
DOI 10.3389/978-2-8325-2621-7

About Frontiers

Frontiers is more than just an open access publisher of scholarly articles: it is a pioneering approach to the world of academia, radically improving the way scholarly research is managed. The grand vision of Frontiers is a world where all people have an equal opportunity to seek, share and generate knowledge. Frontiers provides immediate and permanent online open access to all its publications, but this alone is not enough to realize our grand goals.

Frontiers journal series

The Frontiers journal series is a multi-tier and interdisciplinary set of open-access, online journals, promising a paradigm shift from the current review, selection and dissemination processes in academic publishing. All Frontiers journals are driven by researchers for researchers; therefore, they constitute a service to the scholarly community. At the same time, the *Frontiers journal series* operates on a revolutionary invention, the tiered publishing system, initially addressing specific communities of scholars, and gradually climbing up to broader public understanding, thus serving the interests of the lay society, too.

Dedication to quality

Each Frontiers article is a landmark of the highest quality, thanks to genuinely collaborative interactions between authors and review editors, who include some of the world's best academicians. Research must be certified by peers before entering a stream of knowledge that may eventually reach the public - and shape society; therefore, Frontiers only applies the most rigorous and unbiased reviews. Frontiers revolutionizes research publishing by freely delivering the most outstanding research, evaluated with no bias from both the academic and social point of view. By applying the most advanced information technologies, Frontiers is catapulting scholarly publishing into a new generation.

What are Frontiers Research Topics?

Frontiers Research Topics are very popular trademarks of the *Frontiers journals series*: they are collections of at least ten articles, all centered on a particular subject. With their unique mix of varied contributions from Original Research to Review Articles, Frontiers Research Topics unify the most influential researchers, the latest key findings and historical advances in a hot research area.

Find out more on how to host your own Frontiers Research Topic or contribute to one as an author by contacting the Frontiers editorial office: frontiersin.org/about/contact

Natural products modulate the sensitivity of cancer to Anti-PD-1 based immunotherapy

Topic editors

Qian Ba — Shanghai Jiao Tong University, China

Hang Ma — University of Rhode Island, United States

Jean Christopher Chamcheu — University of Louisiana at Monroe, United States

Xiaoguang Li — Shanghai Jiao Tong University, China

Citation

Ba, Q., Ma, H., Chamcheu, J. C., Li, X., eds. (2023). *Natural products modulate the sensitivity of cancer to Anti-PD-1 based immunotherapy*.

Lausanne: Frontiers Media SA. doi: 10.3389/978-2-8325-2621-7

Table of contents

- 05 **Editorial: Natural products modulate the sensitivity of cancer to anti-PD-1 based immunotherapy**
Jean Christopher Chamcheu, Qian Ba and Hang Ma
- 08 **Chimeric Antigen Receptor-T Cells: A Pharmaceutical Scope**
Alejandrina Hernández-López, Mario A. Téllez-González, Paul Mondragón-Terán and Angélica Meneses-Acosta
- 27 **Immune Checkpoint Inhibitor–Associated Tumor Lysis Syndrome: A Real-World Pharmacovigilance Study**
Li Wang, Xiaolin Li, Bin Zhao, Dan Mei, Jiandong Jiang and Jingli Duan
- 38 **The Current Application and Future Prospects of Astragalus Polysaccharide Combined With Cancer Immunotherapy: A Review**
Fanming Kong, Tianqi Chen, Xiaojiang Li and Yingjie Jia
- 50 **Perifosine, a Bioavailable Alkylphospholipid Akt Inhibitor, Exhibits Antitumor Activity in Murine Models of Cancer Brain Metastasis Through Favorable Tumor Exposure**
Keisuke Taniguchi, Tomo Suzuki, Tomomi Okamura, Akinobu Kurita, Gou Nohara, Satoru Ishii, Shoichi Kado, Akimitsu Takagi, Momomi Tsugane and Yoshiyuki Shishido
- 63 **Targeting GGT1 Eliminates the Tumor-Promoting Effect and Enhanced Immunosuppressive Function of Myeloid-Derived Suppressor Cells Caused by G-CSF**
Zhiqi Xie, Takahiro Kawasaki, Haoyang Zhou, Daisuke Okuzaki, Naoki Okada and Masashi Tachibana
- 74 **Can Natural Products be Used to Overcome the Limitations of Colorectal Cancer Immunotherapy?**
Jiahuan Dong, Yufan Qian, Guangtao Zhang, Lu Lu, Shengan Zhang, Guang Ji, Aiguang Zhao and Hanchen Xu
- 84 **Further investigation of blockade effects and binding affinities of selected natural compounds to immune checkpoint PD-1/PD-L1**
Huifang Li, Navindra P. Seeram, Chang Liu and Hang Ma
- 91 **YIV-906 enhances nuclear factor of activated T-cells (NFAT) activity of T cells and promotes immune checkpoint blockade antibody action and CAR T-cell activity**
Wing Lam, Rong Hu, Shwu-Huey Liu, Peikwen Cheng and Yung-Chi Cheng
- 104 **Development of a population pharmacokinetics and pharmacodynamics model of glucarpidase rescue treatment after high-dose methotrexate therapy**
Yutaka Fukaya, Toshimi Kimura, Yukihiro Hamada, Kenichi Yoshimura, Hiroaki Hiraga, Yuki Yuza, Atsushi Ogawa, Junichi Hara, Katsuyoshi Koh, Atsushi Kikuta, Yuhki Koga and Hiroshi Kawamoto

- 115 **Dietary fungi in cancer immunotherapy: From the perspective of gut microbiota**
Yibing Wei, Dingka Song, Ran Wang, Tingting Li, Hui Wang and Xiaoguang Li
- 127 **Exploring the components and mechanism of *Solanum nigrum* L. for colon cancer treatment based on network pharmacology and molecular docking**
Jin-Fang Chen, Shi-Wei Wu, Zi-Man Shi, Yan-Jie Qu, Min-Rui Ding and Bing Hu
- 141 **Ginsenosides, potential TMPRSS2 inhibitors, a trade-off between the therapeutic combination for anti-PD-1 immunotherapy and the treatment of COVID-19 infection of LUAD patients**
Mei Meng, Rui Gao, Zixue Liu, Fengxiang Liu, Shiyu Du, Yizhi Song and Jian He



OPEN ACCESS

EDITED AND REVIEWED BY
Olivier Feron,
Université catholique de Louvain,
Belgium

*CORRESPONDENCE

Jean Christopher Chamcheu,
✉ chamcheu@ulm.edu
Qian Ba,
✉ qba@shsmu.edu.cn
Hang Ma,
✉ hang_ma@uri.edu

RECEIVED 31 May 2023

ACCEPTED 12 June 2023

PUBLISHED 19 June 2023

CITATION

Chamcheu JC, Ba Q and Ma H (2023),
Editorial: Natural products modulate the
sensitivity of cancer to anti-PD-
1 based immunotherapy.
Front. Pharmacol. 14:1232456.
doi: 10.3389/fphar.2023.1232456

COPYRIGHT

© 2023 Chamcheu, Ba and Ma. This is an
open-access article distributed under the
terms of the [Creative Commons
Attribution License \(CC BY\)](#). The use,
distribution or reproduction in other
forums is permitted, provided the original
author(s) and the copyright owner(s) are
credited and that the original publication
in this journal is cited, in accordance with
accepted academic practice. No use,
distribution or reproduction is permitted
which does not comply with these terms.

Editorial: Natural products modulate the sensitivity of cancer to anti-PD-1 based immunotherapy

Jean Christopher Chamcheu^{1*}, Qian Ba^{2*} and Hang Ma^{3*}

¹School of Basic Pharmaceutical and Toxicological Sciences, College of Pharmacy, University of Louisiana, Monroe, LA, United States, ²School of Medicine, Shanghai Jiao Tong University, Shanghai, China, ³Bioactive Botanical Research Laboratory, Department of Biomedical and Pharmaceutical Sciences, College of Pharmacy, University of Rhode Island, Kingston, RI, United States

KEYWORDS

natural products, immunotherapy, immune checkpoint blockade, cancer immunotherapy, anti-PD-1/PD-L1, sensitivity, resistance

Editorial on the Research Topic

Natural products modulate the sensitivity of cancer to anti-PD-1 based immunotherapy

Immunotherapy has emerged as one of the most promising therapeutic strategies for cancer treatments (Mellman et al., 2011). Among the immunotherapy approaches, immune checkpoint blockade (ICB) is regarded as a front-line immunotherapy for several types of cancer. Blockade of programmed cell death protein 1 (PD-1) and its ligand programmed cell death-ligands 1 (PD-L1) is one of the major ICBs that has been widely used to achieve cancer immunotherapy. Blockade of the interaction between PD-1 and PD-L1 can restore the immunological functions of T cells and exert their anti-tumor effects (Ohaegbulam et al., 2015). Although biologics including monoclonal antibodies (mAbs) targeting PD-1 or PD-L1 have been approved by the U.S. Food and Drug Administration (FDA) for different types of cancers, their application can be limited by drawbacks such as undesired off-target effects and prohibitive costs (Lin et al., 2020). On the contrary, small molecule-based PD-1/PD-L1 inhibitors may show advantages over mAbs, such as fewer side effects and more affordable cost (Wu et al., 2021). Small molecules, especially natural products and their derivatives, have been an important resource for the discovery of anti-cancer drugs. Indeed, a number of clinically approved anti-cancer agents are natural products-based small molecules with varied mechanisms of anti-cancer activity. However, only limited studies have been reported for the development of natural products-based anti-PD-1/PD-L1 agents. This was partially attributed to the challenges including a lack of suitable analytical methods for screening hits from natural products library and less well-characterized biological evaluations of natural products (Liu et al., 2021). Therefore, this Research Topic provides a snippet of published quality reviews of scientific literature and original research communication efforts on the discovery and development of natural products for ICB-based cancer immunotherapy. The published data presented will further increase our understanding of the role of natural bioactive ingredients and derivatives for sensitization of diverse cancers to ICB such as Anti-PD-1 Based Immunotherapy. While these published data highlight the natural products-derived molecules targeting diverse

cancer molecular markers, they also provide promising mechanisms through which to reduce diverse human cancer burdens via targeting immune checkpoints and tumor microenvironments.

The first paper by [Hernández-López et al.](#), is a review that presents chimeric antigen receptor (CAR)-T cell therapy as a promising immunotherapy approach for cancer treatment and discusses the challenges faced by CAR-T cell therapy while highlighting the need for it to meet regulatory requirements (6). This review provides insights into the elements, history, and potential opportunities to improve CAR-T cell therapy, aiming to make it a widely accessible and effective treatment modality for cancer patients.

The second review by [Dong et al.](#) assessed the potential utility of natural products in overcoming the limitations of immunotherapy in colorectal cancer (CRC) treatment. While immune checkpoint inhibitors have shown benefits in certain CRC patients with dMMR/MSI-H, most CRC patients do not respond well to immunotherapy, partly due to internal resistance and immune escape. They discuss the advantages and highlighted the challenges in CRC treatment, explored the immunomodulatory effects of natural products and their bioactive components, and suggested that natural products hold potential as adjuncts in combined CRC immunotherapy approaches.

The third review by [Wei et al.](#), assessed, explored, and provided a comprehensive overview of the crucial role of gut microbiota in cancer development and the role of dietary fungi in cancer immunotherapy. They discussed the advantages of the manipulation of gut microbiota through direct implantation or antibiotic-based depletion and its impact on the overall effectiveness of cancer immunotherapies. They discussed extensively the biological functions, underlying mechanisms, and benefits of dietary fungal supplementation in promoting cancer immunotherapies through the modulation of gut microbiota.

The fourth paper by [Kong et al.](#), is a systematic review highlighting the current application and future potentials of astragalus polysaccharide (APS) in combination with cancer immunotherapy. APS is effective in activating adoptive immunotherapy, including lymphokine-activated killer (LAK) and dendritic cell-cytokine-induced killer treatment (DC-CIK) treatments, and regulates the PD-1/PD-L1 pathway and modulates cytokines, TLR4, NF- κ B, MAPK pathways, and immune cells in the tumor microenvironment. They discussed that the combination of APS and immunotherapy holds great promise toward enhancing treatment efficacy as it activates immune responses while at the same time modulating the tumor microenvironment.

The paper by [Chen et al.](#) employed network pharmacology and molecular docking to investigate the components and mechanisms of *Solanum nigrum* L. (SNL) while providing insights into SNL's therapeutic potential in the treatment of colon cancer. The study along with pathway analysis identified 37 SNL components, 796 target proteins, and 5,356 colon cancer genes, and determined that the key targets were mostly related to several signal transduction pathways, such as PI3K-Akt signaling, drug response, and protein phosphorylation. By molecular docking, the study demonstrated the ability of SNL components, apigenin, and kaempferol, to bind the key target AURKB protein, while exerting anti-colon cancer properties.

In the study by [Lam et al.](#), YIV-906, a natural botanical cancer drug derived from traditional Chinese herbal formulation, demonstrates the ability to enhance T-cell activity and potentiate

ICB and CAR T-cell therapies. YIV-906 was shown to activate T effector cells via upregulation of the expression of CD69, enhanced anti-PD1 therapy, and augmented CAR-T cell killing capability while inhibiting SHP1/2 activities as well as triggering downstream signaling pathways. These, therefore, suggest that YIV-906 is a potential immunomodulator in cancer treatment, supporting ICB and CAR-T cell therapy.

The study by [Meng et al.](#), investigated the potential of ginsenosides as inhibitors of TMPRSS2, a target for COVID-19 prevention and treatment. The role of TMPRSS2 was explored in cancer, focusing on lung adenocarcinoma (LUAD) patients, and its association with anti-PD-1 immunotherapy response and was highlighted that higher TMPRSS2 levels are associated with better prognosis in LUAD, but not in LUSC cohorts. Additionally, TMPRSS2 was found to be positively correlated with poor response to anti-PD-1 therapy, suggesting that TMPRSS2 could serve as a prognostic biomarker and a potential target for immunotherapy combination treatments in LUAD patients who are nonresponsive to anti-PD-1 therapy.

In a clinical trial study by [Fukaya et al.](#), they developed a population pharmacokinetics (popPK) and pharmacodynamics (popPK-PD) model for glucarpidase (CPG2) rescue treatment after high-dose methotrexate (MTX) therapy. This involved a phase 1 analysis in healthy volunteers and a phase 2 analysis in 15 patients who received CPG2 rescue for delayed MTX excretion. The population means pharmacokinetic parameters of MTX were estimated using the final model, and important sampling points for predicting plasma MTX concentrations at 48 h were identified. The study provided clinically significant insights into CPG2-MTX pharmacokinetics as well as Bayesian estimation of plasma MTX concentrations for effective treatment.

In a brief report by [Li et al.](#), they employed a functional assay (pair ELISA) and a PD-L1/PD-L1 binding assay (surface plasmon resonance; SPR) to evaluate a panel of natural products with previously reported anti-PD-1/PD-L1 activity and categorized based on their screening assays responses. The study provides insights into natural product-derived Immune Checkpoint PD-1/PD-L1 inhibitors binding capacities and blockade effects, thus emphasizing the role of using appropriate evaluation methods, including multiple-facet functional assays and target binding techniques.

[Xie et al.](#) investigated the role of myeloid-derived suppressor cells (MDSCs) in tumor progression and their modulation by granulocyte colony-stimulating factor (G-CSF) *in vitro* and in a neutropenic mouse model. They observed, *in vitro* an enhanced proliferation and immunosuppressive activity of MDSCs through the upregulation of gamma-glutamyltransferase (GGT) 1 by G-CSF. G-CSF administration *in vivo* with EL4 lymphoma resulted in increased MDSC numbers and attenuated the anti-cancer effect of chemotherapy. These suggested that aiming at GGT1 on MDSCs can thwart the tumor-promoting properties of G-CSF and proposed GGT1 as a potential combination agent during G-CSF treatment for febrile neutropenia in cancer patients.

[Taniguchi et al.](#) established murine models using human brain metastatic tumor cell lines and evaluate the effectiveness of perifosine, a bioavailable alkylphospholipid Akt inhibitor as a single agent in both ectopic and orthotopic models. Perifosine was found to be favorably distributed in the brain with prolonged localization, and significantly prolonged survival while

inducing complete tumor regression in the orthotopic brain tumor mice group. Perifosine also exhibits strong antitumor responses against subcutaneous tumor growth and was associated with suppression of the PI3K/Akt signaling pathway, tumor cell proliferation, and inducing apoptosis. Therefore, perifosine represents promising for treating metastatic brain cancers.

Wang et al. investigated the occurrence of tumor lysis syndrome (TLS) associated with immune checkpoint inhibitor (ICI) therapies using real-world pharmacovigilance data. They reported that elderly male patients with lung and thymus malignancies were more susceptible to TLS. The onset time of TLS varied among different ICI therapies. The study emphasizes the need for caution regarding TLS as a potential adverse event of ICIs and highlights the importance of further monitoring in clinical practice.

Overall, the 12 papers published on this Research Topic highlighted several natural products that can be characterized appropriately to enhance immunotherapy of diverse human cancers. In summary, the intake of well-characterized natural products is a source of potential cost-effective therapeutics to treat cancer. They can be used in combination with other immunotherapies for the management of diverse cancer as chemopreventive, chemotherapeutics, or as adjuvant treatments. However, further studies using more physiologically relevant models and analytical tools are warranted to determine their efficacy and clinical potency. Therefore, further validation of these natural bioactives would improve cancer immunotherapy and reduce the burdens of advanced metastatic cancers.

Author contributions

All authors listed have made a substantial, direct, and intellectual contribution to the work and approved it for publication.

References

- Lin, X., Lu, X., Luo, G., and Xiang, H. (2020). Progress in PD-1/PD-L1 pathway inhibitors: From biomacromolecules to small molecules. *Eur. J. Med. Chem.* 186, 111876. doi:10.1016/j.ejmech.2019.111876
- Liu, C., Seeram, N. P., and Ma, H. (2021). Small molecule inhibitors against PD-1/PD-L1 immune checkpoints and current methodologies for their development: A review. *Cancer Cell. Int.* 21 (1), 239. doi:10.1186/s12935-021-01946-4
- Mellman, I., Coukos, G., and Dranoff, G. (2011). Cancer immunotherapy comes of age. *Nature* 480 (7378), 480–489. doi:10.1038/nature10673
- Ohaegbulam, K. C., Assal, A., Lazar-Molnar, E., Yao, Y., and Zang, X. (2015). Human cancer immunotherapy with antibodies to the PD-1 and PD-L1 pathway. *Trends Mol. Med.* 21 (1), 24–33. doi:10.1016/j.molmed.2014.10.009
- Wu, Q., Jiang, L., Li, S. C., He, Q. J., Yang, B., and Cao, J. (2021). Small molecule inhibitors targeting the PD-1/PD-L1 signaling pathway. *Acta Pharmacol. Sin.* 42 (1), 1–9. doi:10.1038/s41401-020-0366-x

Funding

Research in JCC's lab receives funding support from a full research project awards from a Louisiana Biomedical Research Network (LBRN)-IDeA Networks of Biomedical Research Excellence (INBRE) award from the National Institute of General Medical Sciences of the National Institutes of Health (NIGMS/NIH) grant number P2O GM103424-18, and a Louisiana Board of Regents Support Fund grant LEQSF (2021-24)-RD-A-22.

Acknowledgments

We thank all the authors for contributing to this Frontiers Research Topic and all the reviewers and invited editors who have helped to make it completed.

Conflict of interest

The authors declare that the research was conducted in the absence of any commercial or financial relationships that could be construed as a potential conflict of interest.

Publisher's note

All claims expressed in this article are solely those of the authors and do not necessarily represent those of their affiliated organizations, or those of the publisher, the editors and the reviewers. Any product that may be evaluated in this article, or claim that may be made by its manufacturer, is not guaranteed or endorsed by the publisher.



Chimeric Antigen Receptor-T Cells: A Pharmaceutical Scope

Alejandrina Hernández-López¹, Mario A. Téllez-González^{1,2}, Paul Mondragón-Terán² and Angélica Meneses-Acosta^{1*}

¹Laboratorio 7 Biotecnología Farmacéutica, Facultad de Farmacia, Universidad Autónoma Del Estado de Morelos, UAEM, Cuernavaca, Mexico, ²Coordinación de Investigación, Centro Médico Nacional "20 de Noviembre" ISSSTE, Mexico city, Mexico

OPEN ACCESS

Edited by:

Peixin Dong,
Hokkaido University, Japan

Reviewed by:

Degang Song,
Janssen Pharmaceuticals, Inc.,
United States
Chu Lin,
Peking University People's Hospital,
China

*Correspondence:

Angélica Meneses-Acosta
angelica_meneses@uaem.mx

Specialty section:

This article was submitted to
Pharmacology of Anti-Cancer Drugs,
a section of the journal
Frontiers in Pharmacology

Received: 04 June 2021

Accepted: 02 August 2021

Published: 20 August 2021

Citation:

Hernández-López A,
Téllez-González MA,
Mondragón-Terán P and
Meneses-Acosta A (2021) Chimeric
Antigen Receptor-T Cells: A
Pharmaceutical Scope.
Front. Pharmacol. 12:720692.
doi: 10.3389/fphar.2021.720692

Cancer is among the leading causes of death worldwide. Therefore, improving cancer therapeutic strategies using novel alternatives is a top priority on the contemporary scientific agenda. An example of such strategies is immunotherapy, which is based on teaching the immune system to recognize, attack, and kill malignant cancer cells. Several types of immunotherapies are currently used to treat cancer, including adoptive cell therapy (ACT). Chimeric Antigen Receptors therapy (CAR therapy) is a kind of ATC where autologous T cells are genetically engineered to express CARs (CAR-T cells) to specifically kill the tumor cells. CAR-T cell therapy is an opportunity to treat patients that have not responded to other first-line cancer treatments. Nowadays, this type of therapy still has many challenges to overcome to be considered as a first-line clinical treatment. This emerging technology is still classified as an advanced therapy from the pharmaceutical point of view, hence, for it to be applied it must firstly meet certain requirements demanded by the authority. For this reason, the aim of this review is to present a global vision of different immunotherapies and focus on CAR-T cell technology analyzing its elements, its history, and its challenges. Furthermore, analyzing the opportunity areas for CAR-T technology to become an affordable treatment modality taking the basic, clinical, and practical aspects into consideration.

Keywords: CAR-T cells therapy, cell and gene therapy, advanced cell therapy, cell manufacturing process, immunotherapy

INTRODUCTION

Cancer is a major health issue worldwide, causing a serious health problem that affects costs on public health, social development and, most importantly, reducing people's life expectancy (Bray et al., 2018; Hassanpour and Dehghani 2017). In a broader context, cancer refers to more than 277 different types of cancer diseases (Hassanpour and Dehghani 2017), which represent major challenges to find out specific diagnosis and treatment. Worldwide, the main incidence of cancer types in adults occurs in the prostate, lung, bronchus, colon, rectum, urinary bladder, breast, and thyroid (Siegel et al., 2019), meanwhile, blood cancer is the main cancer type of concern in children's health (Kolonel and Wilkens). For years, the most effective cancer treatments have included surgery, chemotherapy, radiation therapy and bone marrow transplant (Arruebo et al., 2011), these therapies are considered as the main treatment. Unfortunately, even considering the current technological improvements on such therapies, recurrence and metastasis are still the main causes of death (Bray et al., 2018). In recent years, these common treatments have been challenged with the advent of immunotherapy.

Immunotherapies are designed to harness and manipulate part of the immune system to confer the ability to detect and specifically attack cancer cells (Waldmann 2003). Immunotherapies

TABLE 1 | Six major kinds of cancer immunotherapy.

Cancer immunotherapy	Description	Indications	References
Checkpoint inhibitors	This treatment takes the brakes off the immune system, helping it to identify and attack cancer cells. Checkpoint inhibitor therapies have been discovered and studied for cancer treatment based on CTLA-4 and PD-1	Pleural mesothelioma, classical Hodgkin's lymphoma, Merkel cell and cutaneous squamous cell carcinoma, head and neck cancer, triple negative breast cancer, lung, colorectal, kidney, bladder, cervical, endometrial, liver and stomach cancers, as well non-blood cancers that test positive for the biomarkers MSI-high/dMMR, tumor mutation burden high esophageal squamous cell, renal cell, urothelial carcinoma, and primary mediastinal large B cell lymphoma	Darvin et al. (2018) Sang et al. (2019) Twomey & Zhang (2021)
Cytokines	This treatment promotes the activation of several important specialized cellular functions to boost the body's immune system	Advanced melanomas, kidney, liver, lung, head and neck, breast, ovarian, cervical, prostate, pancreatic, colorectal, bladder, gastric, brain cancers, Sarcomas, hematological malignancies	Berraondo et al. (2019) Parmiani et al. (2000) Qiu et al. (2021)
Monoclonal antibodies (mAbs)	mAbs have a unique antigen specificity that allows them to bind to specific epitopes on cancer cells and kill them by different mechanisms. For example, they can induce apoptotic cell death or the attack by NK cells due to the ADCC action	Non-Hodgkin's and Hodgkin's lymphoma, triple negative breast cancer, melanoma, chronic lymphocytic leukemia, non-small cell lung cancer, chronic myeloid leukemia, acute lymphoblastic leukemia, multiple myeloma, gastric, bladder, breast, colorectal cancers, hairy cell leukemia	Ventola (2017) Golay and Taylor (2020) Zahavi & Weiner (2020) Monajati et al. (2021)
Cancer vaccines	Vaccines teach and stimulate the body's immune system to find, attack and eradicate cancer cells	Cervical, vaginal, vulvar, anal, liver, and prostate cancers	Karlitepe et al. (2015) Miao et al. (2021)
Oncolytic viruses	This treatment uses modified viruses, such as coxsackievirus, adenovirus, reovirus, herpes simplex virus, and measles virus to infect, replicate and kill neoplastic cells	Melanoma and lymph nodes	Anelone et al. (2020) Mondal et al. (2020) Nejad et al. (2021)
Adoptive Cell Therapy (ACT)	This treatment modifies the body's own immune cell to become a cancer treatment drug. ACT can be deployed in different ways such as TIL, TCR, NK or CAR-T therapy	CAR-T therapy for B-cell precursor acute lymphoblastic leukemia, diffuse large B-cell lymphoma, relapsed or refractory follicular lymphoma, mantle cell lymphoma, relapsed or refractory large B-cell lymphomas and multiple myeloma	Maude et al. (2018) Guedan et al. (2019) Rohaan, et al. (2019) Schuster et al. (2019) Iragavarapu and Hildebrandt (2021) Munshi et al. (2021)

(CTLA-4, Cytotoxic T-lymphocyte-associated antigen 4; PD-1 Programmed Death 1; MSI-high, microsatellite instability-high; dMMR, mismatch repair deficient; ADCC, Antibody-dependent cellular cytotoxicity; TIL, Tumor-Infiltrating Lymphocytes; TCR, gene-modified T cells expressing novel T Cell Receptors, NK, Natural Killer cells; CAR, Chimeric Antigen Receptors).

introduce a different perspective into cancer treatment, not only in patients with refractory tumors, but also to ensure long-lasting clinical remission in patients that were historically considered incurable (Dogan and Dranoff 2012; Guedan et al., 2019). Hence, in this paper we intend to expose the general panorama regarding immunotherapies, focusing the effort to the novel CAR-T cell therapy, its components, advantages, and limitations, summarizing the current challenges which need to be overcome and discussing the actual strategies to implement this therapy with a wider scope in benefit of a larger number of patients.

IMMUNOTHERAPY, A NEW APPROACH FOR CANCER TREATMENT

Chemotherapy, radiation, and surgery are the most conventional cancer treatments, nevertheless, they have shown low efficacy and severe adverse effects. Therefore, during the last decade, researchers have addressed the need to improve the inconveniences with conventional cancer therapy, developing new strategies to achieve complete remission of the disease using molecular strategies. Under these circumstances,

immunotherapy arises as a promise for revolutionary cancer treatment, because, compared with conventional therapeutics, it leads to lower side effects and can specifically target cancer cells by regulating the immune system's machinery (Papaioannou et al., 2016; Sang et al., 2019). Therefore, immunotherapy has become an important therapeutic alternative for patients whose immune systems are already compromised due to their advanced disease and/or failure of previous conventional therapies (Ventola, 2017; Charmsaz et al., 2019). **Table 1** covers the six major kinds of available cancer immunotherapies. The most recent immunotherapy that has shown promising results is the Chimeric Antigen Receptor (CAR)-T cell therapy, which is a type of Adoptive Cell Therapy (ACT). This therapeutic strategy entails genetically engineering a patient's T cells to express CARs that recognize, bind, attack and kill tumoral cells (Mirzaei et al., 2017).

A Brief History of Chimeric Antigen Receptor-T Cells Development

To start with the historical review of the discovery of these new technologies, it is necessary to date the first bone marrow transplant for leukemia patients that was reported in 1957 by Thomas and colleagues (Thomas et al., 1957). A few years later,

Miller J. and colleagues reported the immunological function of the thymus, discovering the origin of T cells (Miller, 1961).

However, it was not until 1986, when Steven Rosenberg and colleagues reported a study about Tumor-Infiltrating Lymphocytes (TILs), this therapy consists of cellular isolation of T lymphocytes from a tumor, that is subjected to an *in vitro* culture and expansion to infiltrate them back into the tumor to be treated, hence leading to elimination or clinical resection of the tumor (Rosenberg et al., 1986; Lança and Silva-Santos, 2012; Garber 2019). This report allowed us to fix the gaze on the idea of “Patients’ own immune cells can fight their own cancer”.

Likewise, results of the successful T cell transfections of Sadelain and colleagues in 1992 and their methods publications for retrovirus-mediated gene transfer into primary T-lymphocytes in 1997, allowed genetic modifications providing the means of controlling immunity in an experimental or therapeutic setting (Sadelain and Mulligan, 1992; Sadelain, 1997). Almost at the same time, Zelig Eshhar and colleagues designed a specific activation of cytotoxic lymphocytes through chimeric single chains, using an antibody-binding domain and the γ or ζ subunits of the immunoglobulin on the T-cell receptors, developing the First Generation of CAR-T cells (Eshhar et al., 1993). Five years later, Dr. Sadelain’s group demonstrated that the integration of a co-stimulatory signal like CD28 to a CAR-T enhanced survival, proliferation and remained active, leading to the development of the Second Generation of CARs (Krause et al., 1998). The pioneering work of Dr. Carl June and his group (University of Pennsylvania) led to the development of CAR therapy (Kalos et al., 2011), with the approach of using modified T lymphocytes that carried a CAR to target CD19⁺ leukemic B cells (Varadé et al., 2021). Such an approach was because the expression of the transmembrane glycoprotein CD19 is maintained during differentiation of B lineage at normal (14% in peripheral blood lymphocyte phenotype) (Berron-Ruiz et al., 2016) and neoplastic B cells malignancies (80% of ALL, 88% of B cell lymphomas and 100% of B cell leukemias) (Wang et al., 2012), as well as follicular dendritic cells. Nowadays, CD19 expression is widely used for the diagnosis of leukemias and lymphomas and is used as the main target for the redirection of T lymphocytes against these neoplastic associated molecules (Scheuermann and Racila 1995; Tedder, 2009; Wang et al., 2012). In 2009, Isabelle Rivière group published the manufacturing validation of biologically functional T cells targeted to CD19 antigen basing their work on promising data in the eradication of systemic B cell malignancies. This publication launched phase I clinical trials in chronic lymphocytic leukemia (CLL) and acute lymphoblastic leukemia (ALL) (Hollyman et al., 2009). CD19 expression is widely used for the diagnosis of leukemias and lymphomas and used as the main target for the redirection of T lymphocytes against these neoplastic associated molecules (Scheuermann and Racila 1995; Tedder, 2009; Wang et al., 2012) even though there may be more specific receptors for tumor cells.

The publication of the phase I clinical trial results, proving that CAR-T therapy-induced molecular remissions in adults with chemotherapy-refractory ALL (Brentjens et al., 2013; Grupp et al., 2013), was followed by a scale-up of bioprocess

production. Finally, FDA approved the CD 19 CAR-T cell therapy (Tisagenlecleucel) for ALL in children and young adults (U.S. Food and Drug Administrations, 2021a). In addition, in 2021 the FDA approved the use of CAR-T cells using the B-cell maturation antigen (“BCMA” target (Idecabtagene vicleucel) in multiple myeloma (U.S. Food and Drug Administrations, 2021b).

During the first commercial lustrum of CAR immunotherapy, CAR-T therapy explored different applications in other malignancies associated with the initial biomolecules as large B-cell lymphoma (DLBCL), DLBCL arising from follicular lymphoma and high-grade B-cell lymphoma (YESCARTA U.S. Food and Drug Administrations, 2021c). So far, most studies are carried out on the discovery of other targets such as CD20, CD22, CD30 and new targets in solid tumors to increase the scope of CAR-T therapy (Elahi et al., 2018; Castella et al., 2020).

Profiting the clinical successes, the use of CAR-T cells has also been explored in a variety of cancers (Petersen and Krenciute 2019) such as diffuse large B-cell lymphoma treatments in adults and multiple myeloma (Mullard 2017; Iragavarapu and Hildebrandt 2021; Munshi, et al., 2021) in which the therapeutic products were recently approved by the Food and Drug Administration (FDA, United States). Meanwhile, the European Medicines Agency (EMA) has granted conditional approval, or their authorization is currently under review. CAR-T cells re-targeted against the ubiquitous B-cell antigen, CD19 are a remarkable innovation in the treatment of relapsed and/or refractory (R/R) B-cell acute lymphoblastic leukemia (B-ALL) (Nie et al., 2020). The success of CAR T-cells therapy in cancer is exemplified by numerous clinical trials that have shown that 70–90% complete remission (CR) can be achieved in pediatric and adult patients treated with CD19-directed CAR T-cells (Xu et al., 2019). Based on these growing CAR-T cell immunotherapy achievements, over 500 clinical trials worldwide analyzing CAR-T cells for the treatment of cancer are currently being under evaluation, and the majority are being performed in East Asia (269 trials), followed by the US (225 trials), and Europe (62 ongoing studies) (as registered at clinicaltrials.gov Q3 2020) (Albinger et al., 2021). So far, five CAR-T cell therapy agents were approved by FDA for cancer treatment: Tisagenlecleucel (Kymriah[®]) for treatment of acute lymphoblastic leukemia (ALL) (Mullard 2017), Axicabtagene ciloleucel (Yescarta[™]) for diffuse large B-cell lymphoma (DLBCL) and also FDA-approval for follicular lymphoma in april 2021 (Bouchkouj et al., 2019), Brexucabtagene autoleucel (Tecartus[™]) for treatment of mantle cell lymphoma (MCL) (Al-Juhaishi and Ahmed, 2021), Idecabtagene vicleucel (ABECMA[®]) for treatment of multiple myeloma (Munshi et al., 2021) and Lisocabtagene maraleucel (Breyanzi[®]) for diffuse large B-cell lymphoma treatment (Iragavarapu and Hildebrandt 2021) (Table 2).

Chimeric Antigen Receptor T Cell Immunotherapy

CAR immunotherapy is a successful innovation in cancer therapies achieving impressive results in the treatment of resistant hematological malignancies highlighting its strong

TABLE 2 | Currently approved CAR-T cells products by FDA and EMA. These are the available products up to July 2021.

Brand name	Kymriah	Yescarta	Tecartus	ABECMA	Breyanzi
Generic name	Tisagenlecleucel	Axicabtagene ciloleucel	Brexucabtagene autoleucel	Idecabtagene vicleucel	Lisocabtagene maraleucel
Indication/s	Treatment of pediatric and young adult patients (age 3–25 years) with B-cell ALL that is refractory or in second or later relapse Adult patients with (r/r) LBCL after two or more lines of systemic therapy including DLBCL, HGBL and DLBCL arising from FL	Treatment of adult patients with (r/r) LBCL after two or more lines of systemic therapy, PMBCL, HGBL, and DLBCL arising from FL	Treatment of adult patients with (r/r) MCL	Treatment of adult patients with R/R MM after four or more prior lines of therapy	Treatment of adult patients with r/r DLBCL after two or more lines of systemic therapy, HGBL, PMBCL, and FL grade 3B
Target	CD19	CD19	CD19	BCMA	CD19
Company	Novartis Pharmaceuticals Corporation	Kite Pharma/Gilead	Kite Pharma/Gilead	Bristol Myers Squibb/Bluebird bio	Juno/Bristol Myers Squibb
Price (USD)	\$475,000	\$373,000	\$373,000	\$419,500	\$410,300
Approval date by FDA	LLA; August 2017. DLBCL, HGBL and DLBCL arising from FL; april 2018	LBCL; October 2017 FL; april 2021	July 2020	March 2021	February 2021
Authorization date by EMA	August 2018	August 2018	Conditional approval, October 2020	Recommended granting a conditional marketing authorization, June 2021	PRIME status. Marketing Authorization Application (MAA) is currently under review
Study of efficacy and safety	JULIET for DLBCL ELIANA for B-ALL	ZUMA-1	ZUMA-2	KarMMa	TRANSCEND
Clinical trial	JULIET: NCT02445248 ELIANA: NCT02435849	NCT02348216	NCT02601313	NCT03361748	NCT02631044
Enrolled participants in the clinical trial	115	307	105	149	314
Number of treated patients	79	Data not available	Data not available	Data not available	Data not available
Success rate	83% of patients achieved CR for LLA 65% of patients achieved CR for r/r FL	54% of patients achieved CR. 82% achieved an overall response	67% of patients achieved CR. 92% achieved an overall response	39% of patients achieved CR. 81% achieved an overall response	53% of patients achieved CR. 73% achieved an overall response
Adverse effects	CRS occurred in 79% of pediatric patients, 74% in young adult patients with r/r ALL and 23% in patients with r/r DLBCL NTX occurred in 72% of patients with r/r ALL and 58% of patients with r/r DLBCL	CRS occurred in 94% of patients with LBCL including four patients who had ongoing CRS events at the time of death NTX occurred in 87% of patients with LBCL	CRS occurred in 91% of patients, including one fatality NTX occurred in 81% of patients	CRS occurred in 85% of patients including one fatality NTX of any grade occurred in 28% of patients, including one patient who had ongoing Grade 2 neurotoxicity at the time of death	CRS occurred in 46% of patients including one fatality and two had ongoing CRS at the time of death NTX occurred in 35% of patients. Three patients had fatal NTX and seven had ongoing NTX at the time of death

Large B-cell lymphoma (LBCL), diffuse large B-cell lymphoma (DLBCL), High-grade B-cell lymphoma (HGBL), Follicular lymphoma (FL), Primary mediastinal large B-cell lymphoma (PMBCL), relapsed/refractory mantle cell lymphoma (r/r MCL), relapsed or refractory multiple myeloma (r/r MM), refractory follicular lymphoma (r/r FL), Cytokine release syndrome (CRS), Neurotoxicity (NTX), complete remission (CR), non-Hodgkin lymphoma (NHL), Priority Medicines (PRIME).

potential (Neelapu et al., 2017). CAR-T cell immunotherapy was developed out of the need for T cells to be able to directly recognize tumor cells without the required antigen processing or presentation by professional antigen-presenting cells (Varadé et al., 2021). This immunotherapy is based on T-cell engineering and the use of synthetic (recombinant) receptors, termed CARs, instead of the physiological (native) receptor for the antigen, the TCR (Sadelain et al., 2009). These CARs are based on a specific antibody directed to a target surface molecule and were developed with the intent of combining the tumor recognition capabilities of antibodies with the powerful antitumor effector abilities of T cells.

CAR expression is most often achieved using retroviral- or lentiviral-mediated gene transfer. The T cell's rapidly dividing nature facilitates viral integration, and its ability to establish memory serves to reinforce long-lasting transgene expression (Grosser et al., 2019). Besides, CARs constructions include all the elements necessary for intracellular signaling and activation of helper and cytotoxic T lymphocytes (Singh and McGuirk 2020).

Target Selection

CAR recognition of malignant cells depends on the designed chimeric recognition molecule, not on the traditional

TABLE 3 | Novel targets for hematologic malignancies and solid tumors.

Target	Diseases	Identifier	Status	References
Hematologic malignancies				
BCMA	Multiple myeloma	NCT03502577	Recruiting, phase I	Pont et al. (2019)
		NCT04309981	Recruiting, phase I/II.	
CD38	Multiple myeloma	NCT03464916	Recruiting, phase I	Freitag, et al. (2020)
		NCT03767751	Recruiting, phase I/II.	Nair, et al. (2019)
SLAMF7	Multiple myeloma	NCT04499339	Recruiting, phase I/II.	Rodríguez-Otero et al. (2020)
CD33	Acute myeloid leukemia	NCT03971799	Recruiting, phase I/II.	Freitag et al. (2020)
		NCT03126864	Recruiting, phase I/II.	
CD123	Acute myeloid leukemia	NCT04014881	Recruiting, phase I	Hansrivijit et al. (2019)
		NCT03766126	Not recruiting, phase I	Hoffmann et al. (2018)
CD56	Multiple myeloma	NCT03473496	Recruiting	Freitag et al. (2020)
		NCT03271632	Recruiting, phase I/II.	
CD37	B- and T-cell lymphoma	NCT04136275	Recruiting, phase I/	Scarfo et al. (2018)
Solid tumors				
EGFRVIII	Glioblastoma	NCT03283631	Recruiting temporally suspended, phase I	Martinez and Moon (2019)
GPC3	Hepatocellular carcinoma	NCT03146234	Not recruiting	Da Fonseca and Carrilho (2019)
GD2	Glioma, cervical cancer, sarcoma, neuroblastoma	NCT03373097	Recruiting, phase I/II.	Townsend, et al. (2018)
		NCT02761915	Recruitment completed, phase I	
HER2	CNS tumour	NCT03500991	Recruiting, phase I	Mirzaei, et al. (2017)
		NCT02442297		
		NCT00902044		
Mesothelin	pancreatic cancer, ovarian Cancer, lung Cancer, peritoneal carcinoma, fallopian tube cancer, mesotheliomas Pleural	NCT03054298	Recruiting, phase I	Haas et al. (2019)
		NCT03323944		
Claudin 18.2	Gastric cancer, pancreatic cancer	NCT03874897	Recruiting, phase I	Springuel et al. (2019)
		NCT03159819		
Muc1	Breast Cancer	NCT04020575	Recruiting, phase I	Bamdad et al. (2019)
ROR1	Breast cancer, lung cancer	NCT02706392	Recruiting, phase I	Springuel et al. (2019)

BCMA, B-cell maturation antigen; CD, cluster of differentiation; SLAMF7, SLAM Family Member 7; EGFRVIII, variant III of the epidermal growth factor receptor; GPC3, glypican 3; GD2, disialoganglioside; HER2, human epidermal growth factor receptor 2; Muc1, mucin 1; ROR1, Receptor Tyrosine kinase Like Orphan Receptor 1.

T-lymphocyte receptor (TCR) or human leukocyte antigen (HLA). This interaction between CAR and the target leads to the formation of immune synapses, where contact-dependent cytotoxicity occurs. Hence, choosing a target with high specificity and high coverage is the main objective for these therapies. Unfortunately, nowadays there is no guide with uniform criteria that shows how a target should be properly selected, however, it is important to consider that not only membrane proteins are useful, also carbohydrates and glycolipid molecules can be selected if they adapt to the clinical needs of the desired disease (Wang et al., 2017; Wei et al., 2019).

It is recommended to identify and use a target that achieves adequate coverage of tumor cells with enough specificity to prevent CAR activation in other sites that could lead to serious damage in organs. Hence, this way, it is possible to avoid the main toxic side effects in CAR-T treatment, such as cytokine release syndrome (CRS), and the “off-tumor” effect caused by damage to non-tumor cells (Liu et al., 2019).

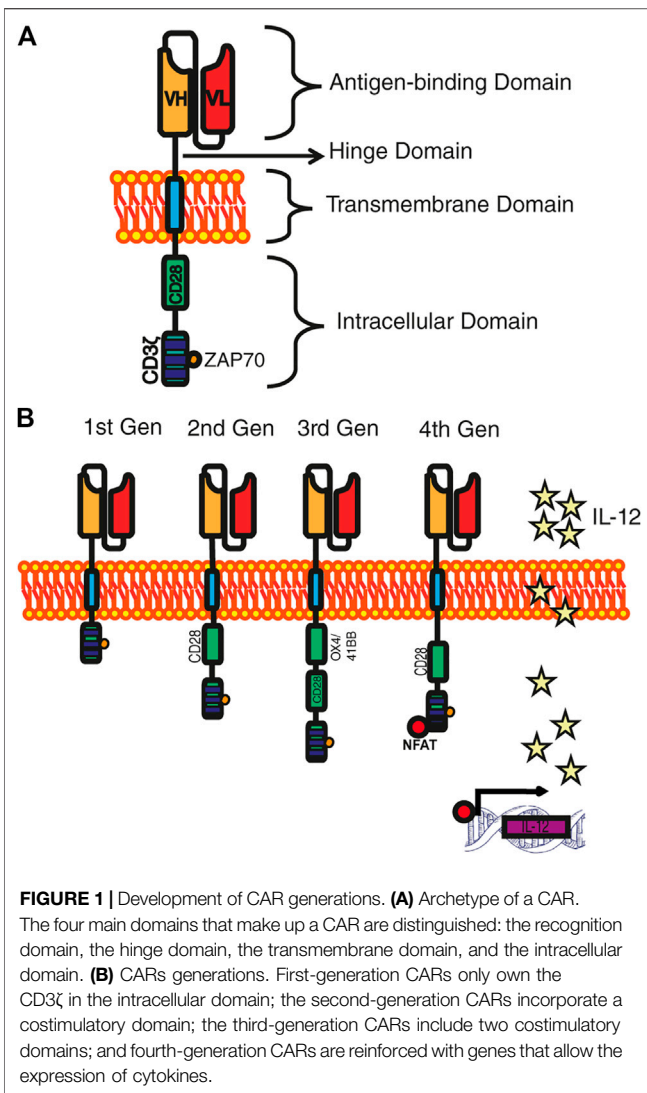
Recently, different types of CAR have been designed to take into consideration the coverage of two selected targets and the specificity for different types of solid tumors that share proteins involved in cell malignancy. Developed strategies are known as, Pooled CAR: two CAR in the same vector; Dual CAR: cross-compliance where the first target has the signaling domain while

the other one has the costimulatory domain, CAR in tandem: where two variable fraction chains are attached to the same antigen-binding domain and some others where activation or function would be inhibited by an inhibitory CAR. The previous designs will further expand CAR-T cell therapy in clinical trials (Fedorov et al., 2013; Hartmann et al., 2017). Since novel targets are currently studied, in a further section, the specific antigens are presented as a strategy to improve the CAR-T cells application (Table 3).

The major advantage of cell-based therapies is the variety of surface proteins that can be used as targets, which allow the specific antigen recognition in an independent manner of the major histocompatibility complex (MHC), in contrast to TCR-mediated antigen recognition (Li et al., 2018; Dwivedi et al., 2019), that deliver remarkable results in the clinic, specifically for the treatment of B cell malignancies (Grupp et al., 2013; Porter et al., 2015).

Chimeric Antigen Receptor Designs

In detail, the CAR is a synthetic receptor that ligates to a surface antigen and transduces the protein target of recognition into a signaling cascade (Brown and Mackall, 2019; Qin et al., 2021). The molecular architecture of CAR consists of four main components: 1) antigen-binding (recognition) domain, which



provides the exclusive recognition of the target molecule based on monoclonal antibodies with variable regions that are linked into a single-stranded fragment (scFv) (Shirasu and Kuroki, 2012); between the recognition and transmembrane domains lies a 2) hinge or spacer domain, which is a structure normally constructed by the flexible hinge sequences of CD8 α , CD28 or the Fc region of immunoglobulins IgG1 or IgG4 (Lee et al., 2019; Roselli et al., 2019), this is in charge of bringing an effective immunological synapse (Fujiwara, et al., 2020). 3) A transmembrane domain, that is the anchor molecule to the cell membrane which impacts the regulation of the amount of CAR signaling into T cells via the control of the CAR surface expression level (Dwivedi et al., 2019). 4) An intracellular signaling domain, that provides the intracellular portion of the TCR invariant chain CD3 ζ , which triggers the phosphorylation of the immunoreceptor tyrosine-based activation motif (ITAM's) domains activates the signaling pathway of ZAP70 (Milone et al., 2009). However, this signal is deficient to activate by itself the resting T cell. Hence, to improve activation, proliferation, and

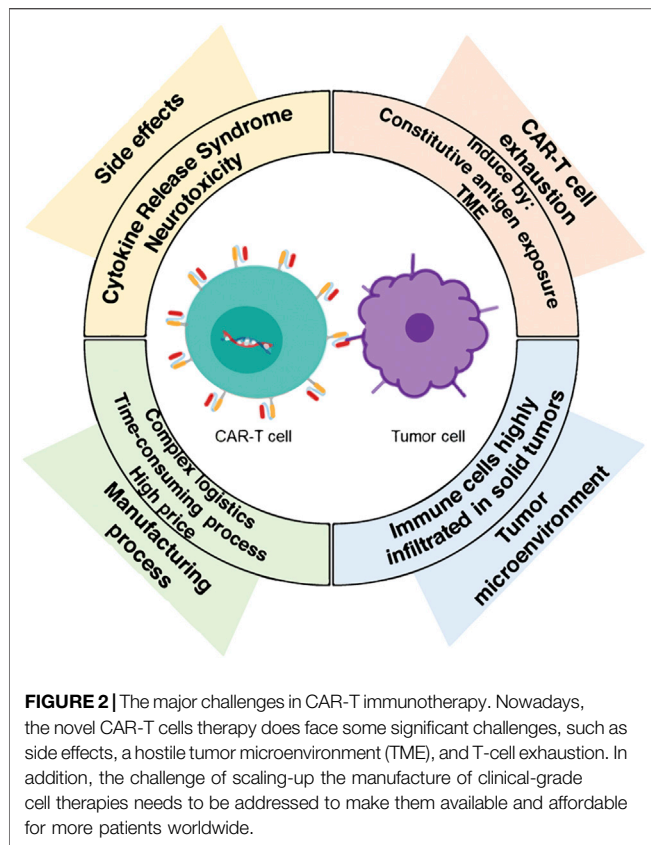
survival the incorporation of the costimulatory domain from other receptors, such as CD28, 4-1BB (CD137), should be included to the intracellular fragment (Ramello et al., 2019) (**Figure 1A**).

Simple CARs classification is given by the number of signaling groups that possess in the intracellular signaling domain, being the first-generation CARs those that in their signaling domain contain CD3 ζ chain as the primary transmitter of endogenous TCR signals (Ghosh et al., 2017). The first generation of chimeric receptors was primarily designed to mimic its T cell activation, a function that is sufficient to trigger cytotoxicity, but not enough to direct a sustained effective T cell response (Sadelain et al., 2009). To broaden T cell function, a different kind of Intracellular signaling domain was designed, mimicking a normal activation of T lymphocytes, and ensuring the presence of a co-stimulatory signal. Diverse co-stimulatory signals have been proposed such as CD28, 4-1BB and OX40, as they normally activate cell survival and proliferation pathways (i.e., PI3K–Akt–mTORC1) (Van Der Stegen et al., 2015). The second-generation of CARs have recently yielded impressive clinical results in patients with B cell malignancies, specifically in acute lymphoblastic leukemia (Brentjens et al., 2011; Maude et al., 2014). The union of two costimulatory domains in the Intracellular signaling domain is called “third-generation” CARs; this strategy increases the differentiation towards T cell effectors (Teff) and improves persistence by prolonging T-cell survival (Hombach et al., 2011). Further research has led to a novel generation of CARs named TRUCK cells (T-cells redirected for universal cytokine killing), also called “fourth generation” CARs that, in addition to costimulatory signal(s), is provided with a “nuclear factor of activated T cell-responsive expression” which can activate an innate immune response through the secretion of an element for an inducible transgenic product like IL-12 or another cytokine, (**Figure 1B**). This CAR-T is expected to be applied in fields of virus infections, auto-immune diseases, or metabolic disorders (Chmielewski et al., 2018; Date and Nair, 2021).

T-Cell Procurement

As the last element, the isolation of T cells is a crucial factor since these types of cells are needed to get a high-quality product. The requirements for CAR-T cell manufacturing process are T cells with CD3/CD4 $^{+}$ and CD3/CD8 $^{+}$ immunophenotype. For T cell harvesting the process starts from the mononuclear cell fraction notwithstanding that the final quantities of contaminating cells are dependent upon the type of blood cell isolation process, counterflow centrifugal elutriation or even the inherent properties of the patient's blood. As a strategy for obtaining viable and high purity of T cells (CD3/CD4 $^{+}$ and CD3/CD8 $^{+}$) additional purification steps are needed; At this point, immunomagnetic isolation has been introduced to shift the density gradient separation (Fesnak and O'Doherty, 2017; Stroncek et al., 2017).

It has even been reported that the impact of CD4/CD8 T-cell selection on the starting apheresis product influences manufacturing feasibility, however, this strategy led to a direct increase in inflammatory toxicities (Shah et al., 2020a; Shah et al., 2020b). Clinical recommended applications of CAR-T-cell



therapy include infusion products at a 2:1 ratio being approximately CD4⁺ CAR-T ($29 \pm 18.1\%$) and CD8⁺ CAR-T ($71 \pm 18.1\%$) (Itzhaki et al., 2020). Taking into consideration that on average one patient receives 3.1×10^6 transduced viable T cells per kilogram of body weight (range, 0.2×10^6 to 5.4×10^6 cells per kilogram) for ALL treatment. Meanwhile, for lymphoma the recommended dose of infused CAR T-cells ranged from $0.66 \times 10^6/\text{kg}$ to $3.3 \times 10^9/\text{m}^2$ (Maude et al., 2018; Cao et al., 2019), with a normal transduction rate around 20–60% (Itzhaki et al., 2020).

Chimeric Antigen Receptor-T Cell Immunotherapy Challenges

CAR-T cell immunotherapy has found its success where conventional therapies fail, becoming a promising emerging technology that represents an important progress for the treatment of cancer malignancies. Furthermore, it also opens new potentials for the treatment of other diseases. However, this therapy is relatively new, and some significant challenges have been observed, mainly related to side effects, toxicity, T-cell exhaustion, and hostile tumor microenvironment (TME) (Figure 2). In addition, the manufacturing process for offering clinical-grade cell therapies at a large-scale production and their distribution are currently time-consuming and costly. Therefore, making CAR-T cell immunotherapy available for as many patients as possible becomes a greater challenge. New

processing techniques, quality control mechanisms and logistic developments are required to overcome these limitations and to develop robust technology. In the next paragraphs, an analysis of such challenges is presented.

Side Effects and Toxicity

After CAR-T cell infusion, close patient monitoring is a crucial part of the treatment protocol due to the potential lethal toxicities of this immunotherapy. Fever, inflammation, abnormal liver enzyme elevation, breath difficulty, chills, confusion, dizziness, lightheadedness, severe nausea, vomiting, and diarrhea are some of reported side effects. All patients have developed long-term B cell aplasia, which can be alleviated by administration of gamma globulins (Swiech et al., 2020; Zhao et al., 2020). There are two main categories of toxicity: Cytokine release Syndrome (CRS) and neurotoxicity (NTX) or CAR-T cell-related encephalopathy syndrome (CRES).

Cytokine Release Syndrome

CRS or “cytokine storm” is a systemic inflammatory response, caused by the release of inflammatory cytokines, such as IL-1, IL-2, IL-6, IL-10, IL-15, interferon (IFN)- γ and tumor necrosis factor (TNF) by a large number of activated lymphocytes (B cells, T cells, and/or natural killer cells) and/or myeloid cells (macrophages, dendritic cells, and monocytes) which result in a wide range of clinical symptoms including fever, fatigue, headache, rash, joint pain and myalgia (Chavez et al., 2019; Riegler et al., 2019). CRS is the most common adverse effect that occurs within a few days after the first infusion of CAR-T cells (the CRS of any grade occurred in 85% of patients). Severe CRS cases are characterized by tachycardia, hypotension, pulmonary edema, cardiac dysfunction, high fever, hypoxia, renal impairment, hepatic failure, coagulopathy, and irreversible organ damage (Park et al., 2018). Fortunately, the effects of CRS can be attenuated by reducing the number of infused T cells and/or by the administration of anti-IL-6 receptor monoclonal antibody (tocilizumab) and steroids (Swiech et al., 2020). Nowadays, the search for different biopharmaceuticals to avoid the CRS is increasing due to COVID-19 treatment, which exhibits a similar CRS profile. This means that the next findings could be useful to improve this type of treatment.

Neurotoxicity

NTX is another common complication of CAR-T cell immunotherapy that occurs in more than 40% of patients (Belin et al., 2020). NTX described as CAR-T cell-related Encephalopathy (CRES) by Neelapu et al. (2018) and, more recently described under the name of ICANS (Immune effector Cell-Associated Neurotoxicity Syndrome) (Lee et al., 2019), is less understood than CRS and usually appears within one to 3 weeks after CAR-T cell infusion, which is frequently correlated with CRS (Siegler and Kenderian, 2020). Patients show a variety of symptoms such as confusion, obtundation, tremors, delirium, word-finding difficulty, and headaches; other symptoms such as aphasia, cranial nerve abnormalities and seizures have also been reported as part of NTX effect (Neill et al., 2020). Nowadays, neurotoxicity management is treated by

administering tocilizumab: an IL-6 receptor antibody; systemic corticosteroids; and dexamethasone (Gust et al., 2018).

The prompt management of toxicities is essential to minimize the mortality associated with this immunotherapy, for that, researchers have developed different safety strategies for overcoming and prevent the CAR-T cells toxicities such as the design of new CARs generations (Andrea et al., 2020; Rafiq et al., 2020). Toxicity management has become a critical step in the success of CAR-T cell immunotherapy. In fact, Tmunity Therapeutics developed a dual PSMA-specific, TGF β -resistant CAR-modified autologous T cells (CAR-T-PSMA-TGF β RDN) for prostate cancer with the objective to expand the use of CAR-T from hematological malignancies to solid tumors. This clinical trial (NCT04227275) had a setback that led to its winding down after two patients died from a type of ICANS. Nevertheless, the study helped to identify the potential barriers of CAR-T therapies against solid tumors, which results in a better understanding of the adverse effects mechanisms that will aid to design safer candidates.

Chimeric Antigen Receptor-T Cell Exhaustion

CAR-T cells have raised enormous interest in cancer immunotherapy due to the high rates of complete remission. Nevertheless, a large fraction of patients that achieve remission have displayed disease relapse within a few years (Maude et al., 2018; Park et al., 2018), the relapse rate varies from 21 to 45% in B-ALL and increases with the follow-up time (Cheng et al., 2019). The treatment failure could be partially explained by CAR-T cells exhaustion induced by tumor microenvironment (TME) created by solid tumors. Similar phenomena appear to extend in hematological malignancies including chronic lymphocytic leukemia (CLL), acute myeloid leukemia (AML), and diffuse large B cell lymphoma (DLBCL), besides to an excessive antigen exposure (Poorebrahim et al., 2020; Shen et al., 2020). The complex and heterogeneous TME affects the activation and function of the infiltrated effector T cells and thus impairs the persistence, proliferation, and potential of the T cells rendering them exhausted (Tahmasebi et al., 2019). CAR-T cells exhaustion refers to a state of dysfunction characterized by physical deletion of antigen-specific T cells due to persisting antigen stimulation, the costimulatory domain of CAR structure and increased expression of inhibitory receptors, usually induced by chronic stimulation, such as cancer (Wherry, 2011; Cheng et al., 2019). *In vitro* CAR-T cell studies have shown that during CAR-T cell exhausting process the loss of functionality against tumors is mainly triggered by the upregulated expression of inhibitory receptors such as PD-1, Lag3, Tim3, TIGIT, and the inhibition of PI3K/AKT pathway through CTLA-4. Nonetheless, cytokines play an important role in T cell activity or exhaustion, for instance, CAR-T cells decrease the ability of interleukin 2 (IL-2), Tumor necrosis factor α (TNF- α), and interferon- γ (IFN- γ) among other cytokines (Tang et al., 2021); Interleukin-5 (IL-5) increased proliferative capacity,

decreased apoptotic state through IL-5 mediated reduction of mTORC1 activity (Alizadeh et al., 2019).

Other factors such as transcriptional factors, metabolism, and epigenetic modification also play an important role in CAR-T cell exhaustion development (Shen et al., 2020). This dysfunctional phenotype is associated with hallmarked loss of the CAR-T cell's capacity of expansion and persistence. That situation compromises the patient's clinical remission (Fry et al., 2018). The reason why CAR-T cells lose *in vivo* persistence and potency remains unknown (Balkhi, 2020), that is why the CAR-T cells exhaustion is a pivotal hurdle for successful CAR-T cell therapies. A possible approach to delay the exhaustion is the engineering of exhaustion-resistant CAR-T cells. Recent reports indicate that the discovery of certain transcription factors like TOX (Seo et al., 2019) and NR4A (Cheng et al., 2019), and the deletion or overexpression of AP-1 family transcription factor c-Jun (Lynn et al., 2019) increases CAR-T cell resistance to exhaustion. Some studies have shown that CAR-T cells equipped with cytokines can enhance their own lifespan and expansion, promoting their own growth and proliferation (Avanzi et al., 2018; Zhao et al., 2020). That is the reason for the TRUCKs development by genetically adding an inducible cytokine-producing cassette (e.g., IL-12) (Zhao et al., 2020). Lately, deleting PD-1 by CAR-T cells engineering (short hairpin RNAs or CRISPR/Cas9), blocking antibodies using PD-1 and blocking the IFN- γ signal have been used to increase the CAR-T therapy efficacy avoiding exhaustion (Cheng et al., 2019; Rafiq et al., 2020). In this case, the discovery of the cellular mechanisms involved during cell proliferation and the maintenance of cell viability are a hindrance to the functioning of this therapy.

Tumor Microenvironment

The success of CAR T-cell immunotherapy has not yet been achieved in solid tumors. A possible reason is that the immunosuppressive nature of the tumor microenvironment (TME) affects the efficacy of adoptive immunotherapy. Solid tumors are highly infiltrated with stromal cells like cancer-associated fibroblasts (CAFs) and suppressive immune cells, including myeloid-derived suppressor cells (MDSCs), tumor-associated macrophages (TAMs), tumor-associated neutrophils (TANs), mast cells, and regulatory T cells (Tregs) which contribute to the establishment of a hostile and immunosuppressive TME capable of interfering the efficacy of CAR-T cell therapy (Martinez and Moon, 2019; Rodríguez-García et al., 2020). Strategies to overcome TME effect, include enabling T cells to resist tumor suppression in TME, such as transgene expression of dominant-negative receptors or signal converters, which can transform suppressive signals into stimulating signals (Tang et al., 2021). Another opportunity to overcome the persistence and exhaustion of CAR-T cells is improving the trafficking delivery of the drug to the tumor site. For CAR-T cells, local injection is a popular investigation among trials. This could be done in an anatomical cavity (pleura, peritoneum), via a device placed surgically (for CNS tumors) or via intra-arterial delivery (such as hepatic artery catheterization), or by direct intratumoral injection (Edeline et al., 2021).

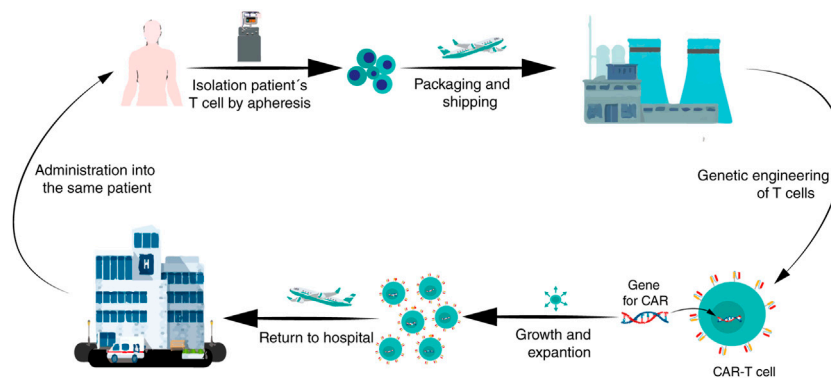


FIGURE 3 | A brief diagram of the CAR-T cells manufacturing process. After enough leukocytes have been harvested from a patient's blood via leukapheresis, T cells are shipped to a biopharmaceutical company where they are genetically engineered to express a CAR on the T cell surface. Then, the CAR-T cells are amplified *in vitro*; after that, the CAR-T cells are returned to the hospital for administration into the patient.

Genetic Alterations

Several reports have highlighted a lack of efficacy and relapses in patients treated with CAR-T cells (Sotillo et al., 2015; Fischer et al., 2017). Few reports have tackled the identification of genomic modifications post CAR-T cell therapy due to vector integration (Nobles et al., 2020). Orlando et al. (2018) incorporated whole-exome DNA-seq and RNA-seq to investigate the extent to which CD19 mutations are the main mechanism causing relapse. They discovered *de novo* CD19 genetic alterations in exons 2–5 in 12 of 12 samples from patients, and loss-of-heterozygosity in 8 of 9 patients, concluding that homozygous mutations in CD19 are the main reason for acquired resistance to CAR-T cell therapy. Asnani et al. (2020) reported similar findings; they described skipping of exon 2 and exons 5–6 in patients with relapsed leukemia after CAR-Tc therapy. Exon 2 is essential for the integrity of CAR-T 19 epitope while exons 5–6 are responsible for the CD19 transmembrane domain (Bagashev et al., 2018). CAR-T cells have been shown to improve the efficacy of immunotherapy; however, further research is needed to explore the impact of genome analysis to identify the prognosis once CAR-T cell transfusion is performed.

Manufacturing Process

The traditional technology to manufacture CAR-T cells consists in: 1) to isolate patient's T-cells (autologous) by apheresis; 2) to ship recovered cells to a central manufacturing site (biopharmaceutical companies) where 3) they are genetically engineered to express a CAR after which 4) they are expanded in the laboratory; then, 5) the CAR-T cells are returned to a hospital to be 6) infused into the patient for tumor eradication (Figure 3) (Roddie et al., 2019). The logistics involved in this traditional manufacturing and treatment with autologous CAR-T cells adds complexity for clinicians and patients because the period in between, referred to as “vein-to-vein time”, ranges between three and 4 weeks in developed countries. This period can be daunting for the patients awaiting treatment and renders the CAR-T treatment complicated for patients with rapidly progressing diseases (Aftab et al., 2020). Nowadays, this therapy presents these main manufacturing challenges and the

picture in developed and underdeveloped countries is very different. Some of such challenges include:

Packaging, Shipping, and Storage of Chimeric Antigen Receptor-T Cells

The clinical manufacture of CAR-T cells is currently a complex process that involves several steps across different geographic locations with multi-technologies and logistics. Any error in timing, transportation methods, cold chain, or storage, would result in cell damage directly impacting therapy efficiency, hence each one of the steps requires careful management, precise sample tracking and adequate preservation technologies to either freeze or cryopreserve patient samples (Papathanasiou et al., 2020). Different shipments with dissimilar temperatures are required throughout the CAR-T cell manufacturing process, therefore, suitable cryopreservation during production is mandatory for quality control tests (Stock et al., 2019).

Current Good Manufacturing Practices

CAR-T cells have a complex preparation process and the cGMP's are a critical and a bottleneck in CAR-T cell production (Wang and Rivière, 2016). The aim of cGMP's is to provide a framework to ensure high-quality production in well-controlled facilities and equipment by well-trained and regularly trained staff. Likewise, it provides strict documentation processes that covers all operation aspects to demonstrate a continuous and adequate compliance (Li et al., 2019). The CAR-T cells manufactured under GMP regulations should provide a system in which the cells will be prepared under controlled, auditable, reproducible conditions that result in providing adequate evidence of identity, safety, purity, and potency (Gee, 2018). The manufacturing protocols must improve reproducibility, cost-effectiveness, and scalability that will enable a broad application of CAR-T cell therapies (Fernández et al., 2019). According to International Organization for Standardization (ISO)5 CAR-T cell manufacturing requires GMP facilities as cell processing clean rooms, that must be equipped with 1) Facilities systems (e.g., air-handlers, 24/7 alarm monitoring systems); 2) Environmental monitoring

equipment (e.g., viable and nonviable particle counters); 3) Manufacturing process equipment (e.g., cell washers, bioreactors); and 4) Analytical equipment (e.g., automatic cell counters, flow cytometers) (Wang and Rivière, 2016). To optimize the GMP facilities the use of automatized manufacturing processes as CliniMACS or Cocoon is feasible to achieve reproducible processes in a closed system. Another key to maintaining a compliant GMP manufacturing environment is the highly skilled staff with extensive knowledge of GMP manufacturing, quality control, and quality assurance (Wang and Rivière, 2016). One complete review of the requirements for CTL019 is presented by Levine et al. (2017), who explain the complete manufacturing process and the challenges involved in each stage.

Production of Lentiviral Vectors

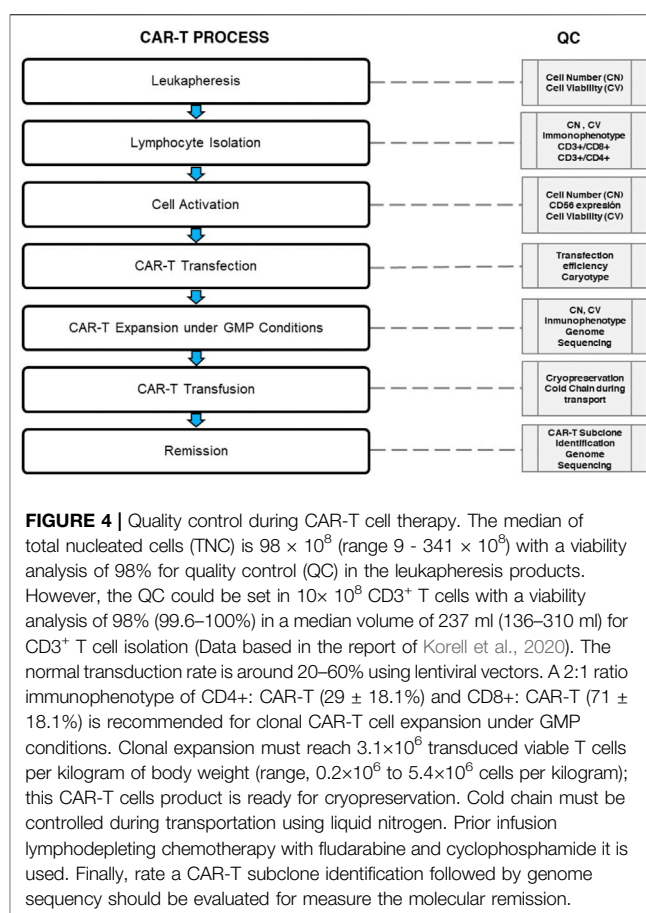
The approval of LV gene therapy products (e.g., Kymriah/Novartis) increased their demand and has created the need to improve their large-scale manufacture to clinical-grade LV (Lester et al., 2018). Nevertheless, the LVs production has challenges, such as their inherent cytotoxicity, low stability, and the dependency on transient transfection impact, both upstream and downstream processes that are reflected in low yielding and cost-ineffective compared to another viral vector (Ferreira et al., 2021). The level of GMP compliance required for the manufacture of LV is a combination of diverse factors including regulatory expertise, compliant facilities, validated and calibrated equipment, starting materials of the highest quality, trained production personnel, scientifically robust production processes, and quality by design approach (Levine et al., 2017; Dasgupta, et al., 2020). In addition, part of the commercialization success of this gene therapy product is the establishment, standardization, and implementation of stable cell lines to produce LVs facilitating GMP-compliant processes, providing an easier scale-up, reproducibility, biosafety, and cost-effectiveness (Ferreira et al., 2021).

Staff and Training

Considering the complex nature of the therapy and its associated high-risk side effects, access to CAR-T cells is highly regulated, making them available only at certified centers and administered by trained staff. All staff involved in CAR-T cell manufacturing (from T cell collection to the manufacturer and back to the clinical unit) require a broad training with satisfactory levels of competency. Such abilities manage complications that could arise during the process hence being able to deliver the product (Yakoub-Agha et al., 2020). Nowadays, there are only a few prepared professionals in this field, however, multidisciplinary collaboration is needed to create greater knowledge in this area. Academic participation is an important fact because the new personnel need to acquire different abilities to manufacture CAR-T cells.

Quality Control

As a living “drug,” a CAR-T cell has a complex preparation process and requires “whole-process quality control”. During the production, well-controlled cold chain transport and storage play



an important role in ensuring the cell products' quality and preventing the bacteria and *mycoplasma* contamination (Li et al., 2019). Current requirements in the CAR-T cell's quality control include the inspection of *ex vivo* transduced T-cell for the replicative virus and of the production materials. Furthermore, it should include a release test of the finished products to confirm identity, purity, safety, and potency, considering CAR-T cell's characteristics as biological products, cell products, and gene therapy products (Figure 4) (Eyles et al., 2019; Li et al., 2019). In addition, the validation of the production process is essential for CAR-T cells to be considered a final product. Moreover, stability studies are needed to verify the storage conditions and their shelf life. Besides, the production of CAR-T cells needs more in-depth studies to evaluate T cells' quality in both relapsed and regression patients. These studies should provide data about the distribution of lymphocyte populations. This information can guarantee efficient cell transduction and propagation ensuring the CAR-T cells' quality, and subsequently it would be reflected in the decrease of CAR-T cells exhaustion in patients. To sum up, quality control is of ultimate importance for the success of CAR-T therapy (Dai et al., 2019).

Scaling Up

CAR-T cells manufacturing should be scalable (that means, to have many single bioreactors for each patient) to have a broader

scope to benefit patients without sacrificing the quality and reproducibility of the products (Dai et al., 2019). Personalized therapies such as autologous cell-therapies require an “intensive scale-up”, that is related to the fact of having many bioreactors to amplify the CAR-T cells for each patient, instead of increasing the volume as in common biopharmaceuticals. Besides, it depends upon the ability to accommodate multiple independent productions in parallel (Wang and Rivière, 2016).

Limited Opportunity for Redosing

CAR-T cells manufacturing does not allow volumetric scale-up, consequently, cells must be prepared as a single batch limiting the quantity of available product. Under this scenario, patients may not have the opportunity to receive a new infusion of their CAR-T cells quickly and easily if needed (Aftab et al., 2020; Papathanasiou et al., 2020).

Time Manufacturing

CAR-T cells can take up to 4 weeks to manufacture, during this window of time, the patients are extremely vulnerable with risk of disease progression and mortality while waiting for infusion (Rafiq et al., 2020). Nevertheless, the use of novel strategies could help to overcome such a limitation, but it is necessary to consider the time required for transporting to prepare the adequate conditions for the patient. This takes around 6 weeks for the treatment to be applied at best.

Pricing and Patient Access

Pricing and patient access is the most important limitation to overcome to disclose the use of CAR-T cells all over the world. The current model of CAR-T cell manufacturing is highly centralized: firstly, the patient's T cells must be transported (often internationally) to the manufacturing facility, secondly, the CAR-T product is returned to the patient for infusion (Hay and Cheung, 2019). The process is complex in each step, resulting in highly costly therapy that ranges between \$373,000 and \$475,000 USD per treatment (hospital expenses associated with the therapy are not considered in such average costs) that neither patients nor the health-care system can afford. This prohibitive cost and the reimbursement gap limit the patient's access and remain unsustainable in socio-economically underdeveloped countries, restricting even more the widespread use of CAR-T cell therapies. Until CAR-T cell therapy becomes affordable, its potential will remain untapped (Yadav et al., 2020).

Regulatory Requirements

Another important bottleneck in cellular products is regulation. The CAR-T cells are globally considered within Advanced Therapy Medicinal Products (ATMP) and these products require licensure (Marks 2019). Regulatory agencies are highly related to standard therapies, but cellular products have special requirements. US or EU regulatory authorities are working to define optimal guidelines that can globally harmonize the requirements for clinical manufacturing of ATMP (Kaiser et al., 2015). Meanwhile underdeveloped countries face a greater challenge because CAR-T therapeutic use in clinics is

highly restricted, resulting in a poor understanding of the regulatory requirements by the authorities.

Strategies to Increase the Use of Chimeric Antigen Receptor-T Cells Technology.

Discovery of New Biomarkers

Biomarkers are of main importance for cancer clinical management, as they can be used to define the criteria to identify the patients suitable for CAR-T therapy, prognosis, prediction of response to treatment and monitoring disease progression. Developing cancer immunotherapy has therapeutic implications and its success varies depending on the type of cancers (Schumacher et al., 2015). On the other hand, CAR-T cell immunotherapy has achieved promising results mainly in patients with hematologic malignancies. On the other side, this type of therapy has more obstacles attacking solid tumors, including immunosuppressive tumor microenvironment (TME), lack of permeation of the CAR-T cells into tumors, limited transport, and specific tumor antigen (Ling, 2020). Despite the significant advances, clinical improvement after CAR-T therapy has not been observed for all the patients who have undergone this immunotherapy. Such differences could rely on molecular response; hence it is necessary to fully understand remission and relapse in CAR-T therapy through biomarkers. Consequently, it is essential to identify the clinical features in the form of biomarkers that drive response, resistance, and adverse effects because of immunotherapies (Townsend et al., 2018). Thus, for the respective CAR-T cell immunotherapy development and success it is essential to broaden the range of cancers that respond to such a kind of immunotherapy with the discovery of new biomarkers. The identification of new biomarkers improves clinical practices for early recognition and minimization of adverse effects while preserving the antitumor activity of the CAR-T cells (Mirzaei et al., 2018), it opens the possibility to target other types of tumors and leads to the development of new strategies for numerous types of cancer treatments, positioning CAR-T cells as a therapeutic option in cancer medicine (Ponterio et al., 2020). The first biomarker for CAR-T - therapy was CD19, a B cell surface protein expressed mainly on malignant B cells. Currently, scientific research is underway to find out biomarkers according to the stage of immunotherapy as follows: biomarkers to define patients baseline status; biomarkers for CAR-T-cell function, CAR-T cell exhaustion, CAR-T cell toxicity and biomarkers for cancer prognosis, response, and relapse (Mirzaei et al., 2018). As for baseline biomarkers, cytokines of the immune system such as IL2, IL-5, IL-7, TNF- α , among others; lactate dehydrogenase (LDH) and CD9 cells, are widely used. Meanwhile, for CAR-T cell function, the following biomarkers have been proposed: CD45RA, CD45RO, CD62L, CCR7, CD27, CD28 (differentiation markers), CD25, CD127, CD57, and CD137 (activation markers) (Wang et al., 2019; Hong et al., 2021). Currently, there are no proven biomarkers that can be used to assess CAR-T cell exhaustion after infusion in patients. However, indirect parameters could be helpful for this purpose; for example, a sustained gain in B-cell recovery

within 3 months after CART-therapy and the detection of LAG3+ cells could be considered due to CAR-T cell exhaustion. As well as high levels of expression of PD-1, LAG-3, TIM-3, and their receptors are associated with T cell exhaustion and poor response to CD19 CAR-T therapy (Hong et al., 2021). Recently a model of T cell exhaustion assessment through flow cytometry has been proposed based upon PD-1 pathway blockade response, identifying three main stages: exhausted progenitors, intermediated exhausted, and terminally exhausted T cells (Beltra et al., 2020). Relapse: IL-6, Protein C reactive, TNF- α , serum calcium, serum phosphate, uric acid (Zhang et al., 2016). In **Table 3**, a summary of novel target antigens selection for CAR-T cells in hematologic malignancies and solid tumors under clinical trials is presented. Despite significant advances in CAR-T therapy, it is essential to continue exploring different cancer cell-type-specific biomarkers to develop more specific therapies.

Allogeneic Chimeric Antigen Receptor-T Cells

Currently, most CAR-T cell immunotherapy is generated using autologous T cells. This represents several disadvantages at different levels. For example, autologous cell therapy is performed for individual patients, the production can be long-time consuming and complicated, resulting in the increase of costs and it can limit the broader application of this therapy. In addition, the challenges due to the use of patient-derived T cells for CAR therapy include weaker proliferation, limited expansion, and low persistence of CAR-T cells. In some cases, CAR-T cell efficacy, most likely due to poor autologous immune cell strength in cancer patients caused by aggressive treatments (Caldwell et al., 2021). One opportunity for improving some manufacturing-related issues is the use of allogeneic CAR-T cells for reducing time delays on autologous cell production. Generating universal CAR-T cells from allogeneic healthy donors could set the stage for overcoming high costs and high time production, making them easily available and with higher quality. Such a fact is very important for patients with aggressive cancers that require urgent therapy (Caldwell et al., 2021). This strategy would broaden the number of patients that could receive this immunotherapy to make CAR-T cell therapy an off-the-shelf treatment at an affordable cost, that be readily available and would increase quality properties in T cells (Cheng et al., 2019). Another advantage is that universal CAR-T cells could provide the possibility of manufacturing clinical-grade CAR-T products against various cancers “on-demand” (Balkhi, 2020). However, it is important to also consider the up-coming challenges and disadvantages for using universal CAR-T cells. For example, immunologic mismatch between donor and recipient, if the administered allogeneic T cells attack healthy recipient tissues, may cause life-threatening graft-versus-host disease (GVHD), and if the recipient’s immune system recognizes and reacts against the allogeneic T cells, these may be rapidly eliminated by the host immune system limiting the expected therapeutic effect (Depil et al., 2020). A possible solution is a genetic elimination or disruption of the TCR gene and/or HLA class I loci on the donor to eliminate GVHD (Cheng et al., 2019), also,

the use of allogeneic anti-CD19 CAR with deleted α -TCR chain and CD52 gene loci has demonstrated effectiveness to eliminate GVHD (Cheng et al., 2019; Balkhi, 2020).

Different allogeneic strategies have appeared to improve immunotherapy challenges such as the use of induced pluripotent stem cells (iPSC). iPSCs offer the opportunity to be unlimitedly cultured *in vitro* and be successfully differentiated towards the lymphoid lineage as to NK lymphocytes that are innate lymphocytes that kill malignant cells in an HLA-independent manner (Kennedy et al., 2012). The use of iPSCs provides unlimited “off-the-shelf” NK cells offering doses without limitations, standardized and cost-effective products (Zeng et al., 2017). iPSCs can generate immune effectors with the capacity of easily being genetically modified to augment their applicability, potency, and persistence (Nianias and Themeli, 2019). The possibility of effortlessly generating NK cells from iPSCs (iPSC-derived NK cells) opens the great option to use the CAR constructions as an alternative to T cells, to produce CAR-iPSCNK cells with rapid responses against malignant cells without causing GVHDs (Euchner et al., 2021). Compared to CAR-T cells, CAR-NK cells offer some more advantages, such as a lack or a decrease in cytokine release syndrome and neurotoxicity in an autologous setting, another point in its favor is the multiple mechanisms for activating cytotoxic activity (NKG2D, KIR’s, CD16, NKp30, NKp44, NKp46), still maintaining its infiltration capacity into solid tumors and into the resistant tumor microenvironment (Xie et al., 2020). CAR-NK preclinical studies showed effectiveness against hematologic malignancy targets (CD19 and CD20), as well as solid tumor targets demonstrating their potential to be an allogeneic therapeutic (Caldwell et al., 2021). Besides CAR-iPSCNK strategy, virus-specific T cells, memory T cells, genetically modified $\alpha\beta$ T cells, and $\gamma\delta$ T cells are other effective ways to tackle allogeneic CAR immunotherapy. All these strategies have in common their effectiveness to attack malignant cells, and the possibility to use CAR construction to improve toxicity effects, costs and efficiency of CAR-T manufacturing, and the persistence of reducing GVHD risk (Martinez and Moon, 2019; Yazdanifar et al., 2020).

Other Strategies to Improve Chimeric Antigen Receptor-T Cells Outcomes

Dual or tandem CARs, consist of the coexpression of two separate CARs in each T cell, which recognize two different antigens rather than one. Some dual CARs have entered clinical trials in hematological malignancies targeting CD19/CD20, and CD19/CD22 (Zah et al., 2016; NCT03241940) and solid tumors. CAR specific for HER2/MUC1 had promising *in vitro* results in a breast cancer model. It is important to mention that dual-target CAR specific HER2/IL13Ra2 showed greater success than single-target CARs in a xenograft glioma model (Martinez and Moon, 2019). Dual CAR is a promising method to address antigen heterogeneity and to prevent the relapse caused by antigen escape (Huang et al., 2020). Synthetic Notch (synNotch) receptors have been applied in CAR-T cells to improve safety. SynNotch receptors recognize one specific tumor antigen and

then transcriptional activation domains are released, promoting the local expression of a CAR (Han et al., 2019). Moreover, synNotch-regulated CAR expression prevents constitutive signaling and exhaustion, maintaining a higher fraction of the T cells in a naïve/stem cell memory state (Choe et al., 2021). Synthetic Notch (synNotch) receptors have been applied in CAR-T cells to improve safety. SynNotch receptors recognized one specific tumor antigen and then transcriptional activation domains were released, promoting the local expression of a CAR (Han et al., 2021). Moreover, synNotch-regulated CAR expression prevents constitutive signaling and exhaustion, maintaining a higher fraction of the T cells in a naïve/stem cell memory state (Choe et al., 2021). Inhibitory chimeric antigen receptor (iCAR), which incorporates inhibitor receptors, such as PD-1 and CTLA-4, play a crucial role in attenuating or terminating T cells response, therefore, they are considered a safety strategy (Yu et al., 2019). iCAR shows antigen-specific suppression of T cell cytokine secretion, cytotoxicity, and proliferation of rapid and selective kills of target cells that only express one antigen, whereas off-target cells, that co-expresses another inhibitory ligand recognized by iCAR, are protected from attack. This allows T cells to distinguish target cells from the off-target cells (Han et al., 2019). With this said, it is important to highlight the following aspects for a successful clinical application: the iCARs' affinity and expression level, the appropriate selection of target antigen and the optimization of the CAR/iCAR ratio (Garrett and Brown, 2014). Currently, Jan and cols., have developed ON and OFF switches for CAR-T cells using lenalidomide, a clinically approved drug, which facilitates the proteasome degradation of several target proteins (Jan et al., 2021). In addition, to efficiently treat solid tumor, innovative combinations strategies such as vaccines, biomaterials, and oncolytic virus are good prospects, because they allow either to directly enhance T cells' function or to recruit endogenous immune cells as well as remodeling the TME (Huang et al., 2020).

Fully Automated Manufacturing Process

Worldwide, the number of patients who require CAR-T cell immunotherapy quickly increases. That is the reason why the standardization of the manufacturing process (following GMP's), the quality control and expanding the production to hospitals making the treatment accessible for a larger number of patients, are highly needed. The industry has developed automated and closed cell manufacturing platforms to adapt to this scenario. Examples of this effort are the automatized platforms Cocoon® (Lonza) and CliniMACS Prodigy (Miltenyi Biotec), both allow reproducible and rapid production of cells, and every step is strictly documented. Cocoon® Platform streamlines patient-scale cell therapy manufacturing making them more efficient, reliable, and flexible. These features speed up CAR-T manufacturing, cut costs and decrease manufacturing failure rates that may be associated with more hands-on methods. In 2020 Lonza and Sheba Medical Center announced the first patient has been treated at Sheba Medical Center with CD19 CAR-T cell immunotherapy manufactured using Lonza's Cocoon Platform. Another example for automated and supervised manufacturing is CliniMACS, which allows T cell activation, transduction, amplification, and final harvesting of CAR-T cells,

with high transduction frequencies and high cell numbers in the same device. This method fully controls the multi-step process through a flexible programming suite (Lock et al., 2017; Köhl et al., 2018).

Network Collaboration

Unfortunately, most of the patients cannot afford CAR-T therapy due to the high costs and the lack of facilities around the world to produce them. The efforts focused on quality production following the GMP's had been successful to a certain extent, but the road is still long to bring this technology to a massive application.

To achieve this, it is necessary to generate a collaborative network between various stakeholders such as the academia, the industry, and the hospitals, for the establishment of adequate and robust legislation for this type of product in each country where such a technology is applied. Thus, universities should provide knowledge and innovation to future professionals for them to do research on new biomarkers discoveries, on the development of stable cell lines, and on developing and validating orthogonal analysis methodologies for the product quality and for them to learn about different production systems. The industry applying GMP's, quality control and automation processes can support the establishment of more standardized and reliable products that have a high quality, and it can also develop on-site production units that allow lower transport and storage costs. Hospitals must have adequate facilities for the management of this technology, with trained personnel in the management of production units *in situ* (if applicable), as well as medical personnel and health professionals for the effective treatment of patients. Encompassing all these activities there must be robust and specific legislation in this area that guarantees the quality of this type of advanced therapy. Additionally, regulation is an essential part of such a process. Nowadays, there is sparse information about regulatory guidelines in different countries, the EMA and FDA guidelines (Iglesias-López et al., 2019) have established the baseline of such requirements for these technologies but the behavior and results on different phases of clinical trials will address novel considerations. One challenge but at the same time one opportunity will be to establish local regulation of these technologies in every country that needs to be approved by competent authorities for smooth implementation of CAR-T cell clinical programs. All this collaborative effort is the key to allow worldwide access to CAR-T cell therapy to a larger number of individuals with cancer.

Finally, the idea of promoting the use of CAR-T cells technology in a greater number of countries rests on its potential application in various diseases in both adults and children. To our knowledge, the application of CAR-T cells technology has been mainly used in developed countries (Elahi et al., 2018), revealing a large gap in the rest of the world. In fact, the only clinical study conducted in Latin America was made in Brazil (Cunha Oct 16, 2019) in a 63-year-old man that was affected by BLBCL. Therefore, it is important to consider that for this technology to be enforceable in developing countries various policies must be created and implemented. On the one hand, technology transfer agreements can be established among centers with experience in the subject and treatment centers in

developing countries, however, this continues to foster scientific-technological dependence. On the other hand, developing countries should work on integrating their own elements (academy-industry-hospital and government), generating treatments of this type but geared to the specific needs of its population and adapting them to the available resources. However, it is important to highlight that in this case, government support is essential to start setting up treatment centers for advanced therapies in hospitals and health institutions. In addition, international support from non-profit institutions in terms of financial resources and support for the training of professionals is also necessary.

DISCUSSION

Current and widely used methods for cancer treatment consist of surgery, chemotherapy, radiation therapy and immunotherapy (mainly monoclonal antibodies). Despite the health care system efforts, with the increasing incidence of cancer, its clinical management continues to be a major challenge. Recently, remarkable progress has been achieved towards adoptive immunotherapies through clinical application and consistent evolution of ACT strategies. Such immunotherapies, in combination with conventional methods have proven major efficiency for cancer treatment. In the last few years, CAR-T cell therapy, a type of ACT, has demonstrated potential in clinical trials, leading to complete and durable responses in patients with late-stage and treatment-refractory disease. In fact, there are currently 5 FDA-approved products on the market, which have been tested in a few hundred patients during clinical trials in developed countries around the world. Furthermore, the first one was approved for commercial use in 2017 but the cost of such a treatment is substantially high (from \$ 375,000.00 to \$475,000.00 without considering operation and indirect costs) so, considering its potential application in the treatment of different types of diseases there is a need to improve the technology to make it more accessible to the world's population.

From a pharmaceutical point of view, CAR-T cells are considered as advanced therapy products or biopharmaceuticals (depending on the country) whose quality must be demonstrated through their identity, safety, and efficacy. This novel technology is the set of synergy between three main elements: the targets (antigens against the CAR will be directed and that, ideally, are required to be only expressed in malignant cells); chimeric receptors (whose sophistication allow to bind to said antigen and that are designed to provide better selectivity towards tumor cells, and properly, T cells (containing CD3 +/CD4 + and CD3 +/CD8 +, in an adequate proportion) that are genetically modified to express the CAR and guarantee the success of such therapy.

Each of the previous three elements presents significant challenges. As discussed in this work, the search for biomarkers is an exhaustive task aimed at identifying target molecules that are specific to a certain type of disease, which will help improve efficacy and reduce adverse effects. Likewise, the improvement in the development of CARs to promote an effective union with the receptor and the generation of an effective immune response against the disease and improve activation, proliferation, and

survival is the subject of study. Furthermore, many efforts are directed at the selection of the T cells used in this technology, such cells must comply with adequate phenotypic characteristics; being genetically stable; being able to transduce within a high percentage (also putting on the table the need of vector optimization for this purpose); being expanded to reach the required levels for the therapy; being enough stable to avoid the cell exhaustion; and, accomplishing all the requirements of a cell therapy product at the level of identity, purity and efficacy. Furthermore, it is necessary to focus on the reduction of adverse effects related to CRS and NTX and in the application of this technology in solid tumors with the idea of increasing the safety and efficacy of this therapy, among other points of improvement.

Alternatively, the need to generate lower-cost production systems, with robust production in each batch (patient-specific), but that meet the necessary quality requirements to be applied to the patient is also a constant challenge. Currently, the use of automated systems applicable *in situ* seems a promising alternative. These processes must be in complete harmony with the requirements established by international and regional health authorities.

Finally, considering all the aspects of this therapy, the multidisciplinary participation of health care professionals in various stages is required. Through intensive collaborations between academia, industry, hospitals, and government, both at the international and regional level, it will be possible to achieve a broader accessibility to this technology to a larger number of patients. This situation should be able to overlap in the case of developing countries, who must seek different strategies by applying their own generated knowledge, making an efficient use of the existing infrastructure, and seeking collaborations at various levels to obtain the necessary information and resources. The implementation of these strategies is likely to increase the number of treatments all over the world.

AUTHOR CONTRIBUTIONS

All authors conceptualized, designed, and assisted with the draft/approval of this manuscript.

FUNDING

The financial support for this work was by I0031-2019-03MACROPRONAI-SALUD-2019 Programa Nacional Estratégico para la Leucemia Infantil, CONACYT postdoctoral fellowship to AH-L (CVU: 253979), CONACYT INFR-2014 226271 and CONACYT doctoral fellowship to MA T-G (02986).

ACKNOWLEDGMENTS

We gratefully acknowledge Facultad de Farmacia, Universidad Autónoma del Estado de Morelos. AH-L (CVU: 253979) is the recipient of a postdoctoral fellowship from CONACYT during development of this work.

REFERENCES

- Aftab, B. T., Sasu, B., Krishnamurthy, J., Gschwend, E., Alcazer, V., and Depil, S. (2020). Toward "Off-The-Shelf" Allogeneic CAR T Cells. *Adv. Cell Gene Ther* 3, 1–11. doi:10.1002/acg2.86
- Al-Juhaishi, T., and Ahmed, S. (2021). Selecting the Optimal CAR-T for the Treatment of B-Cell Malignancies. *Curr. Hematol. Malig. Rep.* 16, 32–39. doi:10.1007/s11899-021-00615-7
- Albinger, N., Hartmann, J., and Ullrich, E. (2021). Current Status and Perspective of CAR-T and CAR-NK Cell Therapy Trials in Germany. *Gene Ther.*, 1–15. doi:10.1038/s41434-021-00246-w
- Alizadeh, D., Wong, R. A., Yang, X., Wang, D., Pecoraro, J. R., Kuo, C. F., et al. (2019). IL15 Enhances CAR-T Cell Antitumor Activity by Reducing mTORC1 Activity and Preserving Their Stem Cell Memory Phenotype. *Cancer Immunol. Res.* 7, 759–772. doi:10.1158/2326-6066.CIR-18-0466
- Andrea, A. E., Chiron, A., Bessoles, S., and Hacein-Bey-abina, S. (2020). Engineering Next-Generation Car-T Cells for Better Toxicity Management. *Int. J. Mol. Sci.* 21, 1–25. doi:10.3390/ijms21228620
- Anelone, A. J. N., Villa-Tamayo, M. F., and Rivadeneira, P. S. (2020). Oncolytic Virus Therapy Benefits from Control Theory. *R. Soc. Open Sci.* 7 (7), 200473. doi:10.1098/rsos.200473
- Arruebo, M., Vilaboa, N., Sáez-Gutierrez, B., Lambea, J., Tres, A., Valladares, M., et al. (2011). Assessment of the Evolution of Cancer Treatment Therapies. *Cancers (Basel)* 3, 3279–3330. doi:10.3390/cancers3033279
- Asnani, M., Hayer, K. E., Naqvi, A. S., Zheng, S., Yang, S. Y., Oldridge, D., et al. (2020). Retention of CD19 Intron 2 Contributes to CART-19 Resistance in Leukemias with Subclonal Frameshift Mutations in CD19. *Leukemia* 34, 1202–1207. doi:10.1038/s41375-019-0580-z
- Avanzi, M. P., Yeku, O., Li, X., Wijewarnasuriya, D. P., van Leeuwen, D. G., ParkCheung, H., et al. (2018). Engineered Tumor-Targeted T Cells Mediate Enhanced Anti-tumor Efficacy Both Directly and through Activation of the Endogenous Immune System. *Cell Rep* 23, 2130–2141. doi:10.1016/j.celrep.2018.04.051
- Bagashev, A., Sotillo, E., Tang, C. H., Black, K. L., Perazzelli, J., Seeholzer, S. H., et al. (2018). CD19 Alterations Emerging after CD19-Directed Immunotherapy Cause Retention of the Misfolded Protein in the Endoplasmic Reticulum. *Mol. Cell Biol.* 38, e00383–18. doi:10.1128/MCB.00383-18
- Balkhi, M. Y. (2020). Challenges and Opportunities to Improve CAR T-Cell Therapy. *Basics Chimeric Antigen Recept. Immunother.* 63, 63–80. doi:10.1016/b978-0-12-819573-4.00005-3
- Bamdad, C., Stewart, A. K., Smaghe, B. J., Glennie, N. D., Huang, P., Moe, S., et al. (2019). First-in-human CAR T for Solid Tumors Targets the MUC1 Transmembrane Cleavage Product. *Cytotherapy* 21 (5), S9. doi:10.1016/j.jcyt.2019.03.563
- Belin, C., Devic, P., Aygnac, X., Dos Santos, A., Paix, A., Sirven-Villars, L., et al. (2020). Description of Neurotoxicity in a Series of Patients Treated with CAR T-Cell Therapy. *Sci. Rep.* 10, 18997. doi:10.1038/s41598-020-76055-9
- Beltra, J. C., Manne, S., Abdel-Hakeem, M. S., Kurachi, M., Giles, J. R., Chen, Z., et al. (2020). Developmental Relationships of Four Exhausted CD8+ T Cell Subsets Reveals Underlying Transcriptional and Epigenetic Landscape Control Mechanisms. *Immunity* 52, 825–841. doi:10.1016/j.immuni.2020.04.014
- Berraondo, P., Sanmamed, M. F., Ochoa, M. C., Etcheberria, I., Aznar, M. A., Pérez-Gracia, J. L., et al. (2019). Cytokines in Clinical Cancer Immunotherapy. *Br. J. Cancer* 120 (1), 6–15. doi:10.1038/s41416-018-0328-y
- Berrón-Ruiz, L., López-Herrera, G., Ávalos-Martínez, C. E., Valenzuela-Ponce, C., Ramírez-Sanjuan, E., Santoyo-Sánchez, G., et al. (2016). Variations of B Cell Subpopulations in Peripheral Blood of Healthy Mexican Population According to Age: Relevance for Diagnosis of Primary Immunodeficiencies. *Allergol. Immunopathol (Madr)* 44, 571–579. doi:10.1016/j.aller.2016.05.003
- Bouchkouj, N., Kasamon, Y. L., de Claro, R. A., George, B., Lin, X., Lee, S., et al. (2019). FDA Approval Summary: Axicabtagene Ciloleucel for Relapsed or Refractory Large B-Cell Lymphoma. *Clin. Cancer Res.* 25, 1702–1708. doi:10.1158/1078-0432.CCR-18-2743
- Bray, F., Ferlay, J., Soerjomataram, I., Siegel, R. L., Torre, L. A., and Jemal, A. (2018). Global Cancer Statistics 2018: GLOBOCAN Estimates of Incidence and Mortality Worldwide for 36 Cancers in 185 Countries. *CA Cancer J. Clin.* 68, 394–424. doi:10.3322/caac.21492
- Brentjens, R. J., Davila, M. L., Riviere, I., Park, J., Wang, X., Cowell, L. G., et al. (2013). CD19-targeted T Cells Rapidly Induce Molecular Remissions in Adults with Chemotherapy-Refractory Acute Lymphoblastic Leukemia. *Sci. Transl. Med.* 5, 177ra38. doi:10.1126/scitranslmed.3005930
- Brentjens, R. J., Riviere, I., Park, J. H., Davila, M. L., Wang, X., Stefanski, J., et al. (2011). Safety and Persistence of Adoptively Transferred Autologous CD19-Targeted T Cells in Patients with Relapsed or Chemotherapy Refractory B-Cell Leukemias. *Blood* 118 (18), 4817–4828. doi:10.1182/blood-2011-04-348540
- Brown, C. E., and Mackall, C. L. (2019). CAR T Cell Therapy: Inroads to Response and Resistance. *Nat. Rev. Immunol.* 19 (2), 73–74. doi:10.1038/s41577-018-0119-y
- Caldwell, K. J., Gottschalk, S., and Talleur, A. C. (2021). Allogeneic CAR Cell Therapy-More Than a Pipe Dream. *Front. Immunol.* 11, 1–12. doi:10.3389/fimmu.2020.618427
- Cao, G., Lei, L., and Zhu, X. (2019). Efficiency and Safety of Autologous Chimeric Antigen Receptor T-Cells Therapy Used for Patients with Lymphoma: A Systematic Review and Meta-Analysis. *Medicine (Baltimore)* 98, e17506. doi:10.1097/MD.00000000000017506
- Castella, M., Caballero-Baños, M., Ortiz-Maldonado, V., González-Navarro, E. A., Suñé, G., Antón-Vidósola, A., et al. (2020). Point-of-care CAR T-Cell Production (ARI-0001) Using a Closed Semi-automatic Bioreactor: Experience from an Academic Phase I Clinical Trial. *Front. Immunol.* 11, 482. doi:10.3389/fimmu.2020.00482
- Charmsaz, S., Collins, D. M., Perry, A. S., and Prencipe, M. (2019). Novel Strategies for Cancer Treatment: Highlights from the 55th IACR Annual Conference. *Cancers (Basel)* 11, 1–11. doi:10.3390/cancers11081125
- Chavez, J. C., Bachmeier, C., and Kharfan-Dabaja, M. A. (2019). CAR T-Cell Therapy for B-Cell Lymphomas: Clinical Trial Results of Available Products. *Ther. Adv. Hematol.* 10, 2040620719841581. doi:10.1177/2040620719841581
- Cheng, J., Zhao, L., Zhang, Y., Qin, Y., Guan, Y., Zhang, T., et al. (2019). Understanding the Mechanisms of Resistance to CAR T-Cell Therapy in Malignancies. *Front. Oncol.* 9, 1237–1239. doi:10.3389/fonc.2019.01237
- Choe, J. H., Watchmaker, P. B., Simic, M. S., Gilbert, R. D., Li, A. W., Krasnow, N. A., et al. (2021). SynNotch-CAR T Cells Overcome Challenges of Specificity, Heterogeneity, and Persistence in Treating Glioblastoma. *Sci. Transl. Med.* 13, eabe7378. doi:10.1126/scitranslmed.abe7378
- Da Fonseca, L. G., and Carrilho, F. J. (2019). Updates in Immunotherapy for Hepatocellular Carcinoma. *Hepatoma Res.* 5, 37. doi:10.20517/2394-5079.2019.012
- Dai, X., Mei, Y., Cai, D., and Han, W. (2019). Standardizing CAR-T Therapy: Getting it Scaled up. *Biotechnol. Adv.* 37, 239–245. doi:10.1016/j.biotechadv.2018.12.002
- Darvin, P., Toor, S. M., Sasidharan Nair, V., and Elkord, E. (2018). Immune Checkpoint Inhibitors: Recent Progress and Potential Biomarkers. *Exp. Mol. Med.* 50 (12), 1–11. doi:10.1038/s12276-018-0191-1
- Dasgupta, A., Tinch, S., Szczur, K., Ernst, R., Shryock, N., Kaylor, C., et al. (2020). Phase I/II Manufacture of Lentiviral Vectors under GMP in an Academic Setting. *Methods Mol. Biol.* 2086, 27–60. doi:10.1007/978-1-0716-0146-4_3
- Date, V., and Nair, S. (2021). Emerging Vistas in CAR T-Cell Therapy: Challenges and Opportunities in Solid Tumors. *Expert Opin. Biol. Ther.* 21 (2), 145–160. doi:10.1080/14712598.2020.1819978
- Depil, S., Duchateau, P., Grupp, S. A., Mufti, G., and Poirot, L. (2020). 'Off-the-shelf' Allogeneic CAR T Cells: Development and Challenges. *Nat. Rev. Drug Discov.* 19, 185–199. doi:10.1038/s41573-019-0051-2
- Dougan, M., and Dranoff, G. (2012). "Immunotherapy of Cancer," in *The Innate Immune Regulation and Cancer Immunotherapy*. Editors R.-F. Wang (New York: Springer-Verlag, 391–414. doi:10.1007/978-1-4419-9914-6_22
- Dwivedi, A., Karulkar, A., Ghosh, S., Rafiq, A., and Purwar, R. (2019). Lymphocytes in Cellular Therapy: Functional Regulation of CAR T Cells. *Front. Immunol.* 9, 3180. doi:10.3389/fimmu.2018.03180
- Edeline, J., Houot, R., Marabelle, A., and Alcantara, M. (2021). CAR-T Cells and BiTEs in Solid Tumors: Challenges and Perspectives. *J. Hematol. Oncol.* 14, 65–12. doi:10.1186/s13045-021-01067-5
- Elahi, R., Khosh, E., Tahmasebi, S., and Esmaeilzadeh, A. (2018). Immune Cell Hacking: Challenges and Clinical Approaches to Create Smarter Generations of Chimeric Antigen Receptor T Cells. *Front. Immunol.* 9, 1717. doi:10.3389/fimmu.2018.01717

- Eshhar, Z., Waks, T., Gross, G., and Schindler, D. G. (1993). Specific Activation and Targeting of Cytotoxic Lymphocytes through Chimeric Single Chains Consisting of Antibody-Binding Domains and the Gamma or Zeta Subunits of the Immunoglobulin and T-Cell Receptors. *Proc. Natl. Acad. Sci. U S A* 90, 720–724. doi:10.1073/pnas.90.2.720
- Euchner, J., Sprissler, J., Cathomen, T., Fürst, D., Schrezenmeier, H., Debatin, K.-M., et al. (2021). Natural Killer Cells Generated from Human Induced Pluripotent Stem Cells Mature to CD56brightCD16+NKp80+/-In-Vitro and Express KIR2DL2/DL3 and KIR3DL1. *Front. Immunol.* 12, 1–11. doi:10.3389/fimmu.2021.640672
- Eyles, J. E., Vessillier, S., Jones, A., Stacey, G., Schneider, C. K., and Price, J. (2019). Cell Therapy Products: Focus on Issues with Manufacturing and Quality Control of Chimeric Antigen Receptor T-Cell Therapies. *J. Chem. Technol. Biotechnol.* 94, 1008–1016. doi:10.1002/jctb.5829
- Fedorov, V. D., Themeli, M., and Sadelain, M. (2013). PD-1- and CTLA-4-Based Inhibitory Chimeric Antigen Receptors (iCARs) Divert Off-Target Immunotherapy Responses. *Sci. Transl. Med.* 5, 215ra172. doi:10.1126/scitranslmed.3006597
- Fernández, L., Fernández, A., Mirones, I., Escudero, A., Cardoso, L., Vela, M., et al. (2019). GMP-compliant Manufacturing of NKG2D CAR Memory T Cells Using CliniMACS Prodigy. *Front. Immunol.* 10, 2361–2372. doi:10.3389/fimmu.2019.02361
- Ferreira, M. V., Cabral, E. T., and Coroadinha, A. S. (2021). Progress and Perspectives in the Development of Lentiviral Vector Producer Cells. *Biotechnol. J.* 16, e2000017–12. doi:10.1002/biot.202000017
- Fesnak, A., and O'Doherty, U. (2017). Clinical Development and Manufacture of Chimeric Antigen Receptor T Cells and the Role of Leukapheresis. *Eur. Oncol. Haematol.* 13, 28–34. doi:10.17925/eoh.2017.13.01.28
- Fischer, J., Paret, C., El Malki, K., Alt, F., Wingerter, A., Neu, M. A., et al. (2017). CD19 Isoforms Enabling Resistance to CART-19 Immunotherapy Are Expressed in B-ALL Patients at Initial Diagnosis. *J. Immunother.* 40, 187–195. doi:10.1097/CJI.0000000000000169
- Freitag, F., Maucher, M., Riester, Z., and Hudecek, M. (2020). New Targets and Technologies for CAR-T Cells. *Curr. Opin. Oncol.* 32 (5), 510–517. doi:10.1097/CCO.0000000000000653
- Fry, T. J., Shah, N. N., Orentas, R. J., Stetler-Stevenson, M., Yuan, C. M., Ramakrishna, S., et al. (2018). CD22-targeted CAR T Cells Induce Remission in B-ALL that Is Naive or Resistant to CD19-Targeted CAR Immunotherapy. *Nat. Med.* 24, 20–28. doi:10.1038/nm.4441
- Fujiwara, K., Tsunai, A., Kusabuka, H., Ogaki, E., Tachibana, M., and Okada, N. (2020). Hinge and Transmembrane Domains of Chimeric Antigen Receptor Regulate Receptor Expression and Signaling Threshold. *Cells* 9 (5), 1182. doi:10.3390/cells9051182
- Garber, K. (2019). Pursuit of Tumor-Infiltrating Lymphocyte Immunotherapy Speeds up. *Nat. Biotechnol.* 37, 969–971. doi:10.1038/d41587-019-00023-6
- Gargett, T., and Brown, M. P. (2014). The Inducible Caspase-9 Suicide Gene System as a "safety Switch" to Limit On-Target, Off-Tumor Toxicities of Chimeric Antigen Receptor T Cells. *Front. Pharmacol.* 5, 235–237. doi:10.3389/fphar.2014.00235
- Gee, A. P. (2018). GMP CAR-T Cell Production. *Best Pract. Res. Clin. Haematol.* 31, 126–134. doi:10.1016/j.beha.2018.01.002
- Ghosh, A., Mailankody, S., Giral, S. A., Landgren, C. O., Smith, E. L., and Brentjens, R. J. (2017). CAR T Cell Therapy for Multiple Myeloma: where Are We Now and where Are We Headed? *Leuk. Lymphoma* 59 (9), 2056–2067. doi:10.1080/10428194.2017.1393668
- Golay, J., and Taylor, R. P. (2020). The Role of Complement in the Mechanism of Action of Therapeutic Anti-cancer mAbs. *Antibodies (Basel)* 9 (4), 58. doi:10.3390/antib9040058
- Grosser, R., Cherkassky, L., Chintala, N., and Adusumilli, P. S. (2019). Combination Immunotherapy with CAR T Cells and Checkpoint Blockade for the Treatment of Solid Tumors. *Cancer Cell* 36, 471–482. doi:10.1016/j.ccell.2019.09.006
- Grupp, S. A., Kalos, M., Barrett, D., Aplenc, R., Porter, D. L., Rheingold, S. R., et al. (2013). Chimeric Antigen Receptor-Modified T Cells for Acute Lymphoid Leukemia. *N. Engl. J. Med.* 368, 1509–1518. doi:10.1056/NEJMoa1215134
- Guedan, S., Ruella, M., and June, C. H. (2019). Emerging Cellular Therapies for Cancer. *Annu. Rev. Immunol.* 37, 145–171. doi:10.1146/annurev-immunol-042718-041407
- Gust, J., Taraseviciute, A., and Turtle, C. J. (2018). Neurotoxicity Associated with CD19-Targeted CAR-T Cell Therapies. *CNS Drugs* 32, 1091–1101. doi:10.1007/s40263-018-0582-9
- Haas, A. R., Tanyi, J. L., O'Hara, M. H., Gladney, W. L., Lacey, S. F., Torigan, D. A., et al. (2019). Phase I Study of Lentiviral-Transduced Chimeric Antigen Receptor-Modified T Cells Recognizing Mesothelin in Advanced Solid Cancers. *Mol. Ther.* 27, 1919–1929. doi:10.1016/j.ymthe.2019.07.015
- Han, D., Xu, Z., Zhuang, Y., Ye, Z., and Qian, Q. (2021). Current Progress in CAR-T Cell Therapy for Hematological Malignancies. *J. Cancer* 12, 326–334. doi:10.7150/JCA.48976
- Han, X., Wang, Y., Wei, J., and Han, W. (2019). Multi-antigen-targeted Chimeric Antigen Receptor T Cells for Cancer Therapy. *J. Hematol. Oncol.* 12, 128–137. doi:10.1186/s13045-019-0813-7
- Hansrivijit, P., Gale, R. P., Barrett, J., and Ciurea, S. O. (2019). Cellular Therapy for Acute Myeloid Leukemia - Current Status and Future Prospects. *Blood Rev.* 37, 100578. doi:10.1016/j.blre.2019.05.002
- Hartmann, J., Schüßler-Lenz, M., Bondanza, A., and Buchholz, C. J. (2017). Clinical Development of CAR T Cells-Challenges and Opportunities in Translating Innovative Treatment Concepts. *EMBO Mol. Med.* 9, 1183–1197. doi:10.15252/emmm.201607485
- Hassanpour, S. H., and Dehghani, M. (2017). Review of Cancer from Perspective of Molecular. *J. Cancer Res. Pract.* 4, 127–129. doi:10.1016/j.jcrpr.2017.07.001
- Hay, A. E., and Cheung, M. C. (2019). CAR T-Cells: Costs, Comparisons, and Commentary. *J. Med. Econ.* 22, 613–615. doi:10.1080/13696998.2019.1582059
- Hoffmann, J. M., Schubert, M. L., Wang, L., Hükelhoven, A., Sellner, L., Stock, S., et al. (2017). Differences in Expansion Potential of Naive Chimeric Antigen Receptor T Cells from Healthy Donors and Untreated Chronic Lymphocytic Leukemia Patients. *Front. Immunol.* 8, 1956. doi:10.3389/fimmu.2017.01956
- Hollyman, D., Stefanski, J., Przybylowski, M., Bartido, S., Borquez-Ojeda, O., Taylor, C., et al. (2009). Manufacturing Validation of Biologically Functional T Cells Targeted to CD19 Antigen for Autologous Adoptive Cell Therapy. *J. Immunother.* 32, 169–180. doi:10.1097/CJI.0b013e318194a6e8
- Hombach, A. A., and Abken, H. (2011). Costimulation by Chimeric Antigen Receptors Revisited The T Cell Antitumor Response Benefits From Combined CD28-OX40 Signalling. *Int. J. Cancer* 129 (12), 2935–2944. doi:10.1002/ijc.25960
- Hong, R., Hu, Y., and Huang, H. (2021). Biomarkers for Chimeric Antigen Receptor T Cell Therapy in Acute Lymphoblastic Leukemia: Prospects for Personalized Management and Prognostic Prediction. *Front. Immunol.* 12, 627764. doi:10.3389/fimmu.2021.627764
- Huang, R., Li, X., He, Y., Zhu, W., Gao, L., Liu, Y., et al. (2020). Recent Advances in CAR-T Cell Engineering. *J. Hematol. Oncol.* 13, 86–19. doi:10.1186/s13045-020-00910-5
- Iglesias-López, C., Agustí, A., Obach, M., and Vallano, A. (2019). Regulatory Framework for Advanced Therapy Medicinal Products in Europe and United States. *Front. Pharmacol.* 10, 1–14. doi:10.3389/fphar.2019.00921
- Iragavarapu, C., and Hildebrandt, G. (2021). Lisocabtagene Maraleucel for the Treatment of B-Cell Lymphoma. *Expert Opin. Biol. Ther.* 28, 1–6. doi:10.1080/14712598.2021.1933939
- Itzhaki, O., Jacoby, E., Nissani, A., Levi, M., Nagler, A., Kubi, A., et al. (2020). Head-to-head Comparison of In-House Produced CD19 CAR-T Cell in ALL and NHL Patients. *J. Immunother. Cancer* 8, 1–10. doi:10.1136/jitc-2019-000148
- Jan, M., Scarfò, I., Larson, R. C., Walker, A., Schmidts, A., Guirguis, A. A., et al. (2021). Reversible ON- and OFF-Switch Chimeric Antigen Receptors Controlled by Lenalidomide. *Sci. Transl. Med.* 13, eabb6295. doi:10.1126/scitranslmed.abb6295
- Kaiser, A. D., Assenmacher, M., Schröder, B., Meyer, M., Orentas, R., Bethke, U., et al. (2015). Towards a Commercial Process for the Manufacture of Genetically Modified T Cells for Therapy. *Cancer Gene Ther.* 22, 72–78. doi:10.1038/cgt.2014.78
- Kalos, M., Levine, B. L., Porter, D. L., Katz, S., Grupp, S. A., Bagg, A., et al. (2011). T Cells with Chimeric Antigen Receptors Have Potent Antitumor Effects. *Sci. Transl. Med.* 3, 1–21. doi:10.1126/scitranslmed.3002842
- Karlitepe, A., Ozalp, O., and Avci, C. B. (2015). New Approaches for Cancer Immunotherapy. *Tumour Biol.* 36 (6), 4075–4078. doi:10.1007/s13277-015-3491-2
- Kennedy, M., Awong, G., Sturgeon, C. M., Ditadi, A., LaMotte-Mohs, R., Zúñiga-Pflücker, J. C., et al. (2012). T Lymphocyte Potential Marks the Emergence of Definitive Hematopoietic Progenitors in Human Pluripotent Stem Cell

- Differentiation Cultures. *Cel Rep* 2, 1722–1735. doi:10.1016/j.celrep.2012.11.003
- Köhl, U., Arsenieva, S., Holzinger, A., and Abken, H. (2018). CAR T Cells in Trials: Recent Achievements and Challenges that Remain in the Production of Modified T Cells for Clinical Applications. *Hum. Gene Ther.* 29, 559–568. doi:10.1089/hum.2017.254
- Kolonel, L. N., and Wilkens, L. R. “Migrant Studies,” in *Cancer Epidemiology and Prevention*. Editors D. Schottenfeld and J. F. Fraumeni Jr. 3rd edn. (New York: Oxford University Press), 189–201.
- Korell, F., Laier, S., Sauer, S., Veelken, K., Hennemann, H., Schubert, M. L., et al. (2020). Current Challenges In Providing Good Leukapheresis Products For Anufacturing of CAR-T Cells For Patients With Relapsed/Refractory NHL or ALL. *Cells* 9 (5), 1225. doi:10.3390/cells9051225
- Krause, A., Guo, H. F., Latouche, J. B., Tan, C., Cheung, N. K. V., and Sadelain, M. (1998). Antigen-dependent CD28 Signaling Selectively Enhances Survival and Proliferation in Genetically Modified Activated Human Primary T Lymphocytes. *J. Exp. Med.* 188, 619–626. doi:10.1084/jem.188.4.619
- Lança, T., and Silva-Santos, B. (2012). The Split Nature of Tumor-Infiltrating Leukocytes: Implications for Cancer Surveillance and Immunotherapy. *Oncoimmunology* 1, 717–725. doi:10.4161/onci.20068
- Lee, D. W., Santomasso, B. D., Locke, F. L., Ghobadi, A., Turtle, C. J., Brudno, J. N., et al. (2019). ASTCT Consensus Grading for Cytokine Release Syndrome and Neurologic Toxicity Associated with Immune Effector Cells. *Biol. Blood Marrow Transpl.* 25, 625–638. doi:10.1016/j.bbmt.2018.12.758
- Lester, J. F., Casbard, A. C., Al-Taei, S., Harrop, R., Katona, L., At-tanoos, R. L., et al. (2018). A Single centre Phase II Trial to Assess the Immunological Activity of TroVax® Plus Pemetrexed/cisplatin in Patients with Malignant Pleural Mesothelioma -the SKOPOS Trial. *Oncoimmunology* 7, e1457597. doi:10.1080/2162402x.2018.1457597
- Levine, B. L., Miskin, J., Wonnacott, K., and Keir, C. (2017). Global Manufacturing of CAR T Cell Therapy. *Mol. Ther. Methods Clin. Dev.* 4, 92–101. doi:10.1016/j.omtm.2016.12.006
- Li, J., Li, W., Huang, K., Zhang, Y., Kupfer, G., and Zhao, Q. (2018). Chimeric Antigen Receptor T Cell (CAR-T) Immunotherapy for Solid Tumors: Lessons Learned and Strategies for Moving Forward. *J. Hematol. Oncol.* 11, 22. doi:10.1186/s13045-018-0568-6
- Li, Y., Huo, Y., Yu, L., and Wang, J. (2019). Quality Control and Nonclinical Research on CAR-T Cell Products: General Principles and Key Issues. *Engineering* 5, 122–131. doi:10.1016/j.eng.2018.12.0010.1016/j.eng.2018.12.003
- Ling, H. (2020). Chimeric-antigen Receptor T (CAR-T) Cell Therapy for Solid Tumor. *IOP Conf. Ser. Mater. Sci. Eng.* 768, 052051. doi:10.1088/1757-899X/768/5/052051
- Liu, B., Yan, L., and Zhou, M. (2019). Target Selection of CAR T Cell Therapy in Accordance with the TME for Solid Tumors. *Am. J. Cancer Res.* 9, 228–241. doi:10.1158/2159-8290.cd-rw2019-112
- Lock, D., Mockel-Tenbrinck, N., Drechsel, K., Barth, C., Mauer, D., Schaser, T., et al. (2017). Automated Manufacturing of Potent CD20-Directed Chimeric Antigen Receptor T Cells for Clinical Use. *Hum. Gene Ther.* 28, 914–925. doi:10.1089/hum.2017.111
- Lynn, R. C., Weber, E. W., Sotillo, E., Gennert, D., Xu, P., Good, Z., et al. (2019). c-Jun Overexpression in CAR T Cells Induces Exhaustion Resistance. *Nature* 576, 293–300. doi:10.1038/s41586-019-1805-z
- Marks, P. (2019). The FDA’s Regulatory Framework for Chimeric Antigen Receptor-T Cell Therapies. *Clin. Transl. Sci.* 12, 428–430. doi:10.1111/cts.12666
- Martinez, M., and Moon, E. K. (2019). CAR T Cells for Solid Tumors: New Strategies for Finding, Infiltrating, and Surviving in the Tumor Microenvironment. *Front. Immunol.* 10, 1–21. doi:10.3389/fimmu.2019.00128
- Maude, S. L., Frey, N., Shaw, P. A., Aplenc, R., Barrett, D. M., Bunin, N. J., et al. (2014). Chimeric Antigen Receptor T Cells for Sustained Remissions in Leukemia. *N. Engl. J. Med.* 371 (16), 1507–1517. doi:10.1056/NEJMoa1407222
- Maude, S. L., Laetsch, T. W., Buechner, J., Rives, S., Boyer, M., Bittencourt, H., et al. (2018). Tisagenlecleucel in Children and Young Adults with B-Cell Lymphoblastic Leukemia. *N. Engl. J. Med.* 378, 439–448. doi:10.1056/nejmoa1709866
- Maude, S. L., Laetsch, T. W., Buechner, J., Rives, S., Boyer, M., Bittencourt, H., et al. (2018). Tisagenlecleucel in Children and Young Adults with B-Cell Lymphoblastic Leukemia. *N. Engl. J. Med.* 378 (5), 439–448. doi:10.1056/NEJMoa1709866
- Miao, L., Zhang, Z., Ren, Z., and Li, Y. (2021). Reactions Related to CAR-T Cell Therapy. *Front. Immunol.* 12, 1501. doi:10.3389/fimmu.2021.663201
- Miller, J. (1961). Immunological Function of the Thymus. *The Lancet* 278, 748–749. doi:10.1016/s0140-6736(61)90693-6
- Milone, M. C., Fish, J. D., Carpenito, C., Carroll, R. G., Binder, G. K., June, C. H., et al. (2009). Chimeric Receptors Containing CD137 Signal Transduction Domains Mediate Enhanced Survival of T Cells and Increased Antileukemic Efficacy In Vivo. *Mol. Ther.* 17 (8), 1453–1464. doi:10.1038/mt.2009.83
- Mirzaei, H. R., Mirzaei, H., Namdar, A., Rahmati, M., Till, B. G., and Hadjati, J. (2018). Predictive and Therapeutic Biomarkers in Chimeric Antigen Receptor T-Cell Therapy: A Clinical Perspective. *J. Cel. Physiol.* 234, 5827–5841. doi:10.1002/jcp.27519
- Mirzaei, H. R., Rodriguez, A., Shepphird, J., Brown, C. E., and Badie, B. (2017). Chimeric Antigen Receptors T Cell Therapy in Solid Tumor: Challenges and Clinical Applications. *Front. Immunol.* 8, 1850. doi:10.3389/fimmu.2017.01850
- Monajati, M., Abolmaali, S. S., and Tamaddon, A. (2021). 2020 FDA/EMA Approvals for New Immunotherapy Drug Technologies and Applications. *J. Glob. Trends. Pharm. Sci.* 7 (2), 81–92. doi:10.30476/tips.2021.91207.1097
- Mondal, M., Guo, J., He, P., and Zhou, D. (2020). Recent Advances of Oncolytic Virus in Cancer Therapy. *Hum. Vaccin. Immunother.* 16 (10), 2389–2402. doi:10.1080/21645515.2020.1723363
- Mullard, A. (2017). FDA Approves First CAR T Therapy. *Nat. Rev. Drug Discov.* 16, 669. doi:10.1038/nrd.2017.196
- Munshi, C. N., Anderson, L. D., Shah, N., Madduri, D., Berdeja, J., Lonial, S., et al. (2021). Idecabtagene Vicleucel in Relapsed and Refractory Multiple Myeloma. *N. Engl. J. Med.* 384, 705–716. doi:10.1056/NEJMoa2024850
- Nair, S., Wang, J. B., Tsao, S. T., Liu, Y., Zhu, W., Slayton, W. B., et al. (2019). Functional Improvement of Chimeric Antigen Receptor through Intrinsic interleukin-15Ra Signaling. *Curr. Gene Ther.* 19 (1), 40–53. doi:10.2174/1566523218666181116093857
- Neelapu, S. S., Locke, F. L., Bartlett, N. L., Lekakis, L. J., Miklos, D. B., Jacobson, C. A., et al. (2017). Axicabtagene Ciloleucel CAR T-Cell Therapy in Refractory Large B-Cell Lymphoma. *N. Engl. J. Med.* 377, 2531–2544. doi:10.1056/NEJMoa1707447
- Neelapu, S. S., Tummala, S., Kebriaei, P., Wierda, W., Gutierrez, C., Locke, F. L., et al. (2018). Chimeric Antigen Receptor T-Cell Therapy - Assessment and Management of Toxicities. *Nat. Rev. Clin. Oncol.* 15, 47–62. doi:10.1038/nrclinonc.2017.148
- Neill, L., Rees, J., and Roddie, C. (2020). Neurotoxicity -CAR T-Cell Therapy: What the Neurologist Needs to Know. *Pract. Neurol.* 20, 287–295. doi:10.1136/practneurol-2020-002550
- Nejad, A. S., Noor, T., Munim, Z. H., and Alikhani My Ghaemi, A. (2021). A Bibliometric Review of Oncolytic Virus Research as a Novel Approach for Cancer Therapy. *Virol. J.* 18, 98. doi:10.1186/s12985-021-01571-7
- Nianias, A., and Themeli, M. (2019). Induced Pluripotent Stem Cell (iPSC)-Derived Lymphocytes for Adoptive Cell Immunotherapy: Recent Advances and Challenges. *Curr. Hematol. Malign. Rep.* 14, 261–268. doi:10.1007/s11899-019-00528-6
- Nie, Y., Lu, W., Chen, D., Tu, H., Guo, Z., Zhou, X., et al. (2020). Mechanisms Underlying CD19-Positive ALL Relapse after Anti-CD19 CAR T Cell Therapy and Associated Strategies. *Biomark. Res.* 8, 1–17. doi:10.1186/s40364-020-00197-1
- Nobles, C. L., Sherrill-Mix, S., Everett, J. K., Reddy, S., Fraietta, J. A., Porter, D. L., et al. (2020). CD19-targeting CAR T Cell Immunotherapy Outcomes Correlate with Genomic Modification by Vector Integration. *J. Clin. Invest.* 130, 673–685. doi:10.1172/JCI130144
- Orlando, E. J., Han, X., Tribouley, C., Wood, P. A., Leary, R. J., Riester, M., et al. (2018). Genetic Mechanisms of Target Antigen Loss in CAR19 Therapy of Acute Lymphoblastic Leukemia. *Nat. Med.* 24, 1504–1506. doi:10.1038/s41591-018-0146-z
- Papaioannou, N. E., Beniata, O. V., Vitsos, P., Tsitsilonis, O., and Samara, P. (2016). Harnessing the Immune System to Improve Cancer Therapy. *Ann. Transl. Med.* 4, 261. doi:10.21037/atm.2016.04.01
- Papathanasiou, M. M., Stamatis, C., Lakelin, M., Farid, S., Titchener-Hooker, N., and Shah, N. (2020). Autologous CAR T-Cell Therapies Supply Chain: Challenges and Opportunities? *Cancer Gene Ther.* 27, 799–809. doi:10.1038/s41417-019-0157-z

- Park, J. H., Rivière, I., Gonen, M., Wang, X., Sénéchal, B., Curran, K. J., et al. (2018). Long-Term Follow-Up of CD19 CAR Therapy in Acute Lymphoblastic Leukemia. *N. Engl. J. Med.* 378, 449–459. doi:10.1056/nejmoa1709919
- Parmiani, G., Rivoltini, L., Andreola, G., and Carrabba, M. (2000). Cytokines in Cancer Therapy. *Immunol. Lett.* 74 (1), 41–44. doi:10.1016/S0165-2478(00)00247-9
- Petersen, C. T., and Krenciute, G. (2019). Next Generation CAR T Cells for the Immunotherapy of High-Grade Glioma. *Front. Oncol.* 9, 1–9. doi:10.3389/fonc.2019.00069
- Pont, M. J., Hill, T., Cole, G. O., Abbott, J. J., Kelliher, J., Salter, A. I., et al. (2019). γ -Secretase Inhibition Increases Efficacy of BCMA-specific Chimeric Antigen Receptor T Cells in Multiple Myeloma. *Blood* 134 (19), 1585–1597. doi:10.1182/blood.2019.000050
- Ponterio, E., De Maria, R., and Haas, T. L. (2020). Identification of Targets to Redirect CAR T Cells in Glioblastoma and Colorectal Cancer: An Arduous Venture. *Front. Immunol.* 11, 1–12. doi:10.3389/fimmu.2020.565631
- Poorebrahim, M., Melief, J., Pico de Coaña Y, L., Wickström, S., Cid-Arregui, A., and Kiessling, R. (2020). Counteracting CAR T Cell Dysfunction. *Oncogene* 40, 421–435. doi:10.1038/s41388-020-01501-x
- Porter, D. L., Hwang, W. T., Frey, N. V., Lacey, S. F., Shaw, P. A., Loren, A. W., et al. (2015). Chimeric Antigen Receptor T Cells Persist and Induce Sustained Remissions in Relapsed Refractory Chronic Lymphocytic Leukemia. *Sci. Transl. Med.* 7, 303ra139. doi:10.1126/scitranslmed.aac5415
- Qin, V. M., D'Souza, C., Neeson, P. J., and Zhu, J. J. (2021). Chimeric Antigen Receptor beyond CAR-T Cells. *Cancers (Basel)* 13, 404. doi:10.3390/cancers13030404
- Qiu, Y., Su, M., Liu, L., Tang, Y., Pan, Y., and Sun, J. (2021). Clinical Application of Cytokines in Cancer Immunotherapy. *Drug Des. Devel Ther.* 27 (15), 2269–2287. doi:10.2147/DDDT.S308578
- Rafiq, S., Hackett, C. S., and Brentjens, R. J. (2020). Engineering Strategies to Overcome the Current Roadblocks in CAR T Cell Therapy. *Nat. Rev. Clin. Oncol.* 17, 147–167. doi:10.1038/s41571-019-0297-y
- Ramello, M. C., Benzaid, I., Kuenzi, B. M., Lienlaf-Moreno, M., Kandell, W. M., Santiago, D. N., et al. (2019). An Immunoproteomic Approach to Characterize the CAR Interactome and Signalosome. *Sci. Signal.* 12 (568), eaap9777. doi:10.1126/scisignal.aap9777
- Riegler, L. L., Jones, G. P., and Lee, D. W. (2019). Current Approaches in the Grading and Management of Cytokine Release Syndrome after Chimeric Antigen Receptor T-Cell Therapy. *Ther. Clin. Risk Manag.* 15, 323–335. doi:10.2147/TCRM.S150524
- Roddie, C., O'Reilly, M., Dias Alves Pinto, J., Vispute, K., and Lowdell, M. (2019). Manufacturing Chimeric Antigen Receptor T Cells: Issues and Challenges. *Cytotherapy* 21, 327–340. doi:10.1016/j.jcyt.2018.11.009
- Rodríguez-García, A., Palazon, A., Noguera-Ortega, E., Powell, D. J., and Guedan, S. (2020). CAR-T Cells Hit the Tumor Microenvironment: Strategies to Overcome Tumor Escape. *Front. Immunol.* 11, 1–17. doi:10.3389/fimmu.2020.01109
- Rodríguez-Otero, P., Prósper, F., Alfonso, A., Paiva, B., and San Miguel, J. F. (2020). CAR T-Cells in Multiple Myeloma Are Ready for Prime Time. *J. Clin. Med.* 9 (11), 3577. doi:10.3390/jcm9113577
- Rohaan, M. W., Wilgenhof, S., and Haanen, J. B. A. G. (2019). Adoptive Cellular Therapies: the Current Landscape. *Virchows Arch.* 474 (4), 449–461. doi:10.1007/s00428-018-2484-0
- Roselli, E., Frieling, J. S., Thorner, K., Ramello, M. C., Lynch, C. C., and Abate-Daga, D. (2019). CAR-T Engineering: Optimizing Signal Transduction and Effector Mechanisms. *BioDrugs* 33 (6), 647–659. doi:10.1007/s40259-019-00384-z
- Rosenberg, S. A., Spiess, P., and Lafreniere, R. (1986). A New Approach to the Adoptive Immunotherapy of Cancer with Tumor-Infiltrating Lymphocytes. *Science* 233, 1318–1321. doi:10.1126/science.3489291
- Sadelain, M., Brentjens, R., and Rivière, I. (2009). The Promise and Potential Pitfalls of Chimeric Antigen Receptors. *Curr. Opin. Immunol.* 21, 215–223. doi:10.1016/j.coi.2009.02.009
- Sadelain, M. (1997). Methods for Retrovirus-Mediated Gene Transfer into Primary T-Lymphocytes. *Methods Mol. Med.* 17, 241–248. doi:10.1385/0-89603-484-4:241
- Sadelain, M., and Mulligan, R. C. (1992). *Efficient Transduction of Murine Primary T Lymphocytes in 8th International Congress of Immunology Ed International Congress of Immunology*. Springer-Verlag.
- Sang, W., Zhang, Z., Dai, Y., and Chen, X. (2019). Recent Advances in Nanomaterial-Based Synergistic Combination Cancer Immunotherapy. *Chem. Soc. Rev.* 48, 3771–3810. doi:10.1039/c8cs00896e
- Scarfo, I., Ormhoj, M., Frigault, M. J., Castano, A. P., Lorrey, S., Bouffard, A. A., et al. (2018). Anti-CD37 Chimeric Antigen Receptor T Cells Are Active against B- and T-Cell Lymphomas. *Blood* 132 (14), 1495–1506. doi:10.1182/blood-2018-04-842708
- Scheuermann, R. H., and Racila, E. (1995). CD19 Antigen in Leukemia and Lymphoma Diagnosis and Immunotherapy. *Leuk. Lymphoma* 18, 385–397. doi:10.3109/10428199509059636
- Schumacher, T. N., Kesmir, C., and van Buuren, M. M. (2015). Biomarkers in Cancer Immunotherapy. *Cancer Cell* 27, 12–14. doi:10.1016/j.ccell.2014.12.004
- Schuster, S. J., Bishop, M. R., Tam, C. S., Waller, E. K., Borchmann, P., McGuirk, J. P., et al. (2019). Tisagenlecleucel in Adult Relapsed or Refractory Diffuse Large B-Cell Lymphoma. *N. Engl. J. Med.* 380 (1), 45–56. doi:10.1056/NEJMoa1804980
- Seo, H., Chen, J., Samaniego-castruita, D., Wang, Y. H., López-moyado, I. F., Georges, O., et al. (2019). Correction: TOX and TOX2 Transcription Factors Cooperate with NR4A Transcription Factors to Impose CD8⁺ Tcell Exhaustion. *Proc. Natl. Acad. Sci. U. S. A.* 116, 19761. doi:10.1073/pnas.1914896116
- Shah, N. N., Highfill, S. L., Shalabi, H., Yates, B., Jin, J., Wolters, P. L., et al. (2020b). CD4/CD8 T-Cell Selection Affects Chimeric Antigen Receptor (CAR) T-Cell Potency and Toxicity: Updated Results from a Phase I Anti-CD22 CAR T-Cell Trial. *J. Clin. Oncol.* 38, 1938–1950. doi:10.1200/JCO.19.03279
- Shah, N. N., Johnson, B. D., Schneider, D., Zhu, F., Szabo, A., Keever-Taylor, C. A., et al. (2020a). Bispecific Anti-CD20, Anti-CD19 CAR T Cells for Relapsed B Cell Malignancies: a Phase I Dose Escalation and Expansion Trial. *Nat. Med.* 26 (10), 1569–1575. doi:10.1038/s41591-020-1081-3
- Shen, C., Zhang, Z., and Zhang, Y. (2020). Chimeric Antigen Receptor T Cell Exhaustion during Treatment for Hematological Malignancies. *Biomed. Res. Int.* 2020, 1–9. doi:10.1155/2020/8765028
- Shirasu, N., and Kuroki, M. (2012). Functional Design of Chimeric T-Cell Antigen Receptors for Adoptive Immunotherapy of Cancer: Architecture and Outcomes. *Anticancer Res.* 32 (6), 2377–2383.
- Siegel, R. L., Miller, K. D., and Jemal, A. (2019). Cancer Statistics. *CA Cancer J. Clin.* 69, 7–34. doi:10.3322/caac.21551
- Siegler, E. L., and Kenderian, S. S. (2020). Neurotoxicity and Cytokine Release Syndrome after Chimeric Antigen Receptor T Cell Therapy: Insights into Mechanisms and Novel Therapies. *Front. Immunol.* 11, 1–11. doi:10.3389/fimmu.2020.01973
- Singh, A. K., and McGuirk, J. P. (2020). CAR T Cells: Continuation in a Revolution of Immunotherapy. *Lancet Oncol.* 21, e168–e178. doi:10.1016/S1470-2045(19)30823-X
- Sotillo, E., Barrett, D. M., Black, K. L., Bagashev, A., Oldridge, D., Wu, G., et al. (2015). Convergence of Acquired Mutations and Alternative Splicing of CD19 Enables Resistance to CART-19 Immunotherapy. *Cancer Discov.* 5, 1282–1295. doi:10.1158/2159-8290.CD-15-1020
- Springuel, L., Lonz, C., Alexandre, B., Van Cutsem, E., Machiels, J. P. H., Van Den Eynde, et al. (2019). Chimeric Antigen Receptor-T Cells for Targeting Solid Tumors: Current Challenges and Existing Strategies. *BioDrugs* 33 (5), 515–537. doi:10.1007/s40259-019-00368-z
- Stock, S., Schmitt, M., and Sellner, L. (2019). Optimizing Manufacturing Protocols of Chimeric Antigen Receptor T Cells for Improved Anticancer Immunotherapy. *Int. J. Mol. Sci.* 20 (24), 6223. doi:10.3390/ijms20246223
- Stronck, D. F., Lee, D. W., Ren, J., Sabatino, M., Highfill, S., Khuu, H., et al. (2017). Elutriated Lymphocytes for Manufacturing Chimeric Antigen Receptor T Cells. *J. Transl. Med.* 15, 4–11. doi:10.1186/s12967-017-1160-5
- Swiech, K., Malmegrim, K. C. R., and Picanço-Castro, V. (2020). *Chimeric Antigen Receptor T Cells: Development and Production*. Springer Protocols. doi:10.1007/978-1-0716-0146-4
- Tahmasebi, S., Elahi, R., and Esmaeilzadeh, A. (2019). Solid Tumors Challenges and New Insights of CAR T Cell Engineering. *Stem Cell Rev. Rep.* 15, 619–636. doi:10.1007/s12015-019-09901-7
- Tang, L., Zhang, Y., Hu, Y., and Mei, H. (2021). T Cell Exhaustion and CAR-T Immunotherapy in Hematological Malignancies. *Biomed. Res. Int.* 2021, 1–8. doi:10.1155/2021/6616391

- Tedder, T. F. (2009). CD19: a Promising B Cell Target for Rheumatoid Arthritis. *Nat. Rev. Rheumatol.* 5, 572–577. doi:10.1038/nrrheum.2009.184
- Thomas, E. D., Lochte, H. L., Lu, W. C., and Ferrebee, J. W. (1957). Intravenous Infusion of Bone Marrow in Patients Receiving Radiation and Chemotherapy. *N. Engl. J. Med.* 257, 491–496. doi:10.1056/NEJM195709122571102
- Townsend, M. H., Shrestha, G., Robison, R. A., and O'Neill, K. L. (2018). The Expansion of Targetable Biomarkers for CAR T Cell Therapy. *J. Exp. Clin. Cancer Res.* 37, 1–23. doi:10.1186/s13046-018-0817-0
- Twomey, J. D., and Zhang, B. (2021). Cancer Immunotherapy Update: FDA-Approved Checkpoint Inhibitors and Companion Diagnostics. *AAPS J.* 23 (2), 39. doi:10.1208/s12248-021-00574-0
- U.S. Food and Drug Administrations (2021a). *KYMRIAHA (Tisagenlecleucel)*. Available at: <https://www.fda.gov/vaccines-blood-biologics/cellular-gene-therapy-products/kymriah-tisagenlecleucel>.
- U.S. Food and Drug Administrations (2021b). *Abecma (Idecabtagene Vicleucel)*. Available at: <https://www.fda.gov/news-events/pressannouncements/fdaapproves-first-cell-based-gene-therapy-adult-patients-multiple-myeloma>.
- U.S. Food and Drug Administrations (2021c). *YESCARTA (Axicabtagene Ciloleucel)*. Available at: <https://www.fda.gov/vaccines-blood-biologics/cellular-gene-therapy-products/yescarta-axicabtagene-ciloleucel>.
- Van der Stegen, S. J., Hamieh, M., and Sadelain, M. (2015). The Pharmacology of Second-Generation Chimeric Antigen Receptors. *Nat. Rev. Drug Discov.* 14 (7), 499–509. doi:10.1038/nrd4597
- Varadé, J., Magadán, S., and González-Fernández, Á. (2021). Human Immunology and Immunotherapy: Main Achievements and Challenges. *Cell. Mol. Immunol.* 18, 805–828. doi:10.1038/s41423-020-00530-6
- Ventola, C. L. (2017). Cancer Immunotherapy, Part 3: Challenges and Future Trends. *P T.* 42 (8), 514–521. doi:10.1007/978-3-319-17900-1_176
- Waldmann, T. A. (2003). Immunotherapy: Past, Present and Future. *Nat. Med.* 9, 269–277. doi:10.1038/nm0303-269
- Wang, K., Wei, G., and Liu, D. (2012). CD19: a Biomarker for B Cell Development, Lymphoma Diagnosis and Therapy. *Exp. Hematol. Oncol.* 1, 1–7. doi:10.1186/2162-3619-1-36
- Wang, M., Pruteanu, I., Cohen, A. D., Garfall, A. L., Milone, M. C., Tian, L., et al. (2019). Identification and Validation of Predictive Biomarkers to CD19- and BCMA-specific CAR T-Cell Responses in CAR T-Cell Precursors. *Blood* 134, 622. doi:10.1182/blood-2019-122513
- Wang, X., and Rivière, I. (2016). Clinical Manufacturing of CAR T Cells: Foundation of a Promising Therapy. *Mol. Ther. Oncolytics.* 3, 16015. doi:10.1038/mto.2016.15
- Wang, Z., Wu, Z., Liu, Y., and Han, W. (2017). New Development in CAR-T Cell Therapy. *J. Hematol. Oncol.* 10, 1–11. doi:10.1186/s13045-017-0423-1
- Wei, J., Han, X., Bo, J., and Han, W. (2019). Target Selection for CAR-T Therapy. *J. Hematol. Oncol.* 12, 1–9. doi:10.1186/s13045-019-0758-x
- Wherry, E. J. (2011). T Cell Exhaustion. *Nat. Immunol.* 12, 492–499. doi:10.1038/ni.2035
- Xie, G., Dong, H., Liang, Y., Ham, J. D., Rizwan, R., and Chen, J. (2020). CAR-NK Cells: A Promising Cellular Immunotherapy for Cancer. *EBioMedicine* 59, 102975. doi:10.1016/j.ebiom.2020.102975
- Xu, X., Sun, Q., Liang, X., Chen, Z., Zhang, X., Zhou, X., et al. (2019). Mechanisms of Relapse after CD19 CAR T-Cell Therapy for Acute Lymphoblastic Leukemia and its Prevention and Treatment Strategies. *Front. Immunol.* 10, 1–15. doi:10.3389/fimmu.2019.02664
- Yadav, R. K., Ali, A., Kumar, S., Sharma, A., Baghchi, B., Singh, P., et al. (2020). CAR T Cell Therapy: Newer Approaches to Counter Resistance and Cost. *Heliyon* 6, e03779. doi:10.1016/j.heliyon.2020.e03779
- Yakoub-Agha, I., Chabannon, C., Bader, P., Basak, G. W., Bonig, H., Ciceri, F., et al. (2020). Management of Adults and Children Undergoing Chimeric Antigen Receptor T-Cell Therapy: Best Practice Recommendations of the European Society for Blood and Marrow Transplantation (EBMT) and the Joint Accreditation Committee of ISCT and EBMT (JACIE). *Haematologica* 105, 297–316. doi:10.3324/haematol.2019.229781
- Yazdanifar, M., Barbarito, G., Bertaina, A., and Airolidi, I. (2020). F8 T Cells: The Ideal Tool for Cancer Immunotherapy. *Cells* 9, 1–26. doi:10.3390/cells9051305
- Yu, S., Yi, M., Qin, S., and Wu, K. (2019). Next Generation Chimeric Antigen Receptor T Cells: Safety Strategies to Overcome Toxicity. *Mol. Cancer* 18, 125–137. doi:10.1186/s12943-019-1057-4
- Zah, E., Lin, M. Y., Anne, S. B., Jensen, M. C., and Chen, Y. Y. (2016). T Cells Expressing CD19/CD20 Bispecific Chimeric Antigen Receptors Prevent Antigen Escape by Malignant B Cells. *Cancer Immunol. Res.* 4, 498–508. doi:10.1158/2326-6066.CIR-15-0231
- Zahavi, D., and Weiner, L. (2020). Monoclonal Antibodies in Cancer Therapy. *Antibodies* 9, 34. doi:10.3390/antib9030034
- Zeng, J., Tang, S. Y., Toh, L. L., and Wang, S. (2017). Generation of “Off-The-Shelf” Natural Killer Cells from Peripheral Blood Cell-Derived Induced Pluripotent Stem Cells. *Stem Cell Rep.* 9, 1796–1812. doi:10.1016/j.stemcr.2017.10.020
- Zhang, Y., Zhang, W., Dai, H., Wang, Y., Shi, F., Wang, C., et al. (2016). An Analytical Biomarker for Treatment of Patients with Recurrent B-ALL after Remission Induced by Infusion of Anti-CD19 Chimeric Antigen Receptor T (CAR-T) Cells. *Sci. China Life Sci.* 59, 379–385. doi:10.1007/s11427-016-5035-4
- Zhao, Z., Xiao, X., Saw, P. E., Wu, W., Huang, H., Chen, J., et al. (2020). Chimeric Antigen Receptor T Cells in Solid Tumors: a War against the Tumor Microenvironment. *Sci. China Life Sci.* 63, 180–205. doi:10.1007/s11427-019-9665-8

Conflict of Interest: The authors declare that the research was conducted in the absence of any commercial or financial relationships that could be construed as a potential conflict of interest.

Publisher's Note: All claims expressed in this article are solely those of the authors and do not necessarily represent those of their affiliated organizations, or those of the publisher, the editors and the reviewers. Any product that may be evaluated in this article, or claim that may be made by its manufacturer, is not guaranteed or endorsed by the publisher.

Copyright © 2021 Hernández-López, Téllez-González, Mondragón-Terán and Meneses-Acosta. This is an open-access article distributed under the terms of the Creative Commons Attribution License (CC BY). The use, distribution or reproduction in other forums is permitted, provided the original author(s) and the copyright owner(s) are credited and that the original publication in this journal is cited, in accordance with accepted academic practice. No use, distribution or reproduction is permitted which does not comply with these terms.



Immune Checkpoint Inhibitor–Associated Tumor Lysis Syndrome: A Real-World Pharmacovigilance Study

Li Wang^{1†}, Xiaolin Li^{2,3}, Bin Zhao^{2*†}, Dan Mei², Jiandong Jiang³ and Jingli Duan¹

OPEN ACCESS

Edited by:

Sandeep Mittal,
The University of Texas MD Anderson
Cancer Center, United States

Reviewed by:

Aloukick Kumar Singh,
University of Texas MD Anderson
Cancer Center, United States
Ajay Sharma,
University of Texas Health Science
Center at Houston, United States
Yuan Tang,
University of Toledo, United States
Sreejoyee Ghosh,
University of Texas MD Anderson
Cancer Center, United States

*Correspondence:

Bin Zhao
zhaobin@pumch.cn

†ORCID:

Li Wang
orcid.org/0000-0002-6253-9453
Bin Zhao
orcid.org/0000-0001-8555-523X

Specialty section:

This article was submitted to
Pharmacology of Anti-Cancer Drugs,
a section of the journal
Frontiers in Pharmacology

Received: 11 March 2021

Accepted: 04 August 2021

Published: 23 September 2021

Citation:

Wang L, Li X, Zhao B, Mei D, Jiang J
and Duan J (2021) Immune
Checkpoint Inhibitor–Associated
Tumor Lysis Syndrome: A Real-World
Pharmacovigilance Study.
Front. Pharmacol. 12:679207.
doi: 10.3389/fphar.2021.679207

Introduction: Immune checkpoint inhibitors (ICIs) have substantially improved the clinical outcomes of various malignancies. However, the adverse event of tumor lysis syndrome (TLS) has not been included in the National Comprehensive Cancer Network guidelines or drug inserts. In this study, we aimed to establish the relationship between ICI therapies and TLS events using data from a real-world pharmacovigilance database.

Methods: The MedDRA terms of TLS and both generic and brand names of ICIs were retrieved from the FDA Adverse Event Reporting System. Four frequentist algorithms were employed to confirm the association between the TLS and the ICI regimens, involving anti-cytotoxic T lymphocyte antigen-4 (anti-CTLA-4), anti-programmed death receptor-1 (PD-1)/programmed cell death 1 ligand 1 (PD-L1), and anti-(CTLA-4 + PD-1). A descriptive and statistical analysis was performed according to the case information.

Results: One hundred sixty-four TLS cases, where patients underwent anti-CTLA-4 ($n = 14$), anti-(PD-1)/(PD-L1) ($n = 113$), or anti-(CTLA-4 + PD-1) ($n = 37$) therapies, were collected between the first quarter of 2004 and the fourth quarter of 2020. The most coverage-reporting year, age-group, sex, reporter, region, country, and indication were 2020 ($n = 62$), 60–74 years ($n = 65$), males ($n = 105$), physician ($n = 66$), Asia ($n = 80$), Japan ($n = 67$), and lung and thymus malignancies ($n = 40$), respectively. The median TLS onset time associated with anti-CTLA-4, anti-(PD-1)/(PD-L1), and anti-(CTLA-4 + PD-1) therapies was 6 (IQR: 2–39.5), 9 (IQR: 2–40), and 20 (IQR: 7.5–37.75) days, respectively. Mortality distribution of 71 reported death outcomes among three groups was statistically significant. All four algorithm signal values of anti-(CTLA-4 + PD-1) were higher than those of anti-CTLA-4 and anti-(PD-1)/(PD-L1).

Conclusion: Elderly male patients with lung and thymus malignancies are frequently predisposed to TLS. ICI therapies could induce TLS in both solid and hematological malignancies. The rapid onset time and poor outcomes of patients prompt caution from health-care professionals.

Keywords: immune checkpoint inhibitor, tumor lysis syndrome, cytotoxic T lymphocyte antigen-4, programmed death receptor-1, programmed cell death 1 ligand 1, pharmacovigilance

INTRODUCTION

By blocking cytotoxic T-lymphocyte antigen-4 (CTLA-4) or targeting the programmed death receptor-1 (PD-1)/programmed cell death 1 ligand 1 (PD-L1) pathway, immune checkpoint inhibitors (ICIs) have transformed the treatment landscape for a range of neoplasms (Hodi et al., 2010; Borghaei et al., 2015; Brahmer et al., 2015; Le et al., 2015; Reck et al., 2016; Rittmeyer et al., 2017). Since their introduction, both mono- and combined ICI regimens have substantially improved outcomes in patients with solid and hematologic malignancies.

Tumor lysis syndrome (TLS) is a life-threatening condition that can occur when massive malignant cells die and break down quickly, releasing large amounts of nucleic acids, phosphate, potassium, and cytokines into the circulatory system either spontaneously or in response to treatment (Cairo et al., 2010; Howard et al., 2011). According to the Cairo–Bishop classification criteria, laboratory TLS requires two or more metabolic disorders such as hyperuricemia, hyperkalemia, hyperphosphatemia, and hypocalcemia to occur during the same 24-h period within 3 days before the initiation of therapy or up to 7 days thereafter. Clinical TLS is defined as the presence of laboratory TLS along with an increased creatinine level, seizures, or cardiac arrhythmia/sudden cardiac death (Cairo and Bishop, 2004).

The Food and Drug Administration (FDA) Adverse Event Reporting System (FAERS) is a spontaneous reporting system (SRS) database that contains adverse event reports, medication error reports, and product quality complaints. Post-marketing pharmacovigilance is often used to depict the surveillance activities. Data mining algorithms based on disproportionality analysis could assist experts in predicting adverse events of drugs and therapeutic biologic products.

Various immune-related adverse events can occur during treatment with ICIs according to the tumor type, and they commonly involve the gastrointestinal tract, endocrine glands, skin, and liver (Postow et al., 2018). To the best of our knowledge, there are no peer-reviewed pharmacovigilance studies of ICI-induced TLS to date and their possible relationship is not mentioned in the National Comprehensive Cancer Network guidelines (Thompson et al., 2020) or the package inserts (ASTRAZENECA_UK_LTD; BRISTOL_MYERS_SQUIBBa; BRISTOL_MYERS_SQUIBBb; EMD_SERONO_INC; GENENTECH_INC; MERCK_SHARP_DOHME; REGENERON_PHARMACEUTICALS). Therefore, the aim of the present study was to establish the relationship between ICI regimens and TLS adverse events using data from the FAERS database.

METHODS

Data Mapping

Institutional review board approval for the present study was not required as the FAERS database is accessible to the public. The Medical Dictionary for Regulatory Activities (MedDRA) is the international medical coding system developed under the

auspices of the International Council for Harmonisation of Technical Requirements for Pharmaceuticals for Human Use (ICH). “Tumour lysis syndrome” [20000219] is a standardized MedDRA Query (SMQ), which comprises three preferred terms (PTs) “hemorrhagic tumour necrosis” [10054096], “tumour lysis syndrome” [10045170], and “tumour necrosis” [10054094].

The FDA-approved generic (and brand names) of ICIs are ipilimumab (Yervoy®), nivolumab (Opdivo®), pembrolizumab (Keytruda®), cemiplimab (Libtayo®), atezolizumab (Tecentriq®), avelumab (Bavencio®), and durvalumab (Imfinzi®). These ICIs were grouped into “anti-CTLA-4” (ipilimumab only), “anti-(PD-1)/(PD-L1)” (monotherapy of nivolumab, pembrolizumab, cemiplimab, atezolizumab, avelumab, and durvalumab), and “anti-(CTLA-4+PD-1)” (combined therapy of ipilimumab and nivolumab only) in this study. The FDA-approved labels of the seven drugs were downloaded on January 26, 2021, and the latest revised indications were clustered according to the World Health Organization (WHO) classification of tumors.

All four adverse event terms and 14 ICI names were retrieved from the FAERS database. The FAERS allows the output of seven data categories, namely, demographic and administrative, drug information, adverse events, patient outcomes, report source, start and end dates of therapies, and therapeutic indications.

Signal Detection

Based on disproportionality analysis, the frequentist algorithms, including reporting odds ratio (ROR) and proportional reporting ratio (PRR), and the Bayesian algorithms, comprising Bayesian confidence propagation neural network (BCPNN) and multi-item gamma Poisson shrinker (MGPS), were employed to calculate the association between the use of ICIs and cases of TLS (van Puijenbroek et al., 2002; Hauben et al., 2005; Matsushita et al., 2007). Notably, the corresponding signal score metrics are expressed as confidence interval (CI), chi-squared (χ^2) test value, information component (IC), the lower limit of the 95% two-sided CI of the IC (IC025), empiric Bayes geometric mean (EBGM), and the lower 90% one-sided CI of EBGM (EB05) (Chen et al., 2020).

Based on the 2×2 contingency table, a represents reports of the suspected drugs with the adverse drug reaction (ADR) of interest, b represents reports of the suspected drugs without the ADR of interest, c represents reports of other drugs with the ADR of interest, and d represents reports of neither the suspected drugs nor the ADRs of interest. The formulae and criteria of four algorithms for signal detection are given in **Table 1** (Hauben, 2003; Hauben et al., 2005).

Statistical Analysis

A descriptive analysis was conducted to summarize the characteristic of TLS in patients receiving treatment with ICIs. For this, first, patients aged between 30 and 90 years were divided into 15-year groups (30–44 years, 45–59 years, 60–74 years, and 75–90 years), whereas those younger than 30 years or older than 90 years composed the other two groups. Second, the onset time was calculated and compared as the interval days between the start of ICI therapy and the onset of an adverse event; 10-day groups from 0 to 70 days after

TABLE 1 | Formulae and criteria of four algorithms for signal detection.

Algorithm	Formula	Criteria
ROR	$ROR = \frac{(a/c)}{(b/d)}, 95\%CI = e^{\frac{\ln(ROR) \pm 1.96 \sqrt{\left(\frac{1}{a} + \frac{1}{b} + \frac{1}{c} + \frac{1}{d}\right)}}{}}$	95% CI > 1, N ≥ 2
PRR	$PRR = \frac{a/(a+b)}{c/(c+d)}, \chi^2 = \sum \frac{(a-E)^2}{E}, E = \frac{(a+b)(a+c)}{(a+b+c+d)}$	PRR ≥ 2, $\chi^2 \geq 4$, N ≥ 3
BCPNN	$IC = \log_2 \frac{a(a+b+c+d)}{(a+c)(a+b)}, IC025 = e^{\frac{\ln(IC) - 1.96 \sqrt{\left(\frac{1}{a} + \frac{1}{b} + \frac{1}{c} + \frac{1}{d}\right)}}{}}$	IC025 > 0
MGPS	$EBGM = \frac{a(a+b+c+d)}{(a+c)(a+b)}, EB05 = e^{\frac{\ln(EBGM) - 1.64 \sqrt{\left(\frac{1}{a} + \frac{1}{b} + \frac{1}{c} + \frac{1}{d}\right)}}{}}$	EB05 ≥ 2, N > 0

ROR, reporting odds ratio; PRR, proportional reporting ratio; BCPNN, Bayesian confidence propagation neural network; MGPS, multi-item gamma Poisson shrinker; CI, confidence interval; χ^2 , chi-squared; IC, information component; IC025, the lower limit of the 95% two-sided CI of the IC; EBGM, empirical Bayesian geometric mean; EB05, the lower 90% one-sided CI of EBGM; N, number of cases.

TABLE 2 | Summary of immune checkpoint inhibitor indications.

	Tissue or system	Indications	Ipilimumab	Nivolumab	Pembrolizumab	Cemiplimab	Atezolizumab	Avelumab	Durvalumab
1	Hematopoietic and lymphoid	Classical Hodgkin lymphoma	-	6	5	-	-	-	-
		Primary mediastinal large B-cell lymphoma	-	-	6	-	-	-	-
2	Lung and thymus	Non-small-cell lung cancer	5 ^a	2 ^a	2	-	2	-	2
		Small-cell lung cancer	-	3	3	-	4	-	3
		Malignant pleural mesothelioma	6 ^a	4 ^a	-	-	-	-	-
3	Skin	Melanoma	1	1 ^a	1	-	6	-	-
		Merkel cell carcinoma	-	-	14	-	-	1	-
		Cutaneous squamous cell carcinoma	-	-	18	1	-	-	-
4	Genitourinary	Renal cell carcinoma	2 ^a	5 ^a	15	-	-	3	-
		Urothelial carcinoma	-	8	7	-	1	2	1
5	Gastroenteric and hepatic	Esophageal squamous cell carcinoma	-	11	11	-	-	-	-
		MSI-H or dMMR colorectal cancer	3 ^a	9 ^a	9	-	-	-	-
		Gastric cancer	-	-	10	-	-	-	-
		Hepatocellular carcinoma	4 ^a	10 ^a	13	-	5	-	-
6	Head and neck	Squamous cell carcinoma	-	7	4	-	-	-	-
7	Uterine	Cervical cancer	-	-	12	-	-	-	-
		Endometrial carcinoma	-	-	16	-	-	-	-
8	Breast	Triple-negative breast cancer	-	-	19	-	3	-	-
9	Non-specific	MSI-H or dMMR cancer	-	-	8	-	-	-	-
		Tumor mutational burden-high cancer	-	-	17	-	-	-	-

MSI-H or dMMR, microsatellite instability-high or mismatch repair deficient;

^arepresents the combined therapy of ipilimumab and nivolumab; -, not covered.

the onset of adverse events were established, and patients with the onset of adverse events more than 70 days after ICI administration were grouped together. Third, the outcomes considered were death, initial or prolonged hospitalization, life-threatening events, and other serious medical events according to the FAERS database. Additionally, the non-parametric Kruskal–Wallis test was used to compare the presence of TLS in different ICI subgroups. Data mining and statistical analysis were performed using SAS software 9.4 (SAS Inc., Cary, NC, United States).

RESULTS

All FDA-approved indications of the seven drugs are illustrated in **Table 2**. Pembrolizumab had 19 indications, covering eight main tissues or systems in the context of both hematology and solid oncology. The combined therapy of ipilimumab and nivolumab is marked with an a.

We identified 164 TLS cases among individuals receiving treatment with ICIs in the FAERS database, covering 5,709 individual TLS cases and 88,620 adverse events in individuals

TABLE 3 | Demographic and Clinical Characteristics of TLS in patients receiving treatment with ICIs.

	Anti-CTLA-4	Anti-(PD-1)/(PD-L1)	Anti-(CTLA-4+PD-1)	N (%)
Reporting year (N = 164)				
Before 2015	8	0	1	9 (5.49)
2015	2	10	1	13 (7.93)
2016	1	7	1	9 (5.49)
2017	1	15	1	17 (10.37)
2018	0	20	6	26 (15.85)
2019	0	19	9	28 (17.07)
2020	2	42	18	62 (37.80)
Age, years (N = 164)				
<18	0	0	1	1 (0.61)
30–44	2	8	4	14 (8.54)
45–59	1	16	13	30 (18.29)
60–74	9	48	8	65 (39.63)
75–90	2	15	6	23 (14.02)
Unknown	0	26	5	31 (18.90)
Sex (N = 164)				
Female	5	30	7	42 (25.61)
Male	9	69	27	105 (64.02)
Unknown	0	14	3	17 (10.37)
Reporter (N = 164)				
Physician	3	44	19	66 (40.24)
Pharmacist	2	5	4	11 (6.71)
Other health professional	4	21	7	32 (19.51)
Consumer	4	27	3	34 (20.73)
Unknown	1	16	4	21 (12.80)
Region (N = 164)				
Asia	4	55	21	80 (48.78)
Europe	5	22	3	30 (18.29)
North America	4	32	13	49 (29.88)
Oceania	0	2	0	2 (1.22)
South America	1	2	0	3 (1.83)
Country (n = 164)				
Argentina	0	2	0	2 (1.22)
Australia	0	2	0	2 (1.22)
Austria	0	1	0	1 (0.61)
Belgium	0	2	0	2 (1.22)
Canada	0	2	1	3 (1.83)
China	0	7	1	8 (4.88)
France	1	7	1	9 (5.49)
Germany	2	5	2	9 (5.49)
Greece	0	1	0	1 (0.61)
Israel	0	1	0	1 (0.61)
Japan	3	44	20	67 (40.85)
Mexico	0	0	1	1 (0.61)
The Philippines	0	1	0	1 (0.61)
Poland	0	1	0	1 (0.61)
Portugal	1	0	0	1 (0.61)
Spain	0	3	0	3 (1.83)
Thailand	0	2	0	2 (1.22)
Turkey	1	0	0	1 (0.61)
Ukraine	0	1	0	1 (0.61)
The United Kingdom	1	1	0	2 (1.22)
The United States	4	29	11	45 (26.83)
Venezuela	1	0	0	1 (0.61)
Indication (N = 162)				
Hematopoietic and lymphoid tissues	1	12	0	13 (8.02)
Lung and thymus	0	39	1	40 (24.69)
Skin	13	9	13	35 (21.60)
Genitourinary	0	12	11	23 (14.20)
Gastroenterologic and hepatic	0	11	1	12 (7.41)
Unknown	0	6	3	9 (5.56)
Head and neck	0	6	1	7 (4.32)
Soft tissue	0	2	3	5 (3.09)
Gastrointestinal and hepatocellular	0	3	1	4 (2.47)

(Continued on following page)

TABLE 3 | (Continued) Demographic and Clinical Characteristics of TLS in patients receiving treatment with ICIs.

	Anti-CTLA-4	Anti-(PD-1)/(PD-L1)	Anti-(CTLA-4+PD-1)	N (%)
Uterine	0	5	0	5 (3.09)
Unspecific	0	3	1	4 (2.47)
Central nervous system	0	1	2	3 (1.85)
Breast	0	1	0	1 (0.62)
Central nervous system	0	1	0	1 (0.62)
Onset time (days) (N = 81)				
0–10	5	28	7	40 (49.38)
11–20	1	4	4	9 (11.11)
21–30	0	4	4	8 (9.88)
31–40	0	4	2	6 (7.41)
41–50	1	0	2	3 (3.70)
51–60	0	5	2	7 (8.64)
61–70	0	2	1	3 (3.70)
>70	1	4	0	5 (6.17)
Outcome (N = 163)				
Death	13	47	11	71 (43.56)
Hospitalization – initial or prolonged	1	30	16	47 (28.83)
Life-threatening	0	6	2	8 (4.91)
Other serious (important medical event)	0	29	8	37 (22.70)

CTLA-4, cytotoxic T lymphocyte antigen-4; PD-1, programmed death receptor-1; PD-L1, programmed cell death 1 ligand 1; N (%), number of cases (percentage).

receiving treatment with ICIs reported between the first quarter of 2004 and the fourth quarter of 2020. The demographic and clinical profiles of the sample population are summarized in **Table 3**.

From the sample population, anti-CTLA-4, anti-(PD-1)/(PD-L1), and anti-(CTLA-4+PD-1) therapies were administered to 14, 113, and 37 cases, respectively. In the anti-(PD-1)/(PD-L1) group, nivolumab monotherapy was used in most cases ($n = 55$), followed by pembrolizumab ($n = 34$), atezolizumab ($n = 17$), avelumab ($n = 3$), durvalumab ($n = 2$), and cemiplimab ($n = 2$).

Annually, the number of ICI-induced TLS cases has increased gradually, with the most cases reported in 2020 ($n = 62$). Most cases involved individuals aged 60–74 years ($n = 65$). Male individuals ($n = 105$) were more vulnerable than female individuals ($n = 42$), with a mean age of 62.16 ± 16.30 years in male individuals and 62.15 ± 12.72 years in female individuals. Most of the reports indicated that physicians oversaw patient management ($n = 66$). Most cases were from Asia ($n = 80$) in terms of region and Japan ($n = 67$) in terms of country. TLS was reported in 149 cases of solid malignancies and 13 hematologic neoplasms. The top three malignancies were all solid tumors, including lung and thymus cancer ($n = 40$), melanoma ($n = 35$), and renal cell and urothelial carcinoma ($n = 23$).

After excluding records with incorrect entries, 81 cases with TLS onset time were analyzed. The median onset time of TLS in patients on anti-CTLA-4 therapy was 6 (interquartile range [IQR]: 2–39.5) days. The median onset time associated with anti-(PD-1)/(PD-L1) and anti-(CTLA-4 + PD-1) therapies was 9 (IQR: 2–40) and 20 (IQR: 7.5–37.75) days, respectively. There was no significant difference in the onset time among the three groups. Most cases had an onset time of 0–10 days ($n = 40$)—anti-CTLA-4 ($n = 5$), anti-(PD-1)/(PD-L1) ($n = 28$), and anti-(CTLA-4 + PD-1) ($n = 7$) cases.

In total, patient outcomes included death ($n = 71$), initial or prolonged hospitalization ($n = 47$), life-threatening events ($n = 8$),

and other serious medical events ($n = 37$). The distribution of mortality among the three groups was significantly different ($\chi^2 = 18.655$, $p < 0.001$). Among these groups, the fatality rate of patients in the anti-CTLA-4 (92.9%) group was significantly higher than that in the anti-(PD-1)/(PD-L1) group (42.0%), ($\chi^2 = 15.928$, $p < 0.001$) and the anti-(CTLA-4 + PD-1) group (29.7%) ($\chi^2 = 14.823$, $p < 0.001$).

As shown in **Table 4**, based on the criteria for signal detection in each of the four algorithms, anti-CTLA-4, anti-(PD-1)/(PD-L1), and anti-(CTLA-4 + PD-1) therapies were identified. The signal values of combined therapy were higher than those of monotherapies, with an ROR of 6.80 (95% CI: 4.92–9.40), a PRR of 6.78 ($\chi^2 = 181.27$), an IC of 2.75 (IC025 = 1.99), and an EBGM of 6.74 (EB05 = 5.14).

DISCUSSION

To the best of our knowledge, this is the first study to comprehensively evaluate TLS in individuals receiving ICI treatment using data from real-world practice. The present frequentist analysis included the ROR and PRR, which have been utilized by the health authorities outside the United States, whereas the Bayesian analysis included the BCPNN and MGPS, which have been adopted by the WHO Uppsala Monitoring Centre and FAERS (Hauben et al., 2005). Compared with the performance using the receiver operating characteristic curve, area under the curve, and Youden's index, which optimize the sensitivity and specificity levels, the Bayesian approach is superior to the frequentist approach in disproportionality analysis algorithms. The values of Youden's sensitivity, specificity, and index of the four algorithms were as follows: BCPNN, 0.6549, 0.6847, and 0.3396; GPS, 0.6637, 0.6306, and 0.2943; ROR, 0.6549, 0.6577, and 0.3125; and PRR, 0.7080, 0.5856, and 0.2936, respectively (Pham et al., 2019). All four

TABLE 4 | Detected signals of TLS related to ICIs by four algorithms.

Regimen	N	ROR (95%two-sided CI)	PRR (χ^2)	IC (IC025)	EBGM (EB05)
Anti-CTLA-4	14	3.33 (1.97–5.63)	3.33 (22.75)	1.73 (1.02)	3.32 (2.14)
Anti-(PD-1)/(PD-L1)	113	3.92 (3.26–4.73)	3.92 (240.96)	1.95 (1.62)	3.86 (3.30)
Anti-(CTLA-4+PD-1)	37	6.80 (4.92–9.40)	6.78 (181.27)	2.75 (1.99)	6.74 (5.14)

CTLA-4, cytotoxic T lymphocyte antigen-4; PD-1, programmed death receptor-1; PD-L1, programmed cell death 1 ligand 1; N, number of cases; ROR, reporting odds ratio; CI, confidence interval; PRR, proportional reporting ratio; χ^2 , chi-squared; IC, information component; IC025, the lower limit of the 95% two-sided CI of the IC; EBGM, empirical Bayesian geometric mean; EB05, the lower 90% one-sided CI of EBGM.

signal detection algorithms showed that TLS was significantly more frequent in individuals receiving treatment with ICIs than in those not treated with ICIs, whereas individuals receiving the combination therapy of ipilimumab and nivolumab had the highest reports of TLS.

Although the precise mechanism of how ICIs lead to cell lysis remains unclear, administering humanized or fully human ICI monoclonal antibodies may activate an immune response leading to serious and even fatal complications in multiple organs. Among the cellular contents and metabolites released when neoplasm cells lyse, uric acid can induce nephrotoxicity by intrarenal crystallization, renal vasoconstriction, impaired autoregulation, decreased renal blood flow, oxidation, and inflammation; potassium can cause fatal cardiac arrhythmias and secondary hypocalcemia, leading to neuromuscular irritability, dysrhythmia, and seizure; calcium phosphate crystals may precipitate in various organs; and cytokines may cause systemic inflammatory response syndrome and multiorgan failure (Howard et al., 2011). Whether the onset of TLS is associated with the efficacy of ICI therapy or the spontaneous progression of various primary or metastasis neoplasm types remains unclear (Das and Johnson, 2019).

Patients can be classified as those having a high risk (HR), intermediate risk (IR), or low risk (LR) of developing TLS based on three sequential phases (Cairo et al., 2010). First, the diagnosis of laboratory TLS is defined based on any two or more serum values of uric acid ($\geq 476 \mu\text{mol/L}$ or 25% increase from baseline), potassium ($\geq 6.0 \text{ mmol/L}$ or 25% increase from baseline), phosphate ($\geq 2.1 \text{ mmol/L}$ for children/ $\geq 1.45 \text{ mmol/L}$ for adults or 25% increase from baseline), and calcium ($\leq 1.75 \text{ mmol/L}$ or 25% decrease from baseline) within 3 days before or 7 days after the initiation of chemotherapy. Second, the stratification of high-risk disease (HRD), intermediate-risk disease (IRD), and low-risk disease (LRD) according to tumor type, age of the patients, tumor stage, bulk disease, white blood cell (WBC) count, and lactate dehydrogenase (LDH) levels (Cairo and Bishop, 2004).

1) HRD: Burkitt lymphoma/leukemia; acute lymphoblastic leukemia (ALL) with $\text{WBC} \geq 100 \times 10^9/\text{L}$; ALL with $\text{WBC} < 100 \times 10^9/\text{L}$ and $\text{LDH} \geq 2 \times$ upper limit of normal (ULN); acute myeloid leukemia (AML) with $\text{WBC} \geq 100 \times 10^9/\text{L}$; lymphoblastic lymphoma in an advanced stage; lymphoblastic lymphoma in an early stage with $\text{LDH} \geq 2 \times \text{ULN}$; adult T-cell/diffuse large B-cell/peripheral T-cell/transformed/mantle cell lymphoma of children in stage III/IV with $\text{LDH} \geq 2 \times \text{ULN}$; and adult T-cell/diffuse large B-cell/peripheral T-cell/transformed/mantle cell lymphoma of adult with $\text{LDH} > \text{ULN}$ and bulky.

2) IRD: bulky, solid tumors, sensitive to chemotherapy including neuroblastomas, germ cell tumors, and small-cell lung cancer; chronic lymphocytic leukemia-targeted and/or biological therapies; ALL with $\text{WBC} < 100 \times 10^9/\text{L}$ and $\text{LDH} < 2 \times \text{ULN}$; AML with $\text{WBC} \geq 25 \times 10^9/\text{L}$ and $< 100 \times 10^9/\text{L}$; AML with $\text{WBC} < 25 \times 10^9/\text{L}$ and $\text{LDH} \geq 2 \times \text{ULN}$; lymphoblastic lymphoma in an early stage and $\text{LDH} < 2 \times \text{ULN}$; adult T-cell/diffuse large B-cell/peripheral T-cell/transformed/mantle cell lymphoma of children in stage III/IV and $\text{LDH} < 2 \times \text{ULN}$; adult T-cell/diffuse large B-cell/peripheral T-cell/transformed/mantle cell lymphoma of adult with $\text{LDH} > \text{ULN}$ and non-bulky; and anaplastic/large-cell lymphoma of children in stage III/IV.

3) LRD: the remaining solid tumors, myeloma, acute leukemia, and lymphoma not mentioned in HRD and IRD.

The third step is the adjustment according to renal function and renal involvement.

1) HR: IRD with renal dysfunction and/or renal involvement; IRD with normal renal function and uric acid $> \text{ULN}$ or phosphate $> \text{ULN}$ or potassium $> \text{ULN}$.

2) IR: IRD with normal renal function; LRD of lymphoma and leukemia with renal dysfunction and/or renal involvement.

3) LR: LRD of lymphoma and leukemia with normal renal function; LRD of solid tumors and myeloma.

A preliminary search on PubMed did not reveal any report on TLS cases in the context of ICI phase 1 to 3 clinical trials. However, some metabolic disorders in the context of TLS including hyperkalemia and acute kidney injury were occasionally reported in association with pembrolizumab (Langer et al., 2016; Goldberg et al., 2020; Middleton et al., 2020), avelumab (Barlesi et al., 2018), and durvalumab uses (Massard et al., 2016). Currently, just eight case reports of individuals developing TLS while receiving treatment with ICIs or co-chemotherapy have been reported in the PubMed database (Masson Regnault et al., 2017; Fa'ak et al., 2019; Carrier et al., 2020; Magara et al., 2020; Narukawa et al., 2020; Shah et al., 2020; Sugimoto et al., 2020; Yen et al., 2020). All cases involved solid tumors—three cases of metastatic melanoma (Masson Regnault et al., 2017; Magara et al., 2020; Sugimoto et al., 2020), three cases of genitourinary malignancies (Fa'ak et al., 2019; Narukawa et al., 2020; Shah et al., 2020), one case of hepatocellular carcinoma (Yen et al., 2020), and one case of metastatic triple-negative breast cancer (Carrier et al., 2020).

These patients were treated with atezolizumab, nivolumab, or ipilimumab monotherapy (Masson Regnault et al., 2017; Fa'ak et al., 2019; Sugimoto et al., 2020); combined therapy of nivolumab plus ipilimumab (Magara et al., 2020); co-chemotherapy with nanoparticle albumin-bound-paclitaxel and atezolizumab (Carrier et al., 2020); nivolumab plus sorafenib (Yen et al., 2020); pazopanib after nivolumab (Narukawa et al., 2020); or pembrolizumab plus axitinib (Shah et al., 2020). The age range of the patients was 37–79 years, with a mean age of 58.5 years. TLS onset was between 5 and 10 days after the initiation of therapy, with various clinical symptoms such as weakness, fatigue, nausea, vomiting, diarrhea, and abdominal pain. Five out of eight patients died within 3–22 days after hospital admission (Masson Regnault et al., 2017; Narukawa et al., 2020; Shah et al., 2020; Sugimoto et al., 2020; Yen et al., 2020) and one after being discharged for home hospice (Fa'ak et al., 2019).

The neoplasm-related intrinsic factors such as high proliferative rate, large malignancy burden, or high chemotherapy sensitivity might facilitate the onset of TLS (Cairo et al., 2010). The overall incidence of TLS in the real world is unknown; however, the reported TLS incidence is higher in patients with hematologic malignancies than in those with solid neoplasms (Gemici, 2006). In a study on prophylaxis with allopurinol, the overall incidence of TLS in 102 patients with high-grade non-Hodgkin lymphoma adults was 42% (Hande and Garrow, 1993). During treatment with aggressive intravenous hydration, urinary alkalinization, and allopurinol, the incidence of TLS among 218 children with Burkitt acute lymphoblastic leukemia was 16.1% (Wössmann et al., 2003). In a study that included 772 adult patients with AML, 130 patients developed TLS—laboratory TLS was 12% and clinical TLS was 5%; furthermore, clinical TLS was associated with a higher mortality rate (Montesinos et al., 2008). In patients with solid tumors, rare cases of TLS have been reported in 46 patients with metastatic germ cell tumors, 300 patients with small-cell lung cancer, and 90 patients with neuroblastomas, which were considered an IRD (Gemici, 2006). Our study revealed that TLS occurred in 13 cases of hematologic neoplasms and 149 cases of solid malignancies. This may be because ICI indications cover more solid tumors than hematologic malignancies, as shown in **Table 2**. The 13 reported cases of hematologic neoplasm consisted of lymphoma ($n = 6$), plasma cell myeloma ($n = 2$), lymphocytic leukemia ($n = 2$), acute myeloid leukemia ($n = 1$), acute lymphocytic leukemia ($n = 1$), and myelodysplastic syndrome ($n = 1$). These neoplasm types covered the HRD, IRD, and LRD; however, further analysis could not be conducted because data such as WBC count, LDH level, and renal function were not collected in the FAERS. It seems that the off-label usage of ICIs is common in patients with hematologic malignancies as only classical Hodgkin lymphoma and primary mediastinal large B-cell lymphoma were the FDA-approved indications. It was unexpected that TLS occurred more often in solid malignancies, especially those occurring in the lung and thymus, skin, genitourinary, gastroenteric, and hepatic systems. The four therapies, namely, monotherapy of ipilimumab, nivolumab, or pembrolizumab, and

combined therapy of ipilimumab and nivolumab, were applied for the top three indications, non-small-cell lung cancer ($n = 28$), melanoma ($n = 32$), and renal cell carcinoma ($n = 21$), which could have led to the high reporting rates. With the growing application and efficacy of ICIs, awareness of the inherent factors that may predispose patients to potentially adverse effects is increasing. The increasing reports of previously rare cancer types imply that their incidence was previously underestimated.

The patient-related clinical features including pretreatment hyperuricemia or hyperphosphatemia, pre-existing nephropathy or exposure to nephrotoxins, oliguria and/or acidic urine, dehydration, blood volume depletion, elevated serum LDH, or inadequate hydration during treatment may cause the onset of TLS events (Hande and Garrow, 1993; Cairo et al., 2010; Howard et al., 2011). Our study revealed that age may be a risk factor as poor renal function, decreased heart and vascular stature, and complicated concomitant medication use might contribute to various clinical adverse events in elderly individuals. In a real-world pharmacovigilance study between renal adverse events and ICIs, atezolizumab showed a relatively stronger association with adverse events than other ICIs, and combined therapies, compared with monotherapies, strengthened the association. This study also reported sex difference. The average age of male and female patients was the same at around 62 years, although male patients seemed to be more susceptible and vulnerable to TLS than female patients in the three therapy groups. This may be associated with the high incidence of lung cancer, which is the leading cause of cancer deaths in men. In our study, the total TLS cases in male individuals were 2.5-fold higher than those in female individuals, and the number of male and female patients with lung and thymus cancers was 30 and 6, respectively.

Medication-induced TLS has been reported. TLS most often occurs after the initiation of cytotoxic therapy in patients with hematologic malignancies (Cairo et al., 2010). The use of single targeted anticancer drugs, including monoclonal antibodies, tyrosine kinase inhibitors, proteasome inhibitors, chimeric antigen receptor T cells, and proapoptotic agents, or combinations with conventional cytotoxic agents, could lead to an increase in the frequency and severity of TLS (Howard et al., 2016). In most cases, TLS was induced by chemotherapy in individuals with solid tumors (Gemici, 2006). The first FDA-approved drug was ipilimumab in 2011, whereas eight out of nine reported TLS cases involved patients receiving treatment with anti-CTLA-4 before 2015. Nivolumab and pembrolizumab were approved in 2014. From 2015 to 2017, 31 patients on anti-PD-1 regimen developed TLS. The 81 TLS cases in the anti-(PD-1)/(PD-L1) group between 2018 and 2020 accounted for 49% of the total cases; atezolizumab, avelumab and durvalumab, and cemiplimab entered the market in 2016, 2017, and 2018, respectively. The number of TLS cases receiving an anti-(CTLA-4 + PD-1) regimen increased from 2018 because the combined therapy was newly indicated for renal cell carcinoma, microsatellite instability-high (MSI-H), or mismatch repair deficient (dMMR) metastatic colorectal cancer in 2018 and hepatocellular carcinoma in 2020. It is noteworthy that the number of TLS cases has been increasing annually. The top

two reporting countries were Japan ($n = 67$, 40.85%) and the United States ($n = 44$, 26.83%). As the country where the drug was originally developed and first approved for marketing, the annual reports from the United States did not exceed single digits between 2014 and 2020. In Japan, the first 16 TLS cases, involving patients on ipilimumab, nivolumab, a combination of ipilimumab and nivolumab, pembrolizumab, or atezolizumab, were reported to the FAERS before 2018. The increased number of annual reports in 2019 ($n = 15$) and 2020 ($n = 36$) implies the potential relationship between widespread usage, the active reporting behavior, and potential high morbidity. Therefore, it should be confirmed whether the populations in Asia and North America are particularly vulnerable. Among all 5,709 TLS events in FAERS, the medications associated with the high occurrence of TLS were venetoclax ($n = 315$), rituximab ($n = 256$), doxorubicin ($n = 227$), lenalidomide ($n = 189$), dexamethasone ($n = 180$), bortezomib ($n = 156$), carboplatin ($n = 152$), ibrutinib ($n = 147$), bevacizumab ($n = 120$), cisplatin ($n = 112$), prednisolone ($n = 92$), and cyclophosphamide ($n = 73$). Except for dexamethasone, carboplatin and prednisolone, TLS were labeled in “warnings and precautions” or “adverse drug reaction” sections on all FDA-approved inserts.

Our study emphasized the frequency, severity, and celerity of TLS events, with a noticeable occurrence of 2.87% in a total of 5,709 TLS events, a high ratio (43.56%) of fatality, and a quick onset (within 10 days of starting treatment). Identifying the ICIs related to TLS cases is important as they account for significant morbidity and mortality, unless recognized early and treated appropriately (Howard et al., 2011). ICI combination therapy showed the strongest correlation with TLS; however, the fatality rate in the anti-CTLA-4 monotherapy group was significantly higher than that in the combination therapy group. It is worth noting that 13 out of 14 patients in anti-CTLA-4 group died from 2011 to 2020. There were 12 cases with malignant melanoma, of which, five were metastatic melanoma and one was malignant melanoma of stage IV. The cancer type and stage might be crucial factors influencing the fatality rate.

Based on the rapid onset and effective prevention suggested by the expert panel (Cairo et al., 2010), it is essential to be aware of its causes, the physiologic consequences, and the predisposing risk factors, and to identify patients at high risk for TLS (Coiffier et al., 2008). The reported prophylaxis and treatment involving vigorous hydration to preserve renal function, close monitoring of electrolytes to maintain homeostasis, pretreatment with anti-hyperuricemia agents (allopurinol, febuxostat, or rasburicase), necessary dialysis, and further intensive care unit admission should be routinely performed in clinical practice (Alakel et al., 2017; Wagner and Arora, 2017). Two compassionate use trials reported rasburicase is safe and highly effective in the prophylaxis and treatment of malignancy-associated hyperuricemia in both children and adults (Bosly et al., 2003; Jeha et al., 2005). The issues of underreporting of ADR (Hazell and Shakir, 2006; Lopez-Gonzalez et al., 2009) and the attitude of health-care providers, including physicians (Herdeiro et al., 2005) and pharmacists (Herdeiro et al., 2006), are major factors in pharmacovigilance of SRSs. Therefore, not only health-care providers, who reported most of the cases in our

study, but also the consumers themselves should be aware of TLS and the associated complications as the early recognition and treatment can mitigate the severity of TLS.

Although this study takes advantage of real-world research and novel data mining techniques, there are some limitations to consider. First, the FAERS does not contain data on all ICI treatment and TLS events in the world. Therefore, the incidence of suspected drugs and adverse events could not be calculated. Second, bias might exist based on missing or incorrect clinical information in the database. Third, confirmatory research should be carried out among individuals receiving combined therapy with ICIs and other anticancer medications. Finally, further studies are needed to explore the specific mechanism of how ICIs might induce TLS.

CONCLUSION

We retrieved data from a large pharmacovigilance database and summarized several aspects regarding age, sex, region, country, indication, onset time, and outcome. Based on the early onset, non-specific symptoms, fulminant progression, and inferior outcomes identifying the association between ICIs and TLS are crucial. Oncologists and general clinicians should closely monitor high-risk patients with cancer who might develop TLS after the administration of therapeutic agents.

DATA AVAILABILITY STATEMENT

The original contributions presented in the study are included in the article; further inquiries can be directed to the corresponding author.

ETHICS STATEMENT

Ethical review and approval was not required for the study on human participants in accordance with the local legislation and institutional requirements. Written informed consent for participation was not required for this study in accordance with the national legislation and the institutional requirements.

AUTHOR CONTRIBUTIONS

Conception and design: LW and JD. Data analysis and interpretation: BZ, XL, DM, and JJ. Manuscript writing and final approval: LW and BZ.

ACKNOWLEDGMENTS

We thank Ning Yuan, Mingnan Cao, Weiran Xu, and Qiang Ding for their insightful suggestions. MedDRA[®] trademark is registered by IFPMA on behalf of ICH. We would like to thank Editage (www.editage.cn) for English language editing.

REFERENCES

- Alakel, N., Middeke, J. M., Schetelig, J., and Bornhäuser, M. (2017). Prevention and Treatment of Tumor Lysis Syndrome, and the Efficacy and Role of Rasburicase. *Ott* 10, 597–605. doi:10.2147/ott.s103864
- ASTRAZENECA_UK_LTD Food and Drug Administration Website. durvalumab (imfinzi®). Available at: https://www.accessdata.fda.gov/drugsatfda_docs/label/2020/761069s023s024s025lbl.pdf (Accessed 01 26, 2021).
- Barlesi, F., Vansteenkiste, J., Spigel, D., Ishii, H., Garassino, M., de Marinis, F., et al. (2018). Avelumab versus Docetaxel in Patients with Platinum-Treated Advanced Non-small-cell Lung Cancer (JAVELIN Lung 200): an Open-Label, Randomised, Phase 3 Study. *Lancet Oncol.* 19 (11), 1468–1479. doi:10.1016/s1470-2045(18)30673-9
- Borghaei, H., Paz-Ares, L., Horn, L., Spigel, D. R., Steins, M., Ready, N. E., et al. (2015). Nivolumab versus Docetaxel in Advanced Nonsquamous Non-small-cell Lung Cancer. *N. Engl. J. Med.* 373 (17), 1627–1639. doi:10.1056/NEJMoa1507643
- Bosly, A., Sonet, A., Pinkerton, C. R., McCowage, G., Bron, D., Sanz, M. A., et al. (2003). Rasburicase (Recombinant Urate Oxidase) for the Management of Hyperuricemia in Patients with Cancer. *Cancer* 98 (5), 1048–1054. doi:10.1002/cncr.11612
- Brahmer, J., Reckamp, K. L., Baas, P., Crinò, L., Eberhardt, W. E. E., Poddubskaya, E., et al. (2015). Nivolumab versus Docetaxel in Advanced Squamous-Cell Non-small-cell Lung Cancer. *N. Engl. J. Med.* 373 (2), 123–135. doi:10.1056/NEJMoa1504627
- BRISTOL_MYERS_SQUIBB (2019a). Food and Drug Administration Website. ipilimumab (yervoy®) [Online]. Available at: https://www.accessdata.fda.gov/drugsatfda_docs/label/2020/125377s119lbl.pdf (Accessed 01 26, 2021).
- BRISTOL_MYERS_SQUIBB (2019b). Food and Drug Administration Website. nivolumab (opdivo®) [Online]. Available: https://www.accessdata.fda.gov/drugsatfda_docs/label/2021/125554s090lbl.pdf (Accessed 01 26, 2021).
- Cairo, M. S., and Bishop, M. (2004). Tumour Lysis Syndrome: New Therapeutic Strategies and Classification. *Br. J. Haematol.* 127 (1), 3–11. doi:10.1111/j.1365-2141.2004.05094.x
- Cairo, M. S., Coiffier, B., Reiter, A., and Younes, A. (2010). Recommendations for the Evaluation of Risk and Prophylaxis of Tumour Lysis Syndrome (TLS) in Adults and Children with Malignant Diseases: an Expert TLS Panel Consensus. *Br. J. Haematol.* 149 (4), 578–586. doi:10.1111/j.1365-2141.2010.08143.x
- Carrier, X., Gaur, S., and Philipovskiy, A. (2020). Tumor Lysis Syndrome after a Single Dose of Atezolizumab with Nab-Paclitaxel: A Case Report and Review of Literature. *Am. J. Case Rep.* 21, e925248. doi:10.12659/ajcr.925248
- Chen, G., Qin, Y., Fan, Q. q., Zhao, B., Mei, D., and Li, X. m. (2020). Renal Adverse Effects Following the Use of Different Immune Checkpoint Inhibitor Regimens: A Real-world Pharmacoepidemiology Study of post-marketing Surveillance Data. *Cancer Med.* 9 (18), 6576–6585. doi:10.1002/cam4.3198
- Coiffier, B., Altman, A., Pui, C.-H., Younes, A., and Cairo, M. S. (2008). Guidelines for the Management of Pediatric and Adult Tumor Lysis Syndrome: an Evidence-Based Review. *Jco* 26 (16), 2767–2778. doi:10.1200/jco.2007.15.0177
- Das, S., and Johnson, D. B. (2019). Immune-related Adverse Events and Anti-tumor Efficacy of Immune Checkpoint Inhibitors. *J. Immunotherapy Cancer* 7 (1), 306. doi:10.1186/s40425-019-0805-8
- EMD_SERONO_INC Food and Drug Administration Website. avelumab (bavencio®) [Online]. Available: https://www.accessdata.fda.gov/drugsatfda_docs/label/2020/761049s005lbl.pdf (Accessed 01 26, 2021).
- Fa'ak, F., Vanegas, D., and Osei, K. M. (2019). A Case Report of Atezolizumab Induced Tumor Lysis Syndrome. *Am. J. Case Rep.* 20, 785–789. doi:10.12659/ajcr.915351
- Gemici, C. (2006). Tumour Lysis Syndrome in Solid Tumours. *Clin. Oncol.* 18 (10), 773–780. doi:10.1016/j.clon.2006.09.005
- GENENTECH_INC Food and Drug Administration Website. atezolizumab (tecentriq®) [Online]. Available: https://www.accessdata.fda.gov/drugsatfda_docs/label/2020/761034s031s032lbl.pdf (Accessed 01 26, 2021).
- Goldberg, S. B., Schalper, K. A., Gettinger, S. N., Mahajan, A., Herbst, R. S., Chiang, A. C., et al. (2020). Pembrolizumab for Management of Patients with NSCLC and Brain Metastases: Long-Term Results and Biomarker Analysis from a Non-randomised, Open-Label, Phase 2 Trial. *Lancet Oncol.* 21 (5), 655–663. doi:10.1016/s1470-2045(20)30111-x
- Hande, K. R., and Garrow, G. C. (1993). Acute Tumor Lysis Syndrome in Patients with High-Grade Non-hodgkin's Lymphoma. *Am. J. Med.* 94 (2), 133–139. doi:10.1016/0002-9343(93)90174-n
- Hauben, M. (2003). A Brief Primer on Automated Signal Detection. *Ann. Pharmacother.* 37 (7-8), 1117–1123. doi:10.1345/aph.1C515
- Hauben, M., Madigan, D., Gerrits, C. M., Walsh, L., and Van Puijenbroek, E. P. (2005). The Role of Data Mining in Pharmacovigilance. *Expert Opin. Drug Saf.* 4 (5), 929–948. doi:10.1517/14740338.4.5.929
- Hazell, L., and Shakir, S. A. W. (2006). Under-Reporting of Adverse Drug Reactions. *Drug Saf.* 29 (5), 385–396. doi:10.2165/00002018-200629050-00003
- Herdeiro, M. T., Figueiras, A., Pol?nia, J., and Gestal-Otero, J. J. (2006). Influence of Pharmacists??? Attitudes on Adverse Drug Reaction Reporting. *Drug Saf.* 29 (4), 331–340. doi:10.2165/00002018-200629040-00004
- Herdeiro, M. T., Figueiras, A., Pol?nia, J., and Jesus Gestal-Otero, J. (2005). Physicians??? Attitudes and Adverse Drug Reaction Reporting. *Drug Saf.* 28 (9), 825–833. doi:10.2165/00002018-200528090-00007
- Hodi, F. S., O'Day, S. J., McDermott, D. F., Weber, R. W., Sosman, J. A., Haanen, J. B., et al. (2010). Improved Survival with Ipilimumab in Patients with Metastatic Melanoma. *N. Engl. J. Med.* 363 (8), 711–723. doi:10.1056/NEJMoa1003466
- Howard, S. C., Jones, D. P., and Pui, C.-H. (2011). The Tumor Lysis Syndrome. *N. Engl. J. Med.* 364 (19), 1844–1854. doi:10.1056/NEJMra0904569
- Howard, S. C., Trifilio, S., Gregory, T. K., Baxter, N., and McBride, A. (2016). Tumor Lysis Syndrome in the Era of Novel and Targeted Agents in Patients with Hematologic Malignancies: a Systematic Review. *Ann. Hematol.* 95 (4), 563–573. doi:10.1007/s00277-015-2585-7
- Jeha, S., Kantarjian, H., Irwin, D., Shen, V., Shenoy, S., Blaney, S., et al. (2005). Efficacy and Safety of Rasburicase, a Recombinant Urate Oxidase (Elitek), in the Management of Malignancy-Associated Hyperuricemia in Pediatric and Adult Patients: Final Results of a Multicenter Compassionate Use Trial. *Leukemia* 19 (1), 34–38. doi:10.1038/sj.leu.2403566
- Langer, C. J., Gadgil, S. M., Borghaei, H., Papadimitrakopoulou, V. A., Patnaik, A., Powell, S. F., et al. (2016). Carboplatin and Pemetrexed with or without Pembrolizumab for Advanced, Non-squamous Non-small-cell Lung Cancer: a Randomised, Phase 2 Cohort of the Open-Label KEYNOTE-021 Study. *Lancet Oncol.* 17 (11), 1497–1508. doi:10.1016/s1470-2045(16)30498-3
- Le, D. T., Uram, J. N., Wang, H., Bartlett, B. R., Kemberling, H., Eyring, A. D., et al. (2015). PD-1 Blockade in Tumors with Mismatch-Repair Deficiency. *N. Engl. J. Med.* 372 (26), 2509–2520. doi:10.1056/NEJMoa1500596
- Lopez-Gonzalez, E., Herdeiro, M. T., and Figueiras, A. (2009). Determinants of Under-reporting of Adverse Drug Reactions. *Drug Saf.* 32 (1), 19–31. doi:10.2165/00002018-200932010-00002
- Magara, A., Kato, H., Oda, T., Nakamura, M., Komatsu, H., and Morita, A. (2020). Tumor Lysis Syndrome Associated with Nivolumab Plus Ipilimumab Combination Therapy in a Melanoma Patient. *J. Dermatol.* 47. doi:10.1111/1346-8138.15547
- Massard, C., Gordon, M. S., Sharma, S., Rafii, S., Wainberg, Z. A., Luke, J., et al. (2016). Safety and Efficacy of Durvalumab (MED14736), an Anti-programmed Cell Death Ligand-1 Immune Checkpoint Inhibitor, in Patients with Advanced Urothelial Bladder Cancer. *Jco* 34 (26), 3119–3125. doi:10.1200/jco.2016.67.9761
- Masson Regnault, M., Ofaiche, J., Boulinguez, S., Tournier, E., Rochemaux, P., Paul, C., et al. (2017). Tumour Lysis Syndrome: an Unexpected Adverse Event Associated with Ipilimumab. *J. Eur. Acad. Dermatol. Venereol.* 31 (2), e73–e74. doi:10.1111/jdv.13733
- Matsushita, Y., Kuroda, Y., Niwa, S., Sonehara, S., Hamada, C., and Yoshimura, I. (2007). Criteria Revision and Performance Comparison of Three Methods of Signal Detection Applied to the Spontaneous Reporting Database of a Pharmaceutical Manufacturer. *Drug Saf.* 30 (8), 715–726. doi:10.2165/00002018-200730080-00008
- MERCK_SHARP_DOHME Food and Drug Administration Website. pembrolizumab (keytruda®) [Online]. Available: https://www.accessdata.fda.gov/drugsatfda_docs/label/2020/125514s088lbl.pdf (Accessed 01 26, 2021).
- Middleton, G., Brock, K., Savage, J., Mant, R., Summers, Y., Connibear, J., et al. (2020). Pembrolizumab in Patients with Non-small-cell Lung Cancer of Performance Status 2 (PePS2): a Single Arm, Phase 2 Trial. *Lancet Respir. Med.* 8 (9), 895–904. doi:10.1016/s2213-2600(20)30033-3
- Montesinos, P., Lorenzo, I., Martín, G., Sanz, J., Pérez-Sirvent, M. L., Martínez, D., et al. (2008). Tumor Lysis Syndrome in Patients with Acute Myeloid Leukemia:

- Identification of Risk Factors and Development of a Predictive Model. *Haematologica* 93 (1), 67–74. doi:10.3324/haematol.11575
- Narukawa, T., Hongo, F., Fujihara, A., Ueno, A., Matsugasumi, T., and Ukimura, O. (2020). Pazopanib after Nivolumab-Induced Tumor Lysis Syndrome in a Patient with Metastatic Clear-Cell Renal Cell Carcinoma. *Case Rep. Oncol.* 13 (1), 249–254. doi:10.1159/000506196
- Pham, M., Cheng, F., and Ramachandran, K. (2019). A Comparison Study of Algorithms to Detect Drug-Adverse Event Associations: Frequentist, Bayesian, and Machine-Learning Approaches. *Drug Saf.* 42 (6), 743–750. doi:10.1007/s40264-018-00792-0
- Postow, M. A., Sidlow, R., and Hellmann, M. D. (2018). Immune-Related Adverse Events Associated with Immune Checkpoint Blockade. *N. Engl. J. Med.* 378 (2), 158–168. doi:10.1056/NEJMra1703481
- Reck, M., Rodríguez-Abreu, D., Robinson, A. G., Hui, R., Csőszi, T., Fülöp, A., et al. (2016). Pembrolizumab versus Chemotherapy for PD-L1-Positive Non-small-cell Lung Cancer. *N. Engl. J. Med.* 375 (19), 1823–1833. doi:10.1056/NEJMoa1606774
- REGENERON_PHARMACEUTICALS Food and Drug Administration Website. cemiplimab (libtayo®) [Online]. Available: https://www.accessdata.fda.gov/drugsatfda_docs/label/2020/761097s003lbl.pdf (Accessed 01 26, 2021).
- Rittmeyer, A., Barlesi, F., Waterkamp, D., Park, K., Ciardiello, F., von Pawel, J., et al. (2017). Atezolizumab versus Docetaxel in Patients with Previously Treated Non-small-cell Lung Cancer (OAK): a Phase 3, Open-Label, Multicentre Randomised Controlled Trial. *The Lancet* 389 (10066), 255–265. doi:10.1016/s0140-6736(16)32517-x
- Shah, M., Jain, S., Abe, T., Surapaneni, P. K., and Bhatia, K. (2020). Pembrolizumab-axitinib-induced Tumor Lysis Syndrome in a Patient with Metastatic Renal Cancer. *Clin. Case Rep.* 8 (4), 704–708. doi:10.1002/ccr3.2737
- Sugimoto, S., Terashima, T., Yamashita, T., Iida, N., Kitahara, M., Hodo, Y., et al. (2020). Tumor Lysis Syndrome in a Patient with Metastatic Melanoma Treated with Nivolumab. *Clin. J. Gastroenterol.* 13 (5), 935–939. doi:10.1007/s12328-020-01164-x
- Thompson, J. A., Schneider, B. J., Brahmer, J., Andrews, S., Armand, P., Bhatia, S., et al. (2020). NCCN Guidelines Insights: Management of Immunotherapy-Related Toxicities, Version 1.2020. *J. Natl. Compr. Canc. Netw.* 18 (3), 230–241. doi:10.6004/jnccn.2020.0012
- van Puijnenbroek, E. n. P., Bate, A., Leufkens, H. G. M., Lindquist, M., Orre, R., and Egberts, A. C. G. (2002). A Comparison of Measures of Disproportionality for Signal Detection in Spontaneous Reporting Systems for Adverse Drug Reactions. *Pharmacoepidem. Drug Safe.* 11 (1), 3–10. doi:10.1002/pds.668
- Wagner, J., and Arora, S. (2017). Oncologic Metabolic Emergencies. *Hematology/Oncology Clin. North America* 31 (6), 941–957. doi:10.1016/j.hoc.2017.08.002
- Wössmann, W., Schrappe, M., Meyer, U., Zimmermann, M., and Reiter, A. (2003). Incidence of Tumor Lysis Syndrome in Children with Advanced Stage Burkitt's Lymphoma/leukemia before and after Introduction of Prophylactic Use of Urate Oxidase. *Ann. Hematol.* 82 (3), 160–165. doi:10.1007/s00277-003-0608-2
- Yen, T.-H., Chang, C.-H., and Shiu, S.-I. (2020). Tumor Lysis Syndrome after Combination Therapy of Nivolumab and Sorafenib in a Woman with Advanced Hepatocellular Carcinoma. *Case Rep. Gastroenterol.* 14 (2), 367–372. doi:10.1159/000508583

Conflict of Interest: The authors declare that the research was conducted in the absence of any commercial or financial relationships that could be construed as a potential conflict of interest.

Publisher's Note: All claims expressed in this article are solely those of the authors and do not necessarily represent those of their affiliated organizations, or those of the publisher, the editors, and the reviewers. Any product that may be evaluated in this article, or claim that may be made by its manufacturer, is not guaranteed or endorsed by the publisher.

Copyright © 2021 Wang, Li, Zhao, Mei, Jiang and Duan. This is an open-access article distributed under the terms of the Creative Commons Attribution License (CC BY). The use, distribution or reproduction in other forums is permitted, provided the original author(s) and the copyright owner(s) are credited and that the original publication in this journal is cited, in accordance with accepted academic practice. No use, distribution or reproduction is permitted which does not comply with these terms.

GLOSSARY

ADR adverse drug reaction

ALL acute lymphoblastic leukemia

AML acute myeloid leukemia

BCPNN Bayesian confidence propagation neural network

CI confidence interval

CTLA-4 cytotoxic T lymphocyte antigen-4

EBGM empirical Bayesian geometric mean

FDA Food and Drug Administration

FAERS FDA Adverse Event Reporting System

HR high risk

HRD high-risk disease

ICIs immune checkpoint inhibitors

ICH international council for harmonization of technical requirements for pharmaceuticals for human use

IC information component

IQR interquartile range

IR intermediate risk

IRD intermediate-risk disease

LR low risk

LRD low-risk disease

LDH lactate dehydrogenase

MGPS multi-item gamma Poisson shrinker

PD-1 programmed death receptor-1

PD-L1 programmed cell death 1 ligand 1

PRR proportional reporting ratio

PT preferred term

SMQ standardized medical dictionary for regulatory activities query

SRS spontaneous reporting system

TLS tumor lysis syndrome

ULN upper limit of normal

WBC white blood cell

WHO World Health Organization

χ^2 chi-squared



The Current Application and Future Prospects of Astragalus Polysaccharide Combined With Cancer Immunotherapy: A Review

Fanming Kong^{1,2†}, Tianqi Chen^{1,2†}, Xiaojiang Li^{1,2} and Yingjie Jia^{1,2*}

¹Department of Oncology, First Teaching Hospital of Tianjin University of Traditional Chinese Medicine, Tianjin, China, ²National Clinical Research Center for Chinese Medicine Acupuncture and Moxibustion, Tianjin, China

OPEN ACCESS

Edited by:

Hany Omar,
University of Sharjah, United Arab
Emirates

Reviewed by:

Palanisamy Subramanian,
Gangneung-Wonju National
University, South Korea
Md. Areeful Haque,
International Islamic University
Chittagong, Bangladesh

*Correspondence:

Yingjie Jia
jiayingjie1616@163.com

[†]These authors have contributed
equally to this work

Specialty section:

This article was submitted to
Pharmacology of Anti-Cancer Drugs,
a section of the journal
Frontiers in Pharmacology

Received: 07 July 2021

Accepted: 09 September 2021

Published: 13 October 2021

Citation:

Kong F, Chen T, Li X and Jia Y (2021)
The Current Application and Future
Prospects of Astragalus
Polysaccharide Combined With
Cancer Immunotherapy: A Review.
Front. Pharmacol. 12:737674.
doi: 10.3389/fphar.2021.737674

So far, immunotherapy has been shown to have impressive effects on different cancers in clinical trials. All those immunotherapies are generally derived from three main therapeutic approaches: immune checkpoint inhibitors, immune cell vaccination, and adoptive cellular immunotherapy. Our research systematically reviewed a wide range of clinical trials and laboratory studies of astragalus polysaccharide (APS) and elucidated the potential feasibility of using APS in activating adoptive immunotherapy. Apart from being effective in adaptive “passive” immunotherapy such as lymphokine-activated killer treatment and dendritic cell (DC)–cytokine-induced killer treatment, APS could also regulate the anti-programmed cell death protein 1 (PD-1)/PD-L1 on the surface of the immune cells, as a part in the immune checkpoint inhibitory signaling pathway by activating the immune-suppressed microenvironment by regulating cytokines, toll-like receptor 4 (TLR4), nuclear factor kappa B (NF- κ B), and mitogen-activated protein kinase (MAPK) pathways, and immune cells, such as DCs, macrophages, NK cells, and so on. In view of the multiple functions of APS in immunotherapy and tumor microenvironment, a combination of APS and immunotherapy in cancer treatment has a promising prospect.

Keywords: cancer immunotherapy, traditional Chinese medicine, astragalus polysaccharide, immune checkpoint inhibitors, DC vaccine

INTRODUCTION

Immunotherapy has been shown to have impressive effects on different cancers in clinical trials (Hodi et al., 2010; Kazandjian et al., 2016; Necchi et al., 2017). Till now, all Food and Drug Administration (FDA)–approved cancer immunotherapies included interleukin (IL)-2, interferon (IFN), dendritic cell (DC) vaccine, chimeric antigen receptor-T (CAR-T) cells, anti-programmed cell death protein 1 (PD-1)/PD-L1 mAbs, anti-cytotoxic T lymphocyte antigen-4 (anti-CTLA-4), and so on. In general, all these strategies have been divided into two categories according to their mechanisms (Sanmamed and Chen, 2018; Sanmamed and Chen, 2019).

The first category is to harm cancer cells directly, known as “passive” immunotherapy, using effector cytokines or cells in the immune system. It involves antibody-targeted treatment, adoptive immune cell therapies, and engineered T cells such as CAR-T therapy. Passive immunotherapy enhanced the immune system to much higher levels by cutting-edge means (Kantoff et al., 2010).

The second category is to activate the immune system by regulating endogenous immune functions, known as “active” immunotherapy. It involves 1) enhancement of antigen uptake,

processing, and presentation to T cells by antigen-presenting cells (APCs), such as DC vaccines, with its extension of using agents such as interferons and cytokines to increase APC function; 2) the activation and expansion of naive T cells with DC vaccines, CTLA-4, or PD-1/PD-L1 inhibitor; and 3) enhancement of the effect of the immune response.

So far, the PD-1/PD-L1 inhibitor is an outstanding instance of these methods. PD-1 has been proved to be expressed in different cancers by activated T cells, B cells, natural killer (NK) cells, and bone marrow cells (Ai et al., 2020), while its ligand PD-L1 abounds in different cancers. They combine with each other on the surface of immune cells, leading to immune escape in the tumor microenvironment (TME). Therefore, there are a number of clinical trials researching PD-1/PD-L1 and other combination treatments trying to rejuvenate the regular immune function in TME.

Astragalus membranaceus is a type of tonic traditional Chinese medicine commonly used in Asia, and its main components such as astragalus polysaccharide (APS), astragaloside IV (AS-IV), and flavonoids could effectively improve the immune function of patients with various diseases as has been shown in previous researches (Fu et al., 2014; Auyeung et al., 2016; Zhang J. et al., 2020). It has been shown that APS mainly contained nine monosaccharides, such as Glc, Gal, Ara, Rha, Man, Xyl, Fuc, Fru, and Rib from the dried roots of *Astragalus* spp. Radix Astragali (Liu et al., 2017).

APS is often used clinically. Numerous *in vitro* and *in vivo* researches have validated that it could regulate the immune system (Fu et al., 2014; Auyeung et al., 2016; Chen et al., 2020; Zheng et al., 2020). Its immunomodulatory effect involves factors such as cytokines like ILs, tumor necrosis factors (TNFs), growth factor, and so forth, and immune cells like macrophages within TME (Zheng et al., 2020). Recently, the powerful immunomodulatory activities of APS for immunological checkpoints have attracted a lot of attention. In clinical and laboratory studies, APS has been shown to improve the effect of immunotherapy (Tsao et al., 2021). APS has been shown to drastically suppress the expression of PD-L1 genes and proteins in tumors and prevent the development of melanoma (Wang et al., 2014). This indicates that APS may regulate PD-1–PD-L1 signaling pathways, enhancing the antitumor capability of immune cells. The underlying mechanism of APS on this immune response remains a mystery. However, it has been well-known that TME plays a crucial role in the activation of PD-1–PD-L1 signaling pathways. Meanwhile, many studies have confirmed the multiple regulatory effects of APS on TME; therefore, in this review, we elucidated the effect of APS on TME and its potential ability to enhance that effect of immunotherapy.

Astragalus Polysaccharide Combined With Immune Checkpoint Inhibitors in Clinical Trials.

CTLA-4 and PD-1 inhibitors are two of the commonly used immune checkpoint inhibitors (ICIs) because they can activate and proliferate tumor-specific T cells in TME. Despite the

therapeutic effectiveness against the CTLA-4 and PD-L1/PD-1 signal pathways, only a tiny number of patients have showed long-term responses. The main explanation for that is the severe immune-suppressive TME and decreased antigen presentation capacity in TME compromised the proliferation and survival of infiltrating T cells, and weakened the immune system from preventing additional T cells from migrating into tumor focus (Chen and Mellman, 2017).

The emergence of immune checkpoint blocking has revolutionized the management of advanced non-small cell lung cancer (NSCLC) (Sui et al., 2018). A high neutrophil-to-lymphocyte ratio (NLR) after the ICI treatment was associated with poorer OS. Fifty-three lung cancer patients were treated with ICI combined with APS, and the result showed that APS could normalize the NLR in patients receiving ICI combination treatments, and prolong the overall survival from 25.4 months (control group) to 26.1 months (APS group) (Tsao et al., 2021). Moreover, in another trial with 23 advanced cancer patients treated with ICI, the retrospective analysis presented real-world data of cancer-related fatigue, cachexia, or poor performance status after APS injection. The APS group showed better tolerance of ICI and remarkable Overall survival (OS) and Progression-free survival (PFS) outcomes (Yuan et al., 2021; Lai et al., 2019). In addition, it should be noted that APS can be considered as a novel nanocarrier for the delivery of hydrophobic drugs in chemotherapy and immunotherapy. APS nanomedicine boosted an overall antitumor immunity and caused the radiation-induced abscopal effect, with the ability to prolong the survival rate of tumor-bearing mice, inhibiting the growth of the primary tumor subjected to radiation as well as the secondary tumor distant from the primary lesion. The systematic antitumor immune responses and the immune memory were enhanced in mice after the treatment (Pang et al., 2019).

Based on the above analyses, APS could be used as a potential adjuvant in tumor immunity in ICI immunotherapy. Further researches of these combination administrations should be conducted in the future to further boost each drug's benefits.

Astragalus Polysaccharide Combined With Adoptive Immunotherapy

Over the last four decades, the promising development of adoptive immunotherapy has uncovered various therapeutic techniques in which immune cells are modified and prescribed to eliminate malignant cells. These techniques include tumor-infiltrating lymphocytes, NK cells, DCs, cytokine-induced killer (CIK) cells, DC-CIK cells, and lymphokine-activated killer (LAK) cells.

DCs, as innate immune cells, are the most potent APCs in the body, able to ingest, process, and present antigens, thereby promoting the stimulation of primary T cells. CIK cells induce or directly lead to apoptosis in cancer cells. During this process, cytokines like IL-2 and IFN- γ are released. CIK cells exhibit traits fast multiplying, high antitumoral efficacy, pan-cancer regulation, and great identification capacity. In biological immunotherapy, DCs paired with CIK cells can successfully ameliorate

TABLE 1 | Effect of APS on adaptive immune therapy.

Cell line	Dosage	Effect of APS on adaptive immune therapy	Ref
SKov3 cell	APS 100 mg/L, 3 d	CIK cytotoxicity↑	Xu et al. (2011)
Hela cell in female BALB/c mice	APS 250,500,1000 mg/L, twice a week, 3 w	CIK cytotoxicity↑	Huo and Shan (2016)
Eca-109 cell	APS 100 mg/L, 7 d	DC-CIK cells cytotoxicity↑	Wang et al. (2016)
pDC cell	APS 50,100, 200 mg/L, 1 d	IFN-α↑, TNF-α↑, and IL-6↑ by pDC; CD11c↑, CD80↑, and CD86↑	Liu et al. (2010)
A549 cell	APS 100 mg/L, 2 d	IFN-γ↑, IL-12↑, CD40↑, CD80↑, and HLA↑ in DCs, cytotoxicity of DC-CIK cells↑	Zhang et al. (2009)
LAK cell, Hela cells	APS 1000 mg/L, 3 d	Dead and apoptotic LAK cells↓	Yang and Zhao (1998)
K562 cells	APS 100 mg/L, 2 d	IFN-γ↑, IL-12↑, CD40↑, CD80↑, and HLA↑ in DCs, cytotoxicity of DC-CIK cells↑	Chen and Zhang (2013)
Kunming mice with S180 cell tumor	APS 100 mg/L, 2 d	CD86↑, CD80↑, in DC, TNF-α↑, and IL-12↑	Qiu et al. (2015)
DCs-CIK cell; Hela cell	APS 300 mg/L, 3 d	CD3 ⁺ CD8 ⁺ , CD3 ⁺ CD56 ⁺ , TNF-α, and IFN-γ in DCs-CIK; CD14↓, CD80↑, CD83↑, CD86↑, CD11c↑, HLA-I↑, and HLA-II↑ in DCs; TNF-β↑ and IFN-γ↑	Gong and Ju (2016)
K562 cells	APS 1000 mg/L, 3 d	LAK cytotoxicity ↑	Wang et al. (1995)
BALB/c mice with S180 cell tumor after CTX treatment	200 mg/kg, 8 d	NK cells↑; IL-2↑, IL-3↑, IL-4↑, IL-6↑, and IFN-γ↑	Weng et al. (2003)
HL-60 cells	15 mg/ml, 2 d	MICA expression↑ in HL-60 cells, sensitivity of HL-60 cells↑ to NK cells	Zeng et al. (2012)
Splenic DCs	APS 50,100,200 mg/L, 1 d	CD11c (high) CD45RB (low) DCs↑, Th2 to Th1↑, T lymphocyte immune function↑	Liu et al. (2010)
Spleen of BALB/c mice	0–200 mg/L, 7 d	Macrophage cytotoxicity↑, NK cell cytotoxicity↑, IgG↑ in supernatant	Wang et al. (2008)
pDC cell from CML patients	APS 50,100, 200 mg/L, 1 d	IL-6↑, TNF-α↑ secreted by pDC in treatment-naïve CML patients, IFN-α↑, IL-6↑, TNF-α↑ secreted by pDC in remission stage patients	Liu (2009)

autoimmunity of cancer patients, hence boosting their survival rate and survival time. Thus, CIK cells or DCs cocultured with CIK cells comprising the CIK/DC-CIK cell treatment has emerged as an essential immunotherapy (Li et al., 2018). Many clinical evidence have shown that APS injection combined with CIK cell therapy can control tumor progression in patients with advanced NSCLC and breast cancer, improving the immune function of patients and the symptoms of qi-deficiency syndrome with no obvious adverse reactions. In the control group (CIK cells group), CIK cells were transfused into the vein (100 ml each time, once every W1,3,5 and totally five times, the total number of cells $>1 \times 10^{10}$ /ml). In the combined group (APS injection and CIK cells group), the CIK cell treatment was combined with APS injection, intravenous drip (250 mg qd, 10 days). Ten days is one cycle; both groups received the second cycle of treatment a month later (Zhang, 2011; Zhang et al., 2018b; **Table 1**).

Astragalus Polysaccharide Combined With Vaccine

The inhibition of immune response by the cancer microenvironment has been identified as a major barrier in effective tumor therapies. Apart from blocking immune checkpoints, DC-derived vaccines are acknowledged as a highly prospective method in cancer treatment. DCs are a special type of APCs that link innate and adaptive immune

function, generating an appropriate immune response by uptaking, processing, and expressing antigens of tumors with the major histocompatibility complex (MHC) I and II. Then, they get into the secondary lymph tissue and activate naïve cancer antigen-specific CD4⁺ and CD8⁺ T cells, differentiating these into effector cells. By activating DCs, there is a chance to induce the efficient cancer-specific immune response coordinated by cytotoxic T cells and other cancer-specific immune cells (Shortman and Liu, 2002; Darwin et al., 2018; Azarov et al., 2019; Kong et al., 2019; Wculek et al., 2019). At present, the FDA has authorized sipuleucel-T, which consists of blood cells enriched for APCs such as DCs. In addition, DC vaccines have been proven to be effective in ovarian cancer, liver cancer, lung cancer, melanoma, and glioblastoma immunotherapy *in vivo*. Clinical trials with ovarian cancer and hepatocellular cancer patients have confirmed the safety of DC vaccines (Carreno et al., 2015; Ott et al., 2017; Keskin et al., 2019; Zhang X. et al., 2020; Chen et al., 2021; Ding et al., 2021; Teng et al., 2021).

Though few clinical trials demonstrated the efficacy of APS in the DC vaccines in patients, several experiments have shown that patient's DCs can be characterized and amplified by APS *in vitro*. Some data showed that APS could be used as a helpful enhancer in the DC-based vaccination for cancer immunotherapies (Zhu et al., 2017). Liu et al. (2009) found APS-treated plasmacytoid DCs (pDC) secreted more IFN-α, IL-6, and TNF-α than the untreated group of CML patients at the remission phase,

suggesting that APS can promote the function of pDC from CML. The mechanism might be related to promotion of antitumor cytokines IL-12 and TNF- α by APS (Jing et al., 2014; Qiu et al., 2015).

MECHANISM OF ASTRAGALUS POLYSACCHARIDE COMBINED IMMUNOTHERAPY

The Potential of Astragalus Polysaccharide as an Adjuvant in Immune Checkpoint Inhibitors Therapy

Astragalus Polysaccharide Affect the Expression of PD-L1 in Tumor Microenvironment

Clinical studies have reported that overexpression of PD-L1 is associated with poor prognosis in multiple types of tumors (Gu et al., 2017; Zhao P. et al., 2019; Xie et al., 2019; Carlsson et al., 2020). According to several researches, as an effective method when joined with other cancer therapies, APS reduces PD-L1 expression in TME and plays an essential part in immunotherapy (Chang HL. et al., 2020).

Previous studies have shown that APS may substantially inhibit melanoma development *in vivo* and lower PD-L1 expression in TME, indicating that APS's antitumor mechanism is also related with the PD-1–PD-L1 signaling pathway. In tumor-bearing mice, APS could also boost T lymphocytes proliferation and enhance the release of IL-2 and IFN- γ in the peripheral circulation (Wang et al., 2014). Chang et al. (2020) found that the isolated single-chain fragment variable (scFv) S12 from APS showed the finest binding ability to PD-1, inhibiting PD-L1–based T cell exhaustion. Furthermore, there were no substantial differences between the effect of ixabepilone and APS in tumor inhibition combined with the PD-1 inhibitor, suggesting that APS prevents tumorigenesis or progress with increased T cell activation, enhancing the synergistic effect with anti-PD-L1. Another study found that APS improved chemotherapy by reducing PD-L1 expression in TME via the protein kinase B (Akt)/mammalian target of rapamycin (mTOR)/ribosomal protein S6 kinase beta-1 (p70S6K) pathway. It could also reduce inflammatory-related cytokines and M2 macrophage proportion, induce DC maturation, and improve the T cell–based antitumor function, demonstrating that APS is a feasible supplement in immunotherapy (Huang et al., 2019).

Based on the facts presented above, it is expected that APS can be utilized in concert with PD-1 to promote immune cell infiltration and boost therapeutic outcomes.

The Effects of Astragalus Polysaccharide on Immune Cells Constituents of Tumor Microenvironment

In the TME, cancer cells have selected inhibitory ligands and their receptors that modulate T-cell effector function to enhance tumor tolerance and avoid immune system eradication. In recent years, pharmacological modulators of these pathways along with many other immune cells and cytokines have been extensively studied and used as new immunotherapeutic agents for the treatment of

cancer. Through our review, we found APS has various effects on the immune cells in the TME. Tumor-associated macrophages (TAMs) are macrophages in the TME. Generally, macrophages include M1 and M2 types, which take tumor inhibitory and tumor promotion roles in TME, respectively. M1 generates reactive oxygen species (ROS) and pro-inflammatory cytokines, such as IL-2, IFN- γ , TNF- α , and IL-1 β , which play essential roles in killing tumor cells. By contrast, M2 produce anti-inflammatory cytokines, such as tumor growth factor (TGF)- β and IL-10, promoting cancer progression.

As for macrophages, a study proved that APS can significantly increase the polarization ratio of M1/M2 macrophages in NSCLC cell lines, regulating inflammatory response in the TME (Bamodu et al., 2019). Wei et al. (2019) showed that this function is related to IL-6, TNF- α , iNOS, and CXCL10 through the NOTCH signaling pathway. Another study showed that APS can activate macrophages and release NO and TNF- α via the activation of toll-like receptor 4 (TLR4) and nuclear factor kappa B (NF- κ B)/Rel, with the inhibition of cancer growth (Lee and Jeon, 2005). Furthermore, APS may greatly boost spleen lymphocyte proliferation and phagocytosis in mouse peritoneal macrophages, increasing the production of IL-2, TNF- α , and IFN- γ in peripheral blood (Li et al., 2020).

The role of B cells in tumor progression and antitumor immunity is only beginning to be understood, partially due to their low numbers in the TME compared to T cells. Tumor-infiltrating B cell (TIB) were found to be present in tumor-draining lymph nodes and in tumor-associated tertiary lymphoid structures. TIBs can have both tumor-promoting and antitumor functions. In another study, as for B cells, APS effectively stimulated the proliferation of splenic B cells in C3H/HeJ mice via membrane Ig in a TLR4-independent process. Meanwhile, monoclonal antibodies against TLR4 interrupted APS binding to macrophages, demonstrating a direct communication between APS and TLR4 on the macrophages surface (Shao et al., 2004).

For T cells, APS could apparently inhibit S100 sarcoma growth, increase CD4⁺ T cells expression and IL-2 production, and decrease CD8⁺ T cell and IL-4 levels in peripheral blood (Zou et al., 2012). In addition, APS dramatically prolonged survival in mice and suppressed the development of radiation-treated primary tumor. DCs are central regulators of adaptive immune responses, providing antigen presentation and ligands for co-stimulatory receptors, as well as a suitable cytokine milieu for activation, differentiation, and effector functions of T cells. In addition, APS could enhance the maturation of DCs and increase the membrane expression of MHC. Another investigation found that an APS-related immune reaction was primarily characterized by DC activation, featured with DC maturation and its improved antigen presentation ability via the TLR4 pathway. Mature DCs moved to the lymph nodes and resulted in the augmentation of the ratio of CD4⁺ T/Treg and CD8⁺ T/Treg. Similarly, another research showed APS made splenic DCs differentiate to CD11c (high) CD45RB (low) DCs and activated T lymphocytes with transfer from Th2 to Th1 (Liu et al., 2011; Shao et al., 2006).

For Treg cells, APS might inhibit the tumor growth partly by decreasing Treg with a lower TGF- β and IL-10 mRNA expression in the spleen (Sun et al., 2013). Furthermore, *in vitro*, APS inhibited the development and proliferation of CD4⁺CD25⁺Treg cells dose-dependently and time-dependently. In Hepatic cell carcinoma (HCC) TME, APS suppressed Treg cells by repairing cytokines imbalance and inhibiting FOXP3 expression. SDF-1 was critical in the Treg recruitment in the TME. APS might impede Treg cell migration by affecting SDF-1 via the CXCR4/CXCL12 pathway (Li et al., 2012). For NK cells, a study showed that APS could promote the transformation of mouse peritoneal macrophages to M1 type under the stimulation of tumor cells and increase the production of TNF- α and NO. APS could also improve the antitumor effect of NK cells. The IFN- γ or granzyme B-positive cells in total NK cells were higher than those in the control group (Chai et al., 2019). Myeloid-derived suppressor cells (MDSCs) take part in tumor development in a variety of ways, including angiogenesis stimulation, epithelial-to-mesenchymal transition (EMT), and pre-metastatic niche establishment. They act as a negative regulator of T-cell and NK-cell activities in the TME by hijacking immunological checkpoint pathways. Treatment with APS inhibited tumor development in MDSCs by reducing the proportion of Gr-1⁺CD11b⁺MDSCs and limiting vascular endothelial growth factor (VEGF) and IL-10 expression (Chai et al., 2012).

The Effects of Astragalus Polysaccharide on Immune Cell Constituents of Tumor Microenvironment

The TME is an inflammatory environment that contains a variety of inflammatory and regulatory mediators, such as cytokines IL-1 β and IL-6, as well as chemokines and ROS. In the TME, cytokines are extremely important. TGF- β and IL-10 are the most well-known immunosuppressive mediators in the TME. DCs and T cells are both suppressed by IL-10. Meanwhile, IFN- γ , TNF- α , IL-2, and IL-1 β play crucial parts in killing tumor cells according to previous researches (West et al., 2013; Garriss et al., 2018; Balta et al., 2021). Furthermore, another study showed that intratumoral DC's IL-12 cytokine signaling leads to anti-tumor immunity, and the antitumor cytokines IFN- γ and IL-12 are stimulated by immunotherapy. T-cell-DC interaction involving IFN- γ and IL-12 is required for effective anti-PD-1 cancer treatment. HIF-1 α expression is largely regulated via various cytokines, which involves the cascading of several growth factors and oncogenic cascades (Noman et al., 2014).

APS-activated macrophages, which increase the concentration of nitric oxide (NO) and TNF- α , acting as an upstream inhibitor of tumor cell proliferation with G1 cycle blockage and modulating genes associated with apoptosis, prevent cancer cells growth (Li et al., 2019). In H22-bearing mice, APS could effectively inhibit solid tumor growth and increase body weight and phagocytotic function of macrophages. Furthermore, APS treatment could increase the release of IL-2, IL-12, and TNF- α and decrease the IL-10 level in the serum (Yang et al., 2013; Zhao et al., 2019).

In tumor-bearing mice, APS has synergistic tumor suppressive effects with Adriamycin (ADM). This may be related to its ability

to enhance the level of IL-1 α , IL-6, IL-2, and TNF- α , reduce IL-10, and reduce MDR1 mRNA and p-gp expression levels (Xiao et al., 2009; Tian et al., 2012; Lai et al., 2017). In patients with lung cancer, the expression of IFN- γ and T-bet was strong after the treatment of APS, while the expression intensity of IL-4 and GATA3 decreased significantly (Wei and Tian, 2003; Liao et al., 2020).

In addition, APS could effectively inhibit the growth and metastasis of Lewis lung cancer in mice and LOVO cells (Tie, 2019), enhancing the activity of normal human lymphatic endothelial cells and inhibiting the protein expression of VEGF and EGFR in tumor tissues (Lee et al., 2020).

APS could revert the increased invasion capacity of the HUVECs co-cultured with SCC7901 cells and reduce the high levels of matrix metalloproteinase (MMP)-2, MMP-9, LOX, SNAIL protein, and vimentin mRNA expression and decreased E-cadherin mRNA expression. The macrophage migration inhibitory factor (MIF) is an inflammatory cytokine that promotes the EMT (Youwei and Yeting, 2020). It is related to MMP-13 and AMP-activated protein kinase (AMPK). A study showed that APS reduced MMP-13 and activated AMPK in A549 and CL1-2 cells, reducing the AXL, vimentin, MMP-13, and MIF expressions. These studies revealed that APS plays an essential role in cancer therapy by suppressing and aggressively removing MIF from cancer cells.

According to these studies, we found APS could significantly suppress the levels of TGF- β and IL-10 *in vivo* and *in vitro* while increasing the levels of IFN- γ , TNF- α , IL-2, and IL-1 β , regulating the growth factor VEGF, and reverting the immune-suppressed TME, hopefully to be an adjuvant drug in immunotherapy (Table 2).

Astragalus Polysaccharide Affects the Pathway of Tumor Microenvironment in Immune Checkpoint Signaling

Feng et al. (2021) studied the immunoregulatory effects of APS in RAW264.7 cells via the activation of the NF- κ B p65/MAPK signaling pathway. It enhanced the protein levels of phosphorylated p65, p38, Jun N-terminal kinase, and extracellular signal-regulated kinase. Then, APS enhanced cytotoxicity potential of RAW264.7 cells on 4T1 cells with more NO and cytokines and upregulated gene expressions of TNF- α , IL-6, and iNOS. Furthermore, studies showed that TLR-4 may take part in the process in which APS promotes the cytokine production of RAW264.7 cells. Another study supported the ability of APS to activate TLR-4-related MAPKs, demonstrating that APS activates macrophages through the TLR-4-MAPK-NF- κ B pathway (Wei et al., 2016; Zhu et al., 2018).

MyD88 and TRIF are well-known downstream signaling pathways of the TLR4 signaling pathway, and their divergence leads to the immune function diversity of the TLR4 pathway. APS stimulated the key nodes in TLR4-MyD88-dependent signaling pathway, including MyD88, TRAF-6, TLR4, AP-1, and NF- κ B in the spleen cells to regulate their immune function (Liqing, 2017; Li Y. et al., 2020).

TABLE 2 | Effect of APS on ICI signaling pathway and TME.

Cell line and animal model	Dosage	Effect of APS on ICI signaling pathway and TME	Reference
Non-small cell lung cancer (NSCLC) H441 and H1299 cells	APS(3 mg/kg/d), 16 w	M1 macrophage↑, M2 macrophage↓, DCs maturation↑, T cell-mediated anticancer↑, M1/M2↑, DCs↑, CTL↑, IL-6↓, IL-10↓, NF-κB↓, CD11b↑, and CD31↓	Bamodu et al. (2019)
4T1 and CT26 cells; BALB/c mice	50 µg of APS intraperitoneal injection, 7 days	Cell surface PD-L1↓ via Akt/mTOR/p70S6K pathway	Chang et al. (2020b)
Inbred strain BALB/c mice (approximately 6–8 weeks old, female); the murine mammary carcinoma 4T1 cells and RAW264.7 cells	APS 30, 100, and 300 µg/ml, 24 h	M1↑, notch ligand↑, iNOS↑, TNF-α↑, and CXCL10↑	Wei et al. (2019)
BALB/c mice; RAW264.7 and 4T1 cells	APS 50, 100, 200, 500, and 1,000 µg/ml, 24 h	Spleen lymphocytes↑ peritoneal macrophages phagocytosis, IL-2, TNF-α, and IFN-γ in peripheral blood	Li et al. (2020a)
RAW264.7 and 4T1 cells; B6C3F1 mice	APS (10, 50, and 100 µg/ml), 24 h	NO↑, iNOS↑ through NF-κB/Rel ↑	Lee and Jeon, (2005)
RAW 264.7 cells; MCF-7 and RAW264.7 murine BALB/c mice with 4T1 allograft tumors	APS 1000 µg/ml, 24 h 50 µg of APS, 7 days	NO↑, TNF-α↑, IL-6↑ M1/M2↑, Ki-67↓, CD25↑, and anti-PD-1 antibody titers, IL-2↑, IFN-γ↑ (scFv) S12 from APS	Li et al. (2019) Chang et al. (2020a)
C57BL/6j (H-2b) mice	APS 10, 50, 100 and 250 µg/ml for 24 h	BM-derived DC maturation↑, CD11c↑, I-A/I-E↑, IL-12↑ in DC, DC endocytic↓	Shao et al. (2006)
H22-bearing mice	APS 100, 400 mg/kg/d, 10 d	Spleen and thymus indexes↑, macrophages phagocytotic↑, IL-2↑, IL-12↑, TNF-α↑, and IL-10↓	Yang et al. (2013)
Female Balb/c mice (6–8 weeks) with irradiated tumor. <i>In vitro</i> : NIH3T3, HUVEC, 4T1, and bone marrow-derived dendritic cells (BMDC)	APS nanoparticles (ANPs) (equal to 20 mg/kg APS). After each dose of radiation, DNP and ANP (20 mg/kg, 3 times) were injected into the irradiated tumor; <i>in vitro</i> , ANP (equal to 50 µg/ml APS) for 24 h	DC activation↑, maturation↑, antigen presentation↑ through TLR4 pathway. CD4 ⁺ T/Treg↑, CD8 ⁺ T/Treg↑, IFN-γ↑, effector memory T cell↑	Pang et al. (2019)
Fresh tissue samples from 31 patients with HCC	APS 10, 50, 100, 150, and 200 ug/ml for 24, 48, and 72 h	CD4 ⁺ CD25 ⁺ Treg↓ through cytokine balance and FOXP3mRNA↓ in TME. Treg cell migration↓ by SDF-1↓ or CXCR4/CXCL12 pathway↓. Th2 cytokines IL-10↓ and IL-4↓, Th1 cytokines IFN-γ↑	Li et al. (2012)
C57BL/6 mice (7–8 weeks) with B16-F10 melanoma	APS 0.1 g/kg, 10 d	T cell↑, IL-2↑, IFN-γ↑ in peripheral blood, PD-1 mRNA↓ in spleen, PD-L1, PD-L2↓ in tumor	Wang et al. (2014)
S100 sarcoma mice	APS 50, 100, 200 mg/kg, 12 d	CD4 ⁺ T↑, CD8 ⁺ T↓, IL-2↑, IL-4↓	Zou et al. (2012)
Peripheral blood mononuclear cell (PBMC) of 18 cancer patients and 6 control patients	10% Astragalus injection, 48 h	IFN-γ↑, T-bet↑, IL-4↓, GATA3↓, IL-6↓	Wei and Tian, (2003)
SCID mice injected with A549 cells, lung adenocarcinoma A549 and CL1-2 cells	APS 10,40, and 160 mg/kg injected intraperitoneally	AXL↓, vimentin↓, macrophage migration inhibitory factor (MIF)↓, E-cadherin↑, MMP-13↓, AMPK↑	Liao et al. (2020)
RAW264.7 cells	APS 25, 50, and 100 µg/ml	NO↑, TNF-α↑, IL-6↑, iNOS↑, p-p65↑, p-p38↑, Jun N-terminal kinase↑ via NF-κB p65/MAPK signaling↑ pathway	Feng et al. (2021)
23 patients with metastatic disease	500 mg, 250 mg, 3 times/week, 4 w	IL-1β↓, IL-4↓, IL-6↓, IL-13↓, IL-17↓, MCP-1↓, GM-CSF↓, VEGF↓, TGF-β1↓, IFN-γ ↓, and IL-10↓ and IL-12↓	Huang et al. (2019)
RAW264.7 cells on 4T1 cells	APS 1 µg/ml, 100 ng/ml, 24 h	NO↑ and gene expressions of TNF-α↑, IL-6↑, iNOS↑ through TLR4, TLR4-related MAPKs↑, pERK↑, pJNK, phosphorylated p38↑, translocation of NF-κB↑, of IκB-α↓	Wei et al. (2016)
YAC-1 C57BL/6(H-2Kb) peritoneal macrophage	APS 10 mg/ml, 7 days	Abdominal macrophages to M1, TNF-α↑, IL-12↑ NO in macrophage↑; NKG2-mediated NK cell function↑	Chai et al. (2019)
C57BL/6J with Lewis lung cancer cell	100, 50, 25 mg/kg, qd, 3 w	VEGF↓ and EGFR↓ in tumor tissues	Zhao et al. (2019a)
BALB/c, nude, and NOD SCID mice HCT116	50 µg of APS, 7 d	Neutralize VEGF in mice; scFv 4E effectively inhibited human umbilical vein endothelial cells induced by VEGF <i>in vitro</i>	Lee et al. (2020)
SCC-25 BALB/c nude mice	APS 10, 25, 50 mg/kg, tid, 1 w	Ki67↓, VEGF↓, pJAK2/pSTAT3↓ by JAK2/STAT3/c-myc	Deng et al. (2019)
LOVO cell	APS 1.5 mg/ml, 48 h	VEGF-C mRNA↓, HLEC↑	Tie (2019)
C57BL/6 male mice with B16-F10 melanoma	APS 150, 300 mg/kg, 0.2 ml gavage, qd, 14 d	IL-10↓, TGF-β↓, VEGF↓, IFN-γ↑, TNF-α↑, Gr-1 ⁺ CD11b ⁺ myeloid derived suppressor cells	Chai et al. (2012)
EPC in 20 patients	APS 10 mg/kg, 7 d	IL-12↓, IL-6↓ VEGF↓, TREM-1↓, EGFR↓ in p-AKT-AKT-VEGF signal pathway	Sun et al. (2020)

(Continued on following page)

TABLE 2 | (Continued) Effect of APS on ICI signaling pathway and TME.

Cell line and animal model	Dosage	Effect of APS on ICI signaling pathway and TME	Reference
SGC7901 cells; HUVEC cells	APS 10 mg/ml, 48 h	Invasiveness↓, MMP-2↓, MMP-9↓, LOX↓, Snail↓ protein and vimentin mRNA expression↓, and increased E-cadherin mRNA expression↑	Youwei and Yeting (2020)
BMSCs	APS 50 µg/ml, 42 d	α-SMA↓, FAP↓, STAT3↓, p65↓ through pathways of IL-6/STAT3 and TNF-α/NF-κB	Zhang et al. (2018c)
BMSCs and A549 cells	APS 100 µg/ml, 16 h	IL-1β↑, TNF-α↑, IL-6 ↑, NO↑, TIPE2↓, pERK↑, pJNK↑, p-P38↑ with the activation of the MAKIP signaling pathway	Zhu et al. (2018)
MSC; A549	APS 50 µg/ml, 7 d	Expression of acetylated H4K5↓, acetylated H4K8↓, and acetylated H3K9↓, RAS↓, ERK↑, NF-κB p65↑, p-p56↓, TP53↑, caspase-3↑ in MAPK/NF-κB pathway	Zhang et al. (2019)
Hepatocellular carcinoma H22-bearing mice	APS 100, 200, 400 mg/kg, 15 days, qd	Spleen and thymus indexes↑, IL-2↑, IL-6↑, and TNF-α↑, Bax↑, Bcl-2↓	Lai et al. (2017)
H22 cells; S100 cells	APS 50, 100 mg/kg, 10 days, qd	IL-2↑, IL-6↑, IL-12↑, TNF-α↑	Xiao et al. (2009)
Caco2 cell	APS 400 µg/ml, 24 h	APS could suppress the LPS-induced MyD88-TRAF6 activation by a TRIF-dependent way, IL-1β↓, IL-8↓, and TNF-α↓	Liqing (2017)
H22 tumor-bearing mice	APS 100 mg/kg, 24 h	IL-1α↑, IL-2↑, IL-6↑, TNF-α↑, IL-10↓, MDR1 mRNA↓, P-GP↓	Li et al. (2020b)
Female BALB/c mice and female C3H/HeJ mice	APS 50, 100, 200 mg/kg, 0.2 ml, qd, 10 days	APS activates B cells via membrane Ig in a TLR4-independent manner, peritoneal macrophages activation IL-1β↑ and TNF-α↑ in BALB/c mice	Tian et al. (2012)

In a clinical trial, the general situation of patients after APS treatment was significantly improved. APS could significantly reduce the levels of IL-6, IL-12, VEGF, and EGFR to protect cells from esophageal carcinoma (EPC) injury through the pAKT-AKT-VEGF signal pathway in a study by Sun et al. (2020). Another study showed APS inhibits the growth of SCC-25 xenograft tumors, increases the survival rate, and downregulates the expression levels of Ki-67 and VEGF by inhibiting the JAK2/STAT3/c-myc signaling pathway (Deng et al., 2019). As for the Bone mesenchymal stem cells (BMSC), APS had inhibited the conversion of BMSCs to TAFs induced by IL-6 and TNF-α, related to the regulation of the pathways of IL-6/STAT3 and TNF-α/NF-κB. APS improved cell morphology, decreased cell proliferation, and cell cycle disruption. The MAPK/NF-κB pathway, TP53, caspase-3, acetylated H4K5, acetylated H4K8, and acetylated H3K9 were included in this regulatory process (Liqing, 2017; Zhang et al., 2018; Zhang et al., 2019).

These discoveries are significant for us to understand the molecular mechanism of APS on TME. On the basis of the above facts, it is fair to believe APS might successfully increase the immunological activity of the TME along with the ICIs (Figure 1).

Astragalus Polysaccharide Increases the Efficacy of Immunoadoptive Therapy

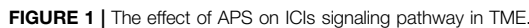
Many studies have suggested that APS could increase the expression of CD40, CD80, and HLA-DR on the surface of DCs (Peng and Luhang, 2006). It could increase the DCs and DC-CIK cells proliferation. APS-treated DCs have the most typical

structures and phenotypic markers of DCs (CD86 and HLA-DR). Liu et al. found that APS increased the amount of IFN-α, TNF-α, and IL-6 generated by pDC and promoted the differentiation of pDC (Chen et al., 2009). These results suggested that APS can enhance human humoral and cellular immunity through the pDC pathway and can be expected to be an effective adjuvant in pDC-based immunotherapy with the effect of TLR9 on pDCs. Moreover, after being processed by APS, DC-CIK cells were more powerful than ordinary DC-CIK cells in antitumor reaction. The combination of APS and DC-CIK cells led to an enhanced killing ability of A549, K562, and esophageal Eca-109 cancer cells. In addition, the cytotoxicity toward Hela and SKOV3 cells in the CIK cells combined with APS group was higher than those in the CIK cells group. *In vivo* results showed that CIK combined with APS inhibited the growth of Hela-implanted tumors significantly, and the inhibitory rate was 80.6% (Peng and Luhang, 2006; Chen et al., 2009; Liu et al., 2010; Gong and Ju, 2016).

According to these studies, APS exerts cytotoxic effects on cancer cells by synergizing the cytotoxicity of CIK cells against tumor cells. These properties of APS are beneficial to the treatment of leukemia, lung cancer, ovarian cancer, cervical cancer, and many other malignant tumors (Zhang et al., 2009; Xu et al., 2011; Chen and Zhang, 2013; Huo and Shan, 2016; Wang et al., 2016).

Astragalus Polysaccharide Could Enhance the Cytotoxicity of Other Immunotherapy

Wang et al. (2008) showed that APS could significantly enhance activation of peritoneal macrophages and splenic



It could be concluded that APS has various kinds of effects on the immune system through LAK cells, NK cells, and so on.

On the other hand, ASP may improve the hypothalamic–pituitary–adrenal (HPA) axis and has been shown to exert hepatoprotective, hematopoietic neuroprotective, cardiovascular-protective, antidiabetic, and antioxidant effects (Si et al., 2015; Xie et al., 2016). APS pretreated mice showed a significant decrease in alanine aminotransferase, NF- κ B expression, aspartate aminotransferase, and lactate dehydrogenase levels and increased antioxidant enzymes. On top of these, APS is a suitable candidate for adjuvant medicines without serious safety concerns, as they are often eaten in the diet for a long time (Liu et al., 2014; Xie et al., 2016).

As for the side effect of APS, in a randomized, double-blind study, APS injection could effectively reduce cancer-related fatigue in advanced cancer patients (310 subjects), and the efficacy of high-dose (500 mg/day) and low-dose (250 mg/day) groups of APS injection was statistically similar. Patients with higher KPS may benefit more from treatment. Five symptoms have been classified as treatment-related adverse events with over 2% incidence, such as rash, pyrexia, feeling cold, chills, and hypersensitivity. More than 90% of the reported adverse events were not related to APS treatment. However, more clinical data are needed to verify the safety of APS in cancer patients and its effect on cancer patients (Wang et al., 2019).

In light of aforementioned studies, it is expected that APS could exert more function in immunotherapy in the future. Nonetheless, there are still some limitations. Firstly, in terms of the effect on adverse events in immunotherapy, such as CTLA-4 or PD-1, the mechanism of APS remains a mystery. Thus, further studies are needed to confirm the feasibility of APS in immunotherapy-related adverse events. Secondly, it is still need to be explore about APS pharmacokinetics and its difference through gut and blood. Thirdly, the investigation about its side effects is still incomplete, which should be elaborated in more clinical trials in the future. Researches collected in this review were mostly conducted in China which might cause some limitations and bias. Therefore, more global researches should be carried out to verify the efficiency of APS. There is still a lot to be desired related to the all-round functions of APS and its indications and contraindications in immunotherapy.

CONCLUSION

Our research systematically reviewed a wide range of clinical trials and laboratory studies, elucidating the potential plausibility of using APS in activating adoptive immunotherapy, as an immunological adjuvant in the future. We found that APS could play a positive part in the immune checkpoint inhibitory signaling pathways by activating the immune-

suppressed microenvironment with regulated cytokines, TLR4, NF- κ B, and MAPK pathways and immune cells such as macrophages, NK cells, DCs, and so on. Also, this review contributes to an understanding of APS as an adjunctive therapy to ICIs by optimizing the immunity balance in the TME and primarily elucidates the underlying mechanism of APS on the microenvironment and immunotherapy systematically.

To conclude, the combination of APS and immunotherapy in cancer treatment has a bright prospect; however, direct effectiveness and the mechanism of APS integrated with ICI on the tumor microenvironment need more confirmations and clinical researches.

AUTHOR CONTRIBUTIONS

In this review, the concept and design were conducted by TC and FK. TC and FK drafted the manuscript. Tables and diagrams were generated by YJ and FK. Critical revision of the manuscript was conducted by XL and YJ. All authors read and approved the final manuscript.

FUNDING

This work is supported by the National Natural Science Foundation of China (No. 81403220 and No. 81904151), Tianjin Health and family planning-high level talent selection and training project, Tianjin Science and Technology Plan Projects (No. 17ZXMFSY00190) and Tianjin Traditional Chinese Medicine Research Project, Tianjin health and family planning commission (No. 2017003).

ACKNOWLEDGMENTS

We thank Hunghsien Tseng for his logistical work for us, and he always backs us up.

REFERENCES

- Ai, L., Xu, A., and Xu, J. (2020). Roles of PD-1/PD-L1 Pathway: Signaling, Cancer, and beyond. *Adv. Exp. Med. Biol.* 1248, 33–59. doi:10.1007/978-981-15-3266-5_3
- Auyeung, K. K., Han, Q. B., and Ko, J. K. (2016). Astragalus Membranaceus: A Review of its Protection against Inflammation and Gastrointestinal Cancers. *Am. J. Chin. Med.* 44 (1), 1–22. doi:10.1142/s0192415x16500014
- Azarov, I., Peskov, K., Helmlinger, G., and Kosinsky, Y. (2019). Role of T Cell-To-Dendritic Cell Chemoattraction in T Cell Priming Initiation in the Lymph Node: An Agent-Based Modeling Study. *Front. Immunol.* 10, 1289. doi:10.3389/fimmu.2019.01289
- Balta, E., Wabnitz, G. H., and Samstag, Y. (2021). Hijacked Immune Cells in the Tumor Microenvironment: Molecular Mechanisms of Immunosuppression and Cues to Improve T Cell-Based Immunotherapy of Solid Tumors. *Int. J. Mol. Sci.* 22 (11). doi:10.3390/ijms22115736
- Bamodu, O. A., Kuo, K. T., Wang, C. H., Huang, W. C., Wu, A. T. H., Tsai, J. T., et al. (2019). Astragalus Polysaccharides (PG2) Enhances the M1 Polarization of Macrophages, Functional Maturation of Dendritic Cells, and T Cell-Mediated Anticancer Immune Responses in Patients with Lung Cancer. *Nutrients* 11 (10). doi:10.3390/nu11102264
- Carlsson, J., Sundqvist, P., Kosuta, V., Fält, A., Giunchi, F., Fiorentino, M., et al. (2020). PD-L1 Expression Is Associated with Poor Prognosis in Renal Cell Carcinoma. *Appl. Immunohistochem. Mol. Morphol.* 28 (3), 213–220. doi:10.1097/pai.0000000000000766
- Carreno, B. M., Magrini, V., Becker-Hapak, M., Kaabinejadian, S., Hundal, J., Petti, A. A., et al. (2015). Cancer Immunotherapy: A Dendritic Cell Vaccine Increases the Breadth and Diversity of Melanoma Neoantigen-specific T Cells. *Science* 348 (6236), 803–808. doi:10.1126/science.aaa3828
- Chai, C., Ma, Q., Zhou, L., Niu, J., Wang, T., Shi, Y., et al. (2019). Astragalus Polysaccharide Can Enhance the Anti-tumor Effect of Mouse Macrophages and Natural Killer Cells. *Chin. J. Microbiol. Immunol.* 39 (4), 292–297.
- Chai, W., He, X., Zhu, J., Lv, C., Zhao, H., Lv, A., et al. (2012). Immunoregulatory Effects of astragalus Polysaccharides on Myeloid Derived Suppressor Cells in B16-F10 Tumor Bearing Mice. *Chin. J. Basic Med. Traditional Chin. Med.* 18 (1), 63–65.

- Chang, F. L., Tsai, K. C., Lin, T. Y., Yang, T. W., Lo, Y. N., Chen, W. C., et al. (2020a). Astragalus Membranaceus-Derived Anti-programmed Death-1 Monoclonal Antibodies with Immunomodulatory Therapeutic Effects against Tumors. *Biomed. Res. Int.* 2020, 3415471. doi:10.1155/2020/3415471
- Chang, H. L., Kuo, Y. H., Wu, L. H., Chang, C. M., Cheng, K. J., Tyan, Y. C., et al. (2020b). The Extracts of Astragalus Membranaceus Overcome Tumor Immune Tolerance by Inhibition of Tumor Programmed Cell Death Protein Ligand-1 Expression. *Int. J. Med. Sci.* 17 (7), 939–945. doi:10.7150/ijms.42978
- Chen, C. J., Li, Z. L., Fu, Q., Liu, Y., Lei, X., Wu, H. C., et al. (2009). Effect of Astragalus Polysaccharides on the Phenotype and Functions of Human Dendritic Cells *In Vitro*. *Nan Fang Yi Ke Da Xue Xue Bao* 29 (6), 1192–1194.
- Chen, D. S., and Mellman, I. (2017). Elements of Cancer Immunity and the Cancer-Immune Set point. *Nature* 541 (7637), 321–330. doi:10.1038/nature21349
- Chen, H., Tan, J., Li, X., Li, H., Wu, W., Wu, Y., et al. (2021). Myeloid and Plasmacytoid Dendritic Cell Combined Vaccines Loaded with Heat-Treated Tumor Cell Lysates Enhance Antitumor Activity in Murine Lung Cancer. *Oncol. Lett.* 21 (2), 90. doi:10.3892/ol.2020.12351
- Chen, H., and Zhang, L. (2013). *The Cytotoxicity of Astragalus Polysaccharide Pulsed Dendritic Cells Co-cultured with Cytokine Induced Killers on K562 Cells*. Lanzhou: Lanzhou University.
- Chen, Z., Liu, L., Gao, C., Chen, W., Vong, C. T., Yao, P., et al. (2020). Astragali Radix (Huangqi): A Promising Edible Immunomodulatory Herbal Medicine. *J. Ethnopharmacol.* 258, 112895. doi:10.1016/j.jep.2020.112895
- Darvin, P., Toor, S. M., Sasidharan Nair, V., and Elkord, E. (2018). Immune Checkpoint Inhibitors: Recent Progress and Potential Biomarkers. *Exp. Mol. Med.* 50 (12), 1–11. doi:10.1038/s12276-018-0191-1
- Deng, L., Cai, T., Wang, J., Xia, Y., and Zhou, Z. (2019). Astragalus Polysaccharide Inhibits Oral Squamous Cell Carcinoma Cell Line SCC-25 Xenograft Tumor by Suppressing JAK/STAT3 Signaling Pathway. *CHINESE JOURNAL CLINICAL ANATOMY* 37 (2), 169–173. doi:10.13418/j.issn.1001-165x.2019.02.011
- Ding, Z., Li, Q., Zhang, R., Xie, L., Shu, Y., Gao, S., et al. (2021). Personalized Neoantigen Pulsed Dendritic Cell Vaccine for Advanced Lung Cancer. *Signal. Transduct. Target. Ther.* 6 (1), 26. doi:10.1038/s41392-020-00448-5
- Feng, S., Ding, H., Liu, L., Peng, C., Huang, Y., Zhong, F., et al. (2021). Astragalus Polysaccharide Enhances the Immune Function of RAW264.7 Macrophages via the NF-Kb P65/MAPK Signaling Pathway. *Exp. Ther. Med.* 21 (1), 20. doi:10.3892/etm.2020.9452
- Fu, J., Wang, Z., Huang, L., Zheng, S., Wang, D., Chen, S., et al. (2014). Review of the Botanical Characteristics, Phytochemistry, and Pharmacology of Astragalus Membranaceus (Huangqi). *Phytother. Res.* 28 (9), 1275–1283. doi:10.1002/ptr.5188
- Garris, C. S., Arlauckas, S. P., Kohler, R. H., Trefny, M. P., Garren, S., Piot, C., et al. (2018). Successful Anti-PD-1 Cancer Immunotherapy Requires T Cell-Dendritic Cell Crosstalk Involving the Cytokines IFN- γ and IL-12. *Immunity* 49 (6), 1148–e7 e1147. doi:10.1016/j.immuni.2018.09.024
- Gong, Y., and Ju, X. (2016). *Influence of Four Polysaccharides on Antitumor Effect of Cytokine-Induced Killer Cells and Dendritic Cells*. Jinan: Shandong University Master Thesis, 1–80.
- Gu, L., Chen, M., Guo, D., Zhu, H., Zhang, W., Pan, J., et al. (2017). PD-L1 and Gastric Cancer Prognosis: A Systematic Review and Meta-Analysis. *PLoS One* 12 (8), e0182692. doi:10.1371/journal.pone.0182692
- Hodi, F. S., O'Day, S. J., McDermott, D. F., Weber, R. W., Sosman, J. A., Haanen, J. B., et al. (2010). Improved Survival with Ipilimumab in Patients with Metastatic Melanoma. *N. Engl. J. Med.* 363 (8), 711–723. doi:10.1056/NEJMoa1003466
- Huang, W. C., Kuo, K. T., Bamodu, O. A., Lin, Y. K., Wang, C. H., Lee, K. Y., et al. (2019). Astragalus Polysaccharide (PG2) Ameliorates Cancer Symptom Clusters, as Well as Improves Quality of Life in Patients with Metastatic Disease, through Modulation of the Inflammatory Cascade. *Cancers (Basel)* 11 (8). doi:10.3390/cancers11081054
- Huo, H., and Shan, B. (2016). *Vitro and in Vivo Anti-tumor Effects of CIK Combined with Astragalus Polysaccharides upon Cervical Cancer Hela Cells*. Shijiazhuang: Hebei Medical University, 1–39.
- Kantoff, P. W., Higano, C. S., Shore, N. D., Berger, E. R., Small, E. J., Penson, D. F., et al. (2010). Sipuleucel-T Immunotherapy for Castration-Resistant Prostate Cancer. *N. Engl. J. Med.* 363 (5), 411–422. doi:10.1056/NEJMoa1001294
- Kazandjian, D., Khozin, S., Blumenthal, G., Zhang, L., Tang, S., Libeg, M., et al. (2016). Benefit-Risk Summary of Nivolumab for Patients with Metastatic Squamous Cell Lung Cancer after Platinum-Based Chemotherapy: A Report from the US Food and Drug Administration. *JAMA Oncol.* 2 (1), 118–122. doi:10.1001/jamaoncol.2015.3934
- Keskin, D. B., Anandappa, A. J., Sun, J., Tirosh, I., Mathewson, N. D., Li, S., et al. (2019). Neoantigen Vaccine Generates Intratumoral T Cell Responses in Phase Ib Glioblastoma Trial. *Nature* 565 (7738), 234–239. doi:10.1038/s41586-018-0792-9
- Kong, B. Y., Bolton, H., Kim, J. W., Silveira, P. A., Fromm, P. D., and Clark, G. J. (2019). On the Other Side: Manipulating the Immune Checkpoint Landscape of Dendritic Cells to Enhance Cancer Immunotherapy. *Front. Oncol.* 9, 50. doi:10.3389/fonc.2019.00050
- Lai, X., Xia, W., Wei, J., and Ding, X. (2017). Therapeutic Effect of Astragalus Polysaccharides on Hepatocellular Carcinoma H22-Bearing Mice. *Dose Response* 15 (1), 1559325816685182. doi:10.1177/1559325816685182
- Lee, K. Y., and Jeon, Y. J. (2005). Macrophage Activation by Polysaccharide Isolated from Astragalus Membranaceus. *Int. Immunopharmacol.* 5 (7–8), 1225–1233. doi:10.1016/j.intimp.2005.02.020
- Lee, Y. C., Huang, H. T., Chang, C. D., Chen, C. T., Lin, T. Y., Yang, T. W., et al. (2020). Isolation of Anti-VEGF Monoclonal Antibodies with Neutralizing Effects from an Astragalus-Induced Immune Antibody Library. *Int. Immunopharmacol.* 88, 107007. doi:10.1016/j.intimp.2020.107007
- Li, Q., Bao, J. M., Li, X. L., Zhang, T., and Shen, X. H. (2012). Inhibiting Effect of Astragalus Polysaccharides on the Functions of CD4+CD25 high Treg Cells in the Tumor Microenvironment of Human Hepatocellular Carcinoma. *Chin. Med. J. (Engl)* 125 (5), 786–793.
- Li, W., Hu, X., Wang, S., Jiao, Z., Sun, T., Liu, T., et al. (2020a). Characterization and Anti-tumor Bioactivity of astragalus Polysaccharides by Immunomodulation. *Int. J. Biol. Macromol.* 145, 985–997. doi:10.1016/j.jbiomac.2019.09.189
- Li, W., Hu, X., Wang, S., Wang, H., Parungao, R., Wang, Y., et al. (2018). Detection and Evaluation of Anti-cancer Efficiency of Astragalus Polysaccharide via a Tissue Engineered Tumor Model. *Macromol. Biosci.* 18 (11), e1800223. doi:10.1002/mabi.201800223
- Li, W., Song, K., Wang, S., Zhang, C., Zhuang, M., Wang, Y., et al. (2019). Anti-tumor Potential of astragalus Polysaccharides on Breast Cancer Cell Line Mediated by Macrophage Activation. *Mater. Sci. Eng. C Mater. Biol. Appl.* 98, 685–695. doi:10.1016/j.msec.2019.01.025
- Li, Y., Xu, Y., Pan, C., Ren, Z., and Yang, X. (2020b). TRIF Is Essential for the Anti-inflammatory Effects of Astragalus Polysaccharides on LPS-Infected Caco2 Cells. *Int. J. Biol. Macromol.* 159, 832–838. doi:10.1016/j.jbiomac.2020.05.005
- Liao, C. H., Yong, C. Y., Lai, G. M., Chow, J. M., Cheng, C. F., Fang, C. L., et al. (2020). Astragalus Polysaccharide (PG2) Suppresses Macrophage Migration Inhibitory Factor and Aggressiveness of Lung Adenocarcinoma Cells. *Am. J. Chin. Med.* 48 (6), 1491–1509. doi:10.1142/s0192415x20500731
- Liqing, Z. (2017). *A Study on Immunomodulatory Mechanism of Astragalus Polysaccharides Mediated by Tlr4-Mediated Myd88 Dependent Signaling Pathway*. Chongqing: Chongqing Medical University, 1–55.
- Liu, L., Zhang, Y., Lu, S., Sun, Y., and He, G. (2010). Regulation on Function and Maturation of Plasmacytoid Dendritic Cells by Astragalus Polysaccharide. *Cell Mol. Immunol.* (8), 712–715. doi:10.3969/j.issn.1000-484X.2010.08.009
- Liu, P., Zhao, H., and Luo, Y. (2017). Anti-Aging Implications of Astragalus Membranaceus (Huangqi): A Well-Known Chinese Tonic. *Aging Dis.* 8 (6), 868–886. doi:10.14336/ad.2017.0816
- Liu, Y., Liu, F., Yang, Y., Li, D., Lv, J., Ou, Y., et al. (2014). Astragalus Polysaccharide Ameliorates Ionizing Radiation-Induced Oxidative Stress in Mice. *Int. J. Biol. Macromol.* 68, 209–214. doi:10.1016/j.jbiomac.2014.05.001
- Necchi, A., Joseph, R. W., Lorient, Y., Hoffman-Censits, J., Perez-Gracia, J. L., Petrylak, D. P., et al. (2017). Atezolizumab in Platinum-Treated Locally Advanced or Metastatic Urothelial Carcinoma: post-progression Outcomes from the Phase II IMvigor210 Study. *Ann. Oncol.* 28 (12), 3044–3050. doi:10.1093/annonc/mdx518
- Noman, M. Z., Desantis, G., Janji, B., Hasmim, M., Karray, S., Dessen, P., et al. (2014). PD-L1 Is a Novel Direct Target of HIF-1 α , and its Blockade under Hypoxia Enhanced MDSC-Mediated T Cell Activation. *J. Exp. Med.* 211 (5), 781–790. doi:10.1084/jem.20131916
- Ott, P. A., Hu, Z., Keskin, D. B., Shukla, S. A., Sun, J., Bozym, D. J., et al. (2017). An Immunogenic Personal Neoantigen Vaccine for Patients with Melanoma. *Nature* 547 (7662), 217–221. doi:10.1038/nature22991

- Pang, G., Chen, C., Liu, Y., Jiang, T., Yu, H., Wu, Y., et al. (2019). Bioactive Polysaccharide Nanoparticles Improve Radiation-Induced Abscopal Effect through Manipulation of Dendritic Cells. *ACS Appl. Mater. Inter.* 11 (45), 42661–42670. doi:10.1021/acsami.9b16814
- Peng, S., and Luhang, Z. (2006). *Regulation on Phenotypic and Functional Maturation of Dendritic Cells by Astragalus Mongholicus Polysaccharides*. Hangzhou: Zhejiang University, 1–41.
- Sanmamed, M. F., and Chen, L. (2018). A Paradigm Shift in Cancer Immunotherapy: From Enhancement to Normalization. *Cell* 175 (2), 313–326. doi:10.1016/j.cell.2018.09.035
- Sanmamed, M. F., and Chen, L. (2019). A Paradigm Shift in Cancer Immunotherapy: From Enhancement to Normalization. *Cell* 176 (3), 677. doi:10.1016/j.cell.2019.01.008
- Shao, B. M., Xu, W., Dai, H., Tu, P., Li, Z., and Gao, X. M. (2004). A Study on the Immune Receptors for Polysaccharides from the Roots of Astragalus Membranaceus, a Chinese Medicinal Herb. *Biochem. Biophys. Res. Commun.* 320 (4), 1103–1111. doi:10.1016/j.bbrc.2004.06.065
- Shortman, K., and Liu, Y. J. (2002). Mouse and Human Dendritic Cell Subtypes. *Nat. Rev. Immunol.* 2 (3), 151–161. doi:10.1038/nri746
- Si, M. W., Yang, M. K., and Fu, X. D. (2015). Effect of Hypothalamic-Pituitary-Adrenal axis Alterations on Glucose and Lipid Metabolism in Diabetic Rats. *Genet. Mol. Res.* 14 (3), 9562–9570. doi:10.4238/2015.August.14.19
- Sui, H., Ma, N., Wang, Y., Li, H., Liu, X., Su, Y., et al. (2018). Anti-PD-1/PD-L1 Therapy for Non-small-cell Lung Cancer: Toward Personalized Medicine and Combination Strategies. *J. Immunol. Res.* 2018, 6984948. doi:10.1155/2018/6984948
- Sun, S., He, X., Chai, W., Lv, C., Wang, P., Lv, A., et al. (2013). Effects of Astragalus Polysaccharide on Treg Cells in Tumor-Bearing Mice. *Chin. J. Exp. Traditional Med. Formulae* 19 (12), 176–178. doi:10.11653/syfx2013120176
- Sun, X., Wang, L., Liu, C., and Zang, W. (2020). Therapeutic Effects and Mechanism of Ginseng Polysaccharide on colon Carcinoma and Inflammatory Factors via pPKA-PKA-VEGF Signaling Pathway. *Guangdong Med. J.* 41 (21), 2187–2191. doi:10.13820/j.cnki.gdxx.20194330
- Teng, C. F., Wang, T., Shih, F. Y., Shyu, W. C., and Jeng, L. B. (2021). Therapeutic Efficacy of Dendritic Cell Vaccine Combined with Programmed Death 1 Inhibitor for Hepatocellular Carcinoma. *J. Gastroenterol. Hepatol.* 36, 1988–1996. doi:10.1111/jgh.15398
- Tian, Q. E., Li, H. D., Yan, M., Cai, H. L., Tan, Q. Y., and Zhang, W. Y. (2012). Astragalus Polysaccharides Can Regulate Cytokine and P-Glycoprotein Expression in H22 Tumor-Bearing Mice. *World J. Gastroenterol.* 18 (47), 7079–7086. doi:10.3748/wjg.v18.i47.7079
- Tsao, S. M., Wu, T. C., Chen, J., Chang, F., and Tsao, T. (2021). Astragalus Polysaccharide Injection (PG2) Normalizes the Neutrophil-To-Lymphocyte Ratio in Patients with Advanced Lung Cancer Receiving Immunotherapy. *Integr. Cancer Ther.* 20, 1534735421995256. doi:10.1177/1534735421995256
- Wang, C. H., Lin, C. Y., Chen, J. S., Ho, C. L., Rau, K. M., Tsai, J. T., et al. (2019). Karnofsky Performance Status as a Predictive Factor for Cancer-Related Fatigue Treatment with Astragalus Polysaccharides (PG2) Injection-A Double Blind, Multi-Center, Randomized Phase IV Study. *Cancers (Basel)* 11 (2). doi:10.3390/cancers11020128
- Wang, G., Lin, W., Zhao, R., and Lin, N. (2008). Effects of Six Polysaccharides Extracted from Plants on the Immunological Cells of Mice. *Wei Sheng Yan Jiu* 37 (5), 577–580.
- Wang, G., Ding, G., Shi, X., Wu, Y., Lou, D., Yang, X., et al. (1995). Regulation of Astragalus Polysaccharide and Interleukin-2 to Lak Cytotoxicity. *CHINESE JOURNAL MICROECOLOGY* 7 (6), 11–15. doi:10.13381/j.cnki.cjm.1995.06.004
- Wang, G., and Lou, D. (1992). Enhancing Effect of Astragalus Polysaccharide on LAK Cytotoxicity. *Chin. J. Public Health* 11 (4), 233.
- Wang, G., Zhou, Z., Lou, D., Shi, X., Liang, Z., Wu, Y., et al. (1994). Study of the Antitumor Effect with Astragalus Polysaccharide and IL-2/Lak. *Chin. J. Immunol.* 10 (6), 359–361.
- Wang, J., Han, Q., Wang, B., Yan, X., Li, W., Zhang, M., et al. (2016). Effect of Astragalus Polysaccharide Induced DCs Co-cultured with CIK Cells on Eca-109 Cells. *ACTA CHINESE MEDICINE* 31 (4), 478–481. doi:10.16368/j.issn.1674-8999.2016.04.136
- Wang, J., Wang, J., Zhang, T., and Cheng, X. (2014). Regulatory Effect of Astragalus Polysaccharin on Expression of PD-1/PD-Ls Molecules in Melanoma Mice. *Shanghai Univ. Traditional Chin. Med.* 28 (5), 74–79. doi:10.16306/j.1008-861x.2014.05.019
- Wculek, S. K., Amores-Iniesta, J., Conde-Garrosa, R., Khouili, S. C., Melero, I., and Sancho, D. (2019). Effective Cancer Immunotherapy by Natural Mouse Conventional Type-1 Dendritic Cells Bearing Dead Tumor Antigen. *J. Immunother. Cancer* 7 (1), 100. doi:10.1186/s40425-019-0565-5
- Wei, H., and Tian, Z. (2003). *The Pathogenesis and Reversal of Th2 Tumor*. Jinan: Shan Dong University, 1–121.
- Wei, W., Li, Z. P., Bian, Z. X., and Han, Q. B. (2019). Astragalus Polysaccharide RAP Induces Macrophage Phenotype Polarization to M1 via the Notch Signaling Pathway. *Molecules* 24 (10). doi:10.3390/molecules24102016
- Wei, W., Xiao, H. T., Bao, W. R., Ma, D. L., Leung, C. H., Han, X. Q., et al. (2016). TLR-4 May Mediate Signaling Pathways of Astragalus Polysaccharide RAP Induced Cytokine Expression of RAW264.7 Cells. *J. Ethnopharmacol.* 179, 243–252. doi:10.1016/j.jep.2015.12.060
- Weng, L., Liu, Y., Liu, X., Zhang, Y., Zhao, L., and Deng, X. (2003). Astragalus Polysaccharide Powder Injection on Secretion of Mouse Spleen Cells Influence of Cytokines and NK Killing Ability. *Study J. Traditional Chin. Med.* 21 (9), 1522–1524. doi:10.13193/j.archctcm.2003.09.112.wengl.062
- West, E. E., Jin, H. T., Rasheed, A. U., Penaloza-Macmaster, P., Ha, S. J., Tan, W. G., et al. (2013). PD-L1 Blockade Synergizes with IL-2 Therapy in Reinvigorating Exhausted T Cells. *J. Clin. Invest.* 123 (6), 2604–2615. doi:10.1172/jci67008
- Wojtukiewicz, M. Z., Rek, M. M., Karpowicz, K., Górka, M., Polityńska, B., Wojtukiewicz, A. M., et al. (2021). Inhibitors of Immune Checkpoints-PD-1, PD-L1, CTLA-4-New Opportunities for Cancer Patients and a New challenge for Internists and General Practitioners. *Cancer Metastasis Rev.* doi:10.1007/s10555-021-09976-0
- Xiao, S., Ren, M., Liu, M., Li, R., and Li, M. (2009). Effect of astragalus Polysaccharides Onthe Level of IL-2, IL-6, IL-12 andTNF- α Intumor-Bearing Mice. *Sichuan J. Physiol. Sci.* 31 (1), 7–8.
- Xie, J. H., Jin, M. L., Morris, G. A., Zha, X. Q., Chen, H. Q., Yi, Y., et al. (2016). Advances on Bioactive Polysaccharides from Medicinal Plants. *Crit. Rev. Food Sci. Nutr.* 56 Suppl 1 (Suppl. 1), S60–S84. doi:10.1080/10408398.2015.1069255
- Xie, M., Huang, X., Ye, X., and Qian, W. (2019). Prognostic and Clinicopathological Significance of PD-1/pd-L1 Expression in the Tumor Microenvironment and Neoplastic Cells for Lymphoma. *Int. Immunopharmacol.* 77, 105999. doi:10.1016/j.intimp.2019.105999
- Xu, Y., Liu, X., and Qu, F. (2011). Effects of Chinese Medicine Polysaccharides Combined with Adoptive Immunotherapy on Ovarian Cancer. *Chin. J. Exp. Traditional Med. Formulae* 17 (21), 231–234. doi:10.13422/j.cnki.syfxj.2011.21.006
- Yang, B., Xiao, B., and Sun, T. (2013). Antitumor and Immunomodulatory Activity of Astragalus Membranaceus Polysaccharides in H22 Tumor-Bearing Mice. *Int. J. Biol. Macromol.* 62, 287–290. doi:10.1016/j.ijbiomac.2013.09.016
- Yang, H., and Zhao, G. (1998). Death and Apoptosis of LAK Cell during Immunologic Assault and the Rescuing Effects of APS. *CHINESE JOURNAL CLINICAL ONCOLOGY* 25 (9), 669–672.
- Youwei, T., and Yeting, L. (2020). Effects of Astragalus Polysaccharides on *In Vitro* Cell Metastasis of SGC7901 Induced by Non-contact Co-cultured HUVECs Cells. *Chin. Traditional Patent Med.* 42 (4), 887–892. doi:10.3969/j.issn.1001-1528.2020.04.012
- Zeng, P. Y., Deng, L. L., Yue, L. L., and Zhang, L. S. (2012). Effect of astragalus Polysaccharide on Sensitivity of Leukemic Cell Line HL-60 to NK Cell Cytotoxicity and its Mechanism. *Zhongguo Shi Yan Xue Ye Xue Za Zhi* 20 (4), 880–883.
- Zhang, J., Wu, C., Gao, L., Du, G., and Qin, X. (2020a). Astragaloside IV Derived from Astragalus Membranaceus: A Research Review on the Pharmacological Effects. *Adv. Pharmacol.* 87, 89–112. doi:10.1016/bs.apha.2019.08.002
- Zhang, S., Mu, X., Wang, H., and Jiang, S. (2009). Enhancement of the Cytotoxic Effect of Cytokine Induced Killers by Dendritic Cells Pulsed with astragalus Polysaccharides. *Cell Mol. Immunol.* 25 (2), 140–142.
- Zhang, X., He, T., Li, Y., Chen, L., Liu, H., Wu, Y., et al. (2020b). Dendritic Cell Vaccines in Ovarian Cancer. *Front. Immunol.* 11, 613773. doi:10.3389/fimmu.2020.613773
- Zhang, X. P., Li, Y. D., Luo, L. L., Liu, Y. Q., Li, Y., Guo, C., et al. (2018a). Astragalus Saponins and Liposome Constitute an Efficacious Adjuvant Formulation for Cancer Vaccines. *Cancer Biother. Radiopharm.* 33 (1), 25–31. doi:10.1089/cbr.2017.2369

- Zhang, X. (2011). *The Clinical Observation of Radix Astragali Polysaccharide Inoculation Fluid union DC-CIK Cure Lacking in Vital Energy Syndrome Breast Cancer Patient*. Fuzhou: Fujian University of Traditional Chinese Medicine, 1–34.
- Zhang, Y., Jia, Y., Li, X., Wang, L., Du, M., and Zhang, X. (2018b). Clinical Observation on Astragalus Polysaccharide Injection Combined with CIK Cells Treating NSCLC Patients with Qi Deficiency Syndrome. *Chin. Traditional Herbal Drugs* 49 (7), 1647–1651. doi:10.7501/j.issn.0253-2670.2018.07.024
- Zhang, Y., Luo, Y., Liu, Y., Wang, L., Xu, X., Feng, C., et al. (2018c). Effects of Astragalus Polysaccharides on Pathways of IL-6/STAT3 and TNF- α /NF- κ B in Process of Differentiation from. *BMSCs TAFs Chin. J. Inf. TCM* 25 (10), 54–59. doi:10.3969/j.issn.1005-5304.2018.10.013
- Zhang, Y. M., Liu, Y. Q., Liu, D., Zhang, L., Qin, J., Zhang, Z., et al. (2019). The Effects of Astragalus Polysaccharide on Bone Marrow-Derived Mesenchymal Stem Cell Proliferation and Morphology Induced by A549 Lung Cancer Cells. *Med. Sci. Monit.* 25, 4110–4121. doi:10.12659/msm.914219
- Zhao, L., Zhong, Y., Liang, J., Gao, H., and Tang, N. (2019a). Effect of Astragalus Polysaccharide on the Expression of VEGF and EGFR in Mice with Lewis Transplantable Lung Cancer. *J. Coll. Physicians Surg. Pak* 29 (4), 392–394. doi:10.29271/jcpsp.2019.04.392
- Zhao, P., Li, L., Jiang, X., and Li, Q. (2019b). Mismatch Repair Deficiency/microsatellite Instability-High as a Predictor for Anti-PD-1/pd-L1 Immunotherapy Efficacy. *J. Hematol. Oncol.* 12 (1), 54. doi:10.1186/s13045-019-0738-1
- Zheng, Y., Ren, W., Zhang, L., Zhang, Y., Liu, D., and Liu, Y. (2020). A Review of the Pharmacological Action of Astragalus Polysaccharide. *Front. Pharmacol.* 11, 349. doi:10.3389/fphar.2020.00349
- Zhu, J., Zhang, Y., Fan, F., Wu, G., Xiao, Z., and Zhou, H. (2018). Tumor Necrosis Factor- α -Induced Protein 8-like-2 Is Involved in the Activation of Macrophages by Astragalus Polysaccharides In vitro. *Mol. Med. Rep.* 17 (5), 7428–7434. doi:10.3892/mmr.2018.8730
- Zou, P., Zhao, C., Li, P., Xiaoyan, Y., and Huang, H. (2012). Effects of Astragalus Polysaccharides on Anti-s180 Sarcoma and Immuno-Logical Regulation. *ACTA ACADEMIAE MEDICINAE ZUNYI* 35 (1), 17–20.

Conflict of Interest: The authors declare that the research was conducted in the absence of any commercial or financial relationships that could be construed as a potential conflict of interest.

Publisher's Note: All claims expressed in this article are solely those of the authors and do not necessarily represent those of their affiliated organizations, or those of the publisher, the editors, and the reviewers. Any product that may be evaluated in this article, or claim that may be made by its manufacturer, is not guaranteed or endorsed by the publisher.

Copyright © 2021 Kong, Chen, Li and Jia. This is an open-access article distributed under the terms of the Creative Commons Attribution License (CC BY). The use, distribution or reproduction in other forums is permitted, provided the original author(s) and the copyright owner(s) are credited and that the original publication in this journal is cited, in accordance with accepted academic practice. No use, distribution or reproduction is permitted which does not comply with these terms.



Perifosine, a Bioavailable Alkylphospholipid Akt Inhibitor, Exhibits Antitumor Activity in Murine Models of Cancer Brain Metastasis Through Favorable Tumor Exposure

Keisuke Taniguchi^{1*}, Tomo Suzuki^{1†}, Tomomi Okamura¹, Akinobu Kurita¹, Gou Nohara², Satoru Ishii², Shoichi Kado¹, Akimitsu Takagi¹, Momomi Tsugane¹ and Yoshiyuki Shishido¹

¹ Yakult Central Institute, Yakult Honsha Co., Ltd., Tokyo, Japan, ² Pharmaceutical Research & Development Department, Yakult Honsha Co., Ltd., Tokyo, Japan

OPEN ACCESS

Edited by:

Peixin Dong,
Hokkaido University, Japan

Reviewed by:

Mari Iida,
University of Wisconsin-Madison,
United States
Xiangyi Ma,
Huazhong University of Science and
Technology, China

*Correspondence:

Keisuke Taniguchi
keisuke-taniguchi@yakult.co.jp

[†]These authors share first authorship

Specialty section:

This article was submitted to
Pharmacology of Anti-Cancer Drugs,
a section of the journal
Frontiers in Oncology

Received: 06 August 2021

Accepted: 19 October 2021

Published: 04 November 2021

Citation:

Taniguchi K, Suzuki T, Okamura T, Kurita A, Nohara G, Ishii S, Kado S, Takagi A, Tsugane M and Shishido Y (2021) Perifosine, a Bioavailable Alkylphospholipid Akt Inhibitor, Exhibits Antitumor Activity in Murine Models of Cancer Brain Metastasis Through Favorable Tumor Exposure. *Front. Oncol.* 11:754365. doi: 10.3389/fonc.2021.754365

Metastatic brain tumors are regarded as the most advanced stage of certain types of cancer; however, chemotherapy has played a limited role in the treatment of brain metastases. Here, we established murine models of brain metastasis using cell lines derived from human brain metastatic tumors, and aimed to explore the antitumor efficacy of perifosine, an orally active allosteric Akt inhibitor. We evaluated the effectiveness of perifosine by using it as a single agent in ectopic and orthotopic models created by injecting the DU 145 and NCI-H1915 cell lines into mice. Initially, the injected cells formed distant multifocal lesions in the brains of NCI-H1915 mice, making surgical resection impractical in clinical settings. We determined that perifosine could distribute into the brain and remain localized in that region for a long period. Perifosine significantly prolonged the survival of DU 145 and NCI-H1915 orthotopic brain tumor mice; additionally, complete tumor regression was observed in the NCI-H1915 model. Perifosine also elicited much stronger antitumor responses against subcutaneous NCI-H1915 growth; a similar trend of sensitivity to perifosine was also observed in the orthotopic models. Moreover, the degree of suppression of NCI-H1915 tumor growth was associated with long-term exposure to a high level of perifosine at the tumor site and the resultant blockage of the PI3K/Akt signaling pathway, a decrease in tumor cell proliferation, and increased apoptosis. The results presented here provide a promising approach for the future treatment of patients with metastatic brain cancers and emphasize the importance of enriching a patient population that has a higher probability of responding to perifosine.

Keywords: brain cancer, metastasis, signaling pathway, PI3K, AKT, apoptosis

INTRODUCTION

The development of metastases adversely affects both quality of life and survival, and 20–40% of all cancer patients eventually experience brain metastasis (1). Any type of tumor can spread to the brain; however, the types of cancer that are most likely to metastasize to the brain are lung, breast, colorectal, renal, and melanoma, whereas gastrointestinal and prostate cancers are less frequent (2). Despite recent

progress in the field of molecular targeted therapy, strategies to effectively treat metastatic brain tumors remain insufficient (3). Consequently, an urgent need remains for the development of effective therapies for these patients. Brain tumors, regardless of whether they are primary or metastatic, are difficult to control, and curative surgery frequently is not a feasible option. Most anticancer agents have limited access to the central nervous system (CNS) following systemic administration. One of the primary causes of this is the blood-brain barrier (BBB) that leads to relatively ineffective drug concentrations within the CNS tissue, a characteristic of a number of chemotherapeutic drugs. This, in turn, hinders the antitumor efficacy of these drugs in the brain following local or systemic administration (4). Based on this, antineoplastic agents that can penetrate the CNS and achieve long-term and high-level exposure are likely to be effective in the treatment of primary and metastatic brain tumors.

PI3K/Akt signaling has been implicated in various malignant cancers and is one of the key signal transduction cascades involved in the control of cellular proliferation, invasion, and survival (5–12). Akt is acknowledged as a major downstream effector of PI3K; Akt becomes fully activated through its phosphorylation at both T308 and S473 (6, 7). Constitutive Akt activation has been demonstrated to render tumor cells highly invasive (5). Additionally, Akt activation has been reported to induce epithelial-to-mesenchymal transition by regulating matrix metalloproteinases, ultimately resulting in increased invasiveness and metastasis (5, 13, 14). Thus, the PI3K/Akt pathway is considered as an attractive target for cancer therapy, and several inhibitors targeting this pathway are currently under evaluation in preclinical and clinical studies (5, 15, 16). Perifosine is the first orally bioactive alkylphospholipid that is currently being tested in clinical trials (16–19). Although the specific mechanisms underlying the anti-cancer activity of perifosine remain to be fully elucidated, perifosine is known to bind to the pleckstrin-homology domain that targets Akt activity by perturbing the membrane translocation of Akt (17–20).

To date, the potential role of perifosine in the context of metastatic brain cancers has not been thoroughly examined. Herein, we sought to evaluate the usefulness of human metastatic brain tumor models, using tumor cell lines originating from human brain metastatic sites, to assess the effectiveness of perifosine against these tumor models. Our results indicated that orally administered perifosine was efficiently delivered into tumor tissues and exhibited powerful antitumor efficacy. Our findings support the concept that prolonged exposure to a high level of perifosine at the tumor site and the suppression of Akt pathway activation are both vital events underlying *in vivo* antitumor activity. Given these encouraging findings, perifosine appears to be a promising candidate for the future treatment of patients with metastatic brain cancers.

MATERIALS AND METHODS

Human Cancer Cell Lines

The primary glioblastoma cell line U-87 MG, the hormone-refractory prostate cancer cell line DU 145, and the large cell lung

cancer cell line NCI-H1915 (hereinafter “H1915”) were purchased from the American Type Culture Collection (ATCC, Manassas, VA). DU 145 and H1915 cell lines were originally isolated from a brain metastasis. All cell lines were maintained according to the supplier’s instructions and routinely tested for mycoplasma contamination using MycoAlerTM (Lonza, Walkersville, MD, USA).

Chemicals, Antibodies, and Reagents

Perifosine was obtained from Aeterna Zentaris GmbH (Frankfurt, Germany). For the *in vitro* assays, perifosine was dissolved in dimethyl sulfoxide (DMSO), and the final concentration of DMSO was adjusted to 0.1%. For the *in vivo* studies, perifosine was dissolved in physiological saline (FUSO Pharmaceutical Industries, Ltd., Osaka, Japan). The antibodies used in this study are listed in **Supplementary Table 1**. EnVision System HRP-Labelled Polymer Secondary antibody was purchased from Agilent Technologies (Santa Clara, CA, USA). All other reagents were obtained from Sigma-Aldrich (St. Louis, MO, USA) unless otherwise specified.

Dose Response Curves for IC₅₀ Determination

Dose response curves were generated for perifosine to determine the inhibitory concentration required to achieve 50% cell death (IC₅₀ values). Briefly, cells were grown overnight in 96-well plates and then left untreated or treated with perifosine at different concentrations. After 48 h, the extent of cell viability was assessed according to a WST-8 dye-based assay (Kishida Chemical, Osaka, Japan) as described previously (21). For each treatment condition, the mean values from triplicate wells were calculated.

Development of Tumor Xenograft Models

Five-week-old male BALB/c nude mice were purchased from Japan SLC, Inc. (Shizuoka, Japan).

Protocol Number 1 (Intracranial Tumor Transplantation)

Brain tumors were initiated using the cerebral injection procedure. Tumor cells can either be injected “freehand” or through the use of stereotactic instruments. The hole in the skull can be created either by simply pricking with a two-step injection needle (tip: 27G, 3 mm; Natsume Seisakusyo, Tokyo, Japan) or through the use of a small drill (1 mm anterior and 2 mm to the right of the bregma) (22–27). We preliminarily confirmed that all intracranial orthotopic brain metastasis mice created using U-87 MG, DU 145, and H1915 cells, but none of the sham-operated mice, exhibited abnormalities such as emaciation, falling, ataxic gait, and/or stupor over time, and all mice reached an endpoint when they were not treated, regardless of any differences between the two procedures (n = 3–15). Based on these findings, we selected the freehand method owing to our need to inoculate large numbers of mice, as this method increases throughput relative to the use of the stereotactic frame. Briefly, mice were anesthetized by inhalation of 1.5% isoflurane (Mylan Seiyaku Ltd., Tokyo, Japan). The dorsal head surface of mice was disinfected with 70% alcohol. A 3 mm two-step injection

needle attached to a microsyringe (Hamilton Company, Reno, NV, USA) was inserted into a unilateral injection site to create a hole in the skull, and the needle was inserted intracranially at 3 mm below the skull surface. U-87 MG (1×10^6), DU 145 (5×10^5), or H1915 (7×10^5) cells suspended in 5 μ L PBS were then injected (day 0). The sham-operated mice underwent the same procedures but did not receive tumor cell injections.

Protocol Number 2 (Subcutaneous Tumor Transplantation)

DU 145 (7×10^6 cells in 0.1 mL) or H1915 (3×10^6 cells in 0.1 mL) cells were subcutaneously inoculated into the right flank of mice and allowed to form a palpable tumor.

Evaluation of Antitumor Activity

We designed a loading (180 mg/kg) and maintenance (45 mg/kg) dosing regimen for a series of experiments, with the aim of efficiently delivering perifosine into tumor sites. The chemotherapy experiments were performed using two different protocols as described below.

Protocol Number 1 (Intracranial Orthotopic Brain Metastasis Models)

Prior to the initiation of efficacy studies, we preliminarily examined tumor growth at the injection site to provide a rationale for treatment schedules, histologically detected viable tumor cells at three days after tumor cell injection (day 3), and determined the characteristics of growth tendencies on day 7. Although therapy is often initiated as early as within two days of inoculation owing to rapidly progressive diseases in preclinical models (28–30), we selected “day 3” or “day 7” as the initial day of treatment based on this preliminary result and in anticipation of clinical use of perifosine.

The animals were assigned homogeneously to each test group based on the body weight on day 3. The animals were treated orally with either vehicle or perifosine with a 5-day-on/2-day-off schedule, as indicated in **Tables 1** and **2**. The survival times of the mice were then tested for 64 days. For humane reasons, the mice were euthanized when they appeared moribund, and this time point was defined as death in our survival analysis. Mortality was monitored by recording the percentage increase in life span (ILS) and median survival time (MST) according to the following formula: $ILS (\%) = (MST \text{ of the treated group} / MST \text{ of the control group} - 1) \times 100$. On day 64, blood was collected from the abdominal vena cava of survived mice under isoflurane anesthesia at 24 h after the final dose. Blood samples were treated with heparin to obtain plasma. Plasma levels of glucose, total cholesterol (T-CHO), total bilirubin (T-BIL), blood urea nitrogen (BUN), creatinine (CRE), alkaline phosphatase (ALP)

were analyzed using an automatic chemistry analyzer (LABOSPECT003, Hitachi High-Tech Co., Tokyo, Japan).

Protocol Number 2 (Subcutaneous Ectopic Tumor Models)

Day “n” denotes the day on which the effects of drugs were estimated, and day “1” denotes the first day of treatment. Once the tumors reached an average volume of 100 mm³, the animals (n = 5) were randomly allocated into two groups based on tumor volume (TV) and then administered orally with either vehicle or a perifosine (180 mg/kg) *loading* dose on day 1 followed by *maintenance* doses of 45 mg/kg (180/45) with a 5-day-on/2-day-off \times 3 cycle schedule. Tumor growth was monitored until day 22 by measuring two perpendicular diameters with a digital caliper (Mitutoyo, Kanagawa, Japan), and TV was calculated as shown previously (31, 32). The tumor growth inhibition rate (TGI, %) was calculated using the following formula:

$$TGI(\%) = (1 - \text{mean TV of the perifosine} - \text{treated group} / \text{mean TV in the control group}) \times 100$$

On day 22, xenograft tumors were excised, weighed, and snap-frozen at 4 h following the last dose. The body weight of each mouse was monitored twice each week to assess the systemic toxicity of this therapy. The relative body weight (RBW) at day n was calculated using the following formula:

$$RBW = \text{body weight on day n} / \text{body weight on day 1}$$

Pathological Analysis

Brain or subcutaneous tumors were fixed in 10% formalin for approximately 72 h, embedded in paraffin, and sectioned at 4 μ m thickness. Sections were stained with hematoxylin and eosin (H&E) for morphological observations, and with van Gieson for detection of fibrosis using a standard procedure. For immunostaining, the sections were preincubated with 3% H₂O₂ to block endogenous peroxidases. Sections were then incubated with antibodies against cytokeratin (clone AE1/AE3) and Ki-67 (clone SP6) overnight at 4°C and cleaved caspase-3 for 60 min at room temperature. After rinsing in Tris buffer, the secondary antibody was applied for 30 min at room temperature, and this was followed by the addition of 3,3'-diaminobenzidine (DAB) as a substrate. The sections were then counterstained with hematoxylin. Ki-67, cleaved caspase-3, and van Gieson-stained sections were graded by a pathologist (TS) as follows: -, absent; \pm , minimal; 1+, mild; and 2+, moderate (**Supplementary Figure 1**).

Mechanistic Analysis of Antitumor Effects

Tumor lysates were prepared from mice in each group on day 22 in *Protocol Number 2 (subcutaneous ectopic tumor models)*. Western blot analysis of the phosphorylation/activation patterns of the relevant molecules was performed as previously described (21).

TABLE 1 | Group configuration in the DU 145 intracranial orthotopic brain metastasis model.

Group	Start of administration	Dosing article	Dose (mg/kg)	No. of animals
Control	day 3	Saline	0	5
Perifosine (D3)*	day 3	Perifosine	180/45	5

*180 mg/kg loading dose on day 3, followed by maintenance doses of 45 mg/kg.

TABLE 2 | Group configuration in the H1915 intracranial orthotopic brain metastasis model.

Group	Start of administration	Dosing article	Dose (mg/kg)	No. of animals
Control	day 3	Saline	0	10
Perifosine (D3)*	day 3	Perifosine	180/45	10
Perifosine (D7)*	day 7	Perifosine	180/45	10

*180 mg/kg loading dose on day 3 or 7, followed by maintenance doses of 45 mg/kg.

All the western blots were normalized to β -actin, and protein intensity was quantified using the Image J software (NIH, Bethesda, MD).

Pharmacokinetics of Perifosine

Non-tumor-bearing mice were orally administered a single dose of perifosine at 45 or 180 mg/kg. At 4, 8, 24, 96, 168, and 360 h after the dose, blood was collected from the abdominal vena cava under isoflurane anesthesia, and the brain was resected after exsanguination. In a separate set, the DU 145 and H1915 subcutaneous ectopic tumor models were administered perifosine as either a single dose (45 or 180 mg/kg) or repeated doses (180 mg/kg *loading* dose followed by four consecutive daily doses of 45 mg/kg [180/45]). At 24, 48, 96, 144, and 168 h after the first dose, blood and tumor tissues were obtained in a manner similar to that described above.

The plasma was mixed with an equal volume of 1% formic acid and stored at -80°C . It (10 μL) was then mixed with an equal volume of acetonitrile containing 1% formic acid (FA/ACN) and 180 μL of internal standard (IS) solution (200 ng/mL of ethyl *p*-hydroxybenzoate [EHB] solution in FA/ACN). Next, the supernatant was collected after deproteinization (Sirocco, Waters Corp.) for LC-MS/MS assay analysis. The brain and tumor tissues were mixed with an equal volume (w/v) of 1% formic acid, homogenized, mixed with a 3-fold volume of FA/ACN, and centrifuged at 15,000 rpm ($16,617 \times g$) for 3 min at 4°C to collect the supernatant. The supernatant (20 μL) was mixed with 80 μL of IS solution (200 ng/mL of EHB solution in “FA/ACN”/water [3:1] solution), and the new supernatant was obtained after deproteinization using the LC-MS/MS assay. The maximum plasma drug concentration (C_{max}), the area under the concentration-time curve up to the last sampling time-point ($\text{AUC}_{0-\text{last}}$), the mean residence time (MRT), and the terminal half-life ($T_{1/2}$) were calculated using the mean values at each point. The $\text{AUC}_{0-\text{last}}$ was calculated using the trapezoidal rule. The MRT was calculated as follows: $\text{MRT} = \text{AUMC}/\text{AUC}$ (AUMC: area

$$\text{under moment curve} = \int_{\text{last}}^{\infty} tCdt).$$

Statistical Analysis

Data were analyzed using SAS System Release 8.2 (SAS Preclinical Package, Version. 5.0; SAS Institute Japan Ltd., Tokyo, Japan). The values are expressed as mean \pm standard deviation (SD). Differences in survival among experimental groups were analyzed according to Kaplan-Meier survival curves using the log-rank test. The Student's *t*-test or Welch's *t*-test (F-test; $p < 0.05$) was used to detect the statistical

differences in brain weight, TV, tumor weight, RBW, and protein levels in tumor tissues between two groups. *P* values < 0.05 were considered to be statistically significant.

RESULTS

Brain Tissue Distribution Profiles of Perifosine

To investigate whether perifosine is extensively distributed in brain tissues, we examined the plasma and brain tissue levels of perifosine in normal mice with intact BBBs. Perifosine was administered at doses of 45 or 180 mg/kg, as the maximum tolerated dose of perifosine was confirmed to be 45 mg/kg (once-daily regimen) and 250 mg/kg (once-weekly regimen). The plasma perifosine concentrations reached maximum levels at 24 or 96 h post-dosing and exhibited a gradual decline thereafter (**Figure 1A**). In contrast, brain concentrations increased gradually and remained at high levels for at least up to 360 h (Brain C_{max} : 6.20 μM [2.86 $\mu\text{g/g}$] for 45 mg/kg and 16.22 μM [7.49 $\mu\text{g/g}$] for 180 mg/kg, respectively) (**Figure 1B**). High and rapid distribution in brain tissues was observed in the 180 mg/kg group compared to that observed in the 45 mg/kg group (**Figure 1B**). When calculating the brain-to-plasma ratios for perifosine, a trend toward a higher retention in brain tissues was observed at 360 h post-dosing (**Figure 1C**); however, this was not observed at the earlier time-points. The *in vitro* perifosine IC_{50} values for DU 145 and H1915 were 28.8 μM and 2.5 μM , respectively, at 48 h; these were approximately 1.8-fold higher and 6.5-fold lower, respectively, than the brain C_{max} values after a single oral dose of 180 mg/kg (**Figure 1D**).

Growth Characteristics of Tumor Cell Lines in Intracranial Orthotopic Brain Metastasis Models

Intracranial inoculations were performed using human primary glioblastoma U-87 MG cells and two human metastatic brain tumor cell lines. Of these cell lines, U-87 MG cells formed a unifocal, unilateral tumor in the cerebral parenchyma, which was consistent with previous reports (23, 33) (**Supplementary Figure 2**). Injection with DU 145 cells caused scattered formation of small tumor nests in the cerebral parenchyma near the injection site. These multiple tumors were found separately (**Figures 2A, Ba, b**), unlike a solitary lesion induced by U-87 MG cells. Injection of H1915 cells resulted in multifocal tumors. Tumor cells were observed not only in the brain parenchyma but also in the subarachnoid spaces,

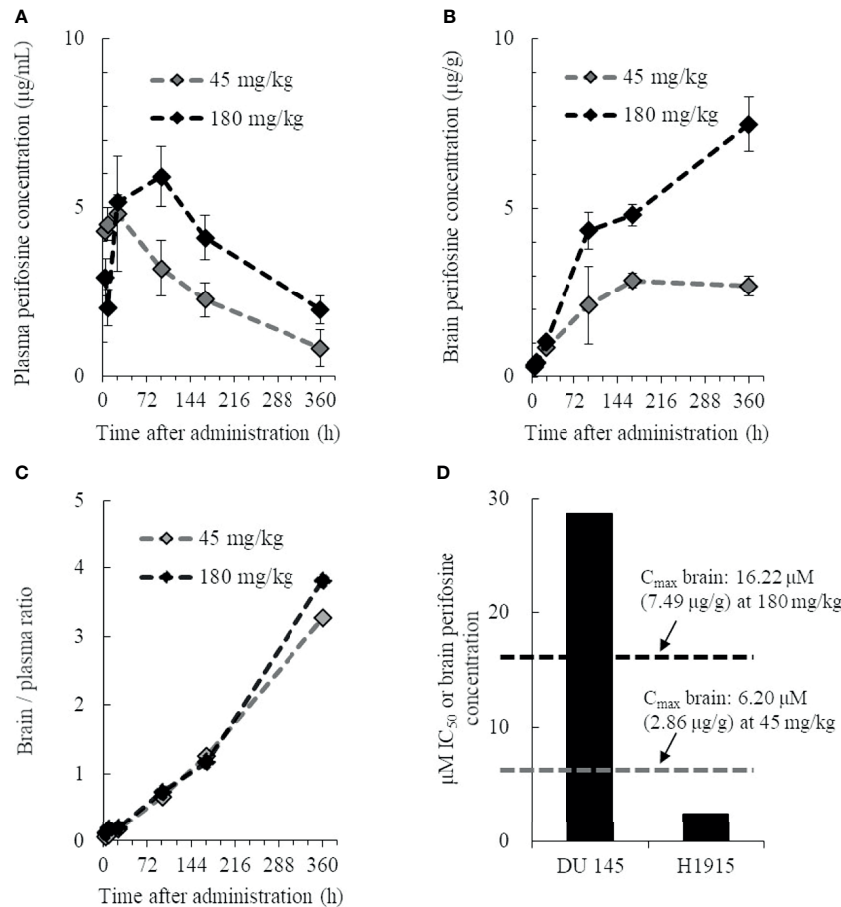


FIGURE 1 | Pharmacokinetic profile of perifosine in plasma and brain tissue. Healthy animals were administered a single oral dose of perifosine, and at six intervals, mice from each group were then euthanized for plasma (A) and brain (B) extraction ($n = 3$). (C) The brain-to-plasma ratio of perifosine was calculated at each time point. (D) Relationship between the brain C_{max} and *in vitro* IC_{50} for DU 145 and H1915 cells.

ventricles, and vascular spaces (all four mice tested; **Figures 2C, Da-g**). Our ability to observe tumor cells even in the left lateral ventricle (**Figure 2Dd**) suggests that this separation was highly unlikely to be caused due to technical reasons, but was instead a result of cell migration; this was also corroborated by the *in vitro* wound-healing assay (**Supplementary Figure 3**). Thus, the H1915 model appeared to closely resemble the clinical features of leptomeningeal carcinomatosis (34–36). The formation of multiple lesions such as leptomeningeal meningitis makes surgical resection impossible, and such patients cannot typically be treated with surgery only (36).

Brain weights of H1915 tumor-bearing mice were increased significantly, with marked enlargement, compared to those of sham-operated mice on day 21 (**Figure 2E**), suggesting that clinical features, including elevated intracranial pressure caused by metastatic brain tumors, were reflected at least in the H1915 model (2, 3). Therefore, these models are likely to provide valuable evaluative tools for predicting the clinical benefits of drug candidates.

Improvement of Survival Following Treatment of Brain Tumor-Bearing Mice With Perifosine

We used the intracranial DU 145 and H1915 models to evaluate the survival benefit of perifosine against metastatic brain tumors. In the DU 145 model, the MST significantly increased to 49.5 (% ILS = 30, $p < 0.01$) upon administration of perifosine from day 3, while the control group exhibited an MST of 38.0 (**Figure 3A**). In the H1915 model, the MST of the control group was 24.5, while eight out of 10 mice survived until the final day of observation (day 64) in the perifosine (D3) group (MST was not reached, $p < 0.001$). Likewise, treatment with perifosine from day 7 onwards significantly prolonged survival compared to that of the control group, where the MST was 59.0 (% ILS = 141, $p < 0.01$) (**Figure 3B**). Although the survival benefit was lower than that of the perifosine (D3) group, four out of 10 mice survived until day 64 in the perifosine (D7) group. Based on the observation that the control mice began to reach the endpoint as early as on day 19 and the time required for perifosine to reach values close

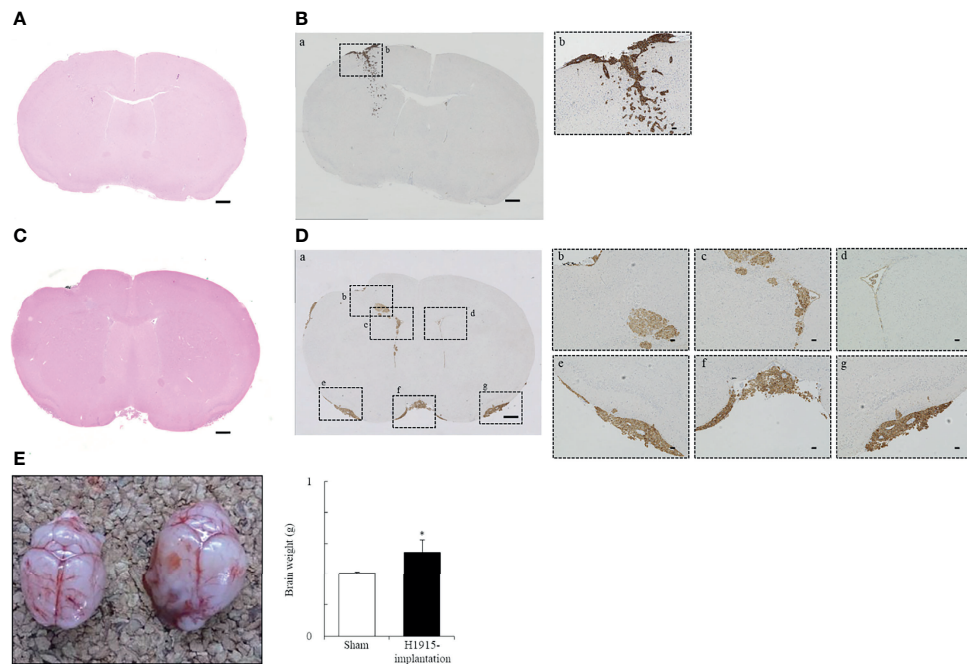


FIGURE 2 | Representative morphological features of tumor cell lines following implantation. **(A–D)** Histological and **(E)** macroscopic images of the brains. Intracranial injection of DU 145 **(A, B)** and H1915 **(C, D)** cells into nude mice shows characteristic tumor growth patterns in brain on day 14. Representative H&E-stained **(A, C)** and cytokeratin (AE1/AE3)-stained **(Ba, Da)** sections are shown (scale bar = 500 μ m). Boxed areas in panels **(Ba)** and **(Da)** show regions depicted in panels **(Bb)** and **(Db–g)**, respectively. Cytokeratin (AE1/AE3) were used to distinguish brain tissues from metastatic DU 145 **(Bb)** and H1915 **(Db–g)** tumors; scale bar = 50 μ m. **(E)** Gross features of representative brains excised from sham-operated (left; $n = 5$) and H1915-implanted (right; $n = 4$) mice on day 21. * $p < 0.05$ versus the sham-operated group.

to C_{\max} in brain tissues was at least four days after administration (**Figure 1B**), it is noteworthy that perifosine resulted in significant survival benefits, even in the perifosine (D7) group.

Some agents targeting the PI3K/Akt signaling pathway are associated with hyperglycemia due to interaction with the insulin-glucose regulatory axis (37, 38). Therefore, hyperglycemia and polyuria are frequently reported adverse effects of PI3K/Akt inhibitors. Here, the bedding of survivors, all of which were mice in perifosine-treated groups, was visibly wet after day 54, suggesting the symptom of polyuria. In order to assess the possibility of hyperglycemia, mice surviving for 64 days were analyzed for the level of glucose in plasma. As a result, perifosine did not induce an increase in plasma glucose when compared to the historical control data. Similarly, there were no severe changes in T-CHO, T-BIL, BUN, CRE, and ALP on day 64 (**Supplementary Figure 4** and **Supplementary Table 2**).

Inhibition of H1915 Tumor Growth in the Brain by Perifosine

In the control group of the H1915 model, the brain weight was clearly higher than that in the normal and sham-operated mice, which is suggestive of aggressive tumor progression and/or cerebral edema (**Figures 3C, D**). In contrast, the brain weights in both the perifosine groups were significantly lower than those in the control group, and these values were almost comparable to the values in the normal and sham-operated groups (**Figures 3C, D**).

Tumor cells were observed multifocally in the control group on day 14 (**Figures 3Ea–c**). However, no apparent viable tumor cells were observed in the perifosine (D3)-treated mice on day 41 in a separate experiment ($n = 2$), thus indicating complete responses (**Figures 3Ed–f**). In agreement with the results of brain weight, it is apparent that perifosine dramatically inhibited H1915 tumor growth.

Perifosine Preferentially Inhibited the Growth of Ectopic H1915 Xenografts

It has been documented that high correlations between *in vitro* and *in vivo* sensitivity of drugs are not always observed (39–41). Although the exact reason for the discrepancies is unknown, this can be explained, at least in part, by the modification of sensitivity through multiple factors in the tumor microenvironment.

Here, we demonstrated that the growth patterns of DU 145 and H1915 were largely different in brain tissues (**Figures 2A–D**). Therefore, we speculated that the growth patterns of both cell lines in brain tissues may have influenced the *in vivo* sensitivity of perifosine.

To confirm this possibility, DU 145 (**Figures 4A–E**) and H1915 (**Figures 4F–K**) cells were subcutaneously inoculated and allowed to form a solitary tumor, and the antitumor effect of perifosine was examined. Perifosine, when used according to the same treatment regimen as was used in the brain orthotopic models, exerted a moderate antitumor effect with a TGI value of

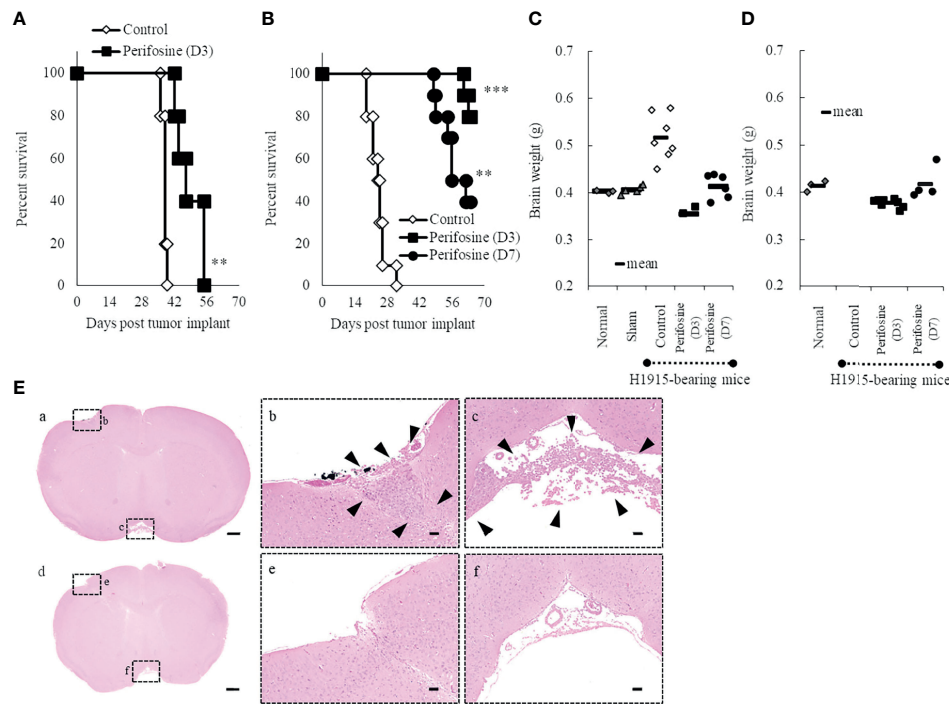


FIGURE 3 | Prolongation of life-span of orthotopic brain metastasis mice with perifosine. Mice were injected intracerebrally with DU 145 (A) or H1915 (B–E) cells on day 0, and the tumor was allowed to establish until day 3 (perifosine [D3]) or day 7 (perifosine [D7]). Mice were treated with either vehicle or perifosine under the conditions indicated in **Tables 1, 2**. (A, B) Survival curve analysis was performed for 64 days, and the death time point was defined when the animals appeared moribund. $^{**}p < 0.01$; $^{***}p < 0.001$ versus the control group. (C, D) The H1915 orthotopic tumor mice were euthanized in a moribund state (C; up to day 63) or at the termination of the experiment (D; on day 64), and each brain was weighed. Although all 10 mice in the control group were euthanized in a moribund state until day 32, the brains were weighed only for seven mice (C). Age-matched normal ($n = 3$) and sham-operated ($n = 5$) mice were included for comparison and euthanized on day 21 (C). (E) Representative H&E-stained images of lesions in the H1915 model are shown; scale bar = 500 μm (a, d) or 50 μm (b, c, e, f). Low (a) and high (b, c) power views in the vehicle-treated mouse on day 14 and low (d) and high (e, f) power views in the perifosine (D3)-treated mouse on day 41. Boxed areas in panels (a) and (d) show regions depicted in panels (b, c, e, f), respectively. Arrowheads indicate tumor cells.

34% in the DU 145 xenograft model, despite the lack of significance [$p = 0.058$ for TV on Day 22 (**Figure 4A**); $p = 0.086$ for tumor weight (**Figure 4C**)]. In accordance with these results, perifosine down-regulated phosphorylation levels of Akt at both Ser473 and Thr308 by 61% ($p = 0.074$) and 44% ($p < 0.05$) respectively without diminishing total Akt protein level in DU 145 xenografts (**Figure 4E**). Meanwhile, perifosine also elicited much stronger antitumor responses against subcutaneous H1915 growth, which included regressions of the established tumor on and after day 7 (93% reduction in TV; **Figures 4F, G**). These results indicated a similar tendency between both *in vitro* cytotoxicity and *in vivo* orthotopic findings, thus demonstrating that perifosine is inherently more potent against H1915 than against DU 145; this was independent of the different growth patterns in brain tissues. Furthermore, perifosine treatment significantly abrogated the Akt signaling pathway in H1915 xenografts on Day 22 (**Figure 4J**), almost consistent with other tumor models (**Supplementary Figure 5**). Notably, both p-Akt and total Akt were reduced at this time point, which is suggestive of an increase in tumor cell death (**Figure 4J**). We also monitored the systemic toxicity of mice receiving this therapy. No adverse effects in general conditions or any treatment-related macroscopic

changes in major organs including the brain, liver, and kidneys were induced by this therapeutically effective regimen. Moreover, as the RBW values were more than 0.8, this therapy was deemed tolerable (**Figures 4D, I**).

Histological examination revealed that the tumor cells were large, round-to-oval, and possessed distinct multiple nucleoli in the clear oval nucleus; all of these characteristics resemble the morphological features of large-cell lung carcinoma (**Figures 4Ka, b**). Although there was still no big difference in H1915-tumor volume between the vehicle and perifosine-treated tumors on day 7, we observed marked morphological changes in tumor cells in response to perifosine treatment, which is suggestive of a decrease in tumor cell proliferation and/or an increase in cell death not only on day 22, but also even at this early stage (**Figures 4Kc–f**).

Perifosine Reduced Cell Proliferation and Induced Apoptosis Preferentially in H1915 Tumor Xenografts

To further investigate the mechanism of perifosine-mediated tumor growth inhibition, the levels of Ki-67 and cleaved caspase-3 were assessed in the DU 145 (**Figures 5A–J**) and H1915

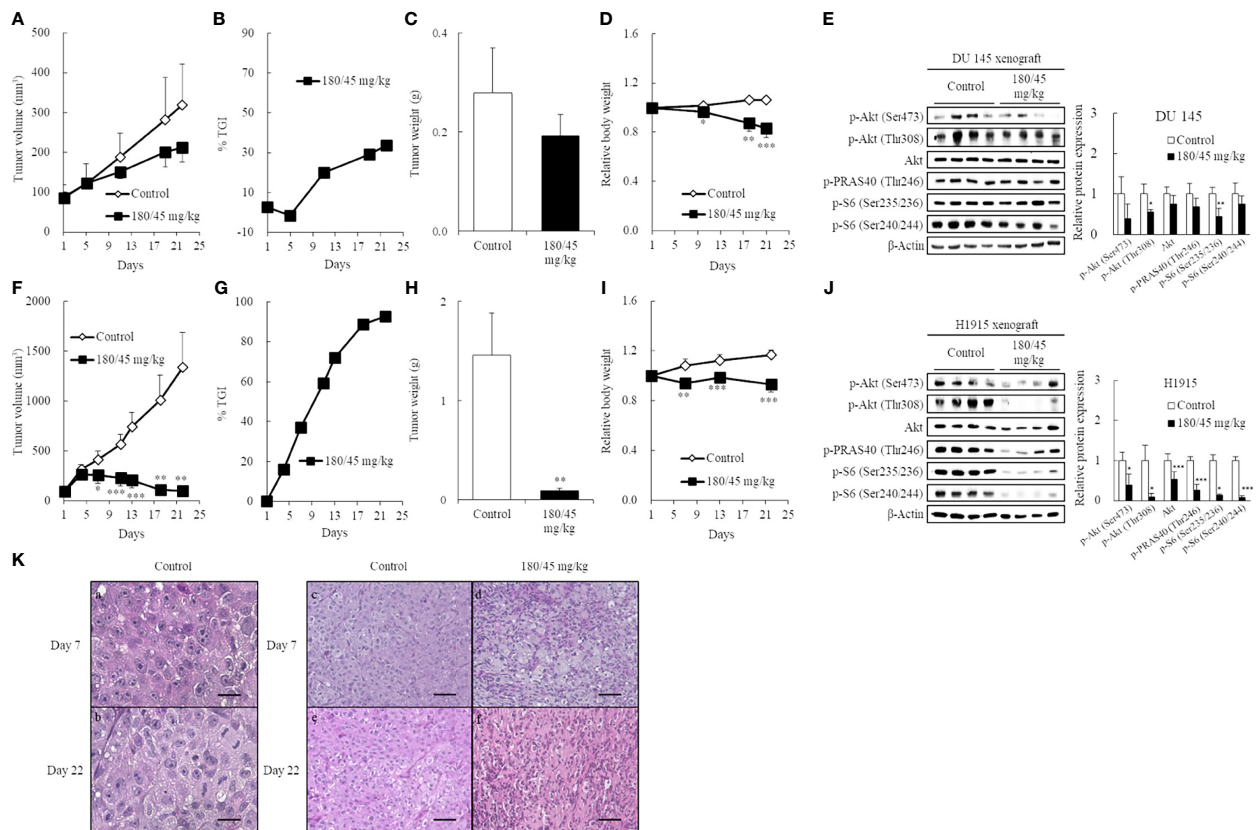


FIGURE 4 | Induction of high antitumor efficacy against ectopic H1915 xenografts in association with blockade of the PI3K/Akt pathway by perifosine. Mice bearing subcutaneous DU 145 (A–E) and H1915 (F–J) tumors were randomized on day 1 and treated orally with either vehicle or perifosine using a 5-day-on/2-day-off \times 3 cycle schedule ($n = 5$). On day 22, xenograft tumors were excised 4 h following the last dose. Changes in TV (A, F), tumor growth inhibition rate (TGI, %) at different days (B, G), tumor weight (C, H), and relative body weight (D, I). The expression level of key molecules was detected by western blot on Day 22 (E, J). Images are representative of at least two independent experiments with similar results. β -actin was used as a loading control. Protein levels were quantified and represented as the percentage of the control group. * $p < 0.05$; ** $p < 0.01$; *** $p < 0.001$ versus the control group. (K) Representative H&E images of the H1915-tumor tissues treated with vehicle (a–c, e) and perifosine (d, f) on days 7 and 22 are shown; scale bar = 20 μ m (a, b) or 50 μ m (c–f). High-power views in the control group suggest that the tumor cells are large, round-to-oval, and possessed distinct multiple nucleoli in the clear oval nucleus (a, b).

(Figures 5K–T) tumors. H1915 tumor cells grew into a solitary solid mass, with central necrosis, in the control group on day 22 (Figure 5K). Perifosine exhibited a marked decrease in tumor cell proliferation, as detected by Ki-67 and increased apoptosis (cleaved caspase-3 staining), compared to that in tumor cells from the control group, and the majority of the residual tumor tissues treated with perifosine were composed largely of collagen fibers (van Gieson) and well-formed granulomas, which are thought to be formed by the effect of perifosine (Table 3 and Figures 5K–T). Consistently, an increase in the number of tumor cells with apoptotic morphology such as apoptotic body formation and nuclear condensation was observed in the H1915 tumor mass of the perifosine-treated animals (Table 3).

Regarding the DU 145 xenografts, although an increase in the number of cleaved caspase-3 positive tumor cells was detected in response to perifosine treatment, there were no obvious differences in the morphological observations, staining patterns of Ki-67, and van Gieson staining between the control and perifosine groups (Table 3 and Figures 5A–J). Special and

immunohistochemical stains revealed the changes underlying the antitumor responses to perifosine, thus indicating consistency with the above-mentioned findings.

Perifosine Preferably Accumulates in H1915 Tumor Xenografts

It has been documented that drug accumulation differs among tumor xenografts (42). Herein, we hypothesized that the different sensitivities to perifosine depend on the differences in drug levels between DU 145 and H1915 xenografts, and characterized the pharmacokinetic properties of perifosine (Figure 6 and Supplementary Table 3).

The plasma concentration of perifosine gradually increased, reached C_{max} at 24 or 48 h after a single dose of 45 or 180 mg/kg, respectively, and then decreased slowly (Figures 6A, D). There were no apparent differences in plasma C_{max} and AUC between the DU 145 and H1915 subcutaneous transplantation models. Although the tumor levels of perifosine remained almost stable at 48 h and beyond in both models (Figures 6B, E), some

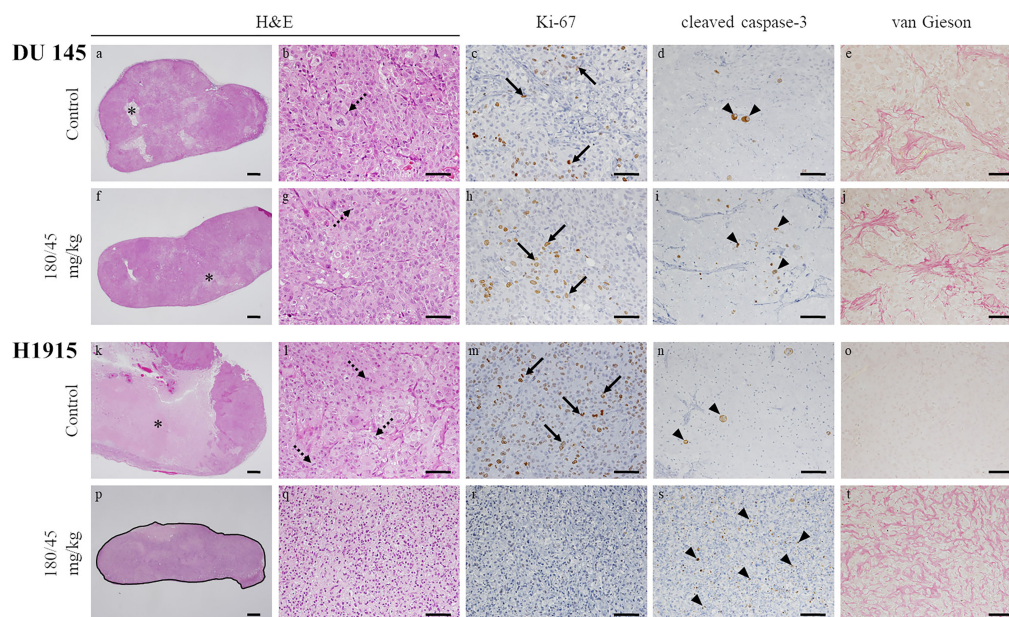


FIGURE 5 | Morphological changes in subcutaneous tumor xenografts evoked by oral administration of perifosine. The resected tumors in **Figures 4C, H** were analyzed by H&E staining, immunohistochemical staining for Ki-67 and cleaved caspase-3, and special staining for van Gieson. Representative images of the DU 145 (**A–J**) and H1915 (**K–T**) tumor tissues treated with vehicle (**A–E, K–O**) and perifosine (**F–J, P–T**) are shown; scale bar = 500 μ m (**A, F, K, P**) or 50 μ m (**B–E, G–J, L–O, Q–T**). Granulomatous lesion is delineated by a solid black line (**P**). Perifosine induced granuloma formation around the H1915 tumor lesion (**P**). Necrosis (asterisks), mitotic figures (dotted arrows), Ki-67-positive cells (arrows), and cleaved caspase-3-positive cells (arrowheads).

differences were observed. In the H1915 tumor xenografts, the AUC of perifosine was 10.7-fold (45 mg/kg) and 6.5-fold (180 mg/kg) higher than that in the DU 145 xenografts; this was corroborated by the data demonstrating that perifosine was favorably delivered into the H1915 tumor tissues, where the tumor-to-plasma ratios were much higher in the H1915 model (**Figures 6C, F**, and **Supplementary Table 3**). These findings indicate H1915-preferential targeting of perifosine and are closely consistent with the above-mentioned results, which showed anti-proliferative activity *in vitro* and antitumor activity in orthotopic and ectopic tumor models were much

stronger against H1915 than against DU 145 (**Figures 1D, 3**, and **4**). Although tumor perifosine concentrations after repeated oral administrations in the 180/45 mg/kg group were higher than those after single doses in the 45 and 180 mg/kg groups, the difference was slight (**Figures 6B, E**).

DISCUSSION

In the current study, we reported the usefulness of human metastatic brain tumor models and the effectiveness of

TABLE 3 | Histopathological evaluation, on day 22, of the tumor tissues treated with perifosine.

Model	Group (n = 5)	necrosis (H&E)					apoptosis: pyknosis/karyorrhexis (H&E)					granuloma (H&E)				
		-	±	1+	2+	3+	-	±	1+	2+	3+	-	±	1+	2+	3+
H1915	Control	0	0	0	4	1	0	5	0	0	0	5	0	0	0	0
	180/45 mg/kg	5	0	0	0	0	0	0	1	4	0	0	0	0	0	5
DU 145	Control	0	4	1	0	0	0	5	0	0	0	5	0	0	0	0
	180/45 mg/kg	0	4	1	0	0	0	2	3	0	0	5	0	0	0	0

Model	Group (n = 5)	proliferation (Ki-67)					apoptosis (cleaved caspase-3)					fibrosis (van Gieson)				
		-	±	1+	2+	3+	-	±	1+	2+	3+	-	±	1+	2+	3+
H1915	Control	0	0	0	5	0	0	5	0	0	0	4	1	0	0	0
	180/45 mg/kg	3	2	0	0	0	0	0	0	5	0	0	0	0	5	0
DU 145	Control	0	0	5	0	0	0	5	0	0	0	0	0	5	0	0
	180/45 mg/kg	0	1	4	0	0	0	1	4	0	0	0	0	5	0	0

-, absent; ±, minimal; 1+, mild; 2+, moderate; 3+, marked. The results shown in **Figure 5** are quantitatively shown in this table.

perifosine in these tumor models. First, we determined that perifosine could distribute into the brain and remain localized there for a prolonged period following oral administration. These data were confirmed in healthy mice with intact BBBs, indicating that perifosine could cross the BBBs. Second, to evaluate the efficacy of perifosine, we established orthotopic xenograft mouse models by injecting the human metastatic brain tumor cell lines DU 145 and H1915 into the brains of these mice. Both models exhibited different apparent growth patterns as compared to those observed using the human glioblastoma cell line U-87 MG. Moreover, multiple tumor lesions were detected remotely from each other in the brain of the H1915 model mice (**Figures 2C, D, and 3E**), indicating that the surgical treatment would be impractical in clinical settings (3). Third, perifosine significantly increased survival for the DU 145 and H1915 orthotopic brain tumor mice, which was also accompanied by complete regression in the H1915 model (**Figures 3B, E**). Fourth, compared to orthotopic tumors, a similar trend of sensitivity to perifosine was observed when the subcutaneous solitary tumors derived from DU 145 and H1915 were treated with perifosine. These findings suggest that the difference in the sensitivity of perifosine against orthotopic tumors was less likely to be attributable to the difference in the growth pattern in brain tissues, but was instead due to intrinsic differences among the cancers themselves. Finally, we confirmed that the suppression level of H1915-tumor growth was associated with the high accumulation of perifosine at the tumor site and the resultant blockage of the PI3K/Akt signaling pathway, decrease in tumor cell proliferation, and increased apoptosis; these findings suggested that these are all indispensable events underlying the *in vivo* antitumor activity of perifosine.

Perifosine is a bioavailable alkylphospholipid consisting of an 18-carbon alkyl chain. Therefore, we hypothesize that perifosine is taken up into the lipid bilayer of vascular endothelial cells due to the lipophilic characteristics of this molecule. It then penetrates the vascular wall and is gradually transferred into the cerebrospinal fluid over a long period. In contrast, as the brain is an organ with a high lipid level, highly lipophilic perifosine is rapidly transferred from cerebrospinal fluid to brain tissues and accumulates there. As a result, the level of perifosine in the cerebrospinal fluid is always low, and perifosine continues to be transferred from the blood to the cerebrospinal fluid owing to a concentration gradient. Thus, we expect that the unidirectional penetration of perifosine from blood to brain tissues passing through cerebrospinal fluid is continuous, ultimately resulting in long-term retention in brain tissues (**Figures 1A–D**). Additionally, the involvement of flippases and scramblases has been proposed as one possible mechanism of perifosine uptake in cancers (43). It has been documented that flippases drive inward-directed translocation of phospholipids across the plasma membrane, and scramblases transfer lipids from the inner to the outer and from the outer to the inner leaflet of the plasma membrane (44–46). Therefore, flippases and scramblases may be vital for uptake of the alkylphospholipid perifosine by cancer cells and may play a crucial role in modulating the response rate. Although the precise mechanism underlying the accumulation of perifosine in tumor tissues has not

yet been fully elucidated, we believe that the enhanced exposure at the target site could enable perifosine to exhibit its antitumor activity.

A research group reported that perifosine monotherapy did not exhibit enough antitumor activity to prolong survival in a genetically engineered mouse model of brainstem gliomas (47). The group described that this may be attributable to poor drug delivery into the brainstem due to the BBBs. However, we administered perifosine at 180/45 mg/kg for nine cycles in the present study, whereas this research group only dosed perifosine at 30 mg/kg for one week. Therefore, we predict that the discrepancy between their data and ours may be due to differences in the experimental settings, as we demonstrated here that perifosine was efficiently transferred into the brain and exhibited encouraging antitumor efficacy.

In this study, we found that perifosine did not induce an increase in plasma glucose, which is one of the on-target adverse events of PI3K/Akt inhibitors. Reportedly, an increase in plasma glucose levels returns to baseline levels within 24 h after an Akt inhibitor AZD5363 treatment, suggesting a transient phenomenon as observed for a PI3K inhibitor copanlisib (38, 48). Therefore, the result here implies that a rise in plasma glucose level, if any, was transient. In our preliminary study, all three mice with H1915 intracranial xenograft tumors that received only six cycles of perifosine similarly survived until the end of the observation period. Based on this, we speculate that we could reduce the dose of perifosine; this research strategy will be employed in our future studies.

Here, we reported that perifosine continued to be retained in the brain for a long period. Although high perifosine concentration in the brain is a vital factor to facilitate therapeutic effects against brain tumors, it could lead to unfavorable side effects associated with CNS disorders. Therefore, it is crucial to determine whether perifosine causes undesirable CNS dysfunction in patients and not just in mice. However, this concern appears to have been recently addressed clinically, where no symptoms associated with CNS disorders were noted in patients, to date, with the exception of manageable toxicities such as anemia, diarrhea, and nausea (49, 50).

Our study does possess a few limitations that are worth noting. Specifically, despite the high degree of homology in the amino acid content of an ATP-dependent efflux transporter, P-glycoprotein in different species and its function may differ across different species (51, 52). It is therefore meaningful for us to examine the species differences, in future studies. Regardless, to our knowledge, our study reports the first evidence of a successful therapy using perifosine against metastatic brain tumors and provides potentially beneficial information for this patient population.

In conclusion, we clearly demonstrated that orally administered perifosine exhibited promising antitumor efficacy in H1915 intracranial orthotopic and ectopic tumor models in association with blockade of the PI3K/Akt pathway. Our results support the concept that long-term exposure to a high level of perifosine at the tumor site and suppression of PI3K/Akt pathway activation are crucial events underlying the *in vivo*

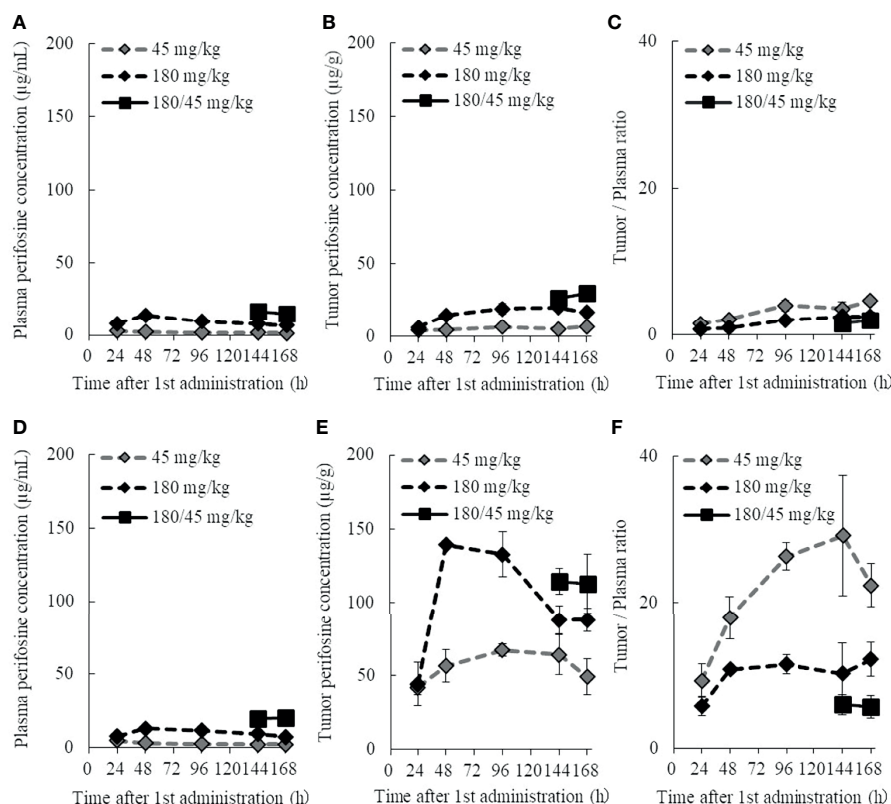


FIGURE 6 | Plasma and tumor pharmacokinetic profiles of perifosine after single and repeated doses. Nude mice with DU 145 (A–C) and H1915 (D–F) subcutaneous xenograft tumors were randomized and treated with single doses of 45 and 180 mg/kg perifosine or a 5-day repeated dose of 180/45 mg/kg (180 mg/kg loading dose followed by maintenance doses of 45 mg/kg) perifosine. Plasma (A, D) and tumor (B, E) samples were collected at the indicated points. Chronological changes in tumor-to-plasma ratios of perifosine are shown for DU 145 (C) and H1915 (F) models ($n = 3$, except at 48-h time point for the 180 mg/kg group in (E, F), where $n = 2$ due to tumor sample processing error).

antitumor activity of perifosine. Although it is important to validate our findings using clinical specimens, the preclinical evidence presented here reveals a promising future approach for the treatment of patients with metastatic brain cancers and emphasizes the importance of enriching a patient population that has a higher probability of responding to perifosine.

DATA AVAILABILITY STATEMENT

The original contributions presented in the study are included in the article/**Supplementary Material**. Further inquiries can be directed to the corresponding author.

ETHICS STATEMENT

The animal study was reviewed and approved by the Animal Experimental Committee of the Yakult Central Institute.

AUTHOR CONTRIBUTIONS

KT, TS, and AT conceived and designed the study. KT, TS, TO, AK, and MT conducted the experiments and prepared the figures and tables. KT provided data analysis and wrote the original draft. GN, SI, SK, AT, MT, and YS supervised the research. All authors have read and approved the final manuscript.

ACKNOWLEDGMENTS

The authors thank Ms. Rika Morita for expert technical assistance.

SUPPLEMENTARY MATERIAL

The Supplementary Material for this article can be found online at: <https://www.frontiersin.org/articles/10.3389/fonc.2021.754365/full#supplementary-material>

REFERENCES

- Hanibuchi M, Kim SJ, Fidler IJ, Nishioka Y. The Molecular Biology of Lung Cancer Brain Metastasis: An Overview of Current Comprehensions and Future Perspectives. *J Med Invest* (2014) 61:241–53. doi: 10.2152/jmi.61.241
- Navarro-Olvera JL, Ariñez-Barahona E, Esqueda-Liquidano MA, Muñoz-Cobos A. Brain Metastases: Literature Review. *Rev Med Hosp Gen Mex* (2017) 80:60–6. doi: 10.1016/j.hgm.2016.04.006
- Wanleenuwat P, Iwanowski P. Metastases to the Central Nervous System: Molecular Basis and Clinical Considerations. *J Neurol Sci* (2020) 412:116755. doi: 10.1016/j.jns.2020.116755
- Nakayama A, Takagi S, Yusa T, Yaguchi M, Hayashi A, Tamura T, et al. Antitumor Activity of TAK-285, an Investigational, Non-Pgp Substrate HER2/EGFR Kinase Inhibitor, in Cultured Tumor Cells, Mouse and Rat Xenograft Tumors, and in an HER2-Positive Brain Metastasis Model. *J Cancer* (2013) 4:557–65. doi: 10.7150/jca.6689
- Agarwal E, Chaudhuri A, Leiphrakpam PD, Haferbier KL, Brattain MG, Chowdhury S. Akt Inhibitor MK-2206 Promotes Anti-Tumor Activity and Cell Death by Modulation of AIF and Ezrin in Colorectal Cancer. *BMC Cancer* (2014) 14:145. doi: 10.1186/1471-2407-14-145
- Grabinski N, Bartkowiak K, Grupp K, Brandt B, Pantel K, Jücker M. Distinct Functional Roles of Akt Isoforms for Proliferation, Survival, Migration and EGF-Mediated Signaling in Lung Cancer Derived Disseminated Tumor Cells. *Cell Signal* (2011) 23:1952–60. doi: 10.1016/j.cellsig.2011.07.003
- Altomare DA, Testa JR. Perturbations of the AKT Signaling Pathway in Human Cancer. *Oncogene* (2005) 24:7455–64. doi: 10.1038/sj.onc.1209085
- Bellacosa A, Kumar CC, Di Cristofano A, Testa JR. Activation of AKT Kinases in Cancer: Implications for Therapeutic Targeting. *Adv Cancer Res* (2005) 94:29–86. doi: 10.1016/S0065-230X(05)94002-5
- Testa JR, Tsichlis PN. AKT Signaling in Normal and Malignant Cells. *Oncogene* (2008) 24:7391–3. doi: 10.1038/sj.onc.1209100
- Tokunaga E, Oki E, Egashira A, Sadanaga N, Morita M, Kakeji Y, et al. Deregulation of the Akt Pathway in Human Cancer. *Curr Cancer Drug Targets* (2008) 8:27–36. doi: 10.2174/156800908783497140
- Brugge J, Hung MC, Mills GB. A New Mutational Activation in the PI3K Pathway. *Cancer Cell* (2007) 12:104–7. doi: 10.1016/j.ccr.2007.07.014
- Huang WC, Hung MC. Induction of Akt Activity by Chemotherapy Confers Acquired Resistance. *J Formos Med Assoc* (2009) 108:180–94. doi: 10.1016/S0929-6646(09)60051-6
- He L, Liu X, Yang J, Li W, Liu S, Liu X, et al. Imbalance of the Reciprocally Inhibitory Loop Between the Ubiquitin-Specific Protease Usp43 and EGFR/PI3K/AKT Drives Breast Carcinogenesis. *Cell Res* (2018) 28:934–51. doi: 10.1038/s41422-018-0079-6
- Mao Y, Xi L, Li Q, Wang S, Cai Z, Zhang X, et al. Combination of PI3K/Akt Pathway Inhibition and PIK1 Depletion Can Enhance Chemosensitivity to Gemcitabine in Pancreatic Carcinoma. *Transl Oncol* (2018) 11:852–63. doi: 10.1016/j.tranon.2018.04.011
- Ippen FM, Grosch JK, Subramanian M, Kuter BM, Liederer BM, Plise EG, et al. Targeting the PI3K/Akt/mTOR Pathway With the Pan-Akt Inhibitor GDC-0068 in PIK3CA-Mutant Breast Cancer Brain Metastases. *Neuro Oncol* (2019) 21:1401–11. doi: 10.1093/neuonc/noz105
- Crespo S, Kind M, Arcaro A. The Role of the PI3K/AKT/mTOR Pathway in Brain Tumor Metastasis. *J Cancer Metastasis Treat* (2016) 2:80–9. doi: 10.20517/2394-4722.2015.72
- Chen MB, Wu XY, Tao GQ, Liu CY, Chen J, Wang LQ, et al. Perifosine Sensitized Curcumin-Induced Anti-Colorectal Cancer Effects by Targeting Multiple Signaling Pathways Both *In Vivo* and *In Vitro*. *Int J Cancer* (2012) 131:2487–98. doi: 10.1002/ijc.27548
- Cirstea D, Hideshima T, Rodig S, Santo L, Pozzi S, Vallet S, et al. Dual Inhibition of Akt/Mammalian Target of Rapamycin Pathway by Nanoparticle Albumin-Bound-Rapamycin and Perifosine Induces Antitumor Activity in Multiple Myeloma. *Mol Cancer Ther* (2010) 9:963–75. doi: 10.1158/1535-7163.MCT-09-0763
- Hilgard P, Klenner T, Stekar J, Nössner G, Kutscher B, Engel J. D-21266, a New Heterocyclic Alkylphospholipid With Antitumor Activity. *Eur J Cancer* (1997) 33:442–6. doi: 10.1016/s0959-8049(97)89020-x
- Fensterle J, Aicher B, Seipelt I, Teifel M, Engel J. Current View on the Mechanism of Action of Perifosine in Cancer. *Anticancer Agents Med Chem* (2014) 14:629–35. doi: 10.2174/1871520614666140309225912
- Taniguchi K, Konishi H, Yoshinaga A, Tsugane M, Takahashi H, Nishisaka F, et al. Efficacy of Combination Treatment Using YHO-1701, an Orally Active STAT3 Inhibitor, With Molecular-Targeted Agents on Cancer Cell Lines. *Sci Rep* (2021) 11:6685. doi: 10.1038/s41598-021-86021-8
- Ozawa T, James CD. Establishing Intracranial Brain Tumor Xenografts With Subsequent Analysis of Tumor Growth and Response to Therapy Using Bioluminescence Imaging. *J Vis Exp* (2010) 13:1986. doi: 10.3791/1986
- Schmidt NO, Ziu M, Cargioli T, Westphal M, Giese A, Black PM, et al. Inhibition of Thromboxane Synthase Activity Improves Glioblastoma Response to Alkylation Chemotherapy. *Transl Oncol* (2010) 3:43–9. doi: 10.1593/tlo.09238
- Bertrand Y, Currie JC, Poirier J, Demeule M, Abulrob A, Fatehi D, et al. Influence of Glioma Tumour Microenvironment on the Transport of ANG1005 via Low-Density Lipoprotein Receptor-Related Protein 1. *Br J Cancer* (2011) 105:1697–707. doi: 10.1038/bjc.2011.427
- Kobayashi N, Allen N, Clendenen NR, Ko LW. An Improved Rat Brain-Tumor Model. *J Neurosurg* (1980) 53:808–15. doi: 10.3171/jns.1980.53.6.0808
- Weizsaecker M, Deen DF, Rosenblum ML, Hoshino T, Gutin PH, Barker M. The 9L Rat Brain Tumor: Description and Application of an Animal Model. *J Neurol* (1981) 224:183–92. doi: 10.1007/BF00313280
- La Regina MC, Culbreth VO, Higashikubo R, Roti Roti JL, Spitz DR. An Alternative Method to Stereotactic Inoculation of Transplantable Brain Tumours in Large Numbers of Rats. *Lab Anim* (2000) 34:265–71. doi: 10.1258/002367700780384708
- Girard E, Ditzler S, Lee D, Richards A, Yagle K, Park J, et al. Efficacy of Cabazitaxel in Mouse Models of Pediatric Brain Tumors. *Neuro Oncol* (2015) 17:107–15. doi: 10.1093/neuonc/nou163
- Tentori L, Leonetti C, Scarsella M, d'Amati G, Portarena I, Zupi G, et al. Combined Treatment With Temozolomide and Poly(ADP-Ribose) Polymerase Inhibitor Enhances Survival of Mice Bearing Hematologic Malignancy at the Central Nervous System Site. *Blood* (2002) 99:2241–4. doi: 10.1182/blood.v99.6.2241
- Xie Q, Thompson R, Hardy K, DeCamp L, Berghuis B, Sigler R, et al. A Highly Invasive Human Glioblastoma Pre-Clinical Model for Testing Therapeutics. *J Transl Med* (2008) 6:77. doi: 10.1186/1479-5876-6-77
- Taniguchi K, Nishiura H, Ota Y, Yamamoto T. Roles of the Ribosomal Protein S19 Dimer and Chemically Induced Apoptotic Cells as a Tumor Vaccine in Syngeneic Mouse Transplantation Models. *J Immunother* (2011) 34:16–27. doi: 10.1097/CJI.0b013e3181fb03ed
- Taniguchi K, Nishiura H, Yamamoto T. Requirement of the Acquired Immune System in Successful Cancer Chemotherapy With Cis-Diamminedichloroplatinum (II) in a Syngeneic Mouse Tumor Transplantation Model. *J Immunother* (2011) 34:480–9. doi: 10.1097/CJI.0b013e31821e7662
- Kang S, Hong J, Lee JM, Moon HE, Jeon B, Choi J, et al. Trifluoperazine, a Well-Known Antipsychotic, Inhibits Glioblastoma Invasion by Binding to Calmodulin and Disinhibiting Calcium Release Channel IP3R. *Mol Cancer Ther* (2017) 16:217–27. doi: 10.1158/1535-7163.MCT-16-0169-T
- Pan Z, Yang G, He H, Yuan T, Wang Y, Li Y, et al. Leptomeningeal Metastasis From Solid Tumors: Clinical Features and its Diagnostic Implication. *Sci Rep* (2018) 8:10445. doi: 10.1038/s41598-018-28662-w
- Nayar G, Ejikeme T, Chongsathidkiet P, Elsamadicy AA, Blackwell KL, Clarke JM, et al. Leptomeningeal Disease: Current Diagnostic and Therapeutic Strategies. *Oncotarget* (2017) 8:73312–28. doi: 10.18632/oncotarget.20272
- Le Rhun E, Preusser M, van den Bent M, Andratschke N, Weller M. How We Treat Patients With Leptomeningeal Metastases. *ESMO Open* (2019) 4:e000507. doi: 10.1136/esmoopen-2019-000507
- Khan KH, Wong M, Rihawi K, Bodla S, Morganstein D, Banerji U, et al. Hyperglycemia and Phosphatidylinositol 3-Kinase/Protein Kinase B/Mammalian Target of Rapamycin (PI3K/AKT/mTOR) Inhibitors in Phase I Trials: Incidence, Predictive Factors, and Management. *Oncologist* (2016) 21:855–60. doi: 10.1634/theoncologist.2015-0248
- Cheung YM, McDonnell M, Hamnvik OR. A Targeted Approach to Phosphoinositide-3-Kinase/Akt/mammalian Target of Rapamycin-Induced Hyperglycemia. *Curr Probl Cancer* (2021). doi: 10.1016/j.crrprcancer.2021.100776. In Press.

39. Benbrook DM. Organotypic Cultures Represent Tumor Microenvironment for Drug Testing. *Drug Discov Today Dis Models* (2006) 3:143–8. doi: 10.1016/j.ddmod.2006.05.005
40. Choi SY, Lin D, Gout PW, Collins CC, Xu Y, Wang Y. Lessons From Patient-Derived Xenografts for Better *In Vitro* Modeling of Human Cancer. *Adv Drug Deliv Rev* (2014) 79–80:222–37. doi: 10.1016/j.addr.2014.09.009
41. Asghar W, El Assal R, Shafiee H, Pitteri S, Paulmurugan R, Demirci U. Engineering Cancer Microenvironments for *In Vitro* 3-D Tumor Models. *Mater Today (Kidlington)* (2015) 18:539–53. doi: 10.1016/j.mattod.2015.05.002
42. Vink SR, Schellens JH, van Blitterswijk WJ, Verheij M. Tumor and Normal Tissue Pharmacokinetics of Perifosine, an Oral Anti-Cancer Alkylphospholipid. *Invest New Drugs* (2005) 23:279–86. doi: 10.1007/s10637-005-1436-0
43. van Blitterswijk WJ, Verheij M. Anticancer Mechanisms and Clinical Application of Alkylphospholipids. *Biochim Biophys Acta* (2013) 1831:663–74. doi: 10.1016/j.bbalip.2012.10.008
44. Lopez-Marques RL, Theorin L, Palmgren MG, Pomorski TG. P4-ATPases: Lipid Flippases in Cell Membranes. *Pflugers Arch* (2014) 466:1227–40. doi: 10.1007/s00424-013-1363-4
45. Suzuki J, Denning DP, Imanishi E, Horvitz HR, Nagata S. Xk-Related Protein 8 and CED-8 Promote Phosphatidylserine Exposure in Apoptotic Cells. *Science* (2013) 341:403–6. doi: 10.1126/science.1236758
46. Suzuki J, Umeda M, Sims PJ, Nagata S. Calcium-Dependent Phospholipid Scrambling by TMEM16F. *Nature* (2010) 468:834–8. doi: 10.1038/nature09583
47. Becher OJ, Hambarzumyan D, Walker TR, Helmy K, Nazarian J, Albrecht S, et al. Preclinical Evaluation of Radiation and Perifosine in a Genetically and Histologically Accurate Model of Brainstem Glioma. *Cancer Res* (2010) 70:2548–57. doi: 10.1158/0008-5472.CAN-09-2503
48. Banerji U, Dean EJ, Pérez-Fidalgo JA, Batist G, Bedard PL, You B, et al. A Phase I Open-Label Study to Identify a Dosing Regimen of the Pan-AKT Inhibitor AZD5363 for Evaluation in Solid Tumors and in PIK3CA-Mutated Breast and Gynecologic Cancers. *Clin Cancer Res* (2018) 24:2050–9. doi: 10.1158/1078-0432.CCR-17-2260
49. Becher OJ, Millard NE, Modak S, Kushner BH, Haque S, Spasojevic I, et al. A Phase I Study of Single-Agent Perifosine for Recurrent or Refractory Pediatric CNS and Solid Tumors. *PLoS One* (2017) 12:e0178593. doi: 10.1371/journal.pone.0178593
50. Hasegawa K, Kagabu M, Mizuno M, Oda K, Aoki D, Mabuchi S, et al. Phase II Basket Trial of Perifosine Monotherapy for Recurrent Gynecologic Cancer With or Without PIK3CA Mutations. *Invest New Drugs* (2017) 35:800–12. doi: 10.1007/s10637-017-0504-6
51. Syvänen S, Lindhe O, Palmer M, Kornum BR, Rahman O, Långström B, et al. Species Differences in Blood-Brain Barrier Transport of Three Positron Emission Tomography Radioligands With Emphasis on P-Glycoprotein Transport. *Drug Metab Dispos* (2009) 37:635–43. doi: 10.1124/dmd.108.024745
52. Katoh M, Suzuyama N, Takeuchi T, Yoshitomi S, Asahi S, Yokoi T. Kinetic Analyses for Species Differences in P-Glycoprotein-Mediated Drug Transport. *J Pharm Sci* (2006) 95:2673–83. doi: 10.1002/jps.20686

Conflict of Interest: KT, TS, TO, AK, GN, SI, SK, AT, MT, and YS are employed by Yakult Honsha Co., Ltd.

Publisher's Note: All claims expressed in this article are solely those of the authors and do not necessarily represent those of their affiliated organizations, or those of the publisher, the editors and the reviewers. Any product that may be evaluated in this article, or claim that may be made by its manufacturer, is not guaranteed or endorsed by the publisher.

Copyright © 2021 Taniguchi, Suzuki, Okamura, Kurita, Nohara, Ishii, Kado, Takagi, Tsugane and Shishido. This is an open-access article distributed under the terms of the Creative Commons Attribution License (CC BY). The use, distribution or reproduction in other forums is permitted, provided the original author(s) and the copyright owner(s) are credited and that the original publication in this journal is cited, in accordance with accepted academic practice. No use, distribution or reproduction is permitted which does not comply with these terms.



Targeting GGT1 Eliminates the Tumor-Promoting Effect and Enhanced Immunosuppressive Function of Myeloid-Derived Suppressor Cells Caused by G-CSF

Zhiqi Xie¹, Takahiro Kawasaki¹, Haoyang Zhou¹, Daisuke Okuzaki^{2,3}, Naoki Okada¹ and Masashi Tachibana^{1,4*}

¹Project for Vaccine and Immune Regulation, Graduate School of Pharmaceutical Sciences, Osaka University, Osaka, Japan,

²Single Cell Genomics, Human Immunology, WPI Immunology Frontier Research Center, Osaka University, Osaka, Japan,

³Genome Information Research Center, Research Institute for Microbial Diseases, Osaka University, Osaka, Japan, ⁴Global Center for Medical Engineering and Informatics, Osaka University, Osaka, Japan

OPEN ACCESS

Edited by:

Peixin Dong,
Hokkaido University, Japan

Reviewed by:

Hiroaki Shime,
Nagoya City University, Japan
Masashi Ikutani,
Hiroshima University, Japan

*Correspondence:

Masashi Tachibana
tacci@phs.osaka-u.ac.jp
orcid.org/0000-0002-0376-508X

Specialty section:

This article was submitted to
Pharmacology of Anti-Cancer Drugs,
a section of the journal
Frontiers in Pharmacology

Received: 11 February 2022

Accepted: 07 April 2022

Published: 25 April 2022

Citation:

Xie Z, Kawasaki T, Zhou H, Okuzaki D,
Okada N and Tachibana M (2022)
Targeting GGT1 Eliminates the Tumor-
Promoting Effect and Enhanced
Immunosuppressive Function of
Myeloid-Derived Suppressor Cells
Caused by G-CSF.
Front. Pharmacol. 13:873792.
doi: 10.3389/fphar.2022.873792

Myeloid-derived suppressor cells (MDSCs) are major immunosuppressive cells that accumulate in tumor-bearing hosts. Since MDSCs suppress anti-tumor immunity and promote tumor progression, they are promising targets for cancer immunotherapy. Granulocyte colony-stimulating factor (G-CSF) is an agent used for the treatment of chemotherapy-induced febrile neutropenia (FN) in patients with cancer. However, several reports have revealed that G-CSF plays crucial immune-related adverse roles in tumor progression through MDSCs. In this study, we showed that MDSCs differentiated in the presence of G-CSF *in vitro* exhibited enhanced proliferation and immunosuppressive activity compared to those differentiated without G-CSF. RNA sequencing analysis demonstrated that G-CSF enhanced the immunosuppressive function of MDSCs by upregulating gamma-glutamyltransferase (GGT) 1. Moreover, in the EL4 lymphoma-bearing neutropenic mouse model, administration of recombinant G-CSF increased the number of MDSCs and attenuated the anti-cancer effect of chemotherapy. We showed that the combination of GGsTop, a GGT inhibitor, could prevent G-CSF-induced tumor growth, without affecting the promotion of myelopoiesis by G-CSF. These results suggest that targeting GGT1 can mitigate G-CSF-induced enhanced immunosuppressive functions of MDSCs and can eliminate the tumor-promoting effect of G-CSF. Furthermore, GGsTop could be an attractive combination agent during G-CSF treatment for FN in patients with cancer.

Keywords: myeloid-derived suppressor cells, granulocyte colony-stimulating factor, GGT1, febrile neutropenia, GGsTop

INTRODUCTION

Myeloid-derived suppressor cells (MDSCs) are immature myeloid cells that accumulate in cancer patients as well as in mouse tumor models. MDSCs play important roles in the suppression of anti-tumor immunity, resulting in the exacerbation of cancer (Fleming et al., 2018; Ostrand-Rosenberg and Fenselau, 2018; Veglia et al., 2021). Phenotypically and morphologically, MDSCs are classified into two subpopulations, namely monocytic (M)-MDSCs with CD11b⁺Ly-6G[−]Ly-6C^{hi} phenotype

and polymorphonuclear (PMN)-MDSCs with CD11b⁺Ly-6G⁺Ly-6C^{int} phenotype (Bronte et al., 2016). M-MDSCs reportedly suppress T cell proliferation via arginase 1 and inducible nitric oxide synthase (iNOS), and PMN-MDSCs show an inhibitory effect via arginase 1 and reactive oxygen species (ROS) (Bronte et al., 2016). However, the mechanisms underlying the immunosuppressive function of MDSCs remain largely unexplored.

Febrile neutropenia (FN) is a deadly complication associated with cancer chemotherapy, usually indicating infection and sepsis, and commonly occurs following the initial cycles of myelosuppressive therapy (Klastersky et al., 2016). Prevention of FN reduces lengthy hospitalization, morbidity, mortality, and risk of chemotherapy reductions and delays (Kuderer et al., 2006; Mehta et al., 2015; Lucas et al., 2018). Granulocyte colony-stimulating factor (G-CSF) is a principal cytokine promoting and mobilizing granulocytes. Recombinant human G-CSF as prophylaxis and therapy has been shown to significantly reduce FN incidence and mortality following chemotherapy (Klastersky et al., 2016; Lucas et al., 2018). However, several observations suggest that G-CSF promotes tumor growth, metastasis, and resistance to chemotherapy by increasing the number of circulating MDSCs (Kawano et al., 2015; Pilatova et al., 2018) and is associated with a poor clinical prognosis (Hollmén et al., 2016; Liu et al., 2020). Although G-CSF has become the main therapeutic agent in cancer therapy for the treatment of neutropenia and prevention of FN, it is necessary to evaluate its impact on tumor-bearing patients. Therefore, considering the possible side effects of G-CSF in promoting tumor progression through MDSCs, there is an urgent need to elucidate the direct mechanism underlying the effect of G-CSF on MDSCs.

MATERIALS AND METHODS

Mice

Female C57BL/6J mice were purchased from Japan SLC (Shizuoka, Japan). All mice were bred and maintained under specific pathogen-free conditions and used for experiments at 6–8 weeks of age. All experimental procedures in this study were performed in accordance with the institutional guidelines for animal experiments at the Osaka University, Japan.

Cell Line

The EL4 cell lines were purchased from the American Type Culture Collection (ATCC) and maintained in RPMI-1640 medium (FUJIFILM Wako, Osaka, Japan) supplemented with 10% fetal bovine serum (FBS; Gibco, CA, United States) and 1% Antibiotic-Antimycotic Mixed Stock Solution (100 ×) (Nacalai Tesque, Kyoto, Japan). Cells were cultured according to the ATCC guidelines and used within 1 month of thawing from an early passage (<3 passages of original vial) lots.

MDSC Differentiation *in vitro*

The *in vitro* differentiation of bone marrow (BM) cells into MDSCs was performed as described previously (Xie et al.,

2018). Briefly, BM cells from C57BL/6J mice were stimulated with 40 ng/ml recombinant Granulocyte-macrophage CSF (GM-CSF) (Peprotech, NJ, United States) for 4 days in the absence or presence of G-CSF (5 ng/ml, BioLegend, CA, United States) and/or GGTsTop (50 mM, FUJIFILM Wako) to examine their effects on MDSCs.

Flow Cytometry Analysis

Cells were pelleted and washed in phosphate-buffered saline (PBS) supplemented with 2% FBS (2% FBS/PBS). The cell suspension was first blocked with TruStain fcX (anti-mouse CD16/32) antibody (BioLegend) for 5 min, and then stained with the following antibodies (Abs) for 15 min at 4°C: APC anti-mouse CD11b, Pacific Blue anti-mouse Gr-1, PE anti-mouse F4/80, FITC anti-mouse CD11c, APC-Cy7 anti-mouse Ly-6C, FITC anti-mouse Ly-6G, Pacific Blue anti-mouse CD4, and FITC anti-mouse CD8α (BioLegend). Next, the cells were washed and resuspended in 2% FBS/PBS. Shortly before performing measurements, a 7-amino actinomycin D viability staining solution (BioLegend) was added to each sample to stain dead cells. Flow cytometry analysis was performed on a BD FACSCanto II flow cytometer (BD Biosciences), and results were analyzed using the FlowJo software (version10.7.0, BD Biosciences).

In vitro Suppression Assay

CD4⁺ T cells or CD8⁺ T cells were isolated from the spleens of C57BL/6J mice using the MojoSort magnetic cell separation system as previously described (Xie et al., 2018) and then labeled with the proliferation dye eFluor 670 (eBioscience, Thermo Fisher Scientific, CA, United States). The eFluor 670-labeled CD4⁺ T cells or CD8⁺ T cells were incubated with *in vitro* differentiated MDSCs at different ratios in a 96-well plate cultured with anti-mouse CD3ε Ab/anti-mouse CD28 Ab (BioLegend). After 3 days of incubation at 37°C in 5% CO₂, the proliferation of CD4⁺ and CD8⁺ T cells determined by the eFluor 670 fluorescence intensity was analyzed using flow cytometry.

Quantitative Reverse Transcription Polymerase Chain Reaction

PMN-MDSCs (Ly-6G⁺Ly-6C^{int}) and M-MDSCs (Ly-6G⁺Ly-6C^{hi}) were purified from *in vitro*-differentiated MDSCs cultured with or without the addition of G-CSF by fluorescence-activated cell sorting (purity >95%; JSAN, Bay bioscience Co., Ltd., Kobe, Japan). Total RNA was extracted from the *in vitro* differentiated MDSCs or sorted MDSC subsets and used to synthesize cDNA using the QuantiTect reverse transcription kit (Qiagen, Hilden, Germany) following the manufacturer's instructions. qRT-PCR was performed using SYBR Premix Ex Taq (Tli RNaseH Plus; TaKaRa, Kusatsu, Japan) on a CFX96 touch real-time PCR detection system (Bio-Rad). The specific primer sequences are listed in **Supplementary Table S1**. Glyceraldehyde 3-phosphate dehydrogenase (*Gapdh*) was used as a reference gene, and relative expressions of other genes were calculated using the 2^{−ΔΔCt} method.

RNA Sequencing Analysis

Total RNA was extracted from cells using the miRNeasy Mini kit (Qiagen) according to the manufacturer's protocol. RNA libraries were prepared for sequencing using a TruSeq stranded mRNA sample prep kit (Illumina, CA, United States) according to the manufacturer's instructions. Whole transcriptome sequencing was performed on RNA samples using the Illumina HiSeq 2500 platform in a 75 bp single-end mode. Volcano plot representation and pathway enrichment analysis of the differentially expressed genes were performed using BioJupies tools with adjusted $p < 0.05$ and fold change > 2 (Torre et al., 2018). Raw data from this study have been submitted to Gene Expression Omnibus (GEO) under the accession number GSE183066.

Gamma-Glutamyltransferase Activity Measurement

MDSCs (1×10^6 cells) were homogenized in 200 μ L of GGT assay buffer and centrifuged at $13,000 \times g$ for 10 min following which the supernatant was collected. After reacting with the GGT substrate at 37°C for 40 min, fluorescence (365/460 nm) was measured using a microplate reader SpectraMax iD5 (Molecular Devices). GGT activity was calculated according to the protocol of the GGT Activity Colorimetric Assay Kit (BioVision, CA, United States).

Glutamate Measurement

The *in vitro* MDSC culture medium was collected on day 4. Next, glutamate concentration was measured using Glutamate Assay Kit-WST (Dojindo, Kumamoto, Japan) according to the manufacturer's protocol. Briefly, a glutamate standard or MDSC culture medium was added to a 96-well microplate; the working solution was then added to each well. After incubating the microplate at 37°C for 30 min, the absorbance was measured at 450 nm using SpectraMax iD5 (Molecular Devices). The glutamate concentration in each sample was calculated using a standard curve.

ROS Level Measurement

Intracellular ROS was assayed using a ROS Assay Kit-Highly Sensitive DCFH-DA (Dojindo) according to the manufacturer's protocol. Briefly, 2×10^5 MDSCs were treated with $2', 7'$ -dichlorofluorescein diacetate (DCFH-DA) working solution and incubated for 30 min. Subsequently, the MDSCs were washed twice with Hanks' Balanced Salt Solution, and ROS production was measured using a BD FACSCanto II flow cytometer (BD Biosciences).

Cyclophosphamide -Induced Neutropenic Tumor Model

EL4 lymphoma cells (4×10^5 cells/mouse) were injected subcutaneously into the lower right flank of C57BL/6J mice. Seven days after inoculation with EL4 cells, mice were intraperitoneally administered a single dose of CPA (100 mg/kg, FUJIFILM Wako) to create a neutropenic mouse

model as described previously (Hattori et al., 1990). Starting from the same day, experimental mice received intraperitoneal injections of PBS, GGTsTop (5 mg/kg, FUJIFILM Wako), and recombinant G-CSF (200 μ g/kg, BioLegend) for six consecutive days. Before administration of the above reagent, mouse retro-orbital blood (approximately 75 μ L) was collected for flow cytometry analysis and determining blood cell counts using a Sysmex XT-2000i automated hematology analyzer (Sysmex) daily. The tumor volume was calculated periodically up to day 15 using the following formula: Tumor Volume (cm^3) = $0.5 \times (\text{Length} \times \text{Width}^2)$.

Statistical Analysis

Significant differences were assessed using Student's *t*-test, or a one- or two-way analysis of variance (ANOVA) using GraphPad Prism 7.0 (GraphPad Software). Statistical significance was set at $p < 0.05$.

RESULTS

G-CSF Regulates the Differentiation and Immunosuppressive Activity of MDSCs

Previous studies have reported that GM-CSF stimulates BM cells to differentiate into MDSCs (hereafter referred to as *in vitro* MDSCs). Freshly isolated BM cells were cultured for 4 days in a medium supplemented with or without G-CSF and GM-CSF to examine whether G-CSF affects the differentiation of *in vitro* MDSCs. G-CSF did not affect the percentage of MDSCs ($\text{CD11b}^+\text{Gr-1}^+$), dendritic cells (DCs; $\text{Gr-1}^-\text{CD11c}^+$), or macrophages ($\text{Gr-1}^-\text{F4/80}^+$) differentiated from BM cells, as shown in **Figure 1A**. The proportion of M-MDSCs with the $\text{CD11b}^+\text{Ly-6G}^-\text{Ly-6C}^{\text{hi}}$ phenotype increased in the presence of G-CSF, whereas PMN-MDSCs with the $\text{CD11b}^+\text{Ly-6G}^+\text{Ly-6C}^{\text{int}}$ phenotype decreased (**Figure 1B**). However, since whole BM cells largely increased with stimulation by G-CSF, there was no change in the number of PMN-MDSCs, and M-MDSCs substantially increased (**Figure 1C**). These results suggest that G-CSF promotes the proliferation of MDSCs, especially M-MDSCs.

Next, we investigated whether G-CSF affected the immunosuppressive activity of *in vitro* MDSCs. Suppression of CD4^+ T cell proliferation was observed in *in vitro* MDSCs that were not treated with G-CSF, and the immunosuppressive activity was impaired with decreasing numbers of MDSCs. Moreover, the immunosuppressive activity of *in vitro* MDSCs was significantly enhanced by G-CSF treatment (**Figure 1D**). Similar results were obtained in the CD8^+ T cell suppression assay (**Figure 1E**). These observations revealed that T cells, especially CD4^+ T cells, were less proliferative when co-cultured with G-CSF-conditioned *in vitro* MDSCs, suggesting that G-CSF strongly enhanced the immunosuppressive activity of *in vitro* MDSCs.

Identifying G-CSF-Induced MDSC Gene Expression Profile Using RNA-Seq

To explore the mechanism by which G-CSF enhances the immunosuppressive function of MDSCs, we first analyzed the

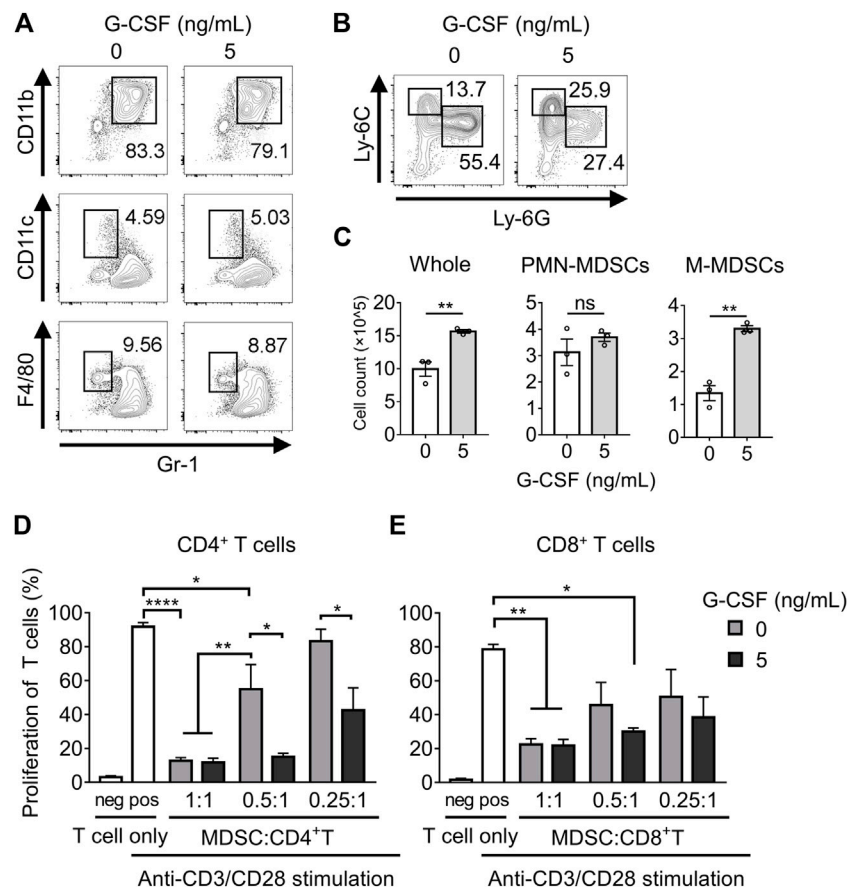


FIGURE 1 | G-CSF regulates the differentiation and immunosuppressive activity of MDSCs. **(A)** Flow cytometry analysis of the percentage of MDSC (CD11b⁺Gr-1⁺), DC (Gr-1⁺CD11c⁺), and macrophage (Gr-1⁺F4/80⁺) populations after 4 days of culture in medium supplemented with GM-CSF (40 ng/ml) with or without G-CSF stimulation (5 ng/ml). **(B)** Flow cytometry analysis of the percentage of PMN-MDSCs (CD11b⁺Ly-6G⁺Ly-6C^{int}) and M-MDSCs (CD11b⁺Ly-6G⁺Ly-6C^{hi}) among CD11b⁺ cells. **(C)** Total numbers of *in vitro* MDSCs and their subset dyed with trypan blue are represented as means ± SEM ($n = 3$, Student's *t*-test: ** $p < 0.01$). **(D)** CD4⁺ or CD8⁺ T cells derived from WT mice were co-cultured with *in vitro* MDSCs under the stimulation of anti-CD3ε/CD28 antibodies. After three-day-culture, T cell proliferation in the absence or presence of MDSCs was examined by flow cytometry. Data are represented as means ± SEM ($n = 5$ pooled with two independent experiments, two-way ANOVA: * $p < 0.05$, ** $p < 0.01$, and **** $p < 0.0001$).

expression of the main immunosuppressive molecules of MDSCs: arginase 1 and iNOS as well as ROS by qRT-PCR or flow cytometry analysis. We found that the mRNA levels of *Arg1* and *Nos2* were significantly upregulated by G-CSF and that ROS levels determined by DCFH-DA also increased (Figures 2A,B). Besides, G-CSF upregulated the expression of *Arg1* and *Nos2* in both PMN-MDSCs and M-MDSCs, indicating that the G-CSF-induced upregulation of those genes was because of the enhanced transcription of the genes but not because of the alteration of the population of MDSC subsets (Figures 2C,D).

Next, we performed an RNA-seq analysis, comparing the gene expression profiles of *in vitro* MDSCs differentiated with or without G-CSF. There were 228 genes differentially expressed with fold change >2 and adjusted $p < 0.05$ when comparing both groups. Among these genes, 89 genes were expressed at higher levels in MDSCs differentiated in the presence of G-CSF than in those differentiated without G-CSF, and 139 genes showed lower expression. Increased expression of *Arg1*, *Nos2*, and *Mpo*, which are the immunosuppressive molecules of MDSCs, was observed

(Figure 2E), consistent with the above results. Additionally, pathway enrichment analysis revealed that the MDSCs differentiated with G-CSF displayed the activation of the cell cycle, metabolism, and DNA replication, which would account for the enhanced proliferation of MDSCs differentiated with G-CSF (Figure 2F).

GGT1 Is Involved in the Enhanced Immunosuppressive Function of MDSCs by G-CSF

Next, among the top 20 upregulated genes by G-CSF, genes associated with poor prognosis (Logrank $p < 0.05$) in more than four cancers, including *Nos2*, proprotein convertase subtilisin/kexin type 9 (*Pcsk9*), PRKC apoptosis WT1 regulator (*Pawr*), and gamma-glutamyltransferase 1 (*Ggt1*), were identified as candidate factors involved in the immunosuppressive ability of MDSCs using the GEPIA web server (Tang et al., 2017) (Supplementary Figure S1). GGT1 is a key enzyme involved in several metabolic

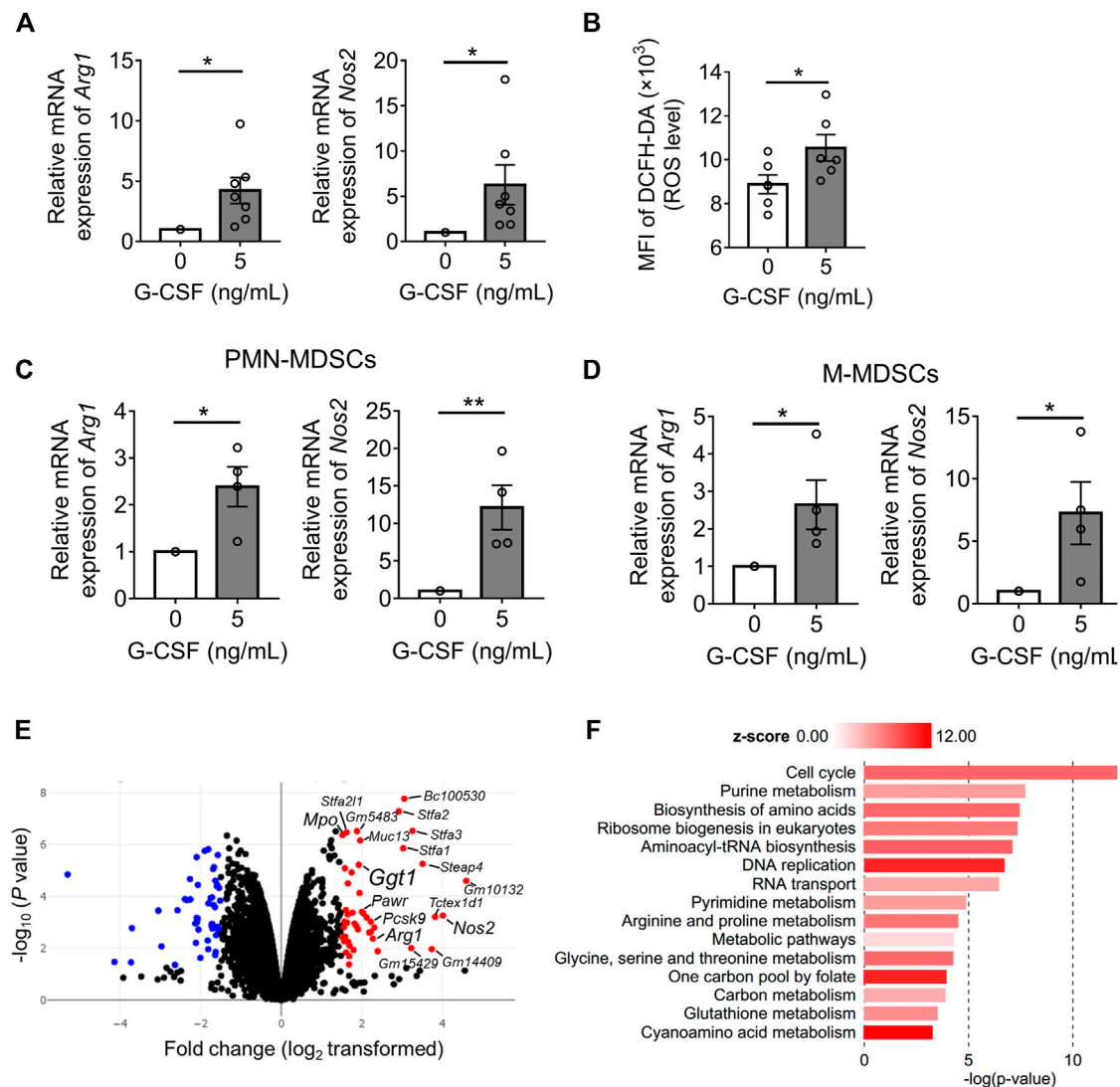


FIGURE 2 | Identifying G-CSF-induced MDSC gene expression profile using by RNA sequencing. **(A)** The mRNA expression of *Arg1* and *Nos2* of *in vitro* MDSCs cultured with GM-CSF with or without the addition of G-CSF was measured by qRT-PCR. Data are represented as means \pm SEM of three independent experiments and normalized to the expression of *Gapdh* housekeeping gene (*Arg1*: $n = 7$; *Nos2*: $n = 7$; Student's *t*-test: * $p < 0.05$). **(B)** Intracellular ROS level was measured by flow cytometry analysis using DCFH-DA (means \pm SEM, $n = 4$ pooled with two independent experiments, Student's *t*-test: * $p < 0.05$). **(C,D)** The mRNA expressions of *Arg1* and *Nos2* in the sorted PMN-MDSCs and M-MDSCs were measured by qRT-PCR (means \pm SEM, $n = 4$ pooled with two independent experiments, Student's *t*-test: * $p < 0.05$, ** $p < 0.01$). **(E)** Volcano plots showing differences in the mRNA expression profile of *in vitro* MDSCs ($n = 2$ biological replicates). **(F)** KEGG pathway enrichment analysis of significantly upregulated gene sets in MDSCs stimulated by G-CSF using BioJuplies tools ($n = 2$ biological replicates).

processes, such as glutathione metabolism and cyanoamino acid metabolism (Verma et al., 2015), which were also enriched and active in MDSCs differentiated with G-CSF (Figure 2F). Furthermore, GGT is expressed on the cell surface, acts as a glutathione hydrolase that increases extracellular cysteinyl glycine and glutamate, and is reported to be associated with the progression of several tumors (Wang et al., 2017; Ince et al., 2020). Thus, to identify novel factors involved in the immunosuppressive ability of MDSCs, we focused on the *Ggt1* gene.

The upregulation of the mRNA of *Ggt1* by G-CSF in MDSCs was verified by qRT-PCR (Figure 3A). Besides, *Ggt1* mRNA

expression was more upregulated in M-MDSCs than in PMN-MDSCs upon G-CSF stimulation, suggesting that M-MDSCs can play an important role in increasing the G-CSF-promoted immunosuppressive effects (Figure 3B). To elucidate whether GGT1 is involved in the enhanced immunosuppressive function of MDSCs by G-CSF, we used GGsTop, a highly selective GGT inhibitor. The GGT activity of MDSCs was enhanced by G-CSF, which was inhibited below the detection limit in the GGsTop alone and G-CSF/GGsTop combination groups (Figure 3C). There was no change in the number of MDSCs in the presence of GGsTop (Figure 3D), suggesting that the inhibition of GGT did not affect the G-CSF-induced

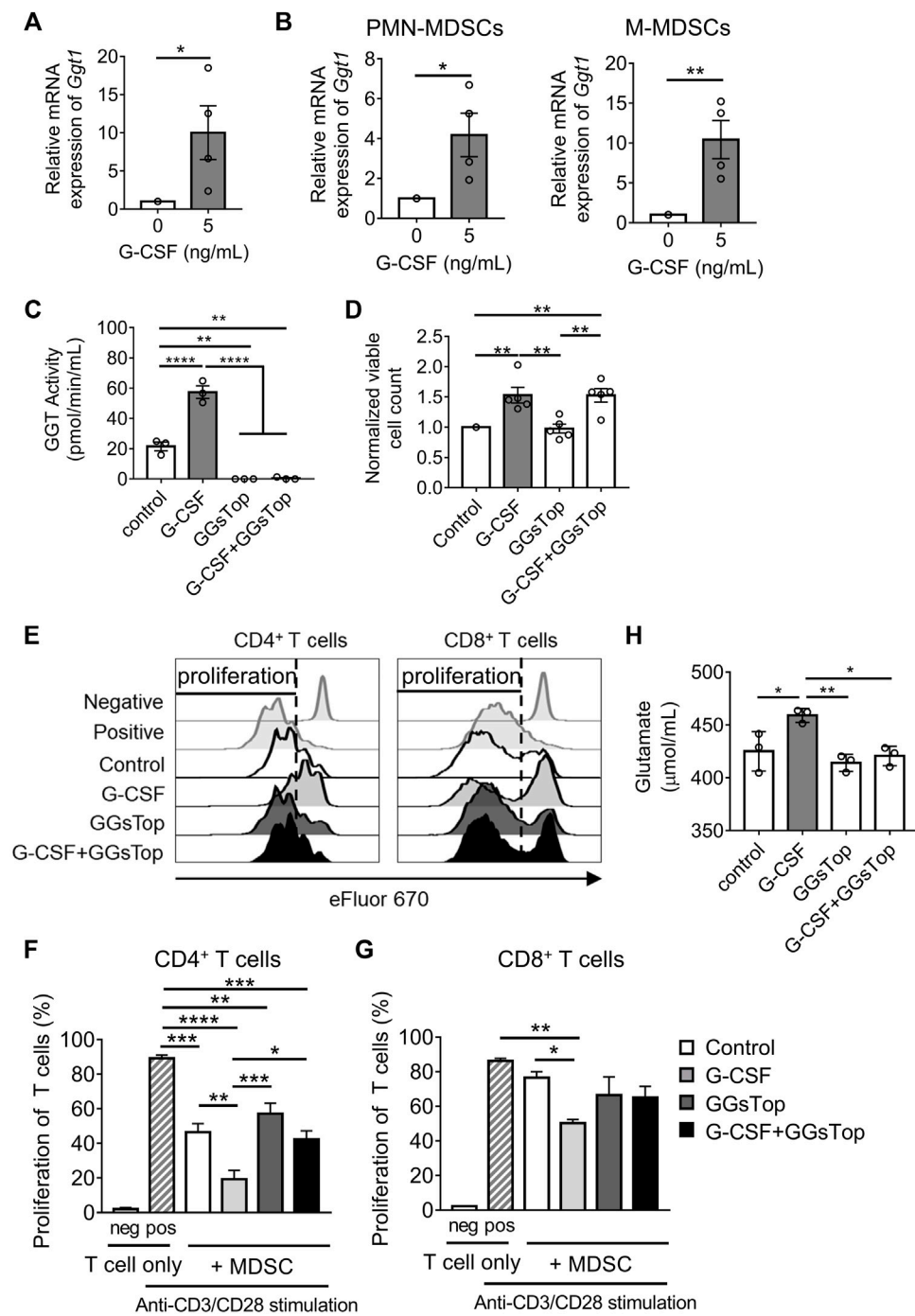


FIGURE 3 | GGT1 is involved in the G-CSF-enhanced immunosuppressive function of MDSCs. **(A)** The mRNA expression of *Ggt1* in *in vitro* MDSCs was measured by qRT-PCR. Data are represented as means \pm SEM of three independent experiments ($n = 4$, Student's *t*-test: * $p < 0.05$). **(B)** The mRNA expression of *Ggt1* in the sorted PMN-MDSCs and M-MDSCs was measured by qRT-PCR (means \pm S.E.M., $n = 4$ pooled with two independent experiments, Student's *t*-test: * $p < 0.05$, ** $p < 0.01$). **(C)** GGT activity of *in vitro* MDSCs cultured with or without the addition of G-CSF and/or GGsTop was measured using a GGT activity assay kit (means \pm SEM, $n = 4$ pooled with two independent experiments, one-way ANOVA: * $p < 0.05$, ** $p < 0.01$, and **** $p < 0.0001$). **(D)** The numbers of *in vitro* MDSCs were measured by trypan blue dye exclusion method (means \pm SEM, $n = 5$ pooled with three independent experiments, one-way ANOVA: ** $p < 0.01$). **(E–G)** MDSCs conditioned with or without G-CSF or GGsTop were combined in a 0.5:1 ratio with eFluor 670-labeled CD4⁺ or CD8⁺ T cells, followed by stimulation with anti-CD3 ϵ /CD28 antibodies. **(E)** Representative histograms of eFluor 670 expressions in CD4⁺ or CD8⁺ T cells. **(F,G)** T cell proliferation was examined by flow cytometry. Data are represented as means \pm SEM (two-way ANOVA: * $p < 0.05$, ** $p < 0.01$, *** $p < 0.001$, and **** $p < 0.0001$). **(H)** The glutamate level was measured from the culture medium of *in vitro* MDSCs by glutamate assay-kit (means \pm SEM, $n = 4$ pooled with two independent experiments, one-way ANOVA: * $p < 0.05$, ** $p < 0.01$).

proliferation of BM cells. Meanwhile, the addition of GGsTop did not affect the proportion and number of M-MDSCs or PMN-MDSCs (**Supplementary Figures S2A,B**). We further investigated whether GGsTop cancels the enhancement of the immunosuppressive activity of *in vitro* MDSCs by G-CSF. Consistent with *Ggt1* expression, the immunosuppressive activity of *in vitro* MDSCs was significantly increased by G-CSF, while the combination of GGsTop and G-CSF attenuated the immunosuppressive activity to the same level as that in the control group (**Figures 3E–G**). Additionally, GGsTop alone did not affect the immunosuppressive activity of *in vitro* MDSCs. Furthermore, we examined the effect of GGsTop alone or the G-CSF/GGsTop combination on *Arg1*, *Nos2*, and ROS expression. The G-CSF/GGsTop combination group downregulated the expression of *Arg1* and *Nos2*. Unexpectedly, GGsTop alone upregulated their expression (**Supplementary Figure S2C**). As *Arg1* and *Nos2* upregulation by GGsTop alone did not increase the immunosuppressive ability of MDSCs (**Figures 3E,F**), suggesting that the upregulation of *Arg1* and *Nos2* did not play a decisive role in increasing the MDSC immunosuppressive ability caused by G-CSF. In addition, GGsTop did not abrogate the expression of ROS caused by G-CSF, suggesting that ROS is not a key factor either (**Supplementary Figure S2D**). These results suggest that inhibition of GGT1 activity eliminates G-CSF-induced enhanced immunosuppressive function of MDSCs, but has no effect on its ability to promote proliferation.

The key role of GGT1 is to hydrolyze glutathione. We speculated that metabolites of glutathione, such as glutamate and cysteinyl glycine, obtained by the action of GGT1, enhance the immunosuppressive function of MDSCs. Elevated glutamate concentrations are commonly observed in tumor patients, and studies indicate that glutamate could regulate the immunosuppressive activity of MDSCs on the proliferation of T cells (Morikawa et al., 2018; Wu et al., 2019). Therefore, we measured the concentration of glutamate to determine whether the level of glutamate is regulated by GGT1. Glutamate levels were increased on treating cells with G-CSF and were decreased on treatment with GGsTop both alone and in combination with G-CSF (**Figure 3H**). GGsTop alone or the G-CSF/GGsTop combination did not significantly reduce glutamate levels compared with the control, which explained why GGsTop alone did not inhibit MDSC-mediated T cell suppression. These observations revealed that elevated GGT activity induced by G-CSF increased glutamate levels, and that GGT1 is a novel factor involved in the enhanced immunosuppressive function of MDSCs induced by G-CSF.

GGsTop Eliminates the Effect of G-CSF in Promoting Tumor Growth

Given that G-CSF enhances the immunosuppressive function and proliferation of MDSCs, it is possible that G-CSF causes side effects through MDSCs when used to prevent FN. We then tested whether G-CSF promoted MDSCs and tumor progression using the EL4 lymphoma-bearing neutropenic mouse model. In the EL4 tumor-bearing mouse model, administration of the anti-

tumor drug CPA reduced white blood cells, including neutrophils, monocytes, and lymphocytes to 50% below the pretreatment value measured using an XT-2000i hematology analyzer, leading to neutropenia (**Figures 4A–D**). CPA strongly inhibited tumor growth (**Figure 4F**). In contrast, the accelerated recovery of white blood cells was observed in mice administered G-CSF after CPA. G-CSF dramatically increased neutrophil and monocyte counts from days 11–13 and facilitated the recovery of lymphocytes to control levels (**Figures 4A–D**), which would reduce the risk associated with CPA-induced neutropenia. Flow cytometry analysis revealed that the proportion of M-MDSCs and PMN-MDSCs in the G-CSF group increased significantly, suggesting that G-CSF promoted neutrophils and monocytes that were morphologically identified using an XT-2000i hematology analyzer to be mixed with most MDSCs (**Figure 4E**). Furthermore, tumor progression was observed after G-CSF administration, suggesting that G-CSF-induced MDSCs attenuated the anti-tumor effect of CPA (**Figure 4F**). Next, we explored whether GGsTop could inhibit the growth of tumors induced by G-CSF while maintaining myelopoiesis by G-CSF. As expected, GGsTop alone did not affect the dynamics of myelopoiesis (**Figures 4A–E**) and tumor progression (**Figure 4F**). The combination of GGsTop and G-CSF promoted the proliferation of white blood cells, neutrophils, and monocytes in the G-CSF group and inhibited tumor growth in the presence of CPA. Consistent with other studies (Jounaidi and Waxman, 2001; Kim et al., 2018), due to CPA drug toxicity and rapid tumor growth in the PBS and GGsTop groups, the biological significance of body weight was shown in the CPA-treated and control mice. Moreover, the results showed that GGsTop was well-tolerated, with no significant decrease observed in the body weight (**Figure 4G**). These results suggest that targeting GGT eliminates the effect of G-CSF in promoting tumor growth. GGsTop could be an attractive combination agent with G-CSF for the treatment of neutropenia in patients with cancer.

DISCUSSION

To date, G-CSF administration is commonly used in the management of cancer patients and dramatically reduces the risks associated with chemotherapy-induced FN (Pilátová et al., 2018). However, an increasing number of studies have found that G-CSF enhances the pro-tumor effects of MDSCs, thereby leading to poor prognosis and chemoresistance in cancers (Hollmén et al., 2016; Liu et al., 2020; Karagiannidis et al., 2021). Therefore, the safety of G-CSF as an adjunct to cancer treatment should be addressed. Although further research is needed, our pre-clinical data showed that G-CSF promotes tumor growth in the CPA-induced neutropenia EL4 tumor-bearing model, which would result from the enhancement of immunosuppressive function and the increase in the number of MDSCs by G-CSF.

To eliminate the side effects of G-CSF, it is necessary to elucidate the direct mechanism underlying the action of G-CSF on MDSCs. We utilized *in vitro* MDSCs and RNA-seq analysis and identified that GGT1 played a pivotal role in enhancing the immunosuppressive function of MDSCs by G-CSF. GGT1 is a member of the GGT family, which also

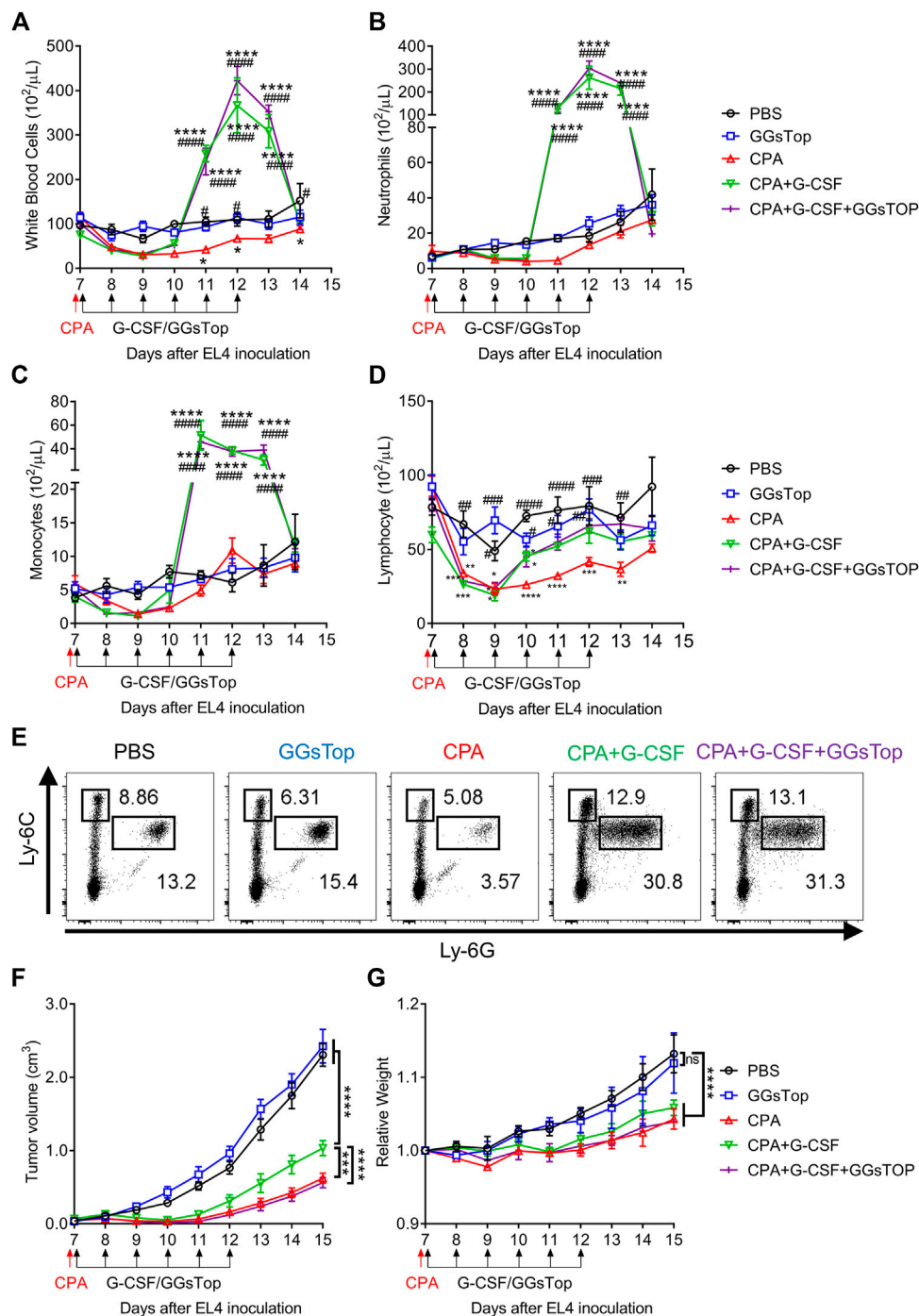


FIGURE 4 | GGTsTop eliminates the effect of G-CSF in promoting tumor growth. **(A–D)** Dynamics of circulating **(A)** white blood cells, **(B)** neutrophils, **(C)** monocytes, and **(D)** lymphocytes was examined using a Sysmex XT-2000i automated hematology analyzer (means \pm SEM, pooled from two independent experiments with $n = 6$, $^*p < 0.05$, $^{**}p < 0.01$, $^{***}p < 0.001$ and $^{****}p < 0.0001$ compared with PBS group by two-way ANOVA; $^{\#}p < 0.05$, $^{\#\#}p < 0.01$, $^{\#\#\#}p < 0.001$ and $^{\#\#\#\#}p < 0.0001$ compared with CPA group by two-way ANOVA). **(E)** Flow cytometric analysis of MDSC subsets in the blood at 4 days after CPA/G-CSF/GGTsTop administration. **(F, G)** Tumor volumes and relative body weight were calculated periodically and are shown as means \pm SEM, pooled from two independent experiments with $n = 6$ ($^{***}p < 0.001$, and $^{****}p < 0.0001$ by two-way ANOVA).

includes other proteins, such as GGT2, GGT3P, GGT4P, GGT5, GGT6, GGT7, and GGT8P. Among these, GGT1 and GGT5 are the only two enzymes with catalytic activity (Takemura et al.,

2021), and the catalytic rate of GGT1 is approximately 46 times faster than that of GGT5 (Wickham et al., 2011). Therefore, GGT1 is the main catalytically active enzyme in the GGT family.

It has been reported that the activity of GGT is increased in cancers resistant to chemotherapy, and the removal of glutathione, the substrate of GGT, in tumors inhibits tumor progression and metastasis (Mena et al., 2007; Hanigan, 2014). Our results also showed that G-CSF upregulated GGT1 expression on MDSCs, while GGsTop canceled the enhanced T cell proliferation inhibitory ability of MDSCs induced by G-CSF. Additionally, we showed that G-CSF increased the level of glutamate in the culture medium. GGT1 hydrolyzes extracellular glutathione to produce glutamate. Glutamate was originally discovered to be the main excitatory neurotransmitter in the central nervous system and can also act as a signaling molecule in other tissues (Affaticati et al., 2011). Recent studies have shown that glutamate could promote the activation of early MDSCs and the high concentrations of extracellular glutamate can suppress T cell activation (Pouloupoulou et al., 2005; Wu et al., 2019). Previously, we found that glutamate signaling through metabotropic glutamate receptor 2/3 increases the potency of the immunosuppressive ability of MDSCs, especially the inhibition of CD4⁺ T cell proliferation, similar to G-CSF (Morikawa et al., 2018). The expression of glutamate receptors differs among different types of T lymphocytes (Pacheco et al., 2007); thus, CD8⁺ T cells may express lower glutamate receptor levels, resulting in the relative resistance of CD8⁺ T cells to the increased suppressive function of MDSCs cultured with G-CSF. These results indicate that the mechanism by which G-CSF enhances the immunosuppressive ability of MDSCs may involve GGT-induced increased glutamate levels.

GGsTop is now commercially available and its beneficial properties, such as being non-toxic, highly selective, and potent irreversible inhibitor of GGT activity, have been reported under a variety of experimental conditions (Kamiyama et al., 2016). For example, it has been reported that GGsTop could quickly and safely treat oral mucositis induced by cancer chemotherapy (Shimamura et al., 2019), reduce hepatic ischemia-reperfusion injury (Tamura et al., 2016), and may protect against chronic experimental autoimmune encephalomyelitis progression (Mendiola et al., 2020). Our results demonstrated its safety and effectiveness in an *in vivo* CPA-induced neutropenic tumor model, indicating that GGsTop can eliminate the effect of G-CSF in promoting tumor growth. Inhibition of GGT1 by GGsTop did not affect the viability and proliferation of MDSCs *in vitro*, as assessed by cell number quantification. The numbers of white blood cells, neutrophils, monocytes, and lymphocytes were similar after 6 days of treatment with GGsTop compared to PBS control *in vivo*. Accordingly, the inhibition of GGT1 by another inhibitor, acivicin, also showed no difference in microglia, macrophages, and whole blood cell numbers, but altered the glutathione metabolism of those cells (Mendiola et al., 2020). These results indicated that inhibiting GGT1 regulated the metabolism and activity of myeloid cells, including MDSCs, but had no effect on their proliferative activity.

In conclusion, our study showed that G-CSF directly enhanced the proliferation and immunosuppressive function of MDSCs and identified GGT1 as a novel factor involved in the enhanced immunosuppressive function of MDSCs induced by G-CSF. Furthermore, our results demonstrated that tumor progression

in the chemotherapy-induced neutropenic mouse model was promoted by G-CSF, and the specific GGT inhibitor, GGsTop, prevented G-CSF-induced EL4 lymphoma progression. Although our findings suggest that GGsTop exerts its effects by targeting GGT1 on MDSCs, GGT1 is also expressed in a variety of cells other than MDSCs, and the possibility that GGsTop functions through other cellular mechanisms cannot be excluded, thus suggesting the requirement for further studies. Our study also still lacks clinical human experimental data to prove the safety and efficacy of GGsTop, the existing results suggest that GGsTop would be effective in future clinical applications. These findings should contribute to the development of safer and more effective treatment strategies for FN in patients with cancer.

DATA AVAILABILITY STATEMENT

The datasets presented in this study can be found in online repositories. The names of the repository/repositories and accession number(s) can be found in the article/Supplementary Material.

ETHICS STATEMENT

The animal study was reviewed and approved by Osaka University.

AUTHOR CONTRIBUTIONS

ZX and MT conceptualized the study, designed the experiments, and wrote the manuscript. ZX and TK performed the experiments. HZ assisted in the acquisition of data. DO helped with the RNA-seq experiment and wrote the associated part of the manuscript. NO helped with the design of the experiments and assisted with discussions. All authors helped with reviewing and revising the manuscript.

FUNDING

This work was supported, in part, by JSPS KAKENHI Grant Number JP19H04049 [Grants-in-aid for Scientific Research (B)] and Suzuken Memorial Foundation (MT). This research was also partially supported by the Platform Project for Supporting Drug Discovery and Life Science Research [Basis for Supporting Innovative Drug Discovery and Life Science Research (BINDS)] from AMED under Grant Numbers JP21am0101084 and JP21am0101123.

SUPPLEMENTARY MATERIAL

The Supplementary Material for this article can be found online at: <https://www.frontiersin.org/articles/10.3389/fphar.2022.873792/full#supplementary-material>

REFERENCES

- Affaticati, P., Mignen, O., Jambou, F., Potier, M. C., Klingel-Schmitt, I., Degrouard, J., et al. (2011). Sustained Calcium Signalling and Caspase-3 Activation Involve NMDA Receptors in Thymocytes in Contact with Dendritic Cells. *Cell Death Differ* 18, 99–108. doi:10.1038/cdd.2010.79
- Bronte, V., Brandau, S., Chen, S. H., Colombo, M. P., Frey, A. B., Greten, T. F., et al. (2016). Recommendations for Myeloid-Derived Suppressor Cell Nomenclature and Characterization Standards. *Nat. Commun.* 7, 12150. doi:10.1038/ncomms12150
- Fleming, V., Hu, X., Weber, R., Nagibin, V., Groth, C., Altevogt, P., et al. (2018). Targeting Myeloid-Derived Suppressor Cells to Bypass Tumor-Induced Immunosuppression. *Front. Immunol.* 9, 398. doi:10.3389/fimmu.2018.00398
- Hanigan, M. H. (2014). Gamma-glutamyl Transpeptidase: Redox Regulation and Drug Resistance. *Adv. Cancer Res.* 122, 103–141. doi:10.1016/B978-0-12-420117-0.00003-7
- Hattori, K., Shimizu, K., Takahashi, M., Tamura, M., Oheda, M., Ohsawa, N., et al. (1990). Quantitative *In Vivo* Assay of Human Granulocyte colony-stimulating Factor Using Cyclophosphamide-Induced Neutropenic Mice. *Blood* 75, 1228–1233. doi:10.1182/blood.v75.6.1228.bloodjournal7561228
- Hollmén, M., Karaman, S., Schwager, S., Lisibach, A., Christiansen, A. J., Maksimow, M., et al. (2016). G-CSF Regulates Macrophage Phenotype and Associates with Poor Overall Survival in Human Triple-Negative Breast Cancer. *Oncoimmunology* 5, e115177. doi:10.1080/2162402X.2015.1115177
- Ince, V., Carr, B. I., Bag, H. G., Koc, C., Usta, S., Ersan, V., et al. (2020). Gamma Glutamyl Transpeptidase as a Prognostic Biomarker in Hepatocellular Cancer Patients Especially with >5 Cm Tumors, Treated by Liver Transplantation. *Int. J. Biol. Markers* 35, 91–95. doi:10.1177/1724600820921869
- Jounaidi, Y., and Waxman, D. J. (2001). Frequent, Moderate-Dose Cyclophosphamide Administration Improves the Efficacy of Cytochrome P-450/cytochrome P-450 Reductase-Based Cancer Gene Therapy. *Cancer Res.* 61, 4437–4444.
- Kamiyama, A., Nakajima, M., Han, L., Wada, K., Mizutani, M., Tabuchi, Y., et al. (2016). Phosphonate-based Irreversible Inhibitors of Human gamma-glutamyl Transpeptidase (GGT). GGSTop Is a Non-toxic and Highly Selective Inhibitor with Critical Electrostatic Interaction with an Active-Site Residue Lys562 for Enhanced Inhibitory Activity. *Bioorg. Med. Chem.* 24, 5340–5352. doi:10.1016/j.bmc.2016.08.050
- Karagiannidis, I., Salataj, E., Said Abu Egal, E., and Beswick, E. J. (2021). G-CSF in Tumors: Aggressiveness, Tumor Microenvironment and Immune Cell Regulation. *Cytokine* 142, 155479. doi:10.1016/j.cyt.2021.155479
- Kawano, M., Mabuchi, S., Matsumoto, Y., Sasano, T., Takahashi, R., Kuroda, H., et al. (2015). The Significance of G-CSF Expression and Myeloid-Derived Suppressor Cells in the Chemoresistance of Uterine Cervical Cancer. *Sci. Rep.* 5, 18217. doi:10.1038/srep18217
- Kim, J. W., Choi, J.-S., Seol, D. J., Choung, J. J., and Ku, S. K. (2018). Immunomodulatory Effects of Kuseonwangdago-Based Mixed Herbal Formula Extracts on a Cyclophosphamide-Induced Immunosuppression Mouse Model. *Evidence-Based Complement. Altern. Med.* 2018, 1–14. doi:10.1155/2018/6017412
- Klastersky, J., de Naurois, J., Rolston, K., Rapoport, B., Maschmeyer, G., Aapro, M., et al. (2016). Management of Febrile Neutropenia: ESMO Clinical Practice Guidelines. *Ann. Oncol.* 27, v111. doi:10.1093/annonc/mdw325
- Kuderer, N. M., Dale, D. C., Crawford, J., Cosler, L. E., and Lyman, G. H. (2006). Mortality, Morbidity, and Cost Associated with Febrile Neutropenia in Adult Cancer Patients. *Cancer* 106, 2258–2266. doi:10.1002/cncr.21847
- Liu, L., Liu, Y., Yan, X., Zhou, C., and Xiong, X. (2020). The Role of Granulocyte Colony-stimulating Factor in Breast Cancer Development: A Review. *Mol. Med. Rep.* 21, 2019–2029. doi:10.3892/mmr.2020.11017
- Lucas, A. J., Olin, J. L., and Coleman, M. D. (2018). Management and Preventive Measures for Febrile Neutropenia. *P T* 43, 228–232.
- Mehta, H. M., Malandra, M., and Corey, S. J. (2015). G-CSF and GM-CSF in Neutropenia. *J. Immunol.* 195, 1341–1349. doi:10.4049/jimmunol.1500861
- Mena, S., Benlloch, M., Ortega, A., Carretero, J., Obrador, E., Asensi, M., et al. (2007). Bcl-2 and Glutathione Depletion Sensitizes B16 Melanoma to Combination Therapy and Eliminates Metastatic Disease. *Clin. Cancer Res.* 13, 2658–2666. doi:10.1158/1078-0432.CCR-06-2642
- Mendiola, A. S., Ryu, J. K., Bardehle, S., Meyer-Franke, A., Ang, K. K., Wilson, C., et al. (2020). Transcriptional Profiling and Therapeutic Targeting of Oxidative Stress in Neuroinflammation. *Nat. Immunol.* 21, 513–524. doi:10.1038/s41590-020-0654-0
- Morikawa, N., Tachibana, M., Ago, Y., Goda, H., Sakurai, F., and Mizuguchi, H. (2018). LY341495, an mGluR2/3 Antagonist, Regulates the Immunosuppressive Function of Myeloid-Derived Suppressor Cells and Inhibits Melanoma Tumor Growth. *Biol. Pharm. Bull.* 41, 1866–1869. doi:10.1248/bpb.b18-00055
- Ostrand-Rosenberg, S., and Fenselau, C. (2018). Myeloid-derived Suppressor Cells: Immune-Suppressive Cells that Impair Antitumor Immunity and Are Sculpted by Their Environment. *J.I.* 200, 422–431. doi:10.4049/jimmunol.1701019
- Pacheco, R., Gallart, T., Lluís, C., and Franco, R. (2007). Role of Glutamate on T-Cell Mediated Immunity. *J. Neuroimmunol.* 185, 9–19. doi:10.1016/j.jneuroim.2007.01.003
- Pilatova, K., Bencsikova, B., Demlova, R., Valik, D., and Zdrzilova-Dubska, L. (2018). Myeloid-derived Suppressor Cells (MDSCs) in Patients with Solid Tumors: Considerations for Granulocyte colony-stimulating Factor Treatment. *Cancer Immunol. Immunother.* 67, 1919–1929. doi:10.1007/s00262-018-2166-4
- Pouloupoulou, C., Markakis, I., Davaki, P., Nikolaou, C., Pouloupoulos, A., Raptis, E., et al. (2005). Modulation of Voltage-Gated Potassium Channels in Human T Lymphocytes by Extracellular Glutamate. *Mol. Pharmacol.* 67, 856–867. doi:10.1124/mol.67.310.1124/mol.67.3
- Shimamura, Y., Takeuchi, I., Terada, H., and Makino, K. (2019). Therapeutic Effect of GGSTop, Selective Gamma-Glutamyl Transpeptidase Inhibitor, on a Mouse Model of 5-Fluorouracil-Induced Oral Mucositis. *Anticancer Res.* 39, 201–206. doi:10.21873/anticancer.13098
- Takemura, K., Board, P. G., and Koga, F. (2021). A Systematic Review of Serum γ -Glutamyltransferase as a Prognostic Biomarker in Patients with Genitourinary Cancer. *Antioxidants (Basel)* 10, 549. doi:10.3390/antiox10040549
- Tamura, K., Hayashi, N., George, J., Toshikuni, N., Arisawa, T., Hiratake, J., et al. (2016). GGSTop, a Novel and Specific γ -glutamyl Transpeptidase Inhibitor, Protects Hepatic Ischemia-Reperfusion Injury in Rats. *Am. J. Physiol. Gastrointest. Liver Physiol.* 311, G305–G312. doi:10.1152/ajpgi.00439.2015
- Tang, Z., Li, C., Kang, B., Gao, G., Li, C., and Zhang, Z. (2017). GEPIA: a Web Server for Cancer and normal Gene Expression Profiling and Interactive Analyses. *Nucleic Acids Res.* 45, W98–W102. doi:10.1093/nar/gkx247
- Torre, D., Lachmann, A., and Ma'ayan, A. (2018). BioJupies: Automated Generation of Interactive Notebooks for RNA-Seq Data Analysis in the Cloud. *Cell Syst* 7, 556. doi:10.1016/j.cels.2018.10.007
- Veglia, F., Sanseviero, E., and Gabrilovich, D. I. (2021). Myeloid-derived Suppressor Cells in the Era of Increasing Myeloid Cell Diversity. *Nat. Rev. Immunol.* 21, 485–498. doi:10.1038/s41577-020-00490-y
- Verma, V. V., Gupta, R., and Goel, M. (2015). "Phylogenetic and Evolutionary Analysis of Functional Divergence Among Gamma Glutamyl Transpeptidase (GGT) Subfamilies". *Biol. Direct* 10, 49. doi:10.1186/s13062-015-0080-7
- Wang, Q., Shu, X., Dong, Y., Zhou, J., Teng, R., Shen, J., et al. (2017). Tumor and Serum Gamma-Glutamyl Transpeptidase, New Prognostic and Molecular Interpretation of an Old Biomarker in Gastric Cancer. *Oncotarget* 8, 36171–36184. doi:10.18632/oncotarget.15609
- Wickham, S., West, M. B., Cook, P. F., and Hanigan, M. H. (2011). Gamma-glutamyl Compounds: Substrate Specificity of Gamma-Glutamyl Transpeptidase Enzymes. *Anal. Biochem.* 414, 208–214. doi:10.1016/j.ab.2011.03.026

- Wu, W. C., Sun, H. W., Chen, J., OuYang, H. Y., Yu, X. J., Chen, H. T., et al. (2019). Immunosuppressive Immature Myeloid Cell Generation Is Controlled by Glutamine Metabolism in Human Cancer. *Cancer Immunol. Res.* 7, 1605–1618. doi:10.1158/2326-6066.CIR-18-0902
- Xie, Z., Ago, Y., Okada, N., and Tachibana, M. (2018). Valproic Acid Attenuates Immunosuppressive Function of Myeloid-Derived Suppressor Cells. *J. Pharmacol. Sci.* 137, 359–365. doi:10.1016/j.jphs.2018.06.014

Conflict of Interest: The authors declare that the research was conducted in the absence of any commercial or financial relationships that could be construed as a potential conflict of interest.

Publisher's Note: All claims expressed in this article are solely those of the authors and do not necessarily represent those of their affiliated organizations, or those of the publisher, the editors, and the reviewers. Any product that may be evaluated in this article, or claim that may be made by its manufacturer, is not guaranteed or endorsed by the publisher.

Copyright © 2022 Xie, Kawasaki, Zhou, Okuzaki, Okada and Tachibana. This is an open-access article distributed under the terms of the Creative Commons Attribution License (CC BY). The use, distribution or reproduction in other forums is permitted, provided the original author(s) and the copyright owner(s) are credited and that the original publication in this journal is cited, in accordance with accepted academic practice. No use, distribution or reproduction is permitted which does not comply with these terms.



Can Natural Products be Used to Overcome the Limitations of Colorectal Cancer Immunotherapy?

Jiahuan Dong^{1,2†}, Yufan Qian^{1†}, Guangtao Zhang^{1,2}, Lu Lu¹, Shengan Zhang¹, Guang Ji¹, Aiguang Zhao^{2*} and Hanchen Xu^{1*}

¹ Institute of Digestive Diseases, Longhua Hospital, Shanghai University of Traditional Chinese Medicine, Shanghai, China,

² Department of Oncology, Longhua Hospital, Shanghai University of Traditional Chinese Medicine, Shanghai, China

OPEN ACCESS

Edited by:

Qian Ba,

Shanghai Jiao Tong University, China

Reviewed by:

Shuji Ogino,

Brigham and Women's Hospital and
Harvard Medical School, United States

Meiyu Peng,

Weifang Medical University, China

*Correspondence:

Aiguang Zhao

aiguangzhao@qq.com

Hanchen Xu

hanson0702@126.com

[†]These authors have contributed
equally to this work

Specialty section:

This article was submitted to
Pharmacology of Anti-Cancer Drugs,
a section of the journal
Frontiers in Oncology

Received: 26 February 2022

Accepted: 08 April 2022

Published: 04 May 2022

Citation:

Dong J, Qian Y, Zhang G, Lu L,
Zhang S, Ji G, Zhao A and Xu H (2022)
Can Natural Products be Used to
Overcome the Limitations of
Colorectal Cancer Immunotherapy?
Front. Oncol. 12:884423.
doi: 10.3389/fonc.2022.884423

Colorectal cancer (CRC) is a common cancer of the digestive system that endangers human health. Immunotherapy is widely used in the treatment of patients with cancer. Some patients with dMMR/MSI-H CRC benefit from treatments that use immune checkpoint inhibitors, but most CRC patients are not sensitive to immunotherapy. Furthermore, internal resistance and immune escape lead to a reduced immunotherapy response. Therefore, the development of an effective combination therapy to improve the response rate to immunotherapy is a goal of cancer research. Natural products are potential candidates for comprehensive cancer treatments due to their wide range of immunomodulatory effects through multifactorial underlying mechanisms. In this review, we summarize the challenges in the treatment of CRC and assess the immunomodulatory effects of natural products and their active components. Our work suggests that natural products represent potential options for combined CRC immunotherapy.

Keywords: colorectal cancer, immunotherapy, immune checkpoint inhibitor, natural products, immunomodulation

INTRODUCTION

The incidence rate and mortality rate of colorectal cancer (CRC) are third and second among all diseases, respectively, and CRC is characterized by a lack of obvious symptoms in the early stage and poor prognosis in the advanced stage (1). The main treatments for CRC are surgery, chemotherapy, radiotherapy, and targeted therapy. The emergence of immunotherapy has provided a transformative new method for the comprehensive treatment of cancer. An important function of the human immune system is to recognize and eliminate tumor cells, a process known as tumor immune surveillance, which

Abbreviations: CRC, Colorectal cancer; dMMR, defective DNA mismatch repair; MSI, Microsatellite instability; MSI-H, Microsatellite instability High; NK cell, Nature killer cell; ICIs, Immune checkpoint inhibitors; PD-1, Programmed cell death 1; CD274(PD-L1), Programmed cell death ligand 1; CTLA4, Cytotoxic T-lymphocyte associated protein 4; IHC, Immunohistochemistry; PCR, Polymerase chain reaction; NGS, Novel next-generation sequencing; ORR, Overall response rate; PFS, Progression-free survival; NCCN, National Comprehensive Cancer Network; VEGF, Vascular endothelial growth factor; pMMR, proficient mismatch repair; MSS, Microsatellite stable; TMB, Tumor mutation burden; NSCLC, Non-small-cell lung cancers; MDSC, Myeloid-derived suppressor cells; OS, Overall survival; PGE2, Prostaglandin E2; IL6, Interleukin 6; AOM, Azoxymethane; DSS, Dextran sodium sulfate; TLR4, Toll-like receptor 4; NF- κ B, Nuclear factor-kappa B; INF γ (INF-gamma), Interferon-gamma; TNF(TNF-alpha), Tumor necrosis factor-alpha; STAT3, Signal transducer and activator of transcription 3.

is mainly performed by antigen-presenting cells, T lymphocytes, B lymphocytes and natural killer (NK) cells (2, 3). Cancer cells inhibit the body's immune system in various ways to avoid the surveillance of the immune system, resulting in tumor immune escape (4, 5). Tumor immunotherapy is a treatment method used to control and eliminate cancer cells by restarting and maintaining the tumor immune cycle and restoring the body's normal antitumor immune response. Tumor immunotherapy mainly involves immune checkpoint inhibitors (ICIs), cellular immunotherapy and cancer vaccines. At present, the administration of ICIs is the most widely used tumor immunotherapy method. Among ICIs, the representative (PDCD1,PD-1) inhibitor, its (CD274,PD-L1) inhibitor, and cytotoxic T-lymphocyte associated protein 4 (CTLA4) restore the ability of immune cells to fight tumors by counteracting the inhibition of the immune system by tumor cells. At present, several ICIs targeting PDCD1(PD-1), CD274(PD-L1) and CTLA4 have been approved for the clinical treatment of various solid tumors, including MSI-H/dMMR CRC (4, 6, 7). However, there are still many challenges in the treatment of CRC with ICIs. MSI-H/dMMR tumors account for 5% of CRC cases, and some patients can benefit from ICIs, but most CRC tumors are still in a "cold" state. Therefore, it is necessary to find methods to transform "cold" tumors into "hot" tumors to make them more sensitive to ICIs.

Natural products, including plants, mushrooms, bacteria, animal metabolism products or organs and even mineral substances, characterized by various structure and activities, are well-known by the researchers gradually in recent years. Some evidence show that natural products have potential immunomodulatory effects and can play a synergistic role when combined with ICIs. So it is more important to explore the mechanisms of nature products for providing strongly clinical evidence. In this review, we summarized the effects of natural products on modulating macrophages, T cells, NK cells and a combination of ICIs.

THE ADVANTAGES AND LIMITATIONS OF ICIS FOR CRC TREATMENT

Currently, the main treatment for resectable CRC is surgery combined with chemotherapy or targeted medicines. However, metastatic CRC treatments remain challenging. According to retrospective analyses, some patients benefit less from 5-FU adjuvant chemotherapy (8, 9) because the molecular mechanism of CRC is different, and it may lead to more heterogeneity.

In 1997, the National Cancer Institute first defined microsatellite instability (MSI), which is a form of genomic instability associated with defective DNA mismatch repair (dMMR) in tumors; two mononucleotide repeats (BAT26 and BAT25) and three dinucleotide repeats (D5S346, D2S123, D17S250) were validated in the detection panel (10). MSI can currently be assessed by immunohistochemistry (IHC), including the expression of MSH2, MSH6, PMS2, MLH1 and polymerase chain reaction (PCR); moreover, novel next-generation sequencing (NGS) has become a new testing option.

Intriguingly, investigators found that MSI-high (MSI-H) CRC is associated with increased neoantigen load and immune infiltration (11–14), which means that immune checkpoint blockade may be an effective method of therapy.

Currently, MSI assessment can influence the selection of clinical medications and predict outcomes in colorectal cancer (15, 16). KEYNOTE-164, a phase II clinical trial, demonstrated that pembrolizumab was effective in MSI-H-dMMR CRC; it displayed a higher overall response rate (ORR) and improved progression-free survival (PFS) (17). KEYNOTE-177, which enrolled patients with stage IV MSI-H-dMMR CRC, demonstrated that the PFS in the pembrolizumab group was prolonged by 8.3 months, with an ORR of 43.8%, and there were fewer treatment-related adverse events in the pembrolizumab group than in the chemotherapy group (18, 19). The PDCD1(PD-1) inhibitor nivolumab showed durable responses and disease control, and 51 patients with metastatic MSI-H CRC had disease control for 12 weeks or longer; these results were similar to the findings of the CheckMate-142 study (20). Meanwhile, nivolumab plus the CTLA4 inhibitor ipilimumab displayed effective responses: 80% of the 119 patients had a disease control rate over 12%, and the investigator-assessed ORR was 55% (21). Considering the dose-dependent effect of ipilimumab, nivolumab combined with a low dose of ipilimumab showed robust and durable clinical benefit, with a 69% ORR and 84% disease control rate until the data cutoff (22). Based on the results of numerous clinical trials, the 2021 NCCN guidelines suggest that patients with advanced or metastatic CRC can use immunotherapy checkpoint blockade for subsequent therapy.

Although the results of clinical trials on dMMR/MSI-H are exciting, the response rates range between 30% and 50%, suggesting that resistance and immune escape still exist (23–25). More clinical trials have focused on the combination of VEGF inhibitors and chemotherapy (26–28); most of the studies are ongoing and the results are pending.

HOW TO MAKE ICIS MORE EFFECTIVE FOR CRC

The incidence of dMMR CRC is approximately 5%, which is far lower than that of proficient mismatch repair (pMMR) CRC (29). The conventional treatment of pMMR/microsatellite stable (MSS) CRC is systematic chemotherapy based on 5-fluorouracil and platinum, and most of patients have lower responses to immunotherapy due to intrinsic resistance. The mechanism may involve low TMB, a lack of tumor antigens and a suppressive microenvironment (30, 31). How to turn "cold" tumors into "hot" tumors is currently a popular topic in academic research.

Some studies have shown that chemotherapy can improve immunogenicity and enhance the efficacy of ICIs (32, 33). Currently, some ongoing clinical trials are exploring chemotherapy combined with angiogenesis medicine and ICIs. A protocol for unresectable metastatic CRC was described in the AtezoTRIBE study that enrolled patients receiving FOLFOXIRI plus bevacizumab; some patients received sequential atezolizumab (34).

A study of chemorefractory MSS mCRC included two cohorts: one was pembrolizumab plus pemetrexed, and in the other oxaliplatin was added for the dose escalation portion of the study (35). Although the trials have not shown the endpoint and some did not consider the microsatellite status, they represent worthwhile attempts.

Meanwhile, antiangiogenic and multitarget drugs also display synergistic sensitivity to ICIs. Innate immunity and immune adoption can directly lead to tumor angiogenesis (36), and the most widely studied VEGF family also drives angiogenesis to promote immune escape and immune suppression (37). Bevacizumab is the first antiangiogenic drug approved for metastatic CRC, NSCLC, metastatic renal cell carcinoma, and recurrent/metastatic cervical cancer (38, 39). Combining bevacizumab with immunotherapy promoted T cell infiltration, enhanced local immune activation and inhibited the expansion of MDSCs in preclinical studies (40, 41). Likewise, the use of bevacizumab combined with ICIs has been studied in many clinical trials, such as those investigating NSCLC, recurrent glioblastoma (42) and ovarian cancer (6, 43, 44); clinical trials for CRC are still ongoing, especially for MSS/pMMR CRC (45–47). In addition, multitarget antiangiogenic drugs show better responses. An open-label, phase II trial that enrolled 25 CRC patients demonstrated that a dose of regorafenib 80 mg can increase sensitivity to nivolumab, and the median PFS was 7.9 months (48). Similarly, a case report showed that in an MSS patient who received fruquintinib plus sindilizumab for six cycles, the lymph nodes became fewer and smaller, and CA199 was decreased (49). In a phase II study of patients with advanced refractory CRC, the median OS was 6.6 months for patients who received durvalumab and tremelimumab compared with the cohort who received supportive care, and the patients accepted the continuation of treatment with TAS-102 or regorafenib after disease progression (50). Not only the clinical report but also the author-selected syngeneic MSS model demonstrated that the combination of the two drugs could inhibit proliferation, induce apoptosis and promote vascular normalization (49). Hence, ICIs combined with antiangiogenic drugs may be a promising method of MSS CRC treatment.

In addition, CRC has some mutations driven by RAS, BRAF, EGFR, HER-2 and POLE, and most of them can impact treatment and prognosis. For example, approximately 10% of patients diagnosed with CRC harbor the BRAF mutation, which is considered a poor prognostic factor, and one third of mutations are associated with MSI (51–54). As shown in the Checkmate-142 study, the ORR was 25% in the BRAF mutation group and similar to that in the combined nivolumab and ipilimumab group (21, 22). A case report suggested that a patient harboring MSS and BRAF V600E mutations responded well to nivolumab and bevacizumab, achieving more than 17 months of PFS (55). However, some studies have reported that the BRAF mutation does not influence the response to immunotherapy (56, 57), and combination therapy needs to be further explored in large samples. Apart from the BRAF V600E mutation, a common oncogenic mutation is RAS mutation, especially KRAS mutation, which accounts for approximately 40% of CRC cases, and is related to poor prognosis and

metastasis (58, 59). In addition, the KRAS mutation in CRC is associated with immune suppression and immune infiltration (60, 61). Some current clinical trials are aimed at investigating these mutations. A phase I/II study enrolled CRC patients with RAS mutations regardless of MSS status to assess the safety and efficacy of the combination of durvalumab and tremelimumab (62). Likewise, a phase II study focused CRC with RAS or BRAF mutations and investigated the use of nivolumab combined with FOLFOXIRI/bevacizumab (63). These studies demonstrate that immunotherapy still has considerable potential for the treatment of CRC mutations.

NATURAL PRODUCTS EXERT MODULATING EFFECTS ON THE IMMUNE SYSTEM IN CRC

In addition to using the above-mentioned methods, researchers have paid attention to natural products. Natural products include the active compounds in plants, mushrooms, bacteria, animal metabolism products or organs and even mineral substances. These products have been explored and used for a thousand years. Some active compounds have proven antitumor, antioxidant, and anti-inflammatory effects (64). However, there are still a number of natural products that have adverse or toxic effects; these products must be used properly or avoided. The specific mechanism of natural products is still unknown and requires further investigation. According to recent evidence, natural products can directly regulate innate immunity and adoptive immunity (65); they play a role in preventing tumor development and modulating immunity (66–68). Thus, natural products show promise as agents in immunotherapy.

First, natural products can influence the immune microenvironment of early CRC in multiple ways, affecting M2 macrophage polarization to M1 to exert an immunomodulation effect. Isoliquiritigenin, a flavonoid derived from licorice, blocks M2 polarization in colitis-related tumorigenesis and inhibits the development of colorectal cancer by downregulating PGE2/IL6 signaling (69). Apple polysaccharides not only prevent the carcinogenesis induced by AOM/DSS in mice but also modulate the M2 to M1 macrophage phenotype and upregulate TLR4/NF- κ B signaling (70). Most basic experiments have adopted the AOM/DSS model or the CAC model to indicate the mechanism by which natural products affect macrophages (70–75). Taken together, these results show that there are many natural products that play important roles in inflammatory cancer transformation *via* different mechanisms, and natural products will intervene in CRC development in the near future.

Natural products can also influence T cells, NK cells and Treg cells. Black raspberries can significantly inhibit CRC progression and increase NK cells in tissues infiltrating the APC^{Min+/-} DSS and AOM/DSS models, and the results were validated in human CRC tissue (76, 77). In addition, Ecklonia cava fucoidan (ECF) not only stimulates NK cell activation and proliferation but also

induces NK cell activation through DCs (78). Moreover, rice hull polysaccharides (RHPS) can enhance NK cell activation and induce the secretion of INFG (INF-gamma) and TNF(TNF-alpha) *in vitro*; they also inhibit tumors in CT-26-bearing mice and enhance NK cell activation *in vivo* (79). It is clear that natural products demonstrate antitumor effects by influencing NK cell activity.

Similarly, natural products can cause T cells to exert immune modulating effects. Another well-known immunomodulatory natural product, curcumin, may suppress the expression of FOXP3 on Tregs and enhance the ability of T cells to kill tumor cells and modulate multiple immune cytokines (80–83). A control study revealed that the administration of curcumin can suppress the transcription of the FOXP3 gene and convert Tregs to Th1 cells by enhancing INFG (INF-gamma) production (84). In an *in vivo* experiment, researchers selected a CT-26 mouse model to compare curcumin and sildenafil combined with anti-PDCD-1(PD-1) and showed that the tumor volume was smaller in the combined treatment group (85). Based on preclinical research, curcumin is a potential natural product, especially when combined with immunotherapy. In addition, natural products can inhibit CRC metastasis by regulating the tumor microenvironment. The natural small molecule bigelovin may inhibit colorectal tumor growth by regulating the tumor immune microenvironment, increasing the T lymphocyte and macrophage populations, and inhibiting liver and lung metastasis of CRC through the IL6/STAT3 pathway (86). Furthermore, natural products can also upregulate IL-17 secretion to stimulate T cell proliferation or differentiation. Gan cao (*Glycyrrhiza uralensis* Fisch.) polysaccharides, especially those of low molecular weight, can upregulate IL-17 and enhance T lymphocyte proliferation (87). The author found that red wine extract could inhibit tumor progression and affect T lymphocyte cell differentiation into T helper 17 cells (88). Other studies have shown that natural products can alleviate tumor growth and modulate immunity by restoring intestinal barriers (89), inducing DC maturation (90) and reducing the accumulation of myeloid-derived suppressor cells (MDSCs) (91). It's noteworthy that quercetin and alantolactone not only can induce immunogenic cell death and cell apoptosis for MSS CRC, but also can reduce immunosuppressive cell population like MDSCs, Treg and so on. This study adjusted nanoformulated codelivery, on the other hand provided a basis for multi-drug combination of nature products (92).

Natural products combined with ICIs demonstrate better responses in patients, and this strategy may be a prospective method for use in the clinic. Many studies have investigated natural products other than curcumin. Atractylenolide I significantly improves the cytotoxic effect of T lymphocytes on tumor cells and promotes the antigen presentation of tumor cells. Atractylenolide I has a synergistic effect in the treatment of CRC when combined with immune checkpoint inhibitors (93). Astragaloside IV can significantly induce M2 macrophages to M1 polarization, decrease the production of anti-inflammatory factors and increase proinflammatory INFG (INF-gamma) in colorectal tumors (94). Meanwhile, astragaloside IV combined with a PDCD1(PD-1) inhibitor exhibited a synergistic effect on

inhibiting tumor growth and T cell infiltration. Inulin, which is derived from dietary fiber, can significantly improve the systemic antitumor efficacy of anti-PDCD-1(PD-1) therapy and effectively slow tumor growth by altering the gut microbiome. Compared with anti-PDCD-1(PD-1) alone, the synergistic use of inulin and anti-PDCD-1(PD-1) significantly increased CT-26 GP70-specific CD8⁺ T cells in mice. Interestingly, by transforming inulin into inulin gel before its use in combination with anti-PDCD-1(PD-1), the effect was improved (95). This suggests that natural products have potential regarding changes in the forms of administered medicines. Many experiments have simulated the combination of natural products and ICIs (96–98). A preclinical study was conducted that explored anti-PDCD-1 (PD-1) alone and in combination with natural products and anti-CTLA4. High-dose vitamin C can decrease tumor volumes combined with anti-PDCD-1(PD-1) and anti-CTLA4 and enhance CD8⁺ T cell cytotoxic activity. This research was conducted not only in CRC but also in breast cancer, pancreatic cancer and melanoma with mismatch repair-deficient tumors with a high mutational burden (99) (**Table 1**).

Natural products combined with ICIs had better results in melanoma, lung cancer and breast cancer studies (100, 101), and they can be gradually extended to the study of pancancer in the future.

CONCLUSION AND PERSPECTIVES

Epidemiologic evidence show that the CRC incidence is strongly related to interaction between the environment exposures and gene alternations (102). Colorectal carcinogenesis includes three major global genetic and epigenetic aberrations: chromosomal instability (CIN), CpG island methylator phenotype (CIMP) and MSI. Although gene factors may lead to the individual risk and increase hereditary susceptibility, CRC are largely affected by diet factors and lifestyle alterations (103), like smoking, alcohol, obesity and so on (104–106). A study demonstrated that high-fat-diet-induced obesity may impair CD8⁺T cell function in the murine tumor microenvironment through the metabolic pathway (107). Conversely lifestyle and diet factors can also affect gene alternation to contribute to the onset of CRC. Similarly smoking was associated with a 59% increased risk of CRC and strongly related to MSI-H and KRAS wild type CRC in a large case-control study which enrolled 4919 participants (108).

Base on the relationship between diet factors or lifestyle and immunity, some researchers addressed a concept of molecular pathological epidemiology (MPE) which could provide the better understanding of environment-tumor-immune interactions (109). Among them, the researches proposed several classes of substance with immunomodulatory effects in CRC, including aspirin, vitamin D, inflammatory diets and omega-3 polyunsaturated fatty acids. Take an example for omega-3 polyunsaturated, a higher intake of marine omega-3 polyunsaturated was associated with the risk of CRC with different density FOXP3⁺ cells (110). Since the introduction of immunotherapies, some patients have benefited, but there are still crucial problems to be solved.

TABLE 1 | Natural products exert modulating effects on the immune system in CRC.

Nature product	Model	Results	Reference
Isoliquiritigenin	AOM/DSS mice Raw267.4 cell Mouse peritoneal macrophages	PGE2 ↓ IL6 ↓ M2 polarization ↓ p-STAT3 ↓ iNOS ↑ CLCX10 ↑	(69)
Apple polysaccharide	AOM/DSS mice Raw267.4 cell	TLR-4 Myd88 p65 ↑	(70)
Vitexin	AOM/DSS mice CAC model	M1 ↑ TNF(TNF-alpha) IL-1β IL6 ↓ NO in tumor tissue ↑	(71)
β-Carotene	AOM/DSS mice U937 cells	IL6 pSTAT3 ↓	(72)
Berberine	AOM/DSS APC ^{Min/+} mice Raw267.4 cell	EGFR-ERK signaling ↓	(73)
Cardamonin	Raw267.4 cell HCT-116	iNOS TNF(TNF-alpha)IL6 ↓ NF-κB ↓	(75)
Black Raspberries	APC ^{Min/+} /DSS AOM/DSS Human CRC tissues	NK cells infiltration ↑	(76)
Elkonina cava fucoidan	CT-26 NK cells and DCs from C57BL/6 spleen	NK cells activation ↑ INFG (INF-gamma) ↑	(78)
Rice hull polysaccharides	NK-92 MI CT-26	NK cells activation ↑ INFG (INF-gamma) ↑	(79)
Curcumin	Advanced CRC patients PBMC	FOXP3+Treg ↓ INFG (INF-gamma) ↑	(84)
Curcumin	CT-26	Tumor volume ↓	(85)
Bigelovin	CT-26 HCT-116	T lymphocyte Macrophage population ↑	(86)
Glycyrrhiza uralensis Fisch.	CT-26	IL-17 ↑ T lymphocyte proliferation ↑	(87)
Red wine extract	CT-26 HCT-116 SW620 MC38	Th17 differentiation ↓	(88)
Dendrobium officinale polysaccharides	AOM/DSS	—	(89)
Maitake Z-fraction	Colon-26 mice	—	(90)
Juglone	CT-26 MDSCs	INFG (INF-gamma) ↑ MDSCs accumulation ↓	(91)
Quercetin and Alantolactone	CT-26 Orthotopic colorectal cancer model	MDSCs Treg IL-10 IL-1β TGF-β CCL-2 ↓	(92)
Atractylenolide I	MC38 MC38-OVA OT-1 mice	CD8 ⁺ T cell ↑	(93)
Astragaloside IV	CT-26 mice	TGF-β IL-10 VEGF-α ↓ INFG (INF-gamma) IL-12 TNF(TNF-alpha) ↑	(94)
Inulin	CT-26 mice	SCFAs (feces) ↑ Induce stem-like Tcf ⁺ PD-1 ⁺ T cell	(95)
Sanguisorbae Radix	Humanized PD-L1 MC38 mice Recombinant Jurkat T cells	Infiltrated cytotoxic T cells ↑	(96)
Pectin	MC38 mice CRC patients fecal microbiota transplantation model	Infiltrated cytotoxic T cells ↑ Butyrate (feces) ↑	(97)
Andrographolide	CT-26 mice	CD8 ⁺ and CD4 ⁺ T cell function ↑ FasL perforin ↑Granzyme B ↑	(98)
High-dose vitamin C	CT-26 MC38	CD8 ⁺ T cell cytotoxic ↑	(99)

Preclinical studies have shown that natural products can exert antitumor effects and modulate immunity by affecting T cells, NK cells, and Tregs in CRC (**Figure 1**). If researches adopt the MPE model and integrate the immunotherapies to the model in the future, that will be a promising method which can provide more accurate strategies for the treatment, especially the field of nature

products which link to the environment and immune. Natural products have some limitations; the ranges of safe doses remain undetermined and adverse effects such as hepatotoxicity and renal toxicity must be controlled. Natural products have the advantages of being easy to obtain and widely used, and they have multiple targets. Natural products have been proven effective in the early

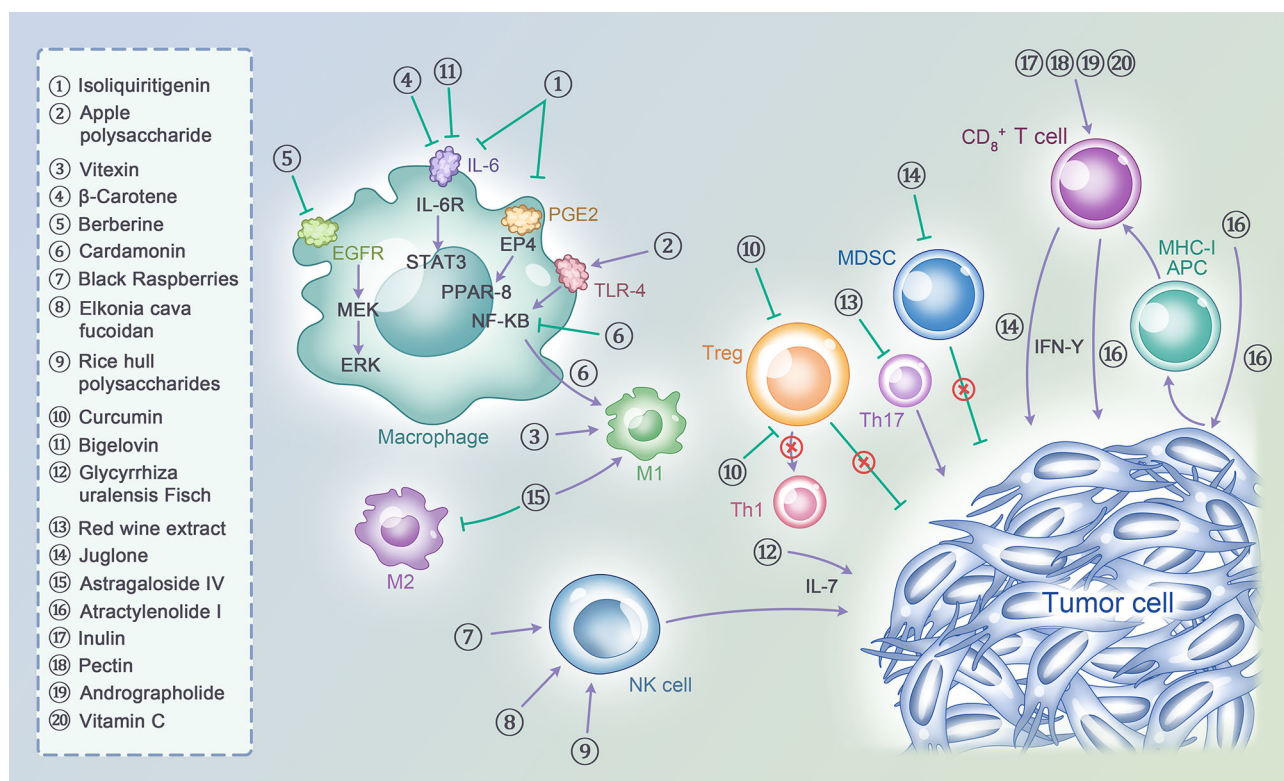


FIGURE 1 | A variety of natural products act on multiple cell subtypes in the tumor immune microenvironment, including T cells, NK cells, Macrophages, MDSCs, Tregs and tumor cells themselves, to exert immunomodulatory effects and thus enhance the ability of anti-tumor immunity.

stage of CRC, especially on the transformation of adenoma to adenocarcinoma, and in advanced cancer stages, natural products can inhibit tumor progression. Meanwhile, combining natural products with ICIs can maximize the antitumor effects by acting on multiple targets.

In summary, natural products can regulate the immune system and enhance immuno-oncological effects, especially when combined with ICIs, which will be a promising strategy in the future that is gradually accepted into clinical practice.

AUTHOR CONTRIBUTIONS

HX and AZ proposed the topic and made the frame. JD and YQ contributed to original draft preparation. GZ, LL, and SZ participated in part of text arrangement and literature

collection. LL and JD participated in the conception and drawing of the image. GJ, AZ, and HX revised the manuscript. All authors contributed to the article and approved the submitted version.

FUNDING

This work was supported by National Nature Science Foundation of China, No. 81874206, 82104466; Shanghai Frontiers Science Center of Disease and Syndrome Biology of Inflammatory Cancer Transformation (2021KJ03-12); Shanghai Rising-Star Program, No. 20QA1409300; and the Program for Young Eastern Scholar at Shanghai Institutions of Higher Learning, No. QD2019034.

REFERENCES

- Bray F, Ferlay J, Soerjomataram I, Siegel RL, Torre LA, Jemal A, et al. Erratum: Global Cancer Statistics 2018: GLOBOCAN Estimates of Incidence and Mortality Worldwide for 36 Cancers in 185 Countries. *CA Cancer J Clin* (2020) 70(4):313. doi: 10.3322/caac.21492
- Boulch M, Grandjean CL, Cazaux M, Bouso P. Tumor Immunosurveillance and Immunotherapies: A Fresh Look From Intravital Imaging. *Trends Immunol* (2019) 40(11):1022–34. doi: 10.1016/j.it.2019.09.002
- Binnewies M, Roberts EW, Kersten K, Chan V, Fearon DF, Merad M, et al. Understanding the Tumor Immune Microenvironment (TIME) for Effective Therapy. *Nat Med* (2018) 24(5):541–50. doi: 10.1038/s41591-018-0014-x

4. Robert C, Thomas L, Bondarenko I, O'Day S, Weber J, Garbe C, et al. Ipilimumab Plus Dacarbazine for Previously Untreated Metastatic Melanoma. *N Engl J Med* (2011) 364(26):2517–26. doi: 10.1056/NEJMoa1104621
5. Hodi FS, O'Day SJ, McDermott DF, Weber RW, Sosman JA, Haanen JB, et al. Improved Survival With Ipilimumab in Patients With Metastatic Melanoma. *N Engl J Med* (2010) 363(8):711–23. doi: 10.1056/NEJMoa1003466
6. Socinski MA, Jotte RM, Cappuzzo F, Orlandi F, Stroyakovskiy D, Nogami N, et al. Atezolizumab for First-Line Treatment of Metastatic Nonsquamous NSCLC. *N Engl J Med* (2018) 378(24):2288–301. doi: 10.1056/NEJMoa1716948
7. Le DT, Uram JN, Wang H, Bartlett BR, Kemberling H, Eyring AD, et al. PD-1 Blockade in Tumors With Mismatch-Repair Deficiency. *N Engl J Med* (2015) 372(26):2509–20. doi: 10.1056/NEJMoa1500596
8. Sargent DJ, Marsoni S, Monges G, Thibodeau SN, Labianca R, Hamilton SR, et al. Defective Mismatch Repair as a Predictive Marker for Lack of Efficacy of Fluorouracil-Based Adjuvant Therapy in Colon Cancer. *J Clin Oncol* (2010) 28(20):3219–26. doi: 10.1200/JCO.2009.27.1825
9. Goldstein J, Tran B, Ensor J, Gibbs P, Wong HL, Wong SF, et al. Multicenter Retrospective Analysis of Metastatic Colorectal Cancer (CRC) With High-Level Microsatellite Instability (MSI-H). *Ann Oncol* (2014) 25(5):1032–8. doi: 10.1093/annonc/mdu100
10. Boland CR, Thibodeau SN, Hamilton SR, Sidransky D, Eshleman JR, Burt RW, et al. A National Cancer Institute Workshop on Microsatellite Instability for Cancer Detection and Familial Predisposition: Development of International Criteria for the Determination of Microsatellite Instability in Colorectal Cancer. *Cancer Res* (1998) 58(22):5248–57PMID: 9823339.
11. Giannakis M, Mu XJ, Shukla SA, Qian ZR, Cohen O, Nishihara R, et al. Genomic Correlates of Immune-Cell Infiltrates in Colorectal Carcinoma. *Cell Rep* (2016) 15(4):857–65. doi: 10.1016/j.celrep.2016.03.075
12. Llosa NJ, Cruise M, Tam A, Wicks EC, Hechenbleikner EM, Taube JM, et al. The Vigorous Immune Microenvironment of Microsatellite Instable Colon Cancer Is Balanced by Multiple Counter-Inhibitory Checkpoints. *Cancer Discovery* (2015) 5(1):43–51. doi: 10.1158/2159-8290.CD-14-0863
13. Becht E, de Reyniès A, Giraldo NA, Pilati C, Buttard B, Lacroix L, et al. Immune and Stromal Classification of Colorectal Cancer Is Associated With Molecular Subtypes and Relevant for Precision Immunotherapy. *Clin Cancer Res* (2016) 22(16):4057–66. doi: 10.1158/1078-0432.CCR-15-2879
14. Lin A, Zhang J, Luo P. Crosstalk Between the MSI Status and Tumor Microenvironment in Colorectal Cancer. *Front Immunol* (2020) 11:2039. doi: 10.3389/fimmu.2020.02039
15. Le DT, Durham JN, Smith KN, Wang H, Bartlett BR, Aulakh LK, et al. Mismatch Repair Deficiency Predicts Response of Solid Tumors to PD-1 Blockade. *Science* (2017) 357(6349):409–13. doi: 10.1126/science.aan6733
16. Luchini C, Bibeau F, Ligtenberg MJL, Singh N, Nottegar A, Bosse T, et al. ESMO Recommendations on Microsatellite Instability Testing for Immunotherapy in Cancer, and its Relationship With PD-1/PD-L1 Expression and Tumour Mutational Burden: A Systematic Review-Based Approach. *Ann Oncol* (2019) 30(8):1232–43. doi: 10.1093/annonc/mdz116
17. Le DT, Kim TW, Van Cutsem E, Geva R, Jäger D, Hara H, et al. Phase II Open-Label Study of Pembrolizumab in Treatment-Refractory, Microsatellite Instability-High/Mismatch Repair-Deficient Metastatic Colorectal Cancer: KEYNOTE-164. *J Clin Oncol* (2020) 38(1):11–9. doi: 10.1200/JCO.19.02107
18. André T, Shiu KK, Kim TW, Jensen BV, Jensen LH, Punt C, et al. Pembrolizumab in Microsatellite-Instability-High Advanced Colorectal Cancer. *N Engl J Med* (2020) 383(23):2207–18. doi: 10.1056/NEJMoa2017699
19. Andre T, Amonkar M, Norquist JM, Shiu KK, Kim TW, Jensen BV, et al. Health-Related Quality of Life in Patients With Microsatellite Instability-High or Mismatch Repair Deficient Metastatic Colorectal Cancer Treated With First-Line Pembrolizumab Versus Chemotherapy (KEYNOTE-177): An Open-Label, Randomised, Phase 3 Trial. *Lancet Oncol* (2021) 22(5):665–77. doi: 10.1016/S1470-2045(21)00064-4
20. Overman MJ, McDermott R, Leach JL, Lonardi S, Lenz HJ, Morse MA, et al. Nivolumab in Patients With Metastatic DNA Mismatch Repair-Deficient or Microsatellite Instability-High Colorectal Cancer (CheckMate 142): An Open-Label, Multicentre, Phase 2 Study. *Lancet Oncol* (2017) 18(9):1182–91. doi: 10.1016/S1470-2045(17)30422-9
21. Overman MJ, Lonardi S, Wong KYM, Lenz HJ, Gelsomino F, Aglietta M, et al. Durable Clinical Benefit With Nivolumab Plus Ipilimumab in DNA Mismatch Repair-Deficient/Microsatellite Instability-High Metastatic Colorectal Cancer. *J Clin Oncol* (2018) 36(8):773–9. doi: 10.1200/JCO.2017.76.9901
22. Lenz HJ, Van Cutsem E, Luisa Limon M, Wong KYM, Hendlisz A, Aglietta M, et al. First-Line Nivolumab Plus Low-Dose Ipilimumab for Microsatellite Instability-High/Mismatch Repair-Deficient Metastatic Colorectal Cancer: The Phase II CheckMate 142 Study. *J Clin Oncol* (2021) 40(2):161–70. doi: 10.1200/JCO.21.01015
23. Vasaikar S, Huang C, Wang X, Petyuk VA, Savage SR, Wen B, et al. Proteogenomic Analysis of Human Colon Cancer Reveals New Therapeutic Opportunities. *Cell* (2019) 177(4):1035–1049.e19. doi: 10.1016/j.cell.2019.03.030
24. Gurjao C, Liu D, Hofree M, AlDubayan SH, Wakiro I, Su MJ, et al. Intrinsic Resistance to Immune Checkpoint Blockade in a Mismatch Repair-Deficient Colorectal Cancer. *Cancer Immunol Res* (2019) 7(8):1230–6. doi: 10.1158/2326-6066.CIR-18-0683
25. Sahin IH, Akce M, Alese O, Shaib W, Lesinski GB, El-Rayes B, et al. Immune Checkpoint Inhibitors for the Treatment of MSI-H/MMR-D Colorectal Cancer and a Perspective on Resistance Mechanisms. *Br J Cancer* (2019) 121(10):809–18. doi: 10.1038/s41416-019-0599-y
26. PD-1 Inhibitors Combined With VEGF Inhibitors for Locally Advanced dMMR/MSI-H Colorectal Cancer. *Nct04715633*. Guangdong Province. Available at: <https://clinicaltrials.gov/ct2/show/NCT04715633?cond=Nct04715633&draw=2&rank=1#studydesc>.
27. An Investigational Immuno-Therapy Study of Nivolumab, and Nivolumab in Combination With Other Anti-Cancer Drugs, in Colon Cancer That Has Come Back or Has Spread (Checkmate142). *NCT02060188* <https://clinicaltrials.gov/ct2/show/NCT02060188?cond=NCT02060188&draw=2&rank=1startwithFebruary11,2014>.
28. PD-1 Inhibitor Combined With Bevacizumab and FOLFIRI Regimen in the Second-Line Treatment of Advanced Colorectal Cancer. *Nct05035381* Tianjin provinces start with September 5, 2021 Available at: <https://clinicaltrials.gov/ct2/show/NCT05035381?cond=Nct05035381&draw=2&rank=1>.
29. Koopman M, Kortman GA, Mekenkamp L, Ligtenberg MJ, Hoogerbrugge N, Antonini NF, et al. Deficient Mismatch Repair System in Patients With Sporadic Advanced Colorectal Cancer. *Br J Cancer* (2009) 100(2):266–73. doi: 10.1038/sj.bjc.6604867
30. Kim CW, Chon HJ, Kim C. Combination Immunotherapies to Overcome Intrinsic Resistance to Checkpoint Blockade in Microsatellite Stable Colorectal Cancer. *Cancers (Basel)* (2021) 13(19):4906. doi: 10.3390/cancers13194906
31. Mlecnik B, Bindea G, Angell HK, Maby P, Angelova M, Tougeron D, et al. Integrative Analyses of Colorectal Cancer Show Immunoscore Is a Stronger Predictor of Patient Survival Than Microsatellite Instability. *Immunity* (2016) 44(3):698–711. doi: 10.1016/j.immuni.2016.02.025
32. Heinhuis KM, Ros W, Kok M, Steeghs N, Beijnen JH, Schellens JHM, et al. Enhancing Antitumor Response by Combining Immune Checkpoint Inhibitors With Chemotherapy in Solid Tumors. *Ann Oncol* (2019) 30(2):219–35. doi: 10.1093/annonc/mdy551
33. Guan Y, Kraus SG, Quaney MJ, Daniels MA, Mitchem JB, Teixeira E, et al. FOLFOX Chemotherapy Ameliorates CD8 T Lymphocyte Exhaustion and Enhances Checkpoint Blockade Efficacy in Colorectal Cancer. *Front Oncol* (2020) 10:586. doi: 10.3389/fonc.2020.00586
34. Antoniotti C, Borelli B, Rossini D, Pietrantonio F, Morano F, Salvatore L, et al. Atezotribe: A Randomised Phase II Study of FOLFOXIRI Plus Bevacizumab Alone or in Combination With Atezolizumab as Initial Therapy for Patients With Unresectable Metastatic Colorectal Cancer. *BMC Cancer* (2020) 20(1):683. doi: 10.1186/s12885-020-07169-6
35. Study of Pembrolizumab With Pemetrexed and Oxaliplatin in ChemoRefractory Metastatic Colorectal Cancer Patients. *Nct03626922*. Available at: <https://clinicaltrials.gov/ct2/show/NCT03626922>.
36. Albin A, Bruno A, Noonan DM, Mortara L. Contribution to Tumor Angiogenesis From Innate Immune Cells Within the Tumor

- Microenvironment: Implications for Immunotherapy. *Front Immunol* (2018) 9:527. doi: 10.3389/fimmu.2018.00527
37. Rahma OE, Hodi FS. The Intersection Between Tumor Angiogenesis and Immune Suppression. *Clin Cancer Res* (2019) 25(18):5449–57. doi: 10.1158/1078-0432.CCR-18-1543
 38. Garcia J, Hurwitz HI, Sandler AB, Miles D, Coleman RL, Deurloo R, et al. Bevacizumab (Avastin®) in Cancer Treatment: A Review of 15 Years of Clinical Experience and Future Outlook. *Cancer Treat Rev* (2020) 86:102017. doi: 10.1016/j.ctrv.2020.102017
 39. Bennouna J, Sastre J, Arnold D, Österlund P, Greil R, Van Cutsem E, et al. Continuation of Bevacizumab After First Progression in Metastatic Colorectal Cancer (ML18147): A Randomised Phase 3 Trial. *Lancet Oncol* (2013) 14(1):29–37. doi: 10.1016/S1470-2045(12)70477-1
 40. Yasuda S, Sho M, Yamato I, Yoshiji H, Wakatsuki K, Nishiwada S, et al. Simultaneous Blockade of Programmed Death 1 and Vascular Endothelial Growth Factor Receptor 2 (VEGFR2) Induces Synergistic Anti-Tumour Effect In Vivo. *Clin Exp Immunol* (2013) 172(3):500–6. doi: 10.1111/cei.12069
 41. Hegde P, Wallin J, Mancao C. Predictive Markers of Anti-VEGF and Emerging Role of Angiogenesis Inhibitors as Immunotherapeutics. *Semin Cancer Biol* (2018) 52:117–24. doi: 10.1016/j.semcancer.2017.12.002
 42. Harter P, Pautier P, Van Nieuwenhuysen E, Reuss A, Redondo A, et al. Atezolizumab in Combination With Bevacizumab and Chemotherapy Versus Bevacizumab and Chemotherapy in Recurrent Ovarian Cancer - A Randomized Phase III Trial (AGO-OVAR 2.29/ENGOT-Ov34). *Int J Gynecol Cancer* (2020) 30(12):1997–2001. doi: 10.1136/ijgc-2020-001572
 43. Reck M, Wehler T, Orlandi F, Nogami N, Barone C, Moro-Sibilot D, et al. Safety and Patient-Reported Outcomes of Atezolizumab Plus Chemotherapy With or Without Bevacizumab Versus Bevacizumab Plus Chemotherapy in Non-Small-Cell Lung Cancer. *J Clin Oncol* (2020) 38(22):2530–42. doi: 10.1200/JCO.19.03158
 44. Reardon DA, Brandes AA, Omuro A, Mulholland P, Lim M, Wick A, et al. Effect of Nivolumab vs Bevacizumab in Patients With Recurrent Glioblastoma: The CheckMate 143 Phase 3 Randomized Clinical Trial. *JAMA Oncol* (2020) 6(7):1003–10. doi: 10.1001/jamaoncol.2020.1024
 45. Mfolfox6+Bevacizumab+PD-1 Monoclonal Antibody in Local Advanced MSS CRC (BASKETII). Nct04895137, Guangdong Province. Available at: <https://clinicaltrials.gov/ct2/show/NCT04895137?cond=Nct04895137&draw=1&rank=1>.
 46. Chemotherapy and Immunotherapy as Treatment for MSS Metastatic Colorectal Cancer With High Immune Infiltrate (POCHI). Nct04262687. Available at: <https://clinicaltrials.gov/ct2/show/NCT04262687?cond=Nct04262687&draw=2&rank=1>
 47. Combination Chemotherapy, Bevacizumab, and/or Atezolizumab in Treating Patients With Deficient DNA Mismatch Repair Metastatic Colorectal Cancer, the COMMIT Study. Nct02997228. Available at: <https://clinicaltrials.gov/ct2/show/NCT02997228?cond=Nct02997228&draw=2&rank=1>.
 48. Fukuoka S, Hara H, Takahashi N, Kojima T, Kawazoe A, Asayama M, et al. Regorafenib Plus Nivolumab in Patients With Advanced Gastric or Colorectal Cancer: An Open-Label, Dose-Escalation, and Dose-Expansion Phase Ib Trial (REGONIVO, Epoc1603). *J Clin Oncol* (2020) 38(18):2053–61. doi: 10.1200/JCO.19.03296
 49. Wang Y, Wei B, Gao J, Cai X, Xu L, Zhong H, et al. Combination of Fruquintinib and Anti-PD-1 for the Treatment of Colorectal Cancer. *J Immunol* (2020) 205(10):2905–15. doi: 10.4049/jimmunol.2000463
 50. Chen EX, Jonker DJ, Loree JM, Kennecke HF, Berry SR, Couture F, et al. Effect of Combined Immune Checkpoint Inhibition vs Best Supportive Care Alone in Patients With Advanced Colorectal Cancer: The Canadian Cancer Trials Group CO.26 Study. *JAMA Oncol* (2020) 6(6):831–8. doi: 10.1001/jamaoncol.2020.0910
 51. Venderbosch S, Nagtegaal ID, Maughan TS, Smith CG, Cheadle JP, Fisher D, et al. Mismatch Repair Status and BRAF Mutation Status in Metastatic Colorectal Cancer Patients: A Pooled Analysis of the CAIRO, CAIRO2, COIN, and FOCUS Studies. *Clin Cancer Res* (2014) 20(20):5322–30. doi: 10.1158/1078-0432.CCR-14-0332
 52. Fariña-Sarasqueta A, van Lijnschoten G, Moerland E, Creemers GJ, Lemmens VEPP, Rutten HJT, et al. The BRAF V600E Mutation is an Independent Prognostic Factor for Survival in Stage II and Stage III Colon Cancer Patients. *Ann Oncol* (2010) 21(12):2396–402. doi: 10.1093/annonc/mdq258
 53. Tran B, Kopetz S, Tie J, Gibbs P, Jiang ZQ, Lieu CH, et al. Impact of BRAF Mutation and Microsatellite Instability on the Pattern of Metastatic Spread and Prognosis in Metastatic Colorectal Cancer. *Cancer* (2011) 117(20):4623–32. doi: 10.1002/cncr.26086
 54. Taieb J, Lapeyre-Prost A, Laurent Puig P, Zaanan A. Exploring the Best Treatment Options for BRAF-Mutant Metastatic Colon Cancer. *Br J Cancer* (2019) 121(6):434–42. doi: 10.1038/s41416-019-0526-2
 55. Fang C, Lin J, Zhang T, Luo J, Nie D, Li M, et al. Metastatic Colorectal Cancer Patient With Microsatellite Stability and BRAF Mutation Showed a Complete Metabolic Response to PD-1 Blockade and Bevacizumab: A Case Report. *Front Oncol* (2021) 11:652394. doi: 10.3389/fonc.2021.652394
 56. Asaoka Y, Ijichi H, Koike K. PD-1 Blockade in Tumors With Mismatch-Repair Deficiency. *N Engl J Med* (2015) 373(20):1979. doi: 10.1056/NEJMc1510353.
 57. Molina-Cerrillo J, San Román M, Pozas J, Alonso-Gordoa T, Pozas M, Conde E, et al. BRAF Mutated Colorectal Cancer: New Treatment Approaches. *Cancers (Basel)* (2020) 12(6). doi: 10.3390/cancers12061571
 58. Andreyev HJ, Norman AR, Cunningham D, Oates J, Dix BR, Iacopetta BJ, et al. Kirsten Ras Mutations in Patients With Colorectal Cancer: The 'RASCAL II' Study. *Br J Cancer* (2001) 85(5):692–6. doi: 10.1054/bjoc.2001.1964
 59. Uhlig J, Cecchini M, Sheth A, Stein S, Lacy J, Kim HS. Microsatellite Instability and KRAS Mutation in Stage IV Colorectal Cancer: Prevalence, Geographic Discrepancies, and Outcomes From the National Cancer Database. *J Natl Compr Canc Netw* (2021) 19(3):307–18. doi: 10.6004/jncn.2020.7619
 60. Liao W, Overman MJ, Boutin AT, Shang X, Zhao D, Dey P, et al. KRAS-IRF2 Axis Drives Immune Suppression and Immune Therapy Resistance in Colorectal Cancer. *Cancer Cell* (2019) 35(4):559–572.e7. doi: 10.1016/j.ccell.2019.02.008
 61. Liu J, Huang X, Liu H, Wei C, Ru H, Qin H, et al. Immune Landscape and Prognostic Immune-Related Genes in KRAS-Mutant Colorectal Cancer Patients. *J Transl Med* (2021) 19(1):27. doi: 10.1186/s12967-020-02638-9
 62. Fumet JD, Isambert N, Hervieu A, Zanetta S, Guion JF, Hennequin A, et al. Phase Ib/II Trial Evaluating the Safety, Tolerability and Immunological Activity of Durvalumab (MEDI4736) (Anti-PD-L1) Plus Tremelimumab (Anti-CTLA-4) Combined With FOLFOX in Patients With Metastatic Colorectal Cancer. *ESMO Open* (2018) 3(4):e000375. doi: 10.1136/esmoopen-2018-000375
 63. Damato A, Iachetta F, Antonuzzo L, Nasti G, Bergamo F, Bordonaro R, et al. Phase II Study on First-Line Treatment of Nivolumab in Combination With Folfotri/Bevacizumab in Patients With Advanced ColoRectal Cancer RAS or BRAF Mutated - NIVACOR Trial (GOIRC-03-2018). *BMC Cancer* (2020) 20(1):822. doi: 10.1186/s12885-020-07268-4
 64. Diederich M. Natural Products Target the Hallmarks of Chronic Diseases. *Biochem Pharmacol* (2020) 173:113828. doi: 10.1016/j.bcp.2020.113828
 65. Samec M, Liskova A, Koklesova L, Samuel SM, Murin R, Zubor P, et al. The Role of Plant-Derived Natural Substances as Immunomodulatory Agents in Carcinogenesis. *J Cancer Res Clin Oncol* (2020) 146(12):3137–54. doi: 10.1007/s00432-020-03424-2
 66. Li TY, Chiang BH. 4-Acetylanthroquinonol B From *Antrodia Cinnamomea* Enhances Immune Function of Dendritic Cells Against Liver Cancer Stem Cells. *BioMed Pharmacother* (2019) 109:2262–9. doi: 10.1016/j.biopha.2018.11.101
 67. Mahmoud YK, Abdelrazek HMA. Cancer: Thymoquinone Antioxidant/Pro-Oxidant Effect as Potential Anticancer Remedy. *BioMed Pharmacother* (2019) 115:108783. doi: 10.1016/j.biopha.2019.108783
 68. Ye H, He X, Feng X. Developing Neobavaisoflavone Nanoemulsion Suppresses Lung Cancer Progression by Regulating Tumor Microenvironment. *BioMed Pharmacother* (2020) 129:110369. doi: 10.1016/j.biopha.2020.110369
 69. Zhao H, Zhang X, Chen X, Li Y, Ke Z, Tang T, et al. Isoliquiritigenin, a Flavonoid From Licorice, Blocks M2 Macrophage Polarization in Colitis-Associated Tumorigenesis Through Downregulating PGE2 and IL-6. *Toxicol Appl Pharmacol* (2014) 279(3):311–21. doi: 10.1016/j.taap.2014.07.001
 70. Sun Y, Diao F, Niu Y, Li X, Zhou H, Mei Q, et al. Apple Polysaccharide Prevents From Colitis-Associated Carcinogenesis Through Regulating

- Macrophage Polarization. *Int J Biol Macromol* (2020) 161:704–11. doi: 10.1016/j.ijbiomac.2020.06.121
71. Chen Y, Wang B, Yuan X, Lu Y, Hu J, Gao J, et al. Vitexin Prevents Colitis-Associated Carcinogenesis in Mice Through Regulating Macrophage Polarization. *Phytomedicine* (2021) 83:153489. doi: 10.1016/j.phymed.2021.153489
 72. Lee NY, Kim Y, Kim YS, Shin JH, Rubin LP, Kim Y. β -Carotene Exerts Anti-Colon Cancer Effects by Regulating M2 Macrophages and Activated Fibroblasts. *J Nutr Biochem* (2020) 82:108402. doi: 10.1016/j.jnutbio.2020.108402
 73. Li D, Zhang Y, Liu K, Zhao Y, Xu B, Xu L, et al. Berberine Inhibits Colitis-Associated Tumorigenesis via Suppressing Inflammatory Responses and the Consequent EGFR Signaling-Involved Tumor Cell Growth. *Lab Invest* (2017) 97(11):1343–53. doi: 10.1038/labinvest.2017.71
 74. Chung KS, Cheon SY, Roh SS, Lee M, An HJ. Chemopreventive Effect of Aster Glehni on Inflammation-Induced Colorectal Carcinogenesis in Mice. *Nutrients* (2018) 10(2):202. doi: 10.3390/nu10020202
 75. James S, James S, Aparna JS, Babu A, Paul AM, Lankadasari MB, Athira SR, et al. Cardamonin Attenuates Experimental Colitis and Associated Colorectal Cancer. *Biomolecules* (2021) 11(5):661. doi: 10.3390/biom11050661
 76. Pan P, Kang S, Wang Y, Liu K, Oshima K, Huang YW, et al. Black Raspberries Enhance Natural Killer Cell Infiltration Into the Colon and Suppress the Progression of Colorectal Cancer. *Front Immunol* (2017) 8:997. doi: 10.3389/fimmu.2017.00997
 77. Huang YW, Lin CW, Pan P, Shan T, Echeveste CE, Mo YY, et al. Black Raspberries Suppress Colorectal Cancer by Enhancing Smad4 Expression in Colonic Epithelium and Natural Killer Cells. *Front Immunol* (2020) 11:570683. doi: 10.3389/fimmu.2020.570683
 78. Zhang W, An EK, Park HB, Hwang J, Dhananjay Y, Kim SJ, et al. Ecklonia Cava Fucoidan has Potential to Stimulate Natural Killer Cells In Vivo. *Int J Biol Macromol* (2021) 185:111–21. doi: 10.1016/j.ijbiomac.2021.06.045
 79. Yang LC, Lai CY, Hsieh CC, Lin WC. Natural Killer Cell-Mediated Anticancer Effects of an Arabinogalactan Derived From Rice Hull in CT26 Colon Cancer-Bearing Mice. *Int J Biol Macromol* (2019) 124:368–76. doi: 10.1016/j.ijbiomac.2018.11.200
 80. Bhattacharyya S, Md Sakib Hossain D, Mohanty S, Sankar Sen G, Chattopadhyay S, Banerjee S, et al. Curcumin Reverses T Cell-Mediated Adaptive Immune Dysfunctions in Tumor-Bearing Hosts. *Cell Mol Immunol* (2010) 7(4):306–15. doi: 10.1038/cmi.2010.11
 81. Shafabakhsh R, Pourhanifeh MH, Mirzaei HR, Sahebkar A, Asemi Z, Mirzaei H. Targeting Regulatory T Cells by Curcumin: A Potential for Cancer Immunotherapy. *Pharmacol Res* (2019) 147:104353. doi: 10.1016/j.phrs.2019.104353
 82. Rahimi K, Ahmadi A, Hassanzadeh K, Soleimani Z, Sathyapalan T, Mohammadi A, et al. Targeting the Balance of T Helper Cell Responses by Curcumin in Inflammatory and Autoimmune States. *Autoimmun Rev* (2019) 18(7):738–48. doi: 10.1016/j.autrev.2019.05.012
 83. Zhao GJ, Lu ZQ, Tang LM, Wu ZS, Wang DW, Zheng JY, et al. Curcumin Inhibits Suppressive Capacity of Naturally Occurring CD4⁺CD25⁺ Regulatory T Cells in Mice In Vitro. *Int Immunopharmacol* (2012) 14(1):99–106. doi: 10.1016/j.intimp.2012.06.016
 84. Xu B, Yu L, Zhao LZ. Curcumin Up Regulates T Helper 1 Cells in Patients With Colon Cancer. *Am J Transl Res* (2017) 9(4):1866–75 PMID: 28469791.
 85. Dent P, Dent P, Booth L, Roberts JL, Poklepovic A, Hancock JF. (Curcumin +sildenafil) Enhances the Efficacy of 5FU and Anti-PD1 Therapies In Vivo. *J Cell Physiol* (2020) 235(10):6862–74. doi: 10.1002/jcp.29580
 86. Li M, Yue GG, Song LH, Huang MB, Lee JK, Tsui SK, et al. Natural Small Molecule Bigelovin Suppresses Orthotopic Colorectal Tumor Growth and Inhibits Colorectal Cancer Metastasis via IL6/STAT3 Pathway. *Biochem Pharmacol* (2018) 150:191–201. doi: 10.1016/j.bcp.2018.02.017
 87. Ayeka PA, Bian Y, Mwitari PG, Chu X, Zhang Y, Uzayisenga R, et al. Immunomodulatory and Anticancer Potential of Gan Cao (Glycyrrhiza Uralensis Fisch.) Polysaccharides by CT-26 Colon Carcinoma Cell Growth Inhibition and Cytokine IL-7 Upregulation In Vitro. *BMC Complement Altern Med* (2016) 16:206. doi: 10.1186/s12906-016-1171-4
 88. Chalons P, Courtaut F, Limagne E, Chalmir F, Cantos-Villar E, Richard T, et al. Red Wine Extract Disrupts Th17 Lymphocyte Differentiation in a Colorectal Cancer Context. *Mol Nutr Food Res* (2020) 64(11):e1901286. doi: 10.1002/mnfr.201901286
 89. Liang J, Li H, Chen J, He L, Du X, Zhou L, et al. Dendrobium Officinale Polysaccharides Alleviate Colon Tumorigenesis via Restoring Intestinal Barrier Function and Enhancing Anti-Tumor Immune Response. *Pharmacol Res* (2019) 148:104417. doi: 10.1016/j.phrs.2019.104417
 90. Masuda Y, Ito K, Konishi M, Nanba H. A Polysaccharide Extracted From Grifola Frondosa Enhances the Anti-Tumor Activity of Bone Marrow-Derived Dendritic Cell-Based Immunotherapy Against Murine Colon Cancer. *Cancer Immunol Immunother* (2010) 59(10):1531–41. doi: 10.1007/s00262-010-0880-7
 91. Wang H, Zou C, Zhao W, Yu Y, Cui Y, Zhang H, et al. Juglone Eliminates MDSCs Accumulation and Enhances Antitumor Immunity. *Int Immunopharmacol* (2019) 73:118–27. doi: 10.1016/j.intimp.2019.04.058
 92. Zhang J, Shen L, Li X, Song W, Liu Y, Huang L. Nanoformulated Codelivery of Quercetin and Alantolactone Promotes an Antitumor Response Through Synergistic Immunogenic Cell Death for Microsatellite-Stable Colorectal Cancer. *ACS Nano* (2019) 13(11):12511–24. doi: 10.1021/acsnano.9b02875
 93. Xu H, Van derJeught K, Zhou Z, Zhang L, Yu T, Sun Y, et al. Attractylenolide I Enhances Responsiveness to Immune Checkpoint Blockade Therapy by Activating Tumor Antigen Presentation. *J Clin Invest* (2021) 131(10):e146832. doi: 10.1172/JCI146832
 94. Liu F, Ran F, He H, Chen L. Astragaloside IV Exerts Anti-Tumor Effect on Murine Colorectal Cancer by Re-Educating Tumor-Associated Macrophage. *Arch Immunol Ther Exp (Warsz)* (2020) 68(6):33. doi: 10.1007/s00005-020-00598-y
 95. Han K, Nam J, Xu J, Sun X, Huang X, Animasahun O, et al. Generation of Systemic Antitumor Immunity via the In Situ Modulation of the Gut Microbiome by an Orally Administered Inulin Gel. *Nat BioMed Eng* (2021) 5(11):1377–88. doi: 10.1038/s41551-021-00749-2
 96. Lee EJ, Kim JH, Kim TI, Kim YJ, Pak ME, et al. Sanguisorbae Radix Suppresses Colorectal Tumor Growth Through PD-1/PD-L1 Blockade and Synergistic Effect With Pembrolizumab in a Humanized PD-L1-Expressing Colorectal Cancer Mouse Model. *Front Immunol* (2021) 12:737076. doi: 10.3389/fimmu.2021.737076
 97. Zhang SL, Mao YQ, Zhang ZY, Li ZM, Kong CY, Chen HL, et al. Pectin Supplement Significantly Enhanced the Anti-PD-1 Efficacy in Tumor-Bearing Mice Humanized With Gut Microbiota From Patients With Colorectal Cancer. *Theranostics* (2021) 11(9):4155–70. doi: 10.7150/thno.54476
 98. Liu W, Fan T, Li M, Zhang G, Guo W, Yang X, et al. Andrographolide Potentiates PD-1 Blockade Immunotherapy by Inhibiting COX2-Mediated PGE2 Release. *Int Immunopharmacol* (2020) 81:106206. doi: 10.1016/j.intimp.2020.106206
 99. Magri A, Germano G, Lorenzato A, Lamba S, Chilà R, Montone M, et al. High-Dose Vitamin C Enhances Cancer Immunotherapy. *Sci Transl Med* (2020) 12(532):eaay8707. doi: 10.1126/scitranslmed.aay8707
 100. Huang J, Liu D, Wang Y, Liu L, Li J, Yuan J, et al. Ginseng Polysaccharides Alter the Gut Microbiota and Kynurenine/Tryptophan Ratio, Potentiating the Antitumor Effect of Antiprogrammed Cell Death 1/Programmed Cell Death Ligand 1 (Anti-PD-1/PD-L1) Immunotherapy. *Gut* (2022) 71(4):734–45. doi: 10.1136/gutjnl-2020-321031
 101. Gao W, Zhang X, Yang W, Dou D, Zhang H, Tang Y, et al. Prim-O-Glucosylcimifugin Enhances the Antitumor Effect of PD-1 Inhibition by Targeting Myeloid-Derived Suppressor Cells. *J Immunother Cancer* (2019) 7(1):231. doi: 10.1186/s40425-019-0676-z
 102. Murphy N, Moreno V, Hughes DJ, Vodicka L, Vodicka P, Aglago EK, et al. Lifestyle and Dietary Environmental Factors in Colorectal Cancer Susceptibility. *Mol aspects Med* (2019) 69:2–9. doi: 10.1016/j.mam.2019.06.005
 103. Keum N, Giovannucci E. Global Burden of Colorectal Cancer: Emerging Trends, Risk Factors and Prevention Strategies. *Nat Rev Gastroenterol Hepatol* (2019) 16(12):713–32. doi: 10.1038/s41575-019-0189-8
 104. Gurjao C, Zhong R, Haruki K, Li YY, Spurr LF, Lee-Six H, et al. Discovery and Features of an Alkylating Signature in Colorectal Cancer. *Cancer Discovery* (2021) 11(10):2446–55. doi: 10.1158/2159-8290.CD-20-1656
 105. Song M, Garrett W, Chan A. Nutrients, Foods, and Colorectal Cancer Prevention. *Gastroenterology* (2015) 148(6):1244–60.e16. doi: 10.1053/j.gastro.2014.12.035

106. Kopp TI, Vogel U, Tjonneland A, Andersen V. Meat and Fiber Intake and Interaction With Pattern Recognition Receptors (TLR1, TLR2, TLR4, and TLR10) in Relation to Colorectal Cancer in a Danish Prospective, Case-Cohort Study. *Am J Clin Nutr* (2018) 107(3):465–79. doi: 10.1093/ajcn/nqx011
107. Ringel AE, Drijvers JM, Baker GJ, Catozzi A, García-Cañaveras JC, Gassaway BM, et al. Obesity Shapes Metabolism in the Tumor Microenvironment to Suppress Anti-Tumor Immunity. *Cell* (2020) 183(7):1848–1866.e26. doi: 10.1016/j.cell.2020.11.009
108. Amitay EL, Carr PR, Jansen L, Roth W, Alwers E, Herpel E, et al. Smoking, Alcohol Consumption and Colorectal Cancer Risk by Molecular Pathological Subtypes and Pathways. *Br J Cancer* (2020) 122(11):1604–10. doi: 10.1038/s41416-020-0803-0
109. Ogino S, Nowak JA, Hamada T, Phipps AI, Peters U, Milner DA Jr, et al. Integrative Analysis of Exogenous, Endogenous, Tumour and Immune Factors for Precision Medicine. *Gut* (2018) 67(6):1168–80. doi: 10.1136/gutjnl-2017-315537
110. Song M, Nishihara R, Cao Y, Chun E, Qian ZR, Mima K, et al. Marine ω -3 Polyunsaturated Fatty Acid Intake and Risk of Colorectal Cancer Characterized by Tumor-Infiltrating T Cells. *JAMA Oncol* (2016) 2(9):1197–206. doi: 10.1001/jamaoncol.2016.0605

Conflict of Interest: The authors declare that the research was conducted in the absence of any commercial or financial relationships that could be construed as a potential conflict of interest.

Publisher's Note: All claims expressed in this article are solely those of the authors and do not necessarily represent those of their affiliated organizations, or those of the publisher, the editors and the reviewers. Any product that may be evaluated in this article, or claim that may be made by its manufacturer, is not guaranteed or endorsed by the publisher.

Copyright © 2022 Dong, Qian, Zhang, Lu, Zhang, Ji, Zhao and Xu. This is an open-access article distributed under the terms of the Creative Commons Attribution License (CC BY). The use, distribution or reproduction in other forums is permitted, provided the original author(s) and the copyright owner(s) are credited and that the original publication in this journal is cited, in accordance with accepted academic practice. No use, distribution or reproduction is permitted which does not comply with these terms.



OPEN ACCESS

EDITED BY

Yuanliang Yan,
Xiangya Hospital, Central South
University, China

REVIEWED BY

Jorge A.R. Salvador,
University of Coimbra, Portugal
Hwan-Suck Chung,
Korea Institute of Oriental Medicine,
South Korea

*CORRESPONDENCE

Chang Liu
hichang813@uri.edu
Hang Ma
hang_ma@uri.edu

SPECIALTY SECTION

This article was submitted to
Pharmacology of Anti-Cancer Drugs,
a section of the journal
Frontiers in Oncology

RECEIVED 15 July 2022

ACCEPTED 25 August 2022

PUBLISHED 12 September 2022

CITATION

Li H, Seeram NP, Liu C and Ma H
(2022) Further investigation of
blockade effects and binding affinities
of selected natural compounds to
immune checkpoint PD-1/PD-L1.
Front. Oncol. 12:995461.
doi: 10.3389/fonc.2022.995461

COPYRIGHT

© 2022 Li, Seeram, Liu and Ma. This is
an open-access article distributed under
the terms of the [Creative Commons
Attribution License \(CC BY\)](#). The use,
distribution or reproduction in other
forums is permitted, provided the
original author(s) and the copyright
owner(s) are credited and that the
original publication in this journal is
cited, in accordance with accepted
academic practice. No use,
distribution or reproduction is
permitted which does not comply with
these terms.

Further investigation of blockade effects and binding affinities of selected natural compounds to immune checkpoint PD-1/PD-L1

Huifang Li, Navindra P. Seeram, Chang Liu* and Hang Ma*

Bioactive Botanical Research Laboratory, Department of Biomedical and Pharmaceutical Sciences,
College of Pharmacy, University of Rhode Island, Kingston, Rhode Island, United States

The breakthrough in the discovery of immune checkpoint PD-1/PD-L1 inhibitors, such as the series of Bristol Myers Squibb synthetic compounds, boosted the research of small molecules with blockade effects on the interaction of PD-1/PD-L1. However, the search for natural products derived PD-1/PD-L1 inhibitors can be impeded by the false positive and/or negative results from the screening assays. Herein, we combined a PD-1/PD-L1 blockade assay (pair ELISA) and a PD-L1/PD-L1 binding assay (surface plasmon resonance; SPR) to evaluate a panel of natural compounds previously reported to show anti-PD-1/PD-L1 activity. The test compounds included kaempferol, cosmosiin, tannic acid, pentagalloyl glucose, ellagic acid, resveratrol, urolithin A, and rifubutin. Based on the analyses of their responses to the combined screening assays, these compounds were categorized into four groups: I) PD-1/PD-L1 inhibitors that can bind to PD-1 and PD-L1; II) PD-1/PD-L1 inhibitors selectively bind to PD-L1 protein; III) PD-1/PD-L1 inhibitors without binding capacity, and IV) PD-1/PD-L1 binders without blockade effect. Discrimination of positive responders in the PD-1/PD-L1 blockade and binding assays can provide useful insights to avoid false outcomes. Examples demonstrated in this study suggest that it is crucial to adopt proper evaluation methods (including using multiple-facet functional assays and target binding techniques) for the search for natural products derived PD-1/PD-L1 inhibitors.

KEYWORDS

immune checkpoint, PD-1/PD-L1, natural products, pair ELISA, surface plasmon resonance, binding affinity

Introduction

Programmed cell death protein 1 (PD-1), a cell surface receptor expressed by T and B cells, is an immune checkpoint that regulates the immune system (1). PD-1 interacts with its ligands, including the programmed cell death-ligand 1 (PD-L1) expressed by antigen-presenting cells or cancer cells, to maintain immune homeostasis. In the tumor microenvironment, when PD-L1 binds to PD-1, T cell's immune responses are undermined, which impairs its function of recognizing cancer cells. Consequently, cancer cells escaping from the immunological surveillance of T cells can lead to the proliferation of cancer cells and the expansion of tumor tissues (2). Thus, disrupting the interaction between PD-1 and PD-L1 has become a promising strategy for cancer immunotherapy. Molecules (e.g. immune checkpoint inhibitors) with blockade effects on the interaction of PD-1/PD-L1 can block the immune escaping signals of cancer cells and, consequently, reactivate immune cells to restore their anti-tumor response. Several antibody-based PD-1 inhibitors (e.g. Pidilizumab and Nivolumab) and PD-L1 inhibitors (e.g. Atezolizumab and Durvalumab) have been approved by the U.S. Food and Drug Administration (FDA) for the treatment of various cancers (3). Although these antibody drugs have shown potent anti-cancer efficacy in clinical trials, they are facing several inherent limitations, such as toxic off-target effects, poor permeability (of the tumor tissues), and immunogenicity, as well as prohibitive costs and challenging quality control (4, 5). On the contrary, compared to antibody drugs, small molecule derived PD-1/PD-L1 inhibitors may display a more favorable safety profile (6). Several synthetic small molecules with potent blockade effects on PD-1/PD-L1 have been developed. For instance, compounds including BMS1166 and BMS202 (by Bristol Myers Squibb Pharma Co.) are designed to directly bind the PD-L1 protein and consequently blockade the interaction of PD-1/PD-L1 (7). The strategy of combining both functional assay (for PD-1/PD-L1 inhibition) and binding characterization (for binding affinity to PD-1/PD-L1 proteins) to search for natural compounds including kaempferol (8), cosmosiin (9), resveratrol (10) and rifabutin (11) with anti-PD-1/PD-L1 effects has been adopted by our group and others. Our group has also summarized the methodologies for the development of small molecule based PD-1/PD-L1 inhibitors utilizing proper functional assays and biophysical methods (12). During the investigation, we noticed that several natural compounds (e.g. punicalagin) were identified as 'false hits' as they showed a detectable binding capacity to PD-1/PD-L1 proteins (characterized by surface plasmon resonance; SPR) but were not active in the PD-1/PD-L1 blockade assay (assessed by pair ELISA). This discrepancy is crucial for screening small molecules based PD-1/PD-L1 inhibitors given that the blockade effect of small molecules and their binding capacity to PD-1/PD-L1 proteins should be scrutinized to avoid false positives. Herein, in this current study, a panel of natural

compounds with previously reported anti-PD-1/PD-L1 activity were selected to study the relationship between their blockade effects on PD-1/PD-L1 interaction (by pair ELISA assay) and binding capacity to the PD-1/PD-L1 proteins (by SPR assay). In addition, a series of natural polyphenols including tannic acid, pentagalloyl glucose, and urolithin A, which have similar chemical structure moieties as punicalagin, were included in the screening. Based on their positive responses to either the blockade assay or the binding affinity assay, these compounds were sorted in four categories: I) PD-1/PD-L1 inhibitors that bind to both PD-1 and PD-L1 proteins; II) PD-1/PD-L1 inhibitors that only bind to PD-L1 protein; III) PD-1/PD-L1 inhibitors without the binding capacity to PD-1/PD-L1 proteins; and IV) PD-1/PD-L1 binders with no blockade effect.

Materials and methods

Chemicals and reagents

BMS202 and BMS1166 were purchased from MedChemExpress LLC (Monmouth Junction, NJ, USA). Rifabutin, kaempferol, tannic acid, and cosmosiin were purchased from Cayman Chemical (Ann Arbor, MI, USA). Ellagic acid and resveratrol were purchased from Sigma Chemical Co. (St. Louis, MO, USA). Urolithin A (13) and pentagalloyl glucose (14) were synthesized and isolated, respectively, by our group as previously reported. Phosphate-buffered saline (PBS, pH 7.2) and dimethylsulfoxide (DMSO) were purchased from Thermo Fisher Scientific (Waltham, MA, USA). The test compounds were dissolved in DMSO (at 100 mM as a stock solution) and stored at -80°C for further use.

PD-1/PD-L1 function assay with pair ELISA

The PD-1/PD-L1 blockade effect was determined by a pair ELISA assay kit (ACRO Biosystems, Newark, DE, USA). Briefly, human PD-L1 (200 ng/per well) was coated into a 96-well microplate and incubated overnight at 4°C. Next, the plate was washed with washing buffer followed by incubating with blocking buffer at room temperature for 1.5 h. Test samples were then added (at concentrations of 10 and 100 µM dissolved in dilution buffer with 0.1% of DMSO) prior to adding human PD-1-biotin (200 ng/per well). The plate was incubated at room temperature for 1 h. After horseradish peroxidase-conjugated streptavidin was added and incubated at room temperature for 1 h, the substrate was added into each well and incubated at room temperature for 20 min. The stop solution was then added to each well followed by measuring the absorbance of each well at a wavelength of 450 nm using a SpectraMax M2 plate reader (Molecular Devices; Sunnyvale, CA, USA).

PD-1/PD-L1 binding assay with SPR

The PD-1/PD-L1 binding affinity of test natural compounds was measured on a SPR Biacore T200 instrument (GE Healthcare; Marlborough, MA, USA). Human PD-L1 and PD-1 proteins (both with a Fc Tag) were purchased from ACRO Biosystems (Newark, DE, USA). Carboxymethylated CM 5 SPR chips were purchased from GE Healthcare (Marlborough, MA, USA). The SPR binding channels were set as: Cell-1, blank immobilization; Cell-2, human PD-L1 protein was immobilized by the injection of protein solution (40 µg/mL) in sodium acetate buffer (10 mM; pH 4.5); Cell-3, human PD-1 protein was immobilized by the injection of protein solution (40 µg/mL) in sodium acetate buffer (10 mM; pH 5.0). Approximately, 5500 and 4500 RU of human PD-1 and PD-L1 proteins, respectively, were immobilized on the flow cells with an amine coupling method.

Results and discussion

Category I: PD-1/PD-L1 inhibitors bind to PD-1 and PD-L1 (tannic acid and kaempferol)

Natural compounds including tannic acid (TA) and kaempferol (Figure 1A) were identified as active PD-1/PD-L1 inhibitors by data from a combination of pair ELISA and the SPR binding assay. TA and kaempferol (10 and 100 µM)

blocked the PD-1/PD-L1 interaction by 11.0 and 36.9% and 4.1 and 63.4%, respectively (Figure 1B). TA and kaempferol also bound to PD-1 and PD-L1 proteins in the SPR measurements (Figures 1C–F). The binding capacity between TA and PD-1 or PD-L1 protein was identical with a comparable K_D value of 1.46×10^{-6} and 1.21×10^{-6} M, respectively. Kaempferol had a stronger binding affinity to PD-1 protein ($K_D = 3.04 \times 10^{-7}$ M) than PD-L1 protein ($K_D = 3.3 \times 10^{-5}$ M). The positive controls, BMS1166 and BMS202, showed a potent blockade effect (99.3 and 87.4% at 10 µM, respectively) and a strong binding affinity to PD-L1 ($K_D = 5.7 \times 10^{-9}$ M and 3.20×10^{-7} M, respectively). The positive results obtained in this category must be carefully examined. Although these compounds, in a manner similar to the positive controls, displayed both blockade effects and binding capacity to PD-1/PD-L1, TA and kaempferol had far less potent anti-PD1/PD-L1 effects as compared to BMS202. This is possibly due to BMS202's distinct mechanism of blocking PD-1/PD-L1 interaction. BMS202 binds to PD-L1 and subsequently induces the dimerization of PD-L1 monomers (15). The complex of dimerized PD-L1 and BMS202 further prevents the interaction with PD-1, which contributes to the dissociation of the PD-1/PD-L1 complex. This principle may not be applicable to the case of natural compounds (e.g. TA and kaempferol) due to the lack of data supporting that they can induce the dimerization of PD-L1, despite they can bind to PD-L1. Moreover, kaempferol's binding affinity to PD-1 protein was 100-fold stronger than PD-L1 protein, whilst TA's PD-1 and PD-L1 binding affinities were

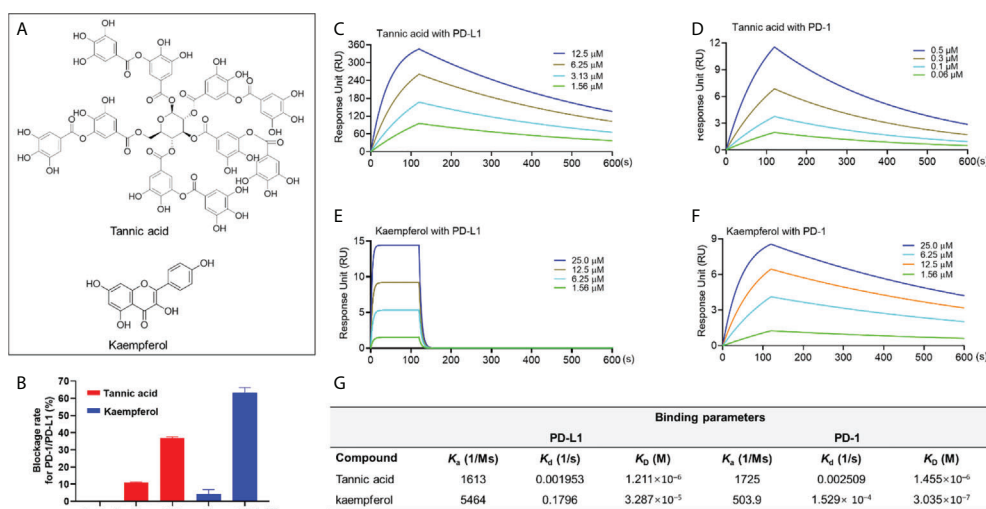


FIGURE 1

Chemical structure of TA and kaempferol (A). Blockade rate of TA and kaempferol (at 10 and 100 µM) on the PD-1/PD-L1 interaction determined by the pair ELISA assay (B). Binding profile of natural compounds at various concentrations with PD-1 and PD-L1 proteins characterized by the SPR measurements. Sensograms of TA with PD-L1 (C) or PD-1 (D) protein at 1.56–12.5 µM and 0.06–0.5 µM, respectively. Sensograms of kaempferol with PD-L1 (E) and PD-1 (F) protein at 1.56–25 µM. Summarized binding parameters including K_a , K_d , and K_D between test compounds and PD-L1 and PD-1 proteins (G).

comparable. This observation suggests that TA and kaempferol did not selectively bind to PD-L1, and thus, may not be able to induce the dimerization of PD-L1 to exert the anti-PD-1/PD-L1 effect. Apart from the ambiguous mechanisms of action, the development of these natural compounds for PD-1/PD-L1 inhibitors can be challenging due to their low druggability (e.g. low bioavailability and non-specific targets) (16). Therefore, further studies using physiological relevant models to examine the effectiveness of compounds in this category are warranted to avoid false positives.

Category II: PD-1/PD-L1 inhibitors selectively bind to PD-L1 protein (resveratrol and cosmosiin)

This group of natural compounds included resveratrol and cosmosiin (Figure 2A), which showed the PD-1/PD-L1 blockade effect in the pair ELISA assay by 43.5 and 55.8%, respectively (at a concentration of 100 μ M). Notably, resveratrol and cosmosiin displayed a selective binding to the PD-L1 protein with a K_D value of 3.79×10^{-5} and 3.32×10^{-6} M, respectively (Figures 3C–E). This is in agreement with a reported study using *in silico* methods (including computational docking and molecular dynamic simulation) to predict that resveratrol can facilitate the

dimerization of PD-L1 (10). However, to date, resveratrol's effect on the dimerization of PD-L1 is not confirmed by experimental data. This limitation is, at least partially, due to the lack of feasible functional assays to evaluate the dimerization of PD-L1. Therefore, specific functional assays, i.e. *PD-L1 dimerization assay*, are crucial for the development of natural compounds based PD-1/PD-L1 inhibitors. Nevertheless, apart from the dimerization of PD-L1, other mechanisms may also be involved in the disruption of PD-1/PD-L1 interaction. For instance, resveratrol was reported to disrupt the PD-1/PD-L1 interaction by altering the structure of PD-L1 protein (*via* post-translational modifications, i.e., N-linked glycosylation), accumulating abnormally glycosylated form of PD-L1, and reducing tumor cells induced cytotoxicity to T cells (10). Therefore, compounds in this category may have the scaffold of lead compounds for PD-1/PD-L1 inhibitors but further structural modifications (by medicinal chemistry) and biological evaluations (with proper functional assays) are warranted.

Category III: PD-1/PD-L1 inhibitors without binding capacity (rifabutin and urolithin A)

Natural compounds in this category only showed a weak blockade effect on the interaction of PD-1/PD-L1. Rifabutin and

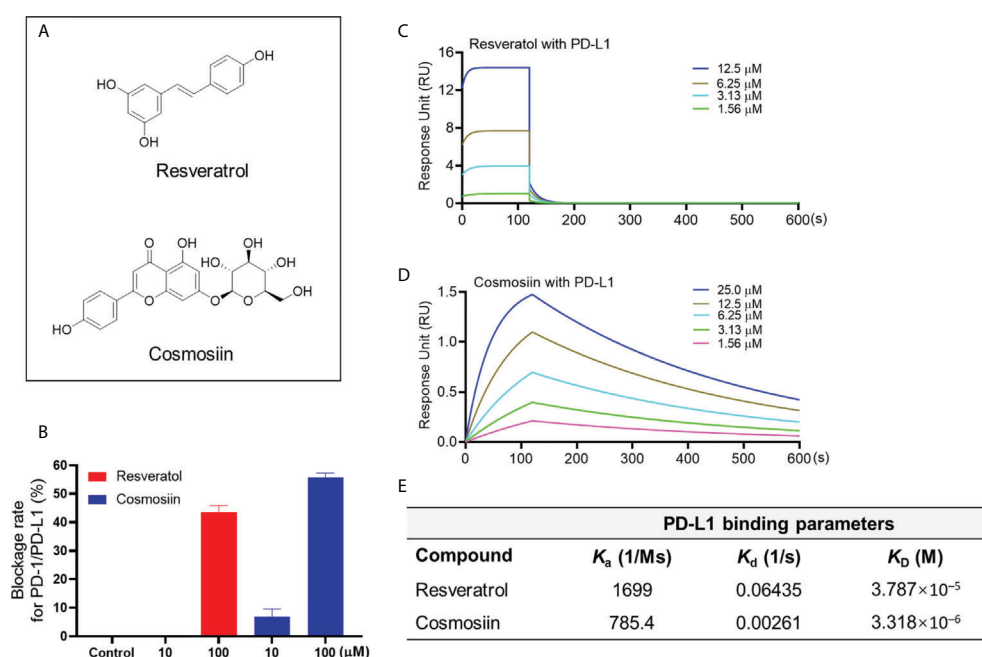


FIGURE 2

Chemical structure of resveratrol and cosmosiin (A). Blockade rate of resveratrol and cosmosiin (at 10 and 100 μ M) on the PD-1/PD-L1 interaction determined by the pair ELISA assay (B). Binding profile of natural compounds at various concentrations with PD-L1 protein characterized by the SPR measurements. Sensograms of resveratrol with PD-L1 (C) protein at 1.56–12.5 μ M. Sensograms of cosmosiin with PD-L1 (D) protein at 1.56–25 μ M. Summarized binding parameters including K_a , K_d , and K_D between test compounds and PD-L1 proteins (E).

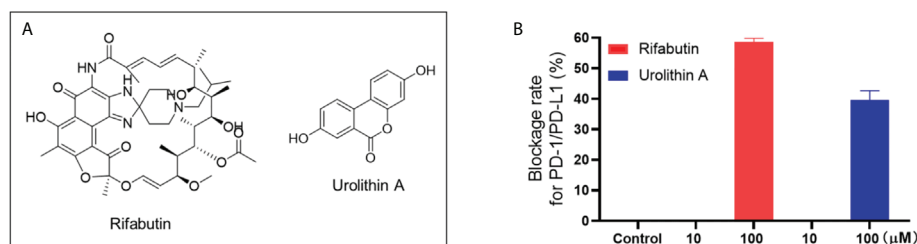


FIGURE 3
Chemical structure of rifabutin and UA (A). Blockade rate of rifabutin and UA (at 10 and 100 μM) on the PD-1/PD-L1 interaction determined by the pair ELISA assay (B).

urolithin A (UA; Figure 3A) blocked the interaction of PD-1/PD-L1 by 58.6 and 39.7% at 100 μM, respectively (Figure 3B). This is in agreement with a reported study showing that rifabutin had a moderate blockade effect of PD-1/PD-L1 in a homogenous AlphaLISA assay ($IC_{50} = 25 \mu M$) (11). Similarly, a study supported the inhibitory effect of UA on PD-1/PD-L1 interaction by showing that urolithins may exert a sensitizing effect in the inhibition of immune checkpoint targeting the PD-1/PD-L1 interaction (17). However, the binding affinity between these compounds and PD-1 or PD-L1 protein was not detectable by the SPR assay. It is possible that these compounds may have shown false positive results. Further functional assays, preferably using cellular or *in vivo* models, are warranted to further evaluate the anti-PD-1/PD-L1 activity of these compounds to avoid false positive outcomes. For instance, a cellular assay, namely, the PD-1/NFAT reporter assay (18), using a recombinant Jurkat cell line, can be used as a functional assay to validate the anti-PD-1/PD-L1 effects of natural compounds.

Category IV: PD-1/PD-L1 binders without blockade effect (pentagalloyl glucose and ellagic acid)

Compounds in this group including two hydrolyzable tannins pentagalloyl glucose (PGG) and ellagic acid (EA; Figure 4A) were able to bind to the PD-L1 proteins. PGG and EA bound to PD-L1 protein with a K_D value of 2.23×10^{-6} and 2.62×10^{-5} M, respectively. PGG and EA also bound to PD-1 protein in the SPR assay with a K_D value of 2.72×10^{-5} and 1.82×10^{-6} M, respectively (Figures 4B–F). However, their blockade effect on the PD-1/PD-L1 interaction was not detected in the pair ELISA assay. To avoid possible false negative results, a PD-L1 dimerization assay should be used to confirm that they are not able to blockade the PD-1/PD-L1 interaction. The challenges shown in these assays were not surprising given that the search for small molecules targeting the PD-1/PD-L1 interface can be challenging. This is because, from a structural perspective, it requires the small molecule inhibitors to be fixed at the center of the PD-L1 homodimer (19), which is a surface

with a deep hydrophobic pocket contributing to molecular interactions between the PD-L1 monomers [see Supplementary Data Figure S1]. Thus, although PGG and EA were able to bind to PD-L1, they may not be able to be located at the desired binding pocket in the PD-L1 dimer complex to exert the blockade effect. Similar to the aforementioned limitation, a PD-L1 dimerization assay should be used to discrete the false negative results from compounds in this category. It should be noted that, apart from the PD-L1 dimerization, other small molecules may confer the anti-PD-1/PD-L1 effects *via* other mechanisms of action of PD-1/PD-L1 interaction. These compounds may also be considered as in a distinct category, which should be further investigated.

Conclusion

A combination of a PD-1/PD-L1 blockade assay (pair ELISA) and a target-binding assay (SPR) was used to screen the PD-1/PD-L1 blockade effect of a series of natural compounds. Based on their responses from the assays, these compounds were categorized into four groups: I) PD-1/PD-L1 inhibitors bind to PD-1 and PD-L1; II) PD-1/PD-L1 inhibitors selectively bind to PD-L1 protein; III) non-binder PD-1/PD-L1 inhibitors, and IV) PD-1/PD-L1 binders without blockade effect. Further functional assays, such as the PD-L1 dimerization assay, should be used to confirm the anti-PD-1/PD-L1 activity to avoid false positive (in the I and III groups) and false negative (in the IV group) outcomes. A promising positive 'hit' should exhibit both potent PD-1/PD-L1 blockade activity and desirable binding affinity with the specific target proteins (i.e. PD-L1). Despite it is challenging to identify natural compounds-based PD-1/PD-L1 inhibitors, compounds in the II group may serve as lead compounds for further structural modifications to improve their PD-1/PD-L1 blockade effect. However, a larger sample size of compounds (e.g. the type II compounds) with promising blockade effect and binding capacity should be included in future studies to evaluate their biological effects in the functional assays. The current study is limited by a confined number of representing compounds included in the bioassays due to, at least partially, the fact that the discovery and development of natural products based PD-1/PD-L1

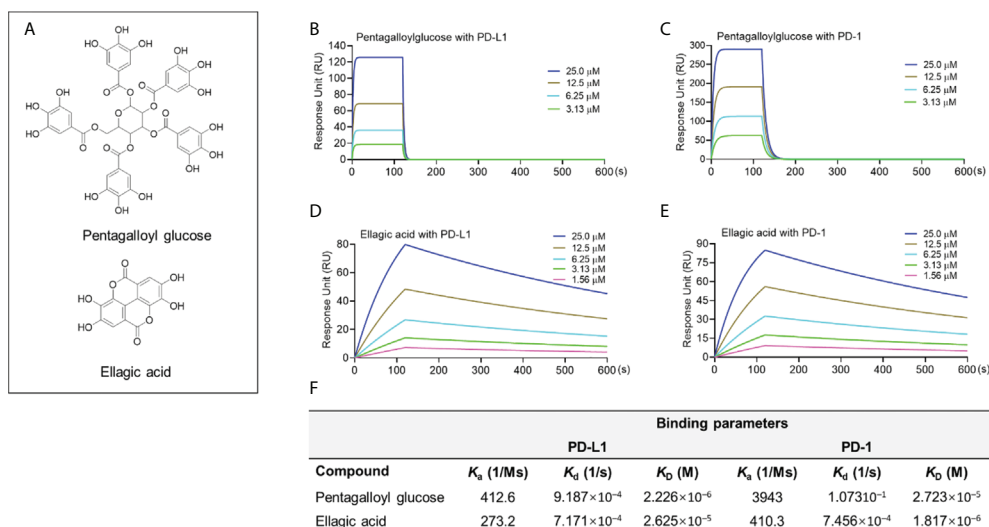


FIGURE 4

Chemical structure of PGG and EA (A). Binding profile of natural compounds at various concentrations with PD-1 and PD-L1 proteins characterized by the SPR measurements. Sensograms of PGG with PD-L1 (B) or PD-1 protein (C) at 3.13–25 μ M. Sensograms of EA with PD-L1 (D) and PD-1 (E) protein at 1.56–25 μ M. Summarized binding parameters including K_a , K_d , and K_D between test compounds and PD-L1 and PD-1 proteins (F).

inhibitors are still in the early stage. In summary, observation demonstrated in the current study suggest that, although natural product may exert PD-L1/PD-L1 blockade effect with target protein binding capacity, their effectiveness should be verified by multiple functional bioassays to exclude false results. Further investigations using medicinal chemistry approaches are warranted to optimize the PD-1/PD-L1 blockade effects of lead natural compounds.

Institutional Development Award (IDeA) Network of Biomedical Research Excellence from the National Institute of General Medical Sciences of the National Institutes of Health under grant number P20GM103430.

Conflict of interest

The authors declare that the research was conducted in the absence of any commercial or financial relationships that could be construed as a potential conflict of interest.

Publisher's note

All claims expressed in this article are solely those of the authors and do not necessarily represent those of their affiliated organizations, or those of the publisher, the editors and the reviewers. Any product that may be evaluated in this article, or claim that may be made by its manufacturer, is not guaranteed or endorsed by the publisher.

Supplementary material

The Supplementary Material for this article can be found online at: <https://www.frontiersin.org/articles/10.3389/fonc.2022.995461/full#supplementary-material>

Data availability statement

The original contributions presented in the study are included in the article/Supplementary Material. Further inquiries can be directed to the corresponding authors.

Author contributions

HL performed the experiments. NS revised the manuscript. CL designed the methods, guided data analysis, and wrote the draft. CL and HM conceived the project and HM extensively edited the manuscript. All authors contributed to the article and approved the submitted version.

Acknowledgments

This research was made possible in part using the Biacore T200 instrument available through the Rhode Island

References

- Chen L, Han X. Anti-PD-1/PD-L1 therapy of human cancer: past, present, and future. *J Clin Invest* (2015) 125(9):3384–91. doi: 10.1172/JCI80011
- Goodman A, Patel SP, Kurzrock R. PD-1–PD-L1 immune-checkpoint blockade in b-cell lymphomas. *Nat Rev Clin Oncol* (2016) 14(4):203–20. doi: 10.1038/nrclinonc.2016.168
- Sunshine J, Taube JM. PD-1/PD-L1 inhibitors. *Curr Opin Pharmacol* (2015) 23:32–8. doi: 10.1016/j.coph.2015.05.011
- Reilly RM, Sandhu J, Alvarez-Diez TM, Gallinger S, Kirsh J, Stern H. Problems of delivery of monoclonal antibodies. pharmaceutical and pharmacokinetic solutions. *Clin Pharmacokinet* (1995) 28(2):126–42. doi: 10.2165/00003088-199528020-00004
- Akinleye A, Rasool Z. Immune checkpoint inhibitors of PD-L1 as cancer therapeutics. *J Hematol Oncol* (2019) 12(1):1–13. doi: 10.1186/S13045-019-0779-5
- Zhan MM, Hu XQ, Liu XX, Ruan BF, Xu J, Liao C. From monoclonal antibodies to small molecules: the development of inhibitors targeting the PD-1/PD-L1 pathway. *Drug Discovery Today* (2016) 21(6):1027–36. doi: 10.1016/J.DRUDIS.2016.04.011
- Ganesan A, Ahmed M, Okoye I, Arutyunova E, Babu D, Turnbull WL, et al. Comprehensive *in vitro* characterization of PD-L1 small molecule inhibitors. *Sci Rep* (2019) 9(1):1–13. doi: 10.1038/S41598-019-48826-6
- Kim JH, Kim YS, Choi JG, Li W, Lee EJ, Park JW, et al. Kaempferol and its glycoside, kaempferol 7-o-rhamnoside, inhibit PD-1/PD-L1 interaction *In vitro*. *Int J Mol Sci* (2020) 21(9):3239. doi: 10.3390/IJMS21093239
- Choi JG, Kim YS, Kim JH, Kim TI, Li W, Oh TW, et al. Anticancer effect of salvia plebeia and its active compound by improving T-cell activity *via* blockade of PD-1/PD-L1 interaction in humanized PD-1 mouse model. *Front Immunol* (2020) 11:598556/FULL. doi: 10.3389/FIMMU.2020.598556/FULL
- Verdura S, Cuyàs E, Cortada E, Brunet J, Lopez-Bonet E, Martin-Castillo B, et al. Resveratrol targets PD-L1 glycosylation and dimerization to enhance antitumor T-cell immunity. *Aging (Albany NY)* (2020) 12(1):8. doi: 10.18632/AGING.102646
- Patil SP, Yoon SC, Aradhya AG, Hofer J, Fink MA, Enley ES, et al. Macrocyclic compounds from ansamycin antibiotic class as inhibitors of PD1–PDL1 protein–protein interaction. *Chem Pharm Bull* (2018) 66(8):773–8. doi: 10.1248/CPB.C17-00800
- Liu C, Seeram NP, Ma H. Small molecule inhibitors against PD-1/PD-L1 immune checkpoints and current methodologies for their development: a review. *Cancer Cell Int* (2021) 21(1):1–17. doi: 10.1186/S12935-021-01946-4
- Yuan T, Ma H, Liu W, Niesen DB, Shah N, Crews R, et al. Pomegranate's neuroprotective effects against alzheimer's disease are mediated by urolithins, its ellagitannin-gut microbial derived metabolites. *ACS Chem Neurosci* (2016) 7(1):26–33. doi: 10.1021/ACSCHEMNEURO.5B00260
- Ma H, Liu W, Frost L, Wang L, Kong L, Dain JA, et al. The hydrolyzable gallotannin, penta- O -galloyl-β- d -glucopyranoside, inhibits the formation of advanced glycation endproducts by protecting protein structure. *Mol Biosyst* (2015) 11(5):1338–47. doi: 10.1039/C4MB00722K
- Zak KM, Grudnik P, Guzik K, Zieba BJ, Musielak B, Dömling A, et al. Structural basis for small molecule targeting of the programmed death ligand 1 (PD-L1). *Oncotarget* (2016) 7(21):30323. doi: 10.18632/oncotarget.8730
- Wang H, Oo Khor T, Shu L, Su ZY, Fuentes F, Lee JH, et al. Plants against cancer: A review on natural phytochemicals in preventing and treating cancers and their druggability. *Anti-cancer Agents medicinal Chem* (2012) 12(10):1281. doi: 10.2174/187152012803833026
- Zitvogel L, Kroemer G. Boosting the immunotherapy response by nutritional interventions. *J Clin Invest* (2022) 132(11):e161483. doi: 10.1172/JCI161483
- Wang X, Martin AD, Negri KR, McElvain ME, Oh J, Wu ML, et al. Extensive functional comparisons between chimeric antigen receptors and T cell receptors highlight fundamental similarities. *Mol Immunol* (2021) 138:137–49. doi: 10.1016/J.MOLIMM.2021.07.018
- Guzik K, Zak KM, Grudnik P, Magiera K, Musielak B, Torner R, et al. Small-molecule inhibitors of the programmed cell death-1/Programmed death-ligand 1 (PD-1/PD-L1) interaction *via* transiently induced protein states and dimerization of PD-L1. *J Medicinal Chem* (2017) 60(13):5857–67. doi: 10.1021/ACS.JMEDCHEM.7B00293



OPEN ACCESS

EDITED BY

Jean Christopher Chamcheu,
University of Louisiana at Monroe,
United States

REVIEWED BY

Venkataswarup Tiriveedhi,
Tennessee State University, United States
Wenbo Yao,
Shaanxi University of Science and
Technology, China
Mulu Tesfay,
University of Arkansas for Medical
Sciences, United States

*CORRESPONDENCE

Yung-Chi Cheng,
✉ yccheng@yale.edu

SPECIALTY SECTION

This article was submitted to
Pharmacology of Anti-Cancer Drugs,
a section of the journal
Frontiers in Pharmacology

RECEIVED 10 November 2022

ACCEPTED 19 December 2022

PUBLISHED 04 January 2023

CITATION

Lam W, Hu R, Liu S-H, Cheng P and
Cheng Y-C (2023), YIV-906 enhances
nuclear factor of activated T-cells (NFAT)
activity of T cells and promotes immune
checkpoint blockade antibody action and
CAR T-cell activity.
Front. Pharmacol. 13:1095186.
doi: 10.3389/fphar.2022.1095186

COPYRIGHT

© 2023 Lam, Hu, Liu, Cheng and Cheng.
This is an open-access article distributed
under the terms of the [Creative Commons
Attribution License \(CC BY\)](#). The use,
distribution or reproduction in other
forums is permitted, provided the original
author(s) and the copyright owner(s) are
credited and that the original publication in
this journal is cited, in accordance with
accepted academic practice. No use,
distribution or reproduction is permitted
which does not comply with these terms.

YIV-906 enhances nuclear factor of activated T-cells (NFAT) activity of T cells and promotes immune checkpoint blockade antibody action and CAR T-cell activity

Wing Lam¹, Rong Hu¹, Shwu-Huey Liu², Peikwen Cheng² and
Yung-Chi Cheng^{1*}

¹Department of Pharmacology, Yale University School of Medicine, New Haven, CN, United States, ²Yiviva Inc, New York, NY, United States

YIV-906 is a systems biology botanical cancer drug, inspired by a traditional Chinese herbal formulation. Results from eight Phase I/II to II clinical studies demonstrated the potential of YIV-906 to prolong survival and improve the quality of life of cancer patients. As an immunomodulator in the tumor microenvironment, YIV-906 can turn cold tumors hot and potentiate anti-tumor activity for different classes of anticancer agents; and as a cytoprotector in the GI, YIV-906 can reduce non-hematological side effects and speed up damaged tissue recovery. YIV-906 enhanced anti-PD1 action against hepatoma in mice by stimulating both innate and adaptive immunity. In a Jurkat cell-staphylococcal superantigen E (SEE)-Raji cell culture model, YIV-906 promoted T cell activation with upregulation of CD69 by enhancing NFAT activity, with or without PD1-PD-L1 interaction. YIV-906 could trigger the phosphorylation of TCR downstream signaling cascades without the involvement of TCR. YIV-906 could inhibit SHP1 and SHP2 activities, which dephosphorylates TCR downstream proteins due to the PD1-PD-L1 interaction. Therefore, YIV-906 could enhance anti-PD1 action to rescue the depressed NFAT activity of Jurkat cells due to the PD1-PD-L1 interaction. In addition, YIV-906 enhanced the NFAT activity and killing capability of Jurkat cells expressing chimeric antigen receptor (CAR-CD19-CD3z) toward CD19 expressing cells, such as Raji cells, with or without PD1-PD-L1 overexpression. Ingredient herb **S** (*Scutellaria baicalensis* Georgi) of YIV-906 and some **S** compounds were found to play key roles in these activities. In conclusion, YIV-906 modulates adaptive immunity by activating T effector cells mainly through its action on SHP1/2. YIV-906 could also facilitate immune checkpoint blockade therapy or CAR-T cell therapy for cancer treatment.

KEYWORDS

YIV-906, NFAT, PD-1, PD-L1, CAR T, SHP1, SHP2

Introduction

YIV-906 is a botanical drug inspired by an 1800-year-old traditional herbal medicine formulation called “Huang Qin Tang,” historically used to treat numerous gastrointestinal (GI) symptoms, including diarrhea, nausea, and vomiting. YIV-906 is composed of four medicinal plants: *Glycyrrhiza uralensis* Fisch (G), *Paeonia lactiflora* Pall (P), *Scutellaria baicalensis* Georgi (S), and *Ziziphus jujuba* Mill (Z). Eight clinical-grade preparations of YIV-906 have been manufactured using cGMP standards over the past 20 years. Batch-to-batch consistency was

established and validated using quality control platforms, including Phytomics (Tilton et al., 2010) and its next-generation Mechanism-based Quality Control platform (Mech QC) that measures the consistency of bioactivities (Lam et al., 2018).

Over 250 patients with liver, pancreatic, colorectal, or rectal cancers have been treated with YIV-906 in combination with different cancer regimens (including irinotecan-based therapies, sorafenib, capecitabine, or chemo-radiation) in nine phase I/II to II clinical studies at numerous research institutions, including Yale University, Stanford University, UPMC Hillman Cancer Center, City of Hope Comprehensive Cancer Center, and Memorial Sloan Kettering (Yen et al., 2009; Saif et al., 2010; Kummar et al., 2011; Saif et al., 2014; Changou et al., 2021). A phase II randomized, double-blinded, placebo-controlled clinical trial (NCT04000737) evaluating the use of YIV-906 in combination with sorafenib as first-line therapy for hepatitis B (HBV+) patients with advanced hepatocellular carcinoma (HCC) is currently enrolling patients in the United States, Mainland China, Hong Kong, and Taiwan. YIV-906 has been observed to prolong patient survival and reduce grade 3/4 non-hematological toxicities including diarrhea, nausea, vomiting, fatigue, and hand-foot syndrome (Yen et al., 2009; Saif et al., 2010; Kummar et al., 2011; Saif et al., 2014; Changou et al., 2021).

In animal studies, YIV-906 reduced irinotecan (CPT-11)-induced intestinal inflammation by inhibiting TNF α , NF- κ B, COX-2, iNOS, and IL6, while promoting intestinal stem/progenitor cell repopulation by potentiating the Wnt signaling pathway (Lam et al., 2010). In irradiation studies, YIV-906 also reduced GI toxicities and promoted GI recovery following radiation treatment (Rockwell et al., 2013). YIV-906 also selectively alters the intestinal bacterial population; however, the change in microbes does not seem to be responsible for YIV-906's action on irinotecan (Lam et al., 2014).

In addition to reducing side effects common to chemotherapy and radiation, YIV-906 can enhance the action for a broad spectrum of anti-cancer agent classes including: immune checkpoint antibodies, multi-kinase inhibitors, topoisomerase inhibitors, anti-metabolites, alkylating agents, anti-microtubule agents, and nucleoside analogs in animals (Liu and Cheng, 2012). In the presence of neoantigens caused by anti-cancer agents, YIV-906 could potentiate innate and/or adaptive immunity potentiation through multiple mechanisms of action. To enhance innate immunity, YIV-906 can potentiate interferon-gamma (IFN γ) action to induce M1-like macrophage polarization simultaneously inhibiting IL4 action to induce M2 macrophage polarization (Lam et al., 2015; Yang et al., 2021). To enhance adaptive immunity, YIV-906 reduces PD1 or counteracts PD-L1 induction caused by anti-PD1, leading to higher T-cell activation-associated gene expression in the tumor (Yang et al., 2021). To help overcome immune suppression, YIV-906 reduces immune tolerance by modulating IDO activity and reducing monocytic MDSC in the tumor (Yang et al., 2021).

Here, we report that YIV-906 and its components can promote T cell activation by modulating nuclear factor of activated T-cells (NFAT) activity. Inhibition of SHP1/2 phosphatases and the induction of protein phosphorylation of T cell receptor signaling cascades could play an integral role in the mechanisms of action. Our studies also suggest that YIV-906 could enhance immune checkpoint blockade antibody action as well as CAR T cell therapy.

Methods and materials

Preparation of herbal extracts

YIV-906 is a complex mixture prepared using a traditional hot water extract of four medicinal plants, *Scutellaria baicalensis* Georgi (S) and *Paeonia lactiflora* Pall. (P) *Glycyrrhiza uralensis* Fisch. (G), and *Ziziphus jujuba* Mill (Z) at a ratio of 3:2:2:2, respectively. It can be consistently prepared batch-to-batch and used in clinical trials. Details of the quality control of YIV-906 can be found in our previous reports (Tilton et al., 2010; Lam et al., 2018). YIV-906 water extract (100 mg/ml) was prepared as a stock for all culture assays.

Cell lines

RPMI1640 (Gibco, cat#11835030)+5%FBS+50ug/ml kanamycin at 37°C with 5%CO₂ incubation was used for cell culture and experiments. Authenticated Jurkat cell lines were purchased from ATCC (Jurkat, Clone E6-1), (T lymphoblast) cells were transfected with pcDNA-PD1-Dyk DNA (Genscript Biotech Corp, OHU263220D) using Lipofectamine LTX (Thermo Fisher Scientific, Cat#15338030) and then selected by G418 200 ug/ml. Authenticated Raji cell lines were purchased from ATCC (Raji-CCL-86TM), (B-lymphocyte) cells were transfected with pcDNA-PD-L1-Dyk DNA (Genscript Biotech Corp, OHU22144D) and then selected by G418 600 ug/ml. Anti-PD1-PE (BioLegend, Cat#A17188B) or Anti-PD-L1(CD274)-APC (Invitrogen, Cat#17-5983-42) were used to confirm the expression of PD1 or PD-L1 in Jurkat cells or Raji cells using a laser flow cytometer (BD, Accuri 6 plus). Jurkat-PD1 cells were transfected with NFAT luciferase reporter DNA, where four repeated NFAT response elements, GGAGGAAAA ACTGTTTCATACAGAAGGCGT (SEQ ID NO. 1) oligos, were inserted into the pGL4.2 vector (Promega, Cat#E6751) and then selected with 0.1ug/ml puromycin. Jurkat-PD1 NFAT-luc TCR $\alpha\beta$ knockout cells were generated by transfecting CRISPR/Cas9-gRNA: eSpCas9-2A-GFP (Genscript Biotech Corp, SC1818) inserted into the targeting sequence using Lipofectamine LTX (Thermo Fisher Scientific, #15338030). The targeting DNA sequences for TCR α and TCR β were CTTCAAGAGCAACAGTGCTG and AGGTCGCTG TGTTTGAGCCA, respectively. PE anti-human $\alpha\beta$ T Cell Receptor Antibody (BioLegend, Cat#306708) was used to confirm the knockout of TCR $\alpha\beta$ using flow cytometry. The targeting sequences for SHP1 (PTPN6) and SHP2 (PTPN11) were ACCTGATCCCCACCCCTGC and AGGCCTAGTAAAAGTAACCC, respectively. Western blot analysis was used to confirm the knockout of SHP1 and SHP2 using anti-SHP1 (BioLegend, Cat#620301) and anti-SHP2 (Cell Signaling, Cat#3397S). Jurkat CART cell establishment: The pSLCAR-CD19-CD3zeta vector (Addgene_135993), pCMV-VSV-G (Addgene_8454), and psPAX2 (Addgene_12260) were transfected into HEK293T for 48h. The lentivirus was concentrated using a Lenti-X concentrator (TakaRa, Cat#631231) according to the manual. Concentrated Lentivirus- pSLCAR-CD19-CD3zeta was transduced into Jurkat-PD1 NFAT-luc cells using polybrene 10ug/ml (Millipore, Cat#TR-1003-G) and then GFP-positive cells were randomly sorted using flow cytometry. Jurka-PD1 NFAT-luc CAR-CD19-CD3zeta clones were randomly selected when NFAT luciferase activity was increased by co-culture with Raji cells overnight.

Stimulation for NFAT of Jurkat cells

Jurkat cells (T cells) were stably transfected with nuclear factor of activated T-cells (NFAT) luciferase reporter DNA and PD1 DNA. For stimulation, 50 μ l of Jurkat cells-PD1 cells at 5×10^5 /ml were co-cultured with 50 μ l of Raji cells at 10^6 /ml in a 1:2 ratio and staphylococcal superantigen E (SEE) (Toxin Technology, Cat#ET404) 1 ng/ml to 10 ng/ml, in the absence or presence of YIV-906 or its components were added to the mixed cells overnight at 37°C with 5%CO₂ incubation. NFAT activity was determined by measuring luciferase activity chemiluminescence. 75 μ l of Jurkat-PD1 cells at 10^6 cells/well with or without wild-type Raji cells or Raji-PD-L1 cells at 2×10^6 cells/well were seeded into round-bottom 96-well plates. In some experiments, InVivoSIM anti-human PD-1 (Nivolumab Biosimilar) (BioXcell, Cat#SIM0003) 18 μ g/ml was added to the cells for 2 h or 24 h before drug and see treatment. 25 μ l of control medium or 25 μ l of 5x concentration of YIV-906 or other drugs were added to the well. 25 μ l of see (5×10 ng/ml) was added to the wells. After overnight incubation at 37°C with 5%CO₂, the cells were lysed using a luciferase lysis buffer which contained luciferin to generate the luminescence. The luminescence was recorded using a luminescence microplate reader. Each data point represents three experiments of triplicate samples from the NFAT luciferase reporter assay.

Flow cytometry analysis

Jurkat-PD1 cells 2×10^5 /ml with or without wild-type Raji cells or Raji-PD-L1 cells (4×10^5 /ml) in 24-well plates were treated with YIV-906 with or without SEE (10 ng/ml and 30 ng/ml), for 48 h. Anti-CD69-FITC (BioLegend, Cat#310904) and anti-PD1-PE (BioLegend, Cat#A17188B) in PBS+1%BSA was used to stain the cells. Anti-PD1-PE was used to separate Jurkat-PD1 cells from mixed cells. The expression of CD69 in the FITC channel was presented as median fluorescence or total Jurkat cell population percentage using a laser flow cytometer (BD, Accuri 6 plus). Cell death of Raji cells (co-cultured with Jurkat-PD1-CAR-CD-19 cells/Raji cells at a 2:1 ratio) was determined by gating CD19⁺ Raji cells (Anti-CD19-perCP, BioLegend, #30228) and Annexin V-PE (BioLegend, #640947) positive and/or Helix-NR positive cells. Each data point represents the average mean of four experiments of triplicate samples of flow cytometry assays.

Following the treatment, the medium was collected for IL2, IFN γ , and IL10 detection using fluorescence bead array (BioLegend: LEGENDplex assays, Human CD8/NK Panel, Cat#740267) according to the to the manufacturer's instructions.

SHP1 and SHP2 enzymatic activity

pNPP assays were used to determine the inhibitory effects of YIV-906 and its components on recombinant human SHP2(PTPN11) and SHP1(PTPN6) (LSBio, WA). Briefly, 20 ng of enzyme with different doses of YIV-906 or its components were reacted in the 100 μ l reaction buffer (5 mM pNPP (p-Nitrophenyl Phosphate), 25 mM Hepes pH 7.3, 2.5 mM EDTA, 2.5 mM DTT, 100 μ g/ml BSA) in a well of a 96-well plate at 37°C for 1 h. 100 μ l of 2N H₂SO₄ were used to stop the reaction. Heated SHP1 or SHP2 (90°C for 15 min) was used as the control in parallel experiments. OD optical 450 nm was measured. The

OD of wells without added drugs was normalized to 1 after subtracting the wells' OD without enzyme. Each data point represents the average mean of three experiments of triplicate samples.

Western blot analysis

Jurkat-PD1 cells 10^6 /ml were placed in 24-well plates and treated with YIV-906 or its constituent herbs for 45 min. The cells were collected at 1000 g centrifugation for 10 min. The cells were prepared with 2X protein loading buffer (Tris pH 6.8 1M, SDS 1%; glycerol; β -mercaptoethanol; bromophenol blue; and distilled water). The samples were then heated to 95°C for 5 min to denature the proteins prior to western blotting. SDS polyacrylamide gel electrophoresis (10% Mini-Protein TGX™ Precast Protein Gels, Bio-Rad) was used to separate the proteins according to their electrophoretic mobility. 20 μ g of Protein extract per 10 μ L per well was used. Migration was performed in a 1X running buffer (Tris/Glycine/SDS) at 185 V for 50 min. Proteins were transferred onto a PVDF membrane in transfer buffer (Tris-CAPS AX, methanol, SDS 10%, distilled water) at 75 V for 1 h. After blotting, the membrane was cut into two parts with an approximate size of 3 cm (height) \times 9 cm (width) to fit into the blocking chamber. The upper part of the membrane was used for probing target proteins with specific antibodies (as described below), and the lower part of the membrane was used for probing GAPDH as a protein loading control for normalization. Non-specific binding sites on the PVDF membrane were blocked with a blocking solution (3% milk powder and 1X TBS-T) for 30 min. The PVDF membrane was then incubated with the primary antibody against the proteins of interest overnight at 4 °C. The primary antibodies used were as follows: P-Lck-Y394 (BioLegend, Cat#933101), P-Zap70-Y319 (Cell Signaling Technology, Cat#2717), P-LAT-Y191 (Cell Signaling Technology, Cat#3584), P-SRC(Fyn)Y416 (Cell Signaling Technology, Cat#6943), P-Pyk2-Y402 (Cell Signaling Technology, Cat#3291), and GAPDH (Cell Signaling Technology Cat# 5174, RRID:AB_10622025). The membrane was washed with TBS-T 1X and incubated with a secondary antibody with horseradish peroxidase-conjugated anti-rabbit IgG 1:5000, (Thermo Fisher Scientific Cat# A27036, RRID:AB_2536099), against the immunoglobulin corresponding to the primary antibody for 1 h at room temperature. The membrane was then washed with TBS-T 1X. The protein bands were detected using chemiluminescence (Super Signal West Dura, Thermo Scientific, Cat#PI34076) and the images were acquired using an X-ray film processor (Fuji Super RX-N). Densitometric scanning was performed using an Epson V600 scanner. ImageJ software (ImageJ, RRID:SCR_003070) was used to quantify the total intensity of the immunoreactive bands. GAPDH was used as an internal control for normalization.

LC-MS analysis for chemical profiles of the metabolites of YIV-906

LC-MS analysis was performed using an Agilent 1200 series HPLC coupled with an AB SCIEX 4000 QTRAP mass spectrometer. The separation was conducted on an Alltima™ HP HPLC column (5 mm, 4.6 \times 250 mm). The mobile phase was acetonitrile (A) and water with 0.1% formic acid (B) with gradient elution: 0 min, 5% A; 10 min, 20% A; 20 min, 25% A; 40 min, 30% A; 45 min, 35% A; 55 min, 45% A; 60 min, 70% A; 62 min, 90% A; 67 min, 90% A; 68 min, 5% A; and 75 min, 5% A. The flow rate was 1.0 ml/min, and the column temperature was set at

30°C. ESI negative mode mass spectrometry of scan rate 4000 amu/s was performed with the following ionization parameters: CAD: High; TEM: 550.00°C; GS1:55.00; GS2:50.00; ihe: ON; IS: 4250.00; DP: 40.00; CES 0.00; CE: 5.00. The mass range for detection was 120–800 amu. Using a custom program integrated with MZmine software, the chemicals were identified based on their retention time, total mass, and ion pair fragment mass.

Statistical analysis

Data was analyzed using one- or two-way analyses of variance (ANOVA) tests (GraphPad Prism 7), correlation analyses (GraphPad Prism, RRID:SCR_002798), and Student's *t*-test distribution (Microsoft Excel, RRID:SCR_016137). Differences were considered statistically significant at $p < 0.05$.

Results

YIV-906 could modulate the nuclear factor of activated T-cells (NFAT) activity and promote CD69 expression in T cells with or without the interaction of PD1 and PD-L1

A cell culture model of Jurkat cells co-cultured with staphylococcal superantigen E (SEE)-Raji cells was established to examine the effects of YIV-906 on T-cell activation. In this cell culture model, YIV-906

was able to promote NFAT activity by approximately one-fold in either the absence (Figure 1A) or presence (Figure 1B) of SEE, which could stimulate NFAT activity about 40-fold in the range of 80 ug/ml to 320 ug/ml, which are non-toxic doses for Jurkat cells and Raji cells.

Effects of different component herbs (at equivalent YIV-906 concentrations): *Glycyrrhiza uralensis* Fisch (G), *Paeonia lactiflora* Pall (P), *Scutellaria baicalensis* Georgi (S), and *Ziziphus jujuba* Mill (Z) on NFAT-mediated transcriptional activity of Jurkat cells was compared. S showed a very similar dose response to YIV-906 in both the absence and presence of SEE (Figures 1A, B); G and P could modulate no more than 20% NFAT activity in the absence or presence of SEE (Figures 1A, B); and Z had no discernable impact on NFAT activity (Figures 1A, B). When comparing two-herb combinations or three-herb combinations (Supplementary Figures S1A–D), only the combinations that included S showed an approximately 1-fold enhancement of NFAT activity in the absence or presence of SEE. We demonstrated that YIV-906 modulates nuclear factor of activated T-cells (NFAT) activity in Jurkat cells. S played the most important role in the modulation of NFAT, conversely G and P might play minor roles in the modulation of NFAT.

To study the impact of PD1-PD-L1 on NFAT activity during T cell activation, Jurkat cells-PD1 cells were co-cultured with PD-L1 over-expressed Raji cells, with or without SEE. YIV-906, S, and combinations with S had similar effects on the basal NFAT activity of Jurkat-PD1 cells, either incubated with Raji (Figure 1A, Supplementary Figures S1A–C) or PD-L1 over-expressed Raji cells (Raji-PD-L1) (Figure 1C, Supplementary Figures S1E–G).

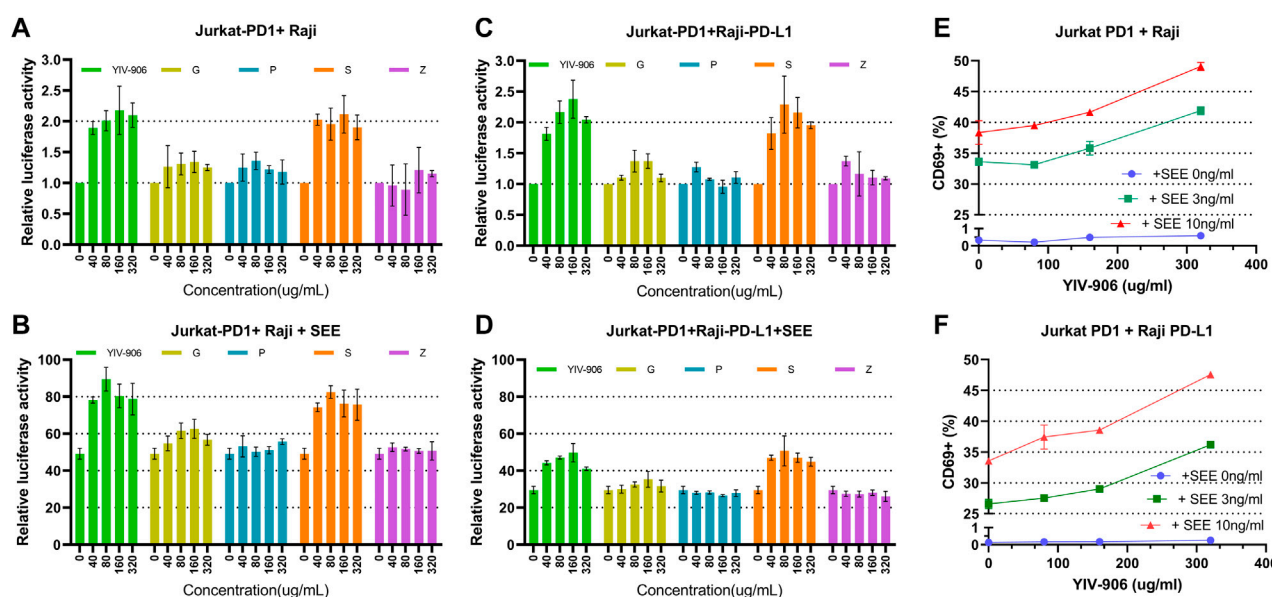


FIGURE 1

Effect of YIV-906 and its component herbs [*Glycyrrhiza uralensis* Fisch (G), *Paeonia lactiflora* Pall (P), *Scutellaria baicalensis* Georgi (S), and *Ziziphus jujuba* Mill (Z)] on NFAT mediated transcriptional activity and CD69 expression of Jurkat cells incubated with wild type Raji cells without or with staphylococcal superantigen E (SEE). Effects of YIV-906 and its single herb on NFAT mediated transcriptional activity of Jurkat cells incubated with Raji cells without SEE (A) and with SEE (B) were compared. The effects of YIV-906 and its single herb on NFAT mediated transcriptional activity of Jurkat-PD1 cells without SEE (C) and with SEE (D) were compared. Equivalent amounts of water extract up to 320 ug/ml were added to Jurkat cells, which were stably transfected with NFAT luciferase reporter, together with Raji cells with or without SEE 10 ng/ml for 24 h before luciferase activity was measured. Each data point represents the average mean of three experiments of triplicate samples from NFAT luciferase reporter assay. Effects of YIV-906 on CD69 expression of Jurkat PD1 cells, when incubated with PD-L1 overexpressed Raji cells (E) or Raji PD-L1 cells (F) in absence or presence of SEE antigen, are determined following 48 h incubation. The expression of CD69 was determined by flow cytometry in which FITC conjugated anti-CD69 was used to determine the expression of CD69 protein on the membrane of Jurkat cells and PE conjugated anti-PD1 was used to gate Jurkat PD1 cell from the mixture of Jurkat/Raji cells. Details of experimental procedures are given in materials and methods.

PD1 Interactions with Jurkat cells and PD-L1 with Raji cells inhibited NFAT activity of Jurkat cells by ~50% (Figure 1B vs. 1D). YIV-906, S, and combinations with S rescued the depressed NFAT activity of Jurkat-PD1 cells (Figure 1D, Supplementary Figures S1F, H). G had a slight impact on NFAT activity under the above conditions (Figures 1C,D and Supplementary Figures S2E–H).

Since NFAT is a very important T cell activation transcriptional factor, the impact of YIV-906 on T cell activation was further studied. CD69 was used as a T cell activation marker. As shown in Figure 1E, YIV-906 enhanced CD69⁺ population (Figure 1E) and the median CD69-fluorescence (Supplementary Figure S2A) of Jurkat-PD1 cells when incubated with Raji cells without SEE, or with 3 ng or 10 ng/ml SEE. The interaction between PD1 and PD-L1 reduced CD69 expression induced by SEE, but YIV-906 could help to restore CD69 expression in Jurkat-PD1 cells (Figure 1F and Supplementary Figure S2B). This result suggested that YIV-906 could modulate NFAT activity of T cells, thereby leading to stronger T cell activation even under PD1-PD-L1 interaction conditions. Since Jurkat cells are a leukemia T cell, their responses may not perfectly reflect the normal conditions. T cells isolated from mice spleen were used to confirm if YIV-906 and S could still promote T cell activation. Results demonstrated that YIV-906 and S treatment could increase CD69⁺ population of CD4⁺ cells (Supplementary Figure S2C) and CD8⁺ cells (Supplementary Figure S2D) isolated from mouse

spleen. This result further supported that YIV-906 and S have potential to promote T cell activation. In further, we will seek collaboration to study the impact of YIV-906 on primary human T lymphocytes.

The action of YIV-906 and S on NFAT does not require TCRαβ

To investigate whether YIV-906 and its components activates NFAT activity through direct activation of TCR, the TCRαβ gene was knocked out from Jurkat-PD1 cells using CRISPR/Cas9 technology (Figure 2A). Jurkat-PD1 TCRαβ knockout (KO) cells did not respond to SEE when co-cultured with Raji cells (Figure 2B). As shown in Figures 2C, D, YIV-906 and S had very similar impacts on NFAT activity in Jurkat-PD1 and Jurkat-PD1 TCRαβ KO cells. These results suggest that TCRαβ are not essential for the action of YIV-906 and its components on NFAT. YIV-906 and its components may have direct downstream targets of TCR αβ.

10R-VIVIT peptide, which is a cell-permeable peptide, could inhibit NFAT activity by blocking calcineurin-mediated dephosphorylation of NFAT. 10R-VIVIT at 25 μM, a non-toxic dose, could inhibit about 70% of NFAT activity of Jurkat-PD1 cells when co-cultured with Raji or Raji-PD-L1 cells (Supplementary Figure

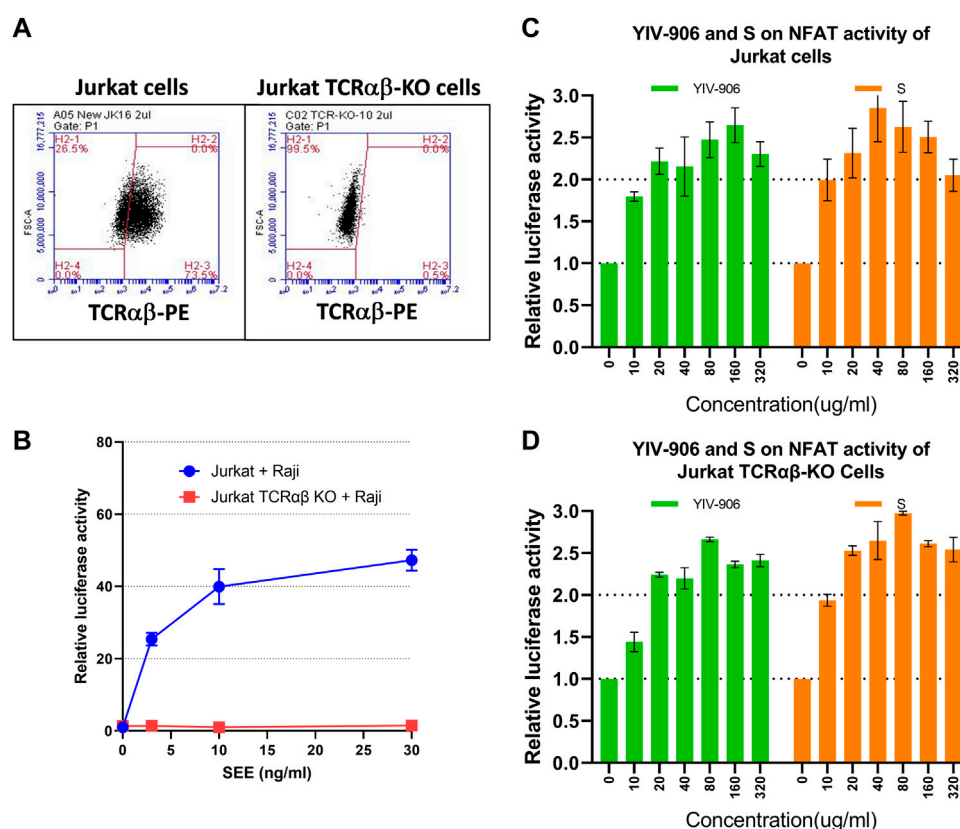


FIGURE 2

Effects of YIV-906 and S on NFAT mediated transcriptional activity of Jurkat cells and T cell receptor-αβ (TCRαβ) knockout Jurkat-cells. Detection of TCRαβ of Jurkat and Jurkat TCRαβ knockout cells (A) by using FITC conjugated anti-TCRαβ and flowcytometry is presented. Effect of SEE on NFAT activity of Jurkat cells or Jurkat TCRαβ KO cells together with Raji wild-type cells (B). Effects of YIV-906 and S on NFAT-mediated transcriptional activity of Jurkat-PD1 cells (C) and Jurkat-PD1 TCRαβ knock-out cells (D) are also shown. Each data point represents the average mean of three experiments of triplicate samples from NFAT luciferase reporter assay. Details of experimental procedures are given in materials and methods.

S3A). Under 10R-VIVIT (25uM) treatment conditions, YIV-906 and S could still promote NFAT activity of Jurkat-PD1 cells with similar magnitude (about 2 folds) without 10R-VIVIT treatment conditions (Supplementary Figure S3B, 3C). Therefore, calcineurin might not be the major target for YIV-906 and S.

YIV-906 and its component herbs could induce protein phosphorylation of T cell receptor downstream cascades

To test whether YIV-906 and its components could directly impact downstream signaling of TCR, their effects on the phosphorylation of T cell receptor downstream cascades, including Lck, Zap70, LAT, Fyn, and Pyk2 in Jurkat cells was examined using western blot analysis. As shown in Figure 3A, treatment with YIV-906 at a dose of 320 ug/ml for 45 min induced the phosphorylation of Lck, Zap70, LAT, Fyn, and Pyk2. By comparing individual herb effects at equivalent concentrations (320 ug/ml), component S was found to play a major role in protein phosphorylation induction by YIV-906 (Figure 3A). Using a C18 column to fractionate YIV-906, higher relative induction activity of protein phosphorylation was observed in 45%–75% acetonitrile/methanol (A/M) fractions (Figure 3B). S was found to have an activity profile similar to YIV-906 (Figure 3C). The 45% A/M fraction of S had a strong effect on P-Zap70-Y319, whereas the 60% A/M fraction of S had a strong effect on P-Lck-Y39, P-LAT-Y191, P-SRC(Fyn)-Y416, and P-Pyk2-Y402 (Figure 3C). The chemicals present in the S fractions are listed in Supplementary Figure S4A and they had been reported in our previous reports (Ye et al., 2007; Zhang et al., 2010). In Supplementary Figure S4A, protein phosphorylation induced by these fractions was indicated using red upward arrows. It should be noted that these chemicals might have different modes of action on the targets.

Some chemicals from active S fractions were studied for their ability to induce protein phosphorylation of T cell receptor downstream cascades, including Lck, Zap70, LAT, Fyn, and Pyk2 in Jurkat cells using western blot analysis. Baicalein strongly induced phosphorylation of all the examined proteins (Figure 3D). Both baicalin and oroxylin A 7-O-beta-D-glucuronide (OA-7-S), at 40 uM, showed some induction effects on P-Zap70-Y394, P-SRC(Fyn)-Y416, and P-Pyk2-Y402 (Figure 3D). These compounds potentially could play a critical role in T cell activation by YIV-906. Some S compounds promoted NFAT activity: Oroxylin A 7-O-beta-D-glucuronide (OA-7-side), baicalein, oroxylin A, and chrysin were able to modulate the basal NFAT activity of Jurkat-PD1 cells incubated with Raji, or PD-L1 over-expressed Raji cells (Figures 3E, F). The measured modulatory effects were independent of TCR $\alpha\beta$ expression (Supplementary Figure S4B, C), but the optimum doses were different. Oroxylin A 7-O-beta-D-glucuronide at 40 uM promote NFAT activity by 2 folds, whereas baicalein, oroxylin A, and chrysin required only 10 to 2.5 uM to have a similar impact on NFAT. In the presence of SEE, oroxylin A 7-O-beta-D-glucuronide, baicalein, oroxylin A, and chrysin showed similar promotional effects as they did on basal NFAT activity. It was also observed that wogonoside, baicalein, oroxylin A, and chrysin inhibited SEE-triggered NFAT activity at concentrations from 20 to 40 uM (Figures 3G, H). Some compounds mentioned above exhibited a biphasic effect on NFAT activity, possibly because these compounds might have multiple modes of action on their target(s) that are associated with the

NFAT pathway. In the tumor microenvironment, overall activity might depend on the composition and internal interactions of compounds within YIV-906, hence no single compound or target can simply explain all activities.

YIV-906 could modulate SHP1 and SHP2 activities, and the response of NFAT to YIV-906 might be dependent on SHP1/2

SHP2 (SH2-containing phosphatase 2, a protein tyrosine phosphatase) is an immediate downstream mediator of PD1 (Marasco et al., 2020; Patsoukis et al., 2020). Once PD1 binds to PD-L1, PD-1 will phosphorylate its immune receptor tyrosine-based inhibitory motif (ITIM) and immune receptor tyrosine-based switch motif (ITSM) to recruit and activate SHP2 (Marasco et al., 2020; Patsoukis et al., 2020). Activated SHP2 initiates T-cell inactivation by dephosphorylating TCR downstream cascade proteins (Marasco et al., 2020; Patsoukis et al., 2020). In the absence of SHP2, SHP1 can replace SHP2 (Celis-Gutierrez et al., 2019). SHP2 inhibitors could block PD1 action and promote T-cell activation for facilitating cancer treatment (Zhao et al., 2019; Yuan et al., 2020). As shown in Figure 4A, YIV-906 showed inhibitory effects on both SHP1 and SHP2 enzyme activities, with stronger potency against SHP1. G and S component herbs of YIV-906 were found to be the key herbs responsible for SHP1 and SHP2 inhibition (Supplementary Figure S5A, B); and some individual chemical compounds in G and S were found to have inhibitory effects on SHP1 and SHP2 (Supplementary Figure S5C, D). These compounds demonstrate selectivity for SHP1 and SHP2, for example, isoliquiritigenin was more potent against SHP1 than SHP2, whereas glycyrrhizic acid showed stronger inhibition of SHP2 than SHP1 (Supplementary Figure S5C, D). Baicalin, oroxylin A 7-O-beta-D-glucuronide, wogonoside, baicalein, chrysin, and oroxylin A from S showed stronger inhibitory effects on SHP2 than on SHP1 (Supplementary Figure S5C, D).

To determine whether TCR downstream protein phosphorylation induced by YIV-906 is dependent on the presence of SHP1 and/or SHP2, SHP1 and/or SHP2 genes were knocked out in Jurkat-PD1 cells using CRISPR-gRNA (Supplementary Figure S6). It appeared that SHP2 and SHP1/2 knockout cells had higher basal levels of protein phosphorylation (Figure 4B and Supplementary Figures S7A–G). SHP2 might be a critical enzyme for maintaining lower levels of TCR downstream protein phosphorylation as well. Comparing to Jurkat cells, SHP1 knockout reduced the phosphorylation of all proteins triggered by YIV-906 (Figure 4B and Supplementary Figures S7A–G). SHP2 knockout did not affect the protein phosphorylation of LCK and LAT triggered by YIV-906 (Figure 4B and Supplementary Figures S7A–G). However, the level of phosphorylation of Zap70, Fyn, and PYK2 in SHP2 knockout cells only slightly increased under YIV-906 treatment (Figure 4B and Supplementary Figures S7A–G). It is interesting to note that LCK, Zap70, and PYK2 in SHP1/2 knockout cells had little or no response to YIV-906 and that a high dose of YIV-906 decreased LAT and Fyn phosphorylation (Figure 4B and Supplementary Figures S7C–G). Overall SHP1 and SHP2 could have different impacts on regulating the basal levels of protein phosphorylation of TCR downstream. Both SHP1 and SHP2 were important to YIV-906 triggering Zap70 and Fyn phosphorylation (Supplementary Figure S7G). Additionally, SHP1 and SHP2 double knockout minimized TCR downstream

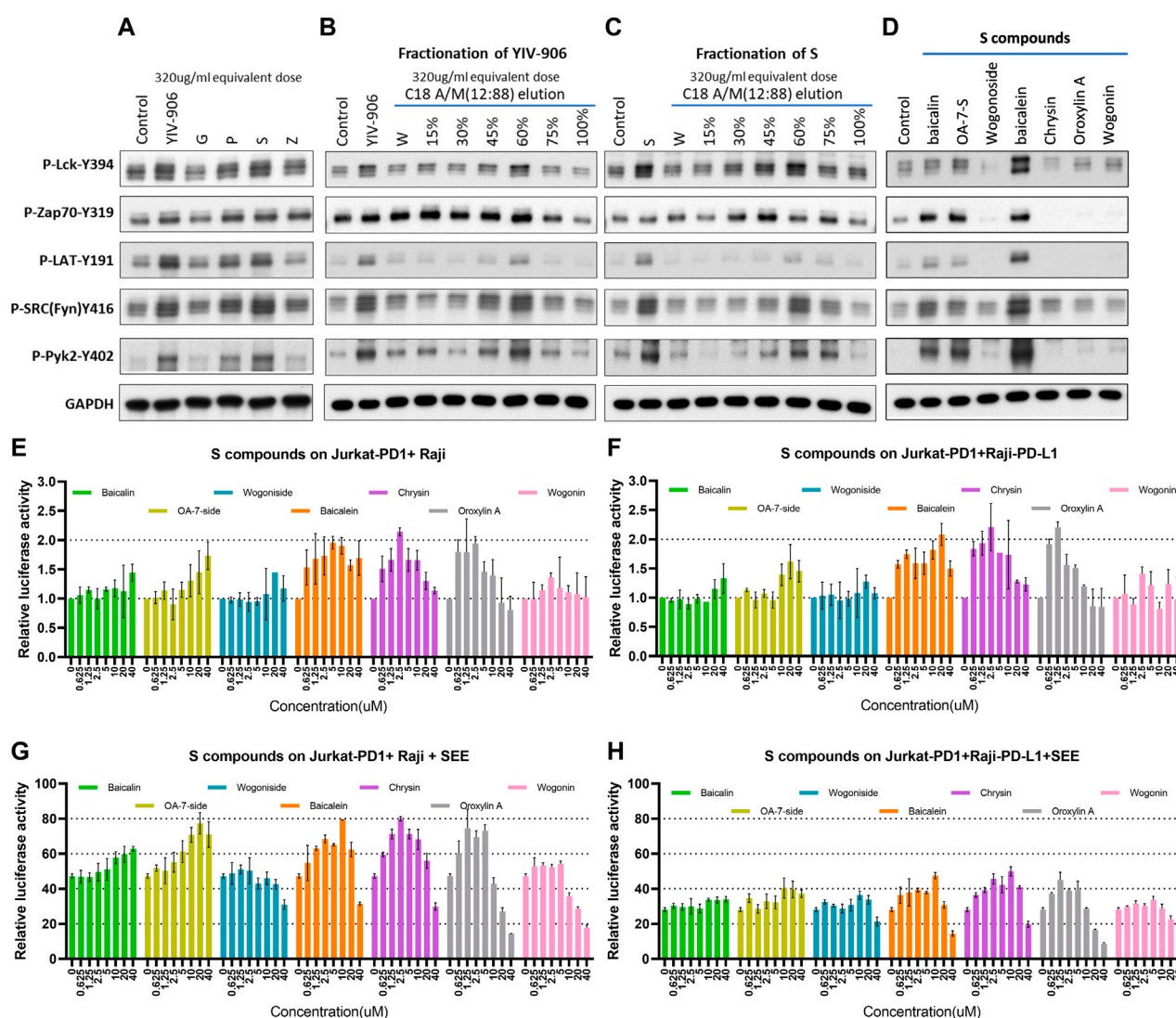


FIGURE 3

Effect of YIV-906 and its component on protein phosphorylation of T cell receptor signaling cascades and NFAT mediated transcriptional response. Effect of YIV-906 and its component herbs (A), the fractions of YIV-906 (B), S (C), and S compounds (D) on protein phosphorylation of T cell receptor signaling cascades including, Lck, Fyn, Zap70, LAT, and Pyk2. Jurkat cells were treated with YIV-906 and its component herbs, the fractions of YIV-906 and S at an equivalent dose of 320ug/ml for 45min. C18 solid phase extract column was used to fractionize YIV-906 and S by eluting with water and increasing percentage of acetonitrile/methanol (A/M). All eluted fractions were dried and reconstituted with water to an equivalent concentration at 100 mg/ml. 20 uM of S was used to treat Jurkat cells for 45 min. Western blot analysis was used to determine the protein phosphorylation using specific antibodies. GAPDH was used to normalize the protein loading. Cropped blots are used in this figure and they have been run under the same experimental conditions. Effects of S compounds on NFAT mediated transcriptional activity of PD1 overexpressed Jurkat cells incubated with Raji cells (E,G) and PD-L1 overexpressed Raji cells (F,H) without and with SEE. S compounds, up to 40 uM, were added to Jurkat-PD1 cells, which were stably transfected with NFAT luciferase reporter and co-culturing with Raji cells or Raji-PD-L1 cells with SEE 10 ng/ml for 24 h before luciferase activity was measured. Details of experimental procedures are given in materials and methods.

protein phosphorylation triggered by YIV-906 (Supplementary Figure S7G).

YIV-906's impacts on promoting NFAT response by SHP1 and SHP2 were studied. As shown in Figure 4C, knockout of SHP1 and/or SHP2 in Jurkat cells reduced but did not completely block NFAT activity triggered by YIV-906 in the absence of SEE. Under PD1-PD-L1 interaction conditions, single knockout of SHP2 but not SHP1 significantly increased NFAT activity (Figure 4D). SHP1/2 knockouts completely rescued the depressed NFAT activity due to PD1-PD-L1 interaction

(Figure 4D). These results support previous findings that PD-1 preferentially binds with SHP-2 over SHP-1 to inhibit TCR response (Celis-Gutierrez et al., 2019). Under Jurkat-PD1-Raji plus SEE conditions, knocking-out SHP1 and/or SHP2 did not have a significant impact on the cells' NFAT response to YIV-906 (Figure 4E). When Jurkat-PD1 cells were co-cultured with Raji-PD-L1 plus SEE, SHP1 or SHP2 knockout only slightly decreased the NFAT response to YIV-906 (Figure 4F), but SHP1/2 double knockout significantly reduced the NFAT response to YIV-906. Overall, our results indicated that YIV-906 could overcome PD1-

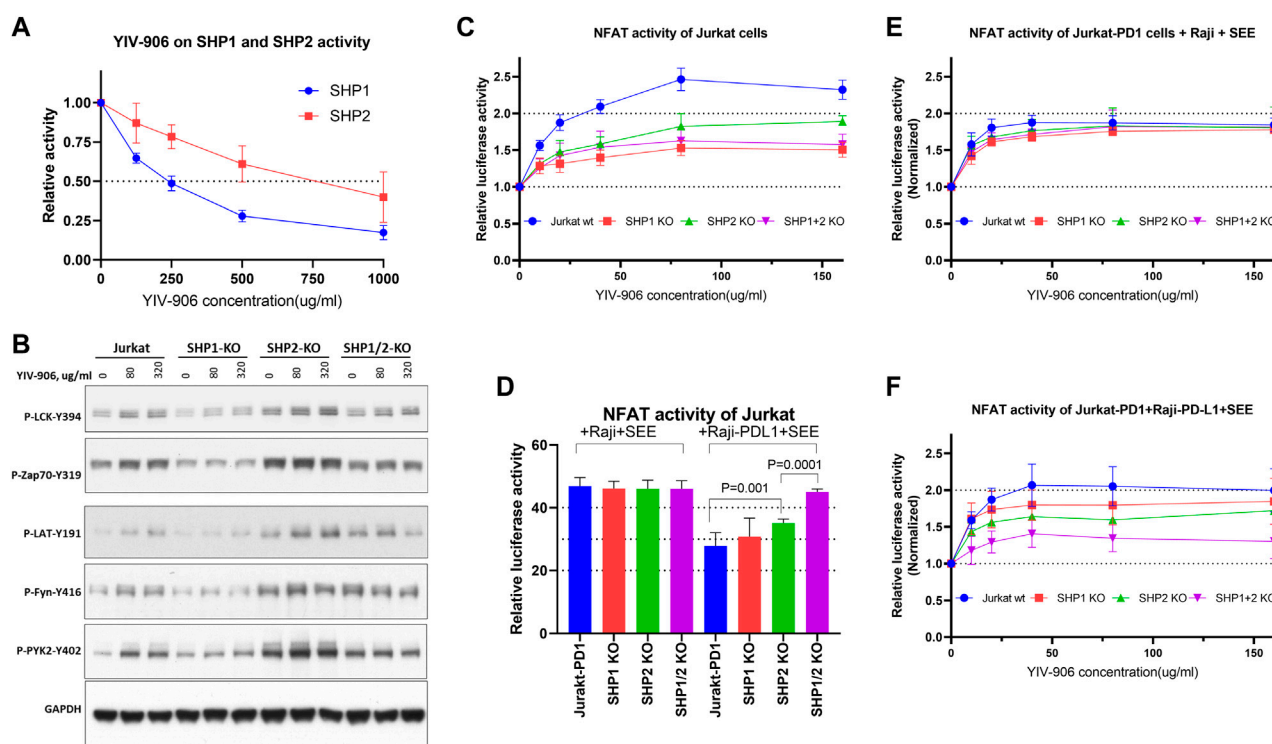


FIGURE 4

Effect of YIV-906 on TCR downstream protein phosphorylation and NFAT mediated transcriptional activity of Jurkat cells in the presence or absence of SHP1 and/or SHP2. **(A)** Effect of YIV-906 on the enzymatic activities of SHP1 and SHP2. Activities of SHP1 and SHP2 were determined by the p-Nitrophenyl Phosphate (pNPP) colorimetric assay. Each data point represents the mean of triplicate samples. **(B)** Effect of YIV-906 on protein phosphorylation of T cell receptor signaling cascades including, Lck, Fyn, Zap70, LAT, and Pyk2. Jurkat cells were treated with YIV-906 for 45 min. Western blot analysis was used to determine the protein phosphorylation using specific antibodies. GAPDH was used to normalize the protein loading. **(C)** NFAT response of Jurkat-PD1 cells with SHP1 and/or SHP2 knockout to YIV-906. **(D)** NFAT activity of Jurkat-PD1 cells with SHP1 and/or SHP2 knocked-out co-cultured with Raji wt or Raji-PD-L1 plus SEE. **(E)** NFAT response of Jurkat-PD1 cells with SHP1 and/or SHP2 knocked-out co-cultured with Raji wt plus SEE. **(F)** NFAT response of Jurkat-PD1 cells with SHP1 and/or SHP2 knocked-out co-cultured with Raji-PD-L1 wt plus SEE 10 ng/ml. Each data point represents the average mean of four experiments of triplicate samples from NFAT luciferase reporter assay. Details of experimental procedures are given in materials and methods.

PD-L1 suppression and promote NFAT activity by affecting SHP1 and SHP2 activity.

YIV-906 could further enhance anti-PD1 antibody action to promote NFAT activity in T cells

As YIV-906 can modulate the antitumor activity of anti-PD1 against tumors in animal models, we investigated whether YIV-906 could cooperate with anti-PD1 to promote NFAT activity for T cell activation. When co-cultured with Jurkat-PD1 and Raji plus SEE, the addition of anti-PD1 (non-therapeutic biosimilar antibody to nivolumab, with the same variable regions) did not affect the NFAT response of Jurkat-PD1 cells to YIV-906, S, or S compounds (Supplementary Figures S8A–D). As shown earlier, co-cultured Jurkat-PD1 cells and Raji-PD-L1 cells inhibited the NFAT activity of Jurkat cells triggered by SEE (Figures 5A, B). YIV-906, S, and S constituent compounds restored any depressed NFAT activity in Jurkat-PD1 cells (Figures 5A, B). As expected, anti-PD1 rescued the depressed NFAT activity of Jurkat-PD1 cells due to PD1 and PD-L1 interactions (Figures 5C, D). Most importantly, YIV-906, S, and S compounds (with different optimum dose) could further enhance anti-PD1 action to promote NFAT activity in Jurkat PD1 cells (Figures 5C,

D). The above results demonstrated that YIV-906 and its components could cooperate with anti-PD1 to promote T-cell activation for immune therapy.

YIV-906 could modulate chimeric antigen receptors triggered NFAT activity of T cells

It is well known that MHC-antigen-TCR interaction recruits CD3 receptors to transduce signals for NFAT activation. Most chimeric antigen receptors (CAR) are composed of an antigen recognition domain, an extracellular hinge region, a transmembrane domain, and co-stimulatory domains such as immunoreceptor tyrosine-based activation motifs (ITAM) of CD3ζ(zeta) (Lindner et al., 2020). Once a chimeric antigen receptor (CAR) binds to its target, a signal is transduced to its ITAM of CD3ζ which further stimulates the downstream cascade leading to NFAT activation (Lindner et al., 2020). Because MHC-antigen-TCR interactions or CAR-target interactions both have the same downstream cascade stimulating NFAT activity, and YIV-906 demonstrated the potential to enhance MHC-antigen-TCR triggered NFAT response, we asked whether YIV-906 could also modulate CAR-triggered NFAT activity. To study this, Jurkat-PD1

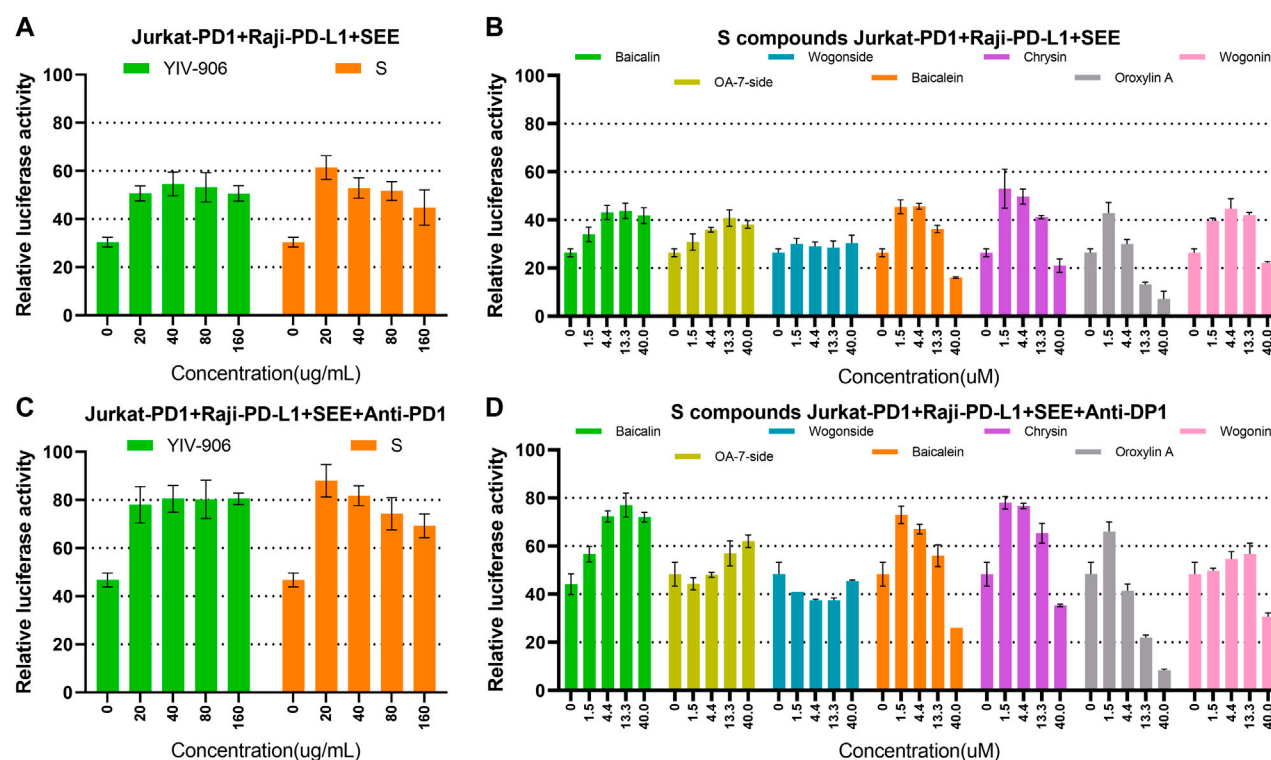


FIGURE 5

Effects of YIV-906, S, and S compounds with or without anti-PD1 on NFAT mediated transcriptional activity of Jurkat cells. (A–B) Effects of YIV-906 (A), S (A) and S compounds (B) on NFAT mediated transcriptional activity of Jurkat-PD1 cells incubated with Raji-PD-L1 cells and SEE 10 ng/ml. (C–D) Effects of YIV-906 (C), S (C) and S compounds (D) on NFAT mediated transcriptional activity of Jurkat-PD1 cells incubated with Raji-PD-L1 cells, SEE 10 ng/ml and anti-PD1 18 ug/ml. Cells and drugs were incubated for 24 h before luciferase activity was measured. Each data point represents the average mean of three experiments of triplicate samples from NFAT luciferase reporter assay. Details of experimental procedures are given in materials and methods.

NFAT luciferase receptor cells were transduced with CAR-CD19⁺CD3ζ(zeta) lentivirus to target CD19 on Raji cells.

YIV-906, S, and S compounds had similar effects on promoting the basal activity of NFAT in both Jurkat-PD1-CAR-CD19 cells (Supplementary Figures S9A, B) and Jurkat-PD1 cells alone (Figure 2C and Supplementary Figures S4B). When Jurkat-PD1-CAR-CD19 cells were co-cultured with Raji cells, a 40-fold increase in NFAT-driven luciferase activity was induced (Figure 6A). Under these conditions, YIV-906, S, and S compounds further promoted NFAT activity triggered (Figure 6A and Supplementary Figures S9C). PD1 and PD-L1 interactions depressed NFAT activity triggered by the interaction CAR-CD19 and CD19 (Figure 6B). YIV-906, S, and S constituent compounds (oroxylin A 7-O-beta-D-glucuronide, wogonoside, baicalein, oroxylin A, and chrysin) could restore this depressed NFAT activity (Supplementary Figures S9D). Depending on the compound, the optimum dose for modulation may be different.

The production of IL2, IFNγ and IL10 were used to monitor the response of Jurkat-PD1-CAR-CD19 cells with or without co-culturing Raji cells or Raji PD-L1 cells. As predicted, co-culturing Jurkat-PD1-CAR-CD19 cells with Raji cells could trigger higher production of IL2 and IFNγ as comparing to Jurkat-PD1 plus Raji cells or Raji PD-L1 cells as well as their single culture (Figures 6C, D, Supplementary Figures S10A–F). YIV-906 and S could further enhance production of IL2 and IFNγ production when

Jurkat-PD1-CAR-CD19 cells were co-cultured with Raji cells (Figures 6C, D). When Jurkat-PD1-CAR-CD19 cells were co-cultured with Raji PD-L1 cells, PD1 and PD-L1 interaction depressed IL2 and IFNγ production (Figures 6C, D). YIV-906 and S could also promote IL2 and IFNγ production under PD1 and PD-L1 interaction conditions (Figures 6C, D). YIV-906 and S had no big impacts on IL10 production in all culturing conditions (Figure 6E and Supplementary Figures S10G–I). Our results indicated that YIV-906 and S could further promote CAR T cell activation by enhancing IL2 and IFNγ production when CAR T cells interact to its target cells.

We further demonstrated that YIV-906 could promote Jurkat-PD1-CAR-CD19 cells to kill Raji cells. As shown in Supplementary Figures S11A, B, Raji or Raji-PD-L1 cell death could be increased by increasing Jurkat-PD1-CAR-CD19 cells in the co-culture. It should be noted that PD1-PD-L1 interaction did reduce Raji-PD-L1 cell death triggered by Jurkat-PD1-CAR-CD19 cells (Fig S11A and S11B). YIV-906 could enhance the Jurkat-PD1-CAR-CD19 cells' killing capability on either Raji or Raji-PD-L1 cells (Figures 6F, G and Supplementary Figures S11A, B). Among the component herbs, S was found to play a key role of YIV-906 to promote Raji or Raji-PD-L1 cell death (Figures 6F, G and Supplementary Figures S11C, D) caused by Jurkat-PD1-CAR-CD19 cells.

K562 cells, which are myelogenous leukemia cell, did not express CD19 as comparing to Raji cells (Supplementary Figures S11E). When K562 cells were co-cultured with Jurkat-PD1-CAR-CD19 cells, no

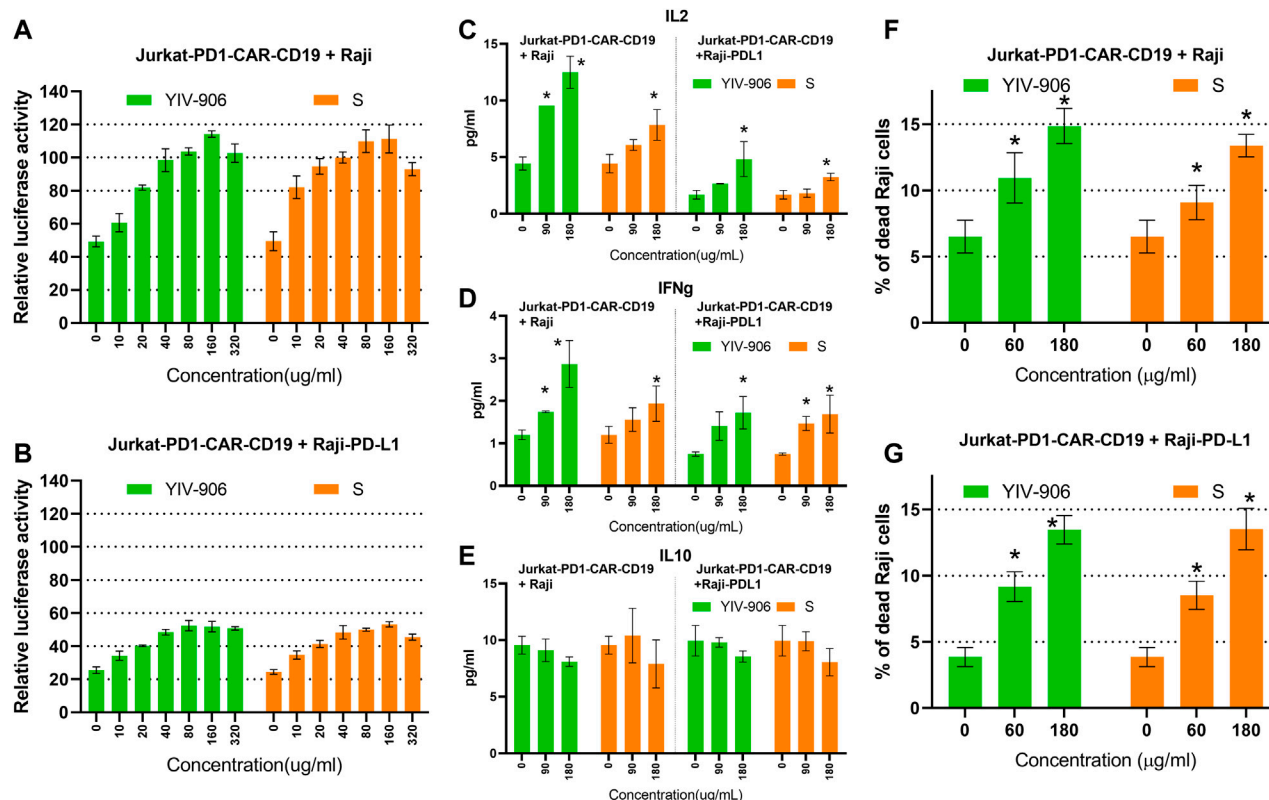


FIGURE 6

Effects of YIV-906, S, and S compounds on NFAT mediated transcriptional activity and of Jurkat cells and cell death of Raji cells triggered by co-culturing Jurkat cells over-expressing chimeric antigen receptor (CAR-CD19⁺CD3z) and Raji or Raji-PD-L1 cells. Effects of YIV-906 and S on NFAT-mediated transcriptional activity of Jurkat-PD1-CAR-CD19 cells incubating with Raji cells (A) or Raji-PD-L1 cells (B). Effect of YIV-906 and S on IL2 (C), IFN γ (D) and IL10 (E) production when Jurkat-PD1-CAR-CD19 cells were co-cultured with Raji or Raji PD-L1. Effects of YIV-906 and S on cell death triggered by incubating Jurkat-PD1-CAR-CD19 cells with Raji cells (F) or Raji-PD-L1 cells (G). Each data point represents the average mean of triplicate samples from NFAT luciferase reporter assay or flow cytometry assay. YIV-906, S (at concentrations up to 320 μ g/ml water extract) were added to Jurkat-PD1-CAR-CD19 cells, which were stably transfected with NFAT luciferase reporter, together with wild type Raji cells or Raji-PD-L1 cells for 24 h before luciferase activity or cytokines of medium were measured. Cytokine fluorescence bead assays were used to quantify IL2, IFN γ , and IL10 of medium following treatments. Annexin V-PE and helix-NR-APC were used to stained dead cells of CD19⁺ Raji cells using flow cytometry and result labeled with * when *p* values of T-test was less than 0.05. Details of experimental procedures are given in materials and methods.

induction of NFAT activity or K562 cell death was observed (Supplementary Figures S11F, G). In addition, YIV-906 and S did not promote cell death of K562 cells when co-cultured with Jurkat-PD1-CAR-CD19 cells. This result demonstrated that Jurkat-PD1-CAR-CD19 cells had selective cytotoxicity on cells with CD19 expression.

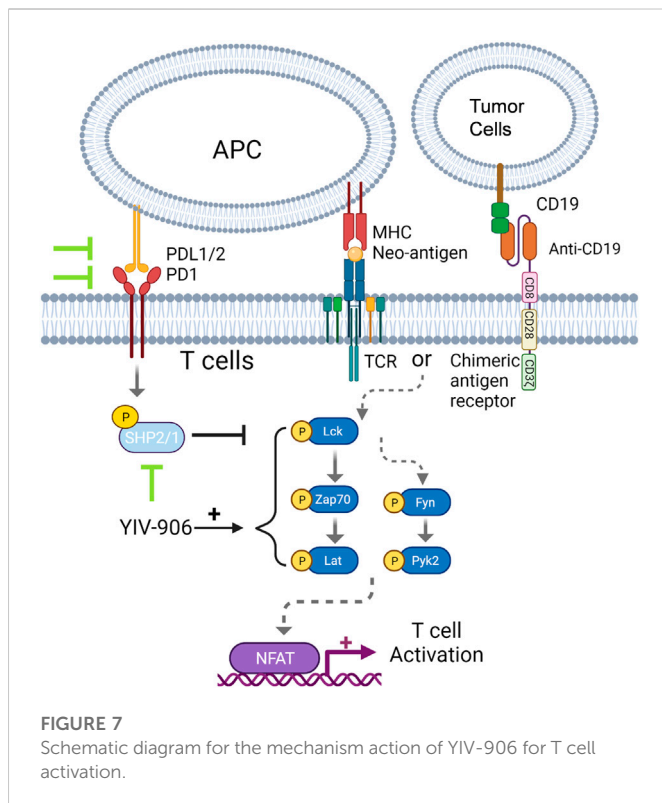
Baicalin, chrysin, and oroxylin A of S (up to 10 μ M, did not cause significant cell death in Raji (Supplementary Figures S12A) or Raji-PD-L1 (Supplementary Figures S12B) when co-cultured, however these compounds promoted the cell killing capability of Jurkat-PD1-CAR-CD19 cells on Raji (Supplementary Figures S12C) or Raji-PD-L1 (Supplementary Figures S12D). These results suggest that YIV-906 and its components might have potential to facilitate CAR T cell therapy for cancer treatment.

Discussion

In recent years, immunotherapy has led to many breakthroughs in cancer treatment. Many therapeutic antibodies and CAR T-cell therapies have been approved for treating different cancer types. Pembrolizumab and nivolumab are the only approved

immunotherapies for pancreatic cancer and colon cancer subtypes, where criteria must have metastatic microsatellite instability-high (MSI-H) or mismatch repair deficiency (dMMR) (Overman et al., 2017; Andre et al., 2020). In general, effector T-cell activation is the key determinant of the cancer immunotherapies' success. However patient responses to immunotherapy are not equal and certain tumor types can have lower responses rates to immune checkpoint inhibitors as compared to others. For example patients with tumors with high PD-L1 expression may have a higher response rate to anti-PD1 antibodies than those with lower expression of PD-L1 (Patel and Kurzrock, 2015). Therefore, many new targets for immunotherapy are currently in clinical trials to determine the optimal treatment. Currently hundreds of regimens are being tested to determine whether they can further promote effector T-cell activation and improve immunotherapy efficacy.

Eight clinical trials using YIV-906 as an adjuvant have been completed with encouraging results (Yen et al., 2009; Saif et al., 2010; Kummur et al., 2011; Saif et al., 2014; Changou et al., 2021). In animal studies, we have demonstrated that YIV-906 can turn "cold tumors" into "hot tumors" when combined with chemotherapy or immune checkpoint antibodies such as anti-



PD1 and anti-PD-L1. Both innate and adaptive immune responses to tumors can be enhanced by YIV-906 during combination treatment. In the case of innate immunity, YIV-906 and its components potentiate IFN γ action to polarize macrophages into becoming M1-like macrophages, while also inhibit IL4 action which prevents M2-like macrophage polarization (Lam et al., 2015; Yang et al., 2021).

In this study, we demonstrated that YIV-906 and its components modulates NFAT activity for T-cell activation. Since YIV-906 still induces NFAT activity in TCR α/β KO Jurkat cells, the critical factor(s) stimulated by YIV-906 should be downstream of TCR. By detecting the phosphorylation of TCR downstream proteins, we found that YIV-906 and compounds in **S** played key roles in inducing the phosphorylation of TCR downstream proteins, including LCK, Zap70, LAT, FYN, and PYK2. We previously reported YIV-906 and its components inhibit phosphatase(s) and prolong ERK1/2 phosphorylation to enhance the action of sorafenib (Lam et al., 2015). Using *in silico* analysis, YIV-906 metabolites were suggested to have a high potential for hitting DUSP3, DUSP5, and DUSP7 phosphatases (Liu et al., 2019). Many inhibitory receptors, including PD1, recruit SHP1 and/or SHP2 phosphatases *via* the phosphotyrosine-based immunoreceptor tyrosine-based inhibitory motif (ITIM) and immunoreceptor tyrosine-based switch motif (ITSM) to inhibit TCR downstream signaling (Chemnitz et al., 2004). SHP1 and SHP2 can limit T cell activation through dephosphorylation of downstream cascade proteins (Lorenz, 2009). We investigated whether YIV-906 promoted T cell activation through SHP1/2 phosphatase(s) inhibition. Our results showed that YIV-906 and certain compounds modulates the enzymatic activity of both SHP1 and SHP2. Using SHP1 and/or SHP2 KO Jurkat cells, we further demonstrated that the induction of TCR protein

phosphorylation triggered by YIV-906 was partially dependent on SHP1 and/or SHP2 under PD1-PD-L1 suppressed condition. It was also demonstrated that SHP1 and SHP2 have different effects on the phosphorylation of different TCR downstream proteins. In the absence of **SEE**, SHP1 and/or SHP2 KO cells showed a lower NFAT response to YIV-906. In addition, SHP1/2 double knockout cells had much lower responses to YIV-906 than SHP1 or SHP2 single knockout cells under the PD1-PD-L1 interaction condition. These results further support the hypothesis that SHP1/2 could be one of the YIV-906s key targets responsible for the induction of TCR downstream protein phosphorylation and NFAT modulation. Since SHP1 and SHP2 could regulate NFAT signaling and they express in many cell types, we are planning to investigate if YIV-906 could also affect NFAT signaling in other cells type, such as NFAT5 activity on Raji cells. It should be noted that LCK phosphorylation and NFAT of SHP1/2 KO cells still showed some response to YIV-906, which suggests that SHP1 and SHP2 were not the only factors responsible for the NFAT modulation caused by YIV-906. Perhaps low-level LCK phosphorylation could still transduce some artifact signal to NFAT. Further investigation is needed to identify the additional mechanisms of action.

SHP2 is the predominant downstream modulator of PD1 to execute immune suppression when PD1 interacts with PD-L1 (Marasco et al., 2020; Patsoukis et al., 2020), SHP2 inhibitors are believed to have the ability to reduce immune resistance due to PD1-PD-L1 interactions. Currently, several clinical trials have been initiated to test SHP2 inhibitors, such as BBP-398 plus nivolumab (NCT05375084), RMC-4630 (SHP2-inhibitor) plus LY3214996 (ERK-inhibitor) (NCT04916236), ET0038 (NCT04528836 and NCT05354843), JAB-3068 (NCT03565003), and ERAS-601 (NCT04670679) as monotherapy or combination treatments for different types of cancer. However, SHP1 could replace SHP2 to transduce the PD1 signal for suppressing TCR downstream protein phosphorylation when SHP2 is knocked out (Celis-Gutierrez et al., 2019). In addition, SHP1 is the predominant executor of the B and T lymphocyte attenuator (BTLA), which interacts with the herpes virus entry mediator (HVEM or TNFRSF14) of APC cells (Steinberg et al., 2011). Activation of SHP1 can also depress TCR signaling (Lorenz, 2009). Furthermore, SHP1 is a key inhibitor of SIRP α (on macrophage)-CD47 (on tumor) for “don’t eat me” signaling (Myers et al., 2020). SHP1 loss increased macrophage phagocytosis of tumor cells, the ratio of effector to regulatory T cells in the E0771 tumor model, and IFN γ in the MC38 tumor model (Myers et al., 2020).

Because of its dual activity on SHP1 and SHP2, YIV-906 offers an appealing alternative to single-action SHP1 or SHP2 specific inhibitors to address the multiple types of immune resistance existing in a complex tumor microenvironment. Furthermore, YIV-906 could also modulate other immune suppression pathways, such as IDO, which activates MDSC (Yang et al., 2021).

Previously we demonstrated that YIV-906 could strongly enhance anti-PD1 antibody action against Hepa 1-6 tumors (mouse hepatoma) in mice. The combination of YIV-906 and anti-PD1 eradicated Hepa 1-6 tumors in mice, and no tumor re-growth was observed when mice were re-challenged with Hepa 1-6 cells, but not when challenged with a second tumor type, such as CMT167 or Pan02 cells (Yang et al., 2021). This suggests that the combination of YIV-906 and anti-PD1 may create a selective tumor-specific vaccination effect. We are currently investigating

whether YIV-906 has the potential to promote vaccine effectiveness, such as in tumor vaccination.

We provided evidence supporting how YIV-906 could affect anti-PD1 activity to enhance the NFAT activity of Jurkat cells. Although the FDA has approved pembrolizumab and nivolumab as second-line monotherapies for the treatment of HCC in patients who have been previously treated with sorafenib, the complete response rate from those clinical trials is only about 3%–6% (El-Khoueiry et al., 2017; Finn et al., 2020). YIV-906 has great potential to increase the response rates and efficacy of these antibodies for HCC treatment. YIV-906 can also activate downstream cascades of TCR, which are the same cascades activated by most CAR constructs, and as predicted, YIV-906 can also promote NFAT activity of Jurkat cells expressing CAR-CD19 to enhance the killing power on tumor cells, independent of PD1-PD-L1 interaction. In this report we demonstrated that YIV-906 could promote two important types of immunotherapies currently in use: immune checkpoint antibodies and CAR T cell therapies. Since YIV-906 can modulate NFAT activity, which is critical for general T-cell activation, YIV-906 may also be combined with other treatments requiring T-cell activation.

Flavonoids such as baicalein, chrysin, and oroxylin A are key components of **S** that show enhanced NFAT activity. Flavonoids, with their various biological functions, are a major class of compounds found in many medicinal herbs used today (Panche et al., 2016). Thus, different flavonoids may have different immunomodulatory activities. In this study, we identified **S** (*Scutellaria baicalensis* Georgi) as the key herbal component responsible for NFAT modulation; this component ingredient has been reported to have an immune modulatory effect on Lewis lung tumor-bearing C57BL/6 mice by decreasing IL-17, IL-10, FOXP3, TGF- β 1, ROR γ t, and IL-6 levels while remarkably increasing IL-2 and IFN- γ levels (Gong et al., 2015). Hesperetin and chrysin can enhance the activity of cytotoxic T lymphocytes *in vitro* (Sassi et al., 2017) or NK activity in BALB/c mice (Sassi et al., 2018). Baicalin-loaded poly (D,L-lactide-co-glycolide) (PLGA) nanoparticles can increase the infiltration of CD4⁺ or CD8⁺ T cells in tumors and induce a CTL cell response *in vivo* (Han et al., 2019). Further exploration of the potential use of flavonoid-containing herbs in the modulation of T cell function is worth considering. It should be noted that YIV-906s action is not identical to **S** or any of its compounds. Thus, the presence of other herbs or their compounds interaction plays a role in modulating the action of **S** in YIV-906.

In summary, YIV-906 can enhance the NFAT activity of effective T cells, partly by inhibiting SHP1/2 and inducing TCR downstream protein phosphorylation. **S** and its component compounds are involved in this process and may have different targets with different potencies within the tumor microenvironment. It is shown here that YIV-906 and perhaps some of its components could be used to modulate T cell activation for facilitating immune checkpoint blockade therapy or CAR T-cell therapy for the treatment of cancer patients (Figure 7).

Data availability statement

The original contributions presented in the study are included in the article/Supplementary Material, further inquiries can be directed to the corresponding author.

Author contributions

WL established cell lines and did luciferase assays, western blotting, flow cytometry and co-wrote the manuscript. RH did SHP1 and SHP2 assays. S-HL provided YIV-906 and co-wrote the manuscript. PC provided YIV-906 and co-wrote the manuscript. Y-CC supervised the project and co-wrote the manuscript.

Funding

This work was supported by Yiviva, Inc. and a research gift from the National Foundation for Cancer Research, United States.

Acknowledgments

Y-CC is a fellow of the National Foundation for Cancer Research (United States).

Conflict of interest

Y-CC is the inventor of YIV-906 for cancer treatment. The patent is owned by the Yale University. Yale University has licensed this patent for Yiviva. S-HL and PC were employed by Yiviva, Inc. WL was a consultant for Yiviva.

The remaining author declares that the research was conducted in the absence of any commercial or financial relationships that could be construed as a potential conflict of interest.

Publisher's note

All claims expressed in this article are solely those of the authors and do not necessarily represent those of their affiliated organizations, or those of the publisher, the editors and the reviewers. Any product that may be evaluated in this article, or claim that may be made by its manufacturer, is not guaranteed or endorsed by the publisher.

Supplementary material

The Supplementary Material for this article can be found online at: <https://www.frontiersin.org/articles/10.3389/fphar.2022.1095186/full#supplementary-material>

References

- Andre, T., Shiu, K. K., Kim, T. W., Jensen, B. V., Jensen, L. H., Punt, C., et al. (2020). Pembrolizumab in microsatellite-instability-high advanced colorectal cancer. *N. Engl. J. Med.* 383, 2207–2218. doi:10.1056/NEJMoa2017699
- Celis-Gutierrez, J., Blattmann, P., Zhai, Y., Jarmuzynski, N., Ruminski, K., Gregoire, C., et al. (2019). Quantitative interactomics in primary T cells provides a rationale for concomitant PD-1 and BTLA coinhibitor blockade in cancer immunotherapy. *Cell Rep.* 27, 3315–3330. doi:10.1016/j.celrep.2019.05.041
- Changou, C. A., Shiah, H. S., Chen, L. T., Liu, S., Luh, F., Liu, S. H., et al. (2021). A phase II clinical trial on the combination therapy of PHY906 plus capecitabine in hepatocellular carcinoma. *Oncologist* 26, e367–e374. doi:10.1002/onco.13582
- Chemnitz, J. M., Parry, R. V., Nichols, K. E., June, C. H., and Riley, J. L. (2004). SHP-1 and SHP-2 associate with immunoreceptor tyrosine-based switch motif of programmed death 1 upon primary human T cell stimulation, but only receptor ligation prevents T cell activation. *J. Immunol.* 173, 945–954. doi:10.4049/jimmunol.173.2.945
- El-Khoueiry, A. B., Sangro, B., Yau, T., Crocenzi, T. S., Kudo, M., Hsu, C., et al. (2017). Nivolumab in patients with advanced hepatocellular carcinoma (CheckMate 040): An open-label, non-comparative, phase 1/2 dose escalation and expansion trial. *Lancet* 389, 2492–2502. doi:10.1016/S0140-6736(17)31046-2
- Finn, R. S., Ryoo, B. Y., Merle, P., Kudo, M., Bouattour, M., Lim, H. Y., et al. (2020). Pembrolizumab as second-line therapy in patients with advanced hepatocellular carcinoma in KEYNOTE-240: A randomized, double-blind, phase III trial. *J. Clin. Oncol.* 38, 193–202. doi:10.1200/JCO.19.01307
- Gong, T., Wang, C. F., Yuan, J. R., Li, Y., Gu, J. F., Zhao, B. J., et al. (2015). Inhibition of tumor growth and immunomodulatory effects of flavonoids and scutebarbatines of *Scutellaria barbata* D. Don in lewis-bearing C57BL/6 mice. *Evid. Based Complement. Altern. Med.* 2015, 630760. doi:10.1155/2015/630760
- Han, S., Wang, W., Wang, S., Wang, S., Ju, R., Pan, Z., et al. (2019). Multifunctional biomimetic nanoparticles loading baicalin for polarizing tumor-associated macrophages. *Nanoscale* 11, 20206–20220. doi:10.1039/c9nr03353j
- Kummar, S., Copur, M. S., Rose, M., Wadler, S., Stephenson, J., O'Rourke, M., et al. (2011). A phase I study of the Chinese herbal medicine PHY906 as a modulator of irinotecan-based chemotherapy in patients with advanced colorectal cancer. *Clin. Colorectal Cancer* 10, 85–96. doi:10.1016/j.clcc.2011.03.003
- Lam, W., Bussom, S., Guan, F., Jiang, Z., Zhang, W., Gullen, E. A., et al. (2010). The four-herb Chinese medicine PHY906 reduces chemotherapy-induced gastrointestinal toxicity. *Sci. Transl. Med.* 2, 45ra59. doi:10.1126/scitranslmed.3001270
- Lam, W., Jiang, Z., Guan, F., Hu, R., Liu, S. H., Chu, E., et al. (2014). The number of intestinal bacteria is not critical for the enhancement of antitumor activity and reduction of intestinal toxicity of irinotecan by the Chinese herbal medicine PHY906 (KD018). *BMC Complement. Altern. Med.* 14, 490. doi:10.1186/1472-6882-14-490
- Lam, W., Jiang, Z., Guan, F., Huang, X., Hu, R., Wang, J., et al. (2015). PHY906(KD018), an adjuvant based on a 1800-year-old Chinese medicine, enhanced the anti-tumor activity of Sorafenib by changing the tumor microenvironment. *Sci. Rep.* 5, 9384. doi:10.1038/srep09384
- Lam, W., Ren, Y., Guan, F., Jiang, Z., Cheng, W., Xu, C. H., et al. (2018). Mechanism based quality control (MBQC) of herbal products: A case study YIV-906 (PHY906). *Front. Pharmacol.* 9, 1324. doi:10.3389/fphar.2018.01324
- Lindner, S. E., Johnson, S. M., Brown, C. E., and Wang, L. D. (2020). Chimeric antigen receptor signaling: Functional consequences and design implications. *Sci. Adv.* 6, eaaz3223. doi:10.1126/sciadv.aaz3223
- Liu, S. H., and Cheng, Y. C. (2012). Old formula, new rx: the journey of PHY906 as cancer adjuvant therapy. *J. Ethnopharmacol.* 140, 614–623. doi:10.1016/j.jep.2012.01.047
- Liu, S. H., He, X., Man, V. H., Ji, B., Liu, J., and Wang, J. (2019). New application of *in silico* methods in identifying mechanisms of action and key components of anti-cancer herbal formulation YIV-906 (PHY906). *Phys. Chem. Chem. Phys.* 21, 23501–23513. doi:10.1039/c9cp03803e
- Lorenz, U. (2009). SHP-1 and SHP-2 in T cells: two phosphatases functioning at many levels. *Immunol. Rev.* 228, 342–359. doi:10.1111/j.1600-065X.2008.00760.x
- Marasco, M., Berteotti, A., Weyershaeuser, J., Thoraus, N., Sikorska, J., Krausz, J., et al. (2020). Molecular mechanism of SHP2 activation by PD-1 stimulation. *Sci. Adv.* 6, eaay4458. doi:10.1126/sciadv.aay4458
- Myers, D. R., Abram, C. L., Wildes, D., Belwafa, A., Welsh, A. M. N., Schulze, C. J., et al. (2020). Shp1 loss enhances macrophage effector function and promotes anti-tumor immunity. *Front. Immunol.* 11, 576310. doi:10.3389/fimmu.2020.576310
- Overman, M. J., McDermott, R., Leach, J. L., Lonardi, S., Lenz, H. J., Morse, M. A., et al. (2017). Nivolumab in patients with metastatic DNA mismatch repair-deficient or microsatellite instability-high colorectal cancer (CheckMate 142): An open-label, multicentre, phase 2 study. *Lancet Oncol.* 18, 1182–1191. doi:10.1016/S1470-2045(17)30422-9
- Panche, A. N., Diwan, A. D., and Chandra, S. R. (2016). Flavonoids: An overview. *J. Nutr. Sci.* 5, e47. doi:10.1017/jns.2016.41
- Patel, S. P., and Kurzrock, R. (2015). PD-L1 expression as a predictive biomarker in cancer immunotherapy. *Mol. Cancer Ther.* 14, 847–856. doi:10.1158/1535-7163.MCT-14-0983
- Patsoukis, N., Duke-Cohan, J. S., Chaudhri, A., Aksoylar, H. I., Wang, Q., Council, A., et al. (2020). Interaction of SHP-2 SH2 domains with PD-1 ITSM induces PD-1 dimerization and SHP-2 activation. *Commun. Biol.* 3, 128. doi:10.1038/s42003-020-0845-0
- Rockwell, S., Grove, T. A., Liu, Y., Cheng, Y. C., Higgins, S. A., and Booth, C. J. (2013). Preclinical studies of the Chinese Herbal Medicine formulation PHY906 (KD018) as a potential adjunct to radiation therapy. *Int. J. Radiat. Biol.* 89, 16–25. doi:10.3109/09553002.2012.717733
- Saif, M. W., Lansigan, F., Ruta, S., Lamb, L., Mezes, M., Elligers, K., et al. (2010). Phase I study of the botanical formulation PHY906 with capecitabine in advanced pancreatic and other gastrointestinal malignancies. *Phytomedicine* 17, 161–169. doi:10.1016/j.phymed.2009.12.016
- Saif, M. W., Li, J., Lamb, L., Kaley, K., Elligers, K., Jiang, Z., et al. (2014). First-in-human phase II trial of the botanical formulation PHY906 with capecitabine as second-line therapy in patients with advanced pancreatic cancer. *Cancer Chemother. Pharmacol.* 73, 373–380. doi:10.1007/s00280-013-2359-7
- Sassi, A., Mokdad Bzeouich, I., Mustapha, N., Maatouk, M., Ghedira, K., and Chekir-Ghedira, L. (2017). Immunomodulatory potential of hesperetin and chrysin through the cellular and humoral response. *Eur. J. Pharmacol.* 812, 91–96. doi:10.1016/j.ejphar.2017.07.017
- Sassi, A., Maatouk, M., El Gueder, D., Bzeouich, I. M., Abdelkefi-Ben Hatira, S., Jemni-Yacoub, S., et al. (2018). Chrysin, a natural and biologically active flavonoid suppresses tumor growth of mouse B16F10 melanoma cells: *In vitro* and *in vivo* study. *Chem. Biol. Interact.* 283, 10–19. doi:10.1016/j.cbi.2017.11.022
- Steinberg, M. W., Cheung, T. C., and Ware, C. F. (2011). The signaling networks of the herpesvirus entry mediator (TNFRSF14) in immune regulation. *Immunol. Rev.* 244, 169–187. doi:10.1111/j.1600-065X.2011.01064.x
- Tilton, R., Paiva, A. A., Guan, J. Q., Marathe, R., Jiang, Z., Van Eyndhoven, W., et al. (2010). A comprehensive platform for quality control of botanical drugs (PhytomicsQC): A case study of Huangqin Tang (HQT) and PHY906. *Chin. Med.* 5, 30. doi:10.1186/1749-8546-5-30
- Yang, X., Lam, W., Jiang, Z., Guan, F., Han, X., Hu, R., et al. (2021). YIV-906 potentiated anti-PD1 action against hepatocellular carcinoma by enhancing adaptive and innate immunity in the tumor microenvironment. *Sci. Rep.* 11, 13482. doi:10.1038/s41598-021-91623-3
- Ye, M., Liu, S. H., Jiang, Z., Lee, Y., Tilton, R., and Cheng, Y. C. (2007). Liquid chromatography/mass spectrometry analysis of PHY906, a Chinese medicine formulation for cancer therapy. *Rapid Commun. Mass Spectrom.* 21, 3593–3607. doi:10.1002/rcm.2832
- Yen, Y., So, S., Rose, M., Saif, M. W., Chu, E., Liu, S. H., et al. (2009). Phase I/II study of PHY906/capecitabine in advanced hepatocellular carcinoma. *Anticancer Res.* 29, 4083–4092.
- Yuan, X., Bu, H., Zhou, J., Yang, C. Y., and Zhang, H. (2020). Recent advances of SHP2 inhibitors in cancer therapy: Current development and clinical application. *J. Med. Chem.* 63, 11368–11396. doi:10.1021/acs.jmedchem.0c00249
- Zhang, W., Saif, M. W., Dutschman, G. E., Li, X., Lam, W., Bussom, S., et al. (2010). Identification of chemicals and their metabolites from PHY906, a Chinese medicine formulation, in the plasma of a patient treated with irinotecan and PHY906 using liquid chromatography/tandem mass spectrometry (LC/MS/MS). *J. Chromatogr. A* 1217, 5785–5793. doi:10.1016/j.chroma.2010.07.045
- Zhao, M., Guo, W., Wu, Y., Yang, C., Zhong, L., Deng, G., et al. (2019). SHP2 inhibition triggers anti-tumor immunity and synergizes with PD-1 blockade. *Acta Pharm. Sin. B* 9, 304–315. doi:10.1016/j.apsb.2018.08.009



OPEN ACCESS

EDITED BY

Jean Christopher Chamcheu,
University of Louisiana at Monroe,
United States

REVIEWED BY

Zachary Taylor,
Cincinnati Children's Hospital Medical
Center, United States
Matthew M Lei,
Massachusetts General Hospital Cancer
Center, United States
Rahul Lall,
University of Florida, United States

*CORRESPONDENCE

Toshimi Kimura
✉ t.kimura.pharm@gmail.com

SPECIALTY SECTION

This article was submitted to
Pharmacology of Anti-Cancer Drugs,
a section of the journal
Frontiers in Oncology

RECEIVED 26 July 2022

ACCEPTED 16 January 2023

PUBLISHED 30 January 2023

CITATION

Fukaya Y, Kimura T, Hamada Y,
Yoshimura K, Hiraga H, Yuza Y, Ogawa A,
Hara J, Koh K, Kikuta A, Koga Y and
Kawamoto H (2023) Development of a
population pharmacokinetics and
pharmacodynamics model of glucarpidase
rescue treatment after high-dose
methotrexate therapy.
Front. Oncol. 13:1003633.
doi: 10.3389/fonc.2023.1003633

COPYRIGHT

© 2023 Fukaya, Kimura, Hamada, Yoshimura,
Hiraga, Yuza, Ogawa, Hara, Koh, Kikuta, Koga
and Kawamoto. This is an open-access
article distributed under the terms of the
Creative Commons Attribution License
(CC BY). The use, distribution or
reproduction in other forums is permitted,
provided the original author(s) and the
copyright owner(s) are credited and that
the original publication in this journal is
cited, in accordance with accepted
academic practice. No use, distribution or
reproduction is permitted which does not
comply with these terms.

Development of a population pharmacokinetics and pharmacodynamics model of glucarpidase rescue treatment after high-dose methotrexate therapy

Yutaka Fukaya¹, Toshimi Kimura^{2*}, Yukihiro Hamada¹,
Kenichi Yoshimura³, Hiroaki Hiraga⁴, Yuki Yuza⁵,
Atsushi Ogawa⁶, Junichi Hara⁷, Katsuyoshi Koh⁸, Atsushi Kikuta⁹,
Yuhki Koga¹⁰ and Hiroshi Kawamoto¹¹

¹Department of Pharmacy, Tokyo Women's Medical University Hospital, Tokyo, Japan, ²Department of Pharmacy, Juntendo University Hospital, Tokyo, Japan, ³Center for Integrated Medical Research, Hiroshima University Hospital, Hiroshima, Japan, ⁴Department of Musculoskeletal Oncology, National Hospital Organization Hokkaido Cancer Center, Sapporo, Japan, ⁵Department of Hematology and Oncology, Tokyo Metropolitan Children's Medical Center, Tokyo, Japan, ⁶Department of Pediatrics, Niigata Cancer Center Hospital, Niigata, Japan, ⁷Department of Pediatric Hematology/Oncology, Osaka City General Hospital, Osaka, Japan, ⁸Department of Hematology/Oncology, Saitama Children's Medical Center, Saitama, Japan, ⁹Department of Pediatric Oncology, Fukushima Medical College, Fukushima, Japan, ¹⁰Department of Perinatal and Pediatric Medicine, Kyushu University, Fukuoka, Japan, ¹¹Department of Pediatric Oncology, National Cancer Center Hospital, Tokyo, Japan

Introduction: Glucarpidase (CPG2) reduces the lethal toxicity of methotrexate (MTX) by rapid degradation.

Methods: In this study, a CPG2 population pharmacokinetics (popPK) analysis in healthy volunteers (phase 1 study) and a popPK-pharmacodynamics (popPK-PD) analysis in patients (phase 2 study, $n = 15$) who received 50 U/kg of CPG2 rescue for delayed MTX excretion were conducted. In the phase 2 study, the first CPG2 treatment at a dose of 50 U/kg was intravenously administered for 5 min within 12 h after the first confirmation of delayed MTX excretion. The second dose of CPG2, with a plasma MTX concentration $>1 \mu\text{mol/L}$, was administered to the patient more than 46 h after the start of CPG2 administration.

Results: The population mean PK parameters (95% CI) of MTX, obtained from the final model *post hoc*, were estimated as follows: $CL_{rMTX} = 2.424 \text{ L/h}$ (95% CI: 1.755–3.093), $V_{cMTX} = 12.6 \text{ L}$ (95% CI: 10.8–14.3), $V_{pMTX} = 2.15 \text{ L}$ (95% CI: 1.60–2.70), and $\alpha = 8.131 \times 10^5$ (4.864×10^5 – 11.398×10^5). The final model, including covariates, was $CL_{rMTX} (\text{L/h})$: $3.248 \times \text{Body Weight}/\text{Serum creatinine}/60$ (CV 33.5%), $V_{cMTX} (\text{L})$: $0.386 \times \text{Body Weight}/\text{body surface area}$ (CV 29.1%), $V_{pMTX} (\text{L})$: $3.052 \times \text{Body Weight}/60$ (CV 90.6%), and $\alpha (\text{L/h})$: 6.545×10^5 (CV 79.8%).

Discussion: These results suggest that the pre-CPG2 dose and 24 h after CPG2 dosing were the most important sampling points in the Bayesian estimation of plasma MTX concentration prediction at 48 h. These CPG2-MTX popPK analysis

and Bayesian estimation of rebound in plasma MTX concentrations are clinically important to estimate $>1.0 \mu\text{mol/L}$ 48 h after the first CPG2 dosing.

Clinical trial registration: <https://dbcentre3.jmacct.med.or.jp/JMACTR/App/JMACTRS06/JMACTRS06.aspx?seqno=2363>, identifier JMA-IIA00078 and <https://dbcentre3.jmacct.med.or.jp/JMACTR/App/JMACTRS06/JMACTRS06.aspx?seqno=2782>, identifier JMA-IIA00097.

KEYWORDS

glucarpidase, methotrexate - adverse effects, safety, pharmacokinetics, pharmacodynamics

1 Introduction

Methotrexate (MTX) is an antineoplastic drug that inhibits fatty acid metabolism. Combination chemotherapy with high-dose MTX (HD-MTX) has been established as the standard regimen for acute lymphoblastic leukemia, malignant lymphoma, and osteosarcoma. HD-MTX causes adverse effects such as nephrotoxicity, hepatotoxicity, severe mucositis, and pancytopenia at a frequency of 1%–10% (1, 2). Treatments such as plasmapheresis, dialysis, and high-dose leucovorin can be used to prevent fatal MTX toxicity; however, these treatments have limited efficacy (2). Nephrotoxicity caused by HD-MTX seems to result mainly from the inhibition of renal tubular excretion of MTX.

In a physiological pathway, most MTX is excreted through the urine as an intact drug by the organic anion transporter-3 (3–5), and less than 10% of MTX is metabolized to relatively inactive 7-hydroxymethotrexate. Other metabolites (less than 5% of MTX) include an inactive metabolite of 2,4-diamino-N10-methylpteroic acid (DAMPA) (3, 4, 6, 7). Glucarpidase (CPG2) is an enzymatic drug (a 390-amino acid homodimer protein with a molecular weight of 83 kDa isolated from the *Pseudomonas* species) that directly decomposes MTX into DAMPA and glutamate (8). Administration of CPG2 is an effective option as an alternative pathway of MTX metabolism if MTX induced acute renal failure and decreased the renal clearance of MTX (8). In Europe and the United States, CPG2 is the only standard drug approved as a therapeutic agent for reducing MTX toxicity caused by delayed MTX excretion. CPG2 rapidly degrades MTX and reduces plasma MTX concentrations by $>95\%$ within 15 min (9–13). A 50-U/kg dose of CPG2 is used in clinical treatment as a theoretically sufficient dose to reduce high plasma MTX concentrations. In an open-label and single-site study, Phillips et al. reported a safe and effective dose of 50 U/kg of CPG2 (14). Several reports have suggested efficacy at doses between 15 and 70 U/kg of CPG2; however, only a few dose-finding studies of CPG2 have been conducted in humans.

We conducted a phase 1 study in which two doses of CPG2 (50 and 20 U/kg) were administered to healthy volunteers (15). Safety was confirmed when 50 U/kg of CPG2 was administered at 48-h intervals. As it is possible that the degradation effect of MTX may be diminished by low doses of CPG2, we set the recommended dose of CPG2 to 50 U/kg and conducted a phase 2 study in Japanese patients receiving HD-MTX.

In this study, we aimed to develop a CPG2 population pharmacokinetics (popPK) analysis in healthy volunteers and a popPK and pharmacodynamics (PD) analysis (popPK-PD) in patients who received CPG2 rescue for delayed MTX excretion. The rebound in plasma MTX concentrations after the administration of CPG2 has been reported (8). Based on the concept of model-informed precision dosing (MIPD), the popPK-PD final model was evaluated using a Bayesian estimation to predict the plasma MTX concentrations.

2 Materials and methods

2.1 Subjects

2.1.1 Phase 1 study

A phase 1 open-label, randomized two-dose (20 and 50 U/kg) study was conducted in healthy volunteers, and a parallel PK study of CPG2 was launched at Hamamatsu University School of Medicine. This study was conducted between November 2011 and January 2012.

2.1.2 Phase 2 study

A phase 2 multicenter collaborative, single-arm uncontrolled study was conducted in patients with delayed excretion of MTX after HD-MTX treatment for cancer. This study was conducted between December 2012 and February 2016 at eight Japanese medical facilities. After treatment with HD-MTX ($\geq 1 \text{ g/m}^2$), CPG2 (50 U/kg) was administered to patients with abnormally high plasma MTX concentrations far above the suggested critical level or elevated serum creatinine levels.

The selection criteria for the treatment of CPG2 were defined by plasma MTX concentrations and time after administration, depending on the status of the patients (Table 1).

Phase 1 and 2 studies were performed in accordance with the Declaration of Helsinki and Guidelines for Good Clinical Practice, with approval from the Human Institutional Review Boards or independent ethics committees for each trial. This investigator-initiated clinical trial was supported by the Center for Clinical Trials of Japan Medical Association (JMACCT). Phase 1 and 2 studies were registered with the JMACCT Clinical Trial Registry (identifiers: JMA-IIA00078 and JMA-IIA00097).

TABLE 1 Selection criteria for the treatment of CPG2.

Plasma MTX concentrations and time after MTX administration
≥50 μmol/L (22 h)
≥5 μmol/L (40 h)
≥2 μmol/L (46 h)
≥1 μmol/L (40 h and patients with acute renal failure ^a)
≥0.4 μmol/L (46 h and patients with acute renal failure ^a)
≥0.3 μmol/L (70 h and >3.5 g/m ² of MTX dose)
≥0.1 μmol/L (70 h and 1–3.5 g/m ² of MTX dose)

CPG2, glucarpidase; MTX, methotrexate.

^aAcute renal failure is defined as meeting either of the following (1) and (2): (1) after 12 h of MTX administration, the serum creatinine level was above the upper limit of the reference, or creatinine clearance or glomerular filtration rate (either calculated or measured) was <70 ml/min; (2) increase the serum creatinine level by two times or more before MTX administration, or by a factor of 1.5, for two consecutive times and increasing.

46 h after the start of CPG2 administration. Supportive care such as leucovorin rescue was continued until a plasma MTX concentration <0.1 μmol/L was obtained; however, CPG2 was not administered for a third time.

2.3 Assay methods

All blood samples were centrifuged for 15 min to separate the plasma. The plasma MTX concentrations for clinical decision-making regarding CPG2 therapy were immediately analyzed at each hospital using a routine assay method. Measurement of the plasma MTX concentrations at each hospital is a commercial immunoassay, and there is a possibility of cross-reactivity between MTX and DAMPA (16). The same samples were also analyzed at the central laboratory using a quantitative validated analytical method by high-performance liquid chromatography (HPLC) that permits the separation of MTX

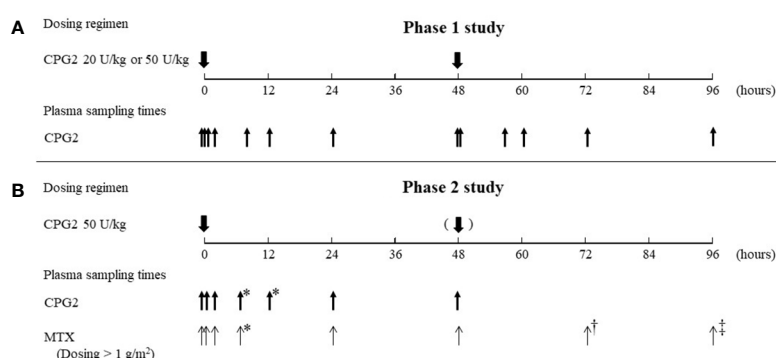


FIGURE 1

Summary of the dosing regimen of CPG2 and blood sampling of CPG2 and MTX. CPG2, glucarpidase; MTX, methotrexate. (A) Blood sampling of CPG2 in the phase 1 study. First dosing of CPG2: before dosing, at 5 and 15 min, and 2, 8, 12, 24, and 48 h (before second dosing of CPG2) after dosing. Second dosing of CPG2: 5 min and 8, 12, 24, and 48 h after dosing. (B) Blood sampling of CPG2 in the phase 2 study. First dosing of CPG2: before dosing, at 20 min, and 2, 5–8*, 12–20*, 24, and 48 h after dosing. Blood sampling of MTX. First dosing of CPG2: before dosing, at 20 min, and 2, 5–8*, 12–20*, 24, 48, 72†, and 96‡ h after dosing. *Before leucovorin dosing; †24 h after and dosing of CPG2; ‡48 h after second dosing of CPG2.

2.2 Dosing regimen, blood sampling, and determination of plasma concentrations of CPG2 and MTX

The sampling times and dosing regimens of CPG2 and MTX for the phase 1 and 2 studies are summarized in Figure 1.

2.2.1 Phase 1 study

A dose of 50 or 20 U/kg of CPG2 was administered intravenously over 5 min. Eight healthy volunteers were allocated to the two-dose groups. All participants received the same second dose of CPG2, 48 h after the first dose.

2.2.2 Phase 2 study

The first CPG2 treatment at a dose of 50 U/kg was intravenously administered for 5 min within 12 h after the first confirmation of delayed MTX excretion. The second dose of CPG2 was administered to patients with a plasma MTX concentration >1 μmol/L more than

metabolites such as DAMPA. Only MTX concentrations measured by HPLC were used for the PK analysis. Plasma samples of MTX and CPG2 were stored at −70°C and −80°C, respectively, until central laboratory analysis. These samples were analyzed by Shin Nippon Biomedical Laboratories, Ltd. (Wakayama, Japan).

The HPLC analysis of plasma MTX concentration was performed using the mobile phase that consisted of formic acid (0.1% vol) and methanol (90:10). The analytical column was an octadecyl silyl (ODS) column (Hydrosphere C18 S-5, 2.0 × 75 mm I.D., YMC CO., Kyoto, Japan). The column temperature was set at 40°C. The flow rate of the mobile phase was set to 0.5 ml/min. MTX-d3 (Toronto Research Chemicals, Inc. Toronto, Canada) was used as an internal standard. The lower limit of quantification (LLOQ) and the upper limit of quantification (ULOQ) of plasma MTX concentrations were 0.5 and 400 ng/ml, respectively.

Plasma CPG2 concentrations were determined using enzyme-linked immunosorbent assay (ELISA) (15). All analytical methods were validated according to the Guidelines on Bioanalytical Method Validation in Pharmaceutical Development in Japan. The calibration

ranges for CPG2 were defined by the LLOQ and ULOQ with seven calibration standards of different concentration levels, including the LLOQ and ULOQ, with a correlation coefficient of ≥ 0.990 . The LLOQ and ULOQ of plasma CPG2 concentrations were 1 ng/ml and 640 μ g/ml, respectively.

2.4 Development of the popPK and popPK-PD models

First, the popPK model of CPG2 was determined from the phase 1 and 2 studies. We then constructed a popPK-PD model that incorporated the degradation reaction of CPG2 into the metabolic clearance of MTX using the Michaelis–Menten equation in the phase 2 study. Simultaneous analysis of all concentration–time and patient physiological data was performed using Phoenix 64 NLME 7.0 (Pharsight Corp., Mountain View, CA, USA), a computer program developed for popPK and popPK-PD analyses. PopPK parameters and their variability were estimated using first-order conditional estimation extended least-squares (FOCE-ELS) methods.

2.5 Development of the CPG2 popPK model

In the first step, popPK analysis of CPG2 was developed in the phase 1 and 2 studies. One- and two-compartment intravenous infusion models with first-order elimination of CPG2 were used to describe the plasma concentration–time courses. Additive and proportional (exponential) error models were compared for interindividual variability in all PK parameters and residual variability in drug concentrations. The additive error model was used for residual variability, which is expressed as follows:

$$C_{ij} = C_{ij}^* + e_{ij}$$

where C_{ij} is the i th measured plasma concentration in the j th individual, C_{ij}^* is the estimated plasma concentration (as observed for PK data), and e_{ij} is the independent identically distributed statistical error with a mean of zero and a variance of σ_e^2 . Exponential interindividual variability models were invoked for all PK parameters as follows:

$$\theta_i = tv\theta \times \exp(n_{i,\theta})$$

where θ_i is the individualized estimated parameter, $tv\theta$ is the typical value of the parameter in the population, and $n_{i,\theta}$ is a random variable with a mean of zero and a variance of ω^2 . In the fitting process, subject demographic and biochemical data were used as covariables in the population model: body weight, height, body surface area (BSA), and age (only in the phase 2 study). The candidate covariate was screened through the simultaneous incorporation of an allometric function on all typical values of PK parameters, such as clearance ($tvCL_{CPG2}$) and distribution volume (tvV_{CPG2}). These were expressed as follows:

$$CL_{CPG2} = tvCL_{CPG2} \times covariate^{\theta_1}$$

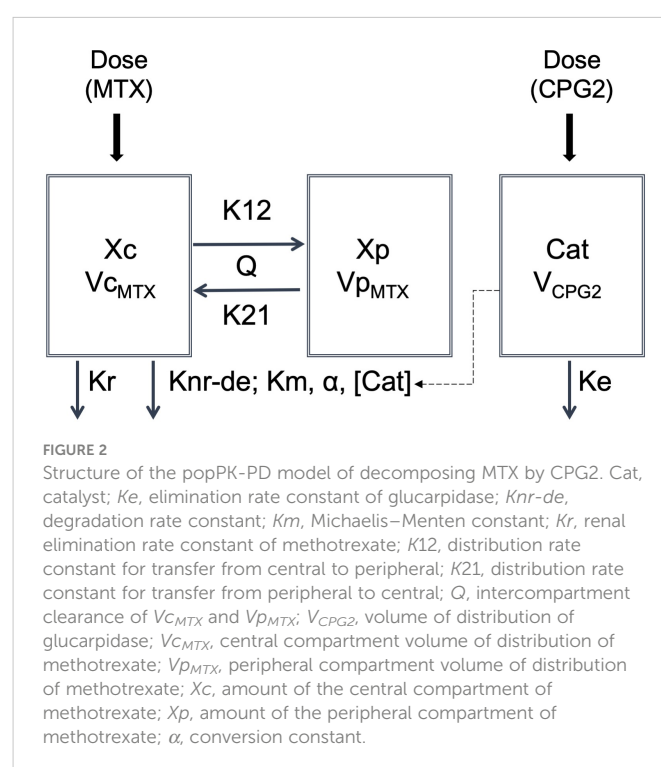
$$V_{CPG2} = tvV_{CPG2} \times covariate^{\theta_2}$$

where θ_1 and θ_2 are the intercept and slope parameters, respectively. An objective function value (OFV; negative value of twice the log-likelihood difference: -2 L.L.d) was calculated for each model in this regression. Covariates such as height, body weight, BSA, age, serum creatinine, and creatinine clearance in each model were determined using the likelihood ratio test based on the degree of freedom of parameters and change in the OFV. Covariates were included in the full model when the likelihood ratio test was decreased in OFV greater than 10.828 (p -value < 0.001). Covariates without multicollinearity were basically considered in the full model. When there was no change in degrees of freedom and multiple covariates were selected, the full model was selected with reference to Akaike's information criterion. The definition of successful in each model analysis was that the standard deviation of all parameters was calculated and the 95% confidence intervals of the parameters were positive values. Each covariate was added using a forward–backward stepwise in the popPK model to validate the final model. The final model determined the most significant model in the likelihood ratio test.

2.6 Development of the popPK-PD model for MTX decomposition by CPG2

In the second step, CPG2-MTX and popPK-PD analyses were performed based on the known popPK properties of MTX. The default structural model of MTX was a two-compartment model using the following differential equations (Figure 2):

$$\begin{aligned} dX_c/dt &= -(Kr + Knr-de + K12) \times X_c + K21 \times X_p \\ dX_p/dt &= K12 \times X_c - (K21 + Ke) \times X_p \end{aligned} \quad (1)$$



$$dXp/dt = K12 \times Xc - K21 \times Xp$$

where Xc and Xp are the amounts of MTX in the central and peripheral compartments, respectively. Kr and $Knr-de$ are elimination constants from the central compartment by renal excretion and metabolic pathways, respectively. $K12$ and $K21$ are the intercompartmental constants between the central and peripheral compartments, respectively. In this differential equation, $dXc/dt = -(Kd \times Xc)$ represents the decomposition of MTX by CPG2 as a catalyst. CPG2 is an enzyme that hydrolyzes MTX to inactive metabolites and is characterized by the Michaelis–Menten equation. Therefore, the metabolism of MTX is as follows (17):

$$dXc/dt = -V_{max} \times [Xc]/(Km + [Xc])$$

where V_{max} is the maximum rate of decomposition, Km (18) is the Michaelis–Menten constant of MTX hydrolysis by CPG2, and $[Xc]$ is the plasma MTX concentration. V_{max} is also a constant for the interaction of the enzyme with its substance and has units of mass/time. Therefore, it can be rearranged based on mass balance as follows:

$$V_{max}(\text{mass/time}) = [\text{catalyst}] \times \alpha(\text{mass/volume} \times \text{volume/time})$$

where α is the conversion constant between V_{max} and the catalyst concentration for a patient-specific parameter, which is the same as the individual clearance.

Equation (1) was rearranged using a constant α and the catalyst concentration, as follows:

$$\begin{aligned} dXc/dt &= -(Kr + K12) \times \\ &Xc + K21 \times Xp - \alpha \times [\text{catalyst}] \times \\ &[Xc]/(Km + [Xc]) \end{aligned}$$

The catalyst concentration was the plasma CPG2 concentration, which was calculated using the patient's individualized CL_{CPG2} and V_{CPG2} , obtained *post hoc* in the popPK analysis of the phase 2 study. To build the popPK model, renal clearance was calculated using the micro rate constants of Kr and distribution volume in the central compartment ($CL_{rMTX} = Kr \times V_{cMTX}$) to incorporate physiological covariates such as height, body weight, BSA, age, serum creatinine, and creatinine clearance. The intercompartmental clearance, Q , of MTX was defined as follows: $Q = K12 \times V_{cMTX} = K21 \times V_{pMTX}$. Model selection and determination of the final model were performed using the same process as in CPG2. A proportional error model was used to determine the residual variability of plasma MTX concentrations: $C_{ij} = C_{ij}^* \times (1 + e_{ij})$.

2.7 Model evaluation

The general goodness-of-fit of the final popPK model of CPG2 and of the CPG2-MTX popPK-PD model was evaluated using the scatter plots of observed plasma concentrations versus predicted plasma concentrations (PRED) based on the mean popPK parameters or individual predicted plasma concentrations (IPRED) using Bayesian estimation and the plots of CWRES versus the relative elapsed time after drug administration. A bootstrap assessment of the

CPG2 popPK final model and CPG2-MTX popPK-PD final model was conducted using Phoenix 64 NLME 7.0 (with 1,000 samples). A visual predictive check (VPC) was used to assess the performance of the final popPK model of CPG2. The 5th, 50th, and 95th percentiles of the distribution of the observed and 1,000 simulated plasma concentrations were calculated and graphically compared.

2.8 Sampling strategy and prediction performance using Bayesian estimation

The sampling strategy and prediction performance of plasma MTX concentrations 48 h after the first administration of CPG2 were investigated using the CPG2-MTX popPK-PD final model by Bayesian estimation in Phoenix 64 NLME 7.0.

To evaluate the best sampling points for the estimation of plasma MTX concentrations at 48 h, the combined multi-sampling MTX concentrations (before CPG2 dosing plus at 20 min, 2 h, 5–8 h, and 24 h after CPG2 dosing) were used. The predicted performance was evaluated using the mean error (ME), mean absolute error (MAE), and root-mean-squared error (RMSE). The ME, MAE, and RMSE were calculated using the predicted plasma MTX concentrations and observed plasma MTX concentrations. We also verified the hit ratio of the estimated plasma MTX concentrations to the observed plasma MTX concentrations over or under 1.0 $\mu\text{mol/L}$, which is the borderline of an additional dose of CPG2, 48 h after the first CPG2 dosing.

3 Results

3.1 Patient characteristics in the phase 1 and 2 studies

Sixteen healthy subjects were randomly allocated to two cohorts (20 U/kg, $n = 8$ or 50 U/kg, $n = 8$) in the phase 1 study. The participant demographics and baseline characteristics did not differ significantly between the two cohorts. The study participants were men (100%) with a mean age of 24.9 years (range, 20–40), height of 169.6 cm (range, 162.6–184.8), and body weight of 60.9 kg (range, 54.3–66.9). The demographic characteristics of the participants in the phase 2 study are shown in Table 2.

The popPK analysis dataset of CPG2 included 192 plasma samples from 16 healthy volunteers in the phase 1 study. Eighty-eight plasma CPG2 samples and 115 plasma MTX samples were used for the CPG2-MTX popPK-PD modeling, which were obtained from 15 patients in phase 2. Scatter plots of plasma CPG2 concentration versus time profiles in the phase 1 and 2 studies are shown in Figure 3.

3.2 Development of the popPK and popPK-PD models

3.2.1 PopPK analysis of CPG2 in the phase 1 and 2 studies

A one-compartment model with intravenous infusion of CPG2 was chosen based on the selection analysis of compartmental models

TABLE 2 Demographic data in phase 2 ($n = 15$).

Characteristics	Number	Percentage (%)
Male	9	60.0
Female	6	40.0
Osteosarcoma	9	60.0
Acute lymphocytic leukemia	3	20.0
Non-Hodgkin's lymphoma	2	13.3
Medulloblastoma	1	6.7
Value (units)	Median	Range
Age (years)	15	1–75
Height (cm)	156.0	78.5–177.5
Weight (kg)	47.0	10.7–78.1
MTX dosage (g)	14.0	1.6–20.0
MTX dosage (g/m ²)	8.0	2.9–14.3
MTX plasma concentration (μmol/L) ^a	51.00	1.02–692.32
White blood cells (/mm ³)	6,840	90–14,690
Hemoglobin (g/L)	8.6	6.3–12.6
Platelet count (10 ⁴ /mm ³)	16.4	3.3–39.7
Blood urea nitrogen (mg/dl)	11.1	7.4–57.0
Serum creatinine (mg/dl)	0.81	0.23–3.47
Albumin (g/dl)	3.5	2.3–4.2
Aspartate aminotransferase (U/L)	53.0	17.0–593.0
Alanine aminotransferase (U/L)	72.0	22.0–685.0
Total bilirubin (mg/dl)	0.60	0.30–1.80
Urine pH	7.8	7.0–8.5

^aMethotrexate plasma concentrations in the decision for CPG2 treatment.

in the phase 1 study (Table 3). In the covariate modeling process with univariate testing, BSA, body weight, and height as covariates on CL and V significantly improved the fit of the model in the phase 1 and 2 studies. In the final model, BSA was identified as a statistically significant covariate of CL and V of CPG2 in the phase 1 and 2 studies. All the popPK parameter estimates for the final model are listed in Table 4. The *post-hoc* analysis by the final model showed the mean popPK parameters of CPG2 as follows: $CL = 0.329$ L/h (range, 0.302–0.356) and $V = 3.17$ L (range, 2.97–3.36) in the phase 1 study and $CL = 0.380$ L/h (range, 0.289–0.470) and $V = 2.04$ L (range, 1.47–2.60) in the phase 2 study.

3.2.2 PopPK-PD analysis of MTX treated with CPG2 in the phase 2 study

In basic model building, Q without interindividual variability made the 95% CI of all other parameters optimal. The estimated $Q = 0.0632$ L/h increased OFV compared with $Q = 0.0778$ L/h, which is the Japanese MTX popPK value reported by Fukuhara et al. Therefore, $Q = 0.0778$ was selected as the fixed value in the exploratory covariate analyses. PK parameters scaled by various subject sizes were used to evaluate the reduction in OFV in the

final model. Body weight/serum creatinine ratio was identified as a covariate for both CL_{MTX} and $V_{p_{MTX}}$, whereas body weight/BSA ratio was a covariate for $V_{c_{MTX}}$. The final model, including covariates, is presented as follows:

$$CL_{MTX} \text{ (L/h)} = 3.248 \times \text{Body Weight/Serum creatinine}/60(\text{CV } 33.5 \%)$$

$$V_{c_{MTX}} \text{ (L)} = 0.386 \times \text{Body Weight/BSA}(\text{CV } 29.1 \%)$$

$$V_{p_{MTX}} \text{ (L)} = 3.052 \times \text{Body Weight}/60(\text{CV } 90.6 \%)$$

$$\alpha = 6.545 \times 10^5(\text{CV } 79.8 \%)$$

where α is a constant to compose a part of the following differential equation:

$$dX_c/dt = -(Kr + K_{12}) \times X_c + K_{21} \times X_p -$$

$$\alpha \times [\text{plasma CPG2 concentration}] \times$$

$$[\text{plasma MTX concentration}]/$$

$$(86 \text{ } \mu\text{mol/L} + [\text{plasma MTX concentration}])$$

Body weight was standardized at 60 kg (58.4 kg; a representative value of body weight in Japan). The *post-hoc* analysis by the final model showed the mean popPK-PD parameters as follows: $CL_{MTX} = 2.424$ L/h (95% CI: 1.755–3.093), $V_{c_{MTX}} = 12.6$ L (95% CI: 10.8–14.3), $V_{p_{MTX}} = 2.15$ L (95% CI: 1.60–2.70), and $\alpha = 8.131 \times 10^5$ (4.864×10^5 – 11.398×10^5).

3.3 Model validation

The goodness-of-fit of the final model for the CPG2 popPK and CPG2-MTX popPK-PD in healthy volunteers and patients was evaluated using PRED, IPRED, and CWRES (Figure 4). All distributions in the plot of observed concentrations against PRED or IPRED display bilateral symmetry around the regression line of $y = x$, since the difference in low plasma MTX concentrations $<0.1 \text{ } \mu\text{mol/L}$ is within a clinically acceptable range of error. CPG2 CWRES was out of range (–5 to 5) in the phase 1 and 2 studies and was only 2/192 (0.1%) and 1/88 (1.1%), respectively, and that of MTX was zero.

VPC plots of CPG2 demonstrated that most observed concentrations were within the 95% prediction intervals of the simulations, and the median lines of the observed and predicted concentrations were similar (Figure 5), indicating good predictive performance of the final model.

Furthermore, bootstrap evaluation of the final model almost concluded normally, and the medians of all estimated popPK and popPK-PD parameters were equal to the values of the final model (Table 4).

3.4 Sampling strategy and performance prediction

The observed plasma concentrations of MTX and Bayes-estimated plasma concentrations, calculated using the CPG2-MTX

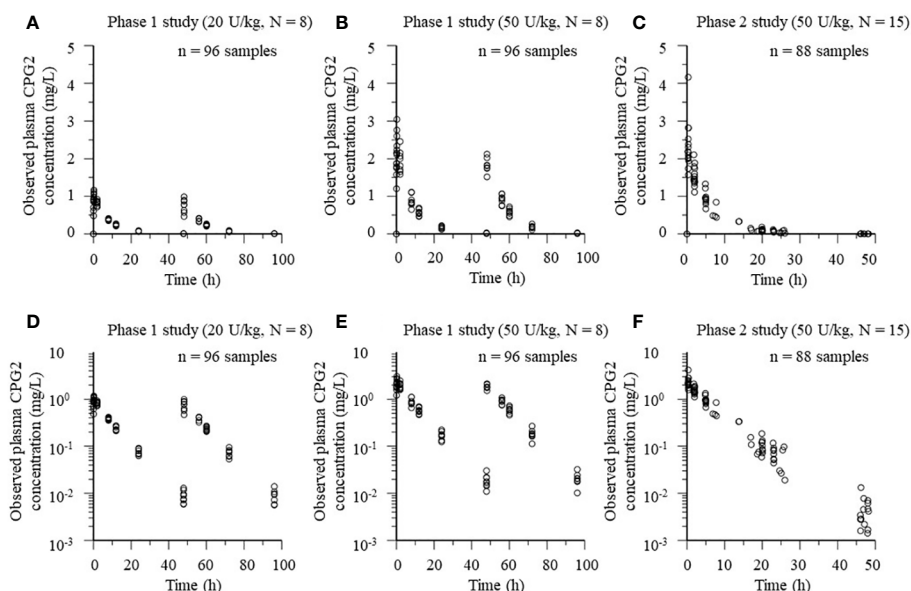


FIGURE 3
Plots of plasma CPG2 concentrations versus time profile in healthy volunteers (phase 1 study) and patients (phase 2 study). (A, B, D, E) Phase 1 study. (C, F) Phase 2 study. (A–C) Observed plasma CPG2 concentrations versus time. (D–F) Observed plasma CPG2 concentrations (logarithmic scale) versus time.

popPK-PD final model versus time for each patient, are presented in Figure 6. The plasma MTX concentration versus time curves showed a graphically good reflection of the alterations of reduced and rebound in plasma MTX concentrations after the administration of CPG2 (Figure 7). The sampling strategies, including the smallest value of predictive performance, were as follows: 2-point sampling (before CPG2 dosing plus 24 h after dosing) and 3-point sampling (before CPG2 dosing plus 20 min and 24 h after dosing), with ME = −0.056 and 0.03, MAE = 0.458 and 0.543, and RMSE = 0.729 and 0.896, respectively. The relationship between sampling points and RMSE is shown in Figure 7.

Additionally, the number of patients with plasma MTX concentrations over and under 1.0 μmol/L was 2 and 13, respectively, at 48 h after the first CPG2 dose. The hit ratio of

Bayesian estimation for plasma MTX concentration over or under 1.0 μmol/L was 93.3% (14/15) using the plasma MTX concentrations at pre-CPG2 dosing and 24 h after CPG2 dosing.

4 Discussion

This study is the first to report popPK for CPG2 and popPK-PD for MTX with CPG2 in healthy volunteers and in patients treated with MTX. The popPK parameters obtained from the phase 1 study were similar to those previously reported in our non-compartmental analysis: $CL = 0.291\text{--}0.347$ L/h and $V = 3.12\text{--}3.67$ L (15). The covariate of the final model was BSA in both phase 1 and 2 studies. However, there was a discrepancy in the final model values for CL in

TABLE 3 Covariate screening of CPG2 in the phase 1 and 2 studies.

Compartment model	Phase 1		Phase 2	
	ΔOFV	p -value	ΔOFV	p -value
1—compartment (basic model)	NC	NC	NC	NC
2—compartment (basic model)	2.0×10^{-5}	1	NA	NA
Covariate model	ΔOFV	p -value	ΔOFV	p -value
$CL_{CPG2} = tvCL_{CPG2} \times BSA^{\theta_1}$	10.736	0.001	32.826	<0.001
$CL_{CPG2} = tvCL_{CPG2} \times Body\ Weight^{\theta_1}$	9.043	0.003	29.660	<0.001
$CL_{CPG2} = tvCL_{CPG2} \times Height^{\theta_1}$	5.780	0.016	30.225	<0.001
$V_{CPG2} = tvV_{CPG2} \times BSA^{\theta_1}$	10.747	0.001	32.133	<0.001
$V_{CPG2} = tvV_{CPG2} \times Body\ Weight^{\theta_1}$	9.597	0.002	30.560	<0.001
$V_{CPG2} = tvV_{CPG2} \times Height^{\theta_1}$	4.610	0.032	25.668	<0.001

CPG2, glucarpidase; MTX, methotrexate; BSA, body surface area; tvCL, typical value of clearance; tvV, typical value of distribution volume; NA, not applicable; NC, not calculated; ΔOFV , change of objective function value.

TABLE 4 The final model and bootstrap validation.

CPG2 popPK final model in phase 1	Parameters	Original estimate	Data (95% CI)	Bootstrap median	Estimates (95% CI)
$CL_{CPG2}(L/h) = tvCL_{CPG2} \times BSA^{\theta_1}$ (CV: 3.2%)	$tvCL_{CPG2}$ (L/h)	0.0590	(0.0244–0.0936)	0.0562	(0.0225–0.1160)
	θ_1	3.227	(2.153–4.302)	3.178	(1.759–4.970)
$V_{CPG2}(L) = tvV_{CPG2} \times BSA^{\theta_2}$ (CV: 6.4%)	tvV_{CPG2} (L)	0.957	(0.447–1.467)	0.863	(0.351–1.617)
	θ_2	2.251	(1.230–3.273)	2.277	(1.148–4.040)
Residual variability (mg/L)		0.170			
CPG2 popPK final model in phase 2	Parameters	Original estimate	Data (95% CI)	Bootstrap median	Estimates (95% CI)
$CL_{CPG2}(L/h) = tvCL_{CPG2} \times BSA^{\theta_1}$ (CV: 17.4%)	$tvCL_{CPG2}$ (L/h)	0.238	(0.203–0.270)	0.241	(0.209–0.281)
	θ_1	1.440	(1.105–1.770)	1.425	(1.068–1.733)
$V_{dCPG2}(L) = tvV_{dCPG2} \times BSA^{\theta_2}$ (CV: 22.1%)	tvV_{dCPG2} (L)	1.200	(1.066–1.330)	1.201	(1.010–1.332)
	θ_2	1.561	(1.391–1.730)	1.557	(1.355–1.812)
Residual variability (mg/L)		0.100			
PopPK-PD final model in phase 2	Parameters	Original estimate	Data (95% CI)	Bootstrap median	Estimates (95% CI)
CL_{rMTX} (L/h) = $tvCL_{rMTX} \times Body\ Weight/Scr/60$ (CV: 33.5%)	$tvCL_{rMTX}$ (L/h)	3.248	(1.783–4.712)	2.912	(2.271–4.209)
V_{cMTX} (L) = $tvV_{cMTX} \times Body\ Weight/BSA$ (CV: 29.1%)	tvV_{cMTX} (L)	0.386	(0.229–0.543)	0.347	(0.256–0.539)
V_{pMTX} (L) = $tvV_{pMTX} \times Body\ Weight/60$ (CV: 90.6%)	tvV_{pMTX} (L)	3.052	(1.698–4.405)	3.348	(2.053–5.344)
$V_{max} = tva \times [CPG2\ concentration]$ (CV: 79.8%)	$tv\alpha$ (L/h)	6.545×10^5	(3.666–9.434)	6.242×10^5	$(4.276 \times 10^5 - 8.686 \times 10^5)$
Q (L/h)		0.0778 (Fixed)			
K_m (μ mol)		86 (Fixed)			
Residual variability		1.414			

CPG2, glucarpidase; MTX, methotrexate; CI, confidence interval; CV, coefficient of variation; BSA, body surface area; Scr, serum creatinine; V_{max} , maximum metabolic velocity; $tvCL_r$, typical value of renal clearance; $tvCL$, typical value of clearance; tvV , typical value of distribution volume; tvV_c , typical value of distribution volume in the central compartment; tvV_p , typical value of distribution volume in the peripheral compartment; α , conversion constant between V_{max} and catalyst concentration; K_m , Michaelis–Menten constant; Q , intercompartmental clearance; θ , covariate as an allometric scale.

the phase 1 and 2 studies. Since the phase 1 study showed that the BSA in healthy adults showed small variations compared with those in the phase 2 study including children, the final model of the phase 2 study is considered to reflect more developmental changes. The mean PK parameters normalized by individual body weight in the phase 1 and 2 studies were $CL = 0.0896$ ml/min/kg, $V_d = 51.9$ ml/kg and $CL = 0.0822$ ml/min/kg, $V_d = 56.0$ ml/kg, respectively. The PK parameters in patients with normal and decreased renal function, reported by the PK study PR001-CLN-005 (14), were $CL = 0.0892$ ml/min/kg, $V_d = 58.0$ ml/kg and $CL = 0.0860$ ml/min/kg, $V_d = 67.9$ ml/kg. Since it has been reported that CPG2 has no intracellular translocation, its distribution in the body estimated from the volume of distribution is considered intravascular (14). Since CPG2 is a protein–enzyme preparation with substance properties that are rapidly metabolized regardless of organ function, it was speculated that the population mean PK parameters of CPG2 are not easily affected by pathological conditions. Therefore, no dose adjustment for CPG2 is recommended

in patients with organ dysfunction. In addition, there was no significant difference in the parameters between the Japanese and foreigners, suggesting no ethnic differences in the PK of this drug.

The mean Japanese PK parameters of MTX previously reported in adults with almost normal renal function are as follows (5): $CL_{rMTX} = 5.39$ L/h, $V_{cMTX} = 25.7$ L, $V_{pMTX} = 2.62$ L, and $Q = 0.0951$ L/h (5). In the phase 2 study, MTX-related renal dysfunction was observed in 57.1% (8/14) of the patients. However, the serum creatinine level, which is one of the indicators of renal function, was 1.23 ± 0.89 mg/dl (mean \pm standard deviation) immediately before CPG2 administration, increased to 1.87 ± 1.78 mg/dl on day 4 after CPG2 administration, and decreased to baseline on day 11. These results suggest that the popPK parameters of MTX in this study are appropriate when considering the body size and renal function.

Rebound plasma MTX concentrations were observed in all the patients after the first administration of CPG2. Therefore, more than 48 h of continued monitoring of plasma MTX concentrations is

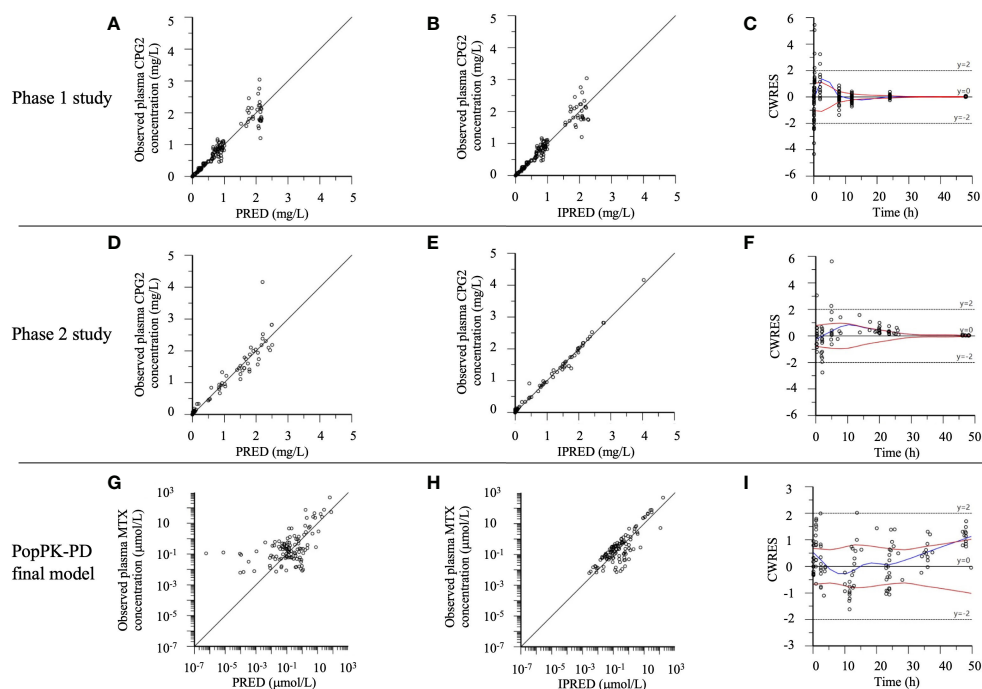


FIGURE 4

The phase 1 and 2 study CPG2, CPG2-MTX popPK-PD final model goodness-of-fit plots. (A–C) Phase 1 study CPG2 final model. (D–F) Phase 2 study CPG2 final model. (G–I) CPG2-MTX popPK-PD final model. (A, D) Observed plasma CPG2 concentrations versus PRED (predicted plasma CPG2 concentrations). (B, E) Observed plasma CPG2 concentrations versus IPRED (individual predicted plasma CPG2 concentration). (C, F, I) CWRES (conditional weighted residuals) versus time. (G) Observed plasma MTX concentrations (logarithmic scale) versus PRED. (H) Observed plasma MTX concentrations (logarithmic scale) versus IPRED.

recommended (8). We verified the performance of the Bayes-estimated plasma MTX concentrations calculated using the CPG2-MTX popPK-PD final model. The RMSE values were gradually increased in order of including sampling points of 24 h, 20 min, 2 h, and 5–8 h. As the number of sampling points increased the RMSE value, the predictive performance tended to decrease. The predictive performance was arithmetically superior when using the plasma MTX

concentrations at pre-CPG2 dosing and 24 h after CPG2 dosing. Bayesian estimation of the plasma MTX concentrations at 48 h based on the obtained popPK-PD model might be useful for MIPD.

This study has several limitations. First, the estimated plasma MTX concentrations at an early time point after CPG2 dosing, based on the CPG2-MTX popPK final model, tended to be underestimated. Therefore, including sampling points within 8 h decreased the

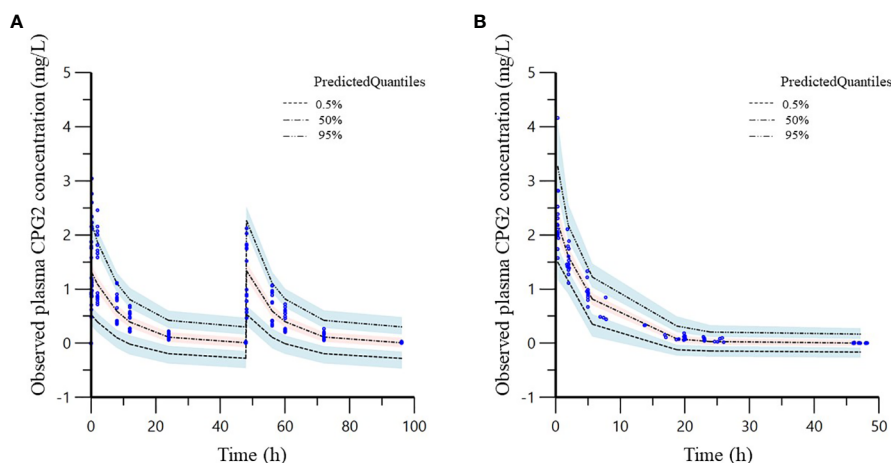


FIGURE 5

Visual predictive check (VPC) of the phase 1 (A) and 2 (B) study CPG2 final model. Quantile deviation (blue shaded) obtained from 1,000 datasets using the final model was superimposed on the observed plasma CPG2 concentration of quantile deviation (red shaded). Blue shaded is 95% confidence intervals for the predicted 5th and 95th percentiles. Red shaded is 95% confidence interval for the predicted 50th percentile. The blue cycles show the observed plasma CPG2 concentrations versus time after CPG2 dosing.

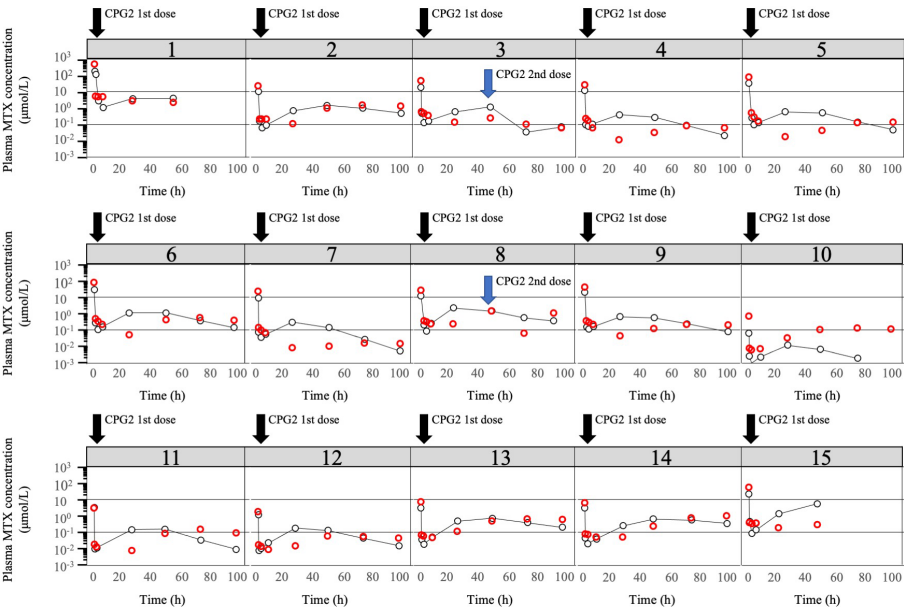


FIGURE 6
Plot of logarithm of observed plasma MTX concentrations and predicted plasma MTX concentrations. Observed plasma MTX concentrations (red cycle) and predicted plasma MTX concentrations (black cycle) using the CPG2-MTX popPK-PD final model versus time in the phase 2 study individual patients ($N = 15$). The two solid black lines represent plasma methotrexate concentrations of 0.1 and 1 $\mu\text{mol/L}$, respectively.

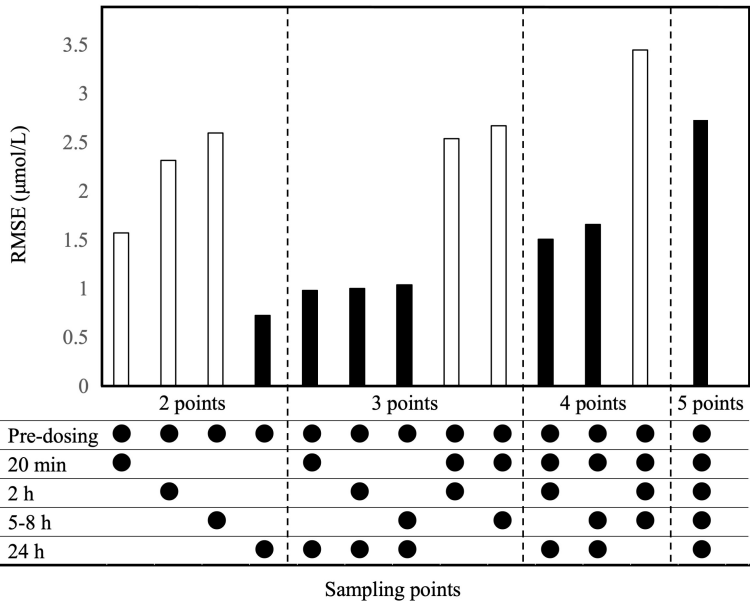


FIGURE 7
Evaluation of RMSE based on the Bayesian estimation of CPG2-MTX popPK-PD final model. Bayesian estimation was conducted for all combinations of sample points. Sampling points are CPG2 pre-dosing, after dosing at 20 min, and 2, 5–8, and 24 h. White bars exclude 24-h values in the sample points, while black bars include 24-h values.

performance of Bayesian estimation of plasma MTX concentrations at 48 h. Second, a fixed value was used for the intercompartmental clearance Q of MTX. This might decrease the performance of Bayesian estimation of rebound in plasma MTX concentrations. Third, renal and extrarenal excretion could not be accurately distinguished because the data did not include urine MTX concentrations. In general, renal clearance is expressed using a glomerular filtration rate as covariate, while extrarenal clearance is

defined as non-glomerular filtration. Accurately, extrarenal clearance and CPG2 clearance of MTX should be shown, but it is difficult to estimate them separately. Non-renal MTX clearance is significantly affected by CPG2 administration because MTX clearance is reduced in patients with delayed MTX excretion. Therefore, the non-renal MTX clearance model was built with CPG2 and unexpected errors (n).
In the phase 2 study, a rebound in plasma MTX concentrations was observed in many cases at a fixed dose (50 U/kg) of CPG2.

However, the plasma MTX concentrations could be managed because the timing of the second dose of CPG2 was predictable. These CPG2-MTX popPK analysis and Bayesian estimation of rebound in plasma MTX concentrations may support early decision-making for the second dose of CPG2.

Data availability statement

The original contributions presented in the study are included in the article/supplementary material, further inquiries can be directed to the corresponding author/s.

Author contributions

HK and TK contributed significantly to the conceptualization and design of the pharmacokinetic study. KY, HH, YY, AO, JH, KK, AK, YK, and HK conducted this trial and collected clinical data. YF, TK, and YH contributed to data analysis and interpretation. YF drafted the manuscript, which was revised by TK and HH. All authors contributed to the article and approved the submitted version.

Funding

This study was supported by the Center for Clinical Trials, Japan Medical Association (identifier: JMA-IIA00078 and JMA-IIA00097).

References

- Green MR, Chamberlain MC. Renal dysfunction during and after high-dose methotrexate. *Cancer Chemother Pharmacol* (2009) 63(4):599–604. doi: 10.1007/s00280-008-0772-0
- Howard SC, McCormick J, Pui CH, Buddington RK, Harvey RD. Preventing and managing toxicities of high-dose methotrexate. *Oncologist* (2016) 21(12):1471–82. doi: 10.1634/theoncologist.2015-0164
- Bleyer WA. The clinical pharmacology of methotrexate: new applications of an old drug. *Cancer* (1978) 41(1):36–51. doi: 10.1002/1097-0142(197801)41:1<36::aid-cnrcr2820410108>3.0.co;2-i
- Seideman P, Beck O, Eksborg S, Wennberg M. The pharmacokinetics of methotrexate and its 7-hydroxy metabolite in patients with rheumatoid arthritis. *Br J Clin Pharmacol* (1993) 35(4):409–12. doi: 10.1111/j.1365-2125.1993.tb04158.x
- Fukuhara K, Ikawa K, Morikawa N, Kumagai K. Population pharmacokinetics of high-dose methotrexate in Japanese adult patients with malignancies: a concurrent analysis of the serum and urine concentration data. *J Clin Pharm Ther* (2008) 33(6):677–84. doi: 10.1111/j.1365-2710.2008.00966.x
- Rhee MS, Galivan J. Conversion of methotrexate to 7-hydroxymethotrexate and 7-hydroxymethotrexate polyglutamates in cultured rat hepatic cells. *Cancer Res* (1986) 46(8):3793–7.
- Donehower RC, Hande KR, Drake JC, Chabner BA. Presence of 2,4-diamino-N10-methylpteroic acid after high-dose methotrexate. *Clin Pharmacol Ther* (1979) 26(1):63–72. doi: 10.1002/cpt.197926163
- Ramsey LB, Balis FM, O'Brien MM, Schmiegelow K, Pauley JL, Bleyer A, et al. Consensus guideline for use of glucarpidase in patients with high-dose methotrexate induced acute kidney injury and delayed methotrexate clearance. *Oncologist* (2018) 23(1):52–61. doi: 10.1634/theoncologist.2017-0243
- Schwartz S, Borner K, Müller K, Martus P, Fischer L, Korfel A, et al. Glucarpidase (carboxypeptidase g2) intervention in adult and elderly cancer patients with renal dysfunction and delayed methotrexate elimination after high-dose methotrexate therapy. *Oncologist* (2007) 12(11):1299–308. doi: 10.1634/theoncologist.12-11-1299
- DeAngelis LM, Tong WP, Lin S, Fleisher M, Bertino JR. Carboxypeptidase G2 rescue after high-dose methotrexate. *J Clin Oncol* (1996) 14(7):2145–9. doi: 10.1200/JCO.1996.14.7.2145
- Widemann BC, Balis FM, Murphy RF, Sorensen JM, Montello MJ, O'Brien M, et al. Carboxypeptidase-G2, thymidine, and leucovorin rescue in cancer patients with methotrexate-induced renal dysfunction. *J Clin Oncol* (1997) 15(5):2125–34. doi: 10.1200/JCO.1997.15.5.2125
- Krause AS, Weihrach MR, Bode U, Fleischhack G, Elter T, Heuer T, et al. Carboxypeptidase-G2 rescue in cancer patients with delayed methotrexate elimination after high-dose methotrexate therapy. *Leuk Lymphoma* (2002) 43(11):2139–43. doi: 10.1080/1042819021000032953
- Buchen S, Ngampolo D, Melton RG, Hasan C, Zoubek A, Henze G, et al. Carboxypeptidase G2 rescue in patients with methotrexate intoxication and renal failure. *Br J Cancer* (2005) 92(3):480–7. doi: 10.1038/sj.bjc.6602337
- Phillips M, Smith W, Balan G, Ward S. Pharmacokinetics of glucarpidase in subjects with normal and impaired renal function. *J Clin Pharmacol* (2008) 48(3):279–84. doi: 10.1177/0091270007311571
- Fukaya Y, Kimura T, Yoshimura K, Umemura K, Kawamoto H. A dose-confirmation phase 1 study to evaluate the safety and pharmacology of glucarpidase in healthy volunteers. *Clin Pharmacol Drug Dev* (2022) 11(3):364–71. doi: 10.1002/cpdd.1010
- Young A, Beriault D, Jung B, Nikonova A, Abosh D, Lee S, et al. DAMPAned methotrexate: A case report and review of the management of acute methotrexate toxicity. *Can J Kidney Health Dis* (2019) 6:1–6. doi: 10.1177/2054358119895078
- Li Z, Gao Y, Yang C, Xiang Y, Zhang W, Zhang T, et al. Assessment and confirmation of species difference in nonlinear pharmacokinetics of atipamezole with physiologically based pharmacokinetic modeling. *Drug Metab Dispos* (2020) 48(1):41–51. doi: 10.1124/dmd.119.089151
- Assessment report by European medicines agency, Voraxaze™ (International non-proprietary name: glucarpidase) (2021). Available at: https://www.ema.europa.eu/en/documents/assessment-report/voraxaze-epar-public-assessment-report_en.pdf (Accessed 27 Aug 2022).

Acknowledgments

We thank Ohara Pharmaceutical Co., Ltd. and BTG International Ltd., which provided the investigational drug and information deemed important to conduct the clinical trial. These companies were not involved in the study design, analysis, interpretation of data, the writing of this article or the decision to submit it for publication.

Conflict of interest

The authors declare that the research was conducted in the absence of any commercial or financial relationships that could be construed as a potential conflict of interest.

Publisher's note

All claims expressed in this article are solely those of the authors and do not necessarily represent those of their affiliated organizations, or those of the publisher, the editors and the reviewers. Any product that may be evaluated in this article, or claim that may be made by its manufacturer, is not guaranteed or endorsed by the publisher.



OPEN ACCESS

EDITED BY

Junmin Zhang,
Lanzhou University, China

REVIEWED BY

Ming Yi,
Zhejiang University, China
Yu Hao,
Sichuan University, China

*CORRESPONDENCE

Xiaoguang Li

✉ lixg@shsmu.edu.cn

Hui Wang

✉ huiwang@shsmu.edu.cn

[†]These authors have contributed equally to this work

SPECIALTY SECTION

This article was submitted to
Pharmacology of Anti-Cancer Drugs,
a section of the journal
Frontiers in Oncology

RECEIVED 07 September 2022

ACCEPTED 27 February 2023

PUBLISHED 08 March 2023

CITATION

Wei Y, Song D, Wang R, Li T, Wang H
and Li X (2023) Dietary fungi in cancer
immunotherapy: From the perspective
of gut microbiota.
Front. Oncol. 13:1038710.
doi: 10.3389/fonc.2023.1038710

COPYRIGHT

© 2023 Wei, Song, Wang, Li, Wang and Li.
This is an open-access article distributed
under the terms of the [Creative Commons
Attribution License \(CC BY\)](#). The use,
distribution or reproduction in other
forums is permitted, provided the original
author(s) and the copyright owner(s) are
credited and that the original publication in
this journal is cited, in accordance with
accepted academic practice. No use,
distribution or reproduction is permitted
which does not comply with these terms.

Dietary fungi in cancer immunotherapy: From the perspective of gut microbiota

Yibing Wei^{1†}, Dingka Song^{1†}, Ran Wang¹, Tingting Li²,
Hui Wang^{1*} and Xiaoguang Li^{1*}

¹State Key Laboratory of Oncogenes and Related Genes, Center for Single-Cell Omics, School of Public Health, Shanghai Jiao Tong University School of Medicine, Shanghai, China, ²College of Medical Technology, Shanghai University of Medicine and Health Sciences, Shanghai, China

Immunotherapies are recently emerged as a new strategy in treating various kinds of cancers which are insensitive to standard therapies, while the clinical application of immunotherapy is largely compromised by the low efficiency and serious side effects. Gut microbiota has been shown critical for the development of different cancer types, and the potential of gut microbiota manipulation through direct implantation or antibiotic-based depletion in regulating the overall efficacy of cancer immunotherapies has also been evaluated. However, the role of dietary supplementations, especially fungal products, in gut microbiota regulation and the enhancement of cancer immunotherapy remains elusive. In the present review, we comprehensively illustrated the limitations of current cancer immunotherapies, the biological functions as well as underlying mechanisms of gut microbiota manipulation in regulating cancer immunotherapies, and the benefits of dietary fungal supplementation in promoting cancer immunotherapies through gut microbiota modulation.

KEYWORDS

cancer, immunotherapy, gut microbiota, dietary intervention, dietary fungi

1 Introduction

The concept of cancer immunotherapy was first carried out by clinicians and immunologists centuries ago, but it had not been widely accepted as a practical option against cancer until recently (1). With the achievement of modern biomedical technologies, various types of immunotherapeutic strategies have been developed, which include the well-known “immune checkpoint blockade (ICB)” therapy (2), represented by the antibodies blocking the cytotoxic T-lymphocyte antigen-4 (CTLA-4) and the programmed cell death 1 (PD-1) and its ligand (PD-L1), as well as the “chimeric antigen receptor T cell (CAR-T)” therapy (3). Besides, many other immunotherapies were also proved to be efficient in treating certain types of cancers (4–7). However, the overall response of cancer patients to immunotherapies varies and serious symptoms were frequently observed, which dampened further utilization of this novel approach (8, 9). For instance, immune-related adverse events (irAEs) were frequently observed in patients

receiving immune-checkpoint inhibitors (ICIs), characterized by excessive inflammation of multiple organs including skin, liver, lung, gastrointestinal tract, endocrine organs, etc. The incidence of irAEs varies among cohorts due to different type of ICIs and cancers (10), however, according to a retrospective study, 91.3% patients were affected by at least one type of irAE following ICI treatments (11). Cytokine release syndrome (CRS), a systemic inflammatory response, was closely associated with patients receiving CAR-T therapies. It was reported that the overall incidence of CRS can be as high as 90% in patients receiving CAR-T treatments (12). Therefore, a comprehensive understanding of the biology of cancer immunotherapy is required to improve its efficiency as well as to eliminate any potential side effects.

In recent years, the emerging role of gut microbiota in human health was emphasized with the development of multi-omic technologies (13). Previous studies have shown that the disruption of gut microbiota homeostasis contributes to the progression of various diseases (14–17). For cancer immunotherapies, the role of gut microbiota in regulating the efficiency as well as side effects of immunotherapy has also been revealed (18), as certain microbial species or related metabolites were shown closely correlated with the higher responsiveness of cancer patients. Nevertheless, the exact molecular mechanisms that how gut microbiota affect the host's response to cancer immunotherapies are still under investigation.

Gut microbiota is composed of trillions of residing microbes, which are strongly affected by consumed nutrients (19); therefore, it is a potential way to manipulate gut microbiota through diet intervention to achieve a better outcome for cancer patients receiving immunotherapies (20). Numerous studies have been conducted on the nutritional value of plant or animal natural products as well as their modulation of gut microbiota and tumor immunotherapy (21, 22). Fungal products as a hot topic in recent years have attracted much attention due to their rich nutritional value and regulating functions to human body, of note, the regulatory role of fungal products on gut microbiota and cancer immunotherapies has been revealed (23). In this review, we will focus on the relationship between intake of natural products and gut microbiota modulation, as well as their biological role and underlying mechanism in cancer immunotherapies.

2 Advances and limitations of current cancer immunotherapies

2.1 Immune checkpoint blockade therapy

Compared with previous standards of care including chemotherapy, radiotherapy, and surgery, immunotherapy is a newly introduced approach, while showing significant improvement in the survival as well as the life quality of cancer patients (24). ICB is one of the most revolutionary technologies based on the theory of “immune surveillance” and the discovery of immune checkpoint molecules including CTLA-4 and PD-1, etc., on T cells (25, 26). Signals transduced by CTLA-4 following CD80/86 binding, and PD-1 following PD-L1 binding inhibit the “hyperactivation” of T cells and are important in preventing

abnormal immune responses commonly seen in autoimmune diseases (27). However, these signals need to be abrogated to enhance the activity of T cells for the clearance of cancer cells (28). According to previous studies, patients treated with monoclonal antibodies against CTLA-4 or PD-1/PD-L1 resulted in dramatic antitumor responses through upregulation of immune activity (29–31). Mechanistic studies revealed that CTLA-4 or PD-1/PD-L1 blockade significantly enhanced T cell receptor (TCR) signals in tumor-specific T cells which leads to stronger tumor-killing activity (32), the infiltration as well as the survival rate of T cells in tumor microenvironment (TME) were also enhanced accordingly (33, 34). Currently, ICB has been approved for use in various types of cancers including melanoma, non-small cell lung cancer (NSCLC), renal cell carcinoma (RCC), squamous cell carcinoma of head and neck (SCCHN), bladder cancer, merkel cell carcinoma, hepatocellular carcinoma, Hodgkin lymphoma as either first-line or second-line treatment (35). Besides, many other agonistic and antagonistic immune checkpoint modulators which target co-stimulatory factors like 4-1BB, ICOS, GITR, OX-40, CD40, etc., are currently under investigation (36).

Along with the achievements in clinical practice, ICB therapy still has many limitations. One notable challenge is the generally low response across different types of cancers (37). Although the efficiency of anti-PD-1/PD-L1 has been clearly addressed in melanoma and NSCLC, the results from other types of cancers are less promising, and the response of individuals to ICB varies, which suggested the effects of other factors including genetics, environment, behavior, and even gut microbiota on the therapeutical efficiency of ICB (38). Another limitation of ICB is the associated side effects, named irAEs (39). IrAEs are excessive inflammatory responses induced by ICB therapies that multiple organs can be affected, even leading to death in some cases. It was reported that the overall irAEs incidence in ICB is around 70–90% (40). The most common symptoms of irAEs involving the skin, gastrointestinal tract, liver, endocrine organs, and lungs, while it varies among different types of cancers and therapies (41). For instance, colitis is the most common type of irAEs in the gastrointestinal tract, which occurred in 10–20% patients receiving ICI treatments (42). Cutaneous irAEs, including rash, pruritus and vitiligo, are also common-seen side effects in ICI therapies, of which approximately 50% patients were affected (43). The exact mechanisms for irAE development are still under investigation, while it was proposed that the over-activated T cell attacking normal tissue, uncontrolled secretion of cytokines, expansion of autoantibodies and even binding of ICI antibodies to normal tissues (the off-target effect) are responsible for the development of irAEs (44, 45).

Interestingly, it has been revealed that gut microbiota may affect the efficacy of ICB therapy as well as the incidence of associated irAEs (46, 47). Fecal material transplantation (FMT) has been shown effective in improving the overall response to PD-1 therapy in patients with melanoma or epithelial tumors, which indicates a substantial role of gut microbiota in modulating host immune response following PD-1 treatment (48, 49). On the other side, one study on melanoma patients receiving anti-CTLA-4 treatment showed that the enrichment of *Bacteroidetes* is strongly

correlated with less frequency of colitis (50), which was supported by others (46, 47). Despite these findings, there is still an urgent need to improve the efficiency as well as eliminate the side effects of ICB, which relies on a deep understanding of the mechanism of the host response to ICB as well as an illustration of the interplay between host immune response, ICB as well as gut microbiota.

In recent years, bispecific antibodies treatment has been recognized as another promising approach in cancer immunotherapies (51). Notably, bispecific antibodies targeting both PD-1/PD-L1 and TGF- β named YM101 and M7824 were developed and achieved superior effects against cancers by overcoming the anti-PD1/PD-L1 drug resistance induced by TGF- β (52–54). Given the established interactions between gut microbiota and cancer immune responses, it would be also worthwhile to investigate the potential effects as well as underlying mechanisms of gut microbiota on the therapeutical efficiency of bispecific antibodies.

2.2 Chimeric antigen receptor therapy

As mentioned earlier, chimeric antigen receptor T cell (CAR-T) therapy is characterized by the genetic modification of T cells to strengthen their capability against cancer cells. Traditionally, T cell activation depends on the interaction between TCR and specific antigens (including tumor cell-associated antigens) presented by the Major Histocompatibility complex (MHC) on the cell surface, which is frequently down-regulated by tumor cells (55). To overcome this, a chimeric antigen receptor protein (which is composed of the ectodomain of cancer antigen-specific B cells and the intracellular domain of T cells) is designed and artificially expressed in normal T cells from patients to produce the CAR-T cells (56). Compared with the normal T cells, CAR-T cells exhibit much higher affinity as well as stronger killing activity against tumor cells both *in vitro* and *in vivo* (57, 58). CAR-T therapy was first developed for treating blood cancers including lymphoma and leukemia and exhibited promising results compared to conventional therapies (59). Currently, CAR-T therapies have been approved for treating various kinds of cancers including relapsed or refractory multiple myeloma, diffuse large B cell lymphoma (DLBCL), high-grade B-cell lymphoma, primary mediastinal large B-cell lymphoma, acute lymphoblastic leukemia (ALL), etc. (60). Additionally, the potential of CAR-T therapy in treating other types of cancers is also evaluated in both clinical and pre-clinical studies (61).

Nevertheless, there are also notable drawbacks of CAR-T therapy, and one of the most challenging issues is the development of tumor resistance to single antigen targeting CAR constructs. Although the administration of CAR-T cells initially yields high response rates, a significant proportion of patients experienced the loss of target antigen expression either partially or completely, which is known as antigen escape (62). It reported that 70–90% of ALL patients show durable responses to CD19 CAR-T therapy in the initial phase; however, it was followed by the downregulation or loss of CD19 antigen expression in 30–70% of the recurrent proportions (63). Consistently, downregulation of other targets including B-cell maturation antigen (BCMA) was also observed in CAR-T treated multiple myeloma patients (64).

Another challenge of CAR-T therapy in clinic is the systemic cytokine release syndrome (CRS), which is characterized by hypotension, cardiac dysfunction, circulatory collapse, respiratory failure, renal failure, multiorgan system failure, etc., and may be life-threatening if not well-controlled (65). Pro-inflammatory IL-1 and IL-6 was identified as the key mediators of CRS in CAR-T therapies; therefore, IL-6/IL-6R blockade has been suggested as potential approaches to eliminate CRS. However, even with the use of tocilizumab, an FDA-approved IL-6R mAb in treating severe CRS, symptoms still persist and eventually lead to patient death (66). To date, an effective strategy against CAR-T therapy-induced CRS is still lacking. In addition, the efficacy of CAR-T therapy on solid tumors is compromised by low ability of tissue infiltration (67), which leads to less promising therapeutic outcomes (68). Localized injection instead of systemic administration was utilized to facilitate tumor infiltration of CAR-T cells, while it is only practical for single tumor lesions/oligometastatic disease (69).

The correlation between gut microbiota and the response/toxicity of CAR-T therapy was recently discovered. According to one cohort study, gut microbiome profile is strongly correlated with response and toxicity following anti-CD19 CAR T cell therapy in B cell malignancy patients, as revealed by distinct bacterial taxa and metabolic pathways in patients treated with/without antibiotics, as well as worse survival and increased neurotoxicity seen in patients exposed to antibiotics (piperacillin/tazobactam, meropenem and imipenem/cilastatin) (70). Nevertheless, there is still largely unknown regarding the role of gut microbiota on CAR-T therapy outcomes and the mechanistic insights are still lacking.

2.3 Other cancer immunotherapies

Beyond the mainstream cancer immunotherapies described above, there are also several other immunotherapies developed or under investigation. IL-2 is a typical example of cytokine therapies and was approved by FDA for treating metastatic renal cell carcinoma in 1992, while the significant toxicities including capillary leak syndrome and multiple organ dysfunction limit the use of IL-2 (71). T cell receptor-engineered T cell (TCR-T) therapy, another subtype of adoptive cell transfer (ACT) therapy just like CAR-T, is characterized by the genetic modification of T cells by implantation with a tumor antigen-specific TCR molecule. The advantage of TCR-T has been well documented in both pre-clinical and clinical studies (72). Beyond that, cancer vaccines and oncolytic virus therapies are also recognized as effective strategies for cancer (4, 5, 61). However, the role of gut microbiota in regulating the efficiency or toxicity of cancer immunotherapies still needs to be addressed.

3 Influence of gut microbiota on cancer immunotherapy

Gut microbiota is a complex community of microorganisms living in digestive tracts, which has the biggest quantities and greatest number of species compared to any other parts of the

body (73). It is well recognized that microbes in human gut play fundamental roles in the well-being of the host. Interactions within constituents of the microbiota (bacteria, viruses, and eukaryotes) as well their relationship with the host immune system influence the development of disease in many ways. For example, it protects the host from pathogens by colonizing mucosal surfaces and secreting various antimicrobial substances, which help enhance the immune response (74). In addition, gut microbiota plays a vital role in digestion and metabolism, controlling epithelial cell proliferation and differentiation, regulating insulin resistance, and brain-gut communication (75). With respect to cancer immunotherapies, the composition, biological activity, and metabolic products derived from gut microbiota were shown to have substantial impacts on efficiency as well as side effects of treatments (Figure 1).

3.1 Gut microbiota affects the efficiency of cancer immunotherapies

The relationship of gut microbiota and anti-PD-1 efficacy in melanoma has been revealed by previous studies. Sivan et al. examined the subcutaneous growth of B16.SIY melanoma in genetically similar C57BL/6 mice raised in two facilities (76). They found that the tumor growth was more aggressive in one group, which was associated with significantly lower intra-tumoral CD8⁺ T cell accumulation and was affected by gut microbiota composition. In line with this, Gopalakrishnan et al. examined the gut microbiota of melanoma patients undergoing anti-PD-1 therapy and observed a significant difference in the diversity and composition of the gut microbiota between responders and non-responders (48). Additionally, a retrospective cohort study found

that exposure to antibiotics in four weeks before CAR-T therapy might reduce patients survival and increase the incidence of neurotoxicity, which underscored the association between gut microbiota and the efficiency of CAR-T therapy (72). The effects of gut microbiota on CAR-T therapy were also proposed and further supported by the observation of close correlation between gut microbial composition and the response to CAR-T therapy (70, 77–79).

The involvement of specific gut microbial species in cancer immunotherapies has also been accessed. Matson et al. examined the stool samples collected from patients with metastatic melanoma before anti-PD-1 immunotherapy and found that *Bifidobacterium longum*, *Collinsella aerofaciens*, and *Enterococcus faecium* were more abundant in responders, indicating the antitumor effects of *Bifidobacterium* species in the context of PD-1 immunotherapy (80). Similarly, previous study showed that the antitumor effects of CTLA-4 blockade depend on distinct *Bacteroides* species, as T cell responses specific for *B. thetaiotaomicron* or *B. fragilis* were associated with the efficacy of CTLA-4 blockade (81).

To determine the biological role of gut microbiota in regulating patients' response to ICB therapy, Davar et al., evaluated the therapeutic efficiency of combined treatment of FMT (from PD-1 responders) and anti-PD-1 administration on patients with PD-1 refractory melanoma (82). It showed that the responders exhibited an increased abundance of taxa that were previously shown to be associated with response to anti-PD-1, increased CD8⁺ T cell activation, and decreased frequency of IL-8 expressing myeloid cells. Additionally, responders had distinct proteomic and metabolomic signatures, and trans-kingdom network analysis revealed the dominant role of gut microbiota in regulating these changes. These results confirmed the effect of gut microbiota in

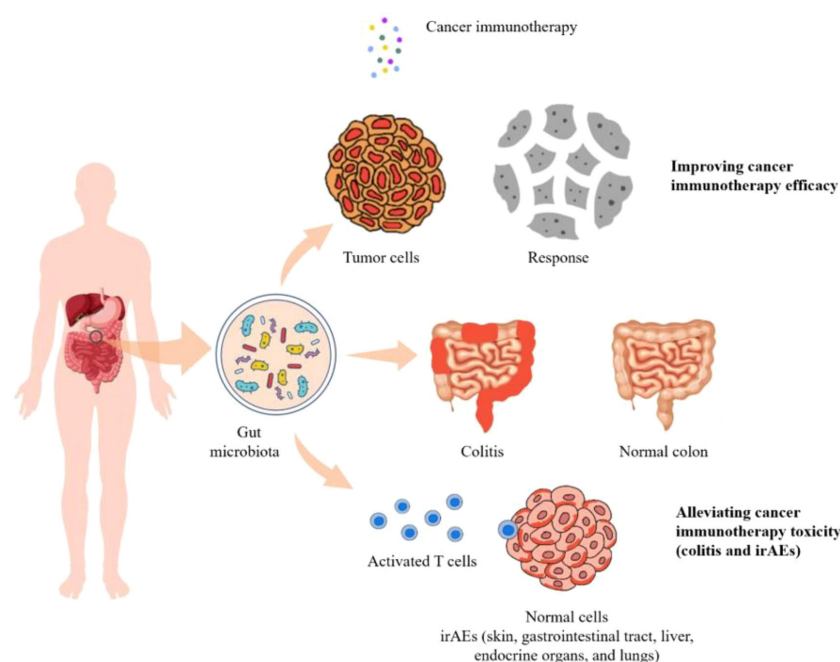


FIGURE 1

The diversity and composition of the gut microbiome can impact the efficacy as well as the toxicity of cancer immunotherapies including colitis and irAEs.

improving anti-PD-1 efficiency against melanoma. In addition to this, gut microbiota had also been found critical in enhancing the efficacy of PD-1 therapy against other cancer types (83).

The biological role of certain gut microbial species in regulating the efficiency of cancer immunotherapies has been addressed by previous studies. It was revealed that *Bifidobacterium* species were beneficial in promoting antitumor immune responses during anti-PD-1 treatment (76). The cause-effect relationship between gut colonization of *B. fragilis* and improved outcome of CTLA-4 blockade therapy has been well demonstrated by fecal material transplantation, and *B. fragilis* implantation approaches (81). In a similar study, Routy et al., uncovered the role of *Akkermansia muciniphila* in regulating the response of melanoma patients to anti-PD-1 treatment (49). Oral supplementation with *A. muciniphila* after fecal material transplantation (FMT) with feces from non-responders significantly restored the efficacy of PD-1 blockade (49). Altogether, these findings highlight the importance of gut microbiota manipulation in improving the efficiency of cancer immunotherapies.

3.2 Gut microbiota affect the toxicities of cancer immunotherapies

Another question regarding gut microbiota in cancer immunotherapies is how the alteration of gut microbes, either in composition or in biological activities, affect the risk of ICB associated toxicities. It showed that the composition of intestinal microbiota can predict whether a patient will develop colitis following treatment with ipilimumab, a monoclonal antibody that blocks CTLA-4 (50). 16S rRNA gene sequencing/16S rDNA sequencing results showed that both the colitis and colitis-free groups had similar microbial compositions before the onset of colitis by ipilimumab administration, however, patients who remained colitis-free following treatment showed a higher proportion of *Bacteroidetes* phylum. Specifically, *Bacteroidaceae*, *Rikenellaceae*, and *Barnesiellaceae* were more abundant in the feces of colitis resistant patients. Metagenomic sequencing analysis further revealed that 4 microbial modules associated with polyamine transport and B vitamin biosynthesis were more abundant in the microbiota of patients who remained colitis-free. In line with this, gut microbiota can also be used for the prediction of side effect risks in anti-PD-1/PD-L1 therapies. According to an observational study, patients with severe irAEs showed higher abundance of *Streptococcus*, *Paecalibacterium*, and *Stenotrophomonas*, while patients with mild irAEs were enriched in *Faecalibacterium* and *Lachnospiraceae* (84). Similarly, another clinical study revealed the distinct compositional differences in gut microbiota between patients who experienced clinically significant or non-significant irAEs (85). In a more comprehensive study led by Dr. Jennifer Wargo, blood, tumor, and gut microbiome of 77 patients with advanced melanoma treated with combined immune checkpoint blockade (CICB) targeting PD-1 and CTLA-4 were profiled, and a significantly higher abundance of *Bacteroides intestinalis* was found in patients with toxicity characterized by colitis and upregulation of mucosal IL-1 β (47). In addition, as mentioned above, exposure to antibiotics was correlated

with a high incidence of neurotoxicity in B cell lymphoma and leukemia patients receiving CD19 CAR-T therapy (70). This indirectly confirmed that the gut microbiota could alleviate the related side effects of CAR-T therapy.

As another common side effect of ICB, colitis is commonly treated with immunosuppressive drugs, including corticosteroids and/or agents targeting tumor-necrosis factor- α (TNF- α), all of such have obvious side effects (86). Clinical evidence showing that colitis and inflammatory bowel disease (IBD) can be successfully treated by gut microbiota manipulation aroused the interest to develop new strategies against ICB-induced colitis (87, 88). It revealed that FMT treatment significantly reduced the incidence and severity of colitis in patients receiving ICB therapies, with a relative increase in the proportion of regulatory T-cells within the colonic mucosa area, although the sample number is too limit (n=2) to draw a firm conclusion (46).

Overall, the biological roles of gut microbiota in regulating efficacy as well as toxicity of cancer immunotherapies have been well documented, which is indicative the future development of new strategies in boosting cancer immunotherapy.

4 Dietary fungi in cancer immunotherapies

4.1 Overview of dietary products, gut microbiota, and cancer immunotherapy

With a deeper understanding of gut microbiota, potential ways to optimize gut microbiota in patients and healthy people have also been evaluated recently. Fecal microbiota transplantation (FMT) and single bacteria transplantation (probiotic administration) have achieved promising results in improving the wellness of patients, however, it may be detrimental for patients exposed to the allogenic strains for FMT and make people vulnerable to chronic diseases such as autoimmune disease (AID) (89, 90). Instead, diet intervention or prebiotic supplementation may be more suitable for the general population as it is considered less harmful and easier to be accepted (91). Meanwhile, the regulatory mechanism of diet intervention on gut microbiota is necessary to be elucidated as a pre-requirement. Researchers have been working in this field for decades and many dietary supplements were identified to have “microbiota-modulating” activity. In general, animal-based diets resulted in higher levels of amino acid fermentation products and lower levels of carbohydrate fermentation products, while the levels of amino acid fermentation products were positively correlated with the amounts of putrefactive, bile-tolerant microbes like *Bacteroides* and *Clostridia*, saccharolytic microbes were increased as well. In contrast, beneficial bacteria, like *Bifidobacteria* and *Eubacteria* were negatively correlated with the consumption of animal products (92). In line with this, high-fat and animal-based diets can promote the growth of *Bilophila wadsworthia*—a bacteria producing hydrogen sulfide (H₂S), which is presumably responsible for GI inflammation (93). Nevertheless, high consumption of polyunsaturated fats fosters *Ruminococcus* growth inside the gut (94). The role of fiber in plant-based diets has been revealed by

several studies. For instance, diets rich in carbohydrates and fiber increase the variety and richness of gut microbiota, characterized by the increase of *Bacteroidetes* and decrease of *Firmicutes/Bacteroidetes* ratio (95). High fiber intake also boosted the outgrowth of *Firmicutes* and *Proteobacteria*, which were usually low in subjects consuming high-fat diets (96). In contrast to that, the high intake of simple sugar instead of fiber resulted in a substantial outgrowth of *Bacteroides* (97). Vegetarian diets do not contain any meat or fish while rich in carbohydrates and fiber. Consumption of vegetarian diets led to increased production of short chain fatty acids (SCFA), which is beneficial in preventing GI inflammation and maintaining the homeostasis of microbial flora in the gut (98). Moreover, it was found that protein consumption increases the diversity of gut microbiota; however, the effects vary depending on the source of proteins. Notably, whey and pea protein consumption increased the levels of *Bifidobacterium* and *Lactobacillus*, while limiting the growth of *Bacteroides fragilis* and *Clostridium perfringens*. In addition, pea protein increased the level of SCFA in GI levels. Meanwhile, an animal-protein-based diet stimulates bile-tolerant anaerobes (90).

Along with the assessment of the role of animal or plant-based diets on gut microbiota, modulating activity of phytochemicals as well as prebiotics on gut microbiota was also evaluated. Phytochemicals, including polyphenols, carotenoids, phytosterols/phytosterols, lignans, alkaloids, have been shown to have positive effects on the modulation of gut microbiota (99). Supplementation of carotenoids such as astaxanthin or retinoic acid help maintains intestinal immune homeostasis by inducing IgA production (100). One study showed that bilberry anthocyanin consumption promoted the efficiency of ICB by modulating the composition of gut microbiota (21). They found that the antitumor efficiency of anti-PD-L1 antibody was enhanced by oral administration of bilberry anthocyanin extracts in a mouse tumor model, which was accompanied by the enrichment of *Clostridia* and *Lactobacillus johnsonii* in feces. Prebiotics, including fructooligosaccharides, galactooligosaccharides, soybean oligosaccharides, inulin, etc., exert benefits in the regulation of gut microbiota by increasing the population of commensals like *Lactobacillus* and *Bifidobacterium* (100). One study reported that orally administered inulin gel could enhance the antitumor efficacy of α -PD-1 therapy via modulating commensal microorganisms in situ, as well as lead to a potent long-lived antitumor effect via eliciting memory CD8⁺ T-cell responses (101). Overall, despite interesting findings on natural products from plants and animals, few studies have investigated natural products from dietary fungus, which may also have potential effects on the regulation of composition as well as biological activity of gut microbes.

4.2 Impact of dietary fungi on gut microbiota

Compared with extensive research on the effect of plants or animal-derived diets on gut microbiota regulation, the role of dietary fungus remained unexplored until recently. *Lentinula edodes* (shiitake) is an edible mushroom enriched with different types of polysaccharides

(102), it showed that administration of heteropolysaccharides from *Lentinula* significantly altered the diversity of microbiota in the small intestine, cecum, colon, and the distal colon (feces) in mice (103). Specifically, the decrease of *Bacteroidetes* was associated with the increase of *Proteobacteria*. Of note, *Chloroflexi*, *Gemmatimonadetes*, *Nitrospirae*, and *Planctomycetes* are exclusively present in treated mice. One study reported that *Lentinula edodes* by-products (LESDF-3) could promote the production of *Bacteroides*, indicating the importance of LESDF on the regulation of gut microbiota (104). In line with this, several studies also demonstrated the biological functions of polysaccharides from *Cordyceps Sinensis*, *Auricularia auricular-judae*, *Ganoderma lucidum*, *Grifola frondose*, *Pleurotus ostreatus*, *Hericium erinaceus*, and wild morels in reshaping gut microbiota and immune regulation (105–111). *Ganoderma lucidum* has long been considered valuable in medication and diet supplementation. According to a recent study, spore oil from *Ganoderma lucidum* has strong immunoenhancing activity, which was correlated with the elevated abundance of several bacterial genera (*Lactobacillus*, *Turicibacter*, and *Romboutsia*) and species (*Lactobacillus intestinalis* and *Lactobacillus reuteri*), as well as reduced level of *Staphylococcus* and *Helicobacter* (112). Those alterations in gut microbiota further resulted in the secretion of a range of key metabolites such as dopamine, prolyl-glutamine, pentahomomethionine, leucyl-glutamine, L-threonine, stearyl-carnitine, dolichyl β -D-glucosyl phosphate to enhance phagocytosis of macrophages and NK cell cytotoxicity. Inulin, a type of natural polysaccharide that exists in various kinds of natural products has been recognized as a powerful probiotic (113), interestingly, β -glucan from dietary fungus also exhibited comparative effects with inulin (114). Specifically, β -glucan could modulate the structure and composition of gut microbiota by inhibiting the proliferation of harmful gut microbiota while upregulating the abundance of beneficial *Bacteroidetes*. Furthermore, both β -glucan and inulin could selectively promote the growth of *Bifidobacterium*. D-glucan from mushrooms also showed similar effects on gut microbiota modulation and thus it can be considered a new type of probiotic. A list of dietary fungi and their roles in modulating gut microbiota is summarized in Table 1.

4.3 Impact of dietary fungi on cancer immunotherapy

Despite the well-known effects of plant-based or animal-based diets on cancer immunotherapy, the relationship between dietary fungus and the efficiency of cancer immunotherapy remains elusive. Previous studies have investigated the role of key components from dietary fungus in cancer immune regulation. The main component of the fungal cell wall is β -Glucan, which has been reported to function as potent immunomodulators to enhance antitumor immune responses by regulating differentiation and function of monocytic myeloid-derived suppressor cells (MDSCs) (115). Consistently, polysaccharides from *Agaricus blazei* Murill stimulated MDSC differentiation from M2 to M1 type, which mediates inhibition of tumor immune evasion via the Toll-like receptor 2 (TLR2) (116). It was later revealed that natural killer (NK) cells, macrophages, and dendritic cells are responsible in

TABLE 1 List of dietary fungi, the bioactive components, and their role in modulating gut microbiota.

Name	Bioactive components	Biological effect on gut microbiota	Reference
<i>Lentinula edodes</i>	LESDF	LESDF-2: upregulating the abundance of <i>Faecalibacterium</i> and <i>Bifidobacterium</i> ; LESDF-3: <i>Bacteroides</i> , <i>Parasutterella</i> , <i>Parabacteroides</i> and <i>Lachnospira</i>	(104)
<i>Cordyceps Sinensis</i>	Polysaccharides	Downregulating the abundance of <i>Bacteroidetes</i> . Upregulating the abundance of <i>Proteobacteria</i> , <i>Actinobacteria</i> and <i>Acidobacteria</i>	(105)
<i>Auricularia auricular-judae</i>	Polysaccharides	Downregulating the abundance of <i>Ruminococcus</i> , <i>Deferribacteres</i> and <i>Actinobacteria</i> compared to control (IBD model)	(106)
<i>Ganoderma lucidum</i>	Polysaccharides	Upregulating the abundance of <i>Blautia</i> , <i>Dehalobacterium</i> , <i>Parabacteroides</i> , and <i>Bacteroides</i> , while downregulating the levels of <i>Aerococcus</i> , <i>Ruminococcus</i> , <i>Corynebacterium</i> and <i>Proteus</i>	(107)
<i>Grifola frondose</i>	Pseudobaptigenin and cyanidin 3-o-xylosylrutinoside	Upregulating the abundance of <i>Paraprevotella</i> , <i>Porphyromonadaceae</i> , <i>Anaerotruncus</i> , <i>Barnesiella</i> , <i>Parasutterella</i> , and <i>Desulfovibrionaceae</i> .	(108)
<i>Pleurotus ostreatus</i>	Polysaccharides	Upregulating the abundance of α -proteobacteria and γ -proteobacteria	(109)
<i>Hericium erinaceus</i>	Polysaccharides, peptides, crude fat, etc.	Upregulating the abundance of <i>Bifidobacterium</i> , <i>Bacteroides</i> and SCFAs-producing bacteria such as <i>Roseburia</i> and <i>Faecalibacterium</i> , etc.	(110)
<i>Wild morels</i>	Polysaccharides	Upregulating the abundance of <i>Bacteroidetes</i> , <i>Lachnospiraceae</i> and the total levels of the SCFA-producing bacteria <i>Lachnospiraceae</i> , <i>Ruminococcaceae</i> , <i>Erysipelotrichaceae</i>	(111)
<i>Ganoderma lucidum</i>	Triterpenes and fatty acids	Downregulating the abundance of <i>Firmicutes</i> while upregulating the abundance of <i>Bacteroidetes</i> .	(112)

mediating fungal products originated antitumor immune response. According to one study, *Agaricus bisporus* polysaccharides MH751906 exerted immunotherapeutic effect on colon cancer by activating gut-residing NK cells, and these activated NK cells played a stable role in killing human colon cancer cells (117). In line with this, another study reported that *Boletus edulis* RNA could also stimulate NK cells against myelogenous leukemia (118). In addition, one study indicated that polysaccharides from *Luchnum* boosted antitumor immune responses by resetting tumor-associated macrophages (TAMs) from the “pro-tumor” M2 to the “antitumor” M1 phenotype (119). Another study uncovered the immunomodulatory activity of polysaccharide–protein complex from *Polyporus rhinocerus*, exerting antitumor effects by activating macrophage-mediated host immune response (120). *Ganoderma lucidum* polysaccharides could partially or completely antagonize the suppression of B16F10 melanoma cells on the viability of peritoneal macrophages, suggesting its potential role in cancer immunotherapy (121). Following study found that the antitumor effect of *Ganoderma lucidum* was from the stimulation of dendritic cell maturation and initiation of the adaptive immune response towards T helper 1 (Th1) polarization *in vivo* (122). Both studies indicated the immunomodulatory mechanism mediated by *Ganoderma lucidum* in the antitumor process. Additionally, polysaccharopeptide (PSP) extracted from *Coriolus versicolor* showed immunotherapeutic effects against tumors *via* strengthening the phagocytosis of macrophages, increasing the expression of cytokines and chemokines, as well as stimulating the infiltration of both dendritic cells and T-cells into tumors (123).

The exact role of dietary fungi in cancer immunotherapy is still largely unknown except for a few studies reported the relevant effects. One study revealed *Cordyceps militaris* polysaccharide

converted immunosuppressive macrophages into M1 phenotype and activated T lymphocytes by inhibiting the PD-1/PD-L1 axis between TAMs and T lymphocytes, which may improve the effectiveness of anti-PD-1/PD-L1 immunotherapy (124). Another study showed that *Ginseng* polysaccharides altered the gut microbiota and kynurenine/tryptophan ratio, potentiating the antitumor effect of PD-1/PD-L1 immunotherapy (125), which elucidated the axis of action of fungal polysaccharides through the gut microbiota to strengthen the antitumor effects of ICB. In addition to enhancing the therapeutic effect of ICB, taking fungal products has also been reported to improve the efficacy of cancer vaccines. Oral ingestion of *Lentinula edodes* mycelia extracts could enhance the antitumor activity of peptide vaccine, which indicated that *Lentinus edodes* extracts play a vital role in cancer immunotherapy (126). Collectively, it is of particular interest to comprehensively understand the role as well as the molecular mechanism of dietary fungus in cancer immunotherapy, and the involvement of gut microbiota in this process also needs to be further addressed. A list of dietary fungi and their roles in modulating host immune response against cancers is summarized in Table 2.

4.4 Clinical studies for dietary fungi on cancer immunotherapy

To date, a few clinical studies have been conducted to evaluate the antitumor activities of fungal products and the underlying mechanisms. It showed that *Grifola frondose* could inhibit lung or breast cancer metastasis and decrease the size of tumors (127), which was achieved by increasing NK cell activity and promoting Th1

response, while with the reduced Th2 activity. Another study showed that *Ganoderma lucidum* polysaccharide has antitumor effects on various types of advanced-stage cancer, which was achieved by stimulating host immune response, including the increased secretion of IL-2, IL-6, IFN- γ , and enhanced NK cell activity, whereas the concentration of IL-1 β and TNF- α was reduced compared with baseline (128). According to a study conducted by Zhao et al., 48 breast cancer patients were treated with *Ganoderma lucidum* spore powder, and it was shown that the concentrations of TNF- α and IL-6 in the serum of patients after treatment decreased significantly, which was accompanied by reduced tumor burden (129). In addition, *Pleurotus cornucopiae* (Oyster mushroom, Tamogitake) was also found to have antitumor effects through host immune regulation. Tanaka et al. conducted a clinical trial to investigate the antitumor activity of *P. cornucopiae*, and it was found that the levels of serum IFN- γ and IL-12 increased along with NK cell activity, suggesting the involvement of Th1 immune response in *P. cornucopiae* directed antitumor activity (130). The antitumor effects on adenocarcinoma as well as the immunomodulation activity of active hexose correlated compound (AHCC, obtained from *Lentinus edodes* of Basidiomycete mushroom) was also evaluated clinically, it showed that AHCC treatment led to the increase of neutrophils, the ratio of CD3⁺/CD4⁺, CD4⁺/CD8⁺, CD3⁺/CD16⁺/CD56⁺ NK cells were also increased accordingly, while the number of lymphocytes and monocytes were reduced (131). In addition, a phase I trial demonstrated the antitumor effect of *Agaricus bisporus* on prostate cancer by modulating IL-15 level and

MDSC activity (132). Recently, several clinical trials are underway to evaluate the antitumor effect of additional fungal extracts and to explore the underlying immunomodulatory mechanisms, while the results have not been reported yet (133). Overall, the antitumor effects of fungal products as well as the molecular mechanisms are well documented, however, most conclusions are drawn only based on small samples. Furthermore, though clinical studies have validated that fungal products can enhance the antitumor effects of chemotherapy and radiotherapy (133), clinical evidence regarding the efficacy of fungal products in cancer immunotherapies is still lacking. Therefore, additional trials are required to investigate the clinical effect of fungal products on cancer immunotherapies. A list of current clinical studies investigating the effects of dietary fungi in different cancers is summarized in Table 3.

5 Conclusion

With the advanced achievement of high-throughput multi-omic technologies including microbial amplicon, meta-genomic, meta-transcriptomic, metabolomic and interatomic analysis in recent years, the biological relevance of gut microbiota on human health has been well recognized. Preclinical studies demonstrated the diverse functions of gut microbe in regulating host immune homeostasis, which is beneficial to protect against many diseases, and in particular, the improvement of cancer immunotherapies. Clinical studies again demonstrated gut microbiota modulating strategies in promoting the

TABLE 2 Biological roles and mechanisms of dietary fungi in treating various types of cancers.

Name	Cancer type	Biological effects on host immune response	Reference
<i>Agaricus blazei Murill</i>	Cervical cancer	<i>Agaricus blazei</i> Murill Polysaccharide selectively block the Toll-like receptor 2 (TLR2) signal to stimulate myeloid-derived suppressor cell differentiation from M2 to M1 type.	(116)
<i>Agaricus bisporus</i>	Colon cancer	<i>Agaricus bisporus</i> polysaccharides activate gut resident natural killer cells.	(117)
<i>Boletus edulis</i>	Myelogenous leukemia	<i>Boletus edulis</i> RNA fraction enhances NK cell activity against Myelogenous Leukemia Cells.	(118)
<i>Luchnum</i>	Sarcoma	<i>Lachnum</i> polysaccharide resets TAMs from pro-tumor M2 to anti-tumor M1 phenotype, resulting in the accumulation of anti-tumor immune cells while decreasing the infiltration of immunosuppressive cells such as myeloid-derived suppressor cells (MDSCs) and Treg cells.	(119)
<i>Ganoderma lucidum</i>	Melanoma	<i>Ganoderma lucidum</i> suppresses the viability, phagocytic activity, NO production, TNF- α production and activity in peritoneal macrophages suppressed by B16F10.	(121)
<i>Ganoderma lucidum</i>	Colon adenocarcinoma, melanoma, and sarcoma	Purified polysaccharide fraction from <i>Ganoderma lucidum</i> exerted antitumor effects by stimulating dendritic cell mature and initiating adaptive immune response towards T helper 1 polarization <i>in vivo</i>	(122)
<i>Coriolus versicolor</i>	Not specified	<i>Coriolus versicolor</i> poly-saccharopeptide promotes the phagocytosis of macrophages, increasing the expression of cytokines and chemokines, and stimulating the infiltration of both dendritic cells and T-cells into tumors.	(123)
<i>Cordyceps militaris</i>	Breast cancer and lung cancer	<i>Cordyceps militaris</i> polysaccharides reset TAMs from a tumour-promoting M2 phenotype to a tumour-killing M1 phenotype by inhibiting the PD-L1/PD-1 axis between TAMs and T lymphocytes to reverse the functional inhibition of T lymphocytes.	(124)
<i>Ginseng</i>	Lung cancer	<i>Ginseng</i> polysaccharides enhance the efficacy of α PD-1 mAb by regulating gut microbiota and decreasing L-kynurenine, as well as the ratio of Kyn/Trp.	(125)
<i>Lentinula edodes</i>	Melanoma	<i>Lentinula edodes</i> mycelia extract enhances peptide vaccine-induced anti-tumor activity by inhibiting the increase of the percentage of Tregs in tumor-bearing hosts.	(126)

TABLE 3 Clinical evidence of dietary fungi in treating different types of cancers.

Name	Cancer Type	Type of study	Main results	Reference
<i>Maitake</i> (<i>Grifola frondosa</i>)	Lung and breast cancer, stage II–IV	Interventional clinical trial, n=10	Maitake D-Fraction could inhibit lung or breast cancer metastasis and decrease the size of tumors, and NK cell activity was significantly elevated.	(127)
<i>Ganoderma lucidum</i>	Advanced-stage cancers arising from various tissues	Interventional clinical trial, n=34	Enhanced host immune responses (a significant increase in IL-2, IL-6, IFN- γ CD56+ cells and NK activity compared with baseline) in patients with advanced-stage cancer.	(128)
<i>Ganoderma lucidum</i>	Breast cancer patients with cancer-related fatigue undergoing endocrine therapy	RCT, n=48	Significant decrease in TNF- α and IL-6 in serum, beneficial effects on cancer-related fatigue and quality of life compared to placebo.	(129)
<i>Lentinula edodes</i>	Adenocarcinoma (pancreatic, lung, colorectal)	Interventional clinical trial, n=7	A consistent increase in neutrophils, the ratio of CD3+/CD4+, CD4+/CD8+, CD3+/CD16+/CD56+ NK cells, while decrease in lymphocytes and monocytes	(131)
<i>Agaricus bisporus</i>	Prostate cancer	Single-arm, unblinded, single-facilit, phase I trial (n=36)	Promising effect against prostate cancer by modulating IL-15 level and MDSC activity.	(132)

outcome of patients. Despite the discovery of various beneficial or harmful microbes/metabolites, however, the underlying mechanism remains unclear, which dampens further development of precise manipulation of gut microbiota. FMT has been proven to be effective in preclinical and clinical studies, while concerns regarding the safety of transferring fecal materials still exist. In 2019, it was reported that 2 patients receiving FMT treatment developed invasive infections caused by multidrug-resistant organisms (MDRO) and one of the patients eventually died (134). FDA of United States warned about potential risk of serious infections caused by MDRO related to the investigational use of FMT (135). Therefore, it is necessary to keep alert to FMT therapy-induced adverse events in further clinical investigation. Diet interventions, on the side, are much less concerning as it has been long accepted as common sense, but the effectiveness in gut microbiota modulation has not been well addressed. To solve this problem, studies have tried to identify the “key gradients” of daily diet or supplements, and polysaccharides, or “diet fiber” was eventually demonstrated to be essential for promoting the growth of commensals and maintaining a healthy gut environment; saturated acid from animal products, on the side, were shown negatively impact the gut microbiota characterized by the outgrowth of harmful microbes and production of pro-inflammatory factors. Regardless, it remains elusive for the effects of many other components, the underlying mechanism has yet to be clarified as well.

Immunotherapies have been demonstrated successful in treating various types of cancers and the improvement of patients' well beings. Meanwhile, the effectiveness varies across individuals along with serious side effects such as neurotoxicity, cytokine release syndrome, colitis, etc. Since gut microbiota was shown closely related to clinical features of cancer patients upon treatment, it is applicable to predict the outcome of any individuals by accessing their gut microbiota. In fact, previous studies have demonstrated the efficiency of such strategies. Beyond that, gut microbiota has also been shown important in regulating the immune response of the host, which highlights its potential role in cancer immunotherapies. To achieve this, many studies have revealed the biological functions of the specific gut microbe and/or metabolites in boosting cancer immunotherapies both pre-clinically and clinically by

FMT or single strain administration. Nevertheless, how diet intervention affects the behavior of gut microbiota and how is it related to cancer immunotherapy remains unclear. These questions need to be addressed by molecular identification of effective factors from diet and the validation of their functions by pre-clinical and clinical interventions.

Fungi have long been used in diet and medications, while their effects on gut microbiota had not been noticed until recently (102). Like plant or animal products, edible fungi contain various types of nutrients which can be recognized by gut microbes. As mentioned, the roles of dietary fungi on gut microbiota were discovered and the effective components were also pinpointed in recent studies. However, systemic screenings of fungi-derived components on gut microbiota are still lacking, which is the pre-requirement for a comprehensive understanding of the interplays between dietary fungi and gut microbes, and more studies are needed to identify the underlying mechanism. Ultimately, investigations of dietary fungi and gut microbiota will pave the way to developing therapies against cancer in combination with current immunotherapeutic approaches.

Author contributions

YW, DS, HW, and XL made substantial contributions to the design, data collection, and writing of this manuscript. RW and TL assisted in data evaluation and helpful discussion. HW and XL supervised the project. All authors contributed to the article and approved the submitted version.

Funding

This study was supported by grants from the National Natural Science Foundation of China (82030099, 81972820), the Natural Science Foundation of Shanghai (22ZR1435900), the National Key R&D Program of China (2018YFC2000700), the Science and Technology Commission of Shanghai Municipality (22DZ2303000), Innovative research team of high-level local universities in Shanghai

and Shanghai Jiao Tong University Key Program of Medical Engineering (YG2021ZD01).

Conflict of interest

The authors declare that the research was conducted in the absence of any commercial or financial relationships that could be construed as a potential conflict of interest.

References

- Waldman AD, Fritz JM, Lenardo MJ. A guide to cancer immunotherapy: From T cell basic science to clinical practice. *Nat Rev Immunol* (2020) 20(11):651–68. doi: 10.1038/s41577-020-0306-5
- Postow MA, Callahan MK, Wolchok JD. Immune checkpoint blockade in cancer therapy. *J Clin Oncol* (2015) 33(17):1974–82. doi: 10.1200/JCO.2014.59.4358
- June CH, O'Connor RS, Kawalekar OU, Ghassemi S, Milone MC. Car T cell immunotherapy for human cancer. *Science* (2018) 359(6382):1361–5. doi: 10.1126/science.aar6711
- Wang RF, Rosenberg SA. Human tumor antigens for cancer vaccine development. *Immunol Rev* (1999) 170:85–100. doi: 10.1111/j.1600-065X.1999.tb01331.x
- Fukuhara H, Ino Y, Todo T. Oncolytic virus therapy: A new era of cancer treatment at dawn. *Cancer Sci* (2016) 107(10):1373–9. doi: 10.1111/cas.13027
- Zhao Q, Jiang Y, Xiang S, Kaboli PJ, Shen J, Zhao Y, et al. Engineered tcr-T cell immunotherapy in anticancer precision medicine: Pros and cons. *Front Immunol* (2021) 12:658753. doi: 10.3389/fimmu.2021.658753
- Fujii S, Shimizu K, Okamoto Y, Kunii N, Nakayama T, Motohashi S, et al. Nkt cells as an ideal anti-tumor immunotherapeutic. *Front Immunol* (2013) 4:409. doi: 10.3389/fimmu.2013.00409
- Tan S, Li D, Zhu X. Cancer immunotherapy: Pros, cons and beyond. *BioMed Pharmacother* (2020) 124:109821. doi: 10.1016/j.biopha.2020.109821
- Kennedy LB, Salama AKS. A review of cancer immunotherapy toxicity. *CA: A Cancer J Clin* (2020) 70(2):86–104. doi: 10.3322/caac.21596
- Martins F, Sofiya L, Sykietis GP, Lamine F, Maillard M, Fraga M, et al. Adverse effects of immune-checkpoint inhibitors: Epidemiology, management and surveillance. *Nat Rev Clin Oncol* (2019) 16(9):563–80. doi: 10.1038/s41571-019-0218-0
- Thapa B, Roopkumar J, Kim AS, Gervaso L, Patil PD, Calabrese C, et al. Incidence and clinical pattern of immune related adverse effects (Irae) due to immune checkpoint inhibitors (Ici). *J Clin Oncol* (2019) 37(15_suppl):e14151–e. doi: 10.1200/JCO.2019.37.15_suppl.e14151
- Yan Z, Zhang H, Cao J, Zhang C, Liu H, Huang H, et al. Characteristics and risk factors of cytokine release syndrome in chimeric antigen receptor T cell treatment. *Front Immunol* (2021) 12. doi: 10.3389/fimmu.2021.611366
- Fan Y, Pedersen O. Gut microbiota in human metabolic health and disease. *Nat Rev Microbiol* (2021) 19(1):55–71. doi: 10.1038/s41579-020-0433-9
- Belkaid Y, Hand TW. Role of the microbiota in immunity and inflammation. *Cell* (2014) 157(1):121–41. doi: 10.1016/j.cell.2014.03.011
- Pascale A, Marchesi N, Marelli C, Coppola A, Luzzi L, Govoni S, et al. Microbiota and metabolic diseases. *Endocrine* (2018) 61(3):357–71. doi: 10.1007/s12020-018-1605-5
- Maiuolo J, Gliozi M, Musolino V, Carresi C, Scarano F, Nucera S, et al. The contribution of gut microbiota-brain axis in the development of brain disorders. *Front Neurosci* (2021) 15:616883. doi: 10.3389/fnins.2021.616883
- Cheng WY, Wu C-Y, Yu J. The role of gut microbiota in cancer treatment: Friend or foe? *Gut* (2020) 69(10):1867. doi: 10.1136/gutjnl-2020-321153
- Zhou C-B, Zhou Y-L, Fang J-Y. Gut microbiota in cancer immune response and immunotherapy. *Trends Cancer* (2021) 7(7):647–60. doi: 10.1016/j.trecan.2021.01.010
- Leeming ER, Johnson AJ, Spector TD, Le Roy CI. Effect of diet on the gut microbiota: Rethinking intervention duration. *Nutrients* (2019) 11(12):2862. doi: 10.3390/nu11122862
- Matson V, Gajewski TF. Dietary modulation of the gut microbiome as an immunoregulatory intervention. *Cancer Cell* (2022) 40(3):246–8. doi: 10.1016/j.ccell.2022.02.014
- Wang L, Jiang G, Jing N, Liu X, Li Q, Liang W, et al. Bilberry anthocyanin extracts enhance anti-Pd-L1 efficiency by modulating gut microbiota. *Food Funct* (2020) 11(4):3180–90. doi: 10.1039/d0fo00255k
- Spencer CN, McQuade JL, Gopalakrishnan V, McCulloch JA, Vetizou M, Cogdill AP, et al. Dietary fiber and probiotics influence the gut microbiome and melanoma immunotherapy response. *Science* (2021) 374(6575):1632–40. doi: 10.1126/science.aaz7015
- Ayeka PA. Potential of mushroom compounds as immunomodulators in cancer immunotherapy: A review. *Evidence-Based Complementary Altern Med* (2018) 2018:7271509. doi: 10.1155/2018/7271509
- Mellman I, Coukos G, Dranoff G. Cancer immunotherapy comes of age. *Nature* (2011) 480(7378):480–9. doi: 10.1038/nature10673
- Kim R, Emi M, Tanabe K. Cancer immunoeediting from immune surveillance to immune escape. *Immunology* (2007) 121(1):1–14. doi: 10.1111/j.1365-2567.2007.02587.x
- Pardoll DM. The blockade of immune checkpoints in cancer immunotherapy. *Nat Rev Cancer* (2012) 12(4):252–64. doi: 10.1038/nrc3239
- Orabona C, Mondanelli G, Puccetti P, Grohmann U. Immune checkpoint molecules, personalized immunotherapy, and autoimmune diabetes. *Trends Mol Med* (2018) 24(11):931–41. doi: 10.1016/j.molmed.2018.08.005
- Zarour HM. Reversing T-cell dysfunction and exhaustion in cancer. *Clin Cancer Res* (2016) 22(8):1856–64. doi: 10.1158/1078-0432.CCR-15-1849
- Rotte A. Combination of ctla-4 and pd-1 blockers for treatment of cancer. *J Exp Clin Cancer Res* (2019) 38(1):255. doi: 10.1186/s13046-019-1259-z
- Forde PM, Chaft JE, Smith KN, Anagnostou V, Cottrell TR, Hellmann MD, et al. Neoadjuvant pd-1 blockade in resectable lung cancer. *N Engl J Med* (2018) 378(21):1976–86. doi: 10.1056/NEJMoa1716078
- Gao J, Navai N, Alhalabi O, Siefker-Radtke A, Campbell MT, Tidwell RS, et al. Neoadjuvant pd-L1 plus ctla-4 blockade in patients with cisplatin-ineligible operable high-risk urothelial carcinoma. *Nat Med* (2020) 26(12):1845–51. doi: 10.1038/s41591-020-1086-y
- Parry RV, Chemnitz JM, Frauwirth KA, Lanfranco AR, Braunstein I, Kobayashi SV, et al. Ctla-4 and pd-1 receptors inhibit T-cell activation by distinct mechanisms. *Mol Cell Biol* (2005) 25(21):9543–53. doi: 10.1128/MCB.25.21.9543-9553.2005
- Nagasaki J, Inozume T, Sax N, Ariyasu R, Ishikawa M, Yamashita K, et al. Pd-1 blockade therapy promotes infiltration of tumor-attacking exhausted T cell clonotypes. *Cell Rep* (2022) 38(5):110331. doi: 10.1016/j.celrep.2022.110331
- Bengsch F, Knoblock DM, Liu A, McAllister F, Beatty GL. Ctla-4/Cd80 pathway regulates T cell infiltration into pancreatic cancer. *Cancer Immunol Immunother* (2017) 66(12):1609–17. doi: 10.1007/s00262-017-2053-4
- Lee JB, Kim HR, Ha SJ. Immune checkpoint inhibitors in 10 years: Contribution of basic research and clinical application in cancer immunotherapy. *Immune Netw* (2022) 22(1):e2. doi: 10.4110/in.2022.22.e2
- Zila N, Hoeller C, Paulitschke V. Novel immune checkpoints beyond pd-1 in advanced melanoma. *memo - Magazine Eur Med Oncol* (2021) 14(2):135–42. doi: 10.1007/s12254-021-00699-0
- Fujiwara Y, Mittra A, Naqash AR, Takebe N. A review of mechanisms of resistance to immune checkpoint inhibitors and potential strategies for therapy. *Cancer Drug Resistance* (2020) 3(3):252–75. doi: 10.20517/cdr.2020.11
- Zhao B, Zhao H, Zhao J. Efficacy of pd-1/Pd-L1 blockade monotherapy in clinical trials. *Ther Adv Med Oncol* (2020) 12:1758835920937612. doi: 10.1177/1758835920937612
- Das S, Johnson DB. Immune-related adverse events and anti-tumor efficacy of immune checkpoint inhibitors. *J ImmunoTher Cancer* (2019) 7(1):306. doi: 10.1186/s40425-019-0805-8
- Michot JM, Bigenwald C, Champiat S, Collins M, Carbone F, Postel-Vinay S, et al. Immune-related adverse events with immune checkpoint blockade: A comprehensive review. *Eur J Cancer* (2016) 54:139–48. doi: 10.1016/j.ejca.2015.11.016
- Geisler AN, Phillips GS, Barrios DM, Wu J, Leung DYM, Moy AP, et al. Immune checkpoint inhibitor-related dermatologic adverse events. *J Am Acad Dermatol* (2020) 83(5):1255–68. doi: 10.1016/j.jaad.2020.03.132
- Dougan M. Checkpoint blockade toxicity and immune homeostasis in the gastrointestinal tract. *Front Immunol* (2017) 8. doi: 10.3389/fimmu.2017.01547
- Villadolid J, Amin A. Immune checkpoint inhibitors in clinical practice: Update on management of immune-related toxicities. *Trans Lung Cancer Res* (2015) 4(5):560–75. doi: 10.3978/j.issn.2218-6751.2015.06.06

Publisher's note

All claims expressed in this article are solely those of the authors and do not necessarily represent those of their affiliated organizations, or those of the publisher, the editors and the reviewers. Any product that may be evaluated in this article, or claim that may be made by its manufacturer, is not guaranteed or endorsed by the publisher.

44. Sullivan RJ, Weber JS. Immune-related toxicities of checkpoint inhibitors: Mechanisms and mitigation strategies. *Nat Rev Drug Discovery* (2022) 21(7):495–508. doi: 10.1038/s41573-021-00259-5
45. Lozano AX, Chaudhuri AA, Nene A, Bacchiocchi A, Earland N, Vesely MD, et al. T Cell characteristics associated with toxicity to immune checkpoint blockade in patients with melanoma. *Nat Med* (2022) 28(2):353–62. doi: 10.1038/s41591-021-01623-z
46. Wang Y, Wiesnoski DH, Helmink BA, Gopalakrishnan V, Choi K, DuPont HL, et al. Fecal microbiota transplantation for refractory immune checkpoint inhibitor-associated colitis. *Nat Med* (2018) 24(12):1804–8. doi: 10.1038/s41591-018-0238-9
47. Andrews MC, Duong CPM, Gopalakrishnan V, Iebba V, Chen WS, Derosa L, et al. Gut microbiota signatures are associated with toxicity to combined ctla-4 and pd-1 blockade. *Nat Med* (2021) 27(8):1432–41. doi: 10.1038/s41591-021-01406-6
48. Gopalakrishnan V, Spencer CN, Nezi L, Reuben A, Andrews MC, Karpinetz TV, et al. Gut microbiome modulates response to anti-Pd-1 immunotherapy in melanoma patients. *Science* (2018) 359(6371):97–103. doi: 10.1126/science.aan4236
49. Routy B, Le Chatelier E, Derosa L, Duong CPM, Alou MT, Daillère R, et al. Gut microbiome influences efficacy of pd-1-Based immunotherapy against epithelial tumors. *Science* (2018) 359(6371):91–7. doi: 10.1126/science.aan3706
50. Dubin K, Callahan MK, Ren B, Khanin R, Viale A, Ling L, et al. Intestinal microbiome analyses identify melanoma patients at risk for checkpoint-Blockade-Induced colitis. *Nat Commun* (2016) 7:10391. doi: 10.1038/ncomms10391
51. Ordóñez-Reyes C, García-Robledo JE, Chamorro DF, Mosquera A, Sussmann L, Ruiz-Patiño A, et al. Bispecific antibodies in cancer immunotherapy: A novel response to an old question. *Pharmaceutics* (2022) 14(6):1243. doi: 10.3390/pharmaceutics14061243
52. Yi M, Zhang J, Li A, Niu M, Yan Y, Jiao Y, et al. The construction, expression, and enhanced anti-tumor activity of Ym101: A bispecific antibody simultaneously targeting tgf- β and pd-L1. *J Hematol Oncol* (2021) 14(1):27. doi: 10.1186/s13045-021-01045-x
53. Yi M, Wu Y, Niu M, Zhu S, Zhang J, Yan Y, et al. Anti-Tgf- β /Pd-L1 bispecific antibody promotes T cell infiltration and exhibits enhanced antitumor activity in triple-negative breast cancer. *J ImmunoTher Cancer* (2022) 10(12):e005543. doi: 10.1136/jitc-2022-005543
54. Knudson KM, Hicks KC, Luo X, Chen JQ, Schlom J, Gameiro SR. M7824, a novel bifunctional anti-Pd-L1/Tgf β trap fusion protein, promotes anti-tumor efficacy as monotherapy and in combination with vaccine. *Oncoimmunology* (2018) 7(5):e1426519. doi: 10.1080/2162402X.2018.1426519
55. Zagzag D, Salnikow K, Chiriboga L, Yee H, Lan L, Ali MA, et al. Downregulation of major histocompatibility complex antigens in invading glioma cells: Stealth invasion of the brain. *Lab Invest* (2005) 85(3):328–41. doi: 10.1038/labinvest.3700233
56. Sadelain M, Brentjens R, Rivière I. The basic principles of chimeric antigen receptor design. *Cancer Discovery* (2013) 3(4):388–98. doi: 10.1158/2159-8290.CD-12-0548
57. Irving BA, Weiss A. The cytoplasmic domain of the T cell receptor zeta chain is sufficient to couple to receptor-associated signal transduction pathways. *Cell* (1991) 64(5):891–901. doi: 10.1016/0092-8674(91)90314-O
58. Makita S, Yoshimura K, Tobinai K. Clinical development of anti-Cd19 chimeric antigen receptor T-cell therapy for b-cell non-Hodgkin lymphoma. *Cancer Sci* (2017) 108(6):1109–18. doi: 10.1111/cas.13239
59. Zhao Z, Chen Y, Francisco NM, Zhang Y, Wu M. The application of car-T cell therapy in hematological malignancies: Advantages and challenges. *Acta Pharm Sin B* (2018) 8(4):539–51. doi: 10.1016/j.apsb.2018.03.001
60. Sengsayadeth S, Savani BN, Oluwole O, Dholaria B. Overview of approved car-T therapies, ongoing clinical trials, and its impact on clinical practice. *eJHaem* (2022) 3(S1):6–10. doi: 10.1002/jha2.338
61. Zareadeh Mehrabadi A, Roozbahani F, Ranjbar R, Farzanehpour M, Shahriari A, Dorostkar R, et al. Overview of the pre-clinical and clinical studies about the use of car-T cell therapy of cancer combined with oncolytic viruses. *World J Surg Oncol* (2022) 20(1):16. doi: 10.1186/s12957-021-02486-x
62. Majzner RG, Mackall CL. Tumor antigen escape from car T-cell therapy. *Cancer Discovery* (2018) 8(10):1219–26. doi: 10.1158/2159-8290.CD-18-0442
63. Sterner RC, Sterner RM. Car-T cell therapy: Current limitations and potential strategies. *Blood Cancer J* (2021) 11(4):69. doi: 10.1038/s41408-021-00459-7
64. García-Guerrero E, Sierrro-Martínez B, Pérez-Simón JA. Overcoming chimeric antigen receptor (Car) modified T-cell therapy limitations in multiple myeloma. *Front Immunol* (2020) 11:1128. doi: 10.3389/fimmu.2020.01128
65. Frey N, Porter D. Cytokine release syndrome with chimeric antigen receptor T cell therapy. *Biol Blood Marrow Transplant* (2019) 25(4):e123–e7. doi: 10.1016/j.bbmt.2018.12.756
66. Giavridis T, van der Stegen SJC, Eyquem J, Hamieh M, Piersigilli A, Sadelain M. Car T cell-induced cytokine release syndrome is mediated by macrophages and abated by il-1 blockade. *Nat Med* (2018) 24(6):731–8. doi: 10.1038/s41591-018-0041-7
67. Marofi F, Motavalli R, Safonov VA, Thangavelu L, Yumashev AV, Alexander M, et al. Car T cells in solid tumors: Challenges and opportunities. *Stem Cell Res Ther* (2021) 12(1):81. doi: 10.1186/s13287-020-02128-1
68. Qian S, Villarejo-Campos P, Guijo I, Hernández-Villafranca S, García-Olmo D, González-Soares S, et al. Update for advance car-T therapy in solid tumors, clinical application in peritoneal carcinomatosis from colorectal cancer and future prospects. *Front Immunol* (2022) 13. doi: 10.3389/fimmu.2022.841425
69. Li H, Wang Z, Ogunnaike EA, Wu Q, Chen G, Hu Q, et al. Scattered seeding of car T cells in solid tumors augments anticancer efficacy. *Natl Sci Rev* (2021) 9(3):nwab172. doi: 10.1093/nsr/nwab172
70. Smith M, Dai A, Ghilardi G, Amelsberg KV, Devlin SM, Pajarillo R, et al. Gut microbiome correlates of response and toxicity following anti-Cd19 car T cell therapy. *Nat Med* (2022) 28(4):713–23. doi: 10.1038/s41591-022-01702-9
71. Jiang T, Zhou C, Ren S. Role of il-2 in cancer immunotherapy. *Oncoimmunology* (2016) 5(6):e1163462. doi: 10.1080/2162402X.2016.1163462
72. Tsimberidou A-M, Van Morris K, Vo HH, Eck S, Lin Y-F, Rivas JM, et al. T-Cell receptor-based therapy: An innovative therapeutic approach for solid tumors. *J Hematol Oncol* (2021) 14(1):102. doi: 10.1186/s13045-021-01115-0
73. Thursby E, Juge N. Introduction to the human gut microbiota. *Biochem J* (2017) 474(11):1823–36. doi: 10.1042/BCJ20160510
74. Cheng HY, Ning MX, Chen DK, Ma WT. Interactions between the gut microbiota and the host innate immune response against pathogens. *Front Immunol* (2019) 10:607. doi: 10.3389/fimmu.2019.00607
75. Aziz Q, Doré J, Emmanuel A, Guarnier F, Quigley EM. Gut microbiota and gastrointestinal health: Current concepts and future directions. *Neurogastroenterol Motil* (2013) 25(1):4–15. doi: 10.1111/nmo.12046
76. Sivan A, Corrales L, Hubert N, Williams JB, Aquino-Michaels K, Earley ZM, et al. Commensal bifidobacterium promotes antitumor immunity and facilitates anti-Pd-L1 efficacy. *Science* (2015) 350(6264):1084–9. doi: 10.1126/science.aac4255
77. Abid MB, Shah NN, Maatman TC, Hari PN. Gut microbiome and car-T therapy. *Exp Hematol Oncol* (2019) 8(1):31. doi: 10.1186/s40164-019-0155-8
78. Schubert ML, Rohrbach R, Schmitt M, Stein-Theoringer CK. The potential role of the intestinal micromilieu and individual microbes in the immunobiology of chimeric antigen receptor T-cell therapy. *Front Immunol* (2021) 12:670286. doi: 10.3389/fimmu.2021.670286
79. Innao V, Allegra AG, Musolino C, Allegra A. New frontiers about the role of human microbiota in immunotherapy: The immune checkpoint inhibitors and car T-cell therapy era. *Int J Mol Sci* (2020) 21(23):8902. doi: 10.3390/ijms21238902
80. Matson V, Fessler J, Bao R, Chongsuwan T, Zha Y, Alegre ML, et al. The commensal microbiome is associated with anti-Pd-1 efficacy in metastatic melanoma patients. *Science* (2018) 359(6371):104–8. doi: 10.1126/science.aao3290
81. Vétizou M, Pitt JM, Daillère R, Lepage P, Waldschmitt N, Flament C, et al. Anticancer immunotherapy by ctla-4 blockade relies on the gut microbiota. *Science* (2015) 350(6264):1079–84. doi: 10.1126/science.aad1329
82. Davar D, Dzutsev AK, McCulloch JA, Rodrigues RR, Chauvin JM, Morrison RM, et al. Fecal microbiota transplant overcomes resistance to anti-Pd-1 therapy in melanoma patients. *Science* (2021) 371(6529):595–602. doi: 10.1126/science.abf3363
83. Wu J, Wang S, Zheng B, Qiu X, Wang H, Chen L. Modulation of gut microbiota to enhance effect of checkpoint inhibitor immunotherapy. *Front Immunol* (2021) 12. doi: 10.3389/fimmu.2021.669150
84. Liu W, Ma F, Sun B, Liu Y, Tang H, Luo J, et al. Intestinal microbiome associated with immune-related adverse events for patients treated with anti-Pd-1 inhibitors, a real-world study. *Front Immunol* (2021) 12:756872. doi: 10.3389/fimmu.2021.756872
85. Hakoziaki T, Richard C, Okuma Y, Derosa L, Elkrief A, Zitvogel L, et al. Gut microbiome to predict efficacy and immune-related toxicities in patients with advanced non-small cell lung cancer treated with anti-Pd-1/Pd-L1 antibody-based immunotherapy. *J Clin Oncol* (2020) 38(15_suppl):3095–. doi: 10.1200/JCO.2020.38.15_suppl.3095
86. Som A, Mandaliya R, Alsaadi D, Farshidpour M, Charabaty A, Malhotra N, et al. Immune checkpoint inhibitor-induced colitis: A comprehensive review. *World J Clin Cases* (2019) 7(4):405–18. doi: 10.12998/wjcc.v7.i4.405
87. Chen P, Xu H, Tang H, Zhao F, Yang C, Kwok LY, et al. Modulation of gut mucosal microbiota as a mechanism of probiotics-based adjunctive therapy for ulcerative colitis. *Microb Biotechnol* (2020) 13(6):2032–43. doi: 10.1111/1751-7915.13661
88. Eindor-Abarbanel A, Healey GR, Jacobson K. Therapeutic advances in gut microbiome modulation in patients with inflammatory bowel disease from pediatrics to adulthood. *Int J Mol Sci* (2021) 22(22):12506. doi: 10.3390/ijms222212506
89. Smith MB, Kelly C, Alm EJ. Policy: How to regulate faecal transplants. *Nature* (2014) 506(7488):290–1. doi: 10.1038/506290a
90. Marrs T, Walter J. Pros and cons: Is faecal microbiota transplantation a safe and efficient treatment option for gut dysbiosis? *Allergy* (2021) 76(7):2312–7. doi: 10.1111/all.14750
91. Clancy AK, Gunaratne AW, Borody TJ. Dietary management for faecal microbiota transplant: An international survey of clinical and research practice, knowledge and attitudes. *Front Nutr* (2021) 8:653653. doi: 10.3389/fnut.2021.653653
92. Shortt C, Hasselwander O, Meynier A, Nauta A, Fernández EN, Putz P, et al. Systematic review of the effects of the intestinal microbiota on selected nutrients and non-nutrients. *Eur J Nutr* (2018) 57(1):25–49. doi: 10.1007/s00394-017-1546-4
93. Ojeda P, Bobe A, Dolan K, Leone V, Martínez K. Nutritional modulation of gut microbiota - the impact on metabolic disease pathophysiology. *J Nutr Biochem* (2016) 28:191–200. doi: 10.1016/j.jnutbio.2015.08.013

94. Szczurek M, Bitkowska P, Chunowski P, Czuchryta P, Krawczyk P, Milanowski J. Diet, microbiome, and cancer immunotherapy—a comprehensive review. *Nutrients* (2021) 13(7):2217. doi: 10.3390/nu13072217
95. Beam A, Clinger E, Hao L. Effect of diet and dietary components on the composition of the gut microbiota. *Nutrients* (2021) 13(8):2795. doi: 10.3390/nu13082795
96. Cronin P, Joyce SA, O'Toole PW, O'Connor EM. Dietary fibre modulates the gut microbiota. *Nutrients* (2021) 13(5):1655. doi: 10.3390/nu13051655
97. Satokari R. High intake of sugar and the balance between pro- and anti-inflammatory gut bacteria. *Nutrients* (2020) 12(5):1348. doi: 10.3390/nu12051348
98. Tomova A, Bukovsky I, Rembert E, Yonas W, Alwarith J, Barnard ND, et al. The effects of vegetarian and vegan diets on gut microbiota. *Front Nutr* (2019) 6:47. doi: 10.3389/fnut.2019.00047
99. Dingeo G, Brito A, Samouda H, Iddir M, La Frano MR, Bohn T. Phytochemicals as modifiers of gut microbial communities. *Food Funct* (2020) 11(10):8444–71. doi: 10.1039/D0FO01483D
100. Lyu Y, Wu L, Wang F, Shen X, Lin D. Carotenoid supplementation and retinoic acid in immunoglobulin a regulation of the gut microbiota dysbiosis. *Exp Biol Med (Maywood)* (2018) 243(7):613–20. doi: 10.1177/1535370218763760
101. Han K, Nam J, Xu J, Sun X, Huang X, Animasahun O, et al. Generation of systemic antitumor immunity Via the in situ modulation of the gut microbiome by an orally administered inulin gel. *Nat BioMed Eng* (2021) 5(11):1377–88. doi: 10.1038/s41551-021-00749-2
102. Valverde ME, Hernández-Pérez T, Paredes-López O. Edible mushrooms: Improving human health and promoting quality life. *Int J Microbiol* (2015) 2015:376387. doi: 10.1155/2015/376387
103. Xu X, Zhang X. Lentinula edodes-derived polysaccharide alters the spatial structure of gut microbiota in mice. *PLoS One* (2015) 10(1):e0115037. doi: 10.1371/journal.pone.0115037
104. Xue Z, Ma Q, Chen Y, Lu Y, Wang Y, Jia Y, et al. Structure characterization of soluble dietary fiber fractions from mushroom lentinula edodes (Berk.) pegler and the effects on fermentation and human gut microbiota in vitro. *Food Res Int* (2020) 129:108870. doi: 10.1016/j.foodres.2019.108870
105. Chen L, Zhang L, Wang W, Qiu W, Liu L, Ning A, et al. Polysaccharides isolated from cordyceps sinensis contribute to the progression of Nash by modifying the gut microbiota in mice fed a high-fat diet. *PLoS One* (2020) 15(6):e0232972. doi: 10.1371/journal.pone.0232972
106. Zhao D, Dai W, Tao H, Zhuang W, Qu M, Chang YN. Polysaccharide isolated from auricularia auricular-judae (Bull.) prevents dextran sulfate sodium-induced colitis in mice through modulating the composition of the gut microbiota. *J Food Sci* (2020) 85(9):2943–51. doi: 10.1111/1750-3841.15319
107. Chen M, Xiao D, Liu W, Song Y, Zou B, Li L, et al. Intake of ganoderma lucidum polysaccharides reverses the disturbed gut microbiota and metabolism in type 2 diabetic rats. *Int J Biol Macromol* (2020) 155:890–902. doi: 10.1016/j.jbiomac.2019.11.047
108. Deng J, Guo W, Guo J, Li Y, Zhou W, Lv W, et al. Regulatory effects of a grifola frondosa extract rich in pseudobaptigenin and cyanidin-3-O-Xylosylrutinoside on glycolipid metabolism and the gut microbiota in high-fat diet-fed rats. *J Funct Foods* (2020) 75:104230. doi: 10.1016/j.jff.2020.104230
109. Song X, Feng Z, Tan J, Wang Z, Zhu W. Dietary administration of pleurotus ostreatus polysaccharides (Pops) modulates the non-specific immune response and gut microbiota diversity of apostichopus japonicus. *Aquacult Rep* (2021) 19:100578. doi: 10.1016/j.aqrep.2020.100578
110. Xie XQ, Geng Y, Guan Q, Ren Y, Guo L, Lv Q, et al. Influence of short-term consumption of hericium erinaceus on serum biochemical markers and the changes of the gut microbiota: A pilot study. *Nutrients* (2021) 13(3):1008. doi: 10.3390/nu13031008
111. Huo W, Qi P, Cui L, Zhang L, Dai L, Liu Y, et al. Polysaccharide from wild morels alters the spatial structure of gut microbiota and the production of short-chain fatty acids in mice. *Biosci Microbiota Food Health* (2020) 39(4):219–26. doi: 10.12938/bmfh.2020-018
112. Wu X, Cao J, Li M, Yao P, Li H, Xu W, et al. An integrated microbiome and metabolomic analysis identifies immunoenhancing features of ganoderma lucidum spores oil in mice. *Pharmacol Res* (2020) 158:104937. doi: 10.1016/j.phrs.2020.104937
113. Vandeputte D, Falony G, Vieira-Silva S, Wang J, Sailer M, Theis S, et al. Prebiotic inulin-type fructans induce specific changes in the human gut microbiota. *Gut* (2017) 66(11):1968. doi: 10.1136/gutjnl-2016-313271
114. Wang H, Chen G, Li X, Zheng F, Zeng X. Yeast β -glucan, a potential prebiotic, showed a similar probiotic activity to inulin. *Food Funct* (2020) 11(12):10386–96. doi: 10.1039/D0FO02224a
115. Tian J, Ma J, Ma K, Guo H, Baidoo SE, Zhang Y, et al. β -glucan enhances antitumor immune responses by regulating differentiation and function of monocytic myeloid-derived suppressor cells. *Eur J Immunol* (2013) 43(5):1220–30. doi: 10.1002/eji.201242841
116. Liu Y, Zhang L, Zhu X, Wang Y, Liu W, Gong W. Polysaccharide agaricus blazei murill stimulates myeloid derived suppressor cell differentiation from M2 to M1 type, which mediates inhibition of tumour immune-evasion Via the toll-like receptor 2 pathway. *Immunology* (2015) 146(3):379–91. doi: 10.1111/imm.12508
117. El-Deeb NM, Ibrahim OM, Mohamed MA, Farag MMS, Farrag AA, El-Aassar MR. Alginate/ κ -carrageenan oral microcapsules loaded with agaricus bisporus polysaccharides Mh751906 for natural killer cells mediated colon cancer immunotherapy. *Int J Biol Macromolecules* (2022) 205:385–95. doi: 10.1016/j.jbiomac.2022.02.058
118. Lemieszek MK, Nunes F, Sawa-Wejksza K, Rzeski W. A king bolete, boletus edulis (Agaricomycetes), rna fraction stimulates proliferation and cytotoxicity of natural killer cells against myelogenous leukemia cells. *Int J Med Mushrooms* (2017) 19(4):347–53. doi: 10.1615/IntJMedMushrooms.v19.i4.50
119. Zong S, Li J, Ye Z, Zhang X, Yang L, Chen X, et al. Lachnum polysaccharide suppresses S180 sarcoma by boosting anti-tumor immune responses and skewing tumor-associated macrophages toward M1 phenotype. *Int J Biol Macromol* (2020) 144:1022–33. doi: 10.1016/j.jbiomac.2019.09.179
120. Liu C, Chen J, Chen L, Huang X, Cheung PC. Immunomodulatory activity of polysaccharide-protein complex from the mushroom sclerotia of polyporus rhinoceros in murine macrophages. *J Agric Food Chem* (2016) 64(16):3206–14. doi: 10.1021/acs.jafc.6b00932
121. Lu J, Sun LX, Lin ZB, Duan XS, Ge ZH, Xing EH, et al. Antagonism by ganoderma lucidum polysaccharides against the suppression by culture supernatants of B16f10 melanoma cells on macrophage. *Phytother Res* (2014) 28(2):200–6. doi: 10.1002/ptr.4980
122. Wang CL, Lu CY, Hsueh YC, Liu WH, Chen CJ. Activation of antitumor immune responses by ganoderma formosanum polysaccharides in tumor-bearing mice. *Appl Microbiol Biotechnol* (2014) 98(22):9389–98. doi: 10.1007/s00253-014-6027-6
123. Dou H, Chang Y, Zhang L. Coriolus versicolor polysaccharopeptide as an immunotherapeutic in China. *Prog Mol Biol Transl Sci* (2019) 163:361–81. doi: 10.1016/bs.pmbts.2019.03.001
124. Bi S, Huang W, Chen S, Huang C, Li C, Guo Z, et al. Cordyceps militaris polysaccharide converts immunosuppressive macrophages into M1-like phenotype and activates T lymphocytes by inhibiting the pd-L1/Pd-1 axis between tams and T lymphocytes. *Int J Biol Macromol* (2020) 150:261–80. doi: 10.1016/j.jbiomac.2020.02.050
125. Huang J, Liu D, Wang Y, Liu L, Li J, Yuan J, et al. Ginseng polysaccharides alter the gut microbiota and Kynurenine/Tryptophan ratio, potentiating the antitumor effect of antiprogrammed cell death 1/Programmed cell death ligand 1 (Anti-Pd-1/Pd-L1) immunotherapy. *Gut* (2022) 71(4):734–45. doi: 10.1136/gutjnl-2020-321031
126. Tanaka K, Ishikawa S, Matsui Y, Kawanishi T, Tamesada M, Harashima N, et al. Combining a peptide vaccine with oral ingestion of lentinula edodes mycelia extract enhances anti-tumor activity in B16 melanoma-bearing mice. *Cancer Immunol Immunother* (2012) 61(11):2143–52. doi: 10.1007/s00262-012-1275-8
127. Kodama N, Komuta K, Nanba H. Effect of maitake (Grifola frondosa) d-fraction on the activation of nk cells in cancer patients. *J Med Food* (2003) 6(4):371–7. doi: 10.1089/109662003772519949
128. Gao Y, Zhou S, Jiang W, Huang M, Dai X. Effects of ganopoly (a ganoderma lucidum polysaccharide extract) on the immune functions in advanced-stage cancer patients. *Immunol Invest* (2003) 32(3):201–15. doi: 10.1081/IMM-120022979
129. Zhao H, Zhang Q, Zhao L, Huang X, Wang J, Kang X. Spore powder of ganoderma lucidum improves cancer-related fatigue in breast cancer patients undergoing endocrine therapy: A pilot clinical trial. *Evid Based Complement Alternat Med* (2012) 2012:809614. doi: 10.1155/2012/809614
130. Tanaka A, Nishimura M, Sato Y, Sato H, Nishihira J. Enhancement of the Th1-phenotype immune system by the intake of oyster mushroom (Tamogitake) extract in a double-blind, placebo-controlled study. *J Tradit Complement Med* (2016) 6(4):424–30. doi: 10.1016/j.jtcm.2015.11.004
131. Del Buono A, Bonucci M, Pugliese S, D'orta A, Fioranelli M. Polysaccharide from lentinus edodes for integrative cancer treatment: Immunomodulatory effects on lymphocyte population. *WCRJ* (2016) 3(1):1–7. <https://www.wcrj.net/article/652>
132. Twardowski P, Kanaya N, Frankel P, Synold T, Ruel C, Pal SK, et al. A phase I trial of mushroom powder in patients with biochemically recurrent prostate cancer: Roles of cytokines and myeloid-derived suppressor cells for agaricus bisporus-induced prostate-specific antigen responses. *Cancer* (2015) 121(17):2942–50. doi: 10.1002/cncr.29421
133. Panda SK, Luyten W. Medicinal mushrooms: Clinical perspective and challenges. *Drug Discovery Today* (2022) 27(2):636–51. doi: 10.1016/j.drudis.2021.11.017
134. DeFilipp Z, Bloom PP, Torres Soto M, Mansour MK, Sater MRA, Huntley MH, et al. Drug-resistant e. coli bacteremia transmitted by fecal microbiota transplant. *New Engl J Med* (2019) 381(21):2043–50. doi: 10.1056/NEJMoa1910437
135. Serious aes linked with investigational faecal microbiota. *Reactions Weekly* (2019) 1759(1):3–. doi: 10.1007/s40278-019-63893-8



OPEN ACCESS

EDITED BY

Hang Ma,
University of Rhode Island, United States

REVIEWED BY

Harikrishna Reddy Rallabandi,
Oklahoma Medical Research Foundation,
United States
Xiaomeng Xie,
China-US (Henan) Hormel Cancer Institute,
China

*CORRESPONDENCE

Bing Hu
✉ beearhu@shutcm.edu.cn

SPECIALTY SECTION

This article was submitted to
Pharmacology of Anti-Cancer Drugs,
a section of the journal
Frontiers in Oncology

RECEIVED 05 December 2022

ACCEPTED 17 February 2023

PUBLISHED 08 March 2023

CITATION

Chen JF, Wu SW, Shi ZM, Qu YJ,
Ding MR and Hu B (2023) Exploring
the components and mechanism of
Solanum nigrum L. for colon cancer
treatment based on network
pharmacology and molecular docking.
Front. Oncol. 13:1111799.
doi: 10.3389/fonc.2023.1111799

COPYRIGHT

© 2023 Chen, Wu, Shi, Qu, Ding and Hu.
This is an open-access article distributed
under the terms of the [Creative Commons
Attribution License \(CC BY\)](#). The use,
distribution or reproduction in other
forums is permitted, provided the original
author(s) and the copyright owner(s) are
credited and that the original publication in
this journal is cited, in accordance with
accepted academic practice. No use,
distribution or reproduction is permitted
which does not comply with these terms.

Exploring the components and mechanism of *Solanum nigrum* L. for colon cancer treatment based on network pharmacology and molecular docking

Jin-Fang Chen^{1,2}, Shi-Wei Wu^{1,2}, Zi-Man Shi^{1,2}, Yan-Jie Qu^{3,4},
Min-Rui Ding³ and Bing Hu^{1,2*}

¹Institute of Traditional Chinese Medicine in Oncology, Longhua Hospital, Shanghai University of Traditional Chinese Medicine, Shanghai, China, ²Department of Oncology, Longhua Hospital, Shanghai University of Traditional Chinese Medicine, Shanghai, China, ³Department of Neurology, Longhua Hospital, Shanghai University of Traditional Chinese Medicine, Shanghai, China, ⁴Department of Traditional Chinese Medicine, Ruijin Hospital, Shanghai Jiao Tong University School of Medicine, Shanghai, China

Background: *Solanum nigrum* L. (SNL) (Longkui) is a Chinese herb that can be used to treat colon cancer. The present study explored the components and mechanisms of SNL in treating colon cancer by using network pharmacology and molecular docking.

Methods: The components of SNL were collected from the TCMSP, ETCM, HERB, and NPASS databases. Meanwhile, the target proteins of these ingredients were collected/predicted by the TCMSP, SEA, SwissTargetPrediction, and the STITCH databases colon cancer-related target genes were identified from TCGA and GTEx databases. The interaction networks were established via Cytoscape 3.7.2. Gene Ontology and KEGG pathways were enriched by using the David 6.8 online tool. Finally, the binding of key components and targets was verified by molecular docking, and the cellular thermal shift assay (CETSA) was used to detect the efficiency of apigenin and kaempferol binding to the AURKB protein in CT26 cells.

Results: A total of 37 SNL components, 796 SNL targets, 5,356 colon cancer genes, and 241 shared targets of SNL and colon cancer were identified. A total of 43 key targets were obtained through topology analysis. These key targets are involved in multiple biological processes, such as signal transduction and response to drug and protein phosphorylation. At the same time, 104 signaling pathways, such as pathways in cancer, human cytomegalovirus infection, and PI3K-Akt signaling pathway, are also involved. The binding of the four key components (i.e., quercetin, apigenin, kaempferol, and luteolin) and the key targets was verified by molecular docking. The CETSA results showed that apigenin and kaempferol were able to bind to the AURKB protein to exert anti-CRC effects.

Conclusions: Quercetin, apigenin, kaempferol, and luteolin are the main components of SNL in treating colon cancer. SNL regulates multiple bioprocesses *via* signaling pathways, such as pathways in cancer, PI3K-Akt, and cell cycle signaling pathways.

KEYWORDS

colon cancer, *Solanum nigrum* L., network pharmacology, molecular docking, compounds, gene ontology, signal pathway, bioactivity

1 Introduction

Colorectal cancer (CRC), including colon and rectal cancers, is a common malignant tumor that threatens human health within a global scope. Its incidence rate ranks top three among all malignant tumors, accounting for 10.0% of the incidence rate of all cancers, with a mortality rate of 9.4% (1). CRC can be treated with surgery, chemotherapy, radiotherapy, targeted therapy and immunotherapy. However, the effect of the treatment is always unsatisfactory. As an important treatment method for CRC, traditional Chinese medicine can inhibit cell proliferation; induce apoptosis, autophagy, and cell senescence; relieve patients' symptoms; improve their quality of life; alleviate the toxic and side effects of chemoradiotherapy; repress metastasis and recurrence; and enhance the long-term treatment effect (2, 3).

Solanum nigrum L. (SNL) (Longkui) is a traditional Chinese medicine that is commonly applied to cancer treatment. SNL can inhibit the proliferation and metastatic potential of RKO CRC cells (4). SNL also induces autophagy and enhances the cytotoxicity of chemotherapy in CRC (5). With cytotoxic activity for MCF-7 cells in human breast cancer, SNL can inhibit cell migration and regulate multiple gene expressions (6). In oral cancer, SNL extracts can activate caspase-9 and caspase-3 and induce mitochondria pathway apoptosis by boosting the production of reactive oxygen species (ROS). Moreover, they can repress cell proliferation through the downregulation of cyclin-dependent kinase 1 (CDK1) and cyclin B1 (7). When applied to treat prostate cancer, SNL can arrest the cell cycle in the G2/M phase and induce cell apoptosis (8). However, the effective components of SNL and its anticancer mechanism remain to be further investigated.

Network pharmacology, an emerging discipline in recent years, can expound the relationships among “drug–gene–disease” from the aspects of the system to reveal the active components and action mechanisms of drugs (9). Chinese herbal medicinal components are complicated with diversified action characteristics and involve multiple target genes and signaling pathways. Hence, they are suitable for network pharmacology studies. In this study, the active components, targets, and related pathways of SNL in the treatment of colon cancer were explored, the “compound–target–pathway” network was established through the network

pharmacology method, the key components and targets of SNL that acted on colon cancer were obtained through network topology analysis and annotated by Gene Ontology (GO) and pathway enrichment, and the binding between key components of SNL and targets was also evaluated *via* molecular docking, expecting to provide a scientific basis for the study and application of SNL.

2 Materials and methods

2.1 Identification of components of SNL

The SNL components were retrieved from the following databases: the Traditional Chinese Medicine Systems Pharmacology Database and Analysis Platform (TCMSP, <http://tcmispw.com/tcmisp.php>) (10), The Encyclopedia of Traditional Chinese Medicine (ETCM, <http://www.tcmip.cn/ETCM/>) (11), the Natural Product Activity and Species Source Database (NPASS, <http://bidd.group/NPASS/index.php>) (12), SymMap (<http://www.symmap.org/>) (13), and HERB (<http://herb.ac.cn/>) (14). The compound properties were inquired from the TCMSP (oral bioavailability (OB) $\geq 20\%$, drug-likeness (DL) ≥ 0.10 , https://old.tcmisp-e.com/load_intro.php?id=29) or ETCM (drug-likeness weight (DW) ≥ 0.49).

2.2 Screening and prediction of compound-related targets

The target genes were retrieved from the TCMSP and ETCM. The target genes in the SNL components were also predicted using Similarity Ensemble Approach (SEA, <https://sea.bkslab.org/>) (15), STITCH (<http://stitch.embl.de/>) (16), and SwissTargetPrediction (<http://swisstargetprediction.ch/>) (17) based on the chemical similarity and pharmacophore model. The SMILE number of compounds was retrieved from PubChem (<https://pubchem.ncbi.nlm.nih.gov/>) and submitted into the SEA, STITCH, and SwissTargetPrediction databases. Next, the targets in active SNL components were predicted by taking Max Tc ≥ 0.4 , confidence score ≥ 0.4 , and probability value ≥ 0.5 as the criteria, and the gene name was converted into its official gene symbol.

2.3 Collection of colon cancer-related protein targets

The Gene Expression Profiling Interactive Analysis (GEPIA2, <http://gepia2.cancer-pku.cn/#index>) online tool (18) was used to identify the differentially expressed genes (fold change (FC) ≥ 2 , q -value < 0.01) of colon adenocarcinoma (COAD) in The Cancer Genome Atlas (TCGA) and Genotype-Tissue Expression (GTEx) databases.

2.4 Network construction and topological analysis

The intersection set between SNL and COAD target genes was acquired using the Venn online tool (<https://www.omicshare.com/tools/Home/Soft/venn>), and overlapped targets were uploaded to the STRING database (<https://string-db.org/>) (19), the protein-protein network (PPI) was constructed, and the targets that satisfied the confidence score of ≥ 0.7 were screened out. Interaction network and topological analysis were conducted *via* Cytoscape 3.7.2 (20), including (1) the compound-target network of SNL, (2) SNL compound-target-pathway network, (3) the compound-overlapped target network, and (4) the compound-key target networks. In the compound-overlapped target network, the target genes that satisfied the degree centrality (DC) $\geq 2 \times$ median DC, betweenness centrality (BC) \geq median BC, and closeness centrality (CC) \geq median CC were screened out as the key targets of SNL acted upon COAD.

2.5 GO and pathway enrichment analysis

The DAVID 6.8 database (<https://david.ncifcrf.gov/>) is an online tool for genetic function annotation (21). The key targets of SNL acted upon COAD were imported into the DAVID 6.8 database, the species were restricted to “Homo sapiens”, and the name of each target gene was converted into their official gene symbols, followed by GO (22) and Kyoto Encyclopedia of Genes and Genomes (KEGG) pathway (23–25) enrichment analysis, and visualized in online tools (<http://www.bioinformatics.com.cn/>, <http://vip.sangerbox.com/home.html>) (26).

2.6 Molecular docking

The protein structures were inquired about in the Protein Data Bank (PDB) (<https://www.rcsb.org/>) database, and the file in PDB format was downloaded (27). After the deletion of the water molecule, macromolecular ligand, and symmetric chain in PyMOL v.3.8 software, the file was saved in the PDB format (28). Operations such as hydrogenation, charge calculation, and addition of atom type were implemented for this protein file using

AutoDockTools (29), and then it was saved in PDBQT format as the receptor. The SDF files of SNL compounds were retrieved from the PubChem database and optimized in the Chem3D 15.1 module of ChemOffice software, and then the SDF format was converted into mol2 format. Next, the root of the ligand was detected, and its rotatable bond was selected in AutoDockTools and exported in PDBQT format as the ligand. The affinity score was obtained by molecular docking in AutoDockTools software, and the binding site was visualized *via* the PLIP website (<https://projects.biotec.tu-dresden.de/plip-web/plip/>) (30) and PyMOL v.3.8 software. The active components with an affinity score ≤ -5 kJ/mol were selected as the criteria for effective binding.

2.7 Cytological experiment

Mouse colon cancer CT26 cells were obtained from the Cell Bank of Type Culture Collection of the Chinese Academy of Sciences (Shanghai, China) and cultured in RPMI1640 medium (Gibco, Grand Island, NY, USA) containing 10% fetal bovine serum (Gibco, Grand Island, NY, USA) in an incubator at 37°C with 5% CO₂ and saturated humidity. Logarithmic growth stage cells were used in the experiment. Cellular thermal shift assay (CETSA) was used to detect the binding efficiency of drugs to the corresponding target proteins in CT26 cells (31, 32). CT26 cells were seeded in 10 cm culture dishes with a density of 5×10^5 cells/ml. CT26 cells were collected 24 h later and washed with cold PBS three times. Cells were resuspended in RIPA lysate buffer containing protease inhibitor cocktail (Beyotime, Shanghai, China). Cell lysates were prepared by centrifugation at 12,000 rpm for 15 min at 4°C, and supernatants were collected. The supernatant was divided into three equal fractions and treated with DMSO, 100 μ M Apigenin (APExBIO, Houston, USA), and 100 μ M Kaempferol (APExBIO, Houston, USA), respectively. After incubating at room temperature for 1 h, the three parts were divided into nine parts (60 μ l each) and heated at different temperatures (50, 55, 60, 65, 70, 75, 80, and 85°C and one aliquot kept at room temperature as control) for 3 min, followed by cooling at room temperature for 3 min. The heated lysates were centrifuged at 15,000 rpm for 20 min at 4°C, and the precipitate and soluble fraction were separated in an ice bath. The supernatant was transferred to a new centrifuge tube, analyzed by SDS-PAGE, and Western blot analysis was performed using aurora kinase B (AURKB; 1:1,000; Beyotime, Shanghai, China).

2.8 Statistical analysis

The data were expressed as mean \pm standard deviation (SD). A two independent sample *t*-test was used when the data satisfy normality distribution and homogeneity of variance. *t*'-test was used when the data satisfy normality distribution but not homogeneity of variance. Non-parametric rank sum test was used for non-normally distributed data. Statistically significant differences were considered at $p < 0.05$.

3 Results

3.1 Active components of SNL

A total of 39 SNL components were acquired from the TCMSP database, 35 from ETCM, 114 from HERB, and 60 from NPASS. Repeated components were deleted and subjected to the OB and DL/DW screening, and then 37 effective compounds were obtained. The targets were collected and predicted in the TCMSP, STITCH, SwissTargetPrediction, and SEA databases, and 796 targets were acquired in total (Table 1; Figure 1). The components that involve over 100 target genes included quercetin, kaempferol, apigenin, and solasodine.

3.2 GO and pathway enrichment analysis of SNL targets

The GO and KEGG enrichment analyses (Figures 2A, B) were performed using the DAVID 6.8 online tool. The results showed that the targets of SNL mainly existed in cell regions, such as the plasma membrane, cytoplasm, nucleus, membrane, mitochondrion, endoplasmic reticulum, and mitochondrial inner membrane, with their molecular functions involving the binding to protein, ATP, zinc ion, enzyme, and sequence-specific DNA. Meanwhile, they were correlated with the activity of transcription factors and protein kinases and took a part in bioprocesses, such as signal transduction, oxidation–reduction process, protein phosphorylation, drug response, inflammatory response, gene expression, cell proliferation, and apoptotic processes (Figure 2A). According to the KEGG pathway analysis results, a total of 148 pathways were affected by the active components of SNL ($p < 0.05$), and those ranking in the top 12 (gene number ≥ 50) included metabolic pathways, pathways in cancer, neuroactive ligand–receptor interaction, PI3K–Akt signaling pathway, non-alcoholic fatty liver disease (NAFLD), Alzheimer’s disease, hepatitis B, MAPK signaling pathway, HTLV-I infection, Huntington’s disease, Parkinson’s disease, and Ras signaling pathway (Figures 2B, 3).

3.3 Identification of SNL targets against COAD

The GEPIA2 online tool screen showed 5,356 genes (i.e., 2,682 upregulated genes and 2,674 downregulated genes) differentially expressed in COAD (Figure 4A; Table 2). The Venn analysis showed 241 overlapped targets of SNL and COAD (Figure 4B). Through the PPI analysis in the STRING database, 215 targets showed high interactions (confidence score ≥ 0.7). A compound-overlapped target network, which consisted of 215 nodes and 930 edges, and the node size was in direct proportion to the degree of centrality, was constructed *via* Cytoscape 3.7.2. By the topological analysis of this network, 43 key targets and 254 interactions were acquired, and all the targets presented high interactions (confidence score ≥ 0.7) (Figure 4C; Table 3). The key targets related to the main

SNL components are listed in Table 4, where the components with a number of key targets of ≥ 5 were quercetin, apigenin, kaempferol, luteolin, adenosine, solasodine, sitosterol, and linoleic acid.

3.4 GO enrichment analysis of SNL key targets

GO and pathway enrichment analyses of key targets were carried out *via* DAVID6.8 online tool. The GO analysis manifested that these targets mainly existed in regions, such as the nucleus, cytoplasm, cytosol, nucleoplasm, plasma membrane, extracellular region, perinuclear region of cytoplasm, centrosome, an integral component of the plasma membrane, and chromatin (Figure 5A). They could also bind to molecules, such as protein, ATP, protein kinase, enzyme, transcription factor, and receptor, which were related to the activity of protein kinase and tyrosine/serine/threonine kinase (Figure 5B). Furthermore, they participated in various bioprocesses, such as signal transduction, response to drug, protein phosphorylation, positive regulation of gene expression, G-protein coupled receptor signaling pathway, regulation of transcription from RNA polymerase II promoter, negative regulation of the apoptotic process, positive regulation of transcription, DNA-templated, and response to xenobiotic stimulus (Figure 5C).

3.5 Pathway enrichment analysis of SNL key targets

According to the pathway enrichment analysis, 104 pathways, including pathways in cancer, human cytomegalovirus infection, PI3K–Akt signaling pathway, Kaposi sarcoma-associated herpesvirus infection, lipid and atherosclerosis, hepatitis C, Epstein–Barr virus infection, cell cycle, measles, cellular senescence, chemokine signaling pathway, and human T-cell leukemia virus 1 infection, were affected by key targets ($p < 0.05$) (Figures 6A, B). The key targets distributed in pathways in cancer are displayed in Figure 7.

3.6 Molecular docking

Quercetin, apigenin, kaempferol, and luteolin were selected and docked with the corresponding key targets by using the AutoDockTools software. The binding sites between compounds and key targets were visualized using the PLIP website and PyMOL v.3.8 software. The lower the binding energy between ligand and receptor, the stabler their binding conformation would be. By screening according to the criterion of affinity score ≤ -5 kJ/mol, four active components (i.e., quercetin, apigenin, kaempferol, and luteolin) could stably bind to the corresponding key targets. Quercetin and CASP3 formed two hydrogen bonds through ASP-2 and SER-251. Apigenin and AURKB formed two hydrogen bonds through HIS-192 and GLY-193. Linoleic acid and CCNA2 formed a hydrogen bond through PRO-155. Kaempferol and AURKB formed

TABLE 1 Characteristics of SNL compounds.

Compounds	CAS	Molecular formula	Molecular weight	DL/DW	Target number
Quercetin	117-39-5	C ₁₅ H ₁₀ O ₇	302.25	0.28	278
Kaempferol	520-18-3	C ₁₅ H ₁₀ O ₆	286.24	0.24	183
Apigenin	520-36-5	C ₁₅ H ₁₀ O ₅	270.24	0.21	137
Solasodine	126-17-0	C ₂₇ H ₄₃ NO ₂	413.64	0.58	121
Luteolin	491-70-3	C ₁₅ H ₁₀ O ₆	286.24	0.25	98
Vanillic acid	121-34-6	C ₈ H ₈ O ₄	168.15	0.696	86
Oleic acid	112-80-1	C ₁₈ H ₃₄ O ₂	282.52	0.14	78
Catechin	154-23-4	C ₁₅ H ₁₄ O ₆	290.27	0.24	78
Adenosine	58-61-7	C ₁₀ H ₁₃ N ₅ O ₄	267.24	0.495	75
Sitosterol	83-46-5	C ₂₉ H ₅₀ O	414.79	0.75	74
Linoleic acid	60-33-3	C ₁₈ H ₃₀ O ₂	278.48	0.14	72
Protocatechuic acid	99-50-3	C ₇ H ₆ O ₄	154.13	0.527	68
(+)-Pinoresinol	487-36-5	C ₁₅ H ₁₂ O ₅	358.4	0.872	61
Medioresinol	40957-99-1	C ₂₁ H ₂₄ O ₇	388.45	0.62	59
(-)-Epicatechin	490-46-0	C ₁₅ H ₁₄ O ₆	290.27	0.24	55
Stigmasterol	83-48-7	C ₂₉ H ₄₈ O	412.77	0.76	53
Glycitein	40957-83-3	C ₁₆ H ₁₂ O ₅	284.28	0.24	45
Daucosterol	474-58-8	C ₃₅ H ₆₀ O ₆	576.95	0.63	43
CLR	57-88-5	C ₂₇ H ₄₆ O	386.73	0.68	43
Scopoletol	92-61-5	C ₁₀ H ₈ O ₄	192.17	0.542	41
Gentisic Acid	490-79-9	C ₇ H ₆ O ₄	154.12	0.527	33
Diosgenin	512-04-9	C ₂₇ H ₄₂ O ₃	414.69	0.81	31
Beta-carotene	7235-40-7	C ₄₀ H ₅₆	536.96	0.58	31
Syringic Acid	530-57-4	C ₉ H ₁₀ O ₅	198.17	0.762	28
Naringenin	67604-48-2	C ₁₅ H ₁₂ O ₅	272.25	0.742	28
Hesperetin	520-33-2	C ₁₆ H ₁₄ O ₆	302.28	0.27	27
PHB	99-96-7	C ₇ H ₆ O ₃	138.12	0.539	25
Tomatidenol	546-40-7	C ₂₇ H ₄₃ NO ₂	413.64	0.58	19
Solanidine	80-78-4	C ₂₇ H ₄₃ NO	397.64	0.563	18
Î-Carotene	7488-99-5	C ₄₀ H ₅₆	536.96	0.58	16
Epigallocatechin	970-74-1	C ₁₅ H ₁₄ O ₇	306.27	0.27	14
Neotigogenin	470-01-9	C ₂₇ H ₄₄ O ₃	416.64	0.81	12
Gentianine	439-89-4	C ₁₀ H ₉ NO ₂	175.18	0.601	12
Tigogenin	77-60-1	C ₂₇ H ₄₄ O ₃	416.64	0.611	11
Gentiopicroside	20831-76-9	C ₁₆ H ₂₀ O ₉	356.32	0.39	6
Syringaresinol	21453-69-0	C ₂₂ H ₂₆ O ₈	418.4	0.737	6
Solanocapsine	639-86-1	C ₂₇ H ₄₆ N ₂ O ₂	430.7	0.67	1

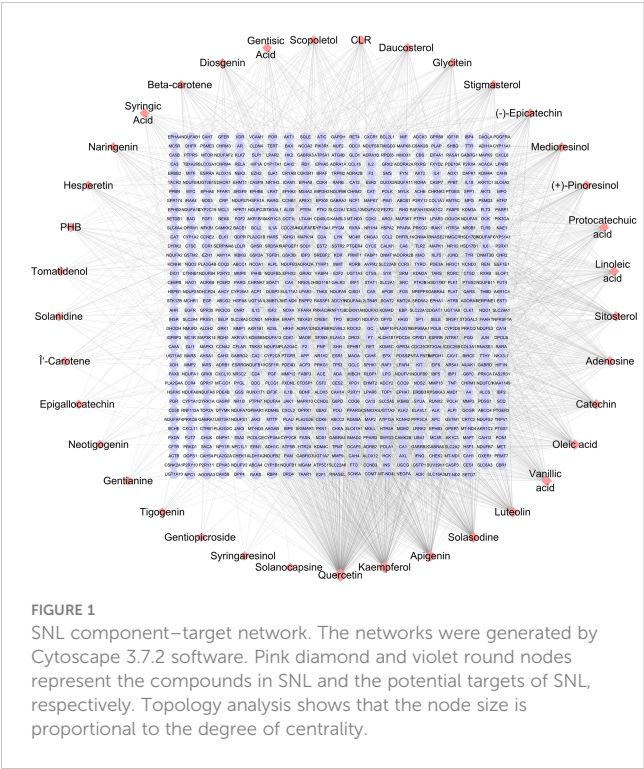


FIGURE 1
SNL component-target network. The networks were generated by Cytoscape 3.7.2 software. Pink diamond and violet round nodes represent the compounds in SNL and the potential targets of SNL, respectively. Topology analysis shows that the node size is proportional to the degree of centrality.

3.7 CETSA

The stability of compound-induced target proteins was examined by CETSA, and the interaction of apigenin and kaempferol with AURKB in CT26 cells was determined by a western blot assay. As shown in Figure 9, the expression of the

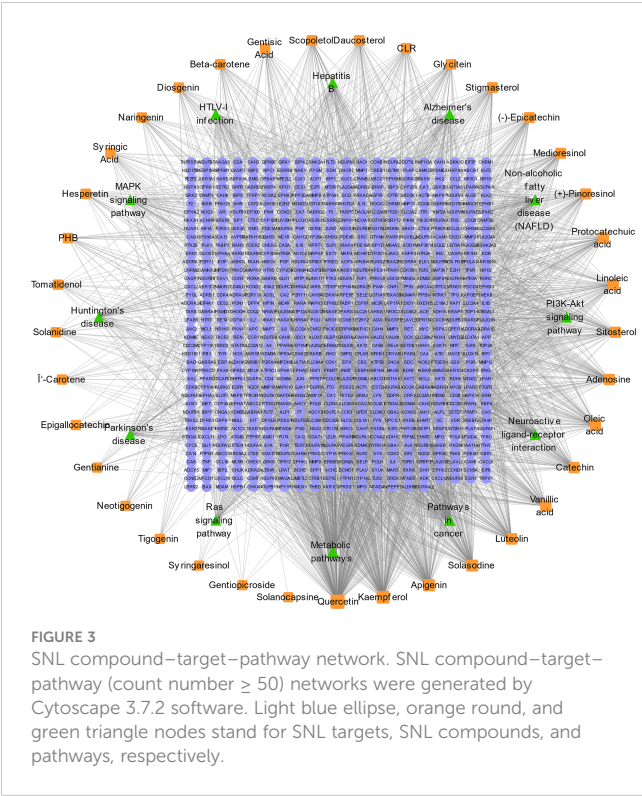


FIGURE 3
SNL compound-target-pathway network. SNL compound-target-pathway (count number ≥ 50) networks were generated by Cytoscape 3.7.2 software. Light blue ellipse, orange round, and green triangle nodes stand for SNL targets, SNL compounds, and pathways, respectively.

AURKB protein decreased continuously with the increase in temperature. The heat stability of the AURKB protein in CT26 cells was significantly higher than that in the control group under the intervention of 100 μM apigenin and 100 μM kaempferol. Taken together, these biophysical binding characteristics suggested that AURKB may be a direct target of apigenin and kaempferol.

4 Discussion

SNL is a commonly clinically used anticancer in traditional Chinese medicine. The antitumor effect of SNL is mainly

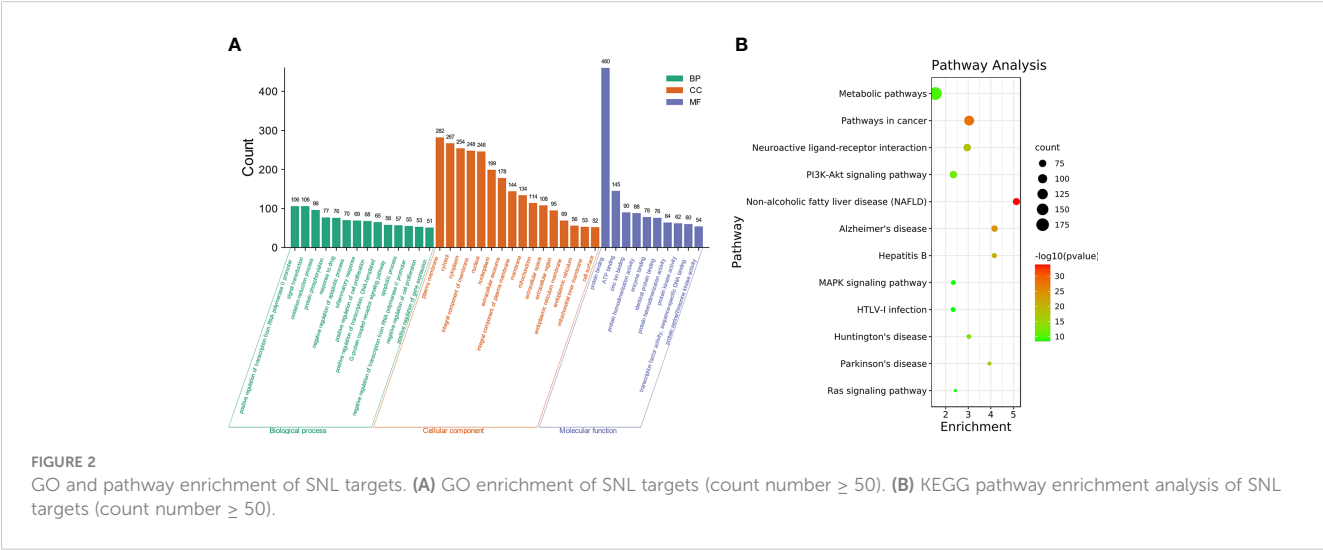
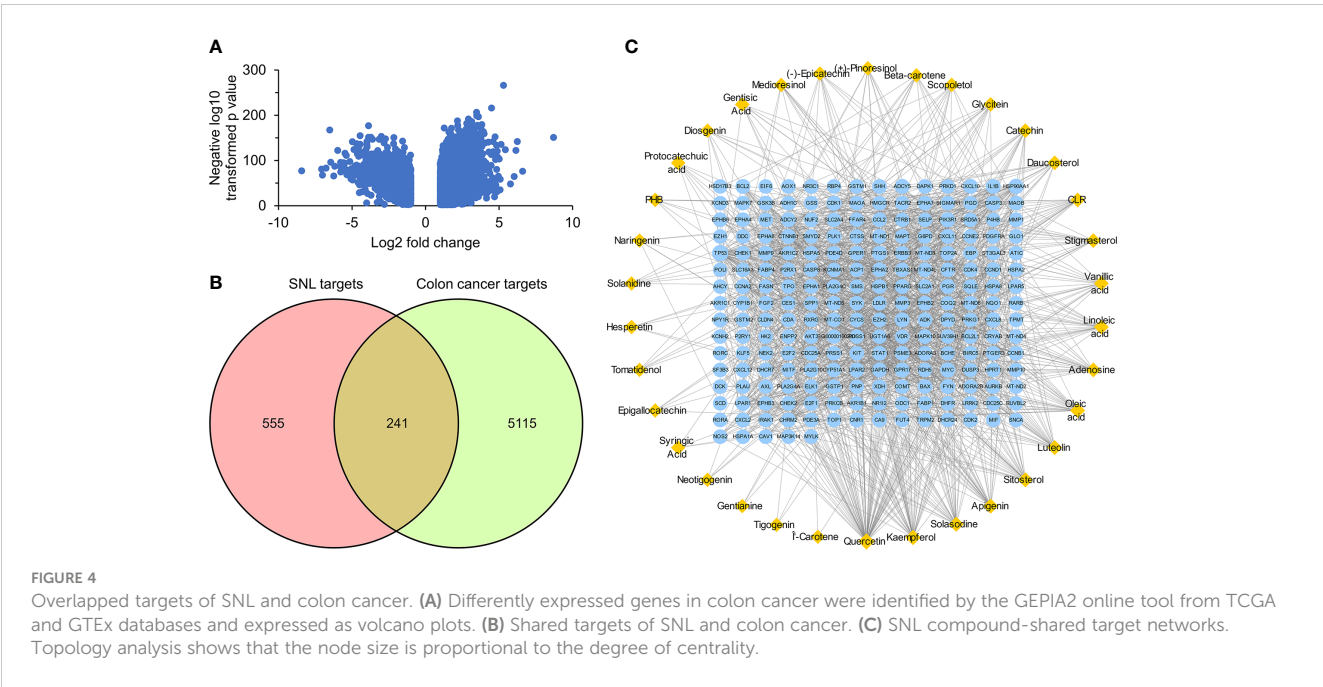


FIGURE 2
GO and pathway enrichment of SNL targets. (A) GO enrichment of SNL targets (count number ≥ 50). (B) KEGG pathway enrichment analysis of SNL targets (count number ≥ 50).



manifested by repressing the proliferation, arresting the cell cycle, inducing cell apoptosis, and inhibiting the cell migration of tumor cells (33–36). However, the active components of SNL and their mechanisms remain unclear. The components and potential targets of SNL were explored through the network pharmacology method. The study results showed that SNL targets existed in multiple cellular areas, involved diversified molecular functions, and were correlated with pathways, such as metabolic pathways, pathways in cancer, neuroactive ligand–receptor interaction, PI3K-Akt signaling pathway, non-alcoholic fatty liver disease (NAFLD), Alzheimer’s disease, hepatitis B, MAPK signaling pathway, HTLV-I infection, Huntington’s disease, Parkinson’s disease, and Ras signaling pathway, suggesting that SNL exerts extensive pharmacological effects in cancers, nervous system diseases, non-alcoholic fatty liver disease, HBV, and HTLV-I virus-related diseases.

The results showed that compounds, such as quercetin, apigenin, kaempferol, luteolin, adenosine, solasodine, sitosterol, and linoleic acid, were the active components of SNL, and quercetin, apigenin, kaempferol, and luteolin were the key components of SNL in treating colon cancer. Quercetin, apigenin, kaempferol, and luteolin are all natural flavonoids that can be used as anticancer agents (37–40). Darband et al. found that quercetin has potential preventive properties in CRC by inhibiting proliferation, metastasis, and angiogenesis, inducing apoptosis, and regulating cell metabolic activities and related signaling pathways (41). In HCT116 cells, apigenin downregulated the expression of Cyclin B1 and its activating partners, Cdc2 and Cdc25c, induced poly (ADP-ribose) polymerase (PARP) cleavage, decreased the expression of procaspase-3, procaspase-8, and procaspase-9, and upregulated the level of LC3-II, suggesting that

TABLE 2 Identified the top 10 up- and downregulated genes in colon cancer.

Upregulated genes			Downregulated genes		
Gene name	log ₂ FC	Adjusted <i>p</i> -value	Gene name	log ₂ FC	Adjusted <i>p</i> -value
RP11-40C6.2	8.703	2.92E–197	DES	–8.427	9.31E–102
CEACAM6	6.596	8.47E–107	MYH11	–7.068	2.41E–104
DPEP1	6.243	2.18E–181	ACTG2	–7.012	1.41E–90
S100P	6.145	5.74E–163	SYNM	–6.771	9.04E–110
LCN2	6.027	1.99E–91	ADH1B	–6.516	3.75E–214
CEACAM5	5.776	1.52E–70	RP11-394O4.5	–6.452	2.41E–128
CLDN2	5.429	3.97E–166	CNN1	–6.243	5.10E–88
ETV4	5.297	0.00E+00	HSPB6	–6.176	1.16E–116
CDH3	5.258	0.00E+00	ADAM33	–5.97	2.11E–160
MMP7	5.129	1.45E–181	LMOD1	–5.782	7.09E–127

TABLE 3 Key targets of SNL that act on colon cancer.

Targets	Official name	Degree	BC	CC
TP53	Cellular tumor antigen p53	68	0.419	0.510
HSP90AA1	Heat shock protein HSP 90-alpha	33	0.062	0.405
MYC	Myc proto-oncogene protein	32	0.043	0.410
CXCL8	Interleukin-8	29	0.043	0.385
CCND1	G1/S-specific cyclin-D1	28	0.024	0.405
PIK3R1	Phosphatidylinositol 3-kinase regulatory subunit alpha	27	0.048	0.376
CASP3	Caspase-3	26	0.047	0.422
CDK1	Cyclin-dependent kinase 1	24	0.007	0.377
CXCL12	Stromal cell-derived factor 1	23	0.042	0.396
LPAR1	Lysophosphatidic acid receptor 1	23	0.021	0.352
CCNA2	Cyclin-A2	23	0.006	0.371
MMP9	Matrix metalloproteinase-9	23	0.099	0.416
LPAR2	Lysophosphatidic acid receptor 2	22	0.011	0.339
CCNB1	G2/mitotic-specific cyclin-B1	21	0.006	0.374
GAPDH	Glyceraldehyde-3-phosphate dehydrogenase	21	0.068	0.420
ADCY2	Adenylate cyclase type 2	20	0.014	0.319
CXCL10	C-X-C motif chemokine 10	20	0.008	0.340
LPAR5	Lysophosphatidic acid receptor 5	20	0.004	0.331
GPR17	Uracil nucleotide/cysteinyl leukotriene receptor	20	0.004	0.331
LYN	Tyrosine-protein kinase Lyn	20	0.033	0.361
FYN	Tyrosine-protein kinase Fyn	20	0.016	0.352
CDK2	Cyclin-dependent kinase 2	20	0.006	0.375
CTNNB1	Catenin beta-1	20	0.018	0.393
CHRM2	Muscarinic acetylcholine receptor M2	19	0.014	0.333
ADCY5	Adenylate cyclase type 5	19	0.010	0.318
CXCL2	C-X-C motif chemokine 2	18	0.003	0.327
IL1B	Interleukin-1 beta	18	0.057	0.370
FGF2	Fibroblast growth factor 2	18	0.014	0.408
ADORA3	Transmembrane domain-containing protein TMIGD3	17	0.009	0.325
PLK1	Serine/threonine-protein kinase PLK1	17	0.004	0.368
CDK4	Cyclin-dependent kinase 4	17	0.014	0.377
EPHA2	Ephrin type-A receptor 2	16	0.038	0.379
STAT1	Signal transducer and activator of transcription 1-alpha/beta	16	0.012	0.391
HSPA8	Heat shock cognate 71 kDa protein	16	0.032	0.385
GSK3B	Glycogen synthase kinase-3 beta	15	0.009	0.380
PSME3	Proteasome activator complex subunit 3	15	0.009	0.366
E2F1	Transcription factor E2F1	15	0.004	0.366
BCL2L1	Bcl-2-like protein 1	14	0.005	0.385
AURKB	Aurora kinase B	14	0.011	0.351

(Continued)

TABLE 3 Continued

Targets	Official name	Degree	BC	CC
CCL2	C–C motif chemokine 2	14	0.011	0.392
EPHB2	Ephrin type-B receptor 2	14	0.009	0.342
PPARG	Peroxisome proliferator-activated receptor gamma	13	0.039	0.386
EZH2	Histone-lysine N-methyltransferase EZH2	13	0.021	0.365

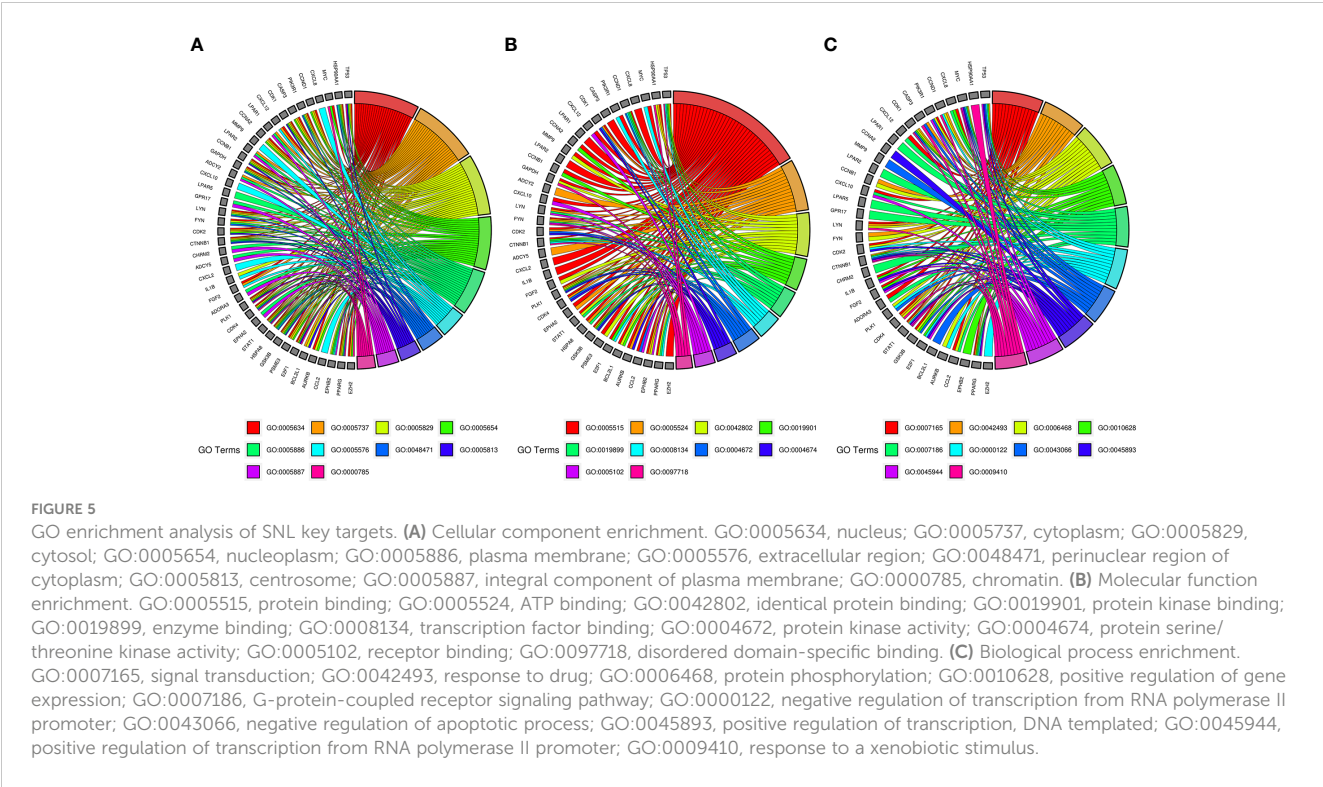
apigenin could regulate the cell cycle and induce apoptosis in HCT116 cells by inhibiting autophagy (42). Kaempferol has a significant antiproliferative and cytotoxic effect on HCT116, HCT15, and SW480 cells, which could promote the cleavage of PARP in HCT116 and HCT15 cells as well as the activation of caspase-8, caspase-9, and caspase-3, phosphor-p38 MAPK, p53, and p21. These changes were reversed after treatment with the ROS inhibitor NAC, the pan-caspase inhibitor z-vad-fmk, and the p38 MAPK inhibitor SB203580. The above results suggested that p38 phosphorylation and caspase activation mediated by ROS and p53 signaling are closely related to kaempferol-induced apoptosis in

CRC cells (43). Luteolin has no effect on the proliferation of CRC cells but could inhibit the migration and invasion of CRC cells by downregulating MMP2, MMP9, and MMP16 *in vitro* and *in vivo*. The expression of miR-384 was downregulated and that of pleiotrophin (PTN) was upregulated compared with adjacent normal tissues, suggesting that the antitumor effects of luteolin were partly mediated through the miR-384/PTN axis (44)..

In addition to the four abovementioned key components, other components also had anti-CRC effects. Linoleic acid facilitates CRC cell apoptosis by inducing oxidative stress and mitochondrial dysfunction (45). Sitosterol activated caspase-9 and caspase-3 and

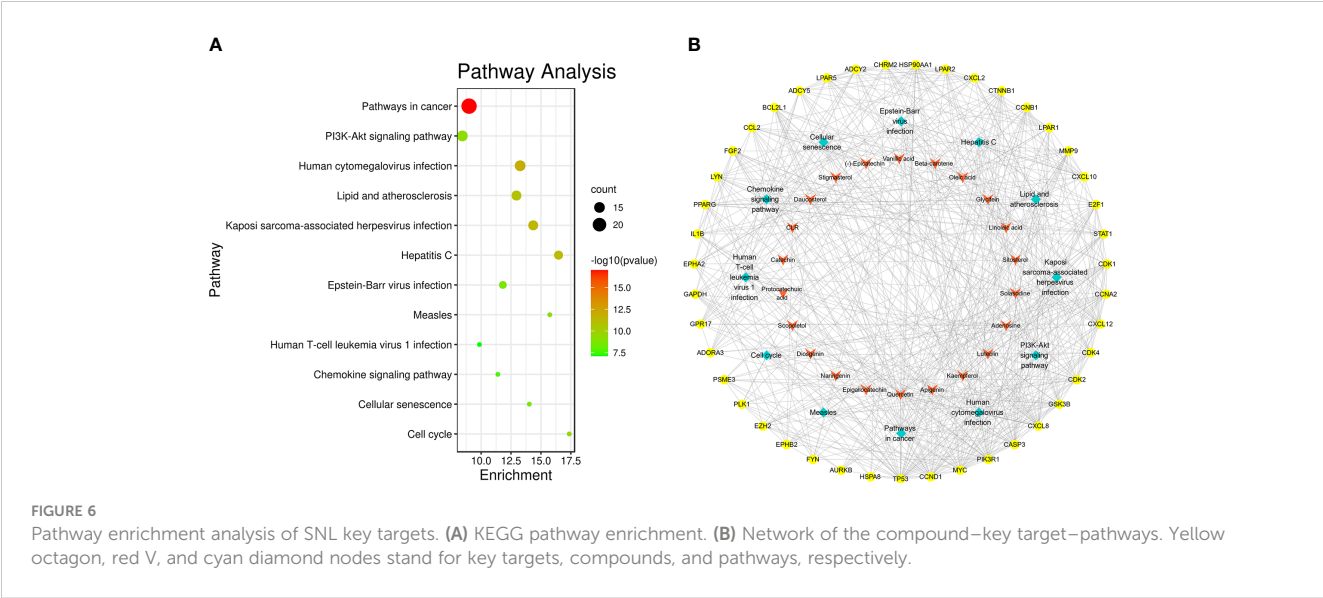
TABLE 4 SNL compounds and related key targets.

Compound	Number of key targets	Targets
Quercetin	22	AURKB, BCL2L1, CASP3, CCL2, CCNB1, CCND1, CDK1, CDK2, CXCL10, CXCL2, CXCL8, E2F1, GSK3B, HSP90AA1, IL1B, MMP9, MYC, PIK3R1, PLK1, PPARG, STAT1, TP53
Apigenin	9	TP53, BCL2L1, CASP3, CCNB1, CCND1, CDK1, GSK3B, MMP9, PSME3
Kaempferol	8	CASP3, CDK1, CHRM2, GSK3B, HSP90AA1, MMP9, PPARG, STAT1
Luteolin	7	ADCY2, CASP3, CCNA2, CCNB1, CDK2, GSK3B, MMP9
Adenosine	6	ADCY5, ADORA3, EZH2, GAPDH, GPR17, HSPA8
Solasodine	5	AURKB, EZH2, FGF2, GSK3B, LYN
Sitosterol	5	CASP3, CHRM2, EPHA2, EPHB2, FGF2
Linoleic acid	5	CHRM2, LPAR1, LPAR2, LPAR5, PPARG
Glycitein	4	CCNA2, CDK4, GSK3B, PPARG
Oleic acid	4	LPAR1, LPAR2, LPAR5, PPARG
Beta-carotene	3	CASP3, CTNNB1, MYC
Vanillic acid	2	CXCL12, FYN
(-)-Epicatechin	2	CASP3, CCL2
Stigmasterol	2	CHRM2, EPHA2
Daucosterol	2	EPHA2, EPHB2
CLR	2	EPHA2, EPHB2
Catechin	1	HSP90AA1
Protocatechuic acid	1	FYN
Scopoletin	1	CASP3
Diosgenin	1	TP53
Naringenin	1	CCL2
Epigallocatechin	1	CXCL8



boosted the CRC cell apoptosis by inhibiting PI3K/Akt and regulating the expressions of Bcl-xl and Bad (46). Solasodine induced the CRC cells' apoptosis by regulating AKT/GSK3B/ β -catenin signaling pathway and activating the caspase cascade (47). By regulating the IL-6/STAT3 pathway, beta-carotene repressed the polarization of M2 macrophages and inhibited the fibroblasts activated by transforming growth factor- β 1 (TGF- β 1) to inhibit the invasion and migration and the epithelial-mesenchymal transition of CRC cells, as well as azoxymethane/dextran sodium sulfate-induced CRC formation (48).

In this study, 43 key targets of SNL were found for the treatment of colon cancer. As serine/threonine kinase, AURKB was able to regulate the G2/M phase of the cell cycle in cell mitosis, and its overexpression was related to the CRC prognosis (49). Glycogen synthase kinase 3 beta (GSK3B) is a multifunctional serine/threonine kinase involved in mediating various cellular functions such as proliferation, apoptosis, metabolism, differentiation, and cell motility (50). Rosales-Reynoso et al. discovered that GSK3B may play a role in tumor progression by regulating the Wnt/ β -catenin pathway and that GSK3B gene variation is associated with



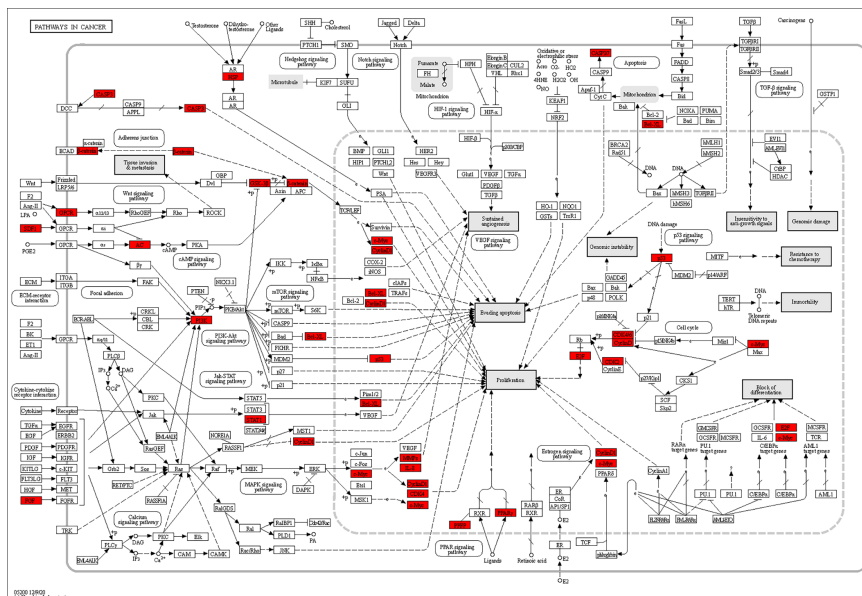


FIGURE 7

Distribution of key targets in pathways in cancer. The red rectangles stand for the key targets. (KEGG Copyright Permission 230270).

tumor location and tumor-node-metastasis (TNM) stage in CRC patients (51). Caspase-3 (CASP3) is an apoptotic executive protein, which can not only inhibit the invasion and metastasis of CRC cells but also increase the sensitivity of tumor cells to radiotherapy and chemotherapy (52). During cell division, cyclin-dependent kinase 2 (CDK2) is a core cell cycle regulator that is active from the late G1-phase to the S-phase. Overexpression of CDK2 leads to abnormal regulation of the cell cycle, which is directly related to the overproliferation of tumor cells. Thus, CDK2 inhibitors could induce antitumor activities (53, 54). CCND1, a type of cyclin, was correlated with the cell cycle and proliferation. Studies have shown that miR-374a could inhibit the PI3K-Akt pathway by lowering the expression of CCND1 to inhibit the proliferation of CRC cells (55). Transcription 1 (STAT1) can repress miR-181a, thereby further inhibiting the phosphatase and tensin homolog (PTEN)/Akt signal transduction and the proliferation of CRC cells (56). In addition, the molecular docking results showed that the key SNL

components, namely, quercetin, apigenin, luteolin, and kaempferol, presented favorable binding activity to the corresponding key targets, such as GSK3B, CDK2, and CASP3. Subsequent CETSA experiments validated these results, showing that AURKB could bind to apigenin and kaempferol and perform the corresponding biological functions.

According to the results of GO and pathway enrichment analysis, the key targets of SNL can bind to protein, ATP, protein kinase, enzyme, transcription factor, and receptor; regulate the activities of tyrosine/serine/threonine kinases; influence pathways in cancer, human cytomegalovirus infection, PI3K-Akt signaling pathway, Kaposi sarcoma-associated herpesvirus infection, lipid and atherosclerosis, hepatitis C, Epstein-Barr virus infection, cell cycle, measles, cellular senescence, chemokine signaling pathway, and human T-cell leukemia virus 1 infection and further took a part in bioprocesses, such as signal transduction, response to the drug, protein phosphorylation, regulation of the apoptotic process, gene

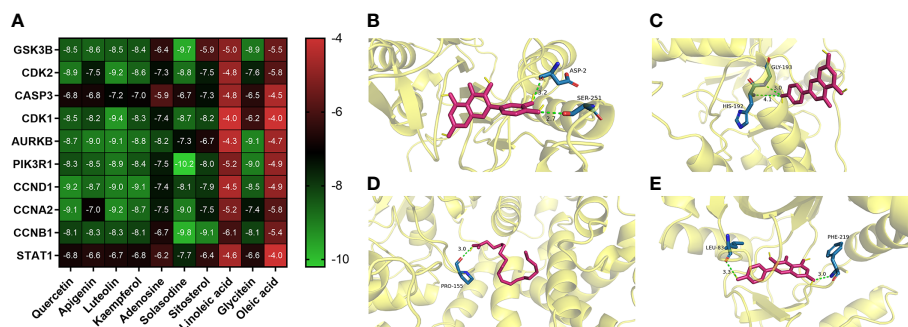


FIGURE 8

Representative molecular docking. (A) Binding affinity score of key compounds and key targets. (B) Quercetin binding with CASP3. (C) Apigenin binding with AURKB. (D) Linoleic acid binding with CCNA2. (E) Kaempferol binding with AURKB.

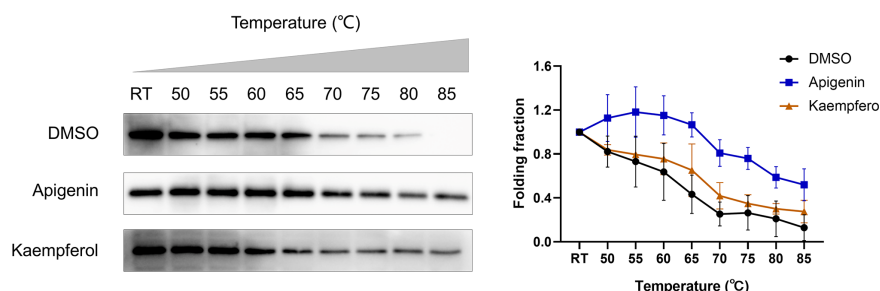


FIGURE 9

Cellular thermal shift assay (CETSA). CETSA was performed in CT26 cells treated with apigenin (100 μ M), kaempferol (100 μ M), or DMSO control. The effect of apigenin and kaempferol on AURKB protein stability was evaluated by Western blot assay. RT, room temperature.

expression, and transcription, DNA-templated, and response to a xenobiotic stimulus.

The pathways in cancer and colorectal cancer were the sets of multiple pathways, including MAPK, p53, PI3K-Akt, Wnt, and Jak-STAT signaling pathways. Mitogen-activated protein kinases (MAPKs) are serine-threonine kinases that could link extracellular signals to fundamental cellular processes such as cell growth, proliferation, differentiation, migration, and apoptosis (57). The MAPK pathway was closely related to the adhesion, angiogenesis, invasion, and migration of CRC cells (58). The Janus kinase (JAK)-signal transducer of activators of transcription (STAT) pathway participated in the proliferation, invasion, and migration of tumor cells, whereas miR-198 could inhibit the proliferation and induce the apoptosis of CRC cells by repressing the JAK-STAT signal transduction (59). The phosphatidylinositol-3 kinase (PI3K)/protein kinase B (Akt) signaling pathway, an important tumor cell pathway, participated in gene transcription and translation, and it was related to the cycle, proliferation, apoptosis, and autophagy of CRC cells (60). As a cancer suppressor gene, p53 could regulate the downstream genes and take a part in DNA repair and regulation of the cell cycle and apoptosis (61). Reactivation and restoration of p53 function hold great potential for the treatment of CRC. The Wnt signaling pathway participates in the regulation of cell cycle, proliferation, and apoptosis and has been suggested as a therapeutic target for CRC treatment (62).

5 Conclusion

In conclusion, the present study demonstrated that the active components of SNL for the treatment of colon cancer include quercetin, apigenin, kaempferol, and luteolin, and the effective targets include AURKB, PIK3R1, CDK1, CDK2, GSK3B, CCNA2, CCND1, CCNB1, CASP3, CCNA2, and STAT1. SNL regulates bioprocesses such as signal transduction, response to the drug, protein phosphorylation, gene expression, and apoptotic process *via* signaling pathways, including pathways in cancer, the PI3K-Akt signaling pathway, cell cycle, cellular senescence, and the chemokine

signaling pathway. The CETSA confirmed that apigenin and kaempferol, the active components of SNL in colon cancer treatment, were able to bind to AURKB. The present study provides a basis for the treatment of CRC by SNL from the perspective of network pharmacology. We identified the main components, targets, and signaling pathways of SNL for the treatment of colon cancer and provided new clues for the R&D of anti-CRC drugs.

Data availability statement

The datasets used and/or analyzed during the current study are available from the corresponding author on reasonable request.

Author contributions

Conception and design: JFC and BH. Administrative support: BH. Provision of study materials: JFC and BH. Collection and assembly of data: JFC, SWW, YJQ and MRD. Data analysis and interpretation: JFC. All authors contributed to the article and approved the submitted version.

Funding

This study was supported by the National Natural Science Foundation of China (grant number 82074352) and the Natural Science Foundation of Shanghai Municipality (grant number 20ZR1458700). The funders had no role in study design, data collection and analysis, the decision to publish, or the preparation of the manuscript.

Conflict of interest

The authors declare that the research was conducted in the absence of any commercial or financial relationships that could be construed as a potential conflict of interest.

Publisher's note

All claims expressed in this article are solely those of the authors and do not necessarily represent those of their affiliated

organizations, or those of the publisher, the editors and the reviewers. Any product that may be evaluated in this article, or claim that may be made by its manufacturer, is not guaranteed or endorsed by the publisher.

References

- Sung H, Ferlay J, Siegel RL, Laversanne M, Soerjomataram I, Jemal A, et al. Global cancer statistics 2020: GLOBOCAN estimates of incidence and mortality worldwide for 36 cancers in 185 countries. *CA Cancer J Clin* (2021) 71(3):209–49. doi: 10.3322/caac.21660
- Deng S, Hu B, An HM. Traditional Chinese medicinal syndromes and treatment in colorectal cancer. *J Cancer Ther* (2012) 3(6A):888–97. doi: 10.4236/jct.2012.326114
- Wang Y, Liu P, Fang Y, Tian J, Li S, Xu J, et al. The effect of long-term traditional Chinese medicine treatment on survival time of colorectal cancer based on propensity score matching: A retrospective cohort study. *Evid Based Complement Alternat Med* (2020) 2020:7023420. doi: 10.1155/2020/7023420
- Hu B, An HM, Shen KP, Shi XF, Deng S, Wei MM. Effect of *Solanum nigrum* on human colon carcinoma RKO cells. *Zhong Yao Cai* (2013) 36(6):958–61. doi: 10.13863/j.issn1001-4454.2013.06.034Chinese
- Tai CJ, Wang CK, Tai CJ, Lin YF, Lin CS, Jian JY, et al. Aqueous extract of *Solanum nigrum* leaves induces autophagy and enhances cytotoxicity of cisplatin, doxorubicin, docetaxel, and 5-fluorouracil in human colorectal carcinoma cells. *Evid Based Complement Alternat Med* (2013) 2013:514719. doi: 10.1155/2013/514719
- Ling B, Xiao S, Yang J, Wei Y, Saktharkar MK, Yang J. Probing the antitumor mechanism of *Solanum nigrum* l. aqueous extract against human breast cancer MCF7 cells. *Bioengineering (Basel)* (2019) 6(4):112. doi: 10.3390/bioengineering6040112
- Uen WC, Lee BH, Shi YC, Wu SC, Tai CJ, Tai CJ. Inhibition of aqueous extracts of *Solanum nigrum* (AESN) on oral cancer through regulation of mitochondrial fission. *J Tradit Complement Med* (2017) 8(1):220–5. doi: 10.1016/j.jtcme.2017.05.011
- Nawab A, Thakur VS, Yunus M, Ali Mahdi A, Gupta S. Selective cell cycle arrest and induction of apoptosis in human prostate cancer cells by a polyphenol-rich extract of *Solanum nigrum*. *Int J Mol Med* (2012) 29(2):277–84. doi: 10.3892/ijmm.2011.835
- Li S, Zhang B. Traditional Chinese medicine network pharmacology: Theory, methodology and application. *Chin J Nat Med* (2013) 11(2):110–20. doi: 10.1016/S1875-5364(13)60037-0
- Ru J, Li P, Wang J, Zhou W, Li B, Huang C, et al. TCMSP: a database of systems pharmacology for drug discovery from herbal medicines. *J Cheminformatics* (2014) 6:13. doi: 10.1186/1758-2946-6-13
- Xu HY, Zhang YQ, Liu ZM, Chen T, Lv CY, Tang SH, et al. ETCM: An encyclopaedia of traditional Chinese medicine. *Nucleic Acids Res* (2019) 47(D1):D976–82. doi: 10.1093/nar/gky987
- Zeng X, Zhang P, He W, Qin C, Chen S, Tao L, et al. NPASS: natural product activity and species source database for natural product research, discovery and tool development. *Nucleic Acids Res* (2018) 46(D1):D1217–22. doi: 10.1093/nar/gkx1026
- Wu Y, Zhang F, Yang K, Fang S, Bu D, Li H, et al. SymMap: An integrative database of traditional Chinese medicine enhanced by symptom mapping. *Nucleic Acids Res* (2019) 47(D1):D1110–7. doi: 10.1093/nar/gky1021
- Fang S, Dong L, Liu L, Guo J, Zhao L, Zhang J, et al. HERB: a high-throughput experiment- and reference-guided database of traditional Chinese medicine. *Nucleic Acids Res* (2021) 49(D1):D1197–206. doi: 10.1093/nar/gkaa1063
- Keiser MJ, Roth BL, Armbruster BN, Ernsberger P, Irwin JJ, Shoichet BK. Relating protein pharmacology by ligand chemistry. *Nat Biotechnol* (2007) 25(2):197–206. doi: 10.1038/nbt1284
- Szklarczyk D, Santos A, von Mering C, Jensen LJ, Bork P, Kuhn M. STITCH 5: Augmenting protein-chemical interaction networks with tissue and affinity data. *Nucleic Acids Res* (2016) 44(D1):D380–4. doi: 10.1093/nar/gkv1277
- Daina A, Michielin O, Zoete V. SwissTargetPrediction: updated data and new features for efficient prediction of protein targets of small molecules. *Nucleic Acids Res* (2019) 47(W1):W357–64. doi: 10.1093/nar/gkz382
- Tang Z, Kang B, Li C, Chen T, Zhang Z. GEPIA2: an enhanced web server for large-scale expression profiling and interactive analysis. *Nucleic Acids Res* (2019) 47(W1):W556–60. doi: 10.1093/nar/gkz430
- Szklarczyk D, Gable AL, Lyon D, Junge A, Wyder S, Huerta-Cepas J, et al. STRING v11: Protein-protein association networks with increased coverage, supporting functional discovery in genome-wide experimental datasets. *Nucleic Acids Res* (2019) 47(D1):D607–13. doi: 10.1093/nar/gky1131
- Shannon P, Markiel A, Ozier O, Baliga NS, Wang JT, Ramage D, et al. Cytoscape: a software environment for integrated models of biomolecular interaction networks. *Genome Res* (2003) 13(11):2498–504. doi: 10.1101/gr.1239303
- Huang DW, Sherman BT, Lempicki RA. Systematic and integrative analysis of large gene lists using DAVID bioinformatics resources. *Nat Protoc* (2009) 4(1):44–57. doi: 10.1038/nprot.2008.211
- Ashburner M, Ball CA, Blake JA, Botstein D, Butler H, Cherry JM, et al. Gene ontology: tool for the unification of biology. the gene ontology consortium. *Nat Genet* (2000) 25(1):25–9. doi: 10.1038/75556
- Kanehisa M, Goto S. KEGG: kyoto encyclopedia of genes and genomes. *Nucleic Acids Res* (2000) 28(1):27–30. doi: 10.1093/nar/28.1.27
- Kanehisa M. Toward understanding the origin and evolution of cellular organisms. *Protein Sci* (2019) 28(11):1947–51. doi: 10.1002/pro.3715
- Kanehisa M, Furumichi M, Sato Y, Kawashima M, Ishiguro-Watanabe M. KEGG for taxonomy-based analysis of pathways and genomes. *Nucleic Acids Res* (2023) 51(D1):D587–92. doi: 10.1093/nar/gkac963
- Shen W, Song Z, Zhong X, Huang M, Shen D, Gao P, et al. Sangerbox: A comprehensive, interaction-friendly clinical bioinformatics analysis platform. *iMeta* (2022) 1:e36. doi: 10.1002/imt2.36
- Burley SK, Berman HM, Bhikadiya C, Bi C, Chen L, Di Costanzo L, et al. RCSB protein data bank: Biological macromolecular structures enabling research and education in fundamental biology, biomedicine, biotechnology and energy. *Nucleic Acids Res* (2019) 47(D1):D464–74. doi: 10.1093/nar/gky1004
- Mooers BHM. Shortcuts for faster image creation in PyMOL. *Protein Sci* (2020) 29(1):268–76. doi: 10.1002/pro.3781
- Trott O, Olson AJ. AutoDock vina: Improving the speed and accuracy of docking with a new scoring function, efficient optimization, and multithreading. *J Comput Chem* (2010) 31(2):455–61. doi: 10.1002/jcc.21334
- Salentin S, Schreiber S, Haupt VJ, Adasme MF, Schroeder M. PLIP: fully automated protein-ligand interaction profiler. *Nucleic Acids Res* (2015) 43(W1):W443–47. doi: 10.1093/nar/gkv315
- Martinez Molina D, Jafari R, Ignatishchenko M, Seki T, Larsson EA, Dan C, et al. Monitoring drug target engagement in cells and tissues using the cellular thermal shift assay. *Science* (2013) 341(6141):84–7. doi: 10.1126/science.1233606
- Jafari R, Almqvist H, Axelsson H, Ignatishchenko M, Lundbäck T, Nordlund P, et al. The cellular thermal shift assay for evaluating drug target interactions in cells. *Nat Protoc* (2014) 9(9):2100–22. doi: 10.1038/nprot.2014.138
- Tuan Anh HL, Tran PT, Thao DT, Trang DT, Dang NH, Van Cuong P, et al. Degalactotigonin, a steroidal glycoside from *Solanum nigrum*, induces apoptosis and cell cycle arrest via inhibiting the egfr signaling pathways in pancreatic cancer cells. *BioMed Res Int* (2018) 2018:3120972. doi: 10.1155/2018/3120972
- Yan X, Li M, Chen L, Peng X, Que ZJ, An HM, et al. α -Solanine inhibits growth and metastatic potential of human colorectal cancer cells. *Oncol Rep* (2020) 43(5):1387–96. doi: 10.3892/or.2020.7519
- Wang X, Zou S, Lan YL, Xing JS, Lan XQ, Zhang B. Solasolone inhibits glioma growth through anti-inflammatory pathways. *Am J Transl Res* (2017) 9(9):3977–989.
- Jain R, Sharma A, Gupta S, Sarethy IP, Gabrani R. *Solanum nigrum*: current perspectives on therapeutic properties. *Altern Med Rev* (2011) 16(1):78–85.
- Russo GL, Russo M, Spagnuolo C, Tedesco I, Bilotto S, Iannitti R, et al. Quercetin: a pleiotropic kinase inhibitor against cancer. *Cancer Treat Res* (2014) 159:185–205. doi: 10.1007/978-3-642-38007-5_11
- Imran M, Aslam Gondal T, Atif M, Shahbaz M, Batool Qaisarani T, Hanif Mughal M, et al. Apigenin as an anticancer agent. *Phytother Res* (2020) 34(8):1812–28. doi: 10.1002/ptr.6647
- Imran M, Salehi B, Sharifi-Rad J, Aslam Gondal T, Saeed F, Imran A, et al. Kaempferol: A key emphasis to its anticancer potential. *Molecules* (2019) 24(12):2277. doi: 10.3390/molecules24122277
- Imran M, Rauf A, Abu-Izneid T, Nadeem M, Shariati MA, Khan IA, et al. Luteolin, a flavonoid, as an anticancer agent: A review. *BioMed Pharmacother* (2019) 112:108612. doi: 10.1016/j.biopha.2019.108612
- Darband SG, Kaviani M, Yousefi B, Sadighparvar S, Pakdel FG, Attari JA, et al. Quercetin: A functional dietary flavonoid with potential chemo-preventive properties in colorectal cancer. *J Cell Physiol* (2018) 233(9):6544–60. doi: 10.1002/jcp.26595
- Lee Y, Sung B, Kang YJ, Kim DH, Jang JY, Hwang SY, et al. Apigenin-induced apoptosis is enhanced by inhibition of autophagy formation in HCT116 human colon cancer cells. *Int J Oncol* (2014) 44(5):1599–606. doi: 10.3892/ijo.2014.2339
- Choi JB, Kim JH, Lee H, Pak JN, Shim BS, Kim SH. Reactive oxygen species and p53 mediated activation of p38 and caspases is critically involved in kaempferol induced apoptosis in colorectal cancer cells. *J Agric Food Chem* (2018) 66(38):9960–7. doi: 10.1021/acs.jafc.8b02656

44. Yao Y, Rao C, Zheng G, Wang S. Luteolin suppresses colorectal cancer cell metastasis via regulation of the miR-384/pleiotrophin axis. *Oncol Rep* (2019) 42(1):131–41. doi: 10.3892/or.2019.7136
45. Lu X, Yu H, Ma Q, Shen S, Das UN. Linoleic acid suppresses colorectal cancer cell growth by inducing oxidant stress and mitochondrial dysfunction. *Lipids Health Dis* (2010) 9:106. doi: 10.1186/1476-511X-9-106
46. Ma H, Yu Y, Wang M, Li Z, Xu H, Tian C, et al. Correlation between microbes and colorectal cancer: Tumor apoptosis is induced by sitosterols through promoting gut microbiota to produce short-chain fatty acids. *Apoptosis* (2019) 24(1-2):168–83. doi: 10.1007/s10495-018-1500-9
47. Zhuang YW, Wu CE, Zhou JY, Chen X, Wu J, Jiang S, et al. Solasodine inhibits human colorectal cancer cells through suppression of the AKT/glycogen synthase kinase-3 β /catenin pathway. *Cancer Sci* (2017) 108(11):2248–64. doi: 10.1111/cas.13354
48. Lee NY, Kim Y, Kim YS, Shin JH, Rubin LP, Kim Y. β -carotene exerts anti-colon cancer effects by regulating M2 macrophages and activated fibroblasts. *J Nutr Biochem* (2020) 82:108402. doi: 10.1016/j.jnutbio.2020.108402
49. Kasap E, Gerciker E, Boyacıoğlu SÖ, Yuceyar H, Yıldırım H, Ayhan S, et al. The potential role of the NEK6, AURKA, AURKB, and PAK1 genes in adenomatous colorectal polyps and colorectal adenocarcinoma. *Tumour Biol* (2016) 37(3):3071–80. doi: 10.1007/s13277-015-4131-6
50. Lin J, Song T, Li C, Mao W. GSK-3 β in DNA repair, apoptosis, and resistance of chemotherapy, radiotherapy of cancer. *Biochim Biophys Acta Mol Cell Res* (2020) 1867(5):118659. doi: 10.1016/j.bbamcr.2020.118659
51. Rosales-Reynoso MA, Zepeda-López P, Saucedo-Sariñana AM, Pineda-Razo TD, Barros-Núñez P, Gallegos-Arreola MP, et al. GSK3 β polymorphisms are associated with tumor site and TNM stage in colorectal cancer. *Arch Iran Med* (2019) 22(8):453–60.
52. Zhou M, Liu X, Li Z, Huang Q, Li F, Li CY. Caspase-3 regulates the migration, invasion and metastasis of colon cancer cells. *Int J Cancer* (2018) 143(4):921–30. doi: 10.1002/ijc.31374
53. Chohan TA, Qian H, Pan Y, Chen JZ. Cyclin-dependent kinase-2 as a target for cancer therapy: Progress in the development of CDK2 inhibitors as anti-cancer agents. *Curr Med Chem* (2015) 22(2):237–63. doi: 10.2174/0929867321666141106113633
54. Tadesse S, Anshabo AT, Portman N, Lim E, Tilley W, Caldon CE, et al. Targeting CDK2 in cancer: challenges and opportunities for therapy. *Drug Discovery Today* (2020) 25(2):406–13. doi: 10.1016/j.drudis.2019.12.001
55. Chen Y, Jiang J, Zhao M, Luo X, Liang Z, Zhen Y, et al. microRNA-374a suppresses colon cancer progression by directly reducing CCND1 to inactivate the PI3K/AKT pathway. *Oncotarget* (2016) 7(27):41306–19. doi: 10.18632/oncotarget.9320
56. Zhang X, Li X, Tan F, Yu N, Pei H. STAT1 inhibits MiR-181a expression to suppress colorectal cancer cell proliferation through PTEN/Akt. *J Cell Biochem* (2017) 118(10):3435–43. doi: 10.1002/jcb.26000
57. Dhillon AS, Hagan S, Rath O, Kolch W. MAP kinase signalling pathways in cancer. *Oncogene* (2007) 26(22):3279–90. doi: 10.1038/sj.onc.1210421
58. Fang JY, Richardson BC. The MAPK signalling pathways and colorectal cancer. *Lancet Oncol* (2005) 6(5):322–7. doi: 10.1016/S1470-2045(05)70168-6
59. Li LX, Lam IH, Liang FF, Yi SP, Ye LF, Wang JT, et al. MiR-198 affects the proliferation and apoptosis of colorectal cancer through regulation of ADAM28/JAK-STAT signaling pathway. *Eur Rev Med Pharmacol Sci* (2019) 23(4):1487–93. doi: 10.26355/eurrev_201902_17106
60. Zhang T, Ma Y, Fang J, Liu C, Chen L. A deregulated PI3K-AKT signaling pathway in patients with colorectal cancer. *J Gastrointest Cancer* (2019) 50(1):35–41. doi: 10.1007/s12029-017-0024-9
61. Slattery ML, Mullany LE, Wolff RK, Sakoda LC, Samowitz WS, Herrick JS. The p53-signaling pathway and colorectal cancer: Interactions between downstream p53 target genes and miRNAs. *Genomics* (2019) 111(4):762–71. doi: 10.1016/j.ygeno.2018.05.006
62. Caspi M, Wittenstein A, Kazelnik M, Shor-Nareznay Y, Rosin-Arbesfeld R. Therapeutic targeting of the oncogenic wnt signaling pathway for treating colorectal cancer and other colonic disorders. *Adv Drug Delivery Rev* (2021) 169:118–36. doi: 10.1016/j.addr.2020.12.010



OPEN ACCESS

EDITED BY

Hang Ma,
University of Rhode Island, United States

REVIEWED BY

Xiaodong Wang,
Swinburne University of Technology,
Australia
Lanzhou Li,
Jilin Agricultural University, China

*CORRESPONDENCE

Jian He,
✉ jih003@sjtu.edu.cn
Yizhi Song,
✉ songyz@sibet.ac.cn
Shiyu Du,
✉ dushiyu@nimte.ac.cn

[†]These authors have contributed equally
to this work

SPECIALTY SECTION

This article was submitted to
Pharmacology of Anti-Cancer Drugs,
a section of the journal
Frontiers in Pharmacology

RECEIVED 31 October 2022

ACCEPTED 09 February 2023

PUBLISHED 13 March 2023

CITATION

Meng M, Gao R, Liu Z, Liu F, Du S, Song Y
and He J (2023), Ginsenosides, potential
TMPRSS2 inhibitors, a trade-off between
the therapeutic combination for anti-PD-
1 immunotherapy and the treatment of
COVID-19 infection of LUAD patients.
Front. Pharmacol. 14:1085509.
doi: 10.3389/fphar.2023.1085509

COPYRIGHT

© 2023 Meng, Gao, Liu, Liu, Du, Song and
He. This is an open-access article
distributed under the terms of the
[Creative Commons Attribution License
\(CC BY\)](https://creativecommons.org/licenses/by/4.0/). The use, distribution or
reproduction in other forums is
permitted, provided the original author(s)
and the copyright owner(s) are credited
and that the original publication in this
journal is cited, in accordance with
accepted academic practice. No use,
distribution or reproduction is permitted
which does not comply with these terms.

Ginsenosides, potential TMPRSS2 inhibitors, a trade-off between the therapeutic combination for anti-PD-1 immunotherapy and the treatment of COVID-19 infection of LUAD patients

Mei Meng^{1†}, Rui Gao^{1†}, Zixue Liu^{1†}, Fengxiang Liu², Shiyu Du^{3,4,5*†},
Yizhi Song^{2*†} and Jian He^{1*†}

¹State Key Laboratory of Oncogenes and Related Genes, Center for Single-Cell Omics, School of Public Health, Shanghai Jiao Tong University School of Medicine, Shanghai, China, ²CAS Key Laboratory of Bio-Medical Diagnostics, Suzhou Institute of Biomedical Engineering and Technology, Chinese Academy of Sciences, Suzhou, China, ³Engineering Laboratory of Nuclear Energy Materials, Ningbo Institute of Materials Technology and Engineering, Chinese Academy of Sciences, Ningbo, China, ⁴School of Materials Science and Engineering, China University of Petroleum (East China), Qingdao, China, ⁵School of Computer Science, China University of Petroleum (East China), Qingdao, China

Background: Acting as a viral entry for coronavirus to invade human cells, TMPRSS2 has become a target for the prevention and treatment of COVID-19 infection. Before this, TMPRSS2 has presented biological functions in cancer, but the roles remain controversial and the mechanism remains unelucidated. Some chemicals have been reported to be inhibitors of TMPRSS2 and also demonstrated other pharmacological properties. At this stage, it is important to discover more new compounds targeting TMPRSS2, especially from natural products, for the prevention and treatment of COVID-19 infection.

Methods: We analyzed the correlation between TMPRSS2 expression, methylation level, overall survival rate, clinical parameters, biological process, and determined the correlation between TMPRSS2 and tumor-infiltrating lymphocytes in the tumor and adjacent normal tissue of adenocarcinoma (LUAD) and squamous cell carcinoma (LUSC) respectively by using various types of bioinformatics approaches. Moreover, we determined the correlation between TMPRSS2 protein level and the prognosis of LUAD and LUSC cohorts by immunohistochemistry assay. Furthermore, the cancer immunome atlas (TCIA) database was used to predict the relationship between the expression of TMPRSS2 and response to programmed cell death protein 1 (PD-1) blocker immunotherapy in lung cancer patients. Finally, the putative binding site of ginsenosides bound to TMPRSS2 protein was built from homology modeling to screen high-potency TMPRSS2 inhibitors.

Abbreviations: ACE2, angiotensin converting enzyme2; FFPE, paraffin embedded; FP, fluticasone propionate; HR, hazard ratio; LUAD, adenocarcinoma; LUSC, squamous cell carcinoma; NSCLC, non-small cell lung cancer; OS, overall survival; PAMPs, pathogen-associated molecular patterns; PD-1, programmed cell death protein 1; PD-L1, cell surface local programmed cells blockade of death ligand 1; RFS, recurrence-free survival; SCLC, small cell lung cancer; TAMs, tumor-associated macrophages; TILs, tumor-infiltrating lymphocytes; TINs, tumor-infiltrating neutrophils; TLRs, Toll-like receptors; TMPRSS2, transmembrane serine protease 2.

Results: We found that TMPRSS2 recruits various types of immunocytes, including CD8⁺, CD4⁺ T cells, B cells and DCs both in LUAD and LUSC patients, and the correlation between TMPRSS2 expression and CD8⁺ and CD4⁺ T cells are stronger in LUAD rather than in LUSC, but excludes macrophages and neutrophils in LUAD patient cohorts. These might be the reason that higher mRNA and protein levels of TMPRSS2 are associated with better prognosis in LUAD cohorts rather than in LUSC cohorts. Furthermore, we found that TMPRSS2 was positively correlated with the prognosis in patient nonresponse to anti-PD-1 therapy. Therefore, we made an inference that increasing the expression level of TMPRSS2 may improve the anti-PD-1 immunotherapy efficacy. Finally, five ginsenosides candidates with high inhibition potency were screened from the natural chemical library to be used as TMPRSS2 inhibitors.

Conclusion: All these may imply that TMPRSS2 might be a novel prognostic biomarker and serve as a potential immunomodulator target of immunotherapy combination therapies in LUAD patients nonresponse to anti-PD-1 therapy. Also, these findings may suggest we should pay more attention to LUAD patients, especially those infected with COVID-19, who should avoid medicating TMPRSS2 inhibitors, such as ginsenosides to gain prophylactic and therapeutic benefits against COVID-19.

KEYWORDS

TMPRSS2, LUAD, biomarker, tumor-infiltrating lymphocytes, prognosis, ginsenosides

1 Introduction

As a major cause of death from tumor all over the world, lung cancer is mainly induced by genetics, environmental factors, age, gender, unreasonable diet, smoking, and other factors (Gao et al., 2022; He et al., 2023). The primary categories of lung malignant tumor are small cell lung cancer (SCLC) and non-small cell lung cancer (NSCLC). Among them, NSCLC is mainly subdivided into adenocarcinoma (LUAD) and squamous cell carcinoma (LUSC) (He et al., 2021a; Li et al., 2021). At present, compared with previous chemotherapy and surgical treatment, more and more targeted therapy and immune checkpoint inhibitor therapy are applied to the treatment of cancer and have become essential for the treatment of lung cancer treatment (Tan and Tan, 2022). Among them, inhibition of the PD-1 axis, including antibody-mediated programmed cell death protein 1 (PD-1) and programmed cell death ligand 1 (PD-L1) blockade, increased the survival rates of many NSCLC patients (Larsen et al., 2019; He et al., 2022; Tan and Tan, 2022). However, immune drugs benefit only a small percentage of patients and poor prognosis is still the leading cause of a high mortality. Therefore, it is indeed necessary to find a factor or modulator that affects the prognosis of lung cancer to assist the existing treatment methods to improve patients' prognosis. Additionally, emerging evidence shows that tumor-infiltrating lymphocytes (TIL), such as tumor-infiltrating neutrophils (TIN) and tumor-associated macrophages (TAM), play a critical role in mediating the response to chemotherapy and achieving better clinical outcomes of different cancers (Stanton and Disis, 2016; Su et al., 2021), and have a great effect on the prognosis of cancer (Benevides et al., 2015; Tariq et al., 2017). So, it is also urgently required to elucidate tumor-immune interactions immunophenotypes, as well as identify novel immunological targets for cancer therapies.

TMPRSS2 encodes a serine protease that contains a receptor type A domain, a type II transmembrane domain, a cysteine-rich scavenger receptor domain, and a protease domain. Serine proteases are known to be involved in a wide range of biological processes (Glowacka et al., 2011). It has been found that TMPRSS2 plays a prominent role in COVID-19 infection. It contributes to the initiation of the spike (S) protein of the coronavirus and, together with angiotensin-converting enzyme 2 (ACE2), assists the virus to enter target cells to infect the host (Hoffmann et al., 2020; He et al., 2021b).

Meanwhile, it is reported that TMPRSS2 was an important factor in cancer development (Hossain and Bostwick, 2013). TMPRSS2 has been demonstrated upregulated in prostate cancer cells by androgenic hormones and downregulated in prostate cancer tissue which is androgen-independent. The silence of TMPRSS2 could inhibit the proliferation of prostate cancer cells (Hossain and Bostwick, 2013). In breast cancer studies, the migratory and metastatic behavior of tumor cells can be promoted by the regulation of TMPRSS2 and its downstream signal pathway *in vitro* (Chi et al., 2020). In addition, studies have shown that patients with cancer are at greater risk of being infected by SARS-CoV-2 (Wang et al., 2021), considering the functions of TMPRSS2 in the COVID-19 infection, medicating the cancer patients infected COVID-19 requires thoughtful consideration.

Ginsenosides, as the main active components of ginseng, have a wide range of pharmacological effects (He et al., 2019), including antioxidant (He, 2017; Yang et al., 2018), antitumor (Zhou et al., 2018), anti-inflammatory (Chen et al., 2019; He and Li, 2015), anti-aging (Sun et al., 2018), etc., among which the antitumor effect is one of the hot spots of research. Many experiments have shown that ginsenosides can inhibit the invasion and metastasis of tumors (Wu et al., 2018). Studies have found that ginsenosides can inhibit the growth of liver cancer (Behrens et al., 2013). In addition, the extracts and metabolites of ginsenoside also have good inhibitory effects on lung cancer (Gao et al., 2013).

In this study, to gain a deeper understanding of how TMPRSS2 affects lung cancer, especially LUAD and LUSC, we used various types of bioinformatic approaches and IHC to determine the relationships between TMPRSS2 expression, methylation level, and OS, clinical parameters, biological process. Furthermore, we examined the correlation between TMPRSS2 and the level of TILs infiltration in tumor and normal tissue respectively. We tried to innovatively provide a novel insight for indicating the prognosis potential of LUAD patients from the perspective of immune infiltration and proposed a theoretical basis and novel therapeutic strategy for lung cancer treatment. In addition, we found that ginsenosides, as the inhibitors of TMPRSS2, play different roles in lung cancer and COVID-19 patients, providing new insights into the prevention and treatment of COVID-19 in lung cancer patients.

2 Materials and methods

2.1 Ethical approval

It was approved by the Independent Ethics Committee of Shanghai Jiao Tong University.

2.2 TMPRSS2 mRNA expression and the prognosis analysis

The mRNA expression level of TMPRSS2 in different types of cancer was identified by using TIMER 2.0 (Li et al., 2020) and UALCAN (Chandrashekar et al., 2017) database and the correlation between the expression of TMPRSS2 and the prognoses of lung cancer was examined by the PrognosScan (Mizuno et al., 2009), TIMER 2.0, GEPIA 2 (Tang et al., 2019) and OncoPrint (Anaya, 2016) database. The threshold was adjusted to a Cox p -value <0.05. The hazard ratio (HR) with 95% confidence intervals (CIs) and log-rank p -value were also determined.

In order to access the level of TMPRSS2 expression in different cell types of patients with lung cancer at single cell level, we utilized TISCH (Sun et al., 2021) to create an interactive gene expression visualization of multiple datasets at single-cell resolution across multiple datasets.

2.3 Clinical parameters analysis

The association between the mRNA expression level of TMPRSS2 and clinicopathological parameters was analyzed by UALCAN (a web tool for visualization of the impact between gene expression and clinicopathological parameters based on the TCGA data) and MEXPRESS (Koch et al., 2015) platform, which is used for integrating and visualizing clinical, expression and methylation data in TCGA at the single-gene level.

2.4 Correlation analysis

We determined the association between the mRNA expression level of TMPRSS2 and survival rate as well as

different cancer staging in LUAD and LUSC (Lánczky and Györfy, 2021). HRs with 95% CIs and log-rank p -values were also computed.

2.5 Methylation analysis

We employed UALCAN to examine the gene methylation levels across a range of clinicopathological features, such as ages and stages. The statistical significance was compared by using t -test. The MEXPRESS platform was also used to identify the level of methylation in the promoter region of TMPRSS2.

2.6 Biological network analysis and GSEA analysis

GeneMANIA (Warde-Farley et al., 2010) is used to create the biological network of TMPRSS2 based on the data relating to function associations, and LinkInterpreter modules in LinkedOmics (Vasaikar et al., 2018), which was used for enrichment analysis in TCGA, was employed for the identification of TMPRSS2 pathways and networks in LUAD and LUSC cohorts. Spearman's correlation coefficient was used to investigate these results.

2.7 Relationship between immune infiltration levels and OS and its association with TMPRSS2 expression

TIMER2.0 was used to examine TMPRSS2 expression level in patients with lung cancer. The association between TMPRSS2 and the immune infiltrating level, including T cells (CD4⁺, CD8⁺), B cells, macrophages, neutrophils, and DCs was studied by using the gene modules in TIMER2.0 (Aran et al., 2015; Li et al., 2016). Log2 RSEM was used to determine gene expression levels. Then we used TIMER2.0 to analyze the relationship between the proportion of certain TILs and OS and the correlation with TMPRSS2 expression.

2.8 Correlation between TMPRSS2 expression and various immune cells in tumor and normal tissue

We employed GEPIA2 to evaluate the differences in the enrichment of different TILs including CD8⁺ T cells, Treg, macrophage, monocyte in the tumor and normal tissue of LUAD and LUSC patients, and further analyzed the enrichment of all T cell subtypes in the same patient cohorts (Danaher et al., 2017; Siemers et al., 2017).

2.9 Immunohistochemical staining for TMPRSS2 in lung cancer cohort tissue microarrays

Two lung cancer tissue microarrays were purchased from Superbiotech (Shanghai, PRC), containing 63 and 78 paired

tumors and adjacent normal tissues from LUAD (LUC1601) and LUSC (LUC1602) patients, respectively. A summary of the clinical pathological information including subtype, tumor/nodal stage, histological grade, and information about patient follow-up. The tissue sections were stained with an anti-TMPRSS2 antibody (ab109131, ABCAM, United States) (dilution: 1: 1000). Following the general standard IHC staining methods, TMAs sections were used to measure the TMPRSS2 protein levels. The staining results were quantified according to the following criteria: for staining degree: 1, weak; 2, intermediate; 3, strong; For the proportion of positive cells: 1, 0–25%; 2, 26–50%; 3, 51–75%; 4, >75%. The staining score was obtained by multiplying staining degree by the proportion, 0–5 was considered low expression, and >5 was high expression.

2.10 Immunophenotyping of LUAD and LUSC patients

The Cancer Immunome Atlas (TCIA) database (Charoentong et al., 2017) contains immunogenomics characterizations of 20 solid cancers from TCGA, enabling comprehensive analysis of tumor immune and genetic profiles. Immunophenogram is used to classify patients who are likely to respond to antibody therapy targeting PD-1 by scoring a panel of immune genes. We analyzed the impact of TMPRSS2 expression on prognosis in the top 100 and bottom 100 patients by ranking the immunophenoscores (IPS) of LUAD and LUSC patients who were likely to respond to PD-1 antibody therapy and representative patients were selected to obtain the corresponding immunophenotype map.

2.11 Molecular docking

Docking calculations were performed by using the computerized protein-ligand docking software, Autodock Vina v.1.2.2 (Morris et al., 2008). TMPRSS2 was docked with the screened ginsenosides to obtain candidate ginsenosides that could be used as TMPRSS2 inhibitors.

2.12 Statistical analysis

HR and P or Cox *p* values based on a log-rank test. Spearman was used to assess the correlation. GraphPad Prism 7.0 was used for statistical analysis of results related to TMAs staining. Student's *t* test was used to compare between 2 groups. Comparison among more than 2 groups was done using one-way analysis of variance (ANOVA). *p* values <0.05 were considered statistically significant.

3 Results

3.1 The variability of TMPRSS2 mRNA expression level across human cancer

Here, we found that TMPRSS2 expression was significantly lower in the tumor tissue of COAD, BRCA, HNSC, KIRC, KIRP,

LIHC, LUAD, LUSC, READ, and THCA, whereas higher in KICH, PRAD, and UCEC compared with adjacent normal tissue (Figure 1A). The differential expression of TMPRSS2 between tumors and paired normal tissue for each of the TCGA tumors in UALCAN is displayed in Figure 1B. The expression of TMPRSS2 was significantly higher in CESC, BLCA, KICH, PRAD and UCEC, whereas lower in BRCA, COAD, KIRP, KIRC, LUAD, LUSC, LIHC, READ compared with adjacent normal tissues (Figure 1B). Integrating above results, we found that the mRNA expression level of TMPRSS2 in LUAD and LUSC tumor tissues is lower than that in the corresponding normal tissues.

3.2 The prognostic potential of TMPRSS2 in cancer

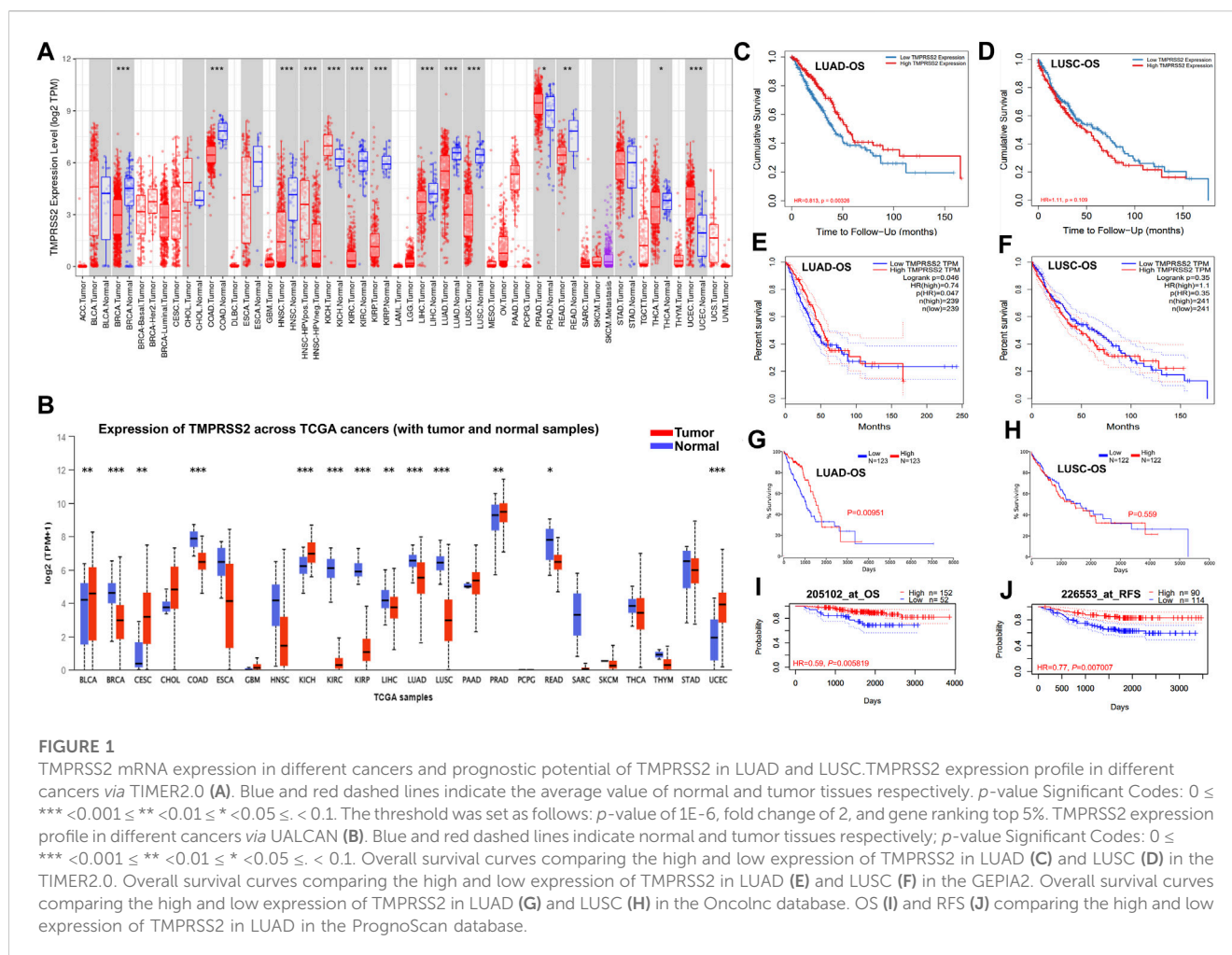
Notably, the expression of TMPRSS2 displays a significant association with OS in several types of cancers, including brain cancer, colorectal cancer, breast cancer, lung cancer, and ovarian cancer. The detailed association between TMPRSS2 mRNA expression and the prognostic potential of different cancers is presented in Supplementary Table S1.

In two lung cancer cohorts (GSE13213 and GSE4573), higher TMPRSS2 expression was associated to favorable outcomes (OS HR = 0.68, 95% CI = 0.51–0.89, Cox *p* = 0.006146; OS HR = 0.83, 95% CI = 0.70–0.99, Cox *p* = 0.042151) (Supplementary Table S1). Therefore, it is conceivable that a high level of TMPRSS2 may be independently linked to better prognoses of lung cancer. HR below 1 implies that TMPRSS2 expression has a protective effect on patients with lung cancer.

The LUAD cohort (GSE31210) demonstrated that a high level of TMPRSS2 was associated with improved OS (Figure 1I) and recurrence-free survival (RFS) (Figure 1J), but there is nonsignificant difference in LUSC cohorts. These data suggested that the expression level of TMPRSS2 shows different prognostic values based on cancer type. Moreover, TMPRSS2's prognosis potential in LUAD and LUSC patient cohorts was also assessed by using the RNA-Seq dataset via TIMER 2.0, GEPIA2 and OncoPrint database, confirming the different association patterns between the level of TMPRSS2 and prognosis in LUAD and LUSC patient's cohorts (Figures 1C–H).

3.3 Expression levels of TMPRSS2 impact the clinicopathological parameters in lung cancer

To better disclose the relevance and impact of the TMPRSS2 expression in LUAD and LUSC patients, the relationship between the mRNA expression level of TMPRSS2 and different clinical characteristics was studied (Supplementary Figure S1; Supplementary Table S2). We discovered that the expression level of TMPRSS2 was significantly different in each stage, different races, and different genders of both LUAD and LUSC patients (Supplementary Figures S1A–C, F–H). Moreover, the mRNA expression level of TMPRSS2 demonstrated age- and smoking-dependent patterns in LUAD and LUSC cohorts (Supplementary Figures 1D, E, I, J;



Supplementary Table S2). These phenomena indicate that the mRNA expression level of TMPRSS2 could impact the clinicopathological parameters of lung cancer but the differences in prognosis patterns between LUAD and LUSC are less affected by the TMPRSS2-dependent clinicopathological parameters. So, there might be some other reasons lying behind.

For a greater understanding of the correlation and mechanism of TMPRSS2 expression level in LUAD and LUSC, we further studied the correlation between TMPRSS2 expression and clinical prognosis in patients with lung cancer with various clinicopathological factors. We found that a higher TMPRSS2 mRNA expression level was associated with a better OS for LUAD patients in the late stage, but worse OS for LUSC patients in the early stage (Table 1). Although both genders experienced better OS with higher TMPRSS2 expression in LUAD, male patients demonstrated better OS in both early and late stages compared with female patients. In addition, race-specific association patterns were observed in LUAD (Table 1). In addition to Asian races, TMPRSS2 has been linked to better OS in White races, and higher TMPRSS2 expression level in mutation burden LUAD was also associated with a better OS. All these results indicate that the expression level of TMPRSS2 has an impact on the prognosis of LUAD and LUSC with different patterns.

3.4 Protein level of TMPRSS2 impacts the clinicopathological parameters of LUAD

We examined TMPRSS2 protein levels in two tissue microarrays containing 63 and 78 paired tumor and normal tissues, respectively, from LUAD and LUSC patient cohorts. Both of those have detailed clinicopathological information, including histological grading, subtype, tumor/nodal stage, and patients' follow-up over 5 years information. TMPRSS2 is mainly expressed in the cytoplasm (Figure 2A). The protein level of the tumor was significantly lower compared to the paired normal tissue in both LUAD and LUSC patient cohorts (Figure 2B). Next, we examined the relationship between TMPRSS2 protein level and the clinical parameters. We found that a higher protein level of TMPRSS2 was associated with a better OS in LUAD patient cohorts rather than in LUSC cohorts (Figure 2C). Moreover, we also found a negative correlation between lower TMPRSS2 levels and clinical stages, and lymph node metastasis status in LUAD patients (Figures 2D, E).

To validate the reliability of our findings, we also analyzed the correlation between TMPRSS2 protein levels in LUAD cohorts and different clinical parameters via UALCAN (Supplementary Table S3). We found a significant decrease in TMPRSS2 protein level in LUAD compared to normal tissues, with the most significant

TABLE 1 Correlation of the mRNA expression level of *TPMRSS2* in different stage and clinical prognostic potential in lung cancer with different clinicopathological factors.

Clinicopathological characteristics	Overall survival					
	LUAD (<i>n</i> = 513)			LUSC (<i>n</i> = 501)		
	N	Hazard ratio	<i>p</i> -value	N	Hazard ratio	<i>p</i> -value
Gender						
Female	270	0.58 (0.390-0.88)	0.0086	129	0.54 (0.25–1.16)	0.11
Male	234	0.55 (0.36–0.84)	0.0051	366	1.28 (0.94–1.75)	0.12
Race						
White	387	0.52 (0.37–0.73)	0.00013	348	1.28 (0.89–1.83)	0.18
Asian	---	---	---	---	---	---
Black/African American mutation burden	52	0.43 (0.12–1.52)	0.18	29	0.51 (0.15–1.79)	0.29
High	255	0.41 (0.22–0.76)	0.0032	240	0.84 (0.57–1.26)	0.41
Low	244	0.47 (0.31–0.72)	0.00039	242	0. (0.93–2.06)	0.11
Stage						
1	270	1.4 (0.84–2.33)	0.2	242	1.64 (1.05–2.55)	0.027
2	119	0.58 (0.32–1.06)	0.073	159	1.17 (0.7–1.95)	0.55
3	81	0.44 (0.24–0.8)	0.0059	83	0.54 (0.29–1.01)	0.05
4	26	0.14 (0.02–1.04)	0.025	---	---	---
Gender + Stage						
Early + male	66	0.45 (0.21–0.98)	0.039	119	1.23 (0.63–2.44)	0.54
Early + female	53	1.55 (0.51–4.69)	0.44	40	0.67 (0.21–2.12)	0.49
Late + male	37	0.38 (0.15–0.97)	0.035	63	0.55 (0.27–1.13)	0.098
Late + female	44	0.44 (0.016–1.19)	0.098	20	0.31 (0.08–1.21)	0.075

Bold values indicate *p* < 0.05.

decrease in solid adenocarcinoma (Supplementary Figures 2A, H). Furthermore, we also found that *TPMRSS2* protein was significantly reduced in male LUAD patients and correlated with higher tumor grade (Supplementary Figures 2D, G). In the pathway-related studies, we found that the protein level of *TPMRSS2* was significantly associated to HIPPO pathway status, mTOR pathway status, WNT pathway status, NRF2 pathway status, P53/Rb-related pathway status, RTK pathway status, SWI-SNF complex status and chromatin modifier status (Supplementary Figures S2I–P), indicating that *TPMRSS2* may function through these pathways in LUAD.

3.5 Low promoter methylation level of *TPMRSS2* impacts the clinicopathological parameters of patients with lung cancer

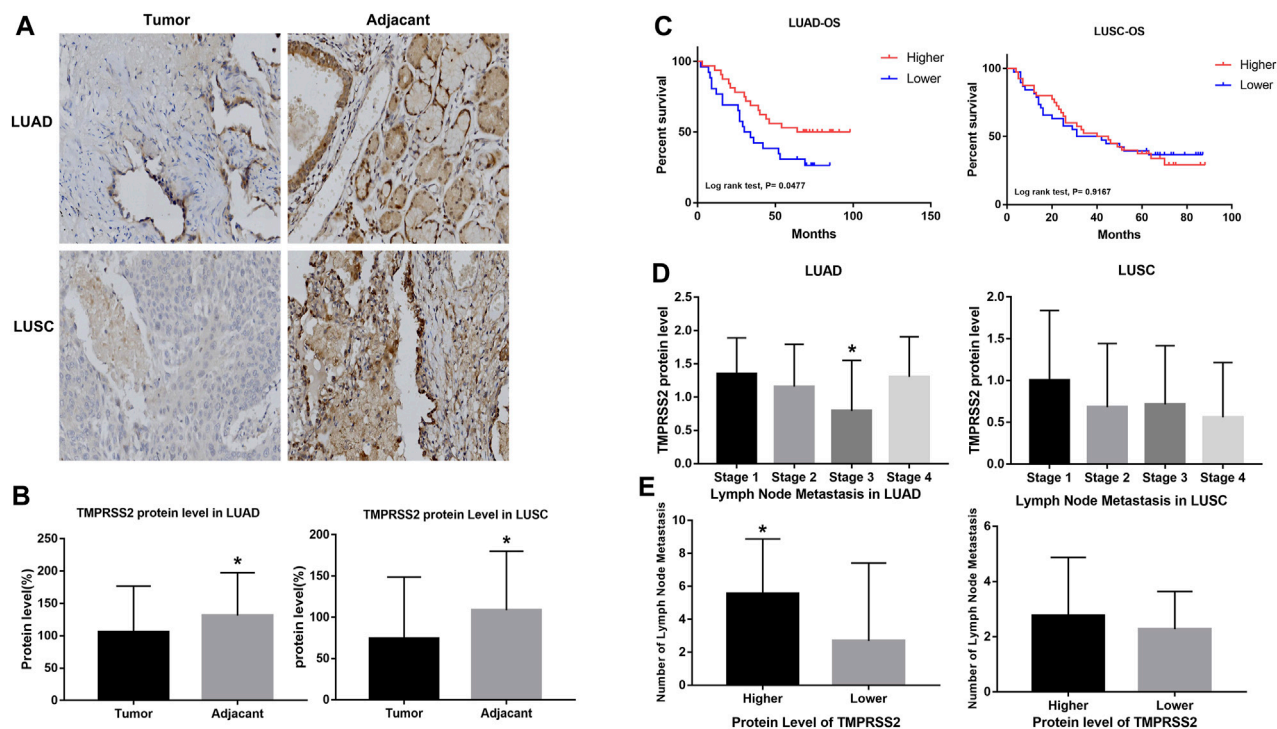
To reveal the mechanism involved in the decreased *TPMRSS2* expression in LUAD and LUSC, we predicted the methylation site and examined the methylation of *TPMRSS2* in tumors and normal tissues of LUAD and LUSC respectively *via* MEXPRESS and UALCAN (Figure 3; Supplementary Tables S4, S5).

Among these CpG locations, CpG41504034 drew our attention, since *TPMRSS2* expression level is significantly negatively correlated with the methylation status in a LUAD cohort, whereas the level of *TPMRSS2* is significantly positively correlated with the methylation status in CpG 41508181 in LUSC patients (Supplementary Table S4).

Moreover, the methylation status in the LUAD patients is significantly lower than that of LUSC on the CpG 41488290, while significantly positively correlated in the LUSC cohort.

We found that 5 CpG sites had significantly higher hypermethylation levels in the tumor tissue compared to paired normal tissue of LUAD and LUSC patients (*p* < 0.0001, Figures 3A, E). A higher level of promoter methylation was detected in the early stage, suggesting that the high levels of *TPMRSS2* promoter methylation were related to earlier stages of lung cancer development (Figures 3B, F). According to the methylation analysis here, the level of *TPMRSS2* may fluctuate throughout the course of lung cancer. Additionally, a similar pattern was observed in the analysis of nodal metastasis, suggesting that the levels of *TPMRSS2* promoter methylation are somehow related to nodal metastasis (Figures 3K, O). Race and age-related methylation patterns of *TPMRSS2* promoters have similar patterns in LUAD and LUSC, respectively; that is, the African-American group, as well as the younger group of these two cohorts, had higher methylation levels of *TPMRSS2* (Figures 3C, G, I, M). In addition, *TPMRSS2* methylation level was also associated with gender, smoking habits and TP53 mutants (Figures 3D, H, J, N, L, P).

The effect of methylation level on prognosis is consistent with the previously found effect of mRNA expression level on prognosis. That is, the level of *TPMRSS2* expression and methylation are basically the same in the two lung cancer subtypes, so we believe that the difference between *TPMRSS2* on LUAD and LUSC prognosis was also not at the methylation level.

**FIGURE 2**

Higher expression of TMPRSS2 protein was correlated with different clinicopathological parameters in LUAD and LUSC cohorts.(A)

Immunohistochemical staining for TMPRSS2 of tumor and adjacent tissue in LUAD and LUSC. Original magnification $\times 40$. TMPRSS2 protein level in tumor and adjacent (B) and overall survival (C) of LUAD and LUSC, $p < 0.05$. (D) Correlation between TMPRSS2 protein level and clinical stage, $p < 0.05$. (E) Correlation between TMPRSS2 protein level and lymph node metastasis, $p < 0.05$.

3.6 Gene ontology of TMPRSS2

In order to investigate the mechanism of TMPRSS2 in biological processes, we performed the GSEA analysis of its related genes. Figure 4A shows 20 TMPRSS2-related proteins based on the analysis of physical interactions, co-expression, co-localization, predicted, genetic interactions, pathway and shared protein domain that was screened through the GENEMANIA database. We found that TMPRSS2 has a high correlation with ACE, KLK2, KLK3, and NGF in protein processing and maturation. In addition, ACE, KLK2, KLK3, and NGF as a gene set positively correlated with prognosis in LUAD but not LUSC (Supplementary Figure S3), which reconfirmed our previous finding that the mRNA expression of TMPRSS2 has different correlation patterns with the prognosis of LUAD and LUSC, that is, the higher the expression level, the better the prognosis.

Furthermore, we used LinkedOmics database to further analyze TMPRSS2-related genes in LUAD and LUSC cohorts. The pathways and networks were identified using LinkInterpreter.

We found that TMPRSS2 functions in LUAD to downregulate regulation of response to cytokine stimulus, T cell activation, defense response to other organism, immune response-regulating signaling pathway, regulation of leukocyte activation, leukocyte migration, interleukin-2 production and cytokine metabolic process (Figure 4B). However, immune-related biological processes were mostly up-regulated in LUSC patients, suggesting that TMPRSS2 is

closely related to immune biology in LUAD and LUSC, and likely in opposite patterns. Further, we found that the relationship between TMPRSS2 and TNF signaling pathway in KEGG pathway analysis showed two diametrically opposite patterns in LUAD and LUSC (Figure 4B). This suggests that: ① the underlying mechanism of the different correlation patterns between the TMPRSS2 mRNA expression level and the prognosis might be the immunity regulatory; ② TMPRSS2 has opposite biological effects on TNF activation.

3.7 TMPRSS2 expression is correlated with immune infiltration level in lung cancer

Tumor-infiltrating lymphocytes are independent predictors of survival in cancers. Therefore, we investigated whether the expression of TMPRSS2 was correlated with immune infiltration levels in lung cancer. We assessed the correlations between TMPRSS2 expression and immune infiltration levels in LUAD and LUSC from TIMER2.0. A significant negative correlation was found between TMPRSS2 expression and tumor purity in LUSC, which suggests that TMPRSS2 may be linked to lymphocyte recruitment to LUSC niches and significant positive correlated to macrophages and neutrophils infiltration levels in LUSC (Figure 5A), while macrophages and neutrophils infiltration were negative correlated to TMPRSS2 expression level in LUAD. In addition, the expression level of

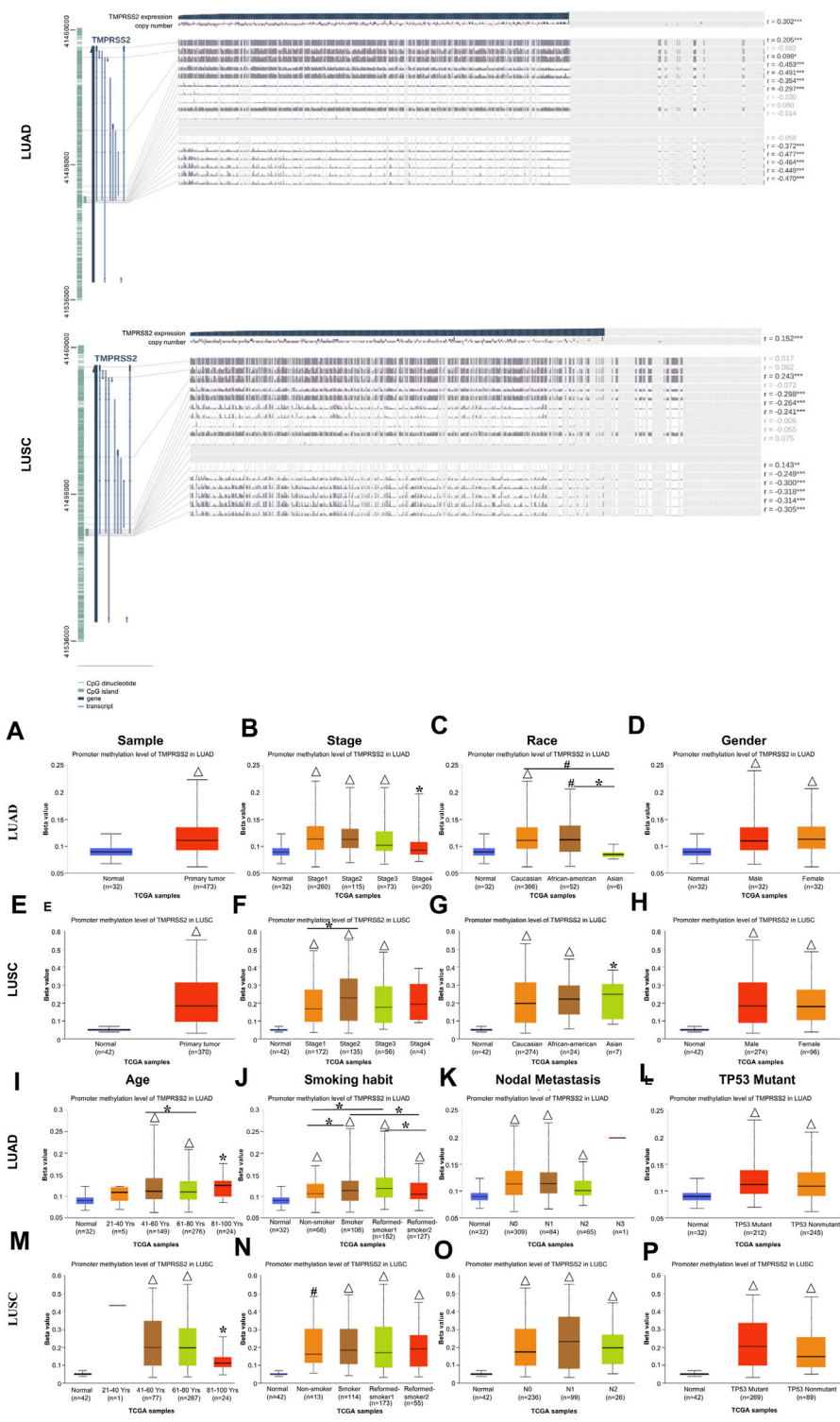
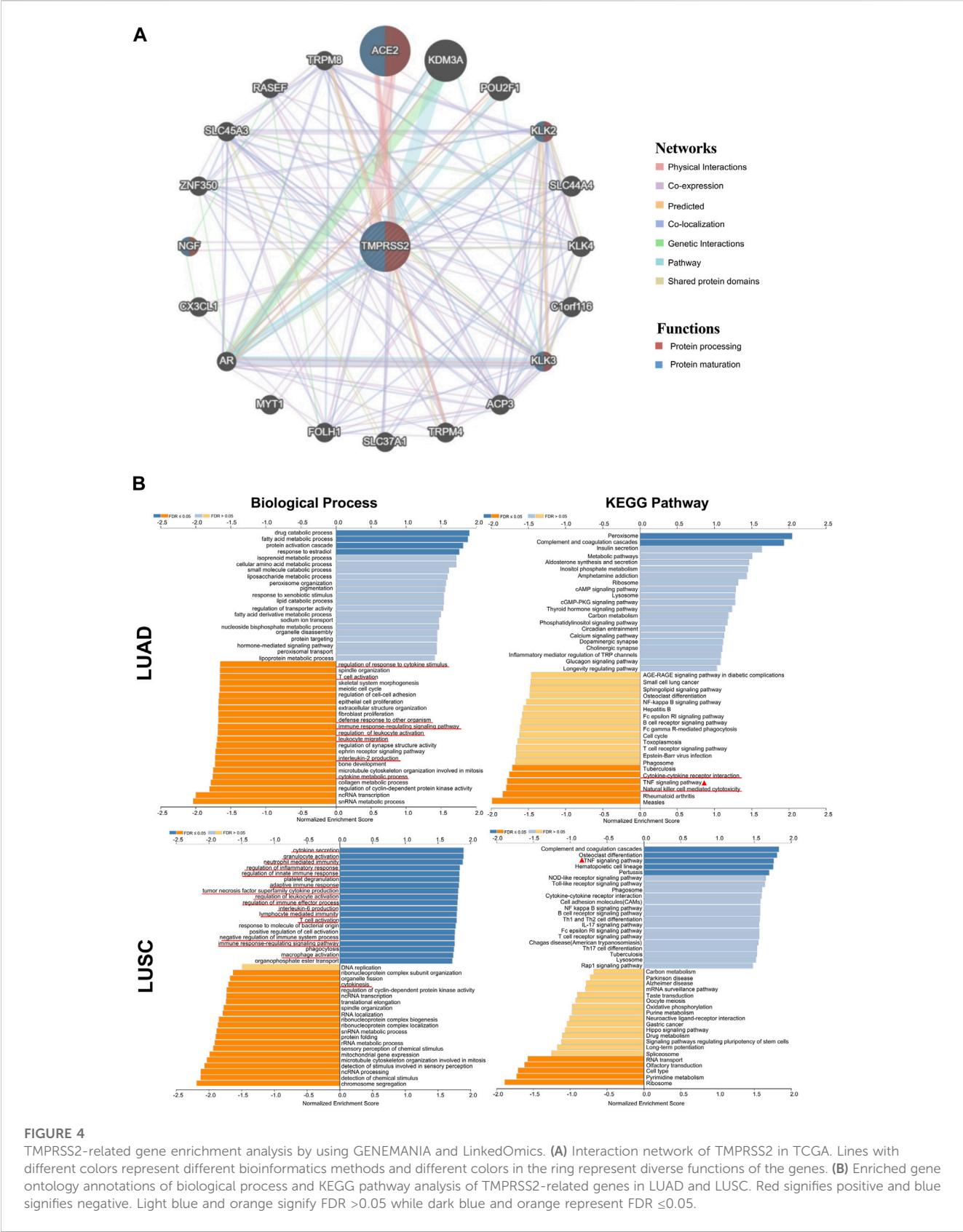


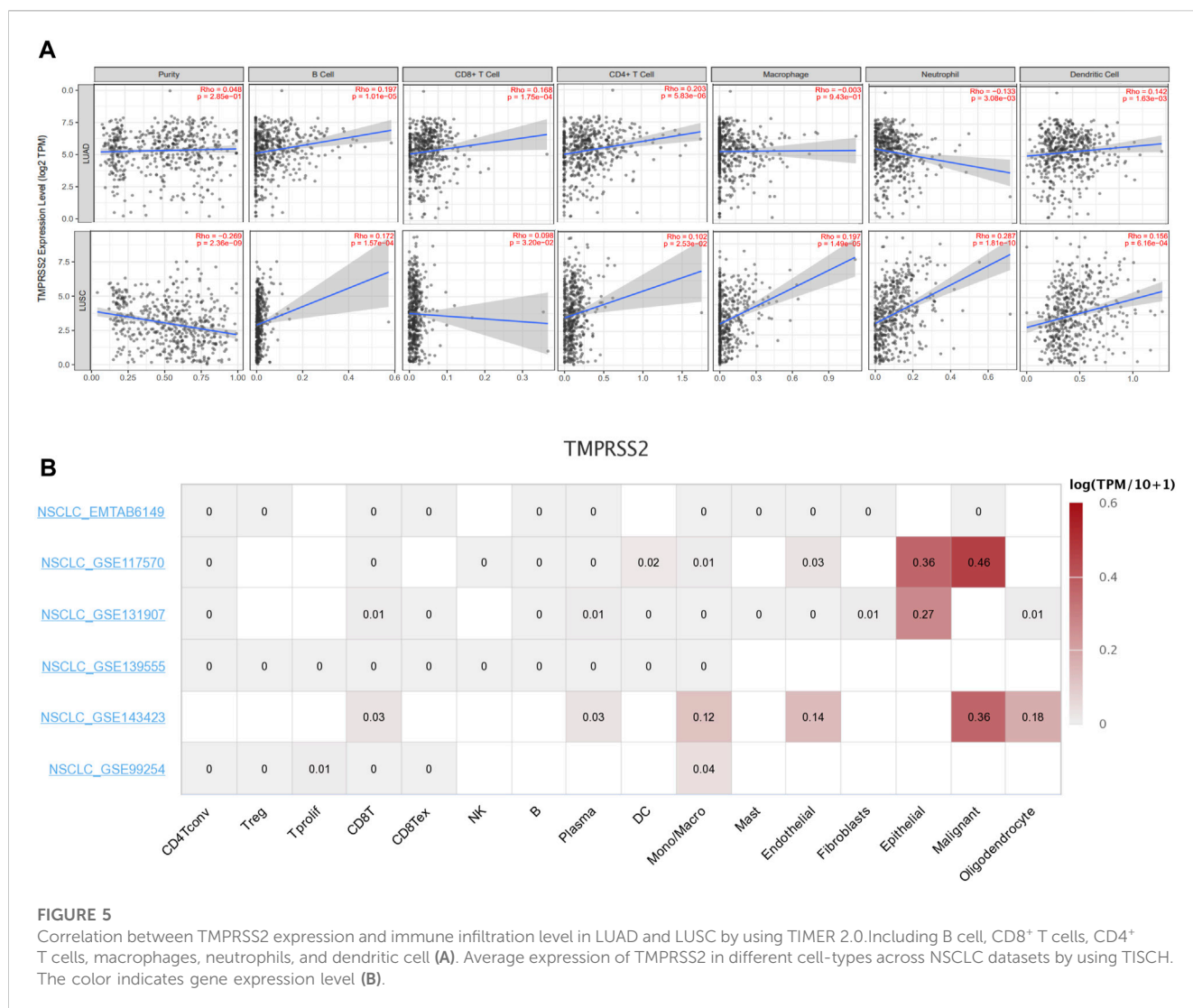
FIGURE 3 Visualization of promoter methylation levels of TMPRSS2 impact the clinicopathological parameters in LUAD and LUSC using MEXPRESS (upper) and UALCAN (lower).The promoter methylation level of TMPRSS2 of sample types (A, E), stage (B, F), race (C, G), gender (D, H), age (I, M), smoking habit (J, N), nodal metastasis status (K, O) and TP53 mutant (L, P) in LUAD and LUSC cohorts respectively. * $p \leq 0.05$, # $p \leq 0.001$, Δ $p \leq 0.0001$.

TMPPRSS2 demonstrated significant positive correlations with infiltrating levels of B cells, CD8⁺ T cells, CD4⁺ T cells, and dendritic cells in both LUAD and LUSC (Figure 5A).

In order to clarify whether the correlation between TMPRSS2 and immune infiltration is due to the recruitment of immune cells by TMPRSS2, or whether immune cells themselves express TMPRSS2, we



used single-cell sequencing data from patients with NSCLC in the TSICH database to study the expression of TMPPRS2 in different cells (Figure 5B) and found that TMPPRS2 was mainly expressed in epithelial cells and malignant cells, but was hardly expressed in immune cells. It indicated that the relationship between the level of TMPPRS2 expression and immune infiltration was correlated with immune cells recruitment by TMPPRS2.



We further explored the prognostic impact of TMPRSS2 expression and immune infiltration in LUAD and LUSC, we studied the relationship between different immune cells and lung cancer OS, and the relationship between the combined effect of TMPRSS2 and immune cells and lung cancer OS respectively (Figure 6). We found that although TMPRSS2 and B cells, CD4⁺T cells are positively correlated in both LUAD and LUSC, the proportion of B cells and CD4⁺T cells and prognosis have different patterns in the two subtypes (Figures 6A–D), that is, the higher the percentage of B cells, the better the prognosis of LUAD, but not LUSC (Figures 6A, C). As for CD4⁺T cells, the higher the percentage of CD4⁺T cells, the worse the prognosis of LUSC (Figure 6D), so the positive correlation between TMPRSS2 expression and CD4⁺T cells will augment the poor prognosis of LUSC; similarly, the higher the proportion of neutrophil, the worse the prognosis of LUSC (Figure 6H), so the positive correlation between TMPRSS2 expression and neutrophil in LUSC will also lead to poor prognosis of LUSC.

We also found that different subtypes of macrophages play different roles in LUAD and LUSC (Figures 6I–L). The high

expression of TMPRSS2 mRNA in LUSC is positively correlated with macrophages, which may be one of the reasons why TMPRSS2 is not a favorable factor for LUSC.

In addition, the infiltration of DCs and the effect of TMPRSS2 expression on prognosis were also diametrically opposite between LUAD and LUSC (Figures 6M, N), which suggested that the underlying mechanism of TMPRSS2 leading to a different prognosis pattern in two lung cancer subtypes might be the recruitment and infiltration of TILs.

Furthermore, we explored the potential prognostic significance of infiltrating cells of T-cell (Tregs, T cell follicular helper, T cell CD4⁺ memory resting and T cell NK) in LUAD and LUSC (Supplementary Figure S4). We found that the infiltration of all these 4 types of T cells correlated to a better prognosis in LUAD rather than in LUSC (Supplementary Figures S4A–H). Moreover, besides Tregs and T cell CD4⁺ memory resting, the expression level of TMPRSS2 augments the positive association between T cell NK and LUAD prognosis (Supplementary Figure S4F). Also, there is a difference in the correlation pattern between the infiltration level of Treg and prognosis in LUAD and LUSC patients (Supplementary Figures S4A, C). It is shown

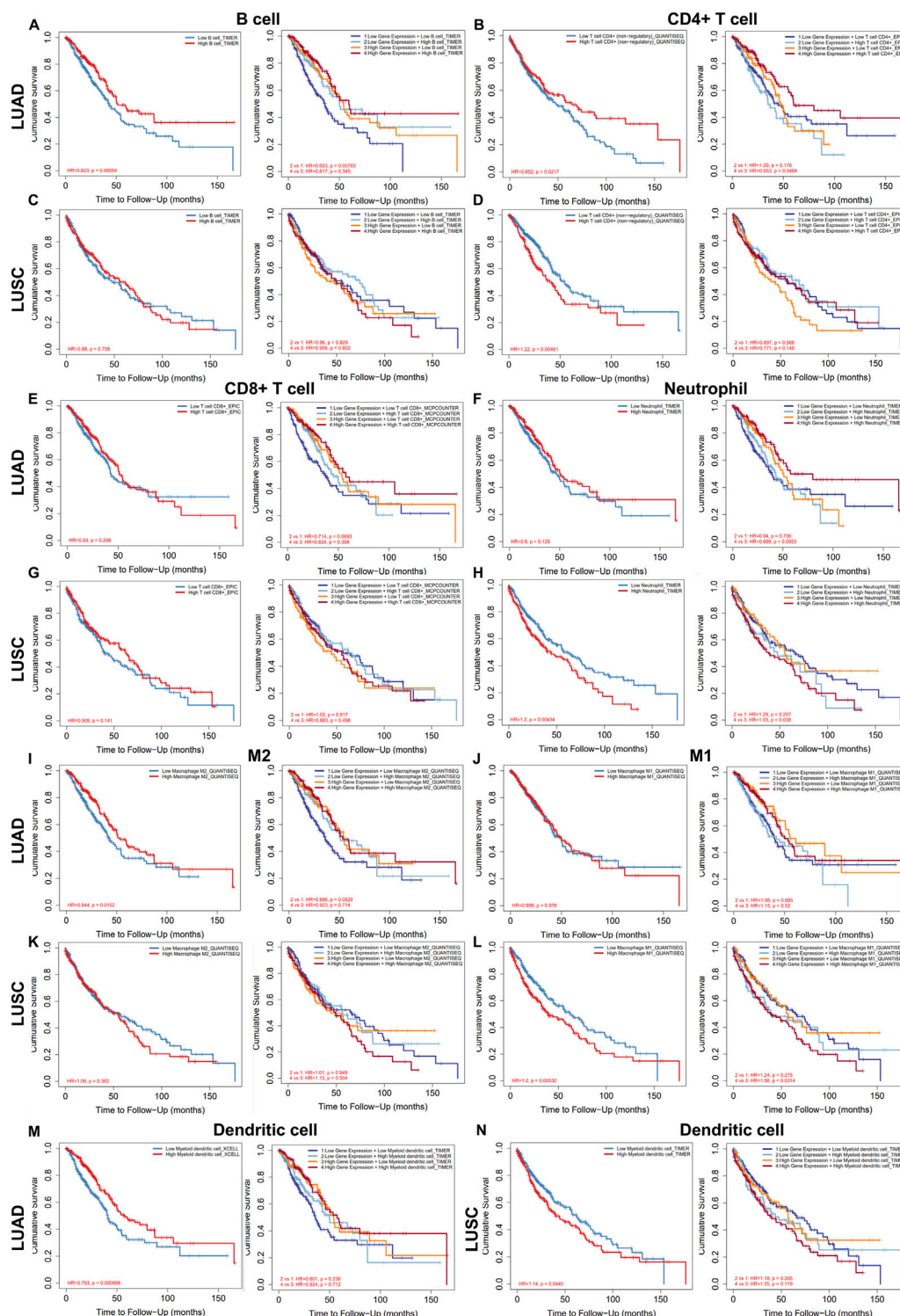


FIGURE 6

Relationship between the level of immune infiltration and OS and its synergy with TMPRSS2 expression in LUAD and LUSC by using TIMER 2.0. Including B cell (A,C), CD4⁺ T cells (B,D), CD8⁺ T cells (E,G), neutrophils (F,H), M2 (I,K), M1 (J,L) and dendritic cell (M,N).

that the higher infiltration level of Treg, the better the prognosis of LUAD whereas the poorer prognosis of LUSC, which implies that the positive correlation between TMPRSS2 and Treg will worsen the poor prognosis of LUSC. These results further illustrate that the underlying mechanism by

which TMPRSS2 leads to different prognostic patterns in LUAD and LUSC may be the recruitment and infiltration of TILs. Therefore, we will study the TILs in the tumor and normal tissue of LUAD and LUSC respectively.

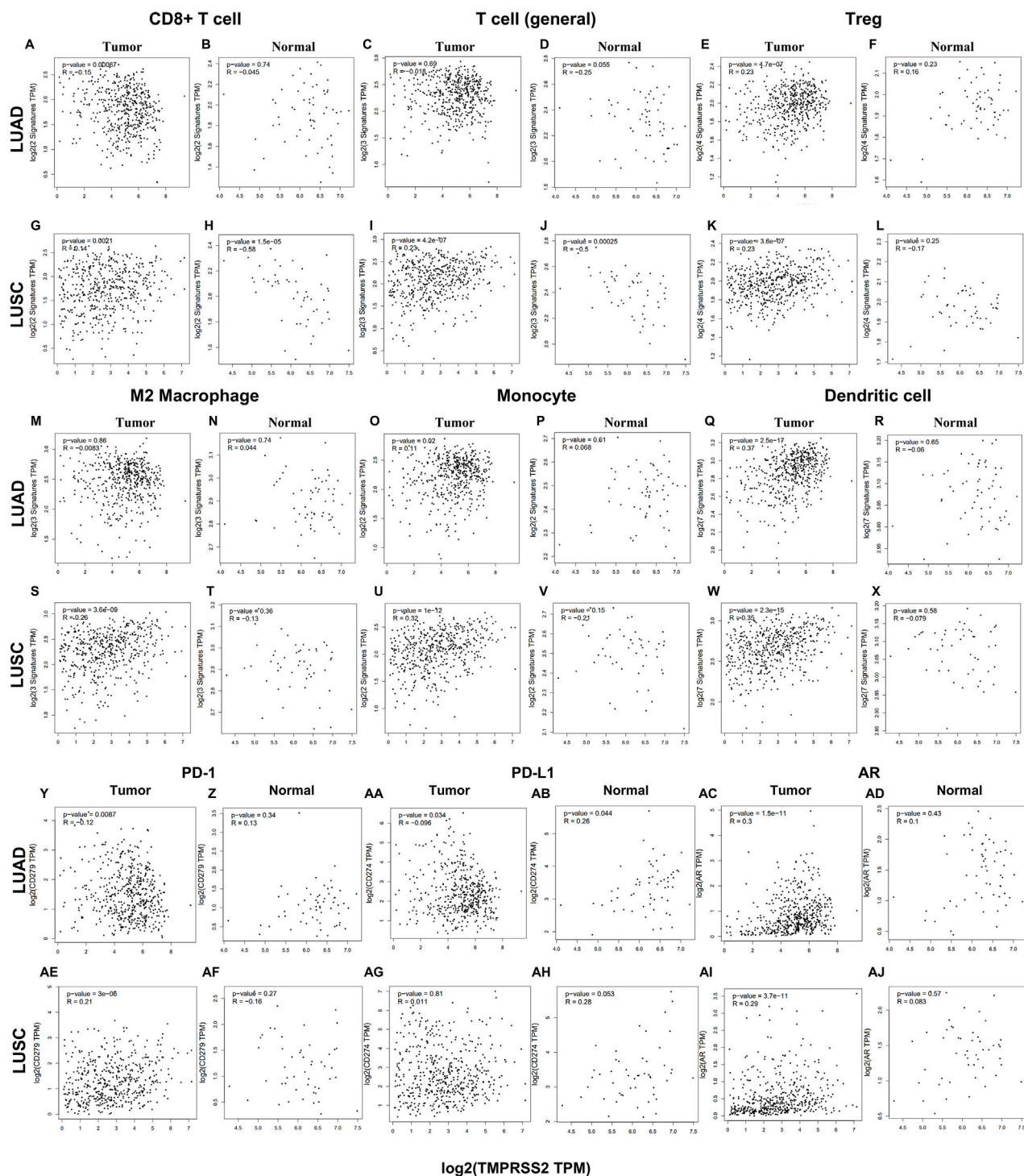


FIGURE 7

Correlation between TMPRSS2 expression and different immune cells in tumor and normal tissue of LUAD and LUSC by using GEPIA2. Markers include general T cell (CD2, CD3D, CD3E); CD8⁺ T cell (CD8A, CD8B); exhausted T cells (CTLA4, PDCD1, LAG3, GZMB and HAVCR2); Treg (CCR8, FOXP3, TGFBI, and STAT5B); monocytes (CD86, CSF1R); M2 macrophages (VSI4, MS4A4A, and CD163); Dendritic cell (CD1C, HLA-DPA1, HLA-DPB1, HLA-DQB1, HLA-DRA, ITGAX, and NRP1). Scatterplots of correlations between TMPRSS2 expression and gene markers of CD8⁺ T cell (A, B), T cell (general) (C, D), Treg (E, F), M2 Macrophage (M, N), Monocyte (O, P), Dendritic cell (Q, R), PD-1 (Y, Z), PD-L1 (AA, AB), AR (AC, AD) in tumor and normal tissue of LUAD; Scatterplots of correlations between TMPRSS2 expression and gene markers of CD8⁺ T cell (G, H), T cell (general) (I, J), Treg (K, L), M2 Macrophage (S, T), Monocyte (U, V), Dendritic cell (W, X), PD-1 (AE, AF), PD-L1 (AG, AH), AR (AI, AJ) in tumor and normal tissue of LUSC.

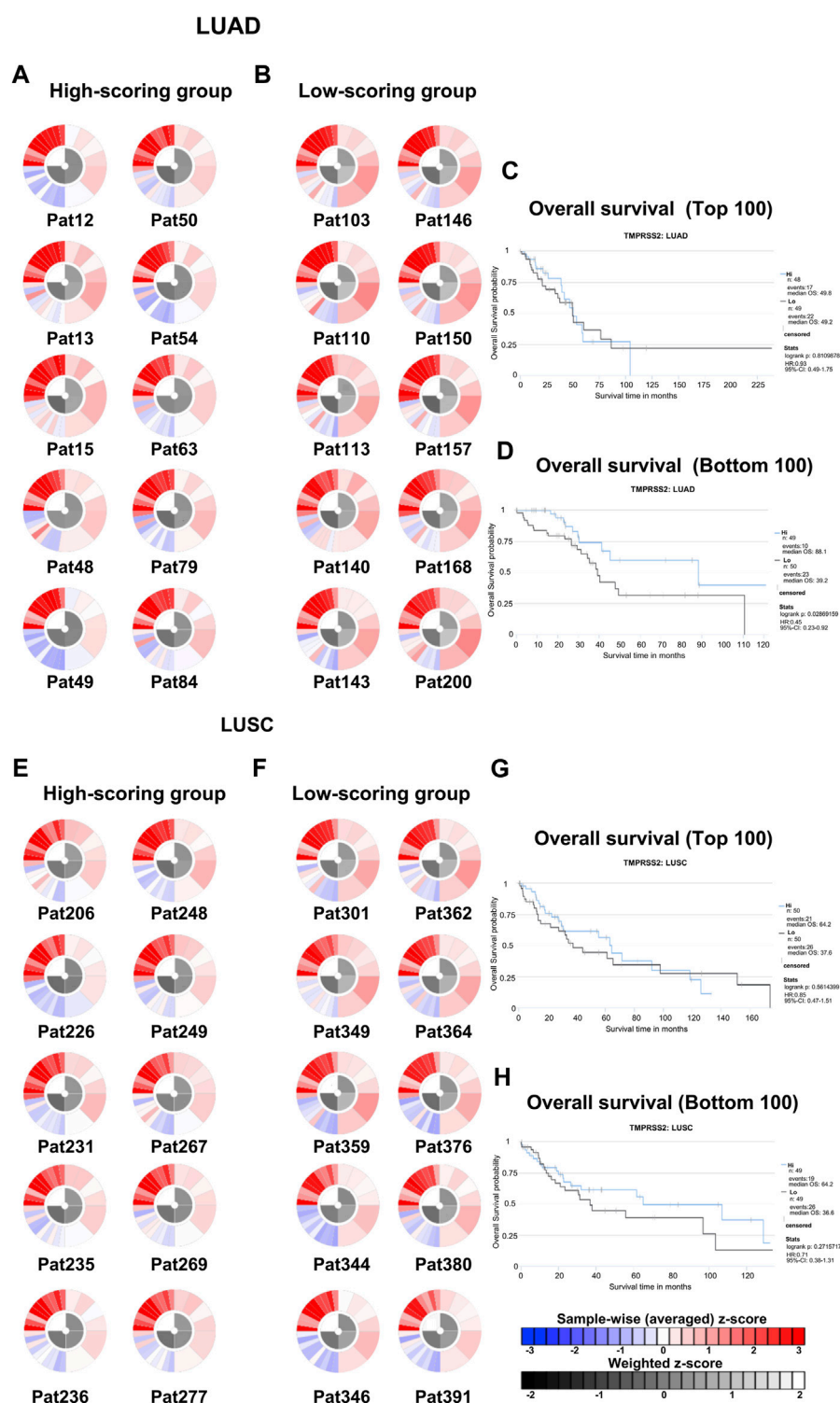
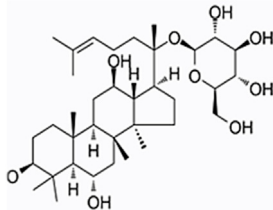
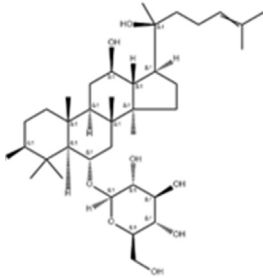
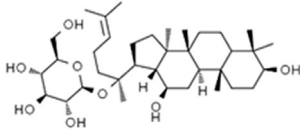
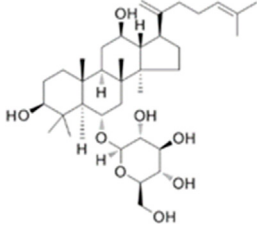
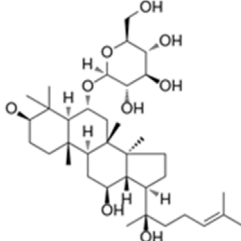


FIGURE 8

Immunophenoscores and overall survival of patients with lung cancer that response to PD-1 blockers immunotherapy in TCIA. **(A)** Immunophenograms for individual patients in the top 100 IPS_PD-1_pos patients with LUAD. The wheel contains individual factors were classified into four categories (clockwise direction), effector cells (EC), suppressor cells (SC), immunomodulators (CP), and MHC molecules (MHC). Effector cells including activated CD4⁺ T cells, activated CD8⁺ T cells, effector memory CD4⁺ T cells, effector memory CD8⁺ T cells. Immunosuppressive cells including MDSC and Treg. Immune checkpoint markers include LAG3, PDCD1, CTLA4, TIGIT, PDCD1LG2, HAVCR2, CD274, IDO1, CD27, ICOS, and B2M. MHC molecules including TAP1, TAP2, HLA-A, HLA-B, HLA-C, HLA-DPA1, HLA-DPB1, HLA-E, and HLA-F in the clockwise direction. The data displayed by the weighted average z-scores for the elements within the particular category ($z > 0$; showed in red, $z < 0$; showed in blue) **(B)** Immunophenograms for individual patients in the bottom 100 IPS_PD-1_pos patients with LUAD. **(C)** Overall survival of the top 100 IPS_PD-1_pos patients with LUAD. **(D)** Overall survival of the bottom 100 IPS_PD-1_pos patients with LUAD. **(E)** Immunophenograms for individual patients in the top 100 IPS_PD-1_pos patients with LUSC. **(F)** Immunophenograms for individual patients in the bottom 100 IPS_PD-1_pos patients with LUSC. **(G)** Overall survival of the top 100 IPS_PD-1_pos patients with LUSC. **(H)** Overall survival of the bottom 100 IPS_PD-1_pos patients with LUSC.

TABLE 2 Five candidate ginsenosides as TMPRSS2 inhibitors.

Compounds	CAS	Formula	MW	Binding energy (kcal/mol)	Scores (kcal/mol)	Ki (uM)	Structure
Ginsenoside F1	53963-43-2	C ₈ H ₁₈ 67ClN	638.88	−6.573	−9.6	0.090228	
Ginsenoside Rh1	63223-86-9	C ₈ H ₂₁ 45ClN	638.87	−6.211	−8.6	0.488831	
Ginsenoside C-K	39262-14-1	C ₈ H ₁₇ 52ClN	622.88	−6.593	−8.5	0.578816	
Ginsenoside Rk3	364779-15-7	C ₈ H ₆ 59ClN	620.86	−6.978	−8	1.347256	
(20R)-Ginsenoside Rh1	80952-71-2	C ₈ H ₁₇ 69ClN	638.9	−7.108	−6.8	10.2337	

3.8 Correlation analysis between TMPRSS2 expression and immune cells in the tumor and normal tissue of lung cancer

To evaluate the relationship between TMPRSS2 and immune infiltrating cells, we focused on the correlations between TMPRSS2 and immune cells, including general T cells, CD8⁺

T cells, Treg, M2 macrophages, monocyte, and DC in tumor and normal tissue of lung cancer. In addition, we also examined the correlation between the expression level of TMPRSS2 and the level of PD-1, PD-L1, and AR (Figure 7). After adjusting by purity, the results demonstrated a significant negative correlation between TMPRSS2 expression level and CD8⁺T cells and T cells (general) in the normal tissue of LUSC (Figures 7H, J). Moreover,

no significant correlation was detected in the normal tissue of M2 macrophages and monocyte in lung cancer cohorts (Figures 7N, P, T, V). The thing that interested us was that different correlation patterns were demonstrated in CD8⁺ T cells and general T cells in tumor and normal tissue in LUAD and LUSC. In the tumor tissue, TMPRSS2 was negatively correlated with CD8⁺ T cells in LUAD cohort but positively correlated in LUSC cohort (Figures 7A, G). General T cells were positively correlated with TMPRSS2 in LUSC cohort but have no correlation with TMPRSS2 in the tumor tissue of LUAD patients (Figures 7C, I).

M2 macrophages are tumor-promoting cells and TMPRSS2 was significantly associated with M2 in the tumor tissue of LUSC rather than in LUAD (Figures 7M, S).

The association between TMPRSS2 and Treg, monocyte and DC is consistent in LUAD and LUSC tumor tissues (Figures 7E, K, O, U, Q, W). In addition, TMPRSS2 was negatively correlated with CD8⁺ T cells and T cells (general) in LUSC normal tissues, but not significant negatively correlated in LUAD normal tissues (Figures 7B, D, H, J).

We also found that TMPRSS2 was positively associated with PD-1, and AR in LUAD normal tissues but the difference was not significant (Figures 7Z, AD). Moreover, the expression level of TMPRSS2 and PD-1 and PD-L1 demonstrated different correlation patterns in the tumor tissue of lung cancer (Figures 7Y, AA, AE, AG). Also, we found that TMPRSS2 was positively related to AR and negatively associated with PD-1 and PD-L1 in LUAD tumor tissue (Figures 7Y, AA, AC), suggesting that TMPRSS2 agonists might be an immunomodulator of LUAD to anti-PD-1 based immunotherapy combination therapies.

So, all these above are indicated that the different prognosis patterns might be induced by the different immune infiltrating patterns. Further research is needed to determine whether TMPRSS2 is crucial in mediating immune cells recruitment and remodeling the tumor microenvironment.

Also, we examined different functional T cells, such as Th1 cells, Th2 cells, Th17 cells, Tfh cells, and Tregs, as well as exhausted T cells, which are all essential elements involved in tumor immune infiltrating. It was found that TMPRSS2 was positively related to naive T-cells, resident memory T-cells, central memory T-cells, exhausted T cells, resting Treg, and Th1-like cells in LUAD normal tissues but the difference was not significant (Supplementary Figures 5B, N, P, R, Z, AD). Moreover, the expression level of TMPRSS2 and the effector memory T-cell, resting Treg, T cell exhaustion, and effector Treg demonstrated different correlation patterns in the tumor tissue of lung cancer (Supplementary Figures 5E, K, Q, W, Y, AE, AA, AG). These might be the reason that higher TMPRSS2 expression levels leading a better prognosis in LUAD patients.

3.9 Prediction of the relationship between TMPRSS2 expression and response to PD-1 blockade immunotherapy in patients with lung cancer

Due to intrinsic immune resistance, only a minority of cancer patients benefit from anti-PD-1 therapy. We used the TCIA

database to investigate whether TMPRSS2 influences the response of patients with lung cancer to anti-PD-1 immunotherapy. We obtained and ranked IPS that predict response to PD-1 blockers in patients with LUAD and LUSC from the TCIA database (Figure 8; Supplementary Table S6). The top 100 and bottom 100 patients were selected for follow-up analysis. Immunophenograms of representative patients were obtained from the top 100 and bottom 100 patients of LUAD and LUSC cohorts respectively (Figures 8A, B, E, F). We found that high-scoring patients and low-scoring patients had different expression patterns. Immunosuppressive cells were enriched in tumors of low-scoring patients compared with the high ones. In addition, we studied the association between the expression of TMPRSS2 and prognosis in high- and low-scoring patients, respectively (Figures 8C, D, G, H). And found that the mRNA expression of TMPRSS2 in LUAD was significantly positive associated with prognosis in low-scoring patients. All these above imply that TMPRSS2 might be an immunomodulator in patients who have no response to anti-PD-1 therapy.

3.10 Screening of candidate TMPRSS2 inhibitors

We obtained a collection of ginsenosides that could serve as TMPRSS2 inhibitors by screening. To evaluate the affinity of the drug candidates for their targets, we performed molecular docking analysis and five ginsenosides that could bind to TMPRSS2 were obtained, namely ginsenoside F1, ginsenoside Rh1, ginsenoside C-K, ginsenoside Rk3 and (20R)-Ginsenoside Rh1, and yielded binding energies per interaction (Table 2). We found that the binding energies of these five ginsenosides to TMPRSS2 were all greater than 6 kcal/mol, indicating that they have good binding activity to TMPRSS2.

Discussion

As a type II transmembrane serine endopeptidase, TMPRSS2 is conserved in many organisms (Shen et al., 2017). It is expressed in many tissues, such as lung, liver and prostate, etc., among which it is mainly expressed in the prostate in an androgen-dependent manner (Lin et al., 1999). TMPRSS2 plays a role in many pathophysiological processes, including digestion, tissue remodeling, inflammation, tumor cell infiltration, apoptosis, and pain (Lam et al., 2015; Thunders and Delahunt, 2020). Emerging researches have demonstrated a functional association between TMPRSS2 and various types of disease, especially tumors (Hong et al., 2020). Whether TMPRSS2 is involved in various tumors' pathogenesis via certain molecular mechanisms remains to be elucidated. TMPRSS2 has been found to inhibit colorectal cancer cell migration (Bowden et al., 2007), and its expression was diminished in cases with P53 mutations (Nishijima et al., 2015). In addition, TMPRSS2 was also taken a key part in HCC by driving the recruitment and differentiation of peritumoral fibroblasts into TAMs (Thunders and Delahunt, 2020). These findings suggest the involvement of TMPRSS2 in TME. Immunotherapy, the new

treatment method available to patients, is associated strongly and consistently with TME.

In this study, we comprehensively studied the mRNA expression, protein level, molecular features of gene expression, DNA methylation, genetic alteration, and protein level of TMPRSS2 in two subtypes of NSCLC relying on various types of computational approaches. Moreover, this finding has been verified by IHC staining study.

According to our study, variations in TMPRSS2 expression level influence prognosis across various cancers, and a higher level of TMPRSS2 associated with better prognosis in LUAD cohorts. Furthermore, our analyses based on databases show that prognosis patterns among lung cancer subtypes differ according to immune infiltration levels. Consequently, our research also offers novel insights into TMPRSS2's possible role in tumor immunology as well as its potential use as a biomarker and novel therapeutic target for lung cancer.

Studies have shown that androgens can promote the exhaustion of CD8⁺T cells by regulating the transcription factor Tcf7, thereby promoting tumor growth. Blockade of androgen receptors can significantly enhance the efficacy of anti-PD-1 therapy (Thunders and Delahunt, 2020). We found that in LUAD, compared with normal tissues, AR was significantly positively correlated with TMPRSS2 in tumor tissues, this was also confirmed in the protein expression levels of TMPRSS2 in different sexes (Figure 7AC; Supplementary Figure S2D). Additionally, we also found a significant decrease of TMPRSS2 in tumor tissues of patients with lung cancer. Also, a significant negative correlation was observed between TMPRSS2 and PD-1 and PD-L1 expression. Furthermore, the correlation between TMPRSS2 and the prognosis of patient who have no response to anti-PD-1 immunotherapy was positive, suggesting that agonists of TMPRSS2 may benefit the treatment of LUAD patients who are not suitable for PD-1 inhibitor therapy. These above suggest that: ① TMPRSS2 might be a new target for combined therapies based on anti-PD-1; ② This combined strategy may significantly extend cancer immunotherapy and improve the clinical benefits of male LUAD patients; ③ Among these, the advanced patients may profit more from the therapeutics above. These conclusions are based on sequencing data from a large database using bioinformatics approaches and IHC study on over one hundred paired tumors and adjacent normal tissues from LUAD and LUSC patients, respectively. In the future, we plan to carry out wet-bench experiments, such as flow cytometry analysis to determine the ratio of different types of immune cells in lung cancer mice model to minimize these limitations mentioned above and to make our conclusions as solid as possible. Ginsenosides, as the main active substances in ginseng, have a wide range of antitumor activities. After relevant screening and molecular docking analysis, five ginsenosides that could bind to TMPRSS2 were finally identified. The selectivity of TMPRSS2 inhibitors will be further evaluated to identify small molecules with higher selectivity for TMPRSS2. In addition, ginsenosides will play a role in the prevention and treatment of COVID-19 as an inhibitor of TMPRSS2. However, as TMPRSS2 inhibition is detrimental to the prognosis of LUAD patients who have no response to anti-PD-1 therapy, its use in the prevention and treatment of COVID-19 in LUAD patient needs to be thoughtfully considered, since the different roles of TMPRSS2 expression level in patients with COVID-19 infection

and in LUAD patients who do not respond to PD-1 treatment, trade-offs need to be made in medicating TMPRSS2 inhibitors, such as ginsenosides to gain prophylactic and therapeutic benefits against COVID-19 and treatment in LUAD patients. The five ginsenoside candidates we selected here are based on virtual screening, so we believe that further pharmacological experiments are necessary to verify our findings. We started to administer these five ginsenoside compounds to LUAD and LUSC mice model to observe the tumor biology and the recruitment of immune cells *in vivo*, which will facilitate to improve the credibility of our findings.

This study provides an overview of TMPRSS2 expression and lung cancer. All these correlations above suggest the potential mechanism where TMPRSS2 regulates T cell functions in LUAD. All these findings suggest that TMPRSS2 takes a vital part in the recruitment and regulation of NK cells and effective T cells, leading to a better prognosis.

Toll-like receptors (TLRs), a type I membrane protein, play a role in recognizing various pathogen-associated molecular patterns (PAMPs) to initiate innate immunity, and are very important for early host defense (Owen et al., 2020). In addition, TLRs maintain tissue homeostasis and promote antitumor effects through activation and modulation of adaptive immune responses. As potent immune stimulators, the binding of TLR agonists to TLRs promotes the maturation of antigen-presenting cells, activates downstream signaling pathways, such as MAP kinases, NFκB, and IRF, and disrupts immunosuppression and tolerance, thereby enhancing innate or treatment-induced antitumor immune response (Owen et al., 2020; Kayesh et al., 2021). A study on primary human nasal epithelial cells found that the TLR3 agonist Poly (I: C) can activate IFN and NFκB signaling pathways after binding to TLR3, thereby increasing the expression levels of ACE2 and TMPRSS2 (Nakazono et al., 2021). Since the TLR agonist poly (I: C) can enhance the expression of TMPRSS2 and act on innate immune cells, this means that the use of TLR agonists in lung cancer will enhance the efficacy of PD-1 targeting adaptive immune cells (Nakazono et al., 2021). Moreover, the researchers found that cancer patients were more vulnerable to SARS-CoV-2 infection and, thus, had worse clinical outcomes (Dai et al., 2020). So this suggests that we should pay more attention to cancer patients in the COVID-19 prophylactic and therapeutic. At the same time, we speculate that LUAD patients infected with COVID-19 may not be suitable for TMPRSS2 inhibitors treatment.

Taken together, our findings may suggest that: ① TMPRSS2 agonists might be an immunomodulator of LUAD patients to anti-PD-1 based immunotherapy combination therapies; ② Gender-dependent AR level difference could be an explanation for the difference in the risk of COVID-19 infection in patients with lung cancer between males and females since the mRNA expression level of AR is significantly positively correlated with TMPRSS2's; ③ Non-TMPRSS2 inhibitor treatment, such as COVID-19 vaccines, should be taken into consideration first in the COVID-19 prophylactic and therapeutic of lung cancer patients, especially LUAD patients.

Conclusion

In this study, we proposed a possible mechanism that explains why TMPRSS2 expression correlates with immune infiltration leads to different prognosis patterns in different types of lung cancer. These

may indicate that TMPRSS2 may be a novel prognostic biomarker for indicating prognostic potential and immune infiltration levels in LUAD and LUSC cohorts and most likely serve as a potential immunomodulator target of immunotherapy combination therapies of nonresponse to anti-PD-1 therapy LUAD patients.

In addition, we identified ginsenosides that can act as TMPRSS2 inhibitors, but due to the different roles of TMPRSS2 expression level in patients with COVID-19 infection and in LUAD patients who do not respond to PD-1 treatment, trade-offs need to be made in medicating TMPRSS2 inhibitors, such as ginsenosides to gain prophylactic and therapeutic benefits against COVID-19 and treatment in LUAD patients.

Data availability statement

The original contributions presented in the study are included in the article/[Supplementary Materials](#), further inquiries can be directed to the corresponding authors.

Author contributions

JH, MM, RG, ZL, and FL: Methodology, reviewing and editing. YS and SD revised and proofread the article. JH: Conceptualization, JH and MM: Writing—original draft.

Funding

This study is supported by the grants of National Science Foundation of China (NSFC 81702730), National Key R&D Program of China (2022YFD2101503) and Start-up Plan for New

Young Teacher of SHSMU (KJ30214190026) of JH, Gusu innovation and entrepreneurship leading talents of Suzhou City (ZXL2021422) and the Primary Research and Development Plan of Jilin Province (20210204117YY) of YS, Key R&D Projects of Zhejiang Province (No. 2019C01060), the National Natural Science Foundation of China (No. 52250005, U20B2021, and 21875271), the Entrepreneurship Program of Foshan National Hi-tech Industrial Development Zone and Zhejiang Public Welfare Applied Research Project (LGJ20E020001) of SD.

Conflict of interest

The authors declare that the research was conducted in the absence of any commercial or financial relationships that could be construed as a potential conflict of interest.

Publisher's note

All claims expressed in this article are solely those of the authors and do not necessarily represent those of their affiliated organizations, or those of the publisher, the editors and the reviewers. Any product that may be evaluated in this article, or claim that may be made by its manufacturer, is not guaranteed or endorsed by the publisher.

Supplementary material

The Supplementary Material for this article can be found online at: <https://www.frontiersin.org/articles/10.3389/fphar.2023.1085509/full#supplementary-material>

References

- Anaya, J. (2016). OncoLnc: Linking TCGA survival data to mRNAs, miRNAs, and lncRNAs. *PeerJ Comput. Sci.* 2 (2), e67. doi:10.7717/peerj-cs.67
- Aran, D., Sirota, M., and Butte, A. J. (2015). Systematic pan-cancer analysis of tumour purity. *Nat. Commun.* 6, 8971. doi:10.1038/ncomms9971
- Behrens, C., Solis, L. M., Lin, H., Yuan, P., Tang, X., Kadara, H., et al. (2013). EZH2 protein expression associates with the early pathogenesis, tumor progression, and prognosis of non-small cell lung carcinoma. *Clin. Cancer Res.* 19 (23), 6556–6565. doi:10.1158/1078-0432.CCR-12-3946
- Benevides, L., da Fonseca, D. M., Donate, P. B., Tiezzi, D. G., De Carvalho, D. D., de Andrade, J. M., et al. (2015). IL17 promotes mammary tumor progression by changing the behavior of tumor cells and eliciting tumorigenic neutrophils recruitment. *Cancer Res.* 75 (18), 3788–3799. doi:10.1158/0008-5472.CAN-15-0054
- Bowden, N. A., Croft, A., and Scott, R. J. (2007). Gene expression profiling in familial adenomatous polyposis adenomas and desmoid disease. *Hered. Cancer Clin. Pract.* 5 (2), 79–96. doi:10.1186/1897-4287-5-2-79
- Chandrasekar, D. S., Bashel, B., Balasubramanya, S. A. H., Creighton, C. J., Ponce-Rodriguez, I., Chakravarthi, B., et al. (2017). Ualcan: A portal for facilitating tumor subgroup gene expression and survival analyses. *Neoplasia* 19 (8), 649–658. doi:10.1016/j.neo.2017.05.002
- Charoentong, P., Finotello, F., Angelova, M., Mayer, C., Efremova, M., Rieder, D., et al. (2017). Pan-cancer immunogenomic analyses reveal genotype-immunophenotype relationships and predictors of response to checkpoint blockade. *Cell. Rep.* 18 (1), 248–262. doi:10.1016/j.celrep.2016.12.019
- Chen, J., Si, M., Wang, Y., Liu, L., Zhang, Y., Zhou, A., et al. (2019). Ginsenoside metabolite compound K exerts anti-inflammatory and analgesic effects via downregulating COX2. *Inflammopharmacology* 27 (1), 157–166. doi:10.1007/s10787-018-0504-y
- Chi, M., Shi, X., Huo, X., Wu, X., Zhang, P., and Wang, G. (2020). Dexmedetomidine promotes breast cancer cell migration through Rab11-mediated secretion of exosomal TMPRSS2. *Ann. Transl. Med.* 8 (8), 531. doi:10.21037/atm.2020.04.28
- Dai, M., Liu, D., Liu, M., Zhou, F., Li, G., Chen, Z., et al. (2020). Patients with cancer appear more vulnerable to SARS-CoV-2: A multicenter study during the COVID-19 outbreak. *Cancer Discov.* 10 (6), 783–791. doi:10.1158/2159-8290.CD-20-0422
- Danaher, P., Warren, S., Dennis, L., D'Amico, L., White, A., Disis, M. L., et al. (2017). Gene expression markers of tumor infiltrating leukocytes. *J. Immunother. Cancer* 5, 18. doi:10.1186/s40425-017-0215-8
- Gao, J. L., Lv, G. Y., He, B. C., Zhang, B. Q., Zhang, H., Wang, N., et al. (2013). Ginseng saponin metabolite 20(S)-protopanaxadiol inhibits tumor growth by targeting multiple cancer signaling pathways. *Oncol. Rep.* 30 (1), 292–298. doi:10.3892/or.2013.2438
- Gao, R., Meng, M., Zhou, X., Yu, M., Li, Z., Li, J., et al. (2022). TRPV1, a novel biomarker associated with lung cancer via excluding immune infiltration. *MedComm* 3 (2), e139. doi:10.1002/mco2.139
- Glowacka, I., Bertram, S., Müller, M. A., Allen, P., Soilleux, E., Pfefferle, S., et al. (2011). Evidence that TMPRSS2 activates the severe acute respiratory syndrome coronavirus spike protein for membrane fusion and reduces viral control by the humoral immune response. *J. Virol.* 85 (9), 4122–4134. doi:10.1128/JVI.02232-10
- He, J. (2017). Bioactivity-guided fractionation of pine needle reveals catechin as an anti-hypertension agent via inhibiting angiotensin-converting enzyme. *Sci. Rep.* 7 (1), 8867. doi:10.1038/s41598-017-07748-x
- He, J., Gao, R., Meng, M., Yu, M., Liu, C., Li, J., et al. (2021). Lysophosphatidic acid receptor 6 (LPAR6) is a potential biomarker associated with lung adenocarcinoma. *Int. J. Environ. Res. Public Health* 18 (21), 11038. doi:10.3390/ijerph182111038

- He, J., Lin, Y., Meng, M., Li, J., Yang, J. Y., and Wang, H. (2021). Construction of a human cell landscape of COVID-19 infection at single-cell level. *Aging Dis.* 12 (3), 705–709. doi:10.14336/AD.2021.0301
- He, J., Meng, M., and Wang, H. (2022). A novel prognostic biomarker LPAR6 in hepatocellular carcinoma via associating with immune infiltrates. *J. Clin. Transl. Hepatol.* 10 (1), 90–103. doi:10.14218/JCTH.2021.00047
- He, J., Qiu, N., Zhou, X., Meng, M., Liu, Z., Li, J., et al. (2023). Resveratrol analog, triacetylresveratrol, a potential immunomodulator of lung adenocarcinoma immunotherapy combination therapies. *Front. Oncol.* 12, 1007653. doi:10.3389/fonc.2022.1007653
- He, J., Wang, H., and Vijj, J. (2019). New insights into bioactive compounds of traditional Chinese medicines for insulin resistance based on signaling pathways. *Chem. Biodivers.* 16 (9), e1900176. doi:10.1002/cbdv.201900176
- He, J., and Li, Y. (2015). Ginsenoside Rg1 downregulates the shear stress induced MCP-1 expression by inhibiting MAPK signaling pathway. *The American Journal of Chinese Medicine* 43 02, 305–317.
- Hoffmann, M., Kleine-Weber, H., Schroeder, S., Krüger, N., Herrler, T., Erichsen, S., et al. (2020). SARS-CoV-2 cell entry depends on ACE2 and TMPRSS2 and is blocked by a clinically proven protease inhibitor. *Cell.* 181 (2), 271–280. e8. doi:10.1016/j.cell.2020.02.052
- Hong, Z., Zhang, W., Ding, D., Huang, Z., Yan, Y., Cao, W., et al. (2020). DNA damage promotes TMPRSS2-ERG oncoprotein destruction and prostate cancer suppression via signaling converged by GSK3 β and WEE1. *Mol. Cell.* 79 (6), 1008–1023. e4. doi:10.1016/j.molcel.2020.07.028
- Hossain, D., and Bostwick, D. G. (2013). Significance of the TMPRSS2:ERG gene fusion in prostate cancer. *BJU Int.* 111 (5), 834–835. doi:10.1111/bju.12120
- Kayesh, M. E. H., Kohara, M., and Tsukiyama-Kohara, K. (2021). An overview of recent insights into the response of TLR to SARS-CoV-2 infection and the potential of TLR agonists as SARS-CoV-2 vaccine adjuvants. *Viruses* 13 (11), 2302. doi:10.3390/v13112302
- Koch, A., De Meyer, T., Jeschke, J., and Van Criekinge, W. (2015). Mexpress: Visualizing expression, DNA methylation and clinical TCGA data. *BMC Genomics* 16 (1), 636. doi:10.1186/s12864-015-1847-z
- Lam, D. K., Dang, D., Flynn, A. N., Hardt, M., and Schmidt, B. L. (2015). TMPRSS2, a novel membrane-anchored mediator in cancer pain. *Pain* 156 (5), 923–930. doi:10.1097/j.pain.0000000000000130
- Lánczky, A., and Györfi, B. (2021). Web-based survival analysis tool tailored for medical research (KMplot): Development and implementation. *J. Med. Internet Res.* 23 (7), e27633. doi:10.2196/27633
- Larsen, T. V., Hussmann, D., and Nielsen, A. L. (2019). PD-L1 and PD-L2 expression correlated genes in non-small-cell lung cancer. *Cancer Commun. (Lond)* 39 (1), 30. doi:10.1186/s40880-019-0376-6
- Li, B., Severson, E., Pignon, J. C., Zhao, H., Li, T., Novak, J., et al. (2016). Comprehensive analyses of tumor immunity: Implications for cancer immunotherapy. *Genome Biol.* 17 (1), 174. doi:10.1186/s13059-016-1028-7
- Li, M., Pei, J., Xu, M., Shu, T., Qin, C., Hu, M., et al. (2021). Changing incidence and projections of thyroid cancer in mainland China, 1983–2032: Evidence from cancer incidence in five continents. *Cancer Causes Control* 32 (10), 1095–1105. doi:10.1007/s10552-021-01458-6
- Li, T., Fu, J., Zeng, Z., Cohen, D., Li, J., Chen, Q., et al. (2020). TIMER2.0 for analysis of tumor-infiltrating immune cells. *Nucleic Acids Res.* 48 (W1), W509–W514. doi:10.1093/nar/gkaa407
- Lin, B., Ferguson, C., White, J. T., Wang, S., Vessella, R., True, L. D., et al. (1999). Prostate-localized and androgen-regulated expression of the membrane-bound serine protease TMPRSS2. *Cancer Res.* 59 (17), 4180–4184.
- Mizuno, H., Kitada, K., Nakai, K., and Sarai, A. (2009). Prognoscan: A new database for meta-analysis of the prognostic value of genes. *BMC Med. Genomics* 2, 18. doi:10.1186/1755-8794-2-18
- Morris, G. M., Huey, R., and Olson, A. J. (2008). Using AutoDock for ligand-receptor docking. *Curr. Protoc. Bioinforma.* 8, 814. doi:10.1002/0471250953.bi0814s24
- Nakazono, A., Nakamaru, Y., Ramezani, M., Kondo, T., Watanabe, M., Hatakeyama, S., et al. (2021). Fluticasone propionate suppresses poly(I:C)-Induced ACE2 in primary human nasal epithelial cells. *Front. Cell. Infect. Microbiol.* 11, 655666. doi:10.3389/fcimb.2021.655666
- Nishijima, J., Hara, T., Ikemoto, K., Oga, A., Kobayashi, K., Kawai, Y., et al. (2015). Clinical significance of ERG rearrangement subtype and its association with increased p53 expression in Japanese and German prostate cancer. *Neoplasma* 62 (2), 278–287. doi:10.4149/neo_2015_033
- Owen, A. M., Fults, J. B., Patil, N. K., Hernandez, A., and Bohannon, J. K. (2020). TLR agonists as mediators of trained immunity: Mechanistic insight and immunotherapeutic potential to combat infection. *Front. Immunol.* 11, 622614. doi:10.3389/fimmu.2020.622614
- Shen, L. W., Mao, H. J., Wu, Y. L., Tanaka, Y., and Zhang, W. (2017). TMPRSS2: A potential target for treatment of influenza virus and coronavirus infections. *Biochimie* 142, 1–10. doi:10.1016/j.biochi.2017.07.016
- Siemers, N. O., Holloway, J. L., Chang, H., Chasalow, S. D., Ross-MacDonald, P. B., Voliva, C. F., et al. (2017). Genome-wide association analysis identifies genetic correlates of immune infiltrates in solid tumors. *PLoS One* 12 (7), e0179726. doi:10.1371/journal.pone.0179726
- Stanton, S. E., and Disis, M. L. (2016). Clinical significance of tumor-infiltrating lymphocytes in breast cancer. *J. Immunother. Cancer* 4, 59. doi:10.1186/s40425-016-0165-6
- Su, X., Lu, Z., Shi, Y., Zhang, R., Long, Q., Bai, S., et al. (2021). Clonal evolution in liver cancer at single-cell and single-variant resolution. *J. Hematol. Oncol.* 14 (1), 22. doi:10.1186/s13045-021-01036-y
- Sun, D., Wang, J., Han, Y., Dong, X., Ge, J., Zheng, R., et al. (2021). Tisch: A comprehensive web resource enabling interactive single-cell transcriptome visualization of tumor microenvironment. *Nucleic Acids Res.* 49 (D1), D1420–D1430. doi:10.1093/nar/gkaa1020
- Sun, J., Jiao, C., Ma, Y., Chen, J., Wu, W., and Liu, S. (2018). Anti-ageing effect of red ginseng revealed by urinary metabolomics using RRLC-Q-TOF-MS. *Phytochem. Anal.* 29 (4), 387–397. doi:10.1002/pca.2758
- Tan, A. C., and Tan, D. S. W. (2022). Targeted therapies for lung cancer patients with oncogenic driver molecular alterations. *J. Clin. Oncol.* 40 (6), 611–625. doi:10.1200/JCO.21.01626
- Tang, Z., Kang, B., Li, C., Chen, T., and Zhang, Z. (2019). GEPIA2: An enhanced web server for large-scale expression profiling and interactive analysis. *Nucleic Acids Res.* 47 (W1), W556–W560. doi:10.1093/nar/gkz430
- Tariq, M., Zhang, J., Liang, G., Ding, L., He, Q., and Yang, B. (2017). Macrophage polarization: Anti-cancer strategies to target tumor-associated macrophage in breast cancer. *J. Cell. Biochem.* 118 (9), 2484–2501. doi:10.1002/jcb.25895
- Thunders, M., and Delahunt, B. (2020). Gene of the month: TMPRSS2 (transmembrane serine protease 2). *J. Clin. Pathol.* 73 (12), 773–776. doi:10.1136/jclinpath-2020-206987
- Vasaikar, S. V., Straub, P., Wang, J., and Zhang, B. (2018). LinkedOmics: Analyzing multi-omics data within and across 32 cancer types. *Nucleic Acids Res.* 46 (D1), D956–D963. doi:10.1093/nar/gkx1090
- Wang, Q., Li, L., Qu, T., Li, J., Wu, L., Li, K., et al. (2021). High expression of ACE2 and TMPRSS2 at the resection margin makes lung cancer survivors susceptible to SARS-CoV-2 with unfavorable prognosis. *Front. Oncol.* 11, 644575. doi:10.3389/fonc.2021.644575
- Warde-Farley, D., Donaldson, S. L., Comes, O., Zuberi, K., Badrawi, R., Chao, P., et al. (2010). The GeneMANIA prediction server: Biological network integration for gene prioritization and predicting gene function. *Nucleic Acids Res.* 38, W214–W220. doi:10.1093/nar/gkq537
- Wu, W., Zhou, Q., Zhao, W., Gong, Y., Su, A., Liu, F., et al. (2018). Ginsenoside Rg3 inhibition of thyroid cancer metastasis is associated with alternation of actin skeleton. *J. Med. Food* 21 (9), 849–857. doi:10.1089/jmf.2017.4144
- Yang, K., Luo, Y., Lu, S., Hu, R., Du, Y., Liao, P., et al. (2018). Salvianolic acid B and ginsenoside Re synergistically protect against ox-LDL-induced endothelial apoptosis through the antioxidative and antiinflammatory mechanisms. *Front. Pharmacol.* 9, 662. doi:10.3389/fphar.2018.00662
- Zhou, Y. D., Hou, J. G., Liu, W., Ren, S., Wang, Y. P., Zhang, R., et al. (2018). 20(R)-ginsenoside Rg3, a rare saponin from red ginseng, ameliorates acetaminophen-induced hepatotoxicity by suppressing PI3K/AKT pathway-mediated inflammation and apoptosis. *Int. Immunopharmacol.* 59, 21–30. doi:10.1016/j.intimp.2018.03.030

Frontiers in Pharmacology

Explores the interactions between chemicals and living beings

The most cited journal in its field, which advances access to pharmacological discoveries to prevent and treat human disease.

Discover the latest Research Topics

[See more →](#)

Frontiers

Avenue du Tribunal-Fédéral 34
1005 Lausanne, Switzerland
frontiersin.org

Contact us

+41 (0)21 510 17 00
frontiersin.org/about/contact



Frontiers in Pharmacology

